The Holocene history of George VI Ice Shelf, Antarctic Peninsula

Smith, James Alexander

THE HOLOCENE HISTORY OF GEORGE VI ICE SHELF, ANTARCTIC PENINSULA

James Alexander Smith

This thesis is submitted in accordance with the regulations for the degree of Doctor of Philosophy at Durham University, Department of Geography, 2005.

DECLARATION

I confirm that no part of the material presented in this thesis has previously been submitted by me or any other person for a degree in this or any other university. In all cases, where it is relevant, material from the work of others has been acknowledged.

The copyright of this thesis rests with the author. No quotation from it should be published without prior written consent and information derived from it should be acknowledged.

Signed: 

Date: 6/5/2005

THE HOLOCENE HISTORY OF GEORGE VI ICE SHELF, ANTARCTIC PENINSULA

James Alexander Smith

ABSTRACT

Meteorological records have shown that the Antarctic Peninsula region has warmed at a rate of 3.7 ± 1.6 °C during the last century. One of the most publicised aspects of this warming has been the retreat and disintegration of several of the regions ice shelves. It is unknown at present however, whether advance and retreat of these ice shelves has occurred repeatedly in response to natural Holocene climate change, or whether their recent collapse is the result of the recent rapid regional warming that has been linked to anthropogenic forcings.

George VI Ice Shelf is the largest ice shelf on the western side of the Antarctic Peninsula and its northern margin marks the southern most latitudinal limit of recent ice shelf retreat. At Ablation Point, on the east coast of Alexander Island, the ice shelf impounds two epishelf lakes: Moutonnée and Ablation. These lakes are tidal, stratified water bodies with a lower marine layer that extends under the ice shelf and an upper freshwater layer whose maximum thickness is determined by the draught of the ice shelf. The first aim of this thesis was to document the physical limnology and sedimentary environment of Moutonnée and Ablation Lakes. Collectively, this information has led to the development of a conceptual model for detecting ice shelf collapse in epishelf lakes and has provided important baseline data for any future changes in the stability of the ice shelf. The second aim was to reconstruct the long-term (Holocene) history of George VI Ice Shelf through detailed analysis of lake sediments from Moutonnée and Ablation Lakes. In addition, this thesis provides a detailed review of the dynamics of George VI Ice Shelf, which provides an important context to any future changes in the configuration of the ice shelf.

Studies of sediment cores extracted from Moutonnée and Ablation Lakes have included; micropaleontology (diatoms/ foraminifera), stable isotope ($\delta^{18}O$, $\delta^{13}C$), geochemistry (C_{org}, N_{org}, C/N ratios) and physical (grain-size/magnetic susceptibility) analyses. Together with the ideas developed in the conceptual model, these data provide robust evidence for one period of past ice shelf absence during the Holocene. The timing of this period has been constrained by 10 AMS ^{14}C dates performed on mono-specific foraminifera samples. These dates suggest that George VI Ice Shelf was absent between ca. 8962 cal. (calibrated) yr B.P. and ca. 7945 cal. yr B.P. This early Holocene absence immediately followed a period of maximum Holocene warmth that is recorded in some Antarctic ice cores and coincides with an influx of warmer ocean water onto the western Antarctic Peninsula shelf at ca. 9000 cal. yr B.P. The absence of the ice shelf during this time interval suggests that early Holocene ocean-atmosphere variability in the Antarctic Peninsula was greater than that measured in recent decades. The lake sediment record from Moutonnée Lake also provides evidence to suggest that Holocene (ca. 8000 to 0 cal yr B.P.) climatic change on the Antarctic Peninsula may have been coupled to atmospheric and/or oceanic changes recorded in the tropical western Pacific Ocean.

ACKNOWLEDGEMENTS

Firstly, I would like to thank my supervisors, Dr. Mike Bentley and Dr. Dominic Hodgson who have provided a constant source of inspiration and guidance throughout my PhD. I am particularly grateful to them for giving me the chance to do work in Antarctica. In addition, I would also like to thank my second supervisors, Dr. Jerry Lloyd (Durham) and Professor Melanie Leng (NIGL, Keyworth), and also Dr. Steve Roberts (BAS) who have provided me with their advice, guidance and shared their technical expertise. I would also like to acknowledge my case-studentship partners, the British Antarctic Survey (BAS), and thank the many people at BAS who have provided me with ideas and advice over the past few years.

My first field season on the Antarctic Peninsula was made even more enjoyable by the company and friendship of Elie 'the Hammer Man' Verleyen. In addition, I would like to thank my fellow PhD students and colleagues at the Department of Geography, Durham University for making my time in Durham so enjoyable. In no particular order of preference; Matthew Wright, Katherine Arrell, Vicky Holliday, Alona Armstrong, Sarah King, Sarah Clement, Alex Jeffrey, Sarah Woodruff, Penny Widdison, Colin McFarlane, Duncan Wishart, Erin McClymont, Elizabeth Mackie, Mike Lim, Nick Rosser, Matt Brain, Toru Higuchi, Dave Roberts, Gordon MacLeod, John Thompson and Simon Nelis. I would also like to thank Derek Coates, Brian Priestly, Eddie Million, Neil Tunstall, Derek Hudspeth and Stella Henderson in the Department of Geography for their invaluable help over the last three years.

Special thanks are reserved for Vicky, who has provided continuous support. Finally this thesis could not have been written without the support, love and encouragement of my family. I wish to dedicate this thesis to them.

LIST OF CONTENTS

List of Figures

Chapter 2 Contemporary and Paleoenvironmental change on the Antarctic Peninsula: Mechanisms and Causes

Chapter 3 George VI Ice Shelf - past history, present behaviour and potential future collapse

List of Tables

LIST OF APPENDICES

Chapter 1
INTRODUCTION AND THESIS AIMS

1.1.Introduction

The Antarctic Peninsula region (AP) (Fig.2.1) encompasses one of the most dynamic climate systems on Earth (Domack et al., 2001). Meteorological records show that the region has warmed at a rate of 3.7 ± 1.6 °C during the last century, several times greater than the global mean (0.6 ± 0.2 °C century^{-1}; Houghton et al., 2001) and quite different to most of the other continental Antarctic station records (Vaughan et al., 2003). Public attention has been focussed on the AP in recent decades due to the rapid disintegration of several ice shelves (see Fox and Vaughan (2001) and references therein) and it is now widely accepted that ice shelf retreat has been caused by atmospheric warming, which appears to be amplified over the AP relative to the rest of the continent. The catastrophic disintegration of the Larsen-B ice shelf in 2002 illustrated the rapidity of ice shelf collapse with the loss of 3,250 km^2 of the ice shelf in a 35-day period and re-awakened the debate about the buttressing effect of ice shelves on grounded glaciers and ice sheets. Early work by Weertman (1974), Hughes (1977) and Thomas (1979) suggested that the removal of buttressing ice shelves could trigger glacier acceleration and drainage of the West Antarctic Ice Sheet (WAIS) thereby leading to rapid eustatic sea-level rise (Lythe et al., 2001). These conclusions were initially discredited by modern theoretical models (Hindmarsh, 1993; Huybrechts and de Wolde, 1999) and limited ground-based observations (Alley and Whillans, 1991; Vaughan, 1993), which argued that the glacier-ice shelf coupling mechanisms were more complex and stable. However, following the collapse of the Larsen-A ice shelf, Rott et al. (2002) and De Angelis and Skvarca (2003) have shown that several glaciers have accelerated significantly.

Similarly Rignot et al. (2004) and Scambos et al. (2004) provided clear evidence of the acceleration of several glaciers feeding into the former Larsen-B following its collapse. Together these studies suggest that ice shelf removal could indeed result in accelerated glacier discharge and thus contribute to eustatic sea level rise.

Not only has the recent warming trend led to ice shelf collapse, but it has modified the local terrestrial environment, expanding the ranges of flowering plants (Fowbert and Lewis Smith, 1994; Convey, 2002), shrinking seasonal snow cover (Fox and Cooper, 1998), causing glacier retreat (Smith et al., 1998) and altering the distribution of penguin species (Fraser et al., 1992). Given the overwhelming evidence for accelerated rates of environmental change (Houghton et al., 2001), it has become increasingly important to understand the long-term history of the region in order to put the recent changes in perspective (e.g. Domack et al., 2003) and to judge their long-term significance. One way to do this is to examine proxy records for environmental change archived on land (geomorphology, lake sediment cores and ice cores) and in the ocean.

Ice shelf collapse is clearly one important aspect of this change and because recent ice shelf collapse has been linked to the recent, rapid atmospheric warming, historical collapse of ice shelves provides a useful proxy for periods of climatic warming in the past. This thesis uses lake sediment records from the AP to provide a long-term (Holocene) perspective on ice shelf stability and investigate the mechanisms for periods of past ice shelf collapse. Such information provides a long-term perspective on the Holocene variability of ice shelves and by inference, on climate.

1.2. Context of Research

This PhD thesis is part of the British Antarctic Surveys (BAS) core program, 'Signals in Antarctica of past Global ChangeS' (SAGES-10K), awarded to Dr. Dominic Hodgson and Dr. Eric Wolff and was enhanced by a NERC-funded project under the Antarctic Funding Initiative (AFI) awarded to Dr. Mike Bentley (University of Durham), Dr. Dominic Hodgson and Professor David Sugden (University of Edinburgh). The PhD work has been completed under a NERC-

CASE studentship (NER/S/S/2001/06527) held between the University of Durham and the British Antarctic Survey and forms a key component of the overall research project. Because of this context, the thesis is clearly structured so that the data generated for this PhD is presented and discussed independently (Chapters 2-6) before drawing in data from other parts of the project to the discussion in Chapter 7.

1.3. Research Aims and Objectives

This thesis has two specific aims:

1. To provide a baseline study of the present-day limnology of Moutonnée and Ablation Lakes in order to develop a conceptual model for detecting ice shelf history from the analysis of the sedimentary record in epishelf lakes.

2. To determine the Holocene history of George VI Ice Shelf.

1.3.1. Research Objectives

To achieve the above aims, the thesis has the following specific objectives:

1. To understand the present day dynamics of George VI Ice Shelf.

2. To retrieve and analyse contemporary material (water samples, lake surface sediments and lake catchment samples) in order to understand the limnology and sedimentology of the modern lake environment and determine the provenance of material deposited in their sediments.

3. To develop a conceptual model for detecting ice shelf loss from the sediments of the epishelf lakes.

4. To retrieve and analyse sediment cores from Moutonnée and Ablation Lakes and to measure their physical, chemical and biological characteristics.

5. To interpret the sediment core data using the conceptual model and thereby identify periods of ice shelf presence or absence.

6. To investigate the mechanisms for any periods of ice shelf absence within the wider context of AP environmental change.

1.4. Thesis Structure

Chapter 2 provides both a contemporary and a historical perspective on climatic changes in the Antarctic Peninsula region. The first section reviews recent atmospheric warming on the Antarctic Peninsula, its environmental impacts, (specifically ice shelf loss), and possible mechanism(s) for the observed changes. The second section reviews what is known about Holocene environmental changes on the Antarctic Peninsula based on information from *multi-proxy* archives on land and in the ocean. This chapter therefore provides an important context for the interpretation (Chapter 7) of the main body of data generated in this PhD thesis. **Chapter 3** provides a detailed review of past history and present behaviour of George VI ice Shelf and concludes with a discussion about its likely future behaviour. **Chapter 4** describes the study sites and outlines the field and laboratory techniques used in this thesis. **Chapter 5** provides baseline data on the present day limnology and sedimentology of Moutonnée and Ablation Lakes, the results of which are then used to develop a conceptual model for ice shelf loss. **Chapter 6** describes the results of multi-proxy analyses of lake sediment cores from Moutonnée and Ablation Lakes and presents the core chronology. **Chapter 7** uses the conceptual model developed in Chapter 5 to interpret the core results from Chapter 6 in terms of the Holocene history of George VI Ice Shelf. These interpretations are then placed in a historical and regional context and their implications discussed. **Chapter 8** presents the conclusions of this thesis, outlines the limitations of the work and makes recommendations for future research.

Chapter 2

CONTEMPORARY AND PALEOENVIRONMENTAL CHANGE ON THE ANTARCTIC PENINSULA: MECHANISMS AND CAUSES

2.1. Introduction

This chapter presents an overview of contemporary and palaeoenvironmental change on the AP and provides the context for the interpretation of the data collected during this PhD study. The first section examines the recent rapid regional warming on the AP and discusses the possible mechanisms. Then it examines recent ice shelf loss on the AP and discusses the possible forcing factors. The second section reviews what is known about past (Holocene) changes on the AP derived from marine, terrestrial and ice core records.

2.2. Recent rapid regional warming on the Antarctic Peninsula

Records of mean annual air temperature between 1950-2000 indicate that three areas of the world have experienced exceptional rates of atmospheric warming relative to the global mean (Hansen et al., 1999). These areas are; northwestern North America, an area centred on the Siberian Plateau, and the Antarctic Peninsula/Bellingshausen Sea (Hansen et al., 2001). In each of these areas mean annual temperatures have increased by 1.5°C since 1950, compared with a global mean of ca. 0.5°C (Folland et al., 2001). Temperature records from the AP show that climate has warmed at a rate of 3.7 ± 1.6 °C over the last century (Vaughan et al., 2003). In contrast, temperatures at the South Pole (Amundsen-Scott Base) appear to have cooled since 1958 (Fig. 2.2 and Table 2.1). Warming of the AP therefore not only appears to be unusual on a global scale but it also differs from the

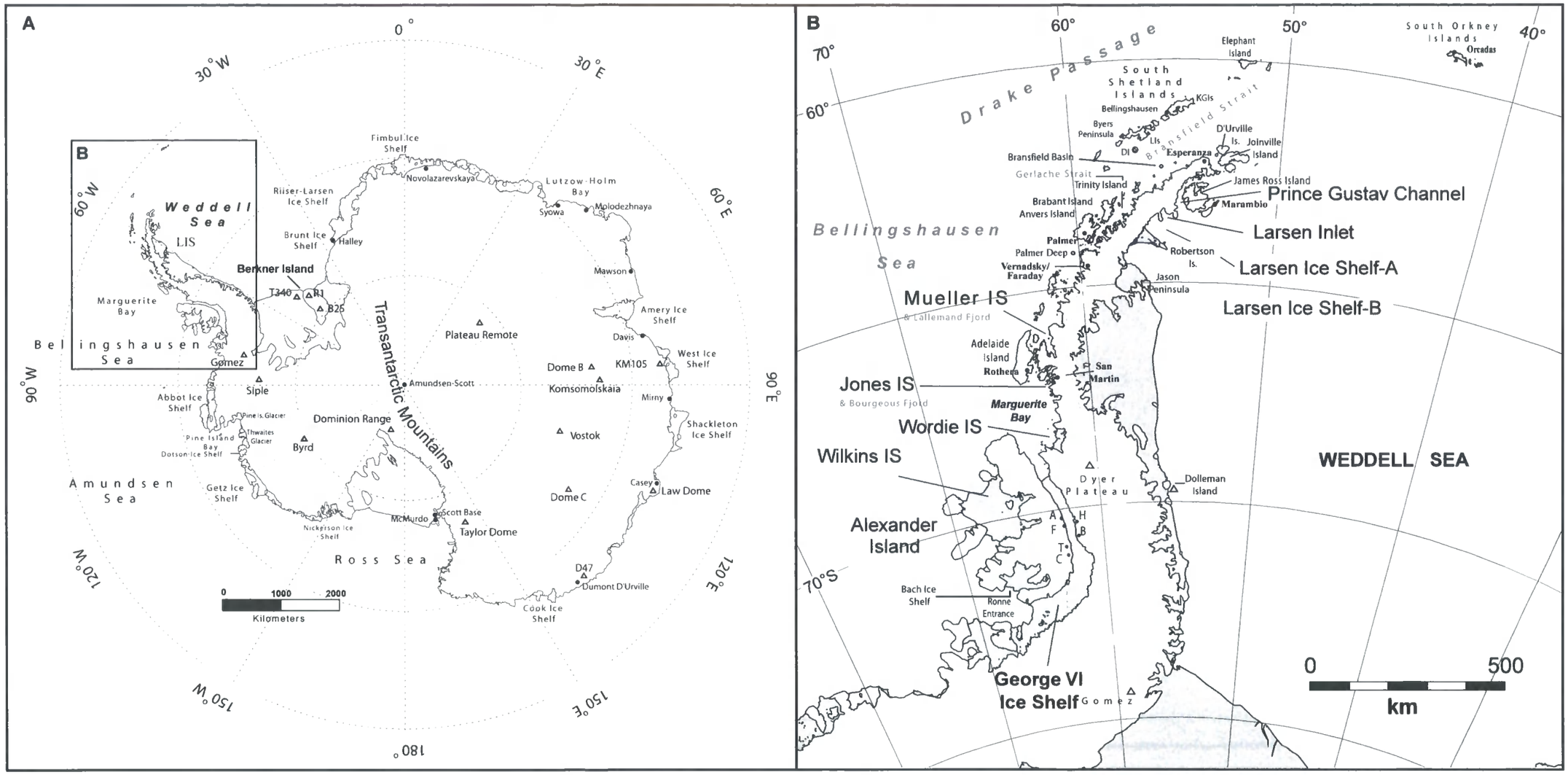

Figure 2.1. Map of Antarctica (A) showing major ice shelves (grey), selected Antarctic stations (black dots) and ice core sites (open triangles). EAIS, East Antarctica Ice Sheet; WAIS, West Antarctic Ice Sheet. (B) Map of the Antarctic Peninsula. Ice Shelves are shown in grey. George VI Ice Shelf is the largest ice shelf on the west side of the Antarctic Peninsula. Also marked on are important field sites referred to throughout the text. [A] Ablation Point, [F] Fossil Bluff, [H] Hobbs Pool, [B] Batterbee Mts, [T] Two Step Cliffs/Mars Oasis, [C] Citadel-Bastion Lake, [DI] Deception Island [LIs] Livingston Island, [KGIs] King George Island. Also shown are Ice Core (triangle) and marine core sites (open circle).

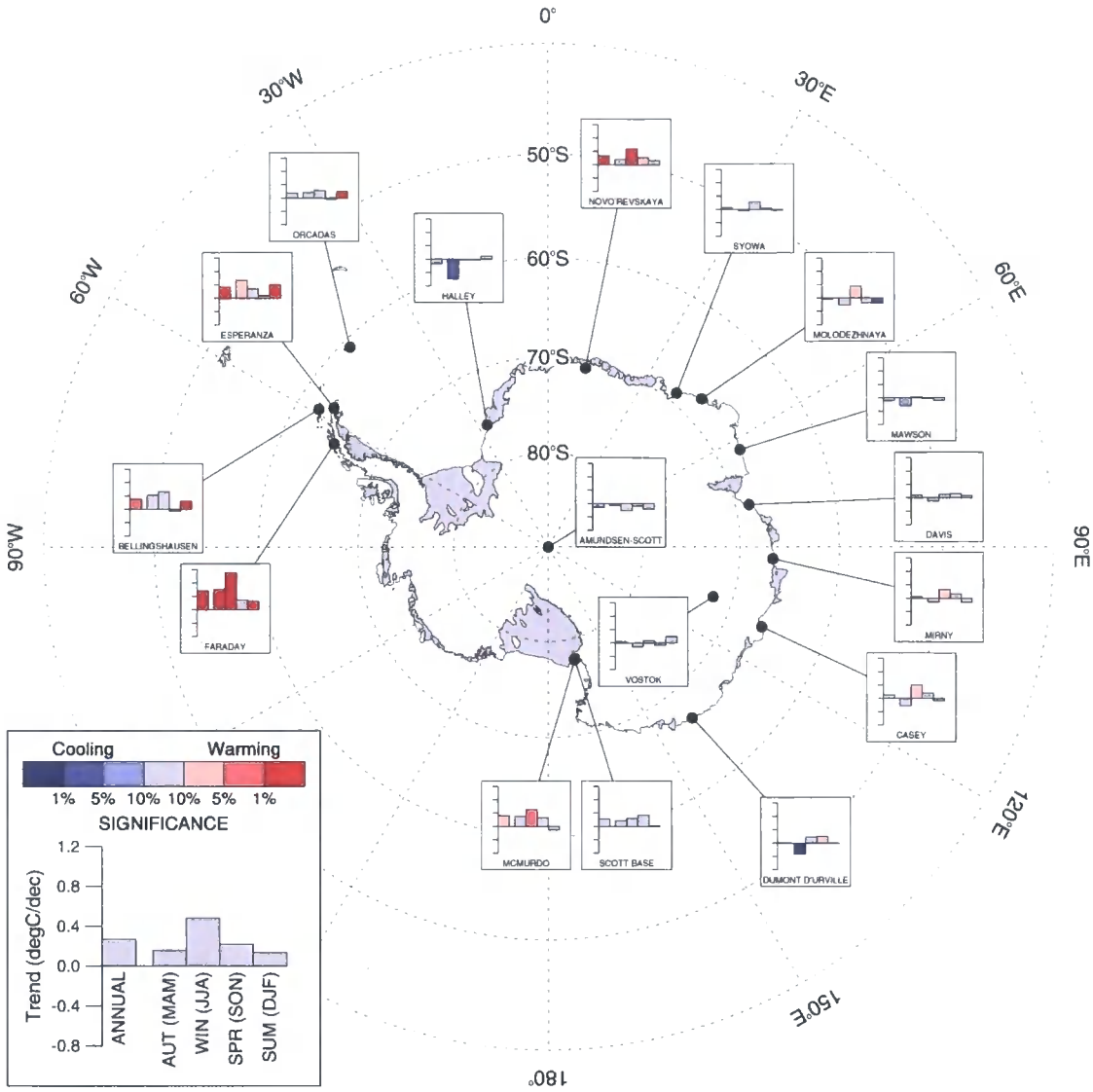

Figure. 2.2. Antarctic near-surface temperature trends between1951-2003 (Minimum of 30 years' data required for inclusion). Data from http://www.antarctica.ac.uk/met/gjma/.

Station	Latitude/S	Longitude/ E	Mean [°C]	Std dev [°C (century)]	Trend [°C (century)]	Years	Significance
Faraday/Vernadsky	65.25	–064.27	–4.0	1.6	5.7 ± 2.0	1951–2001 (51)	1%
Bellingshausen	62.2	–058.97	–2.4	0.8	3.7 ± 2.1	1969–2001 (33)	10%
Esperanza	63.4	–056.98	–5.3	1.2	3.4 ± 1.3	1946–48, 1953–78, 1980–2001 (51)	5%
Orcadas	60.75	–044.72	–4.0	1.2	2.0 ± 1.0	1904–91, 1993–2001	(97) 1%
Halley	75.58	–026.50	–18.6	1.1	0.9 ± 2.2	1957–2000 (44)	Not sig.
Novolazarevskaya	70.77	11.83	–10.3	0.6	2.4 ± 1.2	1962–2001 (40)	10%
Syowa	69	39.58	–10.6	0.8	–0.2 ± 1.7	1960–61, 1967–2001 (37)	Not sig.
Molodezhnaya	67.67	49.85	–11.0	0.6	–0.5 ± 1.5	1964–95, 1997–98 (34)	Not sig.
Mawson	67.6	62.87	–11.2	0.8	–1.1 ± 1.1	1955–2001 (47)	Not sig.
Davis	68.58	77.97	–10.2	0.9	0.4 ± 1.6	1958–63, 1970–2001 (38)	Not sig.
Mirny	66.55	93.02	–11.3	0.8	–0.1 ± 1.2 1	956–2001 (46)	Not sig.
Vostok	78.5	106.9	–55.3	0.8	0.6 ± 1.7	1958–61, 1963–93, 1995, 1997–2001 (39)	Not sig.
Casey	66.28	110.53	–9.3	0.9	1.0 ± 1.8	1958–2001 (44)	Not sig.
Dumont D'Urville	66.67	140.02	–10.8	0.6	0.0 ± 1.3	1956–2001 (46)	Not sig.
McMurdo	77.85	166.66	–17.2	1	3.3 ± 2.3	1957–63, 1965–67, 1969–86, 1988, 1995–96 (31)	Not sig.
Scott Base	77.85	166.76	–19.9	1	2.5 ± 1.8	1958–93, 1995–2001 (43)	Not sig.
Amundsen-Scott	90	0	–49.5	0.6	–2.0 ± 1.0	1958–2001 (44)	10%

Table 2.1. Trends in mean annual air temperature at meteorological stations in Antarctica (adapted from Vaughan et al., 2003). In selecting stations for inclusion Vaughan et al. (2003) rejected records with fewer than 30 years of observations. Records taken from British Antarctic Survey sources are available at http://www.antarctica.ac.uk/climate/surfacetemps. Confidence limits on temperature trends are given at the 1-sigma level (~31.7% significance), but significance level is also shown explicitly with 'not significant' implying anything greater than 10% (Vaughan et al., 2003). See Figure 2.1b for station location.

Antarctic continental mean. What follows is an overview of atmospheric warming on the AP and an outline of the possible reasons why atmospheric warming has been amplified in this area.

Topographically and climatically, the environment on the AP differs to the rest of continental Antarctica (Vaughan et al., 2003). The AP forms an unbroken chain of rugged, alpine topography (Schwerdtfeger, 1984), which forms a climatic barrier separating the warmer Bellingshausen Sea on the west from the cooler Weddell Sea on the east (Fig. 2.3). As a result of this topography the west side of the AP is ca. 7 °C warmer than temperatures at similar altitudes and elevations on the east side (Reynolds, 1981; Morris and Vaughan, 1994; Vaughan et al., 2003). Because of this, temperature-induced surface melting is a more important component of the mass balance of the ice shelves and glaciers on the west side of the AP.

The longest temperature record in Antarctica is from the sub-Antarctic Laurie Island (Orcadas Station; Fig. 2.1b), which began in 1904. Continuous records on the Antarctic Peninsula itself began after the Second World War (Table 2.1). Analysis of three of these records (Faraday, Esperanza and Bellingshausen; Fig. 2.4) by Vaughan et al. (2001) show rates of temperature increase that are an order of magnitude greater than the global mean (Table. 2.1). Shorter-term records also reveal the same warming trend (e.g. Marambio Station; Fig.2.1b) as does the summer-only record from Fossil Bluff on Alexander Island (Fig. 2.1b) (Harangozo et al., 1997). At Faraday station, in addition to the increases in temperature, there has also been an observed increase in winter precipitation since 1956 (Turner et al., 1997).

However, owing to the limited length of these records, it remains difficult to establish precisely when this warming began (Vaughan et al., 2003). The record from Orcadas Station (Fig. 2.4) suggests warming in the sub-Antarctic probably started during the 1930's. Although situated several hundred kilometres north of the AP its subsequent correlation with the post-1950s temperature record from Faraday implies warming may have began on the AP around the same time (Vaughan et al., 2003).

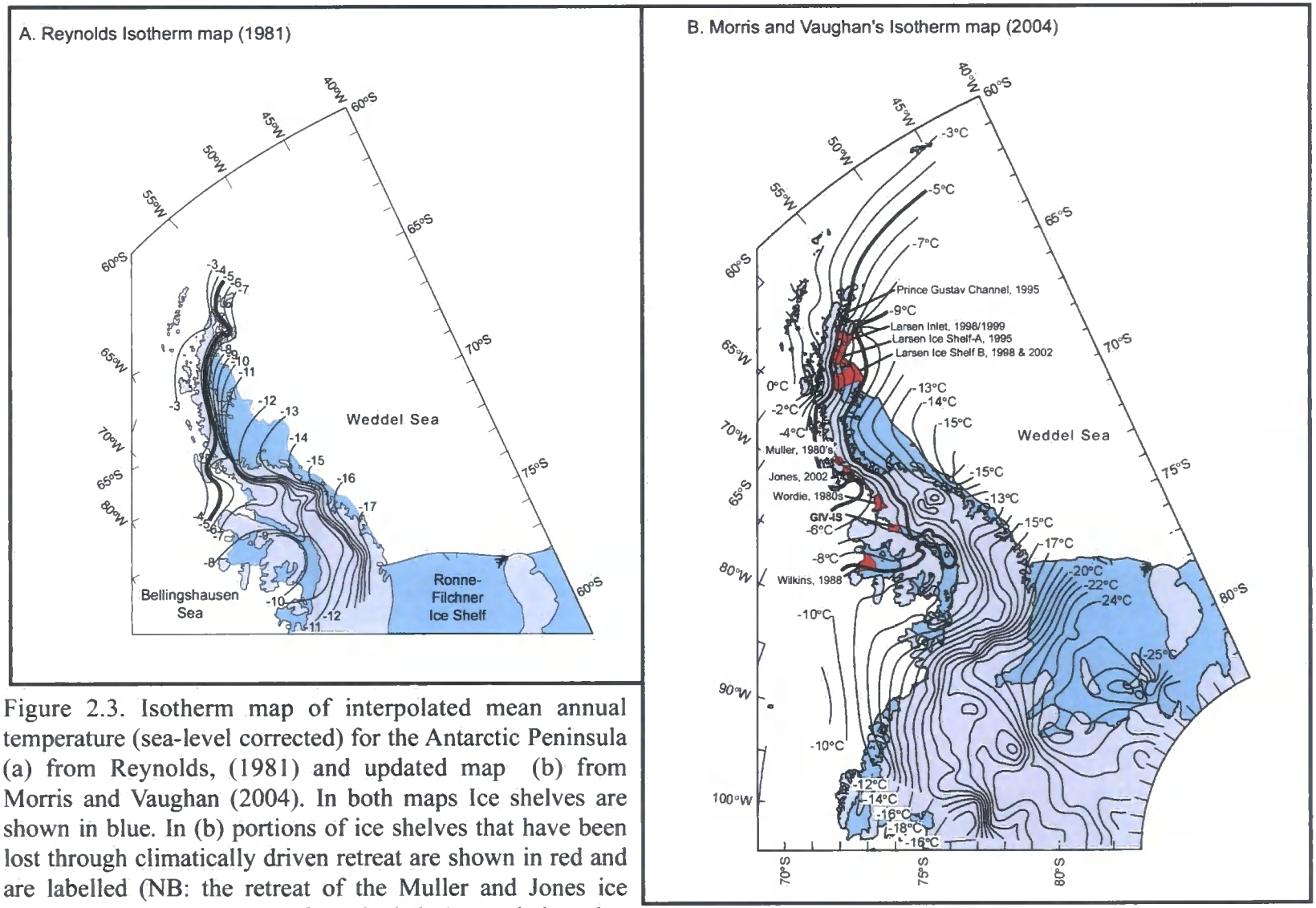

Figure 2.3. Isotherm map of interpolated mean annual temperature (sea-level corrected) for the Antarctic Peninsula (a) from Reynolds, (1981) and updated map (b) from Morris and Vaughan (2004). In both maps Ice shelves are shown in blue. In (b) portions of ice shelves that have been lost through climatically driven retreat are shown in red and are labelled (NB: the retreat of the Muller and Jones ice shelves are shown by a dot of nominal size). Ice shelves that have been lost lie within the key -5 °C to -9 °C isotherm boundary (thick black lines).

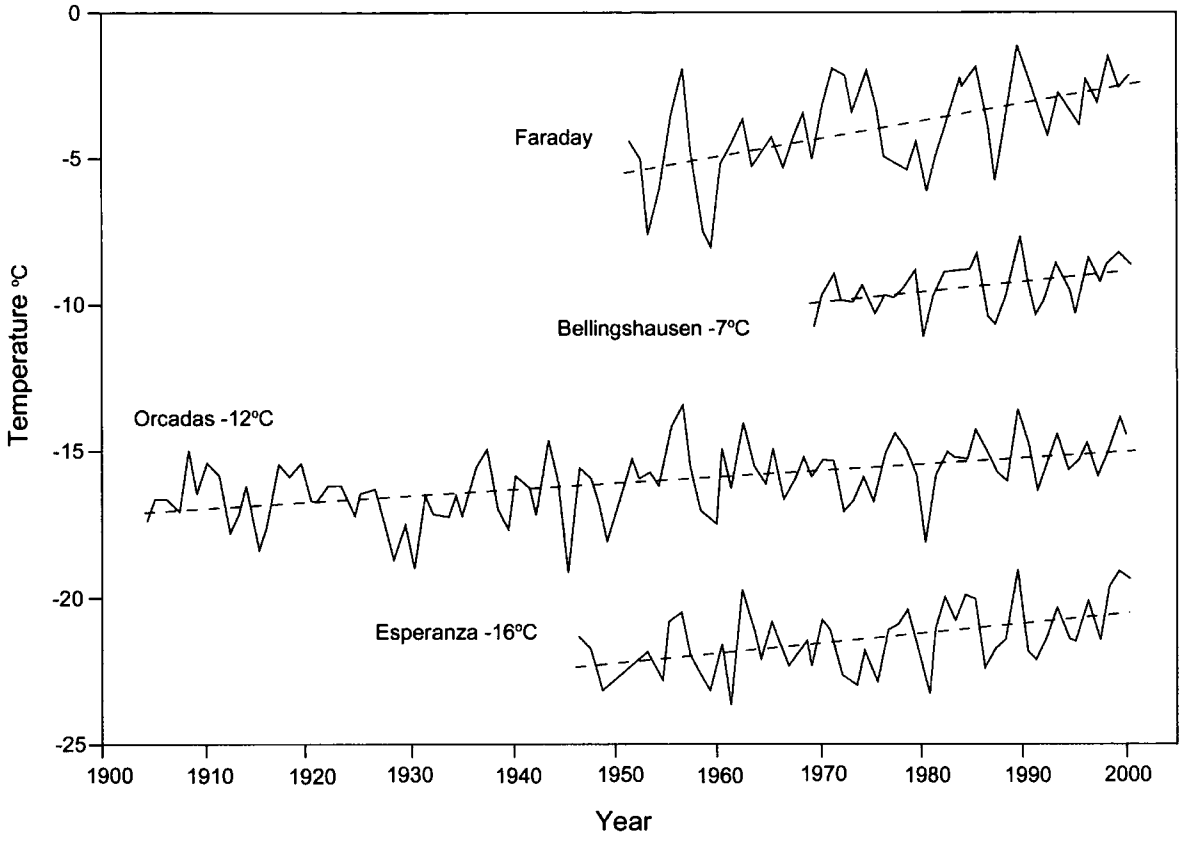

Figure 2.4. Meteorological records of mean annual air temperature from selected bases on the Antarctic Peninsula (from Vaughan et al., 2003). Dashed lines are the trends given in Table 2.1.

2.2.1 Consequences of recent warming

The recent warming trend has affected several environmental parameters on the AP, namely sea-ice extent, terrestrial and marine ecosystems and the distribution and stability of ice shelves, which is described in the next section. Satellite data show a decrease in winter sea-ice extent in the Bellingshausen Sea from mid 1988 through early 1991 (Jacob and Comiso, 1993). Indeed, the west coast of the AP is the only region in Antarctica where a strong correlation between sea-ice extent and near-surface atmospheric temperature is observed (Weatherly et al., 1991). According to Vaughan et al. (2003) this pattern could relate to the fact that the AP acts as a barrier to the eastward transport of sea-ice by the Antarctic Circumpolar Current (ACC) and because, unusually for Antarctica, the sea-ice edge in winter is close to the coast. The impact of the recent rapid regional warming on marine and terrestrial environments has been reviewed by Smith et al. (1999) and Convey (2001). It includes an expansion in the range of flowering plants (Fowbert and Lewis Smith, 1994; Convey, 2001) and shrinking seasonal snow cover (Fox and Cooper, 1998). Quayle et al. (2002) have also documented significant ecological changes (e.g. increased nutrient levels) in several maritime Antarctic lakes. A reorganisation of penguin colonies has also been attributed to recent rapid regional warming (Fraser et al., 1992). For instance, number of Adélie penguins, which require food in and around the pack ice, are declining around Faraday, whilst chinstrap penguins, which usually prefer open water, are increasing (Vaughan et al., 2001).

2.2.1.1. Ice Shelf Retreat

The single most publicised impact of recent AP warming has been the retreat and disintegration of several of the regions ice shelves. On average, AP ice shelves have retreated by ca. 300 km^2 each year since 1980 (Vaughan and Doake, 1996). Atmospheric warming is now considered the key driver in ice shelf retreat (Vaughan and Doake, 1996), but the precise mechanism linking climatic warming and ice shelf disintegration is still debated. This section has three aims: (1) to

provide an introduction to ice shelves on the AP – how they form and why they are important; (2) to explain ice shelf retreat and collapse, how this has been linked to recent climatic warming and our present understanding of the mechanisms; and (3) finally to provide a Holocene perspective on ice shelf variability and climate change for the AP.

2.2.2. Ice Shelves

As the Antarctic ice sheet flows off the continent into the surrounding oceans, there comes a point at which the ice is no longer thick enough to maintain contact with the bed. The point at which flotation occurs is known as the *grounding line*. Where there are high bending stresses across the grounding line, ice tends to break away (or calve). In other areas, the ice sheet passes over this transition intact resulting in floating extensions of the grounded ice sheet – known as *ice shelves*. Ice shelves fringe most of the Antarctic coastlines especially where there are bays, islands or bedrock shoals that constrain them beyond the grounding line by making contact with the ice shelf base (Vaughan and Doake, 1996). It is these topographic constraints that are thought to stabilise many ice shelves. Several different types of ice shelf have been documented, the difference mainly being attributed to different glaciological inputs and outputs (Vaughan, in press) (Table 2.2).

Some believe that ice shelves play a fundamental role in maintaining the stability of the Antarctic ice sheet, specifically the stability of the marine-based West Antarctic Ice Sheet (WAIS) (Mercer, 1978; Weertman, 1974). The WAIS contains 3.8 million km^3 of ice and, if it were to collapse, would raise global eustatic sea level by an estimated 5 m (Lythe et al., 2001). Most of the drainage of the WAIS is concentrated into ice streams, the majority of which flow into the Ross and Weddell seas, where there are extensive ice shelves (the Ross Ice Shelf and the Filchner-Ronne Ice Shelf respectively; Fig. 2.5) (Oppenheimer, 1998). It was first thought that ice shelves acted to buttress or hold back inland ice and their removal would trigger a speeding-up or surge of the inland ice streams, causing rapid depletion of continental ice (Mercer, 1968; Weertman, 1974, 1976; Thomas, 1979). However, this notion was largely discredited by modern theoretical models, which disregard the buttressing effect of ice shelves and suggested that their removal would not

		DOMINANT SOURCE OF INPUT		
		Glacier Input	*Surface* Accumulation	*Basal Accretion*
DOMINANT ROUTE FOR ABLATION	*Iceberg Calving*	**Type A** Wordie Ice Shelf, Antarctic Peninsula	**Type B** None Known	**Type C** Seaward portion of Hell's Gate Ice Shelf, Antarctic
	Surface melting/ Sublimation	**Type D** Landward portion of Hell's Gate Ice Shelf, Antarctica	Not possible	**Type E**
	Basal Melting	**Type F** George VI Ice Shelf, Antarctic Peninsula	**Type G** Wilkins Ice Shelf Antarctic Peninsula	Not possible

Table 2.2. A classification of ice shelves (from Vaughan, in press)

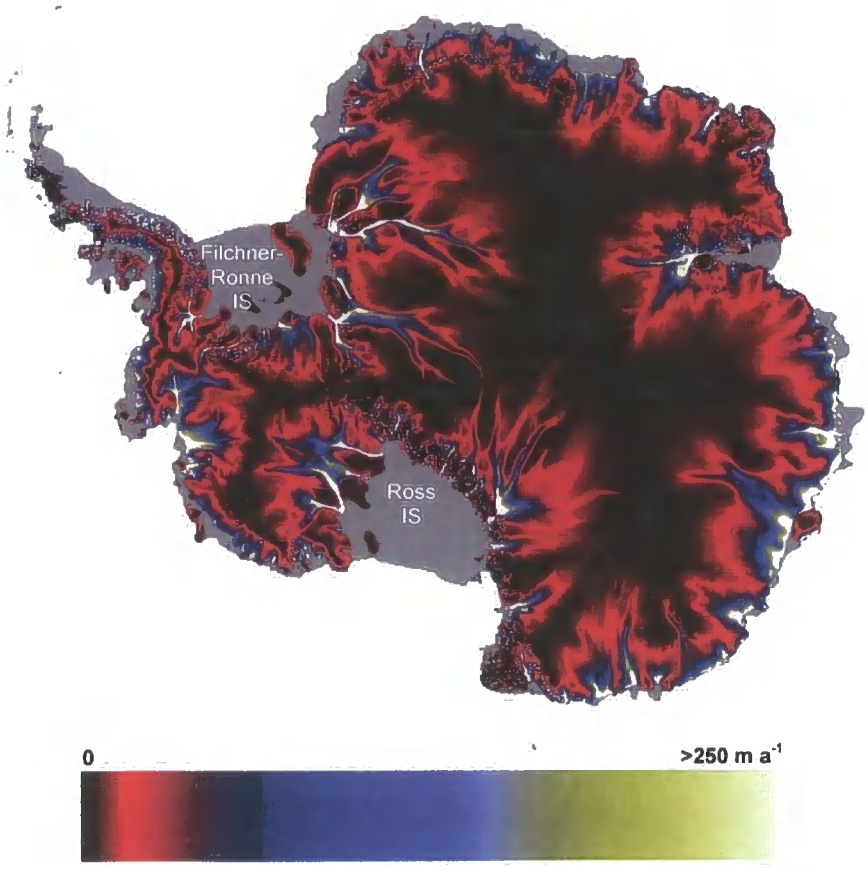

Figure 2.5. Balance velocities calculated for the grounded part of the Antarctic Ice Sheet (from Bamber et al. 2000). Ice shelves and floating ice tongues are gray. Fast flowing ice streams (Blue-yellow) feed into the major ice shelves and are often referred to as the 'arteries' of the West Antarctic Ice Sheet.

affect inland ice (Herterich, 1987; Huybrechts, 1990; Hindmarsh, 1996; Hindmarsh et al., 2001). More recently however, De Angelis and Skvarca (2003), Rignot et al. (2004) and Scambos et al. (2004) have presented compelling observational evidence, of 'surging' or speeding-up of several glaciers following the collapse of the Larsen-A/B and Prince Gustav Channel ice shelves. This discovery calls for a reappraisal of the stabilising role of ice shelves on grounded ice in their upstream catchments (De Angelis and Skvarca, 2003). The importance of this debate is of paramount importance to understanding the role of future global sea-level changes. If ice shelves do 'hold back' grounded ice then their collapse could lead to the increased drainage of continental ice, leading to a potentially rapid rise in eustatic sea level.

2.2.2.1. Climatic Limit for Ice Shelves

In recent decades, several ice shelves on the Antarctic Peninsula have diminished in size, including the Wordie Ice Shelf (Doake and Vaughan, 1991), Prince Gustav Ice Shelf and the ice shelf that formerly occupied the Larsen Inlet, Larsen Ice Shelf-A (Vaughan and Doake, 1996), Muller Ice Shelf (Ward, 1995), Wilkins Ice Shelf (Scambos et al., 2000) and Jones Ice Shelf (Fox and Vaughan, 2003) (Fig. 2.3). Most recently this pattern of retreat has been highlighted by the rapid disintegration of the Larsen-B Ice Shelf (Fig.2.6) (Scambos et al., 2003). Several other AP ice shelves are showing a number of distinct characteristics, which some have interpreted as the first signs of collapse (e.g. George VI Ice Shelf; Lucchitta and Rosanova, 1998).

The possibility that climate controls the viability of ice shelves has been widely discussed. Robin and Adie (1964) first suggested a climatic control on ice shelves. They noted that the distribution of ice shelves apparently corresponded with the 0°C *January* (summer) isotherm, concluding that this marked 'a limit of viability'. This idea was developed further by Reynolds (1981) who compiled a map of mean annual air temperatures for the Antarctic Peninsula (Fig. 2.3a). On this map the distribution of retreating ice shelves indicated that the –5°C *mean annual* isotherm could be interpreted as a proxy for the limit of ice shelf viability (Vaughan and Doake, 1996). Although the 0°C January isotherm is not extensively mapped, it

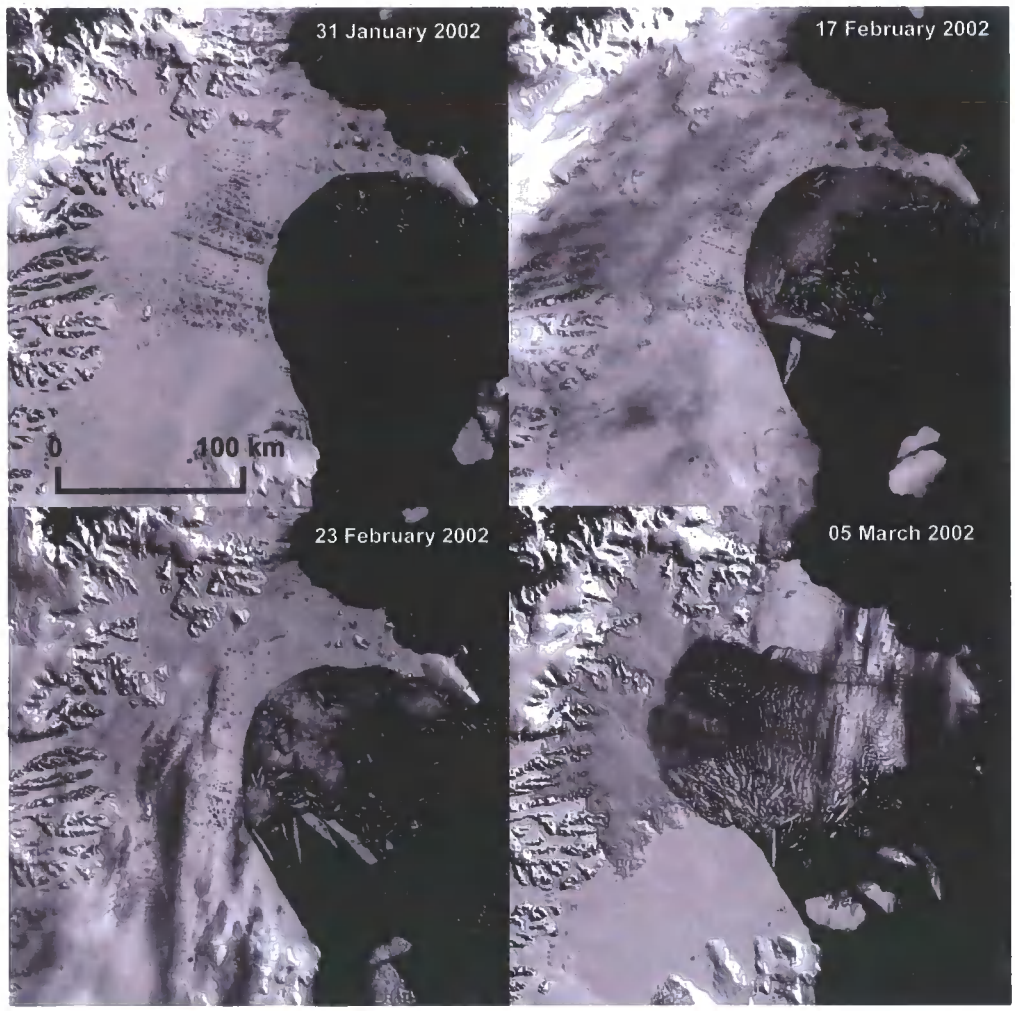

Figure 2.6. Rapid disintegration of the Larsen-B Ice Shelf in 2002. A total of about 3,250 km^2 of shelf area disintegrated in a 35-day period beginning on 31 January 2002. Over the last five years, the shelf has lost a total of 5,700 km^2, and is now about 40 percent the size of its previous minimum stable extent. MODIS images from NASA's Terra satellite, supplied by Ted Scambos, National Snow and Ice Data Center, University of Colorado, Boulder.

appears to coincide with the –5°C mean annual isotherm (Reynolds, 1981; Vaughan and Doake, 1996). For example, at Faraday station, the mean January temperature is approximately 0.5°C whilst the mean annual temperature is –4.4°C. These temperature data have since been updated using new station and borehole temperature data (Morris and Vaughan, 2003). Figure 2.3b shows the updated map, together with the distribution of ice shelves remaining around the AP in 2002 (blue) and those which have shown climatically induced retreat since the beginning of the 20th century (red) (Morris and Vaughan, 2003). The present northerly limit of 'stable' ice shelf distribution closely follows the -9°C isotherm. Ice shelves known to have retreated over the past 100 yrs are bounded by the –9°C and –5°C mean annual isotherms (Fig. 2.3) (Morris and Vaughan, 2003). What is more, the isotherm appears to have been driven south by continuing atmospheric warming on the AP. In the 1940's and 1950's the limit of viability was the position marked by Reynolds' –5 °C isotherm (Fig. 2.3a) (Vaughan and Doake, 1996). In the updated map the limit of ice shelf viability is now the –9 °C isotherm. This change is consistent with the 3.5 °C ± 1.0- 20th century warming on the AP (Morris and Vaughan, 2003). Importantly in the context of this thesis, the –9 °C isotherm viability now covers the northern portion of George VI Ice Shelf, leading some researchers to suggest that it will be the next ice shelf to break-up (Vaughan and Doake, 1996).

The limit of viability for ice shelves based on atmospheric temperature is now widely accepted although some have suggested that ocean temperature (Domack et al., 1995) or tidal amplitude (Holdsworth, 1977) are important factors in ice shelf stability. For example, Domack et al. (1995) proposed that the current extent of ice shelves on the west coast of the AP might be related to the temperature of seawater beneath them. They hypothesised that a recent incursion of Circumpolar Deep Water (CDW) caused the retreat of Müller Ice Shelf. Alternatively, Holdsworth (1977) suggested that the stability of ice shelves was limited by the range of ocean tides and proposed an upper tidal limit of 1-2 m, beyond which ice shelves become unstable. However, a tidal control is now doubtful as tidal range beneath several ice shelves far exceeds this value (Vaughan, 1995).

2.2.2.2. Mechanisms for ice shelf retreat

Although the –9°C mean annual isotherm adequately marks the northern limit of stable ice shelves, it is still uncertain what mechanisms are important during ice shelf retreat (Vaughan and Doake, 1996; Morris and Vaughan, 2003). A common feature of ice shelf retreat is a rapid acceleration preceding the final collapse (Vaughan and Doake, 1996). Remotely sensed imagery has also shown that deeply embayed ice fronts, calving of small elongate bergs in punctuated events, and the presence of melt ponds on the ice-shelf surface are all characteristic of a collapsing ice shelf (Scambos et al., 2000). This was highlighted most dramatically during the final collapse phase of the Larsen-A ice shelf, which lost 1,300 km² in 50 days and the Larsen-B ice shelf, which lost a total of 3,250 km^2 in a 35-day period beginning on 31 January 2002 (Fig. 2.6) (Scambos et al., 2002). These rates are much faster than would be expected from a melting mechanism alone and have been explained in terms of a rapid structural failure following some external forcing (e.g. temperature). Structurally, some embayed ice shelves are like arches, with the 'pillars' being formed by ice rises (places where the ice shelf grounds on shallow parts of the sea bed) and the arch by the smoothly curving (concave) ice shelf front. If too much of the structure between the pillars is removed (analogous to the removal of a keystone from an arch) then the ice shelf collapses (Doake et al., 1998). This hypothesis can explain the rapidity of ice shelf collapse but it still requires some other mechanism to start the process.

Increased meltwater on the ice shelf surface has long been considered to play an important role in ice shelf stability (Robin and Adie, 1964; Mercer, 1978) and could provide the link between atmospheric warming and ice shelf collapse. Mercer (1978) proposed that the downward percolation of surface meltwater and the subsequent release of latent heat on refreezing could potentially eliminate the cold thermal wave that exists in ice shelves from winter freezing thereby raising the pressure melting point. This would effectively create a temperate ice shelf, which at the time of Mercer's original idea, was thought to be unviable. However, the idea of an unstable temperate ice shelf was questioned with the discovery of temperate ice shelves that appear relatively stable. For example, Paren and Cooper, (1988) presented evidence that as ice flows towards the northern margin of George VI Ice

Shelf, it becomes more temperate in character. In 1986, ice near the northern front was between –1.6 to 1.8°C, compared to -10°C further south (Paren and Cooper, 1988). A similar situation has also been observed for the Wilkins Ice Shelf (Swithinbank, 1988). Hence, the idea that a temperate ice shelf is inherently unstable is not necessarily true.

Doake and Vaughan (1991) used a different line of reasoning to pursue the link between ice shelf stability and temperature in an attempt to explain the collapse of the Wordie Ice Shelf. Instead of a direct meltwater connection, they examined the relationship between mass balance (precipitation and ablation) and mean annual temperature. For mean annual temperatures higher than -12°C the net accumulation (N) was a function of the precipitation (P), the mean annual temperature (T) and a parameter (m) related to the ablation rate by

$$N = P - m\,(12 + T)^{n}$$

Where n = 1 for the linear model of Pollard (1980) or n = 2 for the quadratic model of Oerlemans, (1982) and P was assumed, for simplicity, to be independent of T over the small temperature range of interest (Doake and Vaughan, 1991). This analysis revealed a critical temperature, below which net accumulation is positive and above which it is negative. Doake and Vaughan (1991) speculated that small changes in temperature could therefore cause a significant change in the net balance on the Wordie Ice Shelf, effectively changing the balance from accumulation to ablation. They suggested that successive years of net ablation, through increased temperature would lead to deterioration of the ice shelf surface. In addition, rifts and crevasses would no longer be 'healed/glued' by winter accumulation. Together, this would lead to retreat through increased calving. Doake and Vaughan (1991) also saw a role for increased meltwater in the disintegration of Wordie Ice Shelf. Laboratory experiments show that the fracture toughness of ice is reduced at higher temperatures and by the presence of water (Lui and Miller, 1979; Sabo and Schulson, 1989). Like Mercer (1978), Doake and Vaughan (1991) suggested that higher temperature would lead to more free water at the surface which could then percolate down into crevasses. This could increase the pressure at the bottom of crevasses, allowing them to grow into rifts (Robin, 1964) or join together basal

crevasses (Jezek, 1984). These lines of weakness would increase the production of large bergs or 'blocks'. In certain ice shelves (e.g. Brunt), major basal crevasses can form as the ice shelf goes afloat at the grounding line thus creating large blocks. Because of some restriction (e.g. coastline configuration/persistent sea-ice) the blocks are unable to flow away and remain 'glued' together by sea ice and snowfall (Doake and Vaughan, 1991). This type of ice shelf contrasts with more homogeneous ice shelves such as the Ronne, where glaciers and/or ice streams flow unbroken over the grounding line (Doake and Vaughan, 1991). Thus, Doake and Vaughan (1991) conclude that ice-front retreat would be a sensitive function of mean annual air temperature through changes in net balance and through rifting along lines of weakness caused by increased meltwater.

A similar argument has been developed by Scambos et al. (2000) to explain the demise of Larsen-A and B Ice Shelves. They have suggested that most break-up events occurred during longer melt seasons and have been caused by surface melt ponding (Fig. 2.7). Building on the theoretical work of Weertman (1973) and Van der Veen (1998), Scambos et al. (2000) developed a thermodynamic finite-element model to evaluate ice flow and strain. A simple extension of this model allowed them to investigate crack propagation by meltwater. Scambos et al. (2000) suggested that water-filled crevasses penetrate more deeply than air filled crevasses because the water pressure opposes the ice overburden pressure (or lithostatic stress). Their inverse calculation for the Larsen-B Ice Shelf showed that only modest pre-existing crevasse depths (a few tens of meters) are needed for water-filling to induce crevasse-deepening and full thickness fracture (Scambos et al., 2000). In much the same way as Doake and Vaughan's theory, the ice shelf then becomes susceptible to large calving events leading to disintegration. However, not all the ice shelves studied by Scambos et al. (2000) conform to this hypothesis (e.g. George VI Ice Shelf and Amery Ice Shelf). The focus of this study, George VI Ice Shelf has one of the longest histories of melt ponding on its surface but doesn't appear to be in rapid retreat. As will be discussed in greater detail in Chapter 3, this may be due to the compressive stress regime within the ice shelf, which opposes crevasse widening (Scambos et al., 2000). It is also likely that the Amery Ice Shelf (Fig. 2.1) is under compression within the region of frequent annual melting (Swithinbank, 1988; Phillips, 1998; Scambos et al., 2000). Scambos et al. (2000)

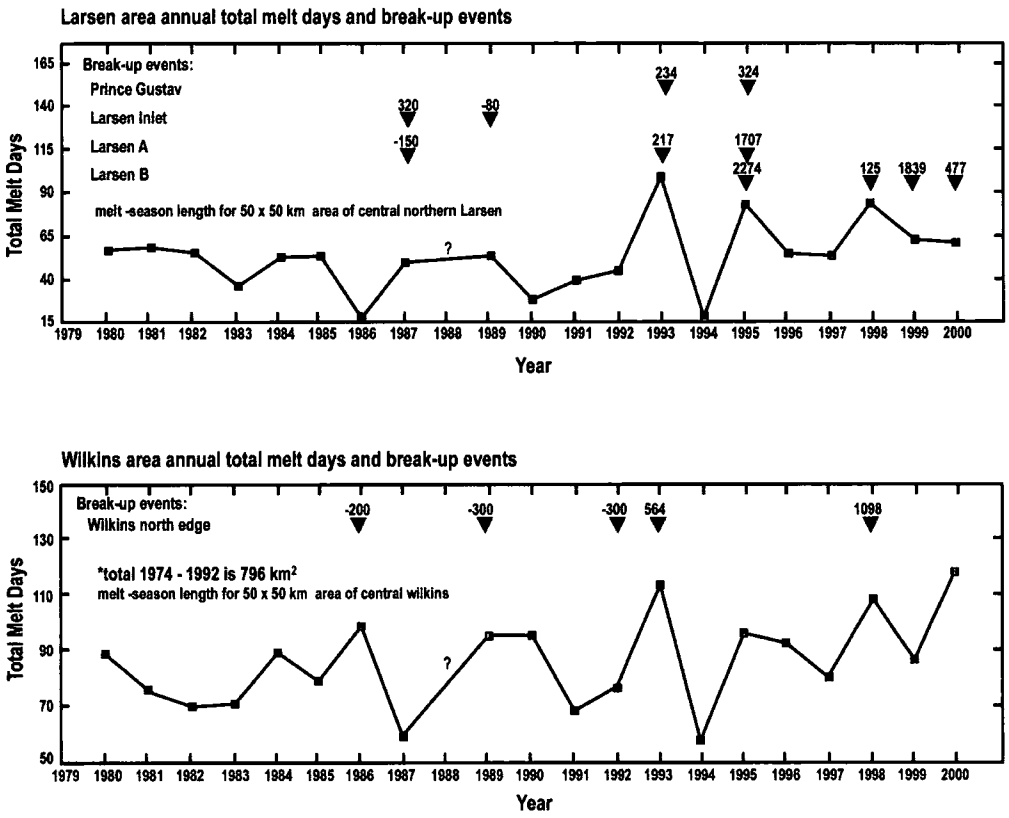

Figure 2.7. Annual total melt days and recent break-up events in the Antarctic Peninsula. Melt-season duration was derived from passive microwave data. All major break-up events (>100 km^2) that can be attributed to a single year are shown (Black arrows). (redrawn from Scambos et al., 2000).

conclude that the most susceptible ice shelves (based on melt activity) to future collapse are the Larsen-C and ice shelves fringing the northern coast of East Antarctica (e.g. Riiser Larsen, Fimbul, West and Shackleton; Fig. 2.1).

More recently Shepherd et al. (2003) have suggested that parts of the Larsen-A and B became susceptible to crevasse fracture through a sustained thinning. They showed from satellite laser altimetry that between 1992 and its disintegration, the Larsen-B ice shelf lowered by up to 0.27 ± 0.11 meters per year. Consistent with the link between atmospheric warming and ice shelf collapse they attributed the thinning to increased surface melting, but also to enhanced melting at the ice shelf base (Shepherd et al., 2003). They stated that, although basal melt rates beneath the Larsen Ice Shelf (LIS) are uncertain, basal melt rates of up to 2-3 m have been observed beneath the nearby Filchner-Ronne Ice Shelf where tidal mixing between local ice shelf water and warmer Weddell Sea Deep Water (WSDW) occurs (Joughin and Padman, 2002). They also note that WSDW has warmed by 0.32°C since 1972 (Robertson et al., 2002) and that large quantities of modified WSDW have been observed in front of Larsen-C with a temperature of 0.65°C above the pressure melting point of ice (Shepherd et al., 2003). From this they argued that ocean-driven melting may provide the link between regional climate warming and the successive disintegration of ice shelves. It is also consistent with the earlier observation of Domack et al. (1995) who suggested a link between the presence of warm Circumpolar Deep Water and the collapse of Müller Ice Shelf.

In summary, amplified atmospheric warming on the AP over the last century has been widely interpreted as the key-forcing factor for ice shelf retreat, but it doesn't necessarily provide the actual mechanism nor can it explain the whole picture (e.g. Shepherd et al., 2003). An important feature of many of the ice shelves that have collapsed on the AP is the relative speed of disintegration once a certain threshold was passed. The rapidity of change implied some internal, structural weakness such as the failure of a structural arch. Mechanisms advanced to explain the inception of this process, all involve enhanced atmospheric warming. For example, Doake and Vaughan (1991) developed a model, which involves the relationship between mass-balance, and mean annual temperature to explain the collapse of the Wordie Ice Shelf. In this model, small changes in the mass balance of the ice shelf, when

combined with structurally weak ice, lead to the increase of large block calving events and thus ice shelf collapse. Similarly, the melt-ponding mechanism developed by Scambos et al. (2000) used to explain the collapse of Larsen-B Ice Shelf relates directly to atmospheric warming, and involves the propagation of structural weaknesses through increased volumes of surface melt water. More recently, several studies have highlighted the importance of changes in ocean circulation under the ice shelf; specifically warm deep-water masses (e.g. CDW and WSDW) but it is still unclear how these changes relate to atmospheric warming. For example, are changes in atmospheric temperature driving changes in CDW and WSDW or are changes in CDW driving atmospheric changes through a series of positive feedbacks?

2.2.3. Mechanisms for recent warming

At presently it is not known what has caused such rapid warming, why it is amplified in the region and whether it will continue. In a recent synthesis, Vaughan et al. (2003) outlined three plausible mechanisms to explain the recent warming; (1) changed ocean circulation; (2) changed atmospheric circulation; and (3) air-sea-ice feedback.

2.2.3.1. Changed ocean circulation

Oceanographic observations have shown the presence of relatively warm Circumpolar Deep Water (CDW) on the continental shelf west of the AP (Hoffman et al., 1996). CDW is the warmest and most saline water mass in the AP region having a salinity maximum of 34.73 ‰ and a temperature maximum of + 2°C (Table 2.3). CDW is usually further split into *Upper Circumpolar Deep Water* (UCDW) and *Lower Circumpolar Deep Water* (LCDW) (Baum, 2001). UCDW is characterized by low oxygen and high nutrient levels (with sources in the Indian and Pacific Oceans) as well as by a relative minimum in temperature south of the *Subantarctic Front* (SAF) induced by the overlying *Antarctic Intermediate Water* (AAIW). LCDW is characterized by high salinity and low nutrients and is derived from *North Atlantic Deep Water* (NADW) (Baum, 2001). The split in CDW takes place in the southwest Atlantic where relatively warm, salty, oxygen rich and

Water Mass	Temperature °C	Salinity ‰	Location
Antarctic Surface Water (AASW)	0.0 to -1.5	34-34.4	All regions
Winter Water	< -1.5	34-34.4	All regions
Circumpolar Deep Water (CDW)	>0	34.6-34.73	All regions except Weddell Sea
Upper CDW (UDCW)	1.5-2.0	34.6-34.7	AP and BrS
Lower CDW (LCDW)	1.3-1.36	34.7-34.73	AP and BrS
Modified CDW (mCDW)	1.0-1.4	34.6-34.7	All regions except Weddell Sea and Oates Coast
Shelf Water	<-1.8	34.2-34.9	Oates Coast, Ross and Weddell Sea, Caird Coast, Princess Martha Coast
High Salinity Shelf Water (HSSW)	-1.9	34.9-34.9	Ross and Weddell Seas, Caird Coast
Low Salinity Shelf Water (LSSW)	<-1.8	34.4-34.6	Ross and Weddell Seas, Caird Coast
Ice Shelf Water			
Shallow Ice Shelf Water (SISW)	<-1.8	34.36-34.42	Ross and Weddell Seas
Deep Ice Shelf Water (DISW)	<-2.0	34.62	Ross and Weddell Seas
Bottom Water			
Low Salinity Bottom Water (LSBW)	-0.1	34.65	Ross Sea
High Salinity Bottom Water (HSBW)	0.5	34.71	Ross Sea
Bransfield Strait Water (BS)	<0.0	34.45-34.6	Bransfield Strait
Modified Weddell Deep Water (MWDW)	-1.8 to -0.5	34.45-34.65	Weddell Sea
Western Shelf Water (WSW)	-1.88	34.7-34.85	Weddell Sea
Eastern Shelf Water (ESW)	-1.88	34.29-34.4	Weddell Sea
Weddell Sea Transitional Water (WSTW)	?	?	Weddell Sea

AP, Antarctic Peninsula; BrS Bransfield Strait

Table 2.3. Summary of the major water masses found on the Antarctic Continental Shelf between 150°E and the Greenwich Meridian (adapted from Hoffman et al., 1998).

nutrient poor NADW meets the Antarctic Circumpolar Current (ACC), splitting the CDW into two parts (Baum, 2001). The upper branch of this split retains the oxygen minimum, with the lower branch also showing an oxygen minimum induced by high oxygen concentrations in both the overlying NADW and the underlying *Antarctic Bottom Water* (Baum, 2001). West of the AP the continental shelf is characterised by UCDW, which is derived from off-slope upwelling in association with the impingement of the ACC (Fig. 2.8 and 2.9) (Domack et al., 2003a). The ACC is the major eastward flowing current in the Southern Ocean. It is principally driven by surface wind stress (the Southern Westerlies), although there is a significant thermohaline component that is not yet well understood (Hofmann et al., 1998). The southern edge of the ACC impinges on the AP shelf as it is channelled by the Southern Westerlies through the Drake Passage into the Atlantic sector of the Southern Ocean forming part of the global ocean circulation cell (Fig. 2.9). The southern edge of the ACC meets a colder (<-1.0 °C) more saline water mass (Weddell Sea Transitional Water, WSTW) driven out of the northwestern Weddell Sea by an East Wind drift (Domack et al., 2003a). The boundary between WSTW and the ACC fluctuates between the southern Bransfield Strait and the southern Gerlache Strait (Fig. 2.1b) (Domack et al., 2003a).

It has been suggested that changes in the physical characteristics (e.g. temperature) of CDW or its rate of upwelling could influence sea ice extent, thus leading to atmospheric feedbacks (Jacobs and Comiso, 1997) (i.e. enhanced CDW = less sea ice = less solar backscatter = warming = less sea ice etc). However, at present it is difficult to assess this hypothesis due to the lack of oceanic measurements, especially time-series data (Vaughan et al., 2003). It has also been suggested that CDW could play an important role in the retreat of ice shelves on the west coast of the AP (Domack et al., 1995). A similar story is now emerging from the east coast of the Antarctic Peninsula (e.g. Shepherd et al., 2003) involving the relatively warm WSDW (Table.2.3). Consistent with this mechanism, some late Holocene climatic changes (e.g. Little Ice Age) have been linked to the withdrawal of CDW from the western continental shelf of the AP (e.g. Shevenell and Kennett, 2002; Ishman and Sperling, 2002).

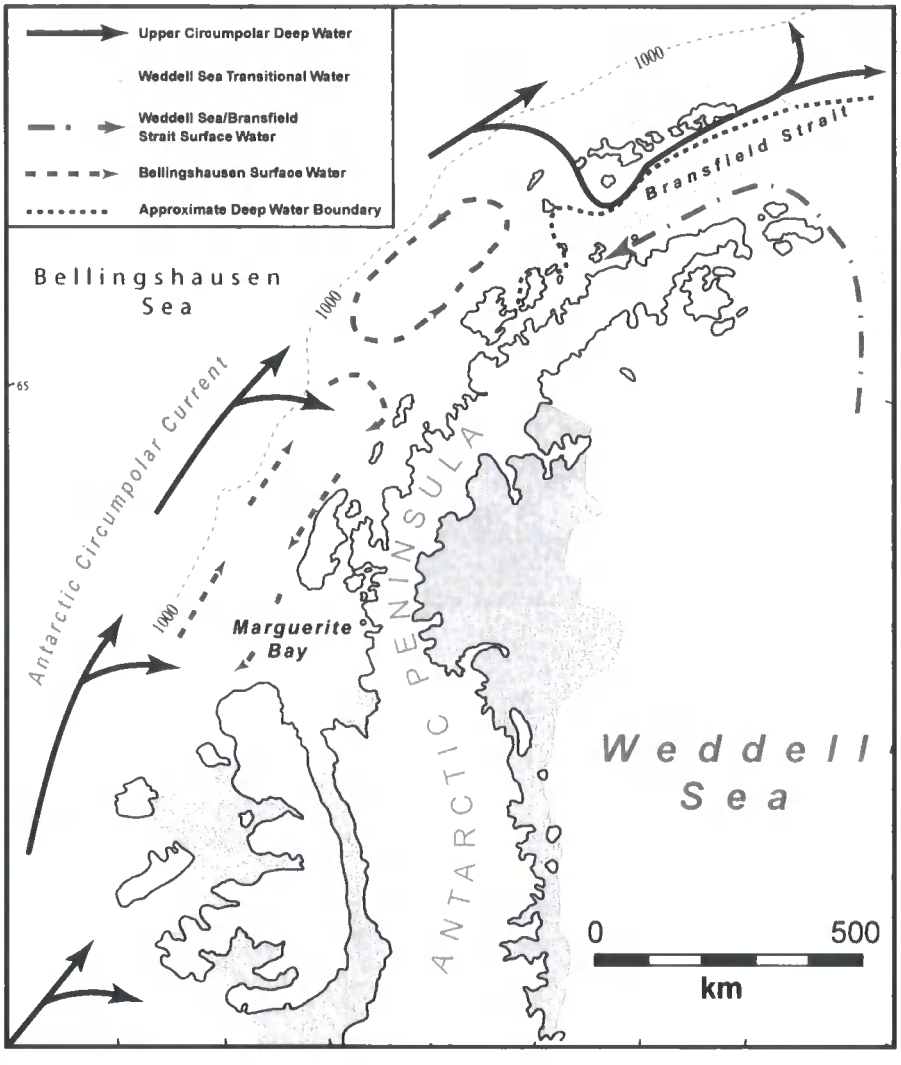

Figure 2.8 : Schematic of oceanographic circulation on the western side of the Antarctic Peninsula (modified from Hofmann et al., (1996) and Ishman and Domack, (1994)). Circumpolar Deep Water circulation is indicated by the solid black lines lines. Arrows suggest general flow direction.

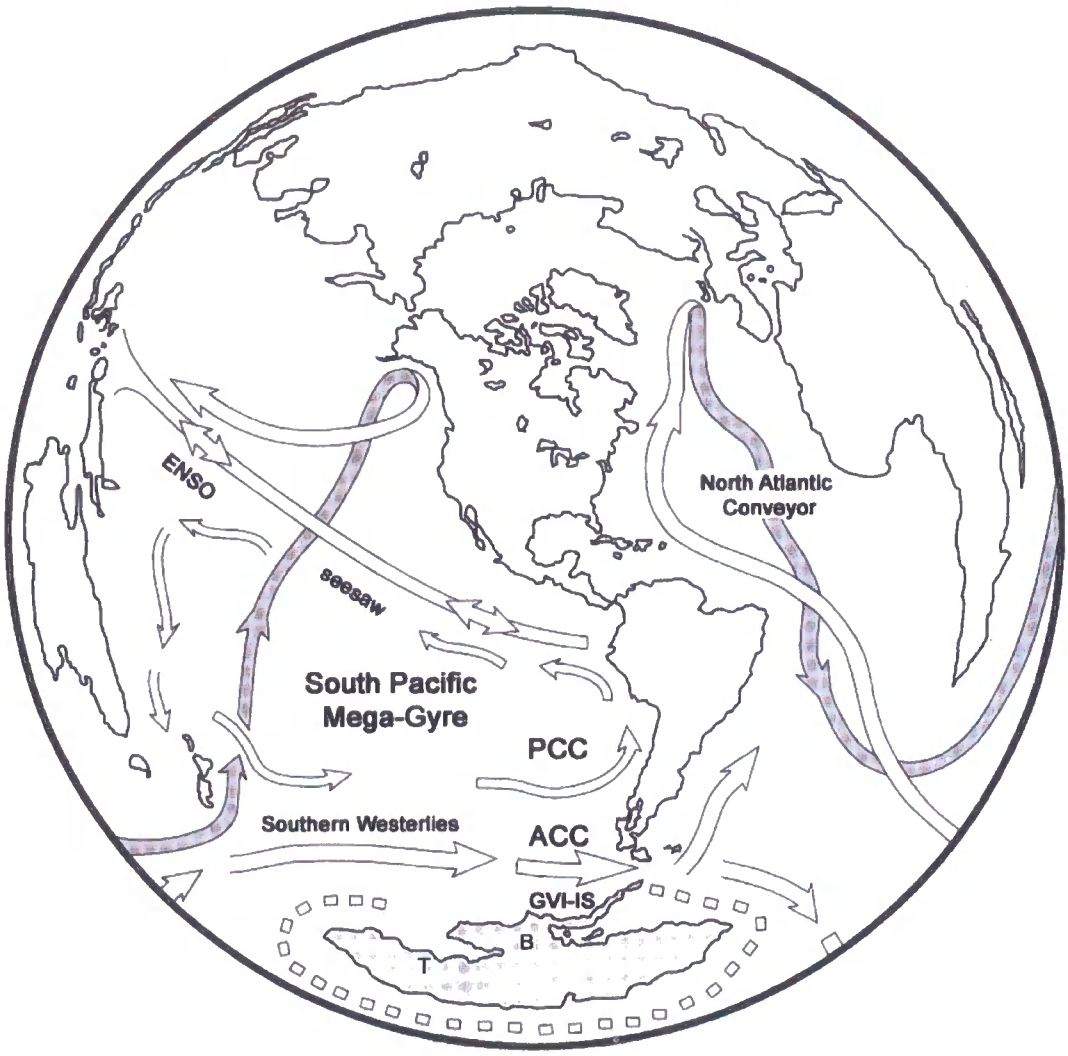

Figure 2.9. Global oceanographic circulation the in context of Antarctic Peninsula and southern Pacific Ocean processes such as El Nino-Southern Oscillation (ENSO), South Pacific Gyre, the Antarctic Circumpolar Current (ACC) and deep water flow contributed by North Atlantic thermohaline processes. Location of the Peru-Chile Current (PCC) is shown together with the location of George VI Ice Shelf (GVI-IS) Byrd Ice Core (B) and Taylor Dome Ice Core (T). The northerly limit of sea-ice is indicated by a bold dashed line (approximate) (modified from Domack and Mayewski, 1999).

2.2.3.2. Changed atmospheric circulation

A second possibility is that large-scale reorganisation of atmospheric circulation over the AP has occurred, advecting warmer air into the region (King and Harangozo, 1998). Atmospheric circulation and surface temperature over the AP are strongly influenced by the position of the circumpolar trough (CPT) of low pressure (Domack et al., 2003a). The position and strength of the CPT varies as part of a large-scale zonally-symmetric mode of the Southern Hemisphere circulation variability in which pressure at all levels varies inversely between middle and high latitudes (Domack et al., 2003a). This mode of variability has been given several names, including the Southern Annular Mode (SAM) or the Antarctic Oscillation (AAO) (Domack et al., 2003a). Within the CPT are regions of low pressure such as the Amundsen and Bellingshausen Sea (ABS) (Vaughan et al., 2003). The ABS low drives northerly winds onto the west coast of the AP, keeping it relatively mild (Vaughan et al., 2003). The steep topography of the AP limits the influence of mild northwest air flow across to the eastern AP. Consequently the near surface temperatures in the west are warmer than those on the east (Fig. 2.3) (King et al., 2003). It has been shown (Marshall and King, 1998) that extremely warm and cold winters on the AP are associated with circulation changes in the ABS. Thus it seems feasible that recent climate changes on the Antarctic Peninsula could be driven by circulation changes in the ABS (Vaughan et al., 2003).

Meteorological data for the ABS part of the AP are however, limited to measurements starting after the mid-1970s, making it difficult to determine with any degree of reliability whether there have been any significant circulation changes in this region (Vaughan et al., 2003). Marshall (2002) has demonstrated a significant increase in upper westerly winds between 1969-2000 based on the analysis of radiosonde station data, but no increase in the northerly winds thought to be associated with warming. A trend to more cyclonic conditions was suggested by increased precipitation at Faraday Station (Turner et al., 1997) but this is at odds with the automatic depression-tracking data of Simmonds and Keay (2000), which indicates a decline in Antarctic cyclone numbers in the ABS over the period 1958-1997. Other studies have established robust links between atmospheric circulation in the ABS and the El-Niño-Southern Oscillation (ENSO) (e.g. Simmonds and

Jacka, 1995; Cullather et al., 1996; Trenberth and Caron, 2000; Yuan and Martinson, 2000) whilst others have suggested a link between ENSO and sea-ice conditions (below). On longer timescales Villalba et al. (1998) have demonstrated that the 20th century (AD 1912-1984) has been characterised by extreme ENSO-related conditions in southern South America. How these processes relate to the climate of the Antarctic Peninsula is still poorly understood (Vaughan et al., 2003), but the possibility that ENSO-related teleconnections are in some way related to climate change on the AP remains an important question to address.

An additional atmospheric explanation for rapid warming in the Peninsula has been suggested by Van den Broeke (1998, 2000), which involves the semi-annual oscillation (SAO), a twice-yearly contraction/expansion of the CPT causing it to grow stronger and move polewards (van Loon and Rodgers, 1984). During this phase, synoptic disturbances are more intense on the AP. In addition, several authors have noted a decrease in SAO strength since the late 1970's (Hurrell and van Loon, 1994; Chen and Yen, 1997). According to van den Broeke (2000) weak SAO years are associated with an enhancement of northerly winds, decreased sea-ice cover in the ABS sector and warming over the AP. These conclusions contrast with Marshall (2002) who re-examined this hypothesis and found no correlation between changes in wind strength and temperature on the AP and weak (or strong) SAO years. Similarly Vaughan et al. (2003) point out that the main changes observed in SAO appear to have occurred after the mid-1970s, later than the first period of significant warming on the AP (1950-1970).

2.2.3.3. Air-sea-ice feedback.

A third mechanism is the amplification of global mean warming by sea-ice-atmosphere feedbacks (Vaughan et al., 2001). The western AP is the only region in Antarctica that shows a strong annual and long-term correlation between sea-ice concentration and air temperature (Weatherly et al., 1991). Sea ice tends to suppress the transfer of heat from the ocean to the atmosphere during winter, and increases the regional albedo (Jacobs and Comiso, 1997; King et al., 2003). Both act to lower air temperatures and favour the production of more sea-ice (Vaughan et al., 2001). The opposite is also true and may account for the recent warming, with the initial

impetus being supplied by local changes in the greenhouse effect, caused by anthropogenic emissions or increased water vapour in the atmosphere (Vaughan et al., 2003). The directionality of the sea-ice-climate feedback is complex given the feedbacks between sea-ice and air temperature and the role CDW plays in controlling sea-ice distribution in the western AP. The relationship is complicated further by the apparent link between ENSO and sea-ice extent (Simmonds and Jacka, 1995; Yuan and Martinson, 2000). Kwok and Comiso (2002) have investigated the relationship between positive, neutral, and negative phases of the Southern Oscillation Index (SOI) and surface meteorological/sea-ice variations in the southern oceans. They found a strong correlation between negative SOI (warm phase of ENSO) over the ABS with decreased sea-ice extent associated with high sea level pressure. The spatial structure of the sea-level pressure-ENSO relationship demonstrated by Kwok and Comiso (2002) exhibit characteristics of the Pacific-South American teleconnection pattern, which has been linked to ENSO by Simmonds (2003) (e.g. Fig. 2.9). Interestingly several recent studies have linked past (Holocene) climatic changes on the AP with ENSO variability (Shevenell and Kennett, 2002; Ishman and Sperling, 2002). However it is unclear at present how these changes relate to variations in sea-ice extent. Finally, some have suggested that climate change in southwest Africa may effect Antarctic sea ice (Stuut et al., 2004).

2.3. Holocene Climate Variability: Terrestrial, Marine & Ice Core Records

The recent rapid regional warming on the Antarctic Peninsula and the collapse of several ice shelves has focused research upon longer-term records of environmental change. Without a long-term perspective of environmental change on the AP it remains difficult to judge the significance of the recent changes in temperature and ice shelf extent. To answer this question, research has concentrated on the Holocene period, particularly looking for analogous temperature maxima, to determine what caused them, what effect they had around the AP, and if they were accompanied by any changes in global sea-level. Several lines of evidence suggest that the climate during the mid-Holocene may have been as warm, or warmer than

at present. This period of climate variability has been given several names including the mid-Holocene hypsithermal (MHH), the Holocene warm interval and the mid-Holocene climatic optimum. Evidence for the MHH has been identified in marine sediment cores (e.g. Shevenell et al., 1996; Yoon et al., 2002; Domack et al., 2003a), lake and terrestrial records (e.g. Hjort et al., 2003) and ice core records (Fig. 2.10) (e.g. Mosley-Thompson and Thompson, 2003). The consensus among these records is that the MHH occurred between ca. 4500 to 3000 cal yr BP (Ingólfsson et al., 2003) in response to enhanced levels of incoming solar radiation, although the marine record from the Palmer Deep (Domack et al., 2001, 2003a) suggests a longer MHH between ca. 9000 and 3500 cal yr BP (Fig. 2.10 and 2.11). The following section will provide a review of Holocene marine and terrestrial proxy records from the AP. All ages are presented as published unless stated otherwise and are reported as calibrated years BP (cal yr BP) or conventional ^{14}C ages (^{14}C yr BP). Holocene ice-core records from the AP will be considered separately.

2.3.1. LGM to mid-Holocene (ca. >30000 – 6000 ka BP)

The Last Glacial Maximum (LGM) provides the natural precursor to Holocene environmental change on the Antarctic Peninsula. The timing of the LGM however is poorly known owing to the lack of well-constrained chronologies for LGM positions of ice margins and the subsequent deglaciation, known as Termination 1 (Bentley, 1999; Ingólfsson et al., 2003). This is largely due to the lack of datable material, and the problems associated with variable carbon reservoirs in the marine environment (See section 4.1). Nevertheless, Sugden and Clapperton (1982) suggested that the last maximum ice extent occurred later than 30000 ^{14}C yr BP and prior to 14000-12000 ^{14}C yr BP based on the terrestrial record. There is strong evidence of grounded ice sheets and outlet glaciers extending onto the continental shelf during the LGM (e.g. Kennedy and Anderson, 1989; Herron and Anderson, 1990; Larter and Bartek, 1991; Anderson et al., 1991a, 1992, 2002; Pope and Anderson, 1992; Banfield and Anderson, 1995; Bart and Anderson, 1996; Larter and Vanneste, 1995; Sloan et al., 1995; Canals et al., 2000; Domack et al., 2001), which have enabled reconstructions of the expanded Antarctic Peninsula ice sheet (APIS) to be made (Fig. 2.12). The oldest ^{14}C dates constraining the minimum ages for ice retreat come from glacial-marine sediments overlying tills on the outer

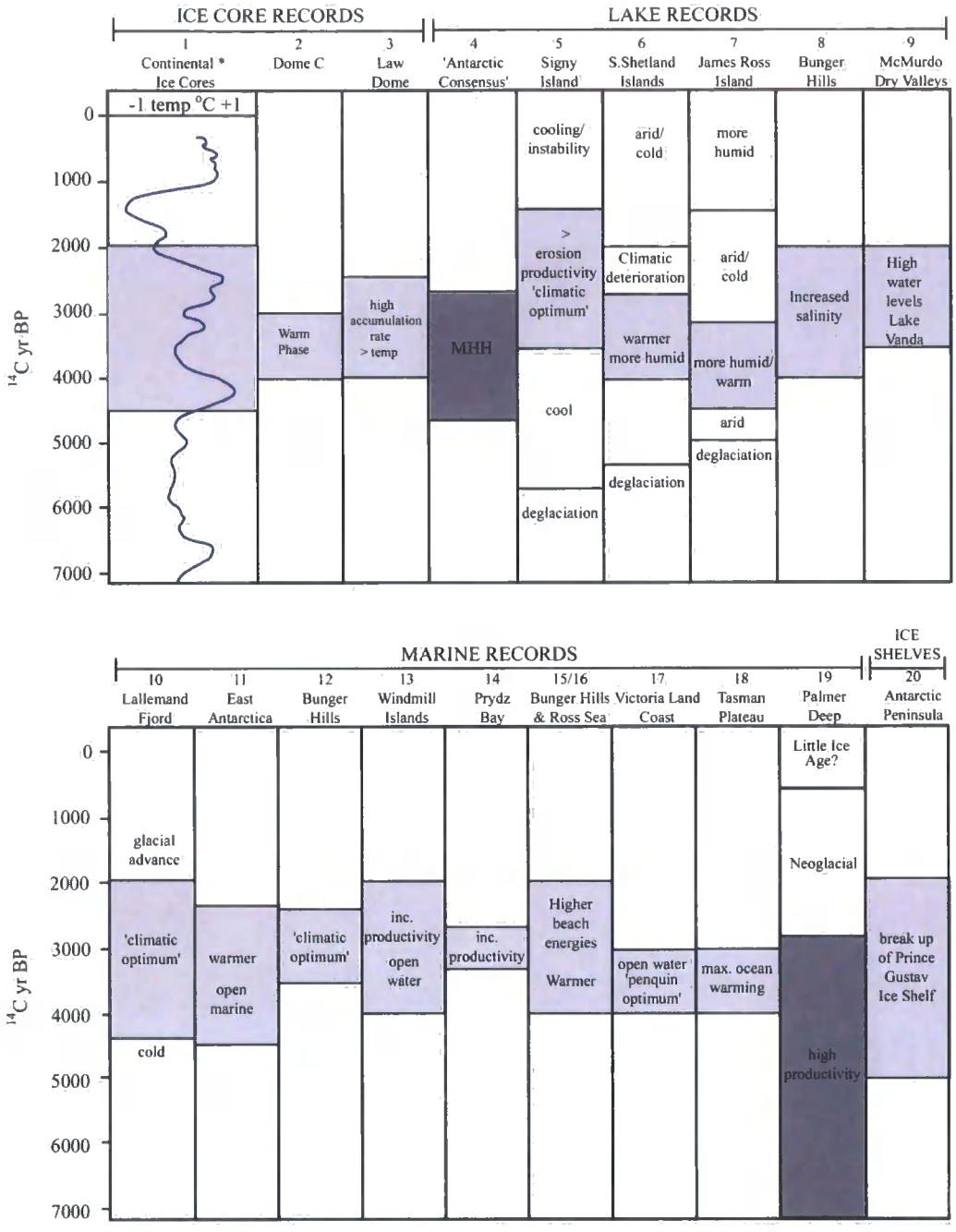

Fig 2.10. Multi-archive compilation showing the mid-Holocene hypsithermal (MHH) as detected in selected ice cores, lake sediments, marine sediments and other records. References: 1 Ciais et al. (1994) *(adjusted to ^{14}C time-scale), 2 Lorius et al.(1990), 3 Goodwin (1993), 4 Ingólfsson et al. (1998), 5 Jones et al. (2000), 6 Björck et al. (1991a), 7 Björck et al. (1996), 8 Roberts et al. (2000a), 9 Smith et al. (1993), 10 Domack et al. (1996), 11 Melles et al. (1997), 12 Kulbe et al. (2001), 13 Hodgson et al. (subm), 14 McMinn (2000), 15 Nichols (1968), 16 Colhoun (1992), 17 Baroni and Orombelli (1994) (note: dates corrected for carbon reservoir), 18 Ikehara et al.(1997), 19 Domack et al.(2001), 20 Pudsey and Evans (2001). Note: dates used in this table are as cited in the original source and have not been independently corrected. (Redrawn from Hodgson et al., 2004)

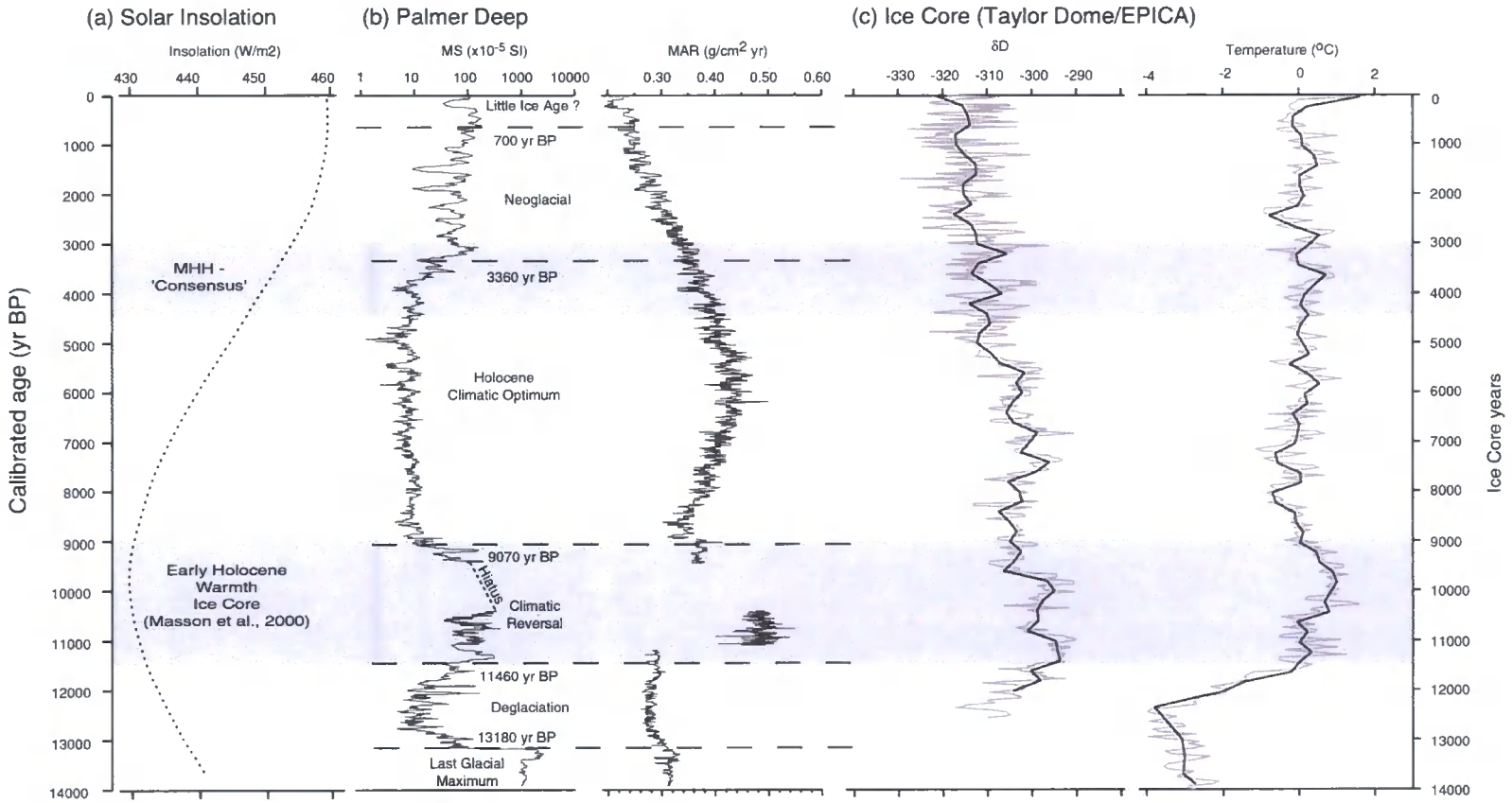

Figure 2.11. Composite diagram of key palaeoevironmental records from the AP: (a) Regional solar insolation at 65°S for December (Berger and Loutre, 1991). Also shown (grey shading) are the key periods of Holocene warmth. *Mid-Holocene Hypsithermal (MHH) consensus derived Ingolofsson et al., (2003) and the Early Holocene opitimum recorded is Antarctic Ice cores (Masson et al., 2000); (b) Magnetic susceptibility (MS), mass accumulation (MAR) records from Palmer Deep plotted against a calibrated time-scale (Domack et al., 2001); (c) Ice core records from Antarctica. Taylor Dome dD record (Steig et al., 1998) and temperature annomaly data from EPICA ice core (200 yr averages) (Masson-Delmotte et al., 2004).

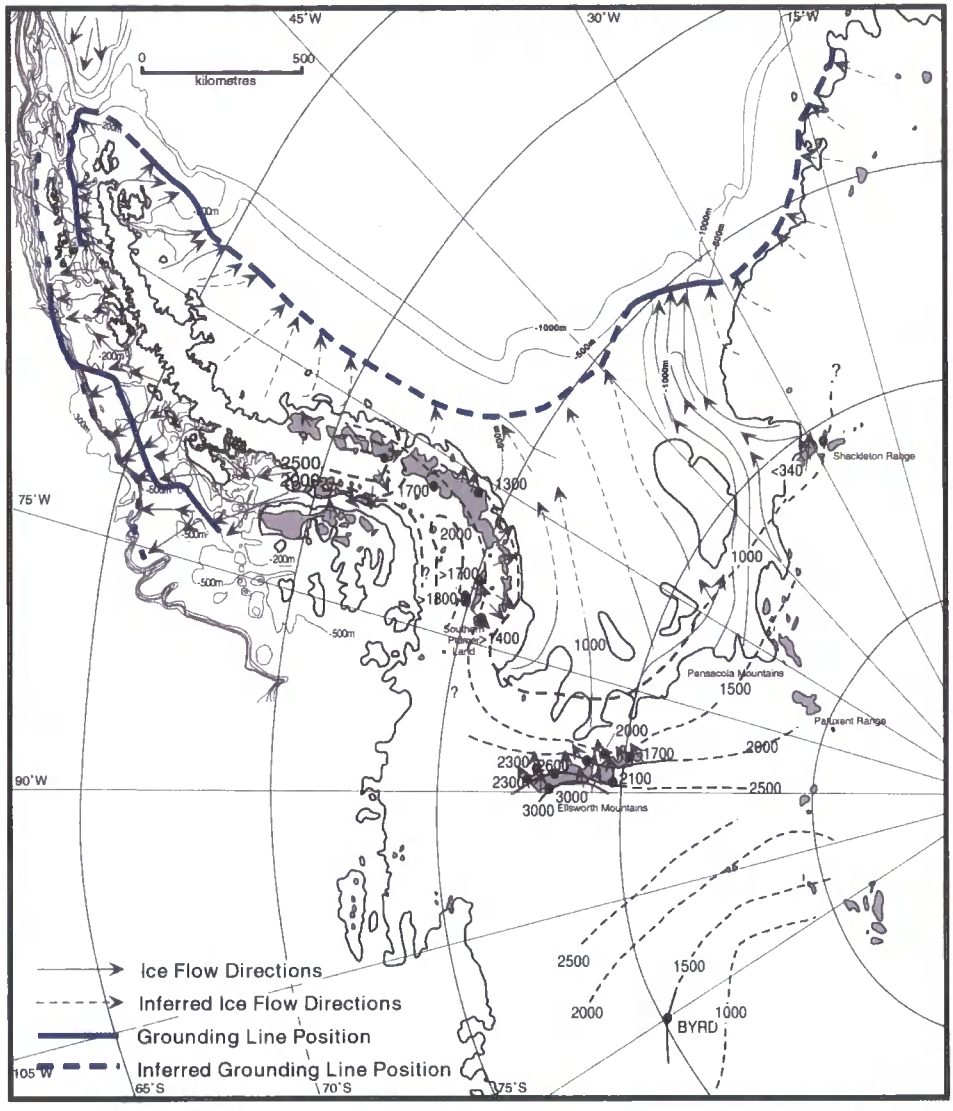

Fig. 2.12. Reconstruction of the Weddell Sea embayment during the LGM (from Bentley and Anderson, 1998). Dots show sites where ice sheet elevations have been constrained by trimlines or over-ridden summits (minimum values). Arrows show flow direction indicators (striations). Contours for the former ice sheet are drawn perpendicular to the flow directions and their altitudes are fixed by the trimlines. Solid lines indicate relatively confident reconstructed contours whereas dashed contours are interpolated and are not well constrained. The elevation of the ice in the interior of West Antarctica is not well-constrained by the reconstruction.

continental shelf (contour lines Fig.2.12) off the west coast of the AP (Banfield and Anderson, 1995; Pope and Anderson, 1992; Pudsey et al., 1994). These ages indicate grounded ice retreat prior to 14000-13000 ^{14}C yr BP for the Bransfield Strait and 12000-11000 ^{14}C yr BP for and Anvers Island. Dates from inner shelf areas and fjords and bays on the AP constrain deglaciation of the inner shelf to as late as 8000-6000 BP (e.g. Harden et al., 1992; Pudsey et al., 1994; Shevenell et al., 1996; Hjort et al., 2001). Deglaciation of Marguerite Bay, based on the relative sea-level curve of Bentley et al. (2005) suggests a minimum age of ca. 9000 ^{14}C yr BP (8368 – 8850 cal yr BP at 1 sigma). In contrast, Domack et al. (2001) have published a record from the Palmer Deep (Fig.2.1b), which shows that the inner shelf further north might have been deglaciated as early as ca. 13000 cal yr BP (Fig. 2.11). From an ice core perspective, available continental records (discussed in more detail below) show a 'climatic optimum' occurred between 11500 and 9000 yr BP when atmospheric temperatures were as warm or warmer than the present day (Masson et al., 2000).

The timing of deglaciation in the presently ice-free terrestrial areas is constrained by minimum ^{14}C ages obtained from fossil mollusc shells from raised marine deposits, peat deposits in moss banks on sub-Antarctic islands, organic matter from lake sediments and fossil penguin remains from coastal rookeries (Ingólfsson et al., 2003). These dates are mostly minimum ages for deglaciation since there are unknown lag times between retreat of ice sheets and glaciers and the colonisation by plants and/or animals (Gore et al., 1997; Ingólfsson et al., 2003). On King George Island a mollusc yielded a minimum age of 9000-8000 yr BP for deglaciation (Sugden and John, 1973; Mäusbacher, 1991). A well-dated lithostratigraphic record from northern James Ross Island implies deglaciation there was prior to ca. 6300 yr BP (Hjort et al., 1997). A similar age has been suggested for deglaciation of Hope Bay (Fig.2.1b) based on ^{14}C from a lake sediment core (Zale, 1994). In the southern part of the AP, ^{14}C dated barnacle fragments from an ice shelf moraine provided minimum ages for deglaciation and possible ice-shelf retreat in George VI Sound of 6500-5700 yr BP (Clapperton and Sugden, 1982; Hjört et al., 2001).

Once glaciers were inside the present coastline, glacial retreat and ice disintegration occurred much more slowly (Ingólfsson et al., 2003). On King George Island,

glaciers were at, or within, their present limits by ca. 6000 yr BP (Martinez-Macchiavello et al., 1996), on northern James Ross Island prior to 4700 yr BP (Hjort et al., 1997) and the Byers Peninsula on Livingston Island deglaciated between 5000-3000 yr BP (Björck et al., 1996). On Elephant Island, ^{14}C dates from the onset of moss-bank formation indicate a minimum date for deglaciation of 5500 BP (Björck et al., 1991). In Marguerite Bay, ^{14}C-dated remains from fossil penguin rookeries suggest initial colonisation occurred between 6500 and 5500 yr BP (Emslie, 2001) which is consistent with marine geological evidence which suggests a minimum age for deglaciation of 7000-6000 yr BP (e.g. Shevenell et al., 1996). Together this data suggests that the transition from glacial to interglacial conditions on the Antarctic Peninsula was broadly completed by ca. 6000 yr BP. Interestingly, many of these records show that some currently ice-free areas were ice-covered until the early to mid-Holocene, which has important implications for retrieving full Holocene records on land.

2.3.2. Mid-Holocene (5700 - 4000 ka BP)

Several records indicate glacial readvances during the mid-Holocene. On King George Island, Mäusbacher (1991) found evidence to suggest increased glacial activity between 5000 and 4000 yr BP, which is consistent with the earlier observations of Sugden and John (1973) who had suggested glacial expansion after 6000 BP. Similarly, Hanson and Flint (1989) provided evidence of a glacial readvance on Brabant Island (Fig.2.1b) after ca. 5300 yr BP. Following a suspected mid-Holocene ice shelf collapse (Sugden and Clapperton, 1980, 1981; Clapperton and Sugden, 1982; Hjört et al., 2001), George VI Ice Shelf is thought to have expanded after 5700 yr BP. Mid-Holocene glacial readvances on James Ross Island and at Hope Bay have also been documented (Hjort et al., 1997; Zale, 1994). Offshore, Yoon et al. (2000) have identified cold waters with extensive sea-ice conditions in fjord margin sediments on King George Island between ca. 6200 and 4000 yr BP, which is consistent with Mäusbacher's (1991) evidence for increased glacial activity. A mid-Holocene cooling is absent, however, in the marine records from Palmer Deep and Lallemand Fjord (e.g. Domack et al., 2001; Shevenell et al., 1996), although a mid-Holocene cool event in the Lallemand Fjord record was noted (Fig. 2.10) (Shevenell et al., 1996). From this Hjört et al. (1997) concluded

that the readvances on land may reflect regional changes in atmospheric conditions, such as increased precipitation associated with warming and increased cyclonic conditions.

2.3.3. Holocene climatic optimum/hypsithermal (ca. 4500 – 2500 ka BP)

It has been suggested that following glacier readvance during the mid-Holocene, the climate of the Antarctic Peninsula warmed between ca. 4500 to 3000 yr BP (Ingólfsson et al., 1998). This mid-Holocene hypsithermal (MHH) appears to have been most marked on the Antarctic Peninsula, but has also been observed elsewhere in Antarctica (Fig. 2.10). Currently the best dated records have been obtained from lake sediments on the South Orkney Islands (Jones et al., 2000) and South Shetland Islands (Schmidt et al., 1990; Björck et al., 1996) which show a period of rapid sedimentation, enhanced productivity and increased species diversity between 4000 – 2000 ^{14}C yr BP. The MHH has also been recognised offshore in marine sediments. The marine record from Lallemand Fjord (Domack et al., 1995; Shevenell et al., 1996) shows an early phase of high productivity between 7500–5800 cal yr BP followed by their 'climatic optimum', again reflected by higher productivity between 4200 and 2700 yr BP. Similarly, a climatic optimum is recognised between 6000 and 2500 cal yr BP from marine cores collected along the western margin of the northern Antarctic Peninsula (Yoon et al., 2002). The marine record from the Palmer Deep (Domack et al., 2001, 2003a) however suggests a more prolonged climatic optimum, that started significantly earlier between ca. 9000 and 3500-2500 cal ka yr BP (Fig. 2.10 and 2.11). It has been suggested that this optimum was caused by the intrusion of warm water onto the western AP continental shelf between ca. 9000-6700 cal yr BP (Leventer et al., 2002). As such the Holocene optimum recorded in the Palmer Deep may reflect oceanic changes, whilst the MHH on land may reflect atmospheric temperature changes.

More recently a small number of studies have highlighted the possibility that some ice shelves may have collapsed in response to the MHH. Former absences of ice shelves on the eastern coast of the Peninsula (e.g. Prince Gustav Ice Shelf (Pudsey and Evans, 2001) and Larsen-A Ice Shelf (Domack et al., 2001; Gilbert and Domack, 2003; Brachfeld et al., 2003) and the coastline of East Antarctica (e.g. Amery Ice Shelf (Hemer and Harris, 2003)) appear to coincide with the MHH.

Pudsey and Evans (2001) provided a long-term perspective on the Prince Gustav Channel Ice Shelf (PGIS) (Fig. 2.1b), which collapsed again in 1995. Sediment cores show that during the period from ~6000 to 1900 cal yr BP (Fig. 2.10) the ice shelf was absent. Since 1900 cal yr BP, the shelf was continuously present until it collapsed in 1995. One problem with this record however is a poor late Holocene chronology. In the absence of marine carbonate (e.g. foraminifera), Pudsey and Evans (2001) were forced to date the acid insoluble organic matter (AIOM) fraction. Each core yielded a surface sediment age of ca. 6000 yr BP which Pudsey and Evans (2001) attributed to the influence of old carbon. To correct their chronology they used a 6000 yr BP (1300 yr Antarctic Marine Reservoir Effect (AMRE) plus local reservoir of 4700 yr BP) correction. Hemer and Harris (2003) showed that the Amery Ice Shelf (AIS) in East Antarctica (Fig. 2.1) retreated at ca. 5700 ^{14}C yr BP. Like Pudsey and Evans, (2001), the Amery Ice Shelf sediments contained no carbonate and the AIOM fraction, derived from surface sediment, yielded an erroneously old core top age (6548 ± 60 ^{14}C yr BP) which Hemer and Harris subtracted from all other (3 further ^{14}C ages) down-core values. As such the ages from these two studies must be treated cautiously. By applying a uniform correction, these studies assume a constant AMRE offset through time. However recent studies (e.g. Crespin et al., 2004) suggest that this is not the case and that the Antarctic Marine Reservoir Effect (AMRE) has varied throughout the Holocene. These problems have led some researchers to concentrate on new and innovative dating techniques. For example, Brachfeld et al. (2003) have successfully developed and applied geomagnetic palaeointensity dating to sediment cores retrieved from beneath the former Larsen-A Ice Shelf. This record indicates the ice retreated between 3800 and 1400 yr BP (similar to the 5000-2000 cal yr BP ice free period suggested by Pudsey and Evans, (2001)) for the more northerly Prince Gustav Channel Ice Shelf) and highlights the potential for utilising such techniques for accurately dating environmental changes on the AP. However, not all marine/lacustrine sediments are suitable for this technique (S. Brachfeld pers. comm.). Thus, at present, and in the absence of sediment that is suitable for geomagnetic palaeointensity dating, any sediment cores that contain carbonate macrofossils such as foraminifera possess a distinct advantage over AIOM in

providing a robust down core chronologies. The issue of obtaining reliable chronologies from the AP is discussed in more detail in Chapter 4.

2.3.4. Neoglacial Period (ca. 2500-0 ka BP)

After ca. 2500 ka BP the climate of the AP became cooler until 1500 yr BP (Björck et al., 1996). On land, several studies suggest that glaciers expanded during this period (e.g. John and Sugden, 1971; John, 1972; Sugden and John, 1973; Curl, 1980; Birkenmajer, 1981; Clapperton and Sugden, 1988; Zale and Karlén, 1989; Clapperton, 1990; Lopez-Martinez et al., 1996). Moraines on James Ross Island suggest an ice re-advance that coincided with the Little Ice Age (LIA) in the Northern Hemisphere (Fig. 2.10), with lichenometric dating yielding ages of ca. AD 1240, 1720 and 1780-1822 (Curl, 1980). Offshore, Barcena et al. (1998) found a significant increase in sea-ice (diatom) taxa after 3000 yr BP in the Bransfield Strait. Similarly, Fabrés et al. (2000) and Khim et al. (2002) studied several marine records form the Bransfield Basin extending back 2850 years, which showed neoglacial cooling as well as a LIA cold-pulse. This is also consistent with the record from the Lallemand Fjord (Shevenell et al., 1996; Taylor et al., 2001), which suggests decreased productivity in the fjord after 3000 yr BP, persistent sea-ice after ca. 2700 yr BP and ice shelf advance into the fjord after ca. 400 yr BP (Fig. 2.10). In the Palmer Deep Leventer et al. (1996) and Kirby et al. (1998) suggested that the Holocene climatic optimum ended at ca. 2500 yr BP and Domack et al. (2003a,b) identify neoglacial cooling beginning at ca. 3500 yr BP and lasting until ca. 150 yr BP. A LIA-type event is also recorded in the Palmer Deep, occurring between ca. 700 and 150 yr BP and is marked by reduced sedimentation and productivity (Domack et al., 2003a,b). The Palmer Deep record also defines a Medieval Warm Period (MWP) between ca. 1150 and 700 yr BP that is characterised by enhanced productivity (Domack et al., 2003a,b) consistent with a record from the Bransfield Basin (e.g. Khim et al., 2002) which shows warming between ca. 1000 and 500 yr BP.

In summary, a review of proxy records from the Antarctic Peninsula support a regionally consistent pattern of palaeoenvironmental change during the Holocene

(Fig.2.10), with events apparently synchronous throughout the region. Specifically, the following conclusions can be made:

1. There is evidence for much more extensive ice cover in the Antarctic Peninsula region than today prior to ca. 14000 yr BP
2. Deglaciation occurred mainly between 14000 and 6000 yrs BP, with outer and middle shelf areas deglaciated between 14000 and 8000 yrs BP and inner shelf areas as late as 6000 yr BP. Deglaciation appears to coincide with an early Holocene climatic optimum between 11500 and 9000 yrs BP recorded in several Antarctic ice cores.
3. There was a mid-Holocene glacial advance in some areas between 5700 and 4000 yr BP.
4. There was a Holocene hypsithermal/optimum with warmer and more humid conditions generally between 4000 and 2500 yr BP. The marine record from the Palmer Deep however recognises an earlier, longer climatic optimum between 9000 and 3000-2500 yr BP.
5. A late Holocene Neoglacial period lasted between 3000 and 2500 yr BP, when the climate became cooler and glaciers and ice shelves expanded
6. Evidence for a Medieval Warm Period has been discovered in some records from about 1150 to 500 yr BP.
7. Evidence for a Little Ice Age type event has been discovered in several records between 700 and 150 yr BP.
8. Recent rapid regional warming 150 yrs to present.

2.3.5. Ice Core Evidence

Information from continental ice cores in the Antarctic has revolutionised our understanding of late Pleistocene climate change and has enabled key assumptions and theories about the earth system to be tested (e.g. Blunier et al., 1998; Petit et al., 1999; Domack and Mayewski, 1999). Unfortunately there are not yet any full Holocene ice-core records from the AP. In addition the few short ice core records which have been retrieved, do not provide a coherent picture, especially of 20th century climatic variability. The situation is set to improve however, as a drilling project currently underway at Berkner Island (Fig. 2.1) is expected to extract an ice

core extending back ca. 10,000+ years (Mulvaney et al., 2002). The aim of this section is to review what is known about ice-core derived climate records from the Peninsula region, before briefly reviewing the Holocene ice core record from elsewhere on the Antarctic continent. In the absence of a Holocene ice core from the AP, possible linkages between ice cores from the Antarctic Peninsula and other continental cores are also discussed.

2.3.5.1. Antarctic Peninsula Ice Cores

There are six ice cores from the AP with century-long isotopic temperature records (Fig. 2.1b): James Ross Island (JRI) (Aristarain et al., 1990), Dolleman Island (DI) (Peel et al., 1992, 1996), T340 on the Ronne-Filchner Ice Shelf (Graf et al., 1988), Dyer Plateau (DP) (Thompson et al., 1994), and the two previous Berkner Island (BI) ice cores R1 and B25 (Mulvaney et al., 2002). In a recent synthesis of AP ice cores, Mosley-Thompson and Thompson (2003) also included two other ice core records in order to expand the temporal and spatial coverage of climate variability. The Siple core (Fig. 2.1) provides a 550-year proxy climate history (Mosley-Thompson et al., 1991; Mosley-Thompson, 1992) that covers nearly the same time interval as the Dyer cores. Whilst the Plateau Remote core in East Antarctica (Mosley-Thompson, 1996) extends both the temporal and spatial coverage and allows possible comparisons between AP ice core records and those from the interior. The locations of these sites are shown in Figure 2.1 and the key feature of each record summarised in Figure 2.13.

Figure 2.13 shows all the *existing* (i.e. minus Berkner Island) multi-century ice core records from the Antarctic Peninsula. The $\delta^{18}O$ record from the Dyer Plateau varies around a long-term mean between 1505-1989. After ca. 1840 there appears to have been a phase of cooling, which lasted until ca. 1920 (Mosley-Thompson and Thompson, 2003) followed by progressive enrichment in $\delta^{18}O$ values, consistent with observed 20th century warming. The pronounced warming observed in the last two decades of this record appear to be the warmest of the past 500 year record. The record from the DP does appear to indicate that recent warming on the Peninsula is exceptional over century-timescales (Vaughan et al., 2003). This is further

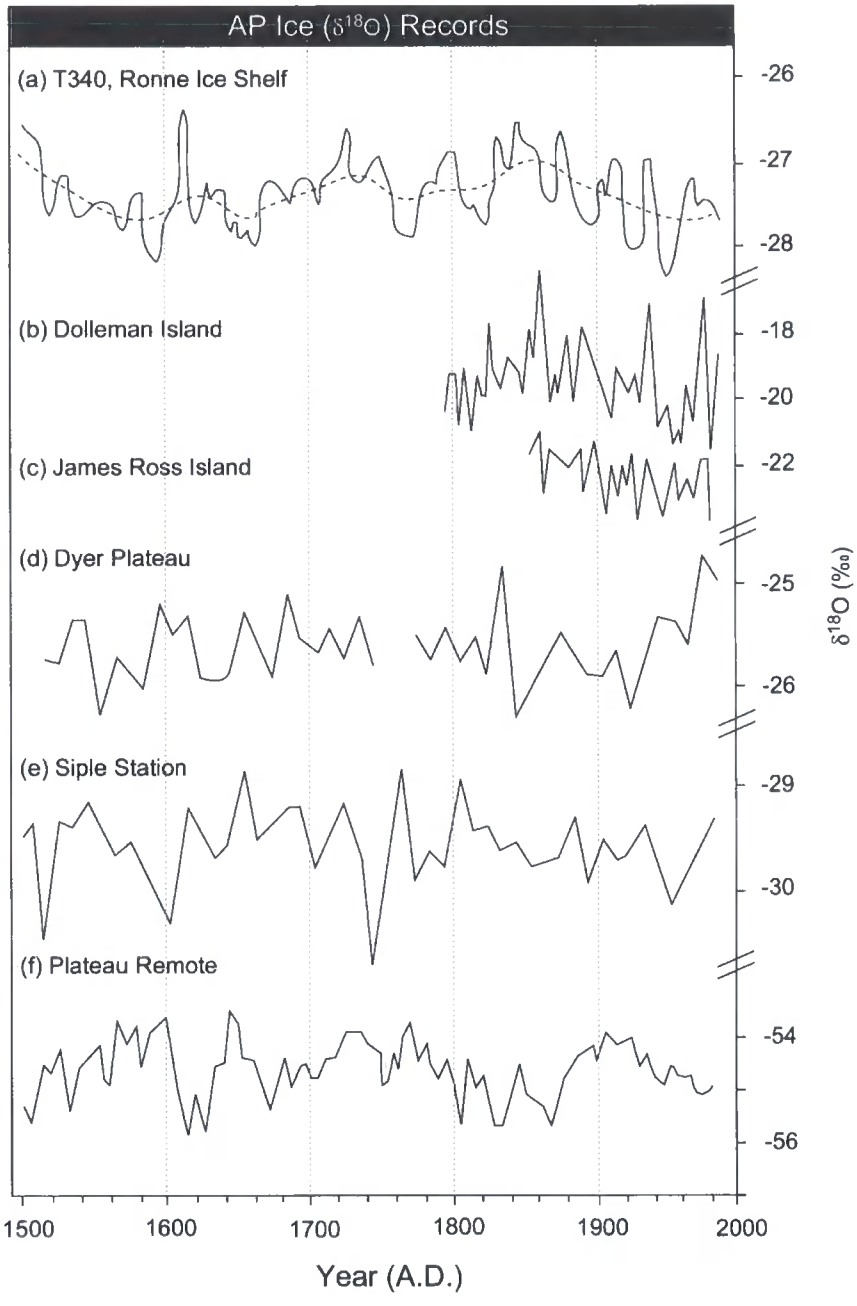

Figure 2.13. The $\delta^{18}O$ isotopic records from five AP ice cores plus Plateau Remote (redrawn Mosley-Thompson and Thompson, 2003): (a) T340 on the Ronne Ice Shelf (Graf et al., 1988); (b) Dolleman Island (Peel, 1992); (c) James Ross Island (Aristarain et al., 1986); (d) decadal averages of $\delta^{18}O$ from the Dyer Plateau (Thompson et al., 1994); (e) decadal averages of $\delta^{18}O$ from the Siple Station (Mosley-Thompson, 1992); and (f) The decadal averages of $\delta^{18}O$, from Plateau Remote (Mosley-Thompson, 1996).

supported by borehole temperature profiles from the Dyer Plateau, which suggest cooling in the late 19th and early 20th century followed by a warming over the last 50 years (Nicholls and Paren, 1993).

The warming trend at DP however, is absent in the JRI, DI and T340 records from the eastern AP and Weddell Sea region. Similarly, the Siple Station ice core shows little variation around the mean (between 1500 and 1986) and no 20th century warming (Vaughan et al., 2003). The $\delta^{18}O$ record from Dolleman Island shows the most pronounced interannual variations observed on the Peninsula between 1938 and 1986, with warming starting around 1960. However, from the mid-19th century to the beginning of inferred warming the record shows an overall cooling trend similar to that at T340 and JRI.

The Plateau Remote record contains century-scale oscillations, with a brief (ca. 30 year) but strong cooling episode in the early 17th century. Following this, conditions remain at or above the long-term mean from 1660 to 1780 after which cooling takes place until 1870. Values indicate rapid warming from the end of the 19th to the beginning of the 20th century followed by a cooling to the present (Mosley-Thompson and Thompson, 2003). The ca. 1200 year long Berkner $\delta^{18}O$ record (not shown) oscillates around a fairly stable mean, lacks much variability and does not appear to record 20th century warming. However, this contrasts with borehole data obtained from Berkner Island (Mulvaney et al., 2002), which suggests a 0.5-1.0 °C temperature increase in the recent past (Mosley-Thompson and Thompson, 2003). With the exception of the Dyer Plateau and Dolleman Island therefore, the ice core isotope records from the AP do not record 20th century warming. Furthermore, whereas the Dyer Plateau record shows warming beginning around 1920, warming in the Dolleman Island record begins much later ca. 1960.

In summary, whilst 20th century warming has been recorded at several meteorological stations across the AP, only one of the AP ice cores (DP) shows warming over the entire century, with Dolleman Island (DI) showing warming only after 1960. It is worth noting however that a similar late 20th century warming has also been observed in a short ice core (Gomez) at the base of the Peninsula

(Fig.2.1b) (Peel et al., 1988). Several studies have investigated this apparent mismatch between the meteorological records warming on the AP and the reconstructed $\delta^{18}O$ temperature trend inferred from ice cores (Peel and Clausen, 1982; Jones et al., 1993, Peel, 1992; Peel et al., 1996). What these studies have revealed is a complex temperature-$\delta^{18}O$ (T-δ) relationship that is strongly influenced by regional atmospheric and/or oceanographic forcings. Jones et al. (1993) found that, in general, the $\delta^{18}O$ records (taken as a proxy for temperature) are at odds with the meteorological observations over the last century. A simple correlation between temperature and both $\delta^{18}O$ and δD from available Peninsula ice cores revealed a R^2 value of 0.25, leaving 75% of the temperature variance unexplained. In a recent review Mosley-Thompson and Thompson (2003) suggest several other factors that could influence the $\delta^{18}O$ ice core record on the Peninsula, such as: (1) temporal changes in moisture sources for different sites; (2) the proximity to the sea ice edge, and hence duration and extent of sea-ice; (3) seasonal differences in the delivery of snowfall to the site; and (4) the glaciological controls on the preservation of the $\delta^{18}O$ signal after snow deposition. Peel et al. (1996) have stated that ice cores exposed to the Weddell Sea may not accurately record regional temperature trends but will instead reflect changes in the local weather systems. This scenario has been invoked to explain the warming trend in the mid-19th century as depicted by T340, DI and JRI ice cores (Fig. 2.13) (Peel et al., 1996). Peel et al. (1996) conclude that ice cores from higher altitudes sites (i.e. Dyer Plateau) along the spine of the Peninsula are more likely to record regional temperature variations than those exposed to local sea ice distributions and local weather systems (e.g. Dolleman Island, James Ross Island).

More recently King and Comiso, (2003) compared new satellite-derived surface temperature data from the AP with four ice core sites (James Ross Island, Dolleman Island, Dyer Plateau and Gomez). They assessed the spatial coherence of temperature variations by correlating time-series of temperature at a base point (i.e. ice core site) with corresponding time series at all other points in the satellite temperature dataset. The resulting maps reproduced in Figure 2.14 highlight regions with which temperature at the base point is highly correlated and may therefore be considered representative. James Ross Island thus appears to be representative of

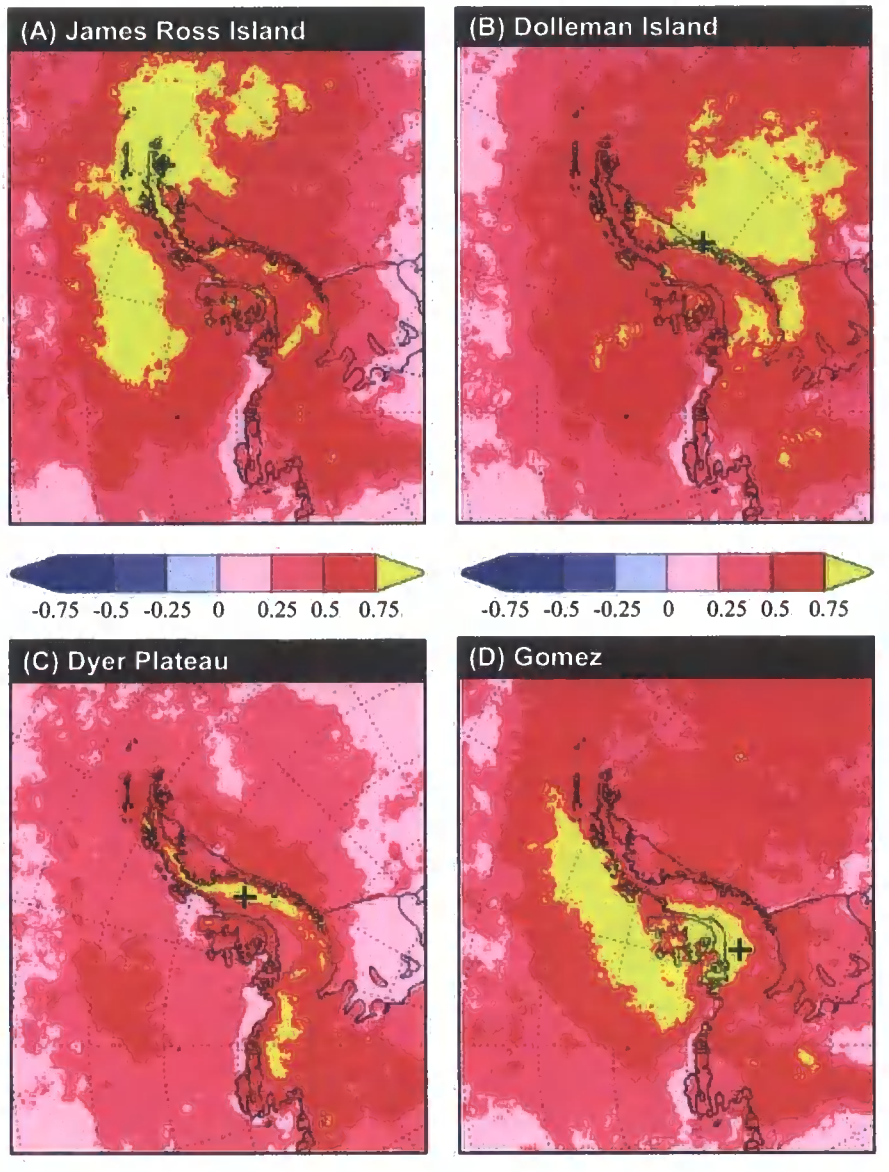

Figure 2.14. Correlation coefficients of winter (June-August) mean surface temperatures at (a) James Ross Island, (b) Dolleman Island, (c) Dyer, and (d) Gomez with other points in the satellite-derived surface temperature dataset. The base point for each map is marked with a black cross (from King and Comiso, 2003). Yellow shading shows areas where there is a high correlation (coefficient >0.75) with temperature variation at ice core site. Thus the yellow areas could be considered as those regions for which the ice core is representative.

the northern tip of the AP and the South Shetland Islands, whilst the Dolleman Island ice core appears to reflect weather conditions in the Weddell Sea (King and Comiso, 2003). Of the interior ice core sites (Siple, Dyer and Gomez), only the short-time record from Gomez correlates with temperature trends on the west side of the AP (Fig.2.12). It is worth noting however that the spatial coherence plots only provide a snapshot in time and do not take into account temporal variability.

The lack of a suitable long-term ice core record from the Antarctic Peninsula and the absence of a single coherent climate reconstruction make any conclusions regarding the long-term nature of climatic changes on the AP from ice cores problematic. In a synthesis of recent warming on the AP, Vaughan et al. (2003) used proxy data (marine/ice core records) to suggest that the rapidity and magnitude of 20^{th} century warming is unprecedented over the past two millennia and is unlikely to be a natural mode of variability. From an ice core perspective, this conclusion can only be viewed as tentative and cannot be tested until a longer ice core record is retrieved.

So, how do other Antarctic ice core records compare to the available Peninsula ice cores? Mosley-Thompson and Thompson (2003) suggested that on millennial time scales the climate in the Antarctic Peninsula may be tightly coupled to that on the East Antarctic Plateau, although they provide no clear evidence why this should be the case. The $\delta^{18}O$ record from Plateau Remote (PR) extends back to 4000 years (Mosley-Thompson et al., 1996) and shows a general cooling trend with three 1200-year oscillations (Fig. 2.13 and 2.15). Warming is inferred between 4000 and 2500 ka, which they note is broadly contemporaneous with more open conditions in Lallemand Fjord (Shevenell et al., 1996) on the west coast of the Peninsula (Fig.2.1b), warmer conditions inferred from depleted ^{18}O values in the high resolution sediment core record from the Bermuda Rise, Sargasso Sea (Keigwin et al., 1996) (Fig. 2.15) and the Holocene hypsithermal recorded in several other Antarctic ice cores. Thus, in the absence of a long AP ice core Mosley-Thompson and Thompson (2003) suggest the Plateau Remote ice core offers a link, through some teleconnection, between the AP and the East Antarctic Plateau. Unfortunately the utility of this record for inferring long-term climatic changes on the AP is again

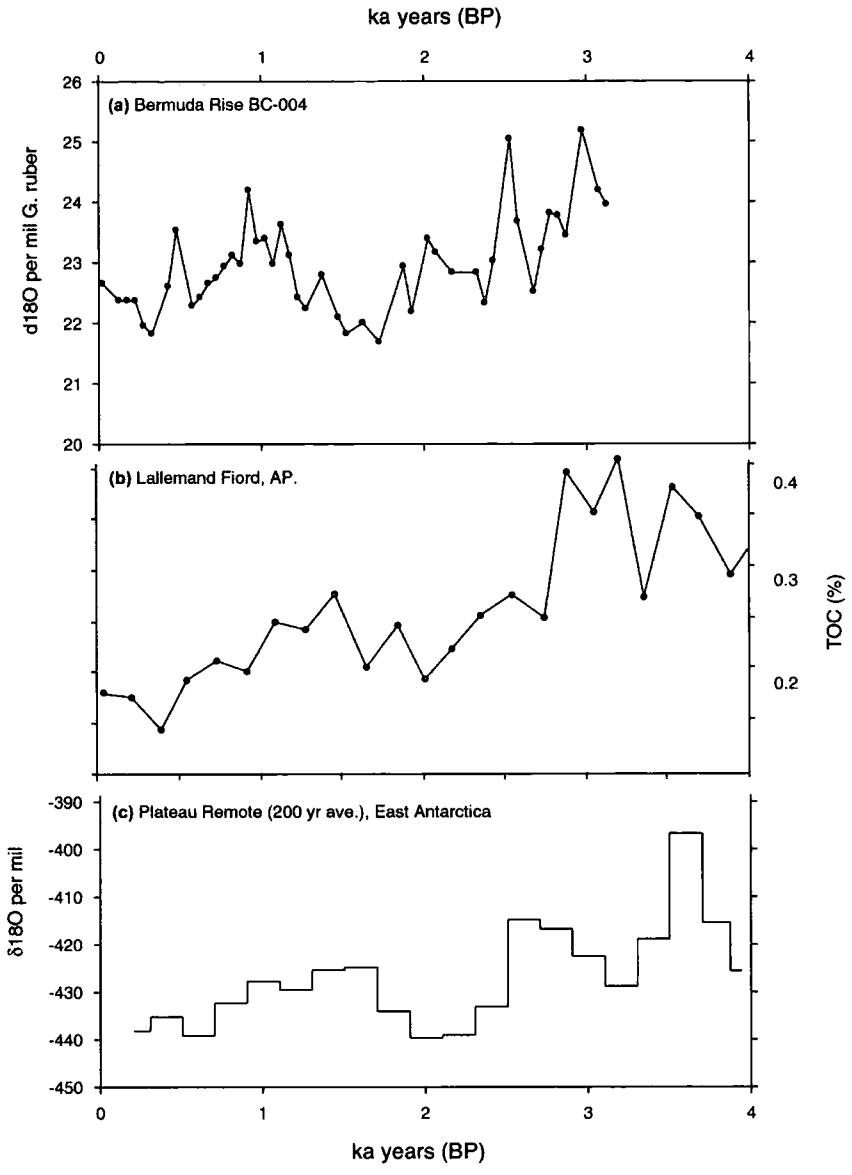

Figure 2.15. Proxy records covering the last four millennia (adapted from Mosley-Thompson and Thompson, 2003): (a) the isotopic abundance in *G. Ruber* tests in a high resolution sediment core from the Bermuda Rise (Keigwin, 1996); (b) Total Organic Carbon (TOC) from a sediment core in the Lallemand Fjord, Antarctic Peninsula (Shevenell et al., 1996); and (c) the 100-year averages of δ18O from an ice core at the Plateau Remote site in East Antarctica (Mosley-Thompson, 1996). The apparent correlation between the Lallemand Fiord TOC record and the Plateau Remote ice core record led Mosley-Thompson and Thompson, (2003) to suggest that Plateau Remore ice core record may record climate changes on the western AP.

limited to the last 4000 years. For a longer-term perspective we must turn our attention to other continental ice cores.

2.3.5.2. Continental and coastal ice cores

In the absence of a full Holocene AP ice core, the longest records, offering entire Holocene $\delta^{18}O$ and δD sequences are located on the central East Antarctic Plateau (Vostok, Dome B, Dome C -EPICA, Komsomolskaia), at coastal sites in East Antarctica (D47, KM105, Law Dome) and on both sides of the Ross Ice Shelf (Byrd, Taylor Dome) and Dominion Range in the Transantarctic Mountains (Fig. 2.16 and locations in Fig.2.1b). In brief, all records appear to shown an early Holocene optimum (11500-9000 yr ago), which Masson et al. (2000) attribute to reduced interhemsipheric heat transport by the global thermohaline circulation following Northern Hemisphere deglaciation (see below) (e.g. Blunier et al., 1997). Secondary warm periods are observed at ca. 8000 to 6000 years ago in the Ross Sea sector (e.g. Taylor Dome, Dominion Range and Byrd) at ca. 6000 to 3000 yr ago at central locations (e.g. Dome B, Vostok) and ca. 3000 years ago at Dome C, Dominion Range and Byrd. Superimposed upon the long-term trend are nine quasi-periodic millennial-scale oscillations, with a spacing of ca. 800 years during warm periods and ca. 1200 years during cooler periods (Masson et al., 2000; Masson-Delmotte et al., 2004).

In terms of the west coast of the AP, the ice cores in the Ross Sea sector (e.g. Taylor Dome and Byrd) are most likely to record Holocene climatic trends (Peel et al., 1994). Research has shown that the moisture budget of Byrd Station and the Ross Sea sector are largely controlled by atmospheric and oceanic processes occurring locally in the Amundsen Sea (Steig et al., 2001) and those occurring in the Southern Pacific Ocean (see Fig. 2.9) (e.g. Southern Westerlies and El Nino-Southern Oscillation; ENSO; Bromwich and Rogers, 2001). Figure 2.17 shows the Holocene ice core records for Taylor Dome, Byrd and Plateau Remote. The EPICA core has also been included since it provides an estimate of temperature changes, although this may not be applicable to the Ross Sea cores. Interestingly, the Plateau Remote ice core profile, suggested by Mosley-Thompson and Thompson (2003) to provide a

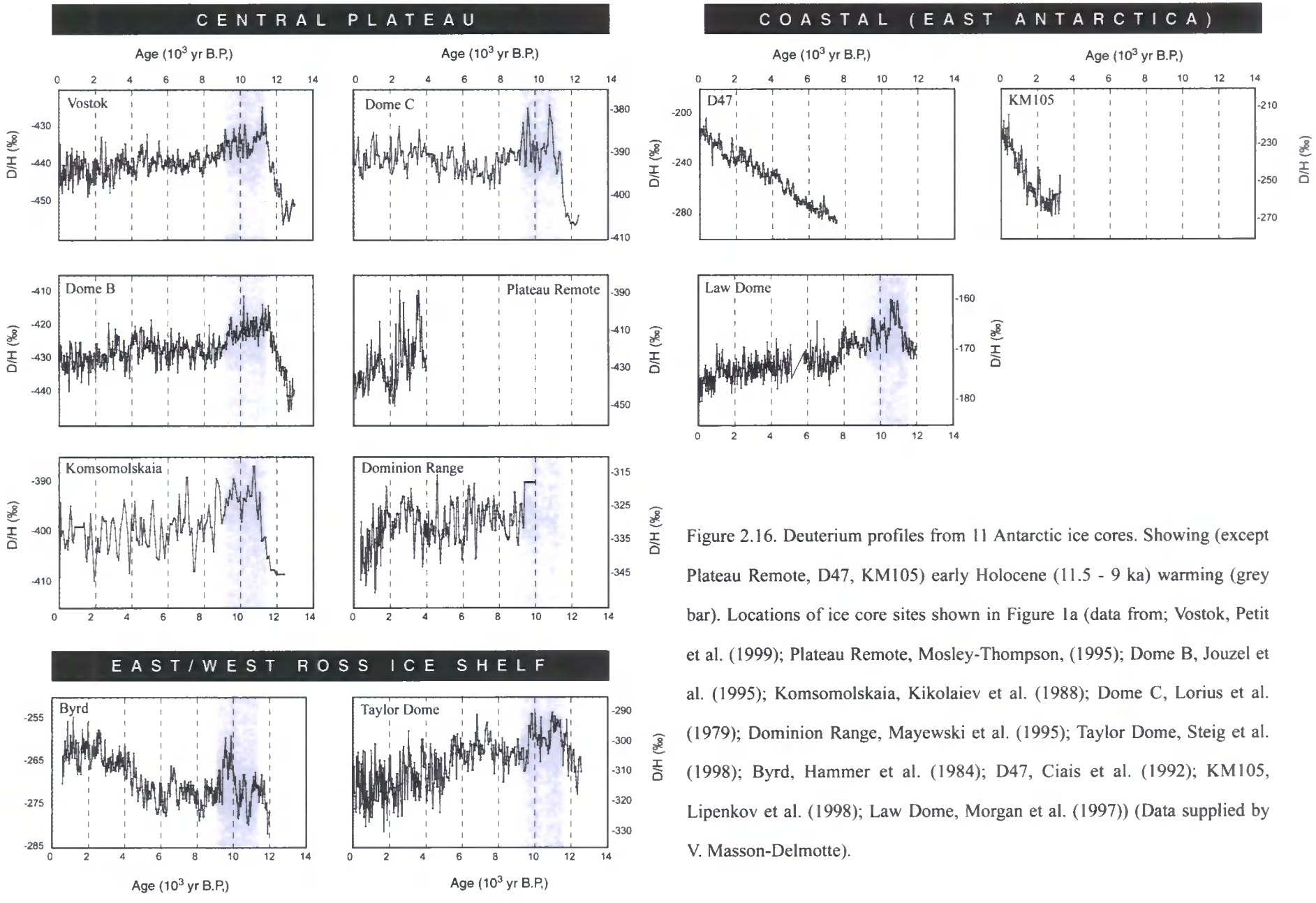

Figure 2.16. Deuterium profiles from 11 Antarctic ice cores. Showing (except Plateau Remote, D47, KM105) early Holocene (11.5 - 9 ka) warming (grey bar). Locations of ice core sites shown in Figure 1a (data from; Vostok, Petit et al. (1999); Plateau Remote, Mosley-Thompson, (1995); Dome B, Jouzel et al. (1995); Komsomolskaia, Kikolaiev et al. (1988); Dome C, Lorius et al. (1979); Dominion Range, Mayewski et al. (1995); Taylor Dome, Steig et al. (1998); Byrd, Hammer et al. (1984); D47, Ciais et al. (1992); KM105, Lipenkov et al. (1998); Law Dome, Morgan et al. (1997)) (Data supplied by V. Masson-Delmotte).

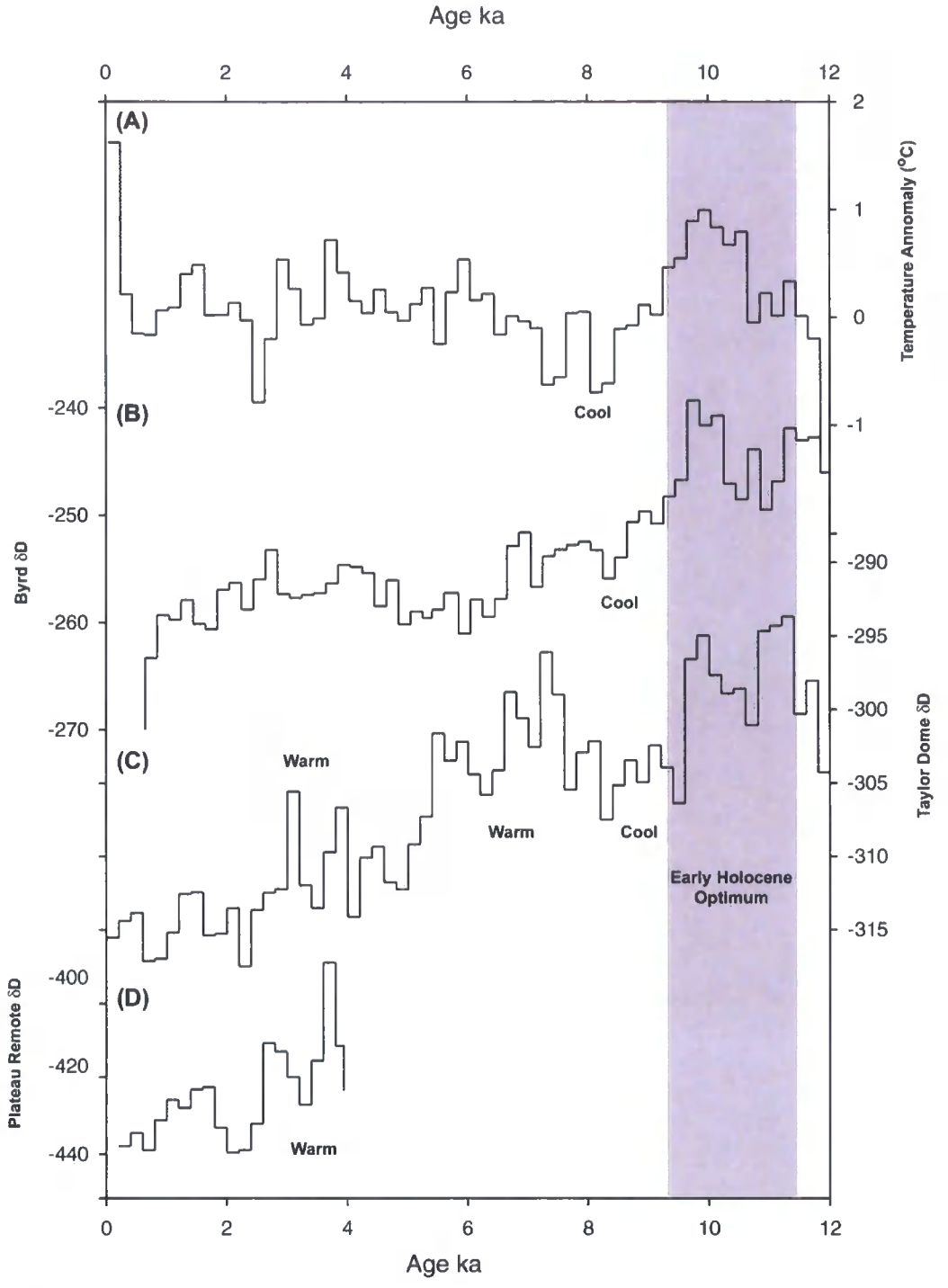

Figure 2.17. Holocene ice cores (200 yr averages) isotopic records from Antarctica which may be representative for climatic change on the Antarctic Peninsula (see text for discussion): (A) Temperature anomaly data from EPICA ice core; (B) Byrd δD (Hammer et al. 1994) and corrected for elevation after Masson et al. (2000); (C) Taylor Dome δD (Steig et al. 1998); (D) Plateau Remote δD (Mosely-Thompson, 1996). All ice cores show an early Holocene climatic optimum (11500 to 9000 yr), followed by cooling ca. 8000 yr. Taylor Dome ice core shows secondary optimums between 7900 and 5900 and between 4000 and 2000. The latter profile is consistent with Plateau Remote, which according to Mosley-Thompson and Thompson (2003) may best record climatic changes on the western side of the AP.

link between the climate of the AP and the interior, is most similar to the Taylor Dome Ice core, which shows a warming interval between 2000 and 4000 yr BP. As noted above, this is also coincident with warmer conditions recorded at Lallemand Fiord on the west coast of the AP. The Byrd and TD records appear divergent in the Mid-Holocene between 8000 and 4000 yr BP but this could reflect elevation changes at Byrd (Steig et al., 2001). Thus as a first approximation, the long continental ice cores from the Ross Sea region, notably Taylor Dome, appear to record Holocene climatic changes similar to those on the west coast of the AP.

2.3.6. Mechanism for Holocene climatic change

In section 2.3 potential mechanisms for the recent (20^{th}-21^{st} Century) AP warming were discussed. These suggested a complex interplay is occurring between, atmospheric (e.g. ENSO/South Westerlies), oceanic (e.g. changes in CDW/ACC) and sea-ice components. A similar story is now beginning to emerge from Holocene palaeoclimatic records on the west coast of the AP. In the absence of a detailed long-term (complete Holocene) ice core record it appears that Taylor Dome and/or Byrd offer the most promising ice core record of Holocene climatic changes. On the AP itself marine sediment sequences represent the best high-resolution palaeoenvironmental archive of oceanographic changes (e.g. Palmer Deep; Domack et al., 2001) and are beginning to provide a framework with which to compare forcing factors of natural variability (e.g. Domack et al., 2003b). The most obvious forcing mechanism is changes in solar insolation as controlled by the precessional index over the last 14,000 years (Fig. 2.11) (Berger and Loutre, 1991). Orbital calculations (Berger and Loutre, 1991) show summertime insolation at high southern latitudes (65°S) has been increasing over much of the Holocene (from ca 10000 yr BP to present; Fig. 2.11). At face value this increase in insolation over the Holocene implies that events such as the MHH may have been initiated through increases in incoming solar insolation, although it cannot explain why the MHH ended at a time of peak solar insolation (Fig. 2.10 and 2.11). In addition, according to Domack et al. (2003a,b) the insolation curve is at odds with the records from the Palmer Deep, which indicates progressive cooling, and reduced sediment accumulation over the last 5,000 years (Fig. 2.11). They suggest that another forcing mechanism is responsible for the millennial-scale change observed in this record

(Domack et al., 2003a,b). One alternative mechanism may be related to changes in ocean circulation (Domack and Mayewski, 1999). The early Holocene optimum recorded in all Antarctic ice cores occurs at the same time as Northern Hemisphere summer insolation maxima (e.g. 11000 yr BP). At the end of the Northern Hemisphere deglaciation, a reduced northern Atlantic thermohaline circulation could contribute to warm conditions in high southern latitudes (Blunier et al., 1997). The end of northern deglaciation was marked by the *switching-on* of North Atlantic circulation, thereby removing the heat from high southern latitudes and ending the early Holocene optimum in Antarctica. This *bipolar seesaw* argues for asynchronous interhemsipheric climate response between Northern and Southern Hemispheres (Broecker, 1998). Several other studies have pursued the link between changing ocean circulation and AP climate change. On millennial time-scales Domack et al. (2003a,b) have suggested a link between climate change on the AP and the South Pacific Gyre through a connection between the Antarctic Circumpolar Current (ACC) and the Peru-Chile Current (PCC) (Fig.2.9). The PCC and ACC occur along the eastern limb of the gyre and therefore reflect changes in its strength of circulation and advection of warmer sub-tropical water (Domack et al., 2003a,b). Concurrent changes in the Palmer Deep record and changes in Central and South America have been linked with this connection (Haug et al., 2001).

Other researchers have suggested a complicated link between the El-Nino Southern Oscillation (ENSO) and climate change on the AP. Past ENSO variability has been inferred from mollusc analysis at archeological sites located on the north and central coast of Peru (Sandweiss et al., 2001) and from palaeolimnological studies in the Galapagos Islands (Steinitz- Kannan et al., 1998). In southwestern Ecuador, the frequency of clastic laminae in a lake record was interpreted as linked to changes in ENSO (Rodbell et al., 1999; Moy et al., 2002). According to this data, El Nino was suppressed prior to 7000 yrs BP, and ENSO variability increased during the Middle and Late Holocene and peaked at 1200 yrs BP. Numerical experiments using a coupled ocean/atmosphere model have shown that seasonal insolation due to changes in the Earth's orbital parameters might explain the suppression of El Nino before 7000 yrs BP and the increasing ENSO variability after that date (Clement et al., 1999, 2000).

On the AP, Shevenell and Kennett (2002) and Ishman and Sperling (2002) have demonstrated strong links between late Holocene oceanographic perturbations in the Palmer Deep record and ENSO, implying that late Holocene oceanic changes (ca. 3600 yr BP to present) on the AP are predominantly driven by atmospheric processes. Interestingly this *teleconnection* is thought to involve Upper Circumpolar Deep Water (UCDW), which has also been implicated in recent climatic change on the AP (Vaughan et al., 2001). Between ca. 9000 and 3700 ka BP the Palmer Deep record is devoid of foraminifera, which Shevenell and Kennett (2002) attribute to the presence of (corrosive) UCDW. They argue that sustained UCDW presence resulted in warmer regional atmospheric temperatures, decreased sea-ice cover and increased primary productivity. They go on to suggest that the presence of UCDW was directly related to decreased westerly wind strength related to ENSO variability. Intervals of increased UCDW in the Palmer Deep appear to correlate with less intense westerly winds, inferred from the sea-salt record of the Siple Dome Ice Core (Kreutz et al., 1997). There is also evidence from the Southern Ocean (Pacific sector) for decreased meridional wind strength (or ENSO) and decreased West Antarctic sea ice during this time period (Stager and Mayewski, 1997). After 3700 yr BP the Palmer Deep sequence exhibits a significant shift in sedimentary character, which is coincident with a southward shift in the Intertropical Convergence Zone (ITCZ) (e.g. Baker et al., 2000; Haug et al., 2001) and an increase in ENSO strength and low-latitude climate variability (Sandweiss et al., 1996; Rodbell et al., 1999). In the Palmer Deep record, Shevenell and Kennett (2003) suggest that this may have resulted in a general increase in the presence of shelf water (replacing UCDW) and westerly wind strength between ca. 3600 and 50 yrs BP resulting in a general cooling. They suggest that predominantly offshore winds could push the southern boundary of the ACC off the western AP continental shelf, thereby depressing the volume of UCDW in Palmer Deep (e.g. Hoffman et al., 1996; Smith et al., 1999). Shevenell and Kennett (2003) also argue that the changes observed in the Palmer Deep record occur too rapidly to reflect teleconnections to the Northern Hemisphere oceanographic system.

Surprisingly, Ishman and Sperling (2002) arrived at a different conclusion for the early Holocene when they analysed the overall foraminiferal composition of the same PD cores. They suggest that between ca 9000 to 3700 yr BP, UCDW was

absent (rather than enhanced) in the PD site and saline shelf water dominated. They do however agree with Shevenell and Kennett (2003) for the late Holocene period (ca. 3700 to 50 yr BP), suggesting a strong teleconnection between the AP and the El Nino-Southern Oscillation. There is a further problem associated with the PD record, in that it appears to record a much longer Holocene oceanic warm signal compared to other AP proxy records (Fig. 2.10 and 2.11). This may, as some have suggested (e.g. Ingólfsson et al., 2003), simply reflect the paucity of terrestrial and ice core records extending beyond 6000-5000 yr BP. Alternatively it could simply reflect the fact that the PD site is recording mainly oceanographic changes, whilst terrestrial (lake, moss bank, ice cores) provide more direct evidence for atmospheric temperature changes. This could imply that the terrestrial and marine records are decoupled, at least for the period prior to the MHH consensus between 4500-2500 yr BP.

In summary, Holocene climate change on the AP appears to reflect the interplay between atmospheric, oceanic and probably solar forcing. The relative importance of each of these variables is still unclear but there appears to be a strong link between atmospheric reorganisations in the tropical Pacific and oceanographic changes around the AP.

2.4. Summary

Temperature records show that the AP has warmed at a rate of 3.7 ± 1.6°C over the last century, a value far greater than the global mean. Several mechanisms have been proposed to explain the recent atmospheric warming including; changed ocean circulation, changed atmospheric circulation and regional sea-ice-atmosphere feedbacks. It has proved difficult to separate these variables and the most likely forcing scenario involves an interplay between several of them. The most publicised aspect of recent warming and central to this thesis has been the collapse of several ice shelves on the AP (e.g. Fox and Vaughan, 2001 and references therein). This has refocused attention on the role of ice shelves in controlling the stability of the West Antarctic Ice Sheet (WAIS) (e.g. de Angelis and Skvarca, 2003; Scambos et al., 2004; Rignot et al., 2004). The link between increased AP temperatures and ice shelf retreat is now firmly established, although more recent studies have suggested

that changes in ocean circulation may play an important role in ice shelf stability (Shepherd et al., 2003). At present it is still largely unknown whether such changes have occurred in the past in response to natural climatic forcing, thereby making it difficult to judge the significance of the rapid warming and ice shelf collapse.

Whilst there is no Holocene ice core record from the Antarctic Peninsula, high-resolution marine (Palmer Deep, Lallemand Fiord) and terrestrial (e.g. Signy Island, James Ross and South Shetland Island) records show that the climate of the AP has varied throughout the Holocene (Fig. 2.10 and 2.11) (Björck et al., 1991; 1996; Shevenell et al., 1996; Jones et al., 2000; Domack et al., 2001). These studies have also suggested that the climate of the Holocene was forced by the complex interplay between atmospheric (e.g. ENSO/Southern Westerlies) and oceanic changes (e.g. CDW/ACC). Notably, ice core records suggest a period of Early Holocene warmth between 11500 and 9000 yr BP (Masson et al., 2000; Masson-Delmotte et al., 2004). The end of this warmth also coincides with the appearance of UCDW on the western continental shelf of the AP and warmer conditions at Palmer Deep (Leventer et al., 2002). A secondary warm interval, widely referred to as the Mid Holocene climatic Hypsithermal or optimum appears to have occurred sometime between 4000 and 2000 ka cal yr BP and has been documented in numerous marine and terrestrial records (see Hodgson et al., 2004 and references therein). Significantly for this thesis, this warm interval has been implicated in the collapse of the Prince Gustav Ice Shelf on the northern tip of the AP and the Larsen-A ice shelf. Although the evidence so far has been restricted to two studies, and these studies have been of recently collapsed ice shelves, this implies that the disappearance of ice shelves on the AP is not unique and advance and retreat of AP ice shelves may have occurred in response to periods of natural climatic forcing.

Chapter 3

GEORGE VI ICE SHELF - PAST HISTORY, PRESENT BEHAVIOUR AND POTENTIAL FUTURE COLLAPSE

3.1. Introduction

George VI Ice Shelf (GVI-IS) is the largest ice shelf on the west coast of the AP, covering a total area of 25,000 km² (Fig. 3.1). The northern margin of GVI-IS marks the southernmost occurrence of recent ice-shelf retreat and according to Vaughan and Doake (1996) is nearing its thermal limit of stability (Fig. 3.1 and Chapter 2). It has shown persistent but minor retreat over the last 20 years and perhaps since 1936 (Lucchitta and Rosanova 1998). If Vaughan and Doake's (1996) prediction is accurate and we are witnessing the first stages of collapse then it is critical that we examine the ice shelf carefully in its pre-collapse phase and re-evaluate what is already known from existing studies of this ice shelf. Such information is essential if we are to gain any insight into mechanisms for ice shelf collapse and to judge the significance of recent ice shelf changes.

The aim of this chapter is threefold. First, to review what is known about the evolution and dynamics of George VI Ice Shelf (GVI-IS). Second, to review what is known about the late Quaternary history of the ice shelf, and whether this can provide information as to its current state and likely behaviour in the future. Thirdly, to discuss mechanisms that could contribute to the collapse of GVI-IS both in the past and the future.

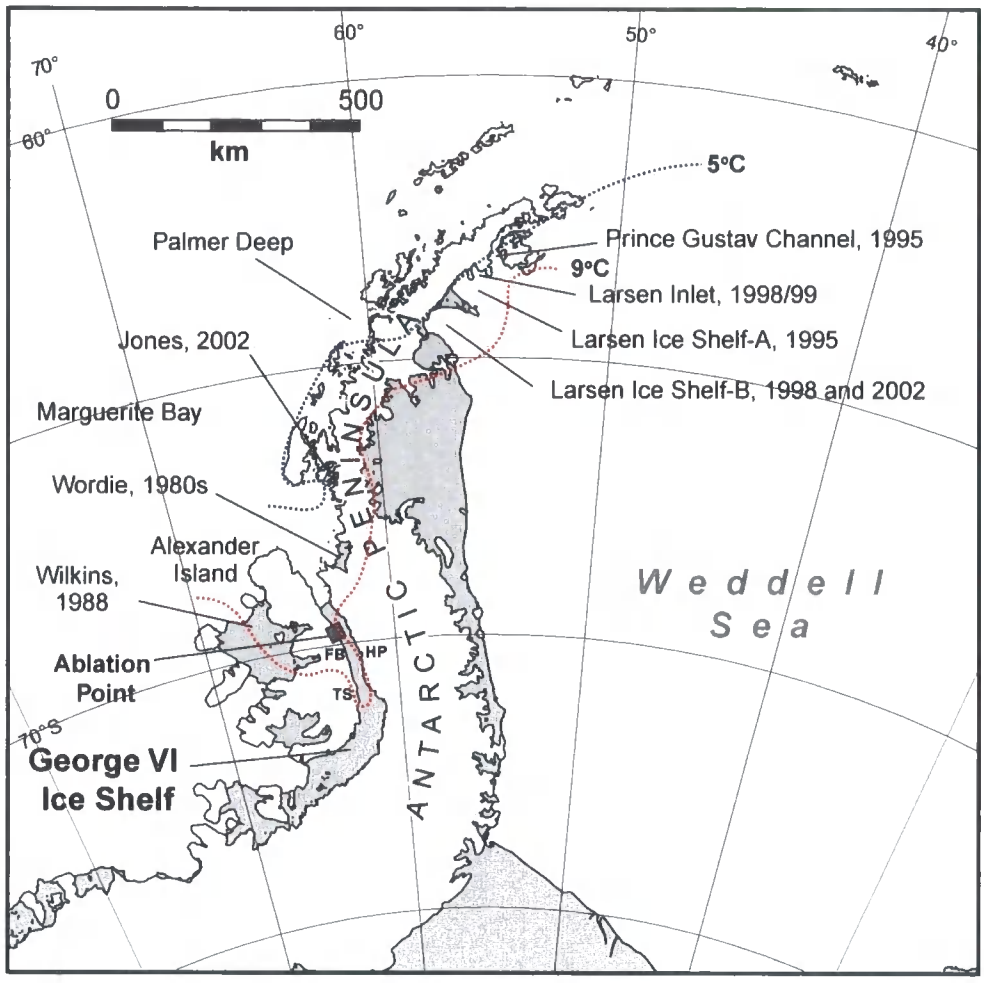

Figure 3.1. Map of the Antarctic Peninsula showing the location of George VI Ice Shelf, the largest ice shelf on the west side of the AP. Ice shelves that have collapsed in the late 20th century (labelled with dates of collapse) lie within a key -5 °C (blue line) to -9 °C (red line) isotherm boundary (taken from Morris and Vaughan 2003). This boundary now covers a large portion of George VI Ice Shelf. Also shown are the locations of Fossil Bluff (FB), Hobbs Pool (HP) and Two Step Cliffs (TS) referred to in the text.

3.2 George VI Ice Shelf – Evolution and dynamics

The first section provides a brief introduction to the geological evolution of George VI Sound its topography and geology, before the glaciology and surface characteristics of the ice shelf are reviewed.

3.2.1. Geological Evolution of George VI Sound

George VI Ice Shelf occupies George VI Sound, a curvilinear channel along the west coast of the AP, separating Alexander Island from Palmer Land (Fig. 3.1). It is 500 km in length with a width of 25 km in the north widening to over 70 km in the south (Maslanyj, 1988). It is the site of a major divide between the Mesozoic fore-arc sediments of Alexander Island and the Lower Cretaceous magmatic arc-related rocks of the Antarctic Peninsula (Crabtree et al., 1985; Maslanyj, 1987).

Since it was first observed from the air by Ellsworth in 1935 (Joerg, 1937) and later travelled over by the British Graham Land Expedition (1934-37) (Rymill, 1938), the origin of George VI Sound has been the source of much debate. It has been variously interpreted as a tectonic valley (Fleming et al., 1938) and/or a structurally controlled glacial or fluvial valley (Nichols, 1953). Many now consider George VI Sound to represent part of a downfaulted rift system along the west side of the Antarctic Peninsula that was probably the result of Tertiary intra-arc extension within the Mesozoic and Cenozoic magmatic arc of the Antarctic Peninsula (Crabtree et al., 1985; Storey and Garrett, 1985; Maslanyj, 1987, 1988). Direct evidence for the age of channel 'opening' however, is still limited. Field evidence indicates that the youngest rocks to have been displaced are Albian age (113-97 Ma) (BAS Geological Map, 1982) but according to Maslanyi (1988) its youthful topography suggests it probably formed since 50 Ma ago along an older more extensive tectonic boundary (Crabtree et al., 1985). This period of time is also correlated with the cessation of magmatism along the Peninsula (Barker, 1982).

3.2.1.1. Geology of George VI Sound

George VI Sound separates two distinct geological terranes (Crabtree et al., 1985). Palmer Land is mainly formed of calc-alkaline volcanic and plutonic rocks that constitute the Mesozoic magmatic arc of the Antarctic Peninsula (Crabtree et al., 1985). In contrast the part of Alexander Island, which borders the sound is made up of thick marine volcaniclastic sedimentary rocks (Fossil Bluff Formation; Taylor et al., 1979), which were derived from the sub-aerial volcanic arc of Palmer Land. The Fossil Bluff Formation, consisting mainly of shale, arkosic sandstone, conglomerate and volcaniclastic and terrestrial (deltaic) material was deposited in a downfaulted marine fore-arc basin during the late Jurassic to early Cretaceous (Suárez, 1976; Bell, 1973). Thus George VI Sound is situated on a remarkable geologic boundary separating sedimentary rocks on the west from crystalline rocks on the east.

3.2.1.2. Sub-glacial topography

The topography of George VI Sound is characterised by deep, steep sided trench slopes and an irregular surface morphology, with bedrock depths ranging from 400 to 1000m (Fig. 3. 2) (Bishop and Walton, 1981; Maslanyj, 1988). Primarily a structural feature, the topography of the channel has subsequently been modified by glacial activity. The most comprehensive study of the topography of the sound has been provided by Maslanyj (1987). The profiles show that the bathymetry of George VI Sound changes along its length (Fig. 3 2). In the north, two lateral troughs up to 800m deep are separated by a central ridge (Fig. 3.2 profile C-D) (Crabtree et al., 1985). This W-shaped cross section is not apparent along the entire length of the sound. Where it is observed, there is a marked asymmetry, being narrower on the western side and deeper and more open on the east (Maslanyj, 1987). It has been suggested that the two lateral troughs were eroded, or at least modified by ice during the last glacial maximum when grounded ice existed in the sound. The deeper eastern trough probably reflected greater ice discharge from the Peninsula (Crabtree et al., 1985). In the central section, the bedrock topography suggests a change in structural trend (Maslanyj, 1987). The profiles indicate the presence of a prominent NE-SW trough, which becomes E-W towards the Ronne

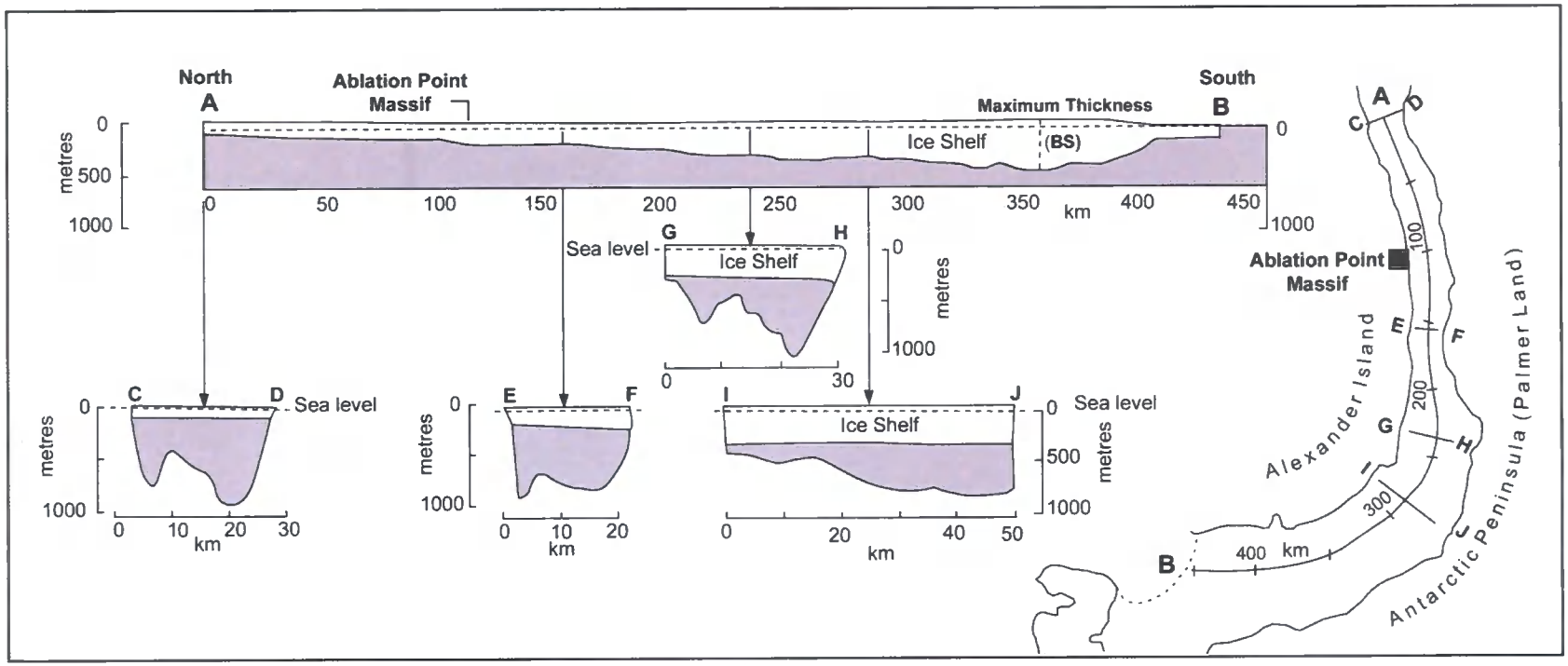

Figure 3.2. Ice-shelf thickness (A-B) along George VI Sound and known bedrock topography. Bedrock soundings along the line C-D were obtained by plumb lines (Potter et al., 1985), along line G-H by seismic shooting (Crabtree et al., 1985) and also along lines E-F and I-K by seismic shooting (Maslanyj, 1987). Grey is marine water and dashed line represents sea-level. Also shown is the location of the inverted basal sill in the ice shelf (BS) referred to in Potter and Paren (1985), which marks the zone of maximum ice shelf thickness, and the location of the Ablation Point Massif (black box) referred to in the text.

Entrance. In the south, hydrographic soundings show a deep channel extends out into the Ronne Entrance, indicating a seaward extension of the trough shown in profile I-J in Figure 3.2. Similarly, in the north a deep-water channel extends for at least 200 km north of George VI Ice Shelf into Marguerite Bay (Maslanyj, 1987; Ó Cofaigh, unpublished data).

3.2.2.Character and Dynamics of George VI Ice Shelf

The thickness of GVI-IS varies from 100m near the northern ice front to a maximum of 600m in the south at 72°50'S, 67°50'W (Fig. 3.2). The thickest region of the ice shelf occurs on a line between the coast of Alexander Island (Fig. 3.2) (72°38'S, 70°10'W) and the AP coastline (73°06'S, 69°10'W) (Potter and Paren, 1985). The ice shelf then thins from this point (Fig. 3.2) towards both ice fronts (Potter and Paren, 1985) making the thickest point appear like an inverted sill in profile (Fig. 3.2). The Ronne Entrance is normally ice free during the summer but the southern margin abuts fast ice. The northern ice front has one small polynya on its western margin during the summer but is otherwise icebound (Potter and Paren, 1985).

The ice shelf receives most of its ice from the AP (46 km^3 a^{-1}) although glacier ice from Alexander Island (12 km^3 a^{-1}) is also significant (Reynolds and Hambrey, 1988). Flow lines constructed for the ice shelf based on the distribution and orientation of surface meltpools shows the majority of ice discharge is towards the northern and southern ends where seasonal calving occurs (Pearson and Rose, 1980; Reynolds and Hambrey, 1988). The ice shelf decelerates as it flows westwards across the sound from c. 400 m a^{-1} near the grounding line to c. 30 m a^{-1} near Alexander Island (Bishop and Walton, 1981; Reynolds and Hambrey, 1988). In some places the ice shelf flows across the sound with a westerly component (Reynolds and Hambrey, 1988), impinging against Alexander Island resulting in a zone of pressure ridges. Where the ice shelf grounds an impressive ice-shelf moraine has been created (Sugden and Clapperton, 1981). At two places near the Ablation Point (Fig. 2.1b) area the grounded ice shelf blocks the mouth of two valleys where it impounds tidal lakes (Heywood, 1977). The environmental setting of these two epishelf lakes is described in more detail later.

In a study of the mass balance of the entire ice shelf it was suggested that GVI-IS is in near-balance, with accumulation matching ablation (Potter et al., 1984, 1988). Ablation occurs in summer at low-lying margins of the ice shelf and throughout the year at the bottom of the ice shelf (Potter and Paren, 1985). The major component of mass wastage is through basal melting, with the balance being maintained by the input of glacier ice from the AP and Alexander Island. To balance accumulation over the catchment with ice losses the calculated equilibrium basal melt rate is 2 ± 0.1 m a^{-1} (Lennon et al., 1982; Potter et al., 1984) but theoretically it could be as high as 10 m a^{-1} at the ice front (Lennon et al., 1982). The calculated basal melt rate agrees well with recent direct measurements using phase sensitive radar, which have yielded a basal melt rate of 2.78 ± 0.08 m yr^{-1} (Corr et al., 2002). By applying the smaller equilibrium basal melt of 2 ± 0.1 m yr^{-1} to the whole ice shelf this equates to 53 km^3a^{-1} total melt at the base of GVI-IS (Potter et al., 1984). To put this in context, although GVI-IS only represents 1.5 % of the total area of all ice shelves in Antarctica, it will, if in equilibrium, supply 10% of the total melt for Antarctica (Potter et al., 1984; Jacobs et al., 1992). If the basal melt value of Corr et al. (2002) is applicable over the whole area then this value will be significantly higher. It is thought that such a high basal melt rate is a direct consequence of intrusions of warm Upper Circumpolar Deep Water (UCDW) from the southeast Pacific Basin which emerges onto the Pacific continental shelf of the AP and extends beneath George VI Ice Shelf (Lennon et al., 1982; Potter and Paren, 1985). Multi-year fast ice occupies the northern entrance of GVI-IS and acts to dampen tidal swell and protect the ice margin. As a result, the ice front advances for several years before breaking back episodically (Potter and Paren, 1985). Calving occurs along natural rifts and fissures, which penetrate the entire depth of the ice shelf along its northern front (Potter and Paren, 1985).

The thermal properties of GVI-IS also change along its length. Based on 10 m depth profiles, Bishop and Walton (1981) noted that the temperature of the ice shelf warms from around -10°C in the central melt-lake area of the ice shelf (~ 70°45' to 71°45'S) to around -2°C near the northern ice front (~70°00'S). Paren and Cooper (1988) investigated this further using thermistor chains installed at three sites

between 70°00' and 70°30'S. Their observations were consistent with those of Bishop and Walton (1981) and show that as ice flows towards the northern ice front it becomes more temperate. Paren and Cooper (1988) suggested that heat from sea water and from the percolation of melt water at the upper surface, both of which release latent heat on re-freezing, progressively warms the ice shelf. Recorded temperatures at mid depth (the coldest level in the ice shelf) were – 6°C at 70°30'S, -4°C at 70°15'S and –1.6°C to –1.8°C at 70°00'S depending on the time of year. These data show that the temperatures near the ice front are warmer than the freezing point of fully saline seawater (Paren and Cooper, 1988).

3.2.3. Surface Features

3.2.3.1. Surface Meltpools

During the austral summer GVI-IS undergoes extensive surface melting (Fig. 3.3 and 3.4). This is most apparent in the central area of the ice shelf from lat. 70°15' to 72°00'S where surface meltwater lakes form (Fig. 3.4) (Reynolds, 1981a; Reynolds and Hambrey, 1988). Surface ponding has been observed on GVI-IS since the early 1940's and begins to appear in December. Between 1989 and 2000 ponding was observed every year except 1994, most frequently and earliest in the region between Fossil Bluff and Ablation Point (Scambos et al., 2000). The distribution of meltpools is still something of an enigma but they appear to occur where; (1) mean annual temperature lies between –6 °C and –10 °C; and (2) the surface net balance is almost zero (Reynolds, 1981a). In addition the compression of the ice shelf from Palmer Land glaciers is thought to inhibit the formation of crevasses, which could otherwise drain the surface meltwater (Reynolds, 1981). Instead, melt water percolates through the upper firn and accumulates on an impermeable ice layer formed by the freezing of the previous summers melt (Pedley et al., 1988). With continued ablation the water levels rise to form freshwater pools, except where they are allowed to drain in areas where the ice shelf is much thinner. Two dominant spatial patterns of meltpools have been identified (Reynolds, 1981a). The primary trend is for large elongate lakes that appear to reflect flow lines within the ice shelf (Fig. 3.3 and 3.4) (Reynolds and Hambrey, 1988). These are intersected by a secondary set of meltpools, which are thought to be wind-induced since they are

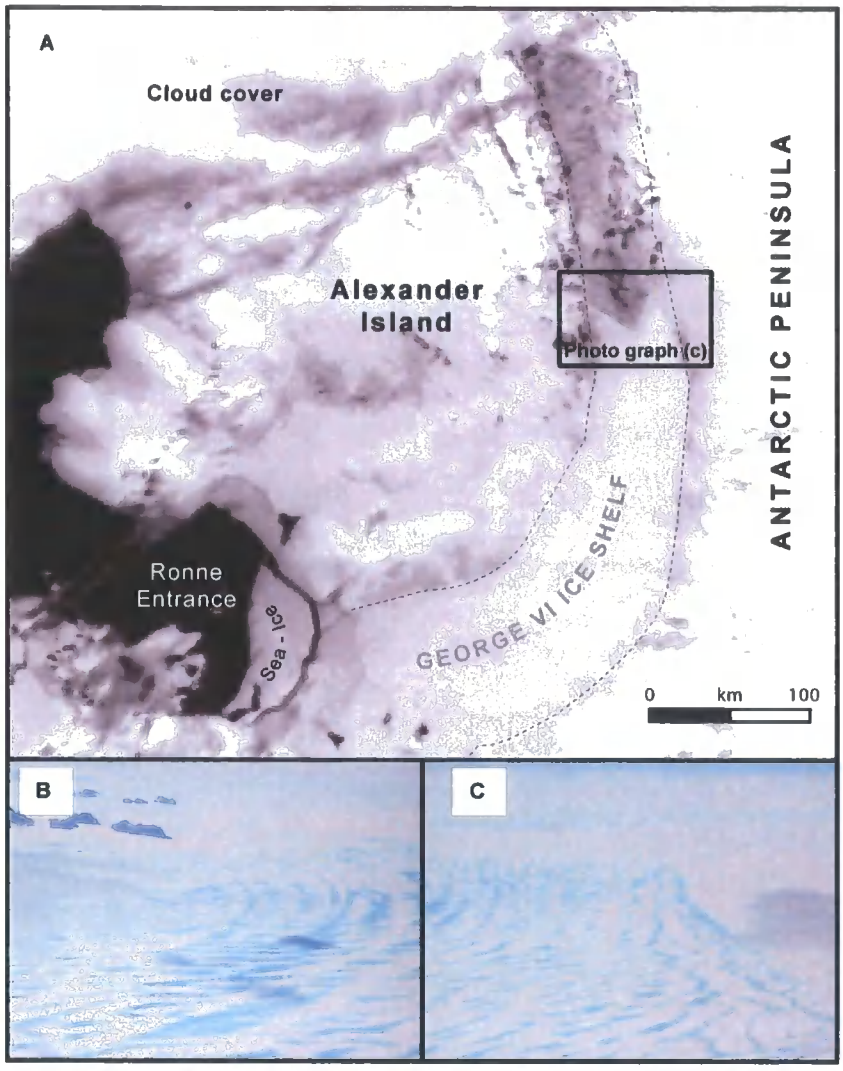

Figure 3.3. Meltpools on George VI Ice Shelf. The distribution of meltpools is restricted to between 70°15' to 72°00'S (area shown in Fig. 3.1 and 3.4.). (a) Radarsat image of GVI-IS and Alexander Island taken on 6/1/2003 (British Antarctic Survey) showing a prominent southern boundary to the area of surface melt. It is worth noting that this is not a processing artefact or image boundary and ground-truthed by low level reconaissance (see below); (b) Oblique aerial photography from an aircraft taken on 6/1/2003 (photo: Adrian Fox) showing the dominant flow patterns (curved bottom to top) and wind induced meltpools (left to right); (c) showing the southern-most limit of the meltpools which forms an abrupt apex (inset in (a)) (photo: Adrian Fox). The horizontal distance in the foreground of photos (a) and (b) is ~ 2-3 km.

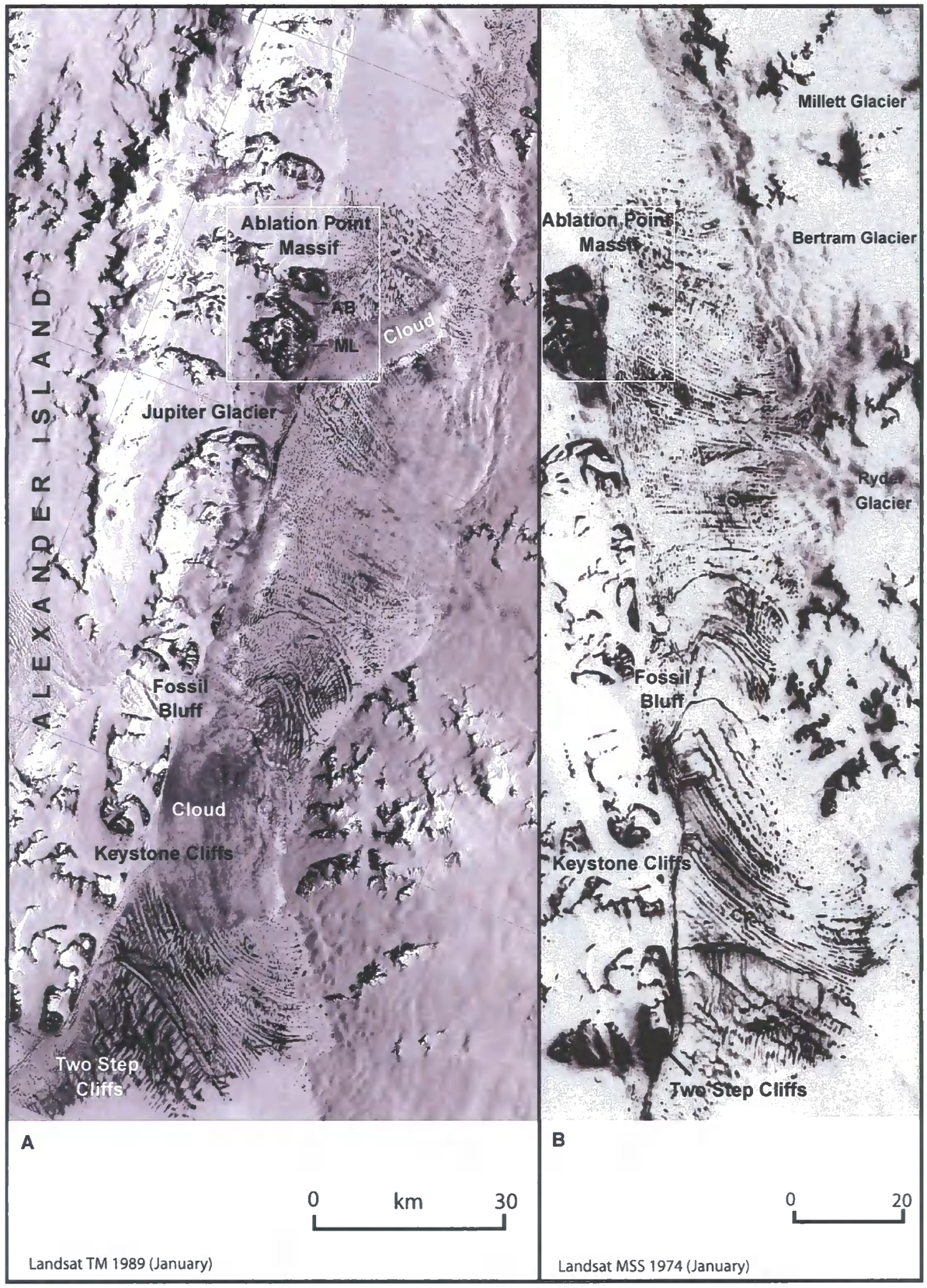

Figure 3.4. Landsat multispectral scanner composite image of central George VI Ice Shelf between Ablation Point in the north and Two Step Cliffs in the South taken in January 1989 (supplied by Peter Fretwell, British Antarctic Survey) (a) and (b) January 1977 (from Reynolds and Hambrey, 1988). The black features on the ice shelf are surface melt-lakes. The geographic distribution of meltpools is almost identical in both images. The location of Ablation (AB) and Moutonnee Lakes (ML in the Ablation Point Massif is also shown.

parallel to the prevailing northerly wind direction (Fig. 3.3 and 3.4) (Reynolds, 1981a). The geographical distribution of meltpools is shown in Figure 3.4, which compares Landsat images taken in 1973 (9th Jan) and 1989 (early-mid Jan). It is difficult to assess quantitatively the relative distribution and volume of meltwater on the surface of the ice shelf but visually the surface pattern of meltpools is remarkably similar between the two images. The overall geographic distribution of meltpools also seems largely unchanged. This suggests that the ice shelf flow regime of GVI-IS has not changed significantly over the last 16 years.

3.2.3.2. Hobbs Pool

Hobbs Pool is adjacent to the coastal mountains of Palmer Land and lies 180 km to the south of the northern ice front (Fig. 3.1) (Pedley et al., 1988). The flow pattern of the glaciers entering the ice shelf in the vicinity of Hobbs Pool has resulted in an area of thin ice between the coastline and the main body of the ice shelf. Unlike other areas of the ice shelf, which are under compression, Hobbs Pool provides a localised drainage route for the surrounding surface melt water. This results in a 155 m thick layer of low-salinity water that is close to freezing point. Colder and more saline water in the lower part of this layer leads to *in-situ* freshwater which lies above it. Significantly, this area of localised basal freezing is thought to play an important role in entraining sediment at the base of GVI-IS and provides a mechanism by which material is transferred from Palmer Land to Alexander Island (Pedley et al., 1988).

3.2.3.3. Epishelf Lakes

At Ablation Point, on the east coast of Alexander Island, the ice shelf impounds two epishelf lakes: Moutonnée and Ablation Lake (Fig. 3.5) (Heywood, 1977). These lakes are tidal, stratified water bodies with a lower marine layer that extends beneath the ice shelf and an upper freshwater layer which is derived from annual melt water and whose maximum thickness is defined by the ice shelf draught. The two lakes offer a unique opportunity to study the history of George VI Ice Shelf since any change in the position of George VI Ice Shelf is likely to leave a detailed signature in the lake sediments. This thesis will use the sedimentary record taken

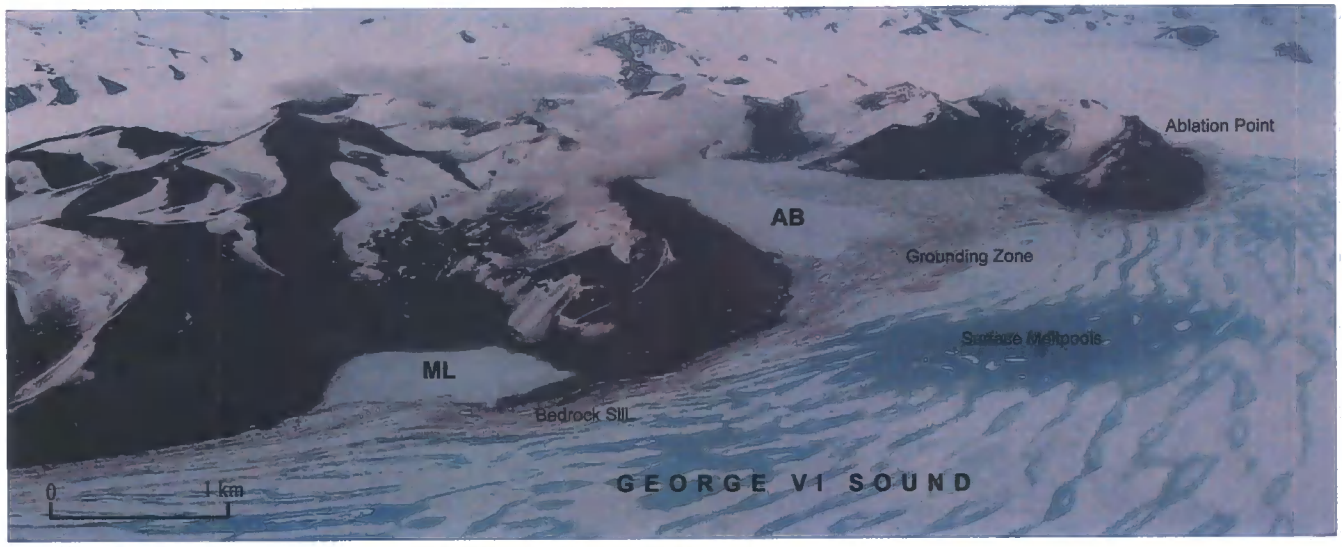

Figure 3.5. Epishelf lakes in the Ablation Point Massif, Alexander Island (location shown in Fig. 3.4). Oblique aerial photograph taken on 6/1/2003 (photo: A. Fox) of Moutonnée Lake (ML) (left) and Ablation Lake (AB) (right). Photograph shows how the ice shelf is prevented from entering Moutonnee Valley by a bedrock sill. In Ablation Valley the ice shelf is grounded along a submerged bedrock bar (Heywood, 1977) and is expressed at the surface as a zone of disturbance. Extensive melting on the surface of GVI-IS is also apparent (e.g. Fig 3.3. and 3.4). The unique environmental setting of ML and AB has been used in this thesis to reconstruct the Holocene history of George VI Ice Shelf.

from these two lakes to reconstruct the Holocene history of GVI-IS. The environmental setting, physical limnology and palaeoclimatic significance of both lakes, plus a conceptual model of how ice shelf presence/absence will effect the lake environment will be discussed in more detail in the following chapters.

3.2.4. Sediment Transfer

Clapperton and Sugden (1982) first reported on the presence of Antarctic Peninsula erratics (granite) along east coast of Alexander Island and specifically on the shoreline of Moutonnée Lake (Fig. 3. 6). The erratics are easily distinguished from the rocks of Alexander Island, which are predominantly sedimentary. The only granitic rocks of Alexander Island are found in a conglomerate (Himalia Formation) but these are easily identified as they are more weathered with a distinctive orange-red weathering rind. This suggests that granite material from the Antarctic Peninsula is transported across George VI Sound by the ice shelf before it is deposited on Alexander Island. Initially this could not be reconciled with the very high melt rates beneath George VI Ice Shelf. However, as noted above Pedley et al. (1988) later provided evidence for localised areas of basal freezing (e.g. Hobbs Pool) where material is frozen onto the base of the ice shelf and gradually makes it way to the ice shelf surface. In addition, it is thought that glacier ice leaving Palmer Land containing embedded rock debris is first subjected to basal freezing, which forces material up into the ice followed by melting as it moves away from the coast and into George VI Sound (Bishop and Walton, 1981; Pedley et al., 1998). Material may also fall directly on the inflowing glaciers or ice shelf and is transported supra, and then, en-glacially. The result of this is that the ice shelf leaves a sedimentological signature of its presence on the west coast of Alexander Island.

3.2.5. Ocean-Ice Shelf Interaction

As noted in section 2.3.1 the dynamics of George VI Ice Shelf are intimately linked to ocean circulation, specifically the presence of Upper Circumpolar Deep Water (UCDW) (Bishop and Walton, 1981; Lennon et al., 1982; Loynes et al., 1984; Potter and Paren, 1985; Potter et al., 1988). UCDW is characterised by salinity (34.73 ‰) and temperatures (+ 2°C) maxima. This relatively warm water is thought

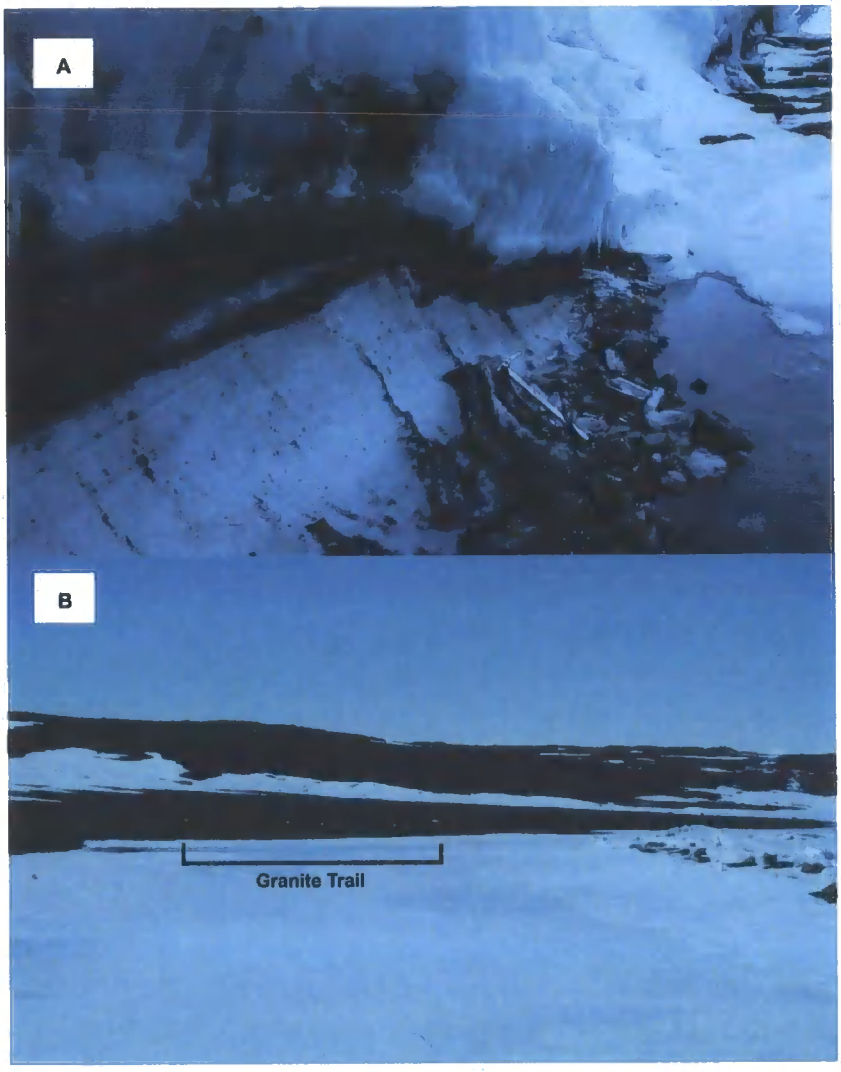

Figure 3.6. Showing (A) englacial debris at the ice shelf front, Moutonnée Lake, where granite clast up to 10 cm x 10 cm were observed (Photograph taken 11/2001); (B) Granite erratics (6 pale dots) along the shoreline of ML (Photograph taken in December 2001). The granite boulders measure up to 40 cm x 40 cm and occur ~ 0.5-1 m above the present lake level.

to drive high basal melt rates at the ice shelf base and is fundamental in controlling the mass balance of the ice shelf. The flux of UCDW only occurs on the Pacific continental shelf of West Antarctica and may be related to a combination of the contiguity and strength of the Antarctic Circumpolar Current (ACC) and the proximity of a cross shelf bathymetric low (Klinck and Smith, 1993; Hofmann and Klinck, 1998; Rebesco et al., 1998). Modeling work suggests that offshore pressure gradients, similar to those created by northeastward ACC flow along the western Antarctic Peninsula, force upslope flow of UCDW within submarine canyon systems (Klinck and Smith, 1993) (refer to Chapter 2 for a more detailed account of AP oceanography).

Oceanographic observations have shown the flux of UCDW beneath GVI-IS results in an increase in both temperature (T) and salinity (S) from the ice shelf base to the sea floor (Potter et al., 1988). Measurements show that the maximum temperature in the sound is 1.10°C, which is 3°C warmer than the freezing point at the base of the ice shelf making it the warmest water below any Antarctic ice shelf (Talbot 1988). Temperature-salinity (T-S) profiles for the northern ice shelf front depict a simple model of fresh ice melting into warm deep water (UCDW), without the influence of the cold continental shelf waters found elsewhere in Antarctica (Fig. 3.7) (Jacobs et al., 1985; Potter et al., 1988). In cross-section, Potter et al. (1988) noted very little lateral variation from the northern ice front but did note a core of unmodified UCDW in the eastern channel trough, whose temperature exceeds 1.05°C. A distinctive feature of southern ice front profiles is that water found at the greatest depth is identical to the deep water in the northern sound and in Marguerite Bay. UCDW is therefore common at both ice fronts. Similar results have also been observed under the ice shelf at Hobbs Pool (Fig. 2.1b), a site 160km from the northern ice shelf front (Potter and Paren, 1985). Together these data suggest that there is direct seawater communication beneath the entire ice shelf.

The T-S profiles for the southern ice front are more complicated (Fig. 3.7b). The waters from the surface to about 200 m exhibit linear T-S trend, confirming that the region is dominated by the melting of ice into warmer water (Potter et al., 1988). Potter et al. (1988) conclude that the waters near the southern ice front and in the

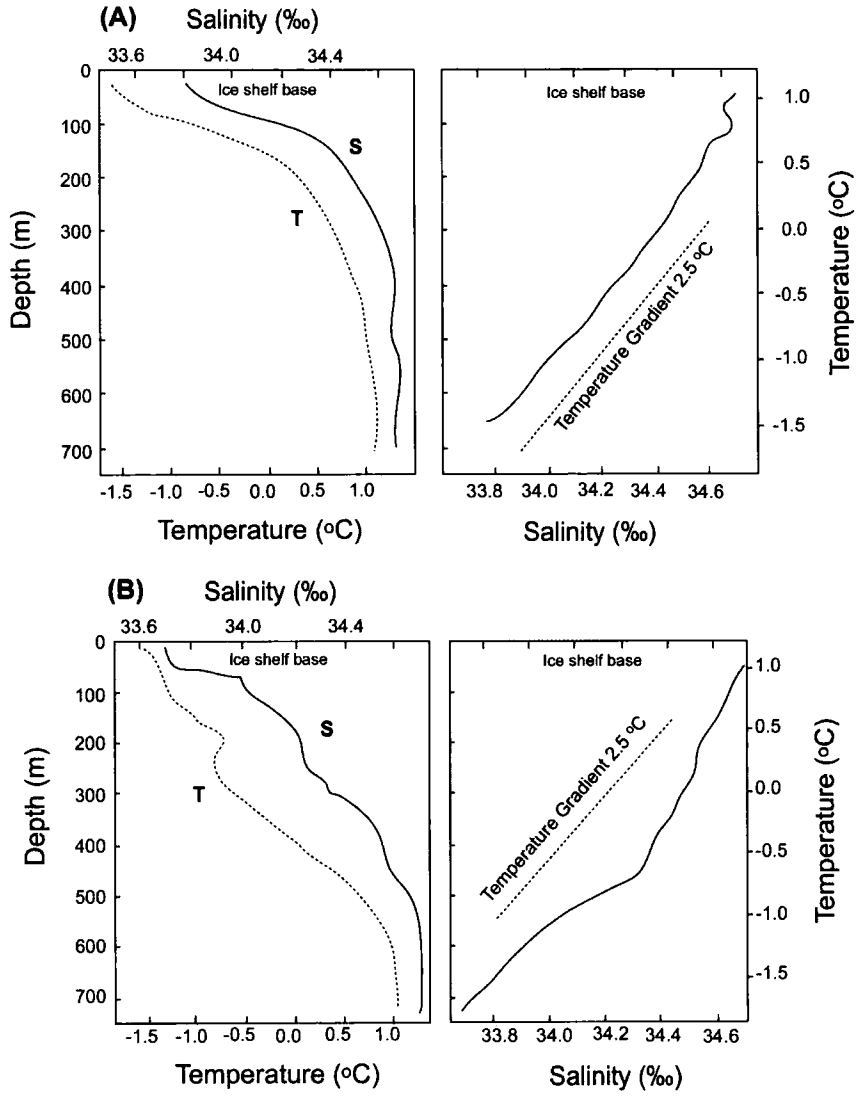

Figure 3.7. Simplified Temperature-Salinity (T-S) profiles from the (a) northern and (b) southern margins of George VI Ice Shelf (from Potter et al., 1988). Northern profiles show characteristic linear melting line of 2.5°C/°/oo. T-S plots for the southern margin show generally the same pattern but the profiles are more complicated. The T-S gradient results from the melting of ice at the base of the ice shelf, resulting in sub-zero, fresh Ice Shelf Water (ISW). This contrast with water at the base of George VI Sound which is characterised by warm, saline Upper Circumpolar Deep Water (UCDW).

Ronne Entrance have T-S curves that are characteristic of open Bellingshausen Sea, which have been subsequently modified by ice melt in the surface layer.

In the north, tidal currents and residual currents are weak and wind driven circulation is minimal. This contrasts with a zone of enhanced outflow 7 km wide and 60 m deep along the western edge of George VI Sound (Fig. 3.8), which implies thermohaline processes dominate circulation beneath the ice shelf. According to Potter and Paren (1985) the accepted circulation model involves dense saline CDW being advected from Marguerite Bay southward beneath the ice shelf where it upwells and melts the base of the ice shelf (Fig. 3.8). The (then buoyant) ice melt is deflected to the west of the channel by the Corriolis effect and advected northward. This process is maintained by melting at the base of the ice shelf, which in turn causes the upwelling of water from greater depth to replace water that has been transported northward (Fig. 3. 8) (Potter and Paren, 1985).

3.2.6. Tidal variations beneath George VI Ice Shelf

Tidal measurements have been made at three lake sites on GVI-IS (Moutonnée, Ablation and Hobbs Pool) and at both ice fronts (e.g. Pedley et al., 1986). Much of the research was carried out during the late 1970's and 1980's (e.g. Bishop and Walton, 1977; Doake, 1978; Cartwright, 1980; Potter et al., 1985; Potter and Paren, 1985; Pedley et al., 1986) and looked at, among other things, the dissipation of tidal energy by ice shelves and tidal and current spectra beneath GVI-IS. This work has revealed peculiarities in the tidal characteristics and behaviour beneath GVI-IS. Notably, there appears to be non-linearity in the tidal spectrum beneath the ice shelf, which suggests that the ice shelf plays an important role in dampening the tidal spectrum.

3.3. Late Quaternary History of GVI-IS

A comprehensive study of the late Quaternary history of George VI Sound was carried-out in the late 1970's by D.E., Sugden and C.M., Clapperton (Sugden and Clapperton, 1980; Clapperton and Sugden, 1982). This study indicated that George

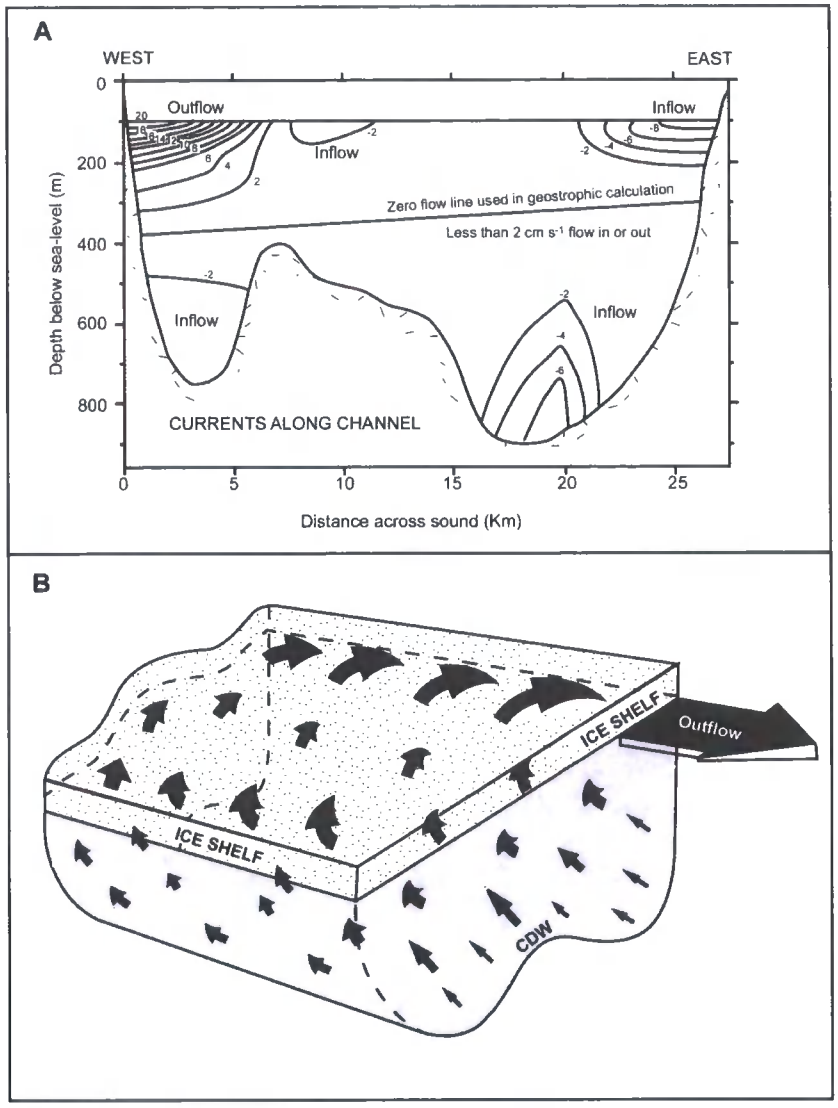

Figure 3.8. (A) Cross section of George VI Sound with calculated geostrophic velocities contoured in cm s-1, showing inflows of CDW (southward) and outflows (northward) (from Potter et al. 1988); (B) Model of CDW circulation beneath GVI-IS. CDW flows southward at depth under the ice. Sensible heat melts the base of the ice shelf causing a buoyant outflow, deflected to the west by the Coriolis effect. The outflow, together with other stirring mechanisms lifts more CDW to the base of the ice shelf, thereby completing the cycle (from Potter and Paren, 1985).

VI Ice Shelf underwent significant changes during the late Quaternary and may have disappeared on at least two previous occasions (Sugden and Clapperton, 1980; Clapperton and Sugden, 1982). The major features of this history are summarised in Figure 3.9 and Table 3.1, and referred to in the text below [numbered points]. Based on detailed geomorphological evidence Clapperton and Sugden (1982) suggested that there was significant expansion of ice during the Wisconsin [2], with an ice cap centred to the west-northwest of the Ablation Point Massif (Fig. 3.4). The ice cap was sufficiently large to override the local topography leaving evidence in the form of eroded and scoured plateau surfaces, abraded roche moutonnées and over steepened valley sides. Estimates of ice thickness, based on the altitude of erratics imply that at the head of Ablation Valley the ice sheet was >800m thick. General flow was to the north, with ice domes centred on Alexander Island and Palmer Land becoming confluent in George VI Sound (Fig. 3.10).

A till deposit in the main valley of the Ablation Point Massif indicates an ice cap of reduced size [3] discharged smaller outlet glaciers over the valley heads and into the main valley leading into George VI Sound. Good examples of this 'valley stage' advance are preserved in Ablation and Moutonnée Valleys [4]. Clapperton and Sugden (1982) suggest that this till deposit was formed during either a significant still stand during recession from the larger ice cap or a separate advance. Following deposition of the valley stage till widespread deglaciation of Alexander Island is thought to have occurred [5]. The presence of Palmer Land erratics on the crests of the valley stage till however, indicate that an ice mass still occupied George VI Sound. Erratics in the valleys of the Ablation Point massif and at Fossil Bluff (Fig. 3.4) imply that ice in George VI Sound at this time reached an altitude ca. 85 m above the present ice surface [6]. The common altitude of the erratics over a 60 km distance indicate that they were deposited at the ice shelf edge, probably whilst the land was still isostatically depressed. This high-stand appears to have been a brief event as no drift limit has been found in association with the erratic line. Isostatic uplift then followed and relative sea-level (and thus the ice shelf) fell in relation to Alexander Island. This period of uplift is represented by an impressive suite of terraces in Ablation and Moutonnée Valleys (Fig. 3. 9).

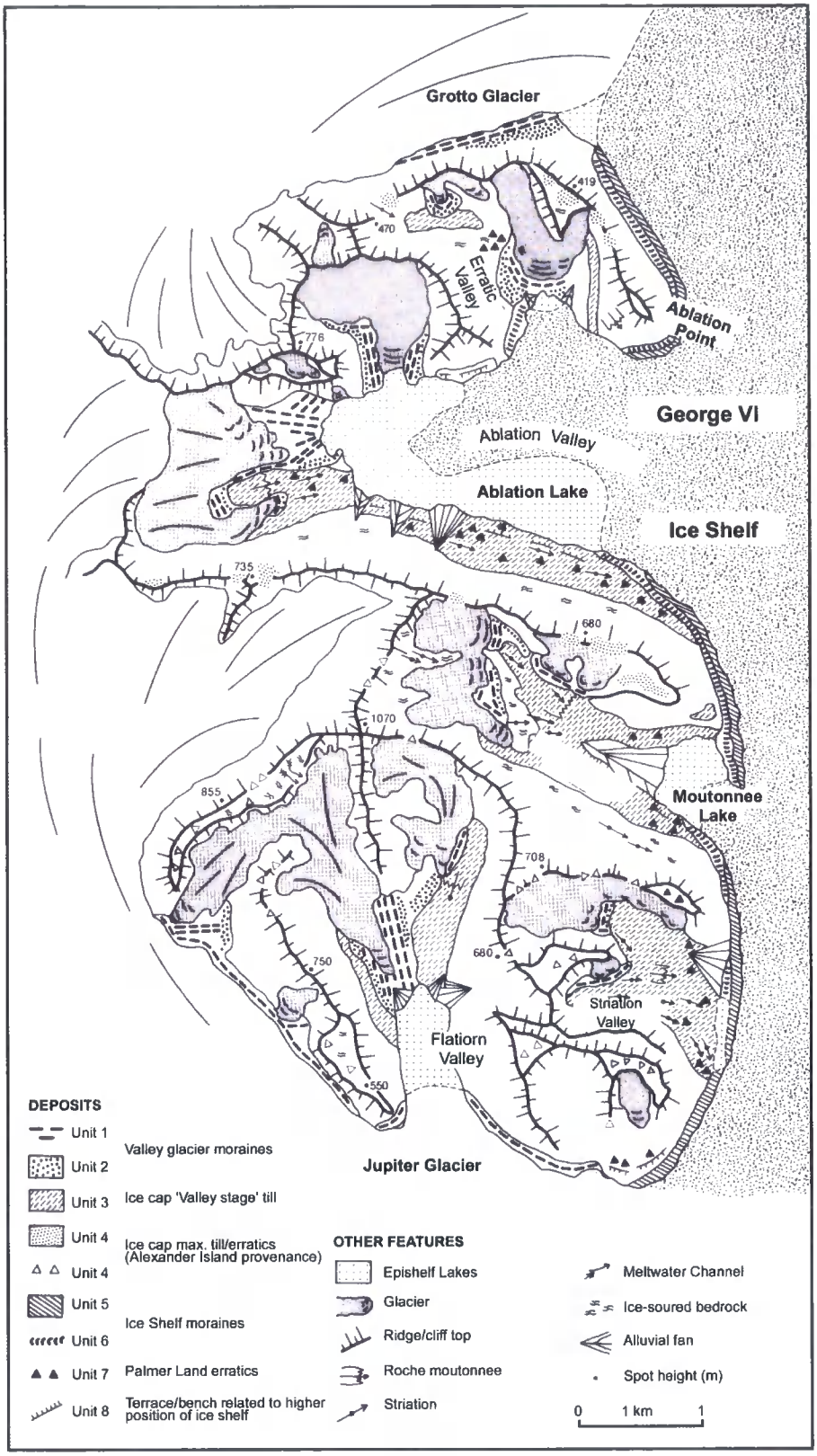

Figure 3.9. Geomorphological map of the Ablation Point Massif, Alexander Island (location shown on Figure 3.4) showing the major features of late Quaternary glaciation discussed in the text (from Clapperton and Sugden, 1982).

	EVENT	CHRONOLOGICAL CONTROL (YRS B.P.)	CHARACTERISTICS & GEOMORPHOLOGICAL EVIDENCE
1	Interglacial or Interstadial	>120,000 (Amino acid) and infinite ^{14}C age	*Hiatella solida* (Mollusc) living in open George VI Sound
2	Wisconsin Maximum	ca. 75,000 (/) or 30,000-18,000 (?)	Ice caps on Palmer Land and on Alexander Island confluent in George VI Sound; *Hiatella* shells incorporated in basal till
3	Ice-cap thinning		Land above 700m exposed; moraines and subglacial meltwater channels formed
4	Valley Stage		Retreat Stadial or Advance of Ablation Massif outlet glaciers to edge of George VI Sound; lateral moraines formed
5	Ice-cap recession		Retreat of outlet glaciers; Ablation Massif valleys and lower valley of Jupiter Glacier becomes free of 'ice-cap' ice
6	Expansion of George VI Ice Shelf		Ice shelf penetrates Ablation Massif valleys to 81m, Fossil Bluff to 85m and Two Step Cliffs to 110m. Palmer Land erratics deposited
7	Collapse of George VI Ice Shelf	*ca.* 6500 (Amino acid and ^{14}C)	*Bathylasma corolliforme* (Barnacles) living in open George VI Sound implying open marine conditions
8	First readvance of Alexander Island valley glaciers		Two terminal moraines deposited at some glaciers
9	George VI Ice Shelf reforms, and advances beyond present limits		Ice-shelf moraine deposited on Alexander Island, incorporating Barnacles; truncates valley-glacier moraines
10	Second readvance of Alexander Island glaciers		Deposition of terminal moraines on top of ice shelf moraine
11	Retreat then readvance, then recession of Alexander Island glaciers and George VI Ice Shelf to present positions		At least 1-3 ice-cored moraines close to valley Glaciers and ice shelf

Table 3.1. Glacial history of George VI Sound Area, West Antarctica (from Clapperton and Sugden, 1982). Numbers are referred to in the text.

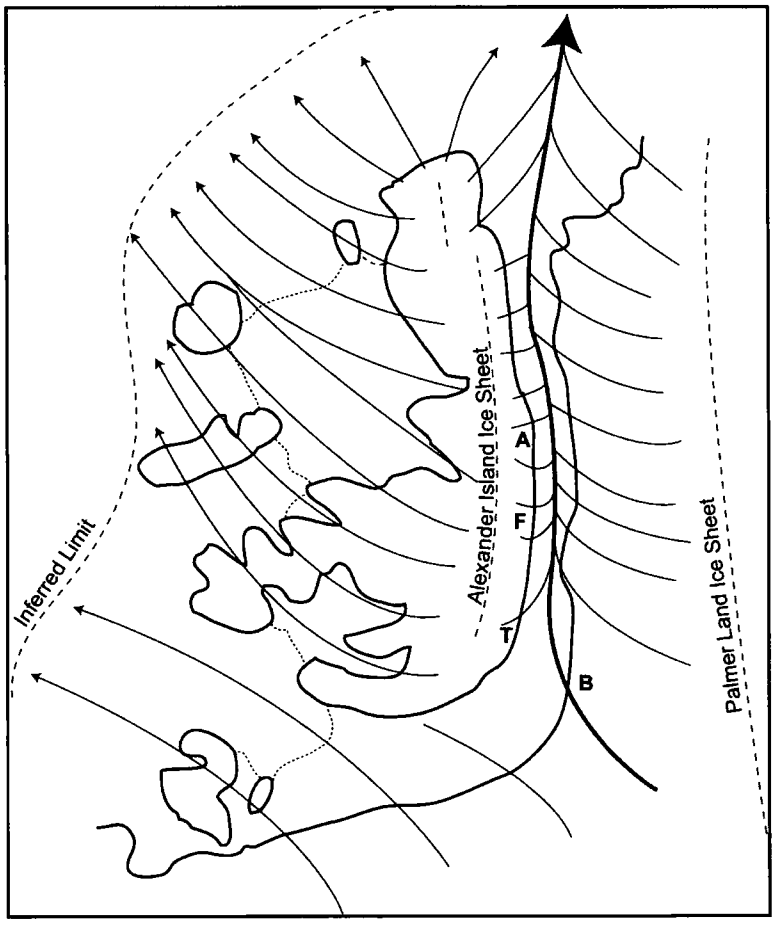

Figure 3.10. Reconstruction of the ice sheet flow lines for George VI Sound during the Last Glacial Maximum (LGM). (A) Ablation Point, (F) Fossil Bluff, (T) Two Step Cliffs, (B) Batterbee Mountains. The main features of the LGM reconstruction are the strong northward flow of grounded ice along George VI Sound, and a broadly west-northwest flow over southwestern Alexander Island (from Clapperton and Sugden, 1982).

At some point during the Holocene, the ice shelf is thought to have collapsed, allowing an open marine fauna (various Mollusca) to exist in George VI Sound [7]. Evidence for this period of instability will be discussed in greater detail below. Before the ice shelf reformed, local valley glaciers on Alexander Island advanced, leaving prominent terminal moraine deposits [8]. As the ice shelf re-formed and expanded it deposited a prominent ice shelf moraine, 500 m further onshore from the present ice shelf edge [9] (Fig. 3.9). This has subsequently been overridden in some places (e.g. Erratic Valley; Fig. 3.9) by local valley glaciers [10]. Following these small oscillations, the ice shelf and valley glaciers have retreated to their present positions [11].

3.3.1. Late Quaternary event chronology

Chronological control on the late Quaternary history outlined above is limited to the discovery of two shell bearing diamicts, one relating to the initial expansion of over-riding ice, sometime during the Wisconsin, and the second relating to a possible Holocene ice shelf collapse. Indication of the timing of last maximum glaciation was obtained from a shelly till 94 to 114 m above the present ice shelf at Two Step Cliffs. Fragments and whole valves of *Hiatella solida* (an infaunal mollusc) yielded finite radiocarbon ages of ca. 32000 yrs BP. In contrast, amino acid ratios suggest a considerably greater age for the shells of ca. 120000 yrs BP or older. The underlying assumption here is that the shells represent ice-free conditions in the sound at some point prior to ca. 32000 yrs BP and that they have been subsequently reworked and deposited by grounded ice sometime in the late Wisconsin. Because of these conflicting ages however it is difficult to say confidently when the event began. The latter point reflects a recurrent problem in the Antarctic of dating carbonate shells, which are controlled by local seawater reservoirs (see Chapter 4) (Berkman et al., 1998; Andrews et al., 1999).

The second suite of dates suggests that George VI Ice Shelf disappeared during the Holocene (Sugden and Clapperton, 1980; Clapperton and Sugden, 1982). Clapperton and Sugden (1982) dated barnacle shells (*Bathylasma corolliforme*) from the ice shelf moraine at Two Step Cliffs. They obtained ages of c. 7200 ^{14}C yr BP, which corresponds to 5900 ^{14}C yr BP after an Antarctic marine reservoir

correction is made (- 1300 yr; Berkman and Forman, 1996; Berkman et al., 1998). Amino Acid Racemization analysis of the shells also suggested a Holocene age. Assuming that barnacles are unable to grow beneath an ice shelf, Clapperton and Sugden (1982) suggested that the George VI ice shelf collapsed in the early to mid-Holocene. Reformation of the ice shelf then bulldozed the shells from their position in George VI Sound to an ice shelf moraine on the coast of Alexander Island.

More recently, Hjort et al. (2001) have produced a suite of supporting AMS radiocarbon dates on individual shells (*Bathylasma corolliforme*) from sites close to those of Clapperton and Sugden (1982). Ages from the ice shelf moraine, using the same reservoir correction as Clapperton and Sugden (1982) confirm a Holocene age (5750-6000 ^{14}C yr BP equivalent to 6550-6850 cal yr BP) for *Bathylasma corolliforme*. Older deposits yielded infinite radiocarbon ages and amino acid ratios indicating an age well before the present interglacial (and possibly dates from MIS5e). Together these results provide evidence that George VI Sound has been free of its ice shelf on at least two occasions during the Late Quaternary. This suggests that the ongoing retreat and collapse of some AP ice shelves might not be unprecedented. However, the interpretation of the shell dates relies on the critical assumption that they cannot grow beneath an ice shelf (Hjort et al., 2001), which has not been robustly tested.

3.4. George VI Ice Shelf – Present behaviour

Over the past century a large body of work has been amassed concerning the evolution, history and dynamics of George VI Ice Shelf. It is clear from this work that it is a complex, and perhaps unique ice shelf. The next two sections will start to examine the recent retreat history of the ice shelf and assess how the ice shelf may behave in future.

3.4.1.Retreat of the northern and southern margins of George VI Ice Shelf

The climatic backdrop to recent ice shelf retreat has already been discussed in Chapter 2. According to Morris and Vaughan, (2003) the present limit of ice shelf

distribution closely follows the -9°C isotherm and ice shelves known to have retreated over the past 100 yrs are bounded by –9°C and –5°C isotherms (Fig. 3.1) (Morris and Vaughan, 2003). It has also been noted that this zone now encompasses the northern margin of George VI Ice Shelf, leading some workers to suggest that it will be the next ice shelf to undergo large-scale retreat or collapse (Vaughan and Doake, 1996).

Retreat of the northern ice front was first noted by Mercer (1978), and later by Lennon et al. (1982) and Potter et al. (1988). Recently Lucchitta and Rosanova (1998) have used historical accounts and satellite imagery to document its twentieth century retreat history. Records show that the ice shelf has undergone persistent retreat over the last 20 years and perhaps since 1936 (first observations by British Graham Land Expedition). Lucchitta and Rosanova (1998) estimate that between 1974 and 1992 an area of 906 km^2 of ice shelf was lost at a retreat rate of 49 $km^2\ a^{-1}$. Between 1992 and 1995 an additional 87 km^2 of the northern margin of George VI Ice Shelf was lost at a retreat rate of 27 $km^2\ a^{-1}$.

A more detailed map of the 20th and 21st century (1947-2001) retreat of GVI-IS has recently been completed by the British Antarctic Survey in collaboration with the United States Geological Survey (USGS) (Fig. 3.11). The map has been compiled using a combination of aerial photographs and satellite imagery and demonstrates that the northern margin has continued to retreat, losing a further 375 km^2 between 1992 and 2001, a retreat rate of 62 $km^2\ a^{-1}$. The map also shows that the southern margin has also retreated since the late 1940's, losing approximately 2,500 km^2 between 1947 and 2001, a retreat rate of 46 $km^2\ a^{-1}$.

Together, these results demonstrate that the retreat rate of GVI-IS significantly outpaces the hypothetical advance rate of a 'stable' ice shelf front. Vaughan and Doake (1996) have defined an ice shelf that is no longer viable as one that undergoes progressive retreat via a series of large calving events, which occur over several years without significant re-advance. Normal (i.e. stable) calving, in contrast, is followed by significant re-advance of the ice shelf (Vaughan and Doake 1996), which has not been observed at either margin of the GVI-IS. Thus, George VI Ice Shelf appears to fit Vaughan and Doake's (1996) definition of being no

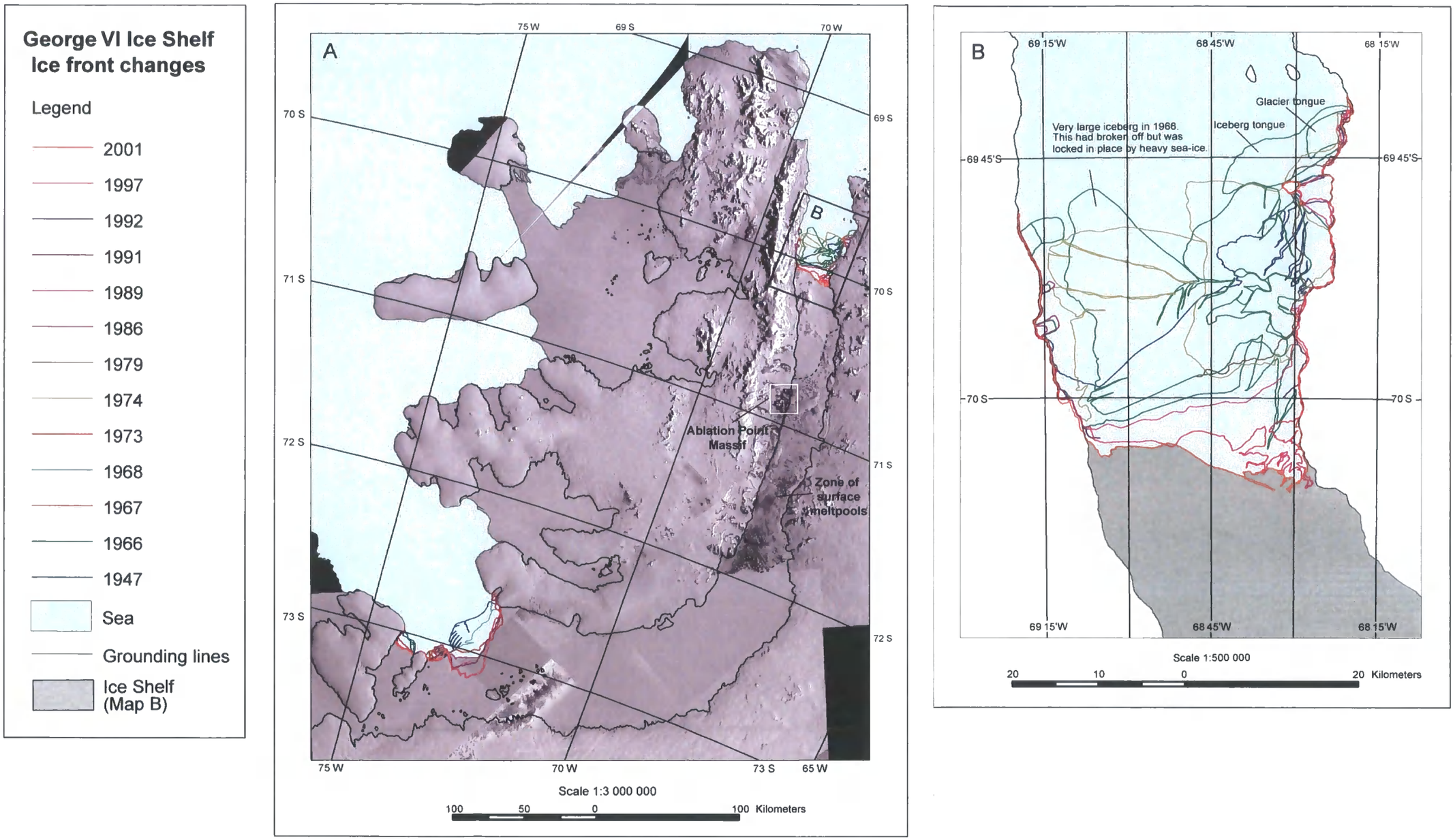

Figure 3.11. (a) Retreat map for the northern and southern margins of George VI Ice Shelf . (b) shows the northern ice front retreat in more detail. The the northern and southern margins of the ice shelf have shown persistent retreat since 1947 without significant re-advance. Also shown are the positions of the Ablation Point Massif (white open box) and the geographical distribution of surface meltpools (dotted line) (map compiled by A. Cook, British Antarctic Survey).

longer viable, which suggests that we may be witnessing the first stages of ice shelf disintegration.

3.5. George VI Ice Shelf – future behaviour?

The recent retreat of GVI-IS appears to be following the behaviour of other AP ice shelves, although it has yet to collapse in a catastrophic Larsen-style break-up event. At face value, the recent changes appear directly related to increased atmospheric temperature, although other forcing mechanisms (e.g. changes in ocean circulation) may also be important. The next section will begin to examine how and if GVI-IS is susceptible to collapse.

3.5.1.Glaciology – A Structural Weakness

In Chapter 2, the structural arch hypothesis (e.g. Doake et al., 1998) was discussed. Although this hypothesis does not provide the initial impetus for ice shelf collapse it has been used to account for the rapidity of ice shelf disintegration (e.g. Wordie/Larsen-B). However, unlike the Wordie and Larsen ice shelves, George VI Ice Shelf has a very small calving front, especially in the north. It is therefore unlikely that a structural arch mechanism will lead to the rapid disintegration of GVI-IS, which is long and narrow.

One other glaciological weakness relates to the temperature regime at the northern ice front. Evidence has shown that the ice towards the northern margin of George VI Ice Shelf is temperate (Potter and Cooper, 1988). The precise reason for this is largely unknown but it may relate to the flow regime in the northern region of the ice shelf, which changes from compressional flow to extensional flow north of about 70°15'S. This change in flow is defined by the northward limit of meltpools (Fig. 3.4), beyond which surface meltwater can drain through the upper firn since the overall compression appears to be reduced. Thus, north of 70°15'S surface water is able to percolate through the upper firn where it refreezes and releases latent heat. The release of latent heat acts to warm the surrounding ice. As noted in Chapter 2, laboratory experiments have demonstrated that the fracture toughness of ice is

reduced at higher temperatures and in the presence of water (Lui and Miller, 1979; Sabo and Schulson, 1989). As such, the ice north of 70°15'S may be more susceptible to crevasse formation and ice shelf break-up. The change in flow also has implications for the meltpool induced break-up hypothesis.

3.5.2. Surface Meltpools – A trigger for collapse?

As noted in Chapter 2, Scambos et al. (2000) have provided evidence to suggest that there is a strong correlation between ice shelf disintegration and melt-ponding. Because water is denser than ice, it exerts a significant outward and downward pressure when it pools on the ice shelf surface and in crevasses. The hydrostatic pressure, under certain conditions in water filled crevasses, is great enough to propagate fractures through the full ice thickness thereby compromising the mechanical integrity of the ice shelf (Scambos et al., 2000). However, as noted in Chapter 2, although this process has played a significant role in the recent collapse of some AP ice shelves (e.g. Larsen-B) it does not appear to be the case for large parts of George VI Ice Shelf, which shows the most extensive melt-pooling and has the longest history of melt-ponding of any AP ice shelves (Reynolds, 1981b; Scambos et al., 2000). This apparent insensitivity to melt pools is largely due to the high compressive forces within the main body of GVI-IS (between 70°15'S and 72°00'S), which effectively counter-acts the hydrostatic pressure thereby keeping the crevasses closed (Scambos et al., 2000). However, the absence of meltpools north of 70°15'S implies that the compressional stresses decrease, thereby allowing the propagation of crevasses and the drainage of surface water. Together with a more temperate ice regime, this may make the northern margin more susceptible to a meltpool-induced retreat. However, excluding the area north of 70°15'S, a meltwater trigger alone is unlikely to destabilise the entire ice shelf.

3.5.3.Circumpolar Deep Water – a potential trigger?

Several studies have linked changes in ocean circulation with climate change on the AP (Vaughan et al., 2001) and ice shelf retreat through enhanced bottom melting (Talbot, 1988; Domack et al., 1995; Lucchitta and Rosanova, 1998; Shepherd et al., 2003). Vaughan et al. (2001) suggested that UCDW could play an important role in

recent atmospheric warming of the AP through a reduction in sea-ice and its associated affects on the regional albedo. A similar argument was also developed by Talbot (1988) who suggested that warm UCDW could contribute to ice shelf disintegration through increased basal melting. Indeed, UCDW has been linked to the recent collapse of the Wilkins Ice Shelf (Lucchitta and Rosanova, 1998) and the retreat of the Müller Ice Shelf (Domack et al., 1995). It is further intriguing that late Holocene climatic changes (e.g. Little Ice Age) have been linked to the withdrawal of UCDW from the western shelf of the AP (e.g. Shevenell and Kennett, 2002; Ishman and Sperling, 2002). A comparable picture is now emerging from the east coast of the AP where Shepherd et al. (2003) have suggested that enhanced bottom melting caused by the presence of warm deep water (Weddell Sea Deep Water, WSDW) may have contributed to the demise of the Larsen-B ice shelf. Superimposed upon the recent atmospheric trends on the AP and the retreat of several ice shelves is the apparent warming of the Southern Ocean over the past 50 years (Gille, 2002). How this relates to UCDW or WSDW is as yet unclear.

It is clear that CDW plays a fundamental role in controlling the climate of the AP, and potentially the stability of some AP ice shelves (e.g. Domack et al., 1995). It is known for example that CDW drives high basal melt rates (ca. 2 ± 0.1 m yr^{-1}) beneath GVI-IS, but it is not known however, if this rate has changed in the past or whether it has changed in response to recent atmospheric and/or ocean warming. There is a growing need therefore to investigate the influence of warm water on the continental shelf and below George VI Ice Shelf and its potential sensitivity to climatic changes. In the absence of contemporary data we must turn to the palaeo record. The question now is whether we can link past changes in CDW with the apparent disintegration of George VI Ice Shelf during the mid-Holocene? As noted in Chapter 2, Howe and Pudsey (1999) have suggested that UCDW flow was unstable until around 12300 yr BP, when enhanced flow was noted. During deglaciation and into the Holocene, at approximately 10000 yr BP, UCDW stabilised, becoming less vigorous. Shevenell and Kennett (2002) have suggested that CDW was present on the continental shelf west of the AP between 9000 and 3500 cal yr BP based on their analysis of $\delta^{18}O$ and $\delta^{13}C$ composition of planktic foraminifera extracted from marine cores from the Palmer Deep (Fig. 2.1b), whilst

the diatom study of Leventer et al. (2001) noted the presence of 'warm water' conditions between 9000 and 6700 cal yr BP at the same site. Surprisingly, Ishman and Sperling (2002) arrived at a different conclusion for the early Holocene when they analysed the overall foraminiferal composition of marine cores from the Palmer Deep. Until the issue of UCDW presence or absence during the mid-Holocene on the western continental shelf is resolved it remains difficult to judge whether UCDW played an important role in the mid-Holocene collapse of GVI-IS. Future research aimed at understanding the long-term history of GVI-IS will be required before the link between UCDW and ice shelf stability can be further investigated

3.5.4. Slow versus catastrophic collapse

One final scenario that needs to be considered is that George VI Ice Shelf may not undergo catastrophic collapse in the style of the Larsen-B ice shelf but instead continue to undergo relatively slow (when compared to other AP ice shelves) retreat. The current rate of retreat appears to conform closely to the southward migration of the –5 °C to –9 °C mean annual isotherms, which is being driven southwards by atmospheric warming on the AP. Thus, if we take the maximum (62 km^2 a^{-1}) $20^{th}/21^{st}$ century retreat rates for the northern and southern margins (46 km^2 a^{-1}) we can obtain a rough estimate of how long the ice shelf will take to disappear if the present retreat rate continues. On the basis that the ice shelf measures about 25, 000 km^2 (Reynolds and Hambrey, 1988) it would take approximately 230 years for the ice shelf to disappear completely. Although this calculation is a gross simplification, which does not take into account variations in ice shelf thickness, which varies from north to south (Fig. 4.2), the rapidity of temperature change (e.g. 3.7 ± 1.6 °C over the last century) and glaciological factors, it does provide a useful approximation, especially for comparison with time intervals in the past when atmospheric temperature may have been similar to, or warmer than, the present day (e.g. Early Holocene optimum).

3.6. Summary

George VI Ice Shelf is the largest ice shelf on the west coast of the AP. It has shown persistent retreat since 1947 and perhaps since the mid-1930's when it was first observed by the British Graham Land Expedition (Lucchitta and Rosanova, 1998). The recent retreat of GVI-IS has led some researchers to suggest that it will be the next ice shelf to undergo large scale retreat, or even collapse (Vaughan and Doake, 1996). Given, the retreat of other AP ice shelves, both on the west side of the AP and the east, it is important that we understand how and why ice shelves are retreating. A large body of evidence regarding the glaciology, ocean-ice shelf interaction and late Quaternary history of GVI-IS has been amassed over the past 50 years. Together with recent changes, this information provides a unique opportunity to study an ice shelf in its pre-collapse phase, and begin to explore the reasons for, and causes of, the ice shelf retreat.

Amplified atmospheric warming on the AP over the last century appears to be directly related to recent ice shelf retreat. However other factors such as changes in ocean circulation are also considered to be important (e.g. Shepherd et al., 2003). At present the key –9 °C mean annual isotherm lies firmly across the northern part of GVI-IS, which according to Morris and Vaughan, (2003), represents the boundary for ice shelf viability. An important feature of many of the ice shelves that have collapsed on the AP is the relative rapidity of disintegration once a certain threshold is passed. The rapidity of change implies some internal, structural weakness (e.g. Doake et al., 1998), but this mechanism does not seem likely to be influential in the collapse of GVI-IS. The melt-ponding mechanism developed by Scambos et al. (2000) offers a link between ice shelf collapse and increased atmospheric temperatures. However, it seems unlikely that this mechanism will play a significant role in the future stability of GVI-IS, due largely to the compressive flow regime within the ice shelf. The meltpool mechanisms, however, may be influential in the retreat of GVI-IS north of 70°15'S, where the flow appears to change from compression to extensional flow.

More recently, several studies have highlighted the importance of changes in ocean circulation; specifically warm deep-water masses (e.g. UCDW and WSDW) but it is still unclear how these changes relate to atmospheric warming. For example, are changes in atmospheric temperature driving changes in UCDW or are changes in UCDW driving atmospheric changes through a series of positive feedbacks? Shevenell and Kennett (2002) believe that the late Holocene UCDW changes observed in the Palmer Deep were controlled by some atmospheric reorganisation, which may have originated in the low-latitude tropical Pacific (see Chapter 2). Their data suggests that atmospheric changes drive perturbations in UCDW. What is clear is that the mass balance of GVI-IS is strongly influenced by UCDW-induced ice shelf melting and without further contemporary records, or proxy data from the past it remains difficult to assess the importance of UCDW to GVI-IS, how long such melt-rates can be maintained and whether they have varied in the past.

In light of these questions it is timely that we attempt to understand in more detail the Holocene history of GVI-IS. The fundamental aim of this thesis is to provide a long-term perspective (Holocene) on GVI-IS through the analysis of sediment cores from two epishelf lakes. The following chapter will document the physical setting of these two lakes and provide an overview of the field techniques, and a detailed account of the laboratory procedures used in this thesis.

Chapter 4
FIELD SETTING, FIELD METHODS AND LABORATORY TECHNIQUES

4.1. Introduction

The previous two chapters have provided a comprehensive review of the recent and past environmental change on the AP (Chapter 2) and a detailed review of George VI Ice Shelf (Chapter 3). This chapter will outline the field methods and laboratory techniques used to reconstruct the Holocene history of GVI-IS. The chapter has three aims. First, to describe the physical setting of the study site (Ablation Point Massif) and document the bathymetry and limnology of Moutonnée and Ablation Lakes. Second, to outline the field techniques used during the 2000-1 and 2001-2 field campaign. Third, to outline and provide the rationale for the laboratory techniques used in this thesis and describe the protocols adopted for each.

4.2. Field Setting

4.2.1. Ablation Point Massif

The Ablation Point massif (Fig. 4.1 and Fig. 3.4 Chapter 3) is one of largest ice-free areas on the AP measuring approximately 18 km from north to south and 10 km from east to west (Clapperton and Sugden, 1982, 1983). It is flanked on either side by two large glaciers (Grotto and Jupiter Glaciers), which flow into GVI-IS. The massif is dissected by five main valleys. Moutonnée, Ablation and Striation Valleys trend east-west whilst Flat Iron and Erratic Valleys trend north-south (Fig. 4.1). Intervening ridge crest altitudes are commonly between 650 m to 750 m with a maximum altitude of over 1000 m. Approximately 17% of the area is covered by permanent snow and ice (Clapperton and Sugden, 1983). This compromises 10

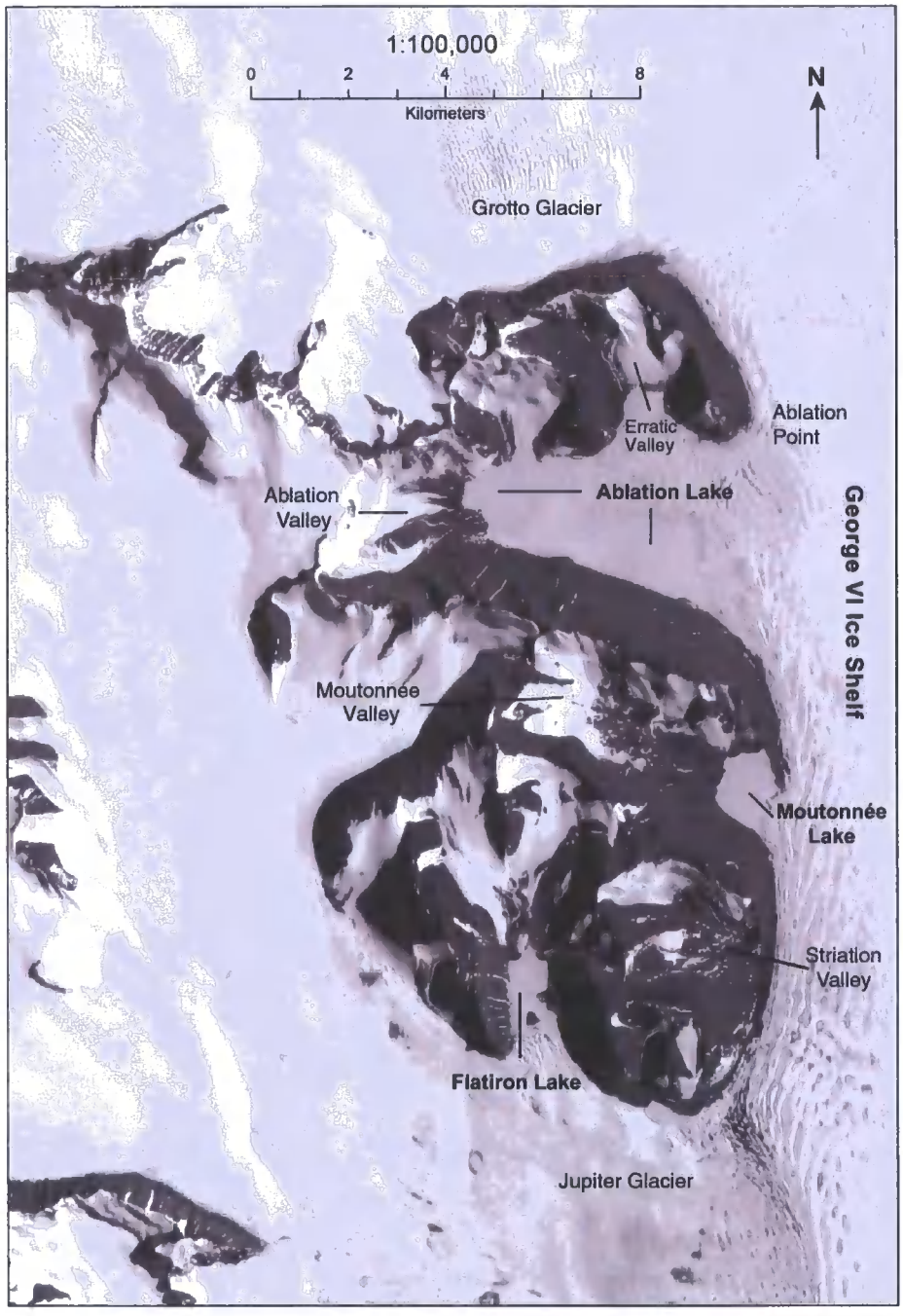

Figure 4.1. Aster (Advanced Spaceborne Thermal Emission and Reflection Radiometer) image of the Ablation Point Massif (location shown in Figures 2.1 (Chapter 2) and 3.4., (Chapter 3) showing, Moutonnée Lake, Ablation Lake and Flatiron Lake (referred to as 'upper lake' by Heywood, 1977). Moutonnee and Ablation Lakes are impounded by George VI Ice Shelf as it impinges against the Ablation Point Massif. Flatiorn Lake, in contrast, is above sea-level and is impounded on its southern side by the Jupiter Glacier (Image supplied by MAGIC, British Antarctic Survey). The late Quaternary history of the masiff is shown 3.9, Chapter 3.

small valley glaciers, 7 cirque and cliff glaciers and numerous permanent snow banks (Clapperton and Sugden, 1983). The majority of these glaciers and snow banks occur on south-facing slopes, reflecting the prevailing wind and snow direction from the south (Clapperton and Sugden, 1983). The geology of the massif is largely sedimentary (Late Jurassic to Early Cretaceous sandstones, mudstones and shales), derived from deeply eroded plutonic and metamorphic terrain, which was subsequently re-deposited in a shallow-marine basin (Elliot, 1974). Volcanic rocks, probably Upper Oxfordian-Kimmeridgian also occur and are exposed rarely on the valley floors and basal parts of several cliffs; they consist mainly of lavas, agglomerates and breccias (Elliot, 1974). As noted in Chapter 3 the massif has undergone a complex late Quaternary history and provides evidence for both ice cap (ca. 75000 yr BP) expansion and local valley glacier variations (summarised in Fig.3.9 and Table 3.1, Chapter 3).

4.2.2. Epishelf Lakes

Within Moutonnée and Ablation valley's, two large epishelf lakes are impounded by GVI-IS, which flows in a westward direction from the AP (Fig. 4.2., also see orientation of meltpools in Figure 3.4 (Chapter 3) which illustrates flow direction). These lakes were first studied in the 1970's (e.g. Heywood and Light, 1975; Heywood, 1977). This work revealed that the lakes are tidal, stratified water bodies each with a lower marine layer that extends under the ice shelf to the ocean, and an upper freshwater layers that is maintained by snow melt and whose maximum thickness is determined by the ice shelf draught (Heywood, 1977). The two lakes are presently at sea-level and provide an exceptional opportunity to investigate the history of GVI-IS since their unique environmental setting means that any change in the position of the ice shelf is likely to leave a detailed record within the lakes sedimentary records. Moutonnée and Ablation Lakes were re-visited during the austral summers of 2000-1 and 2001-2. The site description and physical limnology in the following section is based largely on Heywood's (1977) study, although supplementary data collected for this study is also included.

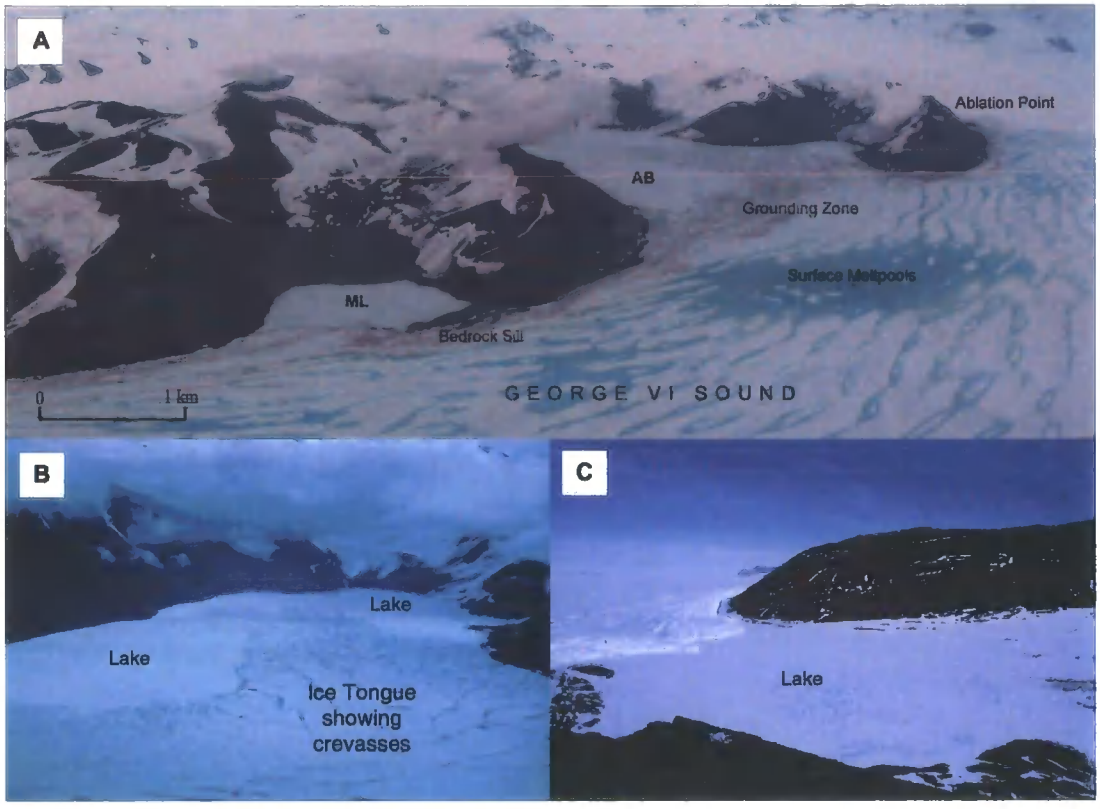

Figure 4.2. Epishelf lakes on Alexander Island. (a) Oblique aerial photograph taken on 6/1/2003 (photo: A. Fox) of Moutonnée Lake (left) and Ablation Lake (right). Photograph shows how the ice shelf is prevented from entering Moutonnée Valley by a bedrock sill. In Ablation Valley the ice shelf is grounded along a submerged bedrock bar (Heywood, 1977) and is expressed at the surface as a zone of disturbance. Extensive melting on the surface of GVI-IS is also apparent (b) Oblique aerial photograph taken from an aircraft in Feburary 1998 (photo: M. Bentley) looking into Ablation Valley at Ablation Lake showing a prominent tongue of the ice shelf (see text). (c) Photograph of Moutonnée Lake taken from the hills above the lake, showing George VI Sound in the background and the impressive ice cliffs (see Fig. 4.3) (ca. 30 m high) at the left-hand (East) edge of the lake.

4.2.2.1.Moutonnée Lake

Moutonnée Lake (ML, 70°51'S, 68°20'W) is impounded on its eastern side by GVI-IS, which is grounded on a partially exposed bedrock sill (Fig. 4.3). At the grounding line the ice shelf front has been forced upwards to form ice cliffs up to 30m high (Fig. 4.3). The height of the ice-cliffs plus the lake water depth at the ice front (or draught) effectively represents the ice shelf thickness at this point. The lake is capped by 2-3 m of ice but, in summer, a narrow moat (~ 2 m wide) forms around the landward shoreline due to advected heat and the inflow of water from catchment snow melt (Fig. 4.3). During winter the lake ice is pushed onshore where it forms small compressional ridges (Fig. 4.3). A small valley glacier exists at the head of the valley, which at some point was much more extensive leaving behind the Valley Stage till (see Fig. 3.9, Chapter 3) (Clapperton and Sugden, 1982). During the summer, extensive moss and cyanobacteria patches develop, especially on the western shoreline of the lake shoreline and on the north facing valley slope (Fig. 4.4). A semi-permanent snow bank exists on the south facing valley side. Detailed bathymetric work (Heywood, 1977; and this study) has revealed that the deepest part of the lake is 55 m (Fig. 4.5). From this point, our measurements show that the lake shallows rapidly to the east where it meets the landward side of the submerged bedrock sill and to the west where it meets the first of two successive shelf areas (Fig. 4.5).

The first vertical profiling of the water chemistry, in late December 1973 (Heywood, 1977), revealed that the lake is stratified with freshwater underlain by saline (marine) water and a two-stepped halocline at 36 m and 44 m (Fig. 4.6). Monitoring of lake water salinity over a tidal cycle revealed that the halocline varied between 36 and 39m depth suggesting some exchange with the seawater beneath the ice shelf (Fig. 4.7). It was concluded that seawater does not penetrate far into the basin but that tidal flow might be sufficient to cause some mixing between the two water masses. However, a mismatch between the timing of tides in ML and under GVI-IS (Cartwright, 1979) suggested that the water exchange was at least partially impeded by grounded ice (e.g. Cartwright et al., 1980). Below ca.44 m the saline monimolimnion is prevented from escaping by the sub-lacustrine bedrock sill

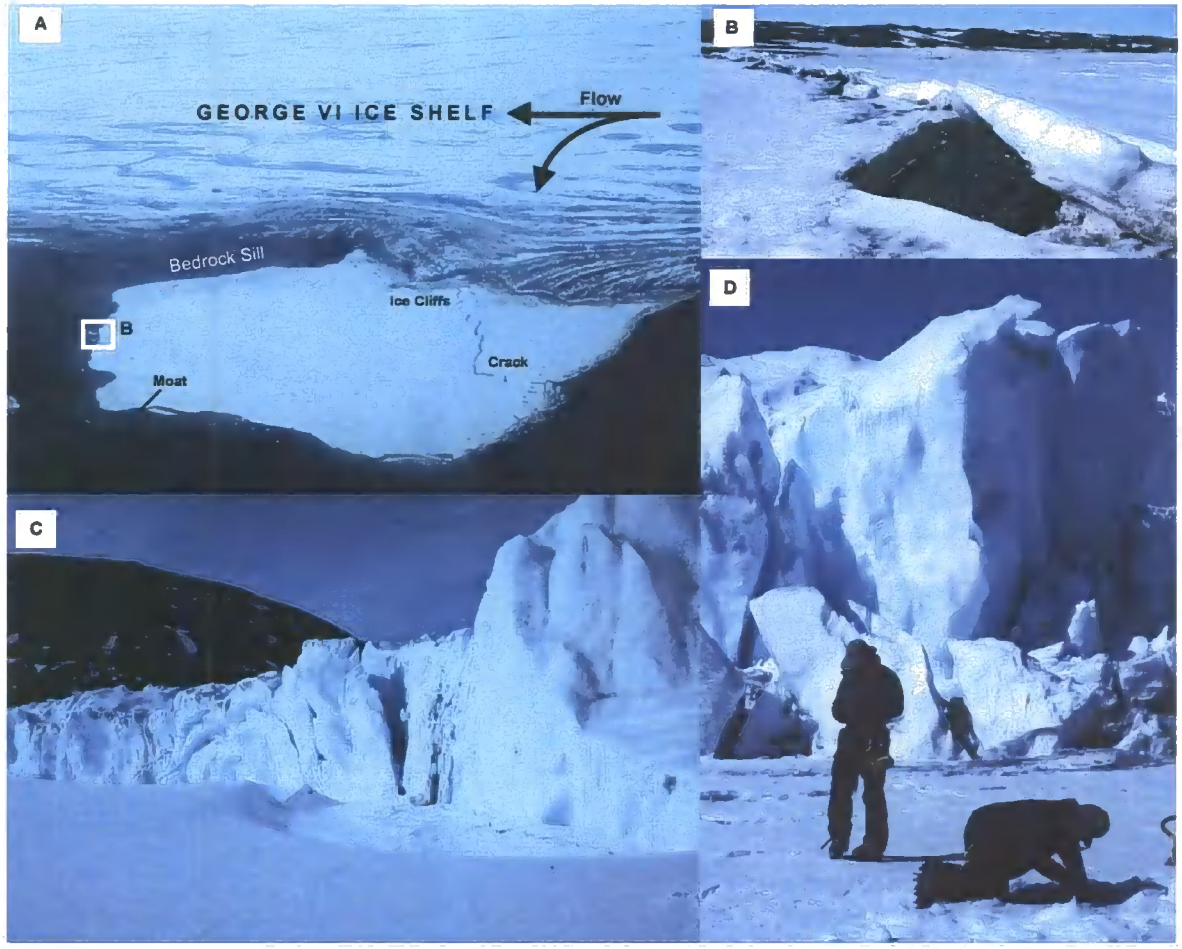

Figure 4.3. (A) Oblique aerial photograph of Moutonnée Lake (ML), showing George VI Ice Shelf, the direction of ice shelf flow, the bedrock sill, ice cliffs and lake moat. The lake ice surface also shows a prominent crack (Photograph taken from an aircraft in Febuary 2003). As the ice shelf meets the lake it causes the lake ice to push forwards, resulting in compressional ridges along the shoreline (B). Ice cliffs in ML with scientists for scale (C,D) (Photograph D.A. Hodgson December 2000).

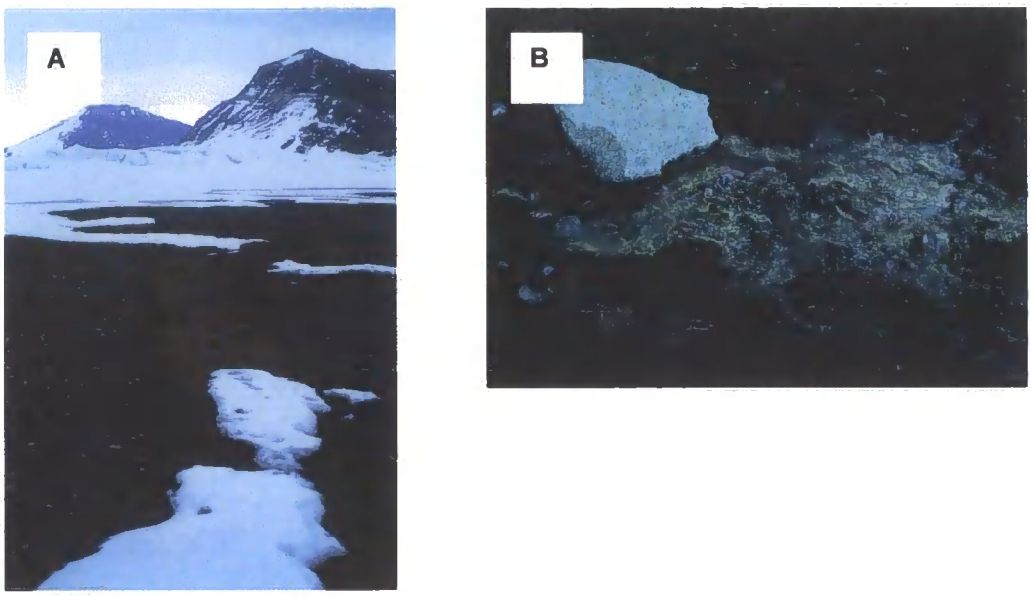

Figure 4.4. (a) Moss along a lake inflow in Ablation Valley (Photograph taken in 2001-2 by D. A. Hodgson) and (b) cyanobacteria/moss patch in Moutonnée Valley (Photograph taken in 2001-2).

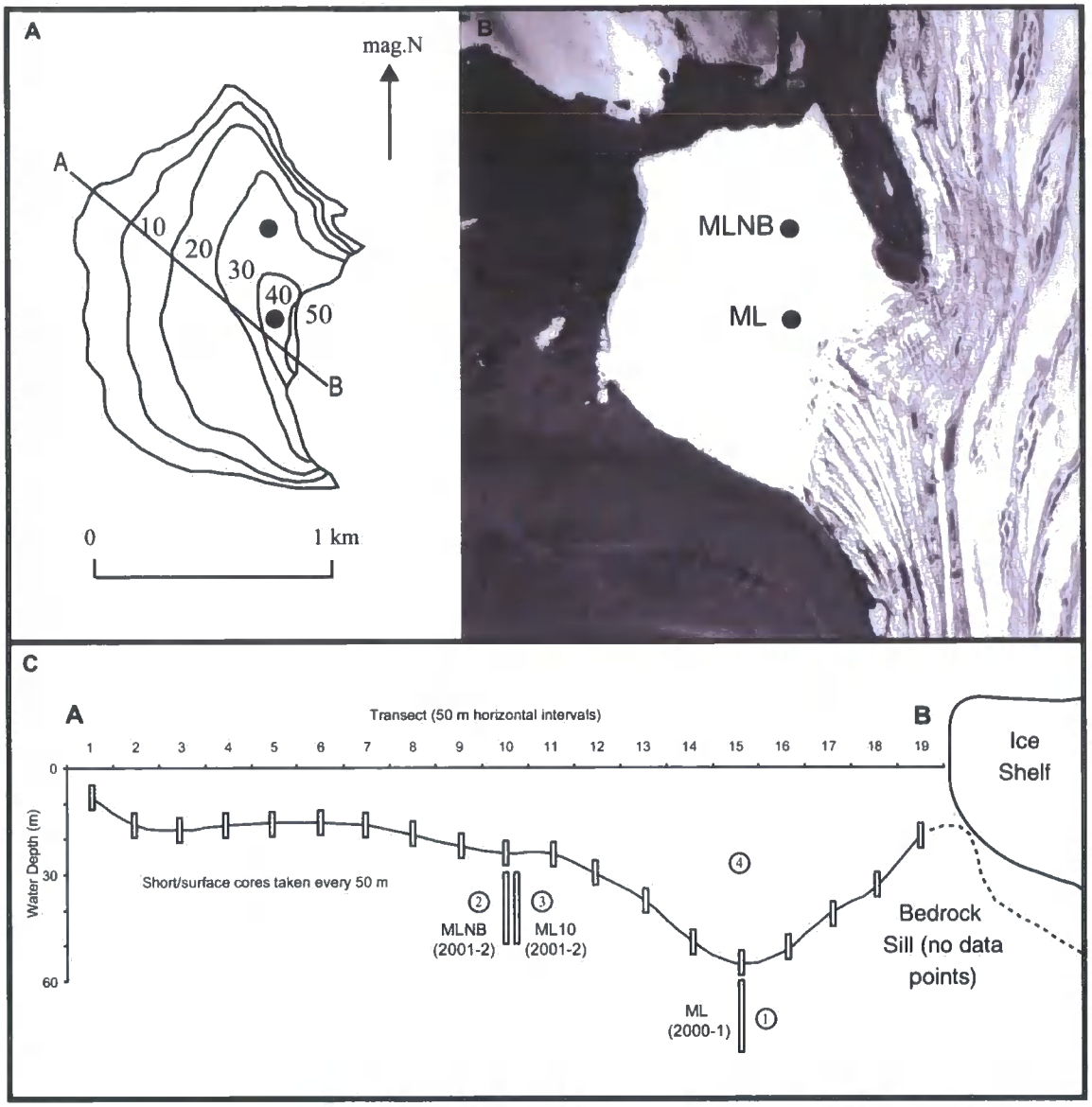

Figure 4.5. Moutonnée Lake bathymetry (A) based on data from Heywood (1977). Also shown are the two principal core sites (ML and MLNB) and A-B transect shown in (C). (B) Shows aerial photograph of ML Lake (BAS archive). (C) shows transect line A-B from ice shelf front to lake shoreline based on echo-sounder measurements made during 2000-1. Surface sediment samples were taken every 50 m in 2000-1. Also shown are the locations of sediment cores (1-3) and sediment traps (4). NB: position of MLNB core projected onto line of surface sediment transect.

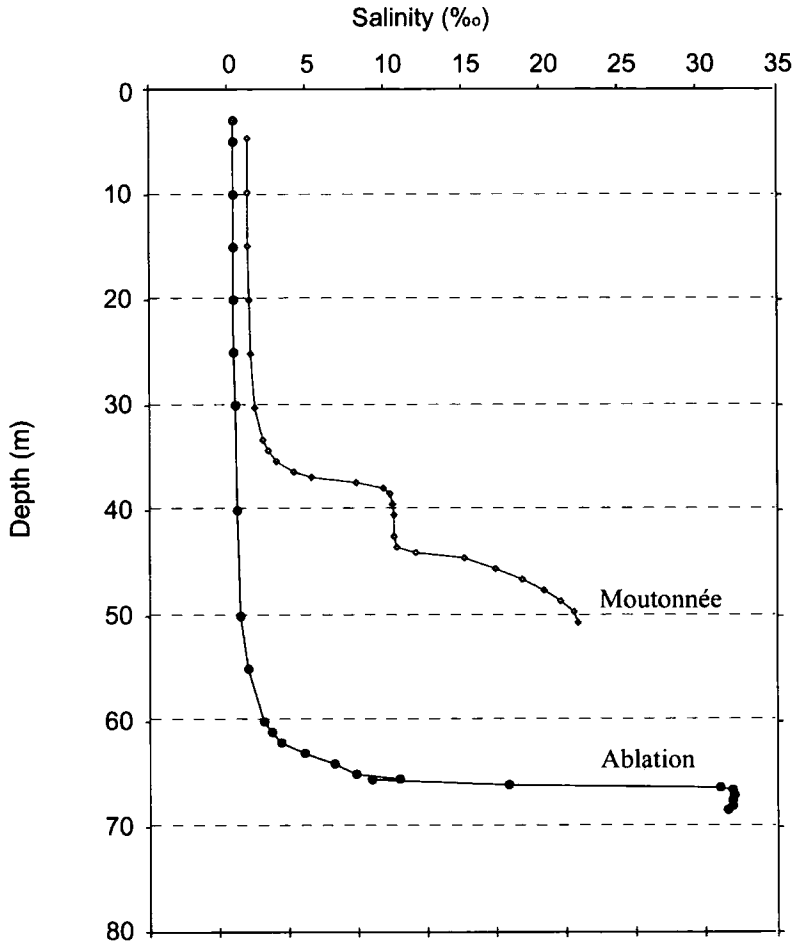

Figure 4.6. Salinity profiles for Moutonnée Lake (blue) and Ablation Lake (Black) measured in 1973 (Heywood, 1977). Moutonnée Lake is characterised by a two-step halocline. This probably reflects the exchange of marine water in a zone between 36 and 39 m and a more stationary saline layer (beneath 39 m) which is prevented (impounded) from escaping the basin by the bedrock sill (see profile in 4.5). In Ablation Lake a very steep halocline occurs between 64 and 66.25 m. CTD profiles were re-measured in 2000 and 2001 and are shown in Chapter 5.

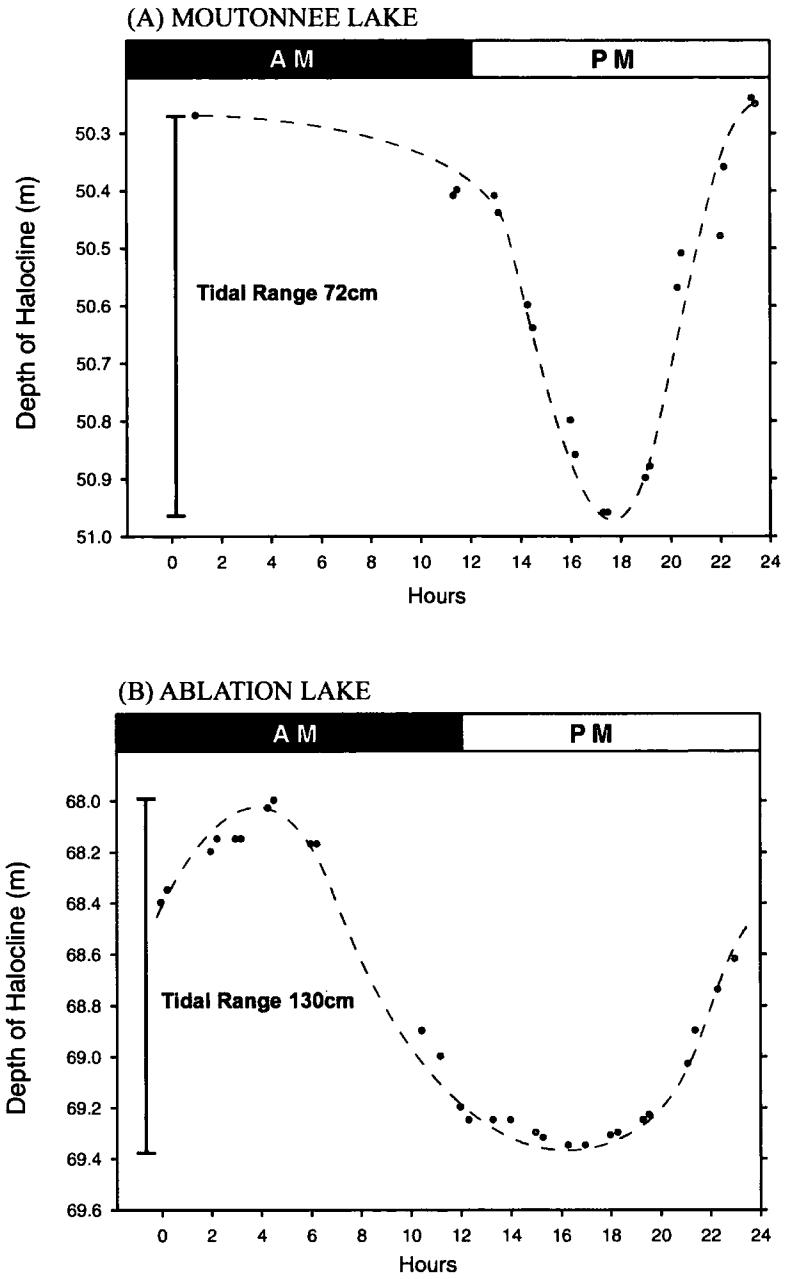

Figure 4.7. Tidal variations recorded in November-December 1973 at (a) Moutonnée and (b) Ablation Lakes (Heywood, unpublished data).

(Heywood, 1977). The saline water is Chlorite dominated (ionic order Cl-Na-SO_4-K-Ca-Mg; Fig. 4.8a) which compares closely with the ionic order of seawater in nearby Marguerite Bay (Heywood, 1977). Nutrient levels (N-NO_2, N-NO_3, P-PO_4) were exceptionally low in the mixolimnion and below detection limits in the monimolimnion (N-NO_3 and P-PO_4, Heywood, 1977).

4.2.2.2. Ablation Lake

Ablation Lake (AB, 70 49'S, 68 27'W) is impounded on its eastern side by GVI-IS, which is only partially grounded on a submerged bedrock bar, with the grounding zones expressed as raised crevassed areas on the surface of the ice shelf (Fig. 4.9 and 4.10). The grounding zone does not completely impede westward flow of GVI-IS, part of which flows over and around the bedrock bar to form a prominent ice tongue extending 2.8 km into Ablation Lake (Fig. 4.9) (Reynolds and Hambrey, 1988). Tides of up to 1.65 m occur in AB causing the lake ice to move up and down with an irregular diurnal rhythm (Fig. 4.9) (Heywood, 1977). Unlike ML a wide (>1 m) seasonal moat does not form in AB due to the high compressive forces exerted by the ice shelf tongue which pushes the lake ice landward forming compression ridges up to 3 m high along the lake shore (Heywood, 1977). Water can be seen between some of these ridges, especially where the lake ice is fractured. The north-facing valley side of Ablation Valley is characterised by rectilinear slopes with a veneer of talus. The foot of the slope has been overprinted by the 'Valley Stage' till (Clapperton and Sugden, 1982), which extends from the mouth of Ablation Valley to the valley head (Fig.3.9 Chapter 3). One other notable feature of the north facing valley side is the outcrop of a mixed granite conglomerate (Himalia Formation) (Fig. 4.11). On the south-facing valley side there are two smaller north-south valleys, both containing small glaciers. The glacier in Erratic Valley (Fig. 4.1 and 4.9) terminates before meeting the ice shelf, whilst the glacier in Unnamed Valley abuts the surface of Ablation Lake (Fig. 4.1 and 4.9). A large glacier occupies the head of Ablation Valley, approximately 1 km west of the present lake shoreline and is the source of significant glacier melt-water during the summer months (Fig. 4.9).

Vertical profiling of the water chemistry in late December 1973 revealed that the lake is stratified with deep freshwater mixolimnion and a single halocline underlain

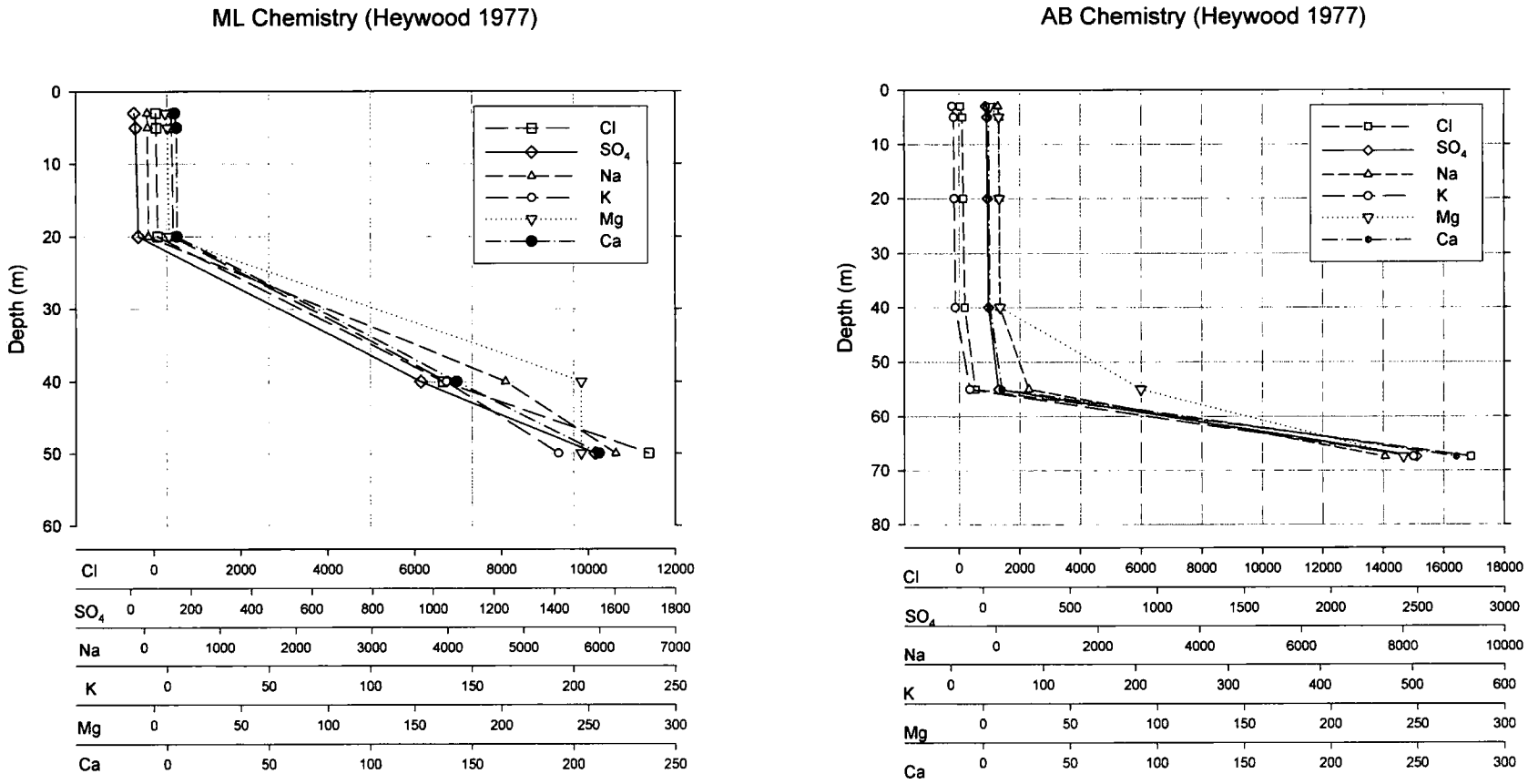

Figure 4.8. Showing elemental water chemistry data from Moutonnée and Ablation Lake sampled in November-December 1973 (Heywood, 1977). NB: the very step chemical gradient in Moutonnée Lake simply reflects the spacing of sampling points above and below the halocline. It is likely that the change in chemical composition of lake water coincides with the halocline seen in Figure 4.6.

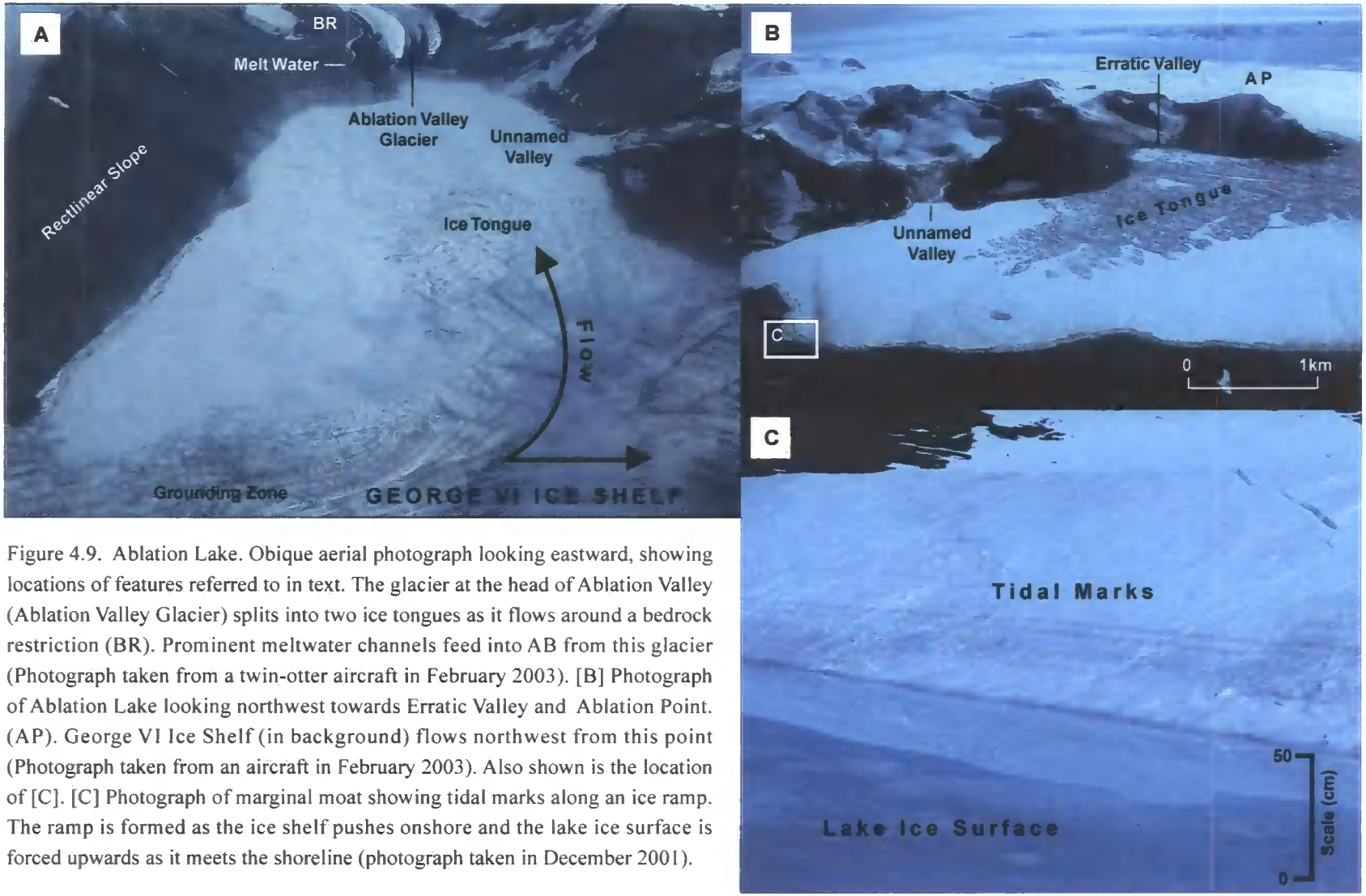

Figure 4.9. Ablation Lake. Obique aerial photograph looking eastward, showing locations of features referred to in text. The glacier at the head of Ablation Valley (Ablation Valley Glacier) splits into two ice tongues as it flows around a bedrock restriction (BR). Prominent meltwater channels feed into AB from this glacier (Photograph taken from a twin-otter aircraft in February 2003). [B] Photograph of Ablation Lake looking northwest towards Erratic Valley and Ablation Point. (AP). George VI Ice Shelf (in background) flows northwest from this point (Photograph taken from an aircraft in February 2003). Also shown is the location of [C]. [C] Photograph of marginal moat showing tidal marks along an ice ramp. The ramp is formed as the ice shelf pushes onshore and the lake ice surface is forced upwards as it meets the shoreline (photograph taken in December 2001).

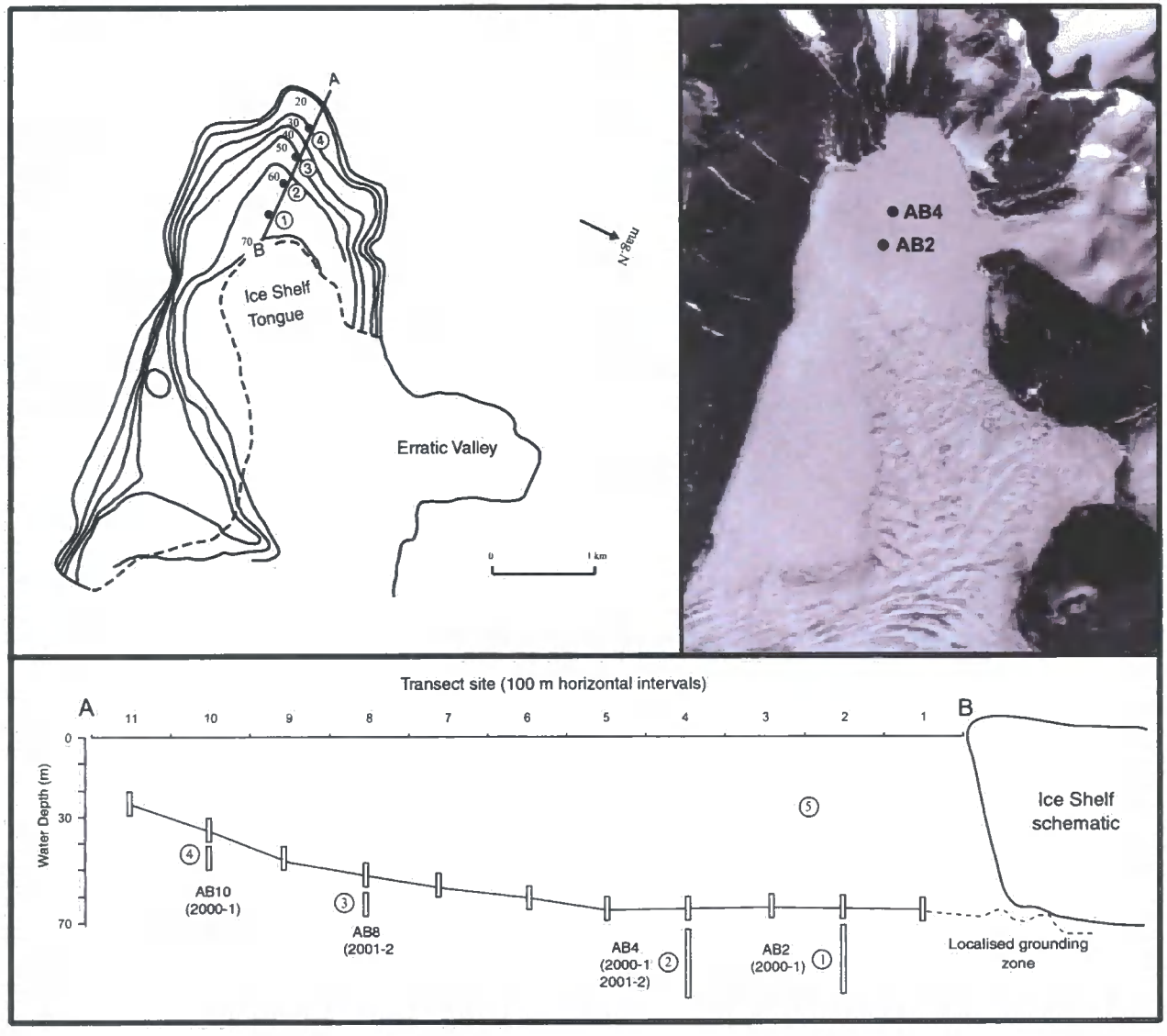

Figure 4.10. (A) Ablation Lake bathymetry based on data from Heywood (1977). (B) Aerial photograph of AB (Aster image, MAGIC, BAS)) showing principal core sites (AB2 and AB4) [C] shows transect line A-B from ice shelf front to lake shoreline based on echo-sounder measurements made during 2000-1. Surface sediment samples were taken every 100 m. Also shown are the locations of sediment core (1-4) and sediment traps (5).

Figure 4.11. South side of Ablation Valley. The Himalia Formation outcrops as a series of pale bands on the upper slopes of the valley and is a mixed granite conglomerate. This represents the only *in-situ* source of granite on Alexander Island.

by a thin saline monimolimnion (Fig. 4.6) (Heywood, 1977). The water below 55 m was Chlorite dominated (ionic order, Cl-Na-SO_4-K-Ca-Mg; Fig. 4.8). Repeated measurements of the position of the halocline over a tidal cycle (Heywood 1977) concluded that the saline layer is in direct contact with the seawater beneath George VI Sound and extends 4km into the lake. This was supported not only by measurements of the water chemistry that revealed no appreciable difference in the chemical composition of the seawater beneath AB, the brackish water from ML and seawater collected further north in Marguerite Bay (Fig. 2.1b Chapter 2), but also the discovery of benthic marine fish (*Trematomus bernacchii*).

4.2.3. Climate of the Ablation Point Massif

The climate of the Ablation Point massif is dominated by the interaction of cyclonic depressions that originate in the southeastern Pacific Ocean and Amundsen-Bellingshausen Sea and the north-to-northeasterly outflow of cold anticyclonic air from the West Antarctic ice sheet (King and Turner, 1998). This interaction is extremely important in determining the long-term climate of the massif with the former bringing relatively warm weather, strong northerly winds and a heavy cloud cover to the Ablation Point area, whilst the latter brings cool stable weather. Mean annual temperature is approximately -1.9°C during summer (December-February) and –17.5°C during winter (June-August) (Harangozo et al., 1997) and annual precipitation is less than 20 cm water equivalent. Analysis of long-term weather data (1961-1994) from nearby Fossil Bluff station (45 km south) has revealed that on multi-decadal time scales, the temperature data appear to reflect the recent rapid warming observed elsewhere on the AP (Vaughan et al., 2003), particularly during summer months (Harangozo et al., 1997). The most pronounced warming at Fossil Bluff appears to have been delayed compared to other central and northern records from the AP and shows the most apparent warming has taken place over the last decade (Harangozo et al., 1997). Figure 4.12 shows the summer temperature plot from Fossil Bluff and confirms that mean annual temperatures have continued to rise. One immediate effect of this temperature rise in the Ablation Point area appears to have been the partial break-up of the lake surface in Moutonnée Lake in late February 1998 (Bentley, pers. comm.) (Fig. 4.13), which occurred during the warmest recorded summer (ca. +1 °C). Break-up of the lake ice has not been

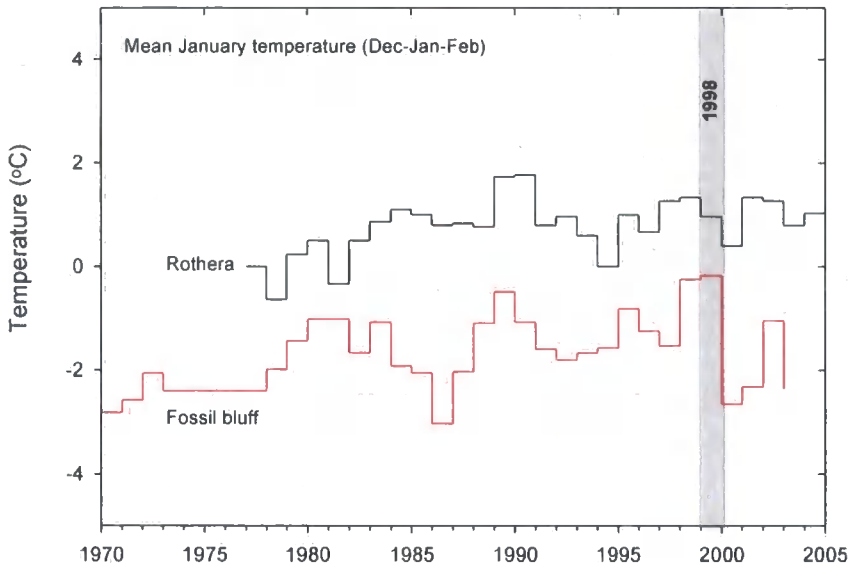

Figure 4.12. Mean summer (January) air temperature at Fossil Bluff Station, Alexander Island (see Fig. 3.4b for location) and nearby Rothera Station (Fig. 2.1). Summer temperatures have gradually warmed since 1968 (Monthly temperature data supplied by Stephen Harangozo, British Antarctic Survey). Break-up of Moutonnée Lake occurred in the summer of 1998 (the warmest summer since records began).

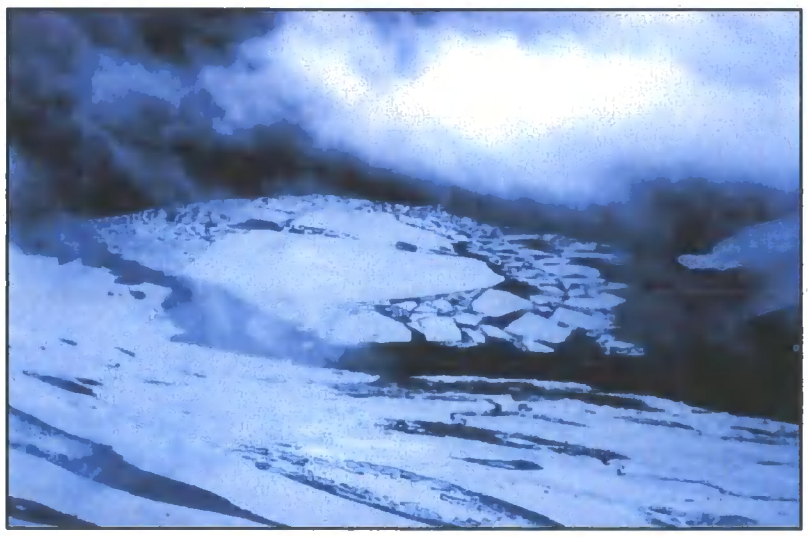

Figure 4.13: Oblique aerial photograph of Moutonnée Lake taken from an aircraft (photo: M. Bentley) showing the partial break-up of Moutonnée Lake surface in late February 1998.

reported by anyone else during the ca. 70 year period that GVI-IS has been visited. It is worth noting however, that late February is towards the end of the normal summer logistical operating season and thus previous ice surface break-up may have occurred without it being observed.

4.3. Field Techniques

It was the hypothesis of this thesis that Moutonnée and Ablation Lakes would contain a detailed record of the Holocene history of George VI Ice Shelf. To test this hypothesis, fieldwork and data collection for the project took place over two successive field seasons; 2000-1 (M.J. Bentley/D.A. Hodgson/P. Noon), and 2001-2 (**J.A. Smith**/M.J. Bentley/D.A. Hodgson/E. Verleyen). The fundamental aim of the fieldwork was to obtain several sediment cores from Moutonnée and Ablation Lakes, together with detailed water chemistry measurements and reference data from each lake catchment. The latter information were collected in order to constrain minerogenic/biogenic inputs into the lake basin and provide a valuable baseline data set that will allow comparisons with earlier measurements (e.g. Heywood, 1977) and to develop a conceptual model for detecting ice shelf histories from epishelf lake sediments. Owing to logistical considerations, primarily the safety of landing aircraft on, and then working on lake ice, fieldwork was carried out between the austral summer months of October and January when mean monthly temperatures remain below freezing. Beyond this 'window of opportunity', the lake ice surface, especially on Moutonnée Lake, can potentially become unstable due to rising temperatures and enhanced surface ablation. The next section will provide an overview of the field techniques employed.

4.3.1. Bathymetry

Bathymetric measurements were carried out on transects from lakeshores to ice fronts during 2000-1 and 2001-2, building on the work of Heywood (1977). Lake ice was drilled using a Jiffy motorised ice drill with a 1 m long, 10 inch diameter auger blade and up to four, 1 m extension rods, depending on ice thickness (Fig. 4.14). Depths were measured using a portable echo sounder, a plumb line, or both. The majority of depth measurements were undertaken using the echo sounder, but

Figure 4.14. Photograph showing the 'jiffy-team' (JAS and Elie Verleyen) drilling through lake ice using a Jiffy drill (photograph by D.A. Hodgson, December 2001).

in some cases the echo sounder appeared to yield incorrect water depths, probably related to the interference of loose ice in the water column. In such cases, water depths were validated using a plumb line.

4.3.2. Sediment cores

Surface sediment cores were collected using a UWITEC short (1.2 m) gravity corer fitted either with a hydraulic core catcher for soft sediments (not used in season 2001-2002) or a steel 'orange-peel' core catcher for consolidated sediment. Long cores were collected using a 2 m UWITEC (KOL. Kolbenlot) cable-operated piston corer (60 mm diameter) mounted on a lightweight aluminium A-frame, with a solid wooden platform (Fig. 4.15). This system has been used with considerable success by a number of researchers, has a maximum operating depth of 150 m, and can collect up to 20 m depth of sediment (Melles et al., 1997; Kulbe et al., 2001; Hodgson et al., 2003). Where we sampled more than 2 m of sediment thickness, two adjacent holes were drilled through the ice (c. 1 m apart) and successively deeper cores taken from alternate holes with an overlap of 10-20 cm as outlined by Hodgson et al. (2003). Intact cores were retrieved in transparent Perspex liners, capped securely and carefully frozen vertically in the field. Surface cores were sectioned at 1 cm intervals in the field, stored in small Whirlpak sample bags and frozen (e.g. Hodgson et al., 2003). All sediment samples were shipped back to the UK in a freezer container (-80°C) on the RSS James Clark Ross.

4.3.3. Water chemistry

Field measurements of conductivity, temperature, pH and dissolved oxygen were carried out at 2 m intervals using a SOLOMAT water quality meter in 2000-1 and YSI 650 water quality meter in 2001-2 in order to measure the present-day water chemistry and also to compare with previous chemistry data collected in the 1970's (Heywood, 1977). Water samples were collected using a UWITEC or Niskin bottle water sampler. Selected samples, which coincided with major changes in water chemistry, were filtered through GF/C (0.45 μm) glass fibre filters and stored in acid-washed Nalgene bottles. The filters were frozen and retained for pigment

Figure 4.15. Sediment coring at Moutonnée Lake (November 2001) using a UWITEC piston corer and aluminium A-frame (from left to right D. Hodgson, E. Verleyen and M. Bentley). Jiffy drill auger blade lying in the foreground and ice cliffs of George VI Ice Shelf are visible in the background.

analyses at BAS HQ.

Additional filtered water samples were collected for $\delta^{18}O$ and $\delta^{13}C$ and D/H analysis and stored in 125 ml acid-washed Nalgene bottles. Twenty ml of $NaOH.BaCl_2$ solution was added to the $\delta^{13}C$ isotope samples to precipitate the bicarbonate. Air was excluded from the bottles and the caps sealed with PVC tape. Samples were stored frozen. To support the interpretation of the isotopic data, Meteorological data collected at nearby Fossil Bluff (~ 45 km further south) (Fig. 2.1b) was used to supply proxy data for the sites. Regular radio communication between our field party at Ablation Point and scientists at Fossil Bluff suggested that the two sites experienced near-identical weather conditions.

4.3.4. Sediment traps

Sediment traps were installed in Moutonnée Lake on 28/11/00 and at Ablation Lake on 11/12/00 to investigate annual sedimentation rates and sediment composition. These consisted of paired traps 30 cm long and 5 cm wide (6:1 aspect ratio) constructed from PVC pipe. At each site the traps were positioned below the major steps in the conductivity profiles (field data from 2000). The traps were suspended in the water column on nylon rope with a sub-surface buoy to maintain rope tension. The traps were suspended from a wooden cross on the lake ice surface and accurate positions recorded both on GPS (precision <10 m) and using a Geodimeter Total Station EDM (precision <mm). Due to late-lying snow cover in 2001-2 the wooden crosses could not be easily re-located. Therefore, traps were re-located using a folding L-shaped probe, lowered through a drilled hole in the ice and then deployed and rotated below the ice to 'snag' or 'catch' the hanging rope of the trap. The traps from Moutonnée Lake (installed on a single rope at depths 22m, 40m and 47m, position 70° 52.123' S, 068°19.635'W) were successfully retrieved on 27/11/01 and the contents of each trap transferred to Nalgene bottles. In the case of the lower-most paired trap the material was transferred immediately into light-tight Nalgene bottles to enable OSL bleaching tests to be carried-out for an allied project (Roberts, unpublished data). Biological sub-samples were preserved in Lugols iodine. We were unable to re-locate the Ablation Lake sediment traps despite exhaustive

searches over several days. A corridor 39m long, and 16.6m wide, aligned 246°M from the original location of the trap was 'swept' with the probe but the traps were not found suggesting either rapid movement of the lake ice or failure of the trap suspension system.

The new position of the ML sediment trap was surveyed using the Geodimeter and it was found to have moved 3.85m in a WNW direction. This is an important result as it demonstrates for the first time that a lake conveyor mechanism (Hendy, 2000; Hendy et al, 2000) is operating at this site (and by inference, probably at AB too). This result will allow us to make better interpretations from our core material as we can identify sediment transport pathways with more confidence (Chapter 5).

4.3.5. Catchment reference datasets – constraining lake inputs

A reference data set comprising soil, moss, cyanobacteria and valley gravels was collected from representative environments within the catchments of each of the lakes. Soil, moss and cyanobacteria were analysed for their elemental carbon (C_{org}), nitrogen (N_{org}) and isotopic carbon ($\delta^{13}C_{org}$) values, whilst the valley gravels were used to aid the interpretation of the lithological and sedimentological composition of the lake sediment. These samples also ensured that the study had a comprehensive reference data set of diatoms samples from the full range of environments in the catchments. Together, this information enables catchment inputs into the lake sediments to be identified and to discriminate them from marine-derived inputs from George VI Sound and its ice shelf.

4.3.6. $\delta^{18}O$ and δD isotopic analysis of ice and snow - constraining lake water source

Ice samples were collected from the ice shelf front to the lakeshore at each site in order to better understand the progressive transition from ice shelf ice to lake ice and also to help interpret the isotopic composition of the lake water. Ten holes were drilled along an east west transect at each site every 100 m. Samples were taken from 5cm, 25cm, 50cm and 75cm depths within the ice at each hole. Blocks of ice

from the ice shelf front were also sampled. The sampling at Moutonnée occurred before any significant melting had taken place within the lake ice, so no water was seen and the ice surface was snow-covered and undegraded. Snow and ice were sampled either as frozen samples in Whirlpak© sealed sample bags with air excluded, or in 20ml Nalgene© screw cap bottles, packed down to minimise the air gap. A selection of ice shelf ice samples and upstanding 'bergs' of ice shelf ice within the lake ice at Ablation were also collected for analysis. Moreover, in order to better understand the isotopic composition of the lake waters we sampled residual winter snow-pack; fresh summer snowfall and blue glacier ice from the catchments for isotope analyses. All $\delta^{18}O$ and δD samples were kept frozen in the field and shipped back to the UK at –80°C on RSS *James Clark Ross*.

4.3.7. Core Site selection

The selection of the core sites were based upon two factors. First, and most importantly, it was based on a detailed understanding of the lake bathymetry, from Heywood (1977) and our own measurements and principles of sediment focusing in lake systems. A second factor was the logistical considerations of collecting the best possible suite of cores in the time available. A summary of core material collected during 2000-1 and 2001-2 relevant to this study is shown in Table 4.1.

4.3.7.1. Moutonnée Lake

The location of core sites in 2000-1 was based on the detailed bathymetric measurements of Heywood (1977) and our own supplementary bathymetric work in 2000. Together this enabled us to select the optimum axis for the surface sediment transect and to identify the basin's 'deep spot' along the transect. Surface sediment samples were collected every 50 m (Fig. 4.5) using the UWITEC short gravity corer. These were collected for two principal reasons. Firstly, to judge the nature of the sediment and thus help determine the most suitable sites for coring operations. Secondly, the transect approach enabled a detailed analysis of ecological and physical changes along a depth transect from the ice shelf front to the lake shoreline and was important in developing the conceptual model for ice shelf

LAKE	Lake & core identifiers	Corer type	Year cored	Lat (°S) Long (°W)	Lake ice thickness (m)	Water depth (m)	Total sediment depth (TSD) recovered (cm)
MOUTONNÉE	**MOUTONNÉE CORE (ML)**	UWITEC-PISTON	00-01	70°52.123'	2.0	51	548
	Moutonnée Short Core (ML-S)	UWITEC-GRAVITY	00-01	68°19.635'			22
	Moutonnée Transect Cores (ML1-19)	UWITEC-GRAVITY	00-01	70°51.937'-70°52.178' 68°19.376'-68°20.612	2.0-2.2	8.1-55	1-27
	MOUTONNÉE NORTH BASIN (MLNB)	UWITEC-PISTON	01-02	70°52.053' 68°019.989'	2.0	34	190
	Moutonnée Lake – Site 10 (ML10)	UWITEC-PISTON	01-02	70°51.827' 68°019.411'	2.0	23.5	75
ABLATION	**ABLATION CORE (AB2)**	UWITEC-PISTON	00-01	70°48.974' 68°27.143'	2.0	65	228
	Ablation Transect Cores (AB1-10)	UWITEC-GRAVITY	00-01	70°48.954'-70°49.126' 68°27.143'-68°28.537'	2.0-2.5	25.21-65.25	0-22
	ABLATION LONG CORE (AB4)	UWITEC-PISTON	01-02	70°48.994'	2.0	73 [echo]	246
	Ablation Surface Core (AB4-S-02)	UWITEC-GRAVITY		68°27.295'		65.25 [plumb]	18
	Ablation Transect Core (AB8-02)	UWITEC-GRAVITY	01-02	70°49.086' 68°28.213'	2.0	47.4	17

Table 4.1. Summary of core data collected from epishelf lakes on Alexander Island, Antarctic Peninsula in 2000-2001 and 2001-2002 seasons. Principal cores discussed in the text are shown in bold. Location of cores in Moutonnée and Ablation Lakes are shown in Figures 4.5 and 4.10.

presence/absence (Chapter 5). Surface sediment material was sub-sampled at 1 cm resolution and transferred into Whirlpak© bags. The deepest part of the basin (short core site ML15) was selected as the primary core site as it is most likely to represent the sediment depo-centre (Last and Smol, 2001). A 22 cm surface sediment core was collected at this site (ML15; 70°52.123'S, 68°19.635'W) using the UWITEC gravity corer fitted with a hydraulic core catcher. The cable-operated piston corer was then deployed a few meters away to collect four successively deeper, overlapping sediment cores. A total sediment depth of 5.48 cm was retrieved before encountering bedrock, sampled as a disk of sandstone at the base of the cutting face of the UWITEC corer. We are therefore confident that this represents the entire sedimentary sequence.

Coring in 2001-2 built on the knowledge and experience gained during the 2000-2001-field season and the preliminary analysis of the 2000-1 cores. The coring system was positioned on one of the 'shelf' sites (ML 10; 70°52.053'S 68°19.989'W) (Fig. 4.5). Three sites were tried within 50 m of this point - each yielded sediment cores c.75 cm long. This indicates that the sediment drape at this site is uniformly thin, when compared to the >5 m core retrieved from the depocentre during 2000-1 season. Due to the coarse nature of the sediments the orange peel core catcher was used throughout. New bathymetric measurements were also undertaken in the northeastern part of the lake to find a sheltered basin in the 'lee' of the bedrock sill and a suitable site for an additional 'shelf' site sediment core. Surface sediments were collected from each access hole to help determine the most suitable site for coring operations. The site chosen at 70°51.827'S 68°19.411'W was informally named the Moutonnée Lake North Basin (MLNB) coring site. Water depth at this site was 34 m, with a ca. 2.5 m lake ice cover. Surface sediment cores were collected from the new site with the UWITEC gravity corer fitted with the orange-peel core catcher. The UWITEC cable-operated piston corer was then deployed to collect a sediment core to 190 cm total sediment depth. This core stopped in very stiff, dewatered and coarse (gravel) sediment, which prevented further penetration. It is therefore less likely that the entire sedimentary sequence was sampled at this site.

4.3.7.2. Ablation Lake

The location of core sites in 2000-1 was based similarly on the detailed bathymetric measurements of Heywood (1977) and our own supplementary bathymetric work in 2000. Together this enabled us to select the optimum axis for the surface sediment transect (from the lake shore to the ice shelf front) and to identify the most suitable site for long-coring. Surface sediment samples were collected every 100 m (Fig. 4.10) using the UWITEC short gravity corer. Firstly, to judge the nature of the sediment and thus help determine the most suitable sites for coring operations. Secondly, the transect approach enabled a detailed analysis of ecological and physical changes in the sediment from the ice shelf front to the lake shoreline. Surface sediment material was sub-sampled at 1 cm resolution and transferred into Whirlpak© bags. Using the bathymetry of Heywood (1977) and our supplementary water depth data taken in 2000-1 the main core site was chosen in a zone ca. 100 m from the first of the pressure ridges in the lake-ice (short core site AB2; 70°48.974'S, 68°27.143'W). The coring site represents a natural deep trough in the basin. The UWITEC cable operated piston corer was deployed at this site to obtain two successively deeper sediment cores with a total sediment depth of 2.33 m. The base of the sequence consisted of a highly dewatered and compacted sediment with multiple clasts, sufficiently dense to cause some deformation of the steel coring tube. It is therefore unclear whether the entire sedimentary sequence was retrieved at this site.

Following the bathymetric transect work in 2000-2001 and previous bathymetric measurements (Heywood, 1977) we were able to immediately take short and long cores from transect site AB4 (Fig. 4.10) (position: 70°48.994' 68°27.295') and transect site AB8 sites (position: 70°49.086' 68°28.213'). An 18 cm surface sediment core was collected from site AB4 using the UWITEC gravity corer fitted with the orange peel core catcher. The main coring site was chosen about 400 m inshore from AB2 because of the coarse-grained nature of sediment encountered at transect point AB2 (Fig. 4.10). The proximity of the ice shelf may have caused a large amount of rain-out of coarse material and so by moving ca. 400 m shorewards, but still staying within the deep basin (see bathymetric transect Fig. 4.10) we would be

more likely to get a complete but finer-grained sedimentary record of ice shelf fluctuations. The UWITEC cable operated piston corer was deployed at this site to collect two successively deeper sediment cores to 2.46 m total sediment depth where highly dewatered and compressed sediment was encountered.

An attempt was made to retrieve a further sediment core from site AB8. This site is in shallower water, but is located on a very low gradient slope (Fig. 4.10). After two abortive attempts a third hole yielded a short core of 17.5 cm of brown-green finely textured clay, silt and fine sand. Long coring was unsuccessful because of striking very coarse material in one hole and the unexpected, undulating local lake floor topography. Because of the latter problem, a detailed bathymetric profile was undertaken along a c. 10-15 m length, which showed that there is a 46 cm transverse gradient at this site as well as the very gentle east-dipping gradient (sloping down to N). Because of this, coring at AB8 was abandoned.

4.4. Analytical Procedures

The following section provides the rationale for the laboratory techniques and explains the procedures adopted for each. A multi-proxy approach was adopted for this thesis to help reconstruct the Holocene history of George VI Ice Shelf. The approach involved a combination of physical, biological and isotopic and elemental techniques. It was hoped that such an approach would provide an unambiguous record of ice shelf variations.

4.4.1. Radiometric Dating

As stated in Chapter 2 the utility of any palaeoenvironmental record is constrained by its ability to be placed in a historical framework. Traditionally, the principal age control on Late Quaternary palaeoenvironmental records in Antarctica has been derived from radiocarbon dating. However, obtaining reliable chronologies using radiocarbon techniques can be problematic, especially when forced, due to lack of carbonate, to date the acid insoluble organic matter (AIOM) fraction (Björck et al., 1991; Berkman et al., 1998; Doran et al., 1999; Domack et al., 1999; Andrews et al., 1999; Jones et al., 2000; Hodgson et al., 2003). In the marine environment this

largely reflects a variable Antarctic marine reservoir effect (AMRE) and the addition of old or new carbon. The radiocarbon reservoir in the Southern Ocean is dominated by the upwelling of deep water at the Antarctic Divergence, which produces radiocarbon ages for living marine species that exceed 1000 years (Broecker, 1963; Stuiver et al., 1983; Gordon and Harkness, 1992; Berkman and Forman, 1996). This 'marine reservoir' has also been affected by natural changes in the production of atmospheric radiocarbon (Bard et al., 1990). An additional problem is the spatial variability of the AMRE (Gordon and Harkness, 1990), which can be influenced by glacial meltwater containing old carbon (Domack et al., 1989; Melles et al., 1994) or regional differences in upwelling around the continent (Berkman et al., 1998). Aside from natural impacts, the Southern Ocean reservoir has been altered by human activities. Throughout the 20th century 'old' radiocarbon from fossil fuels and 'new' radiocarbon from nuclear explosions has added carbon to the atmosphere (Berkman et al., 1998). The 53‰ differences between Δ ^{14}C values of pre-bomb and post-bomb Biogenic carbonates, is almost identical to the c. 50‰ offset for surface seawater south of 50° (Broecker et al., 1985; Berkman and Forman, 1996). The bomb signal has also been observed in long-lived brachiopods from Signy Island (Peck and Brey, 1996). This data implies that the Antarctic marine reservoir has been altered by ca. 500 years during the 20th century due to nuclear testing and fossil fuel combustion (Berkman et al., 1998). Pre-bomb, the radiocarbon content of surface waters around the Antarctic was almost equivalent to the ca. 1300-year age of deep water (Stuiver et al., 1983). Thus as a first approximation, the general radiocarbon reservoir used for samples from the circum-Antarctic marine system is 1300 years (Berkman and Forman, 1996; Berkman et al., 1998).

A further problem, which can influence the radiocarbon ages of marine organisms in the Southern Ocean, are specific 'vital effects' associated with their ecology and composition (Berkman et al., 1998). In an example provided by Berkman et al. (1998), there are significant differences in the radiocarbon age of pre-bomb living calcareous invertebrates assumed to be the same age (1346 ± 104 yrs), penguins (1130 ± 134 yrs) and seals (1424 ± 200 yrs). Similarly the radiocarbon age for post-bomb is offset by 'new' radiocarbon resulting in younger ages for the same taxa:

calcareous invertebrates (901± 227 yrs), penguins (606 ± 388 yrs) and seals (778 ± 412 yrs).

The interpretation of radiocarbon ages from marine sediments is further complicated by the addition of much older organic material (e.g. carbon-bearing rocks/microfossils/macerals) (Eglington et al., 1997; Brachfeld et al., 2003). In the East Antarctic for example, Harris et al. (1996) found a ca. 7000 year offset for modern surface samples, which they attributed to the addition of Jurassic age pollen. It has been suggested that these problems can be overcome by systematically collecting and dating modern carbonaceous/carbonate samples and thus being able to calculate a local offset for the older samples (e.g. Berkman et al., 1998; Andrews et al., 1999). For example, Andrews et al. (1999) has suggested that in such cases, the surface age should be subtracted for all other downcore ages. However, this approach assumes that the surface error is comparable to the downcore error which, as Crespin et al. (2004) have recently noted, is not always the case.

It is also often difficult to obtain reliable ^{14}C from lacustrine environments, but for different reasons (Hall et al., 2000). A lacustrine reservoir effect can occur because of old carbon (from carbonate bearing bedrock, from old CO_2 from glacial ice) or from the lack of aeration of deep water (Hall et al., 2000), leading to erroneously old radiocarbon dates. Recent studies (e.g. Doran et al., 1999; Hodgson et al., 2001; Cremer et al., 2004) however have demonstrated that reliable dates from lacustrine sediments can be obtained through the implementation of several dating techniques (e.g. ^{14}C, ^{210}Pb, ^{137}Cs, OSL) and by systematically dating the various inputs into the lake. Indeed many of the studies referred to in this chapter have successfully overcome these problems by implementing more than one dating technique (e.g. Jones et al., 2000). In addition, where suitable macrofossils are present good chronologies can be obtained (e.g. Jones et al., 2000; Hodgson et al., 2001a). This section outlines the techniques used in this study to obtain a reliable core chronology.

4.4.1.1. ^{210}Pb and ^{137Cs}

Despite low concentrations of ^{210}Pb fallout around continental Antarctica, ^{210}Pb has been used successfully to date sediments in the sub-Antarctic (Appleby et al., 1995), the maritime Antarctic (Ye and Cuihua, 1997) and East Antarctica (Bird et al., 1991; McMinn et al., 1994; Doran et al., 1999). Some of the greatest concentrations of ^{210}Pb have occurred in lakes similar to Moutonnée and Ablation where there is a focussing effect from large catchment areas (e.g. White Smoke Lake, East Antarctica; Doran et al., 2000). Several studies have also recorded well-defined ^{137}Cs peaks, which relate to the fallout from atomic weapons testing in 1964-5 (Appleby et al., 1995).

A pilot ^{137}Cs and ^{210}Pb study was carried out on sediment from the MLNB core to investigate caesium and lead radioisotope concentrations. Initially, it was hoped that it would also allow us to assess the carbon reservoir by comparing ^{14}C ages with a lead or caesium derived chronology. However, the absence of suitable organic material in the upper sections of all our lake sediment cores meant that ^{137}Cs and ^{210}Pb represented the only viable dating technique for providing a core-top chronology.

One cm^3 of dry sediment was finely ground in an agate pestle and mortar and sieved through a 63 μm mesh to remove coarse material. Sediment was then carefully loaded into acid-washed plastic vials designed to fit inside the recess of the detector. Gamma ray detection was recorded over 24 hours using an EG&G Ortec hyper-pure germanium well detector coupled to a 4096 multi-channel analyser (MCA) at the Department of Geography, University of Durham (Donoghue et al., 2004). ^{210}Pb was measured via its gamma emissions between the 45.65-47.55 keV range of interest (ROI), and ^{137}Cs at 659.68-664.33 keV ROI. Post detection analyses of the ROI files followed the procedure of Donoghue et al. (2004).

4.4.1.2. ^{14}C Dating

Despite the problems associated with dating the bulk AIOM fraction of sediment reviewed earlier, four samples were selected from the surface and basal sediments of the ML and AB cores for radiocarbon dating at the NERC Radiocarbon

Laboratory, East Kilbride, UK. A further 11 samples were submitted for Accelerator Mass Spectrometry (AMS) ^{14}C dating. Ten of these dates were based on two mono-specific, handpicked foraminiferal species (either *Globocassidulina biora* or *Cibicides sp*; identification after Igarashi et al., 2001). These posses a distinct advantage over the AIOM dated material since the AMRE for marine carbonate species found on AP is better understood. One other AMS ^{14}C date was obtained from fragments of an algal mat from the surface of the ML long core. Analyses were undertaken at the NERC Radiocarbon Laboratory and at Beta Analytic Inc., Florida. A summary of the material dated, and the location and justification for each date is provided in Table 4.2.

4.4.2. Physical Analyses

Physical analyses (Loss-On-Ignition, Magnetic Susceptibility, Carbonate Content, Grain-Size) were performed in order to describe the sediments and, in cases where multiple cores were taken from the same basin, to aid core correlation. Analyses were carried out at three different laboratories (Table 4.3); (1) British Antarctic Survey (BAS) (M. Barrett and E. Carmichael); (2) Department of Geography, University of Durham (J.A. Smith); and (3) School of GeoSciences, University of Edinburgh (S. Roberts). Where possible inter-lab procedures were standardised. A more detailed account of these methodologies is presented below, including between-laboratory differences.

4.4.2.1. Magnetic Susceptibility

Magnetic susceptibility (MS) has been routinely used in the study of lake sediments (Thompson and Oldfield, 1986; Sandgren and Snowball, 2001 (and references therein)). The majority of magnetic minerals found in lake-sediments are derived from catchment erosion, of either bedrock or surface sediment in the lakes drainage basin (Sandgren and Snowball, 2001). Because of this, changes in the intensity of the magnetic signal of lake core sediments may reflect changes in rates of erosion in the catchment. Since erosion rates are often (but not exclusively) a function of climate, changes in the intensity of the magnetic signal may be useful to infer climate changes. Changes in the magnetic signal also reflect changes in sediment

DATE	SITE	MATERIAL	DEPTH	DATING TECHNIQUE	JUSTIFICATION FOR DATING
1	ML Core	AIOM	Base of ML core	^{14}C (Bulk AIOM)	Range finder date/to obtain a maximum age for the sedimentary sequence
2	ML Core	AIOM	Top of ML core	^{14}C (Bulk AIOM)	Range finder date/to obtain a surface age for the sedimentary sequence
3	AB Core	AIOM	Base of AB core	^{14}C (Bulk AIOM)	Range finder date/to obtain a maximum age for the sedimentary sequence
4	AB Core	AIOM	Top of AB core	^{14}C (Bulk AIOM)	Range finder date /to obtain a surface age for the sedimentary sequence
5	ML Core	Algal material	3cm	^{14}C (AMS On algal fragments)	To investigate possible marine reservoir. Material thought to be freshwater and thus should be unaffected by AMRE problem, thereby potential to provide a local AMRE correction.
6	ML Core	*Globo*	243-246 cm	^{14}C (AMS on carbonate microfossils)	Provide accurate ages for important ecological/environmental changes in core sediments
7	ML Core	*Globo*	252-255 cm	^{14}C (AMS on carbonate microfossils)	
8	ML Core	*Globo*	270-272 cm	^{14}C (AMS on carbonate microfossils)	
9	ML Core	*Globo*	280-281 cm	^{14}C (AMS on carbonate microfossils)	
10	ML Core	*Cibicides*	280-281 cm	^{14}C (AMS on carbonate microfossils)	
11	ML Core	*Globo*	291-293 cm	^{14}C (AMS on carbonate microfossils)	
12	ML Core	*Globo*	494-495 cm	^{14}C (AMS on carbonate microfossils)	
13	ML Core	*Cibicides*	494-495 cm	^{14}C (AMS on carbonate microfossils)	
14	MLNB Core	*Globo*	137-138 cm	^{14}C (AMS on carbonate microfossils)	
15	MLNB Core	*Globo*	162-163 cm	^{14}C (AMS on carbonate microfossils)	
16	MLNB Core	Bulk Sediment	0-30 cm	^{210}Pb & ^{137}Cs	(1) Provide reliable surface ages for the core sediment; and (2) to investigate possible AMRE effects

Table 4.2. Dating methods, material and justification. Abbreviations: *Globo* = *Globocassidulina* species; AIOM=Acid Insoluble Organic Matter; AMRE=Antarctic Marine Reservoir Effect.

LAKE & CORE IDENTIFIERS	ANALYSIS	OPERATOR	LAB.	SEDIMENT DEPTH (CM)	RESOLUTION	METHOD
MOUTONNÉE CORE (ML)	MS	M. Barrett	BAS	**548**	1cm	BP
	LOI	M. Barrett	BAS		1cm	Heiri et al. 2001
	CaCO3	M. Barrett	BAS		1cm	Heiri et al. 2001
	GS/litho	S.J. Roberts	Edin.		4cm	[Coulter Particle Size Analyser LS230]
Moutonnée Short Core (ML-S)	NA	-		**22**	-	
Moutonnée Transect Cores (ML1-19)	GS	**J. A. Smith**	Durham	**1-27**	-	BP
MOUTONNÉE NORTH BASIN (MLNB)	MS	**J. A. Smith**	Durham	**190**	1cm	BL
	LOI	**J. A. Smith**	Durham		2cm	Heiri et al., (2001)
	CaCO3	**J. A. Smith**	Durham		2cm	Heiri et al., (2001)
	GS/litho	**J. A. Smith**	Durham		2cm	[Coulter Particle Size Analyser LS230]
Moutonnée Lake - Site 10 (ML10)	NA	-		**75**	-	
ABLATION CORE (AB2)	MS	M. Barrett	BAS	**228**	1cm	BP
	LOI	M. Barrett	BAS		1cm	Heiri et al., (2001)
	CaCO3	M. Barrett	BAS		1cm	Heiri et al., (2001)
	GS/litho	**J. A. Smith**	Durham		2cm	[Coulter Particle Size Analyser LS230]
Ablation Transect Cores (AB1-10)	GS	**J. A. Smith**	Durham	**0-22**	-	[Coulter Particle Size Analyser LS230]
ABLATION LONG CORE (AB4-02)	MS	E. Carmichael	BAS	**246**	1cm	BP
	LOI	E. Carmichael	BAS		1cm	Heiri et al., (2001)
	CaCO3	E. Carmichael	BAS		1cm	Heiri et al., (2001)
	GS/litho	**J. A. Smith**	Durham		4cm	[Coulter Particle Size Analyser LS230]
Ablation Surface Core (AB4-S-02)	NA	-		**18**	-	
Ablation Transect Core (AB8-02)	GS	**J. A. Smith**	Durham	**17**	1cm	[Coulter Particle Size Analyser LS230]

Table 4.3. Summary of physical analysis by core, operator and laboratory. Abbreviations: [BP] Bartington Pot MS samples; [BL] Bartington Loop MS sensor; [NA] not analysed. Principal cores are in bold.

source. ML and AB have well defined catchments that are uniformly sedimentary in origin, and have a defined magnetic characteristic (ca. 25 mm^3 kg^{-1}). Thus any change in the source of sediment, for example related to changes in the ice shelf, will be recorded in the magnetic signal in the sediment cores. In addition, the magnetic signal within a lake basin is largely homogenised (Thompson and Oldfield, 1986). Consequently, variations in MS can be used to correlate multiple cores taken from the same lake basin (Dearing, 1999).

For this thesis, magnetic susceptibility measurements are used to supplement other proxy records to help establish changes in sediment supply and transport. It also aids core correlation. Magnetic susceptibility readings were undertaken using standard techniques described elsewhere (e.g. Thompson and Oldfield, 1986; Sandgren and Snowball, 2002). Readings were obtained using a Bartington MS2 single sample, dual frequency susceptibility meter (Edinburgh) for the ML-core and a Bartington loop sensor for the MLNB and AB2 and 4 cores (BAS). Although the equipment reads the magnetic signal in different ways (the Bartington MS2 reads from single pot samples whilst the Bartington loop sensor can process entire cores) the end result, or reading is comparable (Wright, 1994). There is a tendency for the loop sensor to smooth the data, since it takes an average magnetic signal from the radius of the core, whereas the signal from pot samples can be influenced by a specific grain or rock component within the selected sample, so may produce a noisier signal. A problem associated with the loop senor, relates to difference in air pressure within the core tube, which can result in a weaker magnetic signal. This can lead to characteristic 'tail/edge effects' in the MS signal. These factors are taken into account when discussing the magnetic susceptibility results.

4.4.2.2. Loss-On-Ignition – Organics and Carbonates

The organic matter of lake sediments is made up of the residue of former biota and is commonly used as a proxy for palaeoproductivty (e.g. Meyers, 1994, 1997; Meyers and Ishiwatari, 1993). The primary source of organic matter is from plants living in or around the lake. This can be divided further into two geochemically distinct groups on the basis of their biochemical compositions: (1) non-vascular plants such as phytoplankton, which contain little or no carbon rich cellulose and

lignin, and (2) vascular plants, such as grasses, trees and lake macrophytes that are mostly absent in the Antarctic. In addition to lacustrine (and in this setting, marine) phytoplankton, benthic cyanobacteria tend to dominate the lake biomass (Hodgson et al., 2003). During the austral summer, extensive algal mats develop, especially on north-facing valley sides (e.g. Heywood, 1977), which may get washed into the lake. However, Heywood (19977) measured the chemical composition of water from several streams entering ML and AB and found them to be entirely deficient in nutrients. Lake and catchment primary productivity is controlled mainly by water temperature and light, the latter being dependent on both the duration and thickness of the ice cover and blanketing snow (Gore, 1997). Because the amount of organic matter in lake sediments is controlled by primary production it can be used as a proxy for climatic changes, specifically temperature and snow cover (e.g. Kulbe et al., 2001).

In this study percentage Loss-On-Ignition (LOI) was used primarily to: (1) obtain a quick estimate of organic matter in the core sediments. This was needed to determine sample weights for elemental carbon and nitrogen (C/N ratios) and $\delta^{13}C$ analysis (discussed below); and (2) to obtain a measure of carbonate content. Elemental carbon analysis was used to infer total organic content. Sequential LOI is a common and widely used method to estimate the organic and carbonate content of sediments (e.g. Dean, 1974; Heiri et al., 2001). In a first reaction organic matter is oxidised at 500-550°C to carbon dioxide and ash. The second reaction requires further heating to evolve CO_2 from the carbonate at 900-1000°C. The weight losses during the reaction are measured by weighing the sample before and after heating (Heiri et al., 2001). Dean (1974) concluded that LOI provides a fast and reliable means of determining carbonate and organic content of sediments. However, it has been suggested that LOI tends to overestimate the amount of organic matter because there is no discrimination between carbon and non-carbon sediment components. More recently Heiri et al. (2001) performed repeat LOI measurements on several hundred sediment samples and found sample size, exposure time, position of samples in the furnace, and laboratory measuring all affected the LOI results. However, by maintaining a consistent sample size throughout the sediment core,

and consistent ignition temperature and exposure time in the furnace, Heiri et al. (2001) concluded that reliable LOI values could be obtained.

Determination of weight percent organic matter and carbonate was based on the sequential heating of samples in a muffle furnace (see Dean, 1974 and references therein) and closely followed the procedure recommended by Heiri et al. (2001). A sub-sample of wet sediment was first transferred to a dry china crucible and weighed to four decimal places using a top pan balance. Samples were then oven-dried at 105°C for 12 hrs and re-weighed to obtain a percentage wet weight. Following this, samples were combusted to ash and carbon dioxide at 550°C for 4 hours (Heiri et al., 2001) in a Carbolite ashing muffle furnace (OAF 11/1). Once cooled in a desiccator, the samples were re-weighed and the amount of organic matter determined using the following equation:

$$LOI_{550} = ((DW_{105} - DW_{550})/DW_{105}) \times 100$$

Where LOI_{550}, represents LOI at 550°C (as a percentage), DW_{105} represents the dry weight of the sample after heating to 550°C (both in grams). The weight loss should then be proportional to the amount of organic carbon contained in the sample (Heiri et al., 2001).

Crucibles were then returned to the furnace at 950°C for two hours. Carbon dioxide is evolved from carbonate, leaving oxide and the samples are re-weighed. Carbonate content (LOI_{950}) is calculated as:

$$LOI_{950} = ((DW_{550} - DW_{950})/DW_{105}) \times 100$$

Where LOI_{950} is the LOI at 950°C (as a percentage), DW_{550} is the dry weight of the sample after combustion of organic matter at 550°C, DW_{950} represents the dry weight of the sample after heating to 950°C and DW_{105} is again the initial dry weight of the sample before the organic combustion.

4.4.2.3. Grain Size

Particle size distribution in lacustrine sediments has been widely used as a primary indicator of energy levels and changes in the sedimentary system (e.g. Syvitski, 1991). Variations in grain-size have been used with considerable success in the Arctic (e.g. Nesje and Dahl (2001) and references therein) and Antarctic (e.g. Björck et al., 1996; Noon et al., 2001) to reconstruct glacier variation and catchment instability, which have been used indirectly to infer climatic changes. In this thesis, grain-size variations are used to help reconstruct changes in sedimentation associated with changing environmental conditions.

The >2 mm (gravel) grain size fraction was determined by dry sieving (e.g. Lewis and McConchie, 1994a,b). For < 2mm grain size fraction, approximately 0.5 g of sediment was transferred into a plastic 50 ml centrifuge tube and weighed on a top pan balance to four decimal places. Ten ml of 10% HCl was added and left overnight (to remove carbonates). A further 20 ml of H_2O_2 was then added and the samples placed in a hot water bath for 2-3 hours at +85°C to remove the organics. Samples were then centrifuged at 4000 rpm for four minutes and half the supernatant decanted off. Tubes were topped up with H_2O and transferred back to the centrifuge for four minutes. 20 ml of H_2O and 2 ml of Sodium Hexametaphosphate ($(NaPO_3)_6$) solution was then added to reduce sediment flocculation. Samples were then analysed on a Coulter Laser Granulometer LS230 particle size analyser equipped with a fluid module and PIDS (Polarisation Intensity Differential Scatter) attachment. This machine uses a 5 mW, 750 nm laser beam and 126 detectors placed at a range of angles up 35° to the laser beam, measuring particle sizes from 0.4 μm-2 mm. Samples were mixed thoroughly before analysis and loaded into the counter vessel until obscuration values of 45-55 % and PIDS values of 8-12 % were obtained. Background readings were undertaken for each run. Samples were run continuously with offsets automatically measured every hour and detectors aligned every two hours; sample run time = 90 seconds; grain size parameters were modelled using the Fraunhofer model with sand/silt/ clay divisional boundaries defined by Wentworth (1922). The sub-2mm grain-size data was exported directly from the Coulter LS2000 software as xls-files and then the relevant grain-size channels extracted using an unpublished (Morgan, 2001)

program. The program GRADISTAT (Blott and Pye, 2001) was then used to split the grain size classes following the Folk and Ward (1957) classification.

4.4.3. Biological Analyses

4.4.3.1. Diatom Analysis

Diatoms are one of the key indicators of environmental change in Antarctic palaeolimnology on account of their sensitivity to changes in water chemistry and the physical environment such as salinity, nutrients and depth (Spaulding and McKnight, 1999). They have also been used with considerable success in the Antarctic to investigate freshwater-marine transitions (e.g. Wasell and Håkansson 1992; Verleyen et al., 2004). In this study, the proportion of marine, freshwater and sea-ice diatoms in core sediments will provide key information on the environmental conditions within the basins at the time of diatom deposition. We have also collected contemporary diatom samples (sediment trap) and surface sediments from ML to help understand the present lake limnology and overall diatom ecology.

For the lake water column samples, up to 5 ml of water was transferred to a UWITEC plankton counter and then analysed under an inverted light microscope. For core material and surface sediment material, diatom preparation followed techniques outlined in Batterbee (1986). Sediment samples was first sieved (0.5 mm) to remove coarse material. Between 0.3-0.4 g of dry sediment were then transferred to 50 ml plastic centrifuge tubes and weighed to four decimal places using a top pan balance. Tubes were then arranged sequentially in test tube racks. 30 ml of 30% H_2O_2 was added to each sample and then observed. If the samples did not react vigorously, they were transferred to a heated water bath for 2-3 + hours at (+ 85°C). After about one hour, samples were lightly shaken and returned to the water bath. Samples were removed from the heat and 1-2 drops of 50% HCl were added to dissolve any carbonates. The digested samples were then rinsed with distilled (d) H_2O and centrifuged for 4 minutes at 1200 rpm. The supernatant was then decanted off and the sediment pellet resuspended. This cleaning step was

repeated four times. On the final wash 1-2 drops of weak ammonia (NH_3) were added to each sample to help keep the clays in suspension (Batterbee, 1986) Centrifuging samples has the advantage of saving time (compared to settling) but it may damage individual valves (Batterbee, 1986). To evaluate possible damage, one sample known to contain diatoms was prepared using both the centrifuge and settling technique to investigate the impact on the diatom valves. No differences were noted (e.g. an increase in the number of fragments) and individual valves appeared to show no signs of attrition. For slide preparation, appropriate suspension concentration was achieved by noting the turbidity and experience from previous test slides (Renberg, 1990). 0.5 ml of suspension was then placed on a cover slip and left to settle overnight. The high refraction mountant Naphrax® was used for mounting the cover slip on the slide. Diatom identification was carried out using a Nikon Alphashot 2 microscope, fitted with a Zeiss 100/1.25 oil immersion objective. Fully quantitative counts were made for each sample by counting the total number of diatom valves on for a known volume of sediment. Species identification and taxonomy was based mainly Wasell and Håkansson, (1992), Roberts and McMinn (1999), Sabbe et al. (2001) and Cremer et al. (2003) and was aided by collaboration with E. Verleyen, K. Sabbe and W. Vyverman at the Laboratory of Prostiology and Aquatic Ecology, University of Gent (Belgium) who specialise in Antarctic diatoms (e.g. Sabbe et al., 2003; Verleyen et al., 2003a,b). Data were plotted using TILIA 2.0B4 (Grimm, 1991), TILIA*GRAPH 2.20 and TGView 1.1.1.1 (Grimm, 2001) and zoned using the cluster analysis program CONISS (Grimm, 2001).

4.4.3.2. Foraminiferal Analysis

Foraminifera are abundant constituents of marine sediments and can provide detailed information concerning palaeoproductivity and bottom water circulation (Murray, 1991). Their distribution is primarily controlled by water temperature, salinity and nutrient supply (Murray, 1991). For example, specific high productivity faunas are associated with upwelling zones and reflect high fluxes of particulate organic matter (e.g. Lutze and Coulbourn, 1984; Corliss and Chen, 1988). Other assemblages are associated with bottom water mass characteristics and substrate

conditions (Douglas and Woodruff, 1981; Murray, 1991) and have been used to infer bottom water routes and distributions (e.g. Corliss, 1983; Mackensen et al., 1990, 1993). The analysis of marine microfossil assemblages can therefore provide a unique source of information on former climatic and oceanographic conditions. In this study, foraminifera present in each was identified to species level in order to assess hydrological changes in the lake basin.

Each sediment sample was wet sieved through 2 mm and 63 μm brass sieves, transferred to a petri dish, dried, weighed and examined for any macro-fossils (e.g. algal flakes). The >2 mm fraction was also dried, weighed and subsequently used to quantify the gravel grain-size fraction. The 2 mm to 63 μm sediment fraction was then resieved through a 125 μm -brass mesh and transferred to plastic petri dishes. Taxonomic work was carried out on the 125 μm –2.00 mm fraction under a Nikon microscope with external bipolar light source (Schott KL1500). Quantitative foraminiferal counts were achieved by counting the total number of tests in a known volume of sediment (foraminifera per gram of sediment). Species identification and taxonomy was based largely on Anderson (1975); Osterman and Kellogg (1979); Loeblich and Tappan (1988); Mackensen et al. (1990, 1993); Schmiedl et al. (1997) and Igarashi et al. (2001). Data were plotted using TILIA 2.0B4 (Grimm, 1991), TILIA*GRAPH 2.20 and TGView 1.1.1.1 (Grimm, 2001) and zoned using the cluster analysis program CONISS (Grimm, 2001).

4.4.4. Geochemistry and Isotopic analyses

4.4.4.1. $\delta^{18}O$, $\delta^{2}H$, $\delta^{13}C_{TDIC}$ analysis of lake water samples

Water samples for stable isotope analysis $\delta^{18}O$, $\delta^{13}C$ and $\delta^{2}H$ were filtered (Whatman GF/C, 0.45 μm) and stored in 125 ml acid-washed Nalgene bottles. Stable isotope analysis of water was determined by CO_2 equilibrium (Epstein and Mayeda, 1953) for ^{18}O and zinc reduction (Kendall and Coplen, 1985) for ^{2}H and isotope compositions are reported in standard delta (δ) notation (e.g. $\delta^{18}O$ and $\delta^{2}H$) using units per mille (‰) versus Vienna Standard Mean Ocean Water (VSMOW).

$$\delta\ (^{18}O, D) \text{ vs. SMOW} = (R_{sample}/R_{vSMOW} - 1)\ x1000$$

Where R is the ratio of $^{18}O/^{16}O$ or $^{2}H/^{1}H$ (Craig, 1961). The analytical precision (1SD) was better than 0.05 and 2 ‰ for $\delta^{18}O$ and $\delta^{2}H$ respectively. Total dissolved inorganic carbon (TDIC) for $^{13}C/^{12}C$ analysis was precipitated in the field by the addition of $BaCl_2$ + NaOH solution. Samples were reacted with anhydrous phosphoric acid *in vacuo* overnight; at a constant 25°C (McCrea, 1950) and the evolved CO_2 measured on a VG Optima mass spectrometer. Isotopic results for carbonate (precipitated total dissolved inorganic carbon) are reported in standard $\delta^{13}C$ notation in per mil (‰) versus VPDB, based on calibration of laboratory standards against NBS-19. Analytical reproducibility was normally better than 0.1 ‰ (2 sigma).

4.4.4.2. $\delta^{18}O$ and $\delta^{13}C$ on Authigenic Carbonate

Authigenic carbonate is precipitated in freshwater lakes as a result of photosynthetic activity (Gat, 1995). Authigenic carbonate is formed when submerged aquatic algae use dissolved CO_2 for photosynthesis leading to a CO_2 deficit in the lake water (Siegenthaler and Eicher, 1986). As a consequence, bicarbonate is decomposed into CO_2 and insoluble carbonate, which precipitates:

$$Ca^{++} + 2HCO_3 = CO_2 + CaCO_3 + H_2O$$

If it is assumed that authigenic carbonate forms in thermodynamic equilibrium with the lake water (Siegenthaler and Eicher, 1986; Talbot, 1990; Gat, 1995) then, variations in $\delta^{18}O$ preserved in precipitates reflect past changes in the isotopic composition of the lake water (Leng et al., 2001). In glacier-fed lakes the $\delta^{18}O$ of authigenic carbonate is a function of meteoric (snow and rain), glacial meltwater inputs versus through-flow and/or evaporation losses. Modern, hydrologically open lakes in Antarctica have $\delta^{18}O$ and $\delta^{2}H$ values which tend to cluster around the regional Global Meteoric Water Line (GMWL) (See Chapter 5) (Hermichen et al., 1985; Gillieson et al., 1990; Richter and Bormann, 1995; Lyons et al., 1998). This scenario is complicated however, by the addition of meltwater derived from older

(e.g. Pleistocene age) glacial ice (Richter and Bormann, 1995; Miller and Aiken, 1996), which can cause significant deviations from the MWL by increasing the input of more depleted waters (rich in ^{16}O) leading to more negative $\delta^{18}O$ values. In this study the $\delta^{18}O$ and $\delta^{13}C$ of authigenic carbonate will be used together with other proxies (e.g. foraminifera and diatoms) to reconstruct past changes in lake hydrology.

For each sample, 2 g of dry sediment was wet sieved at 80 μm. The < 80 μm fraction was collected in 500 ml Pyrex beakers and evaporated at 40°C. Once dry the samples were transferred to 50 ml plastic centrifuge tubes. Fifty ml of Analar-grade NaOH.Cl (5%) was added to each centrifuge tube to oxidise the organic material, and then left for 12 hours. Fifty ml of ultra-pure (MilliQ) water (pH_2O) was added to each sample and then filtered through Whatmans No. 1 filter papers that retained particles to 47 mm ∅ using a vacuum filter pump. 50 ml of pH_2O was then passed through the sample. This step was performed three times. Filter papers were oven dried for 12 hours and placed in a desiccator to cool. Sediment was carefully removed from the filter papers and the samples crushed in an acetone-cleaned agate pestle and mortar. The carbonate samples were measured at the NERC Isotope Geosciences Laboratory (Keyworth, UK). 10 mg of $CaCO_3$ was reacted with anhydrous phosphoric acid in *vacuo* overnight at a constant temperature of 25°C (McCrea, 1950). The liberated CO_2 was separated from water vapour and its stable isotope content of oxygen and carbon measured on a VG Optima mass spectrometer. Results are reported in $\delta^{18}O$ and $\delta^{13}C$ notation in per mil (‰) versus Vienna Peedee belemnite (VPDB), based on calibration of the laboratory standards against NBS-19 and NBS-22. Analytical reproducibility is better than 0.1 ‰ (2 σ) for both isotopes.

4.4.4.3. $\delta^{13}C$ and C/N on Bulk Sediment

The ratio of organic carbon (C_{org}) to nitrogen (N_{org}) content of sediment has been used together with isotope ratios of organic carbon ($^{13}C/^{12}C$; given the notation $\delta^{13}C$) to differentiate between marine and terrestrial sources of organic matter and provide information on past productivity (Macko et al., 1993; Thornton and

McManus, 1994; Muller and Mathesius, 1999). The application of these tracers is based on the existence of differences in C/N and $\delta^{13}C$ between different types of organic matter (Meyers, 1994; Schelske and Hodell, 1995; Ruttenberg and Goni, 1997, and references therein). As a general rule, enrichment of elementary nitrogen and ^{13}C occurs in organic matter of marine origin (Fig. 4.16) (Fontugne and Jouanneau, 1987; Meyers, 1994). During ice shelf presence the C/N ratio will be dominated by terrestrial-derived C and N and will have a likely signature of 8-10 whilst the carbon isotopic composition of the sediment will be depleted in ^{13}C and characterized by freshwater algal values, yielding $\delta^{13}C_{org}$ values between –30 and –25 ‰ (see conceptual model in Chapter 5).

4.4.4.3.1. C/N Ratios

The C/N ratio reflects protein content, which is the most important nitrogen-containing component in living organisms (Muller and Mathesius, 1999). Together with carbohydrates and lipids, proteins account for the greatest part of the organic matter of living organisms. Marine algae generally contain more protein than higher land plants, resulting in a lower C/N ratio (Muller, 1975). In the Antarctic, C/N ratios are on the whole relatively low (~ 4 – 12), due to the absence of vascular plants which commonly contain a higher carbon content (cellulose) resulting in C/N ratios of 20 or greater (Fig. 4.16) (Meyers, 1997). Thus, the C/N ratios of planktonic organisms usually vary between 4 and 7 (Bordovskiy, 1965), zooplankton and phytoplankton have average C/N ratios between 5 and 6 (Redfield et al., 1963; Bordovskiy, 1965), whilst benthic organisms and bacteria are generally very rich in protein and have C/N ratios around 4.2 and 4.1 (Bordovskiy, 1965). Unfortunately, organic compounds are subject to selective degradation and alteration both on their passage through the water column and in the uppermost layer of the sediments (Kulbe et al., 2001). Partial degradation of algal organic matter during sinking can diminish proteinaceous compounds thereby increasing the C/N ratio (Meyers, 1997). Conversely, lower C/N ratios have been observed in ocean sediments due to the absorption of ammonia derived from the decomposition of organic matter accompanied by its recyrstalisation and release of carbon (Meyers, 1997). However, it is thought that the C/N ratio in lacustrine sediments is usually preserved well

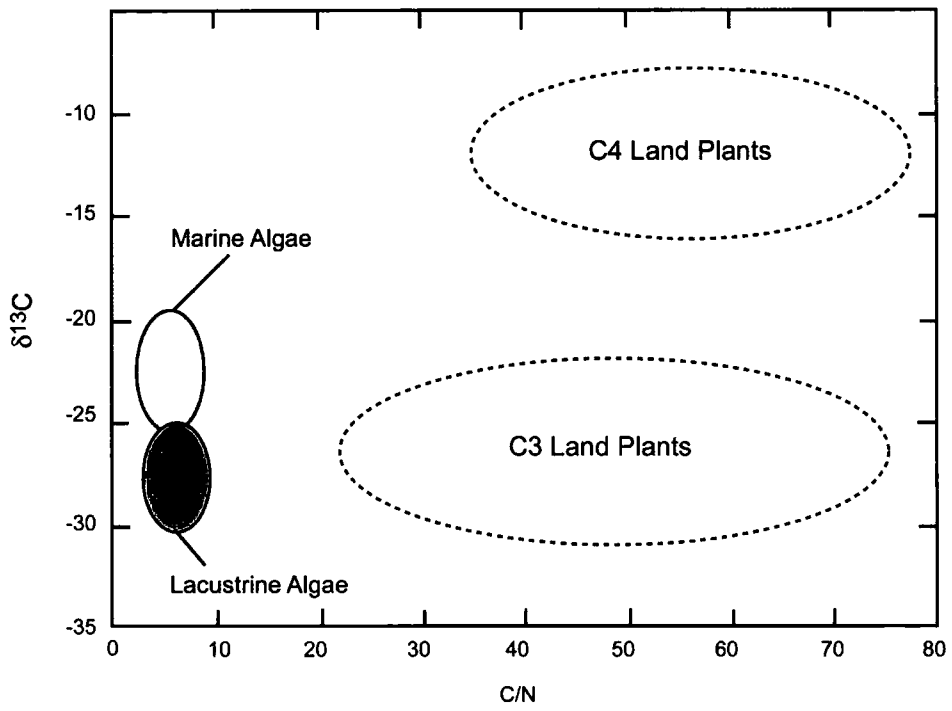

Figure 4.16. Elemental (atomic C/N ratio) and isotopic ($\delta^{13}C$ value) identifiers of bulk organic matter produced by marine algae, lacustrine algae, C3 plants and C4 land plants. Data fields are from Meyers (1994).

enough to reflect the intensity of primary production (Eppleby and Peterson, 1979). There is also a grain-size effect, with different fractions having different C/N ratios that must be borne in mind (e.g. Thompson and Eglington, 1978; Keil et al., 1994; Prahl et al., 1994; Meyers, 1997). Hydrodynamic sorting of sediment can therefore influence C/N ratios, which can potentially bias source discrimination (Meyers, 1997). In general, the C/N ratio in fine sediments is lower compared with coarse sediment (Meyers, 1997). This is because the fine fractions contain a larger proportion of clay minerals, which have a large surface area and negative surface charge, both of which enhance the absorption of ammonia. Their C/N ratio can be depressed by the uptake of inorganic nitrogen (Meyers, 1997). Whilst a grain size effect must be considered, changes in the elemental composition of sedimentary organic matter due to grain size are not normally large enough to erase the larger overall signal from the C/N ratio (Meyer, 1994).

In the Antarctic C/N ratios have been routinely used to assess variations in palaeoproductivity (Lawrence and Hendy, 1989; Björck et al., 1991; Wharton et al., 1993; Doran et al., 1998; McMinn, 2000; Kulbe et al., 2001) with periods of high primary productivity showing higher C/N ratios (e.g. Kulbe et al., 2001). Their use as a source discriminator however is problematic since benthic cyanobacteria and diatoms dominate the overall lake biomass with aquatic mosses forming the highest form of plants (Hodgson et al., 2003), all of which have similar C/N ratios. For this reason, in this study the C/N ratio will be used to assess productivity rates, whilst the $^{13}C/\ ^{12}C$ ratio of organic matter will be used to detect changes in source.

4.4.4.3.2. $\delta^{13}C$ on Organic Matter

Carbon isotope ratios have been used successfully to distinguish between lacustrine and marine-derived algae (Fontugne and Jouanneau, 1987; Meyers, 1994, 1997; Muller and Voss, 1999; Westman and Hedenström, 2002). Emeis et al. (2003) have even suggested a direct link between the $\delta^{13}C_{org}$ value and salinity. Typical values of $\delta^{13}C_{org}$ for freshwater plankton lie between –30 and –25‰, whereas marine plankton have $\delta^{13}C_{org}$ values between –20 and –25‰ (Fig. 4.16). The carbon isotope composition of organic matter is controlled by a number of factors.

Biological production is the most important (McKenzie, 1985) with carbonate precipitation, respiration of organic matter and CO_2 exchange between the water and atmosphere also contributing (Menking et al., 1997). Most photosynthetic plants incorporate carbon into organic matter using the Calvin (C_3) pathway. This preferentially fractionates against ^{12}C to produce a shift of about –20‰ from the isotope ratio of the inorganic carbon source (Meyers, 1997). Organic matter that is produced from atmospheric CO_2 ($\delta^{13}C \sim -7‰$) by land plants using the C_3 pathway has an average $\delta^{13}C_{org}$ (relative to PDB) of ~ -27‰ (Meyers, 1997). Freshwater algae exploit dissolved CO_2, which is usually in equilibrium with atmospheric CO_2 (Meyers, 1997). Because of this, the isotopic composition of lake-derived organic matter is very similar to that from the surrounding catchment (e.g. Nakai, 1972; Benson et al., 1991; Tenzer et al., 1997). For marine algae the source of inorganic carbon is from dissolved bicarbonate, which has a $\delta^{13}C_{org}$ value of ca. 0‰ (Meyers 1997). As a consequence, marine organic matter has $\delta^{13}C_{org}$ values between –20 and –22‰ (Meyers 1994). The ca. 7‰ difference between marine-derived organic matter and lacustrine organic matter can therefore be used to discriminate between sources (e.g. Fontugne and Jouanneau, 1987; Prahl et al., 1994; Meyers, 1994, 1997; Muller and Voss, 1999; Westman and Hedenström, 2002). Furthermore, unlike C/N ratios, the carbon isotope ratio is relatively conservative and unaffected by grain size, making them particularly useful in reconstructing past organic sources in areas of changing depositional processes (Meyer, 1997).

However, some studies have shown that this isotopic partitioning may not always exist in the Antarctic. For example Doran et al. (1994) have reported a very wide range of $\delta^{13}C$ values (-1.9 to –25.7 ‰) for sediments retrieved from Lake Hoare, an oligotrophic lake in Taylor Valley, Antarctica, while highly fractionated values as high as –12 ‰ have been recorded from sea ice (Dunbar and Leventer, 1992; McMinn et al., 1999b). Likewise, Gibson et al. (1999) have reported a range of –5 to –20 ‰ for Ross Sea sediments, whilst Rau et al. (1989) have reported values as low as –28 ‰ for marine algae in the Southern Ocean. The latter value largely reflects the fact that cold waters are capable of holding more dissolved CO_2 than temperate and tropical waters, thereby allowing greater isotopic discrimination by algae. The possibility that the isotopic partitioning between marine and terrestrial

organic algae can break down in Antarctic sediments must therefore be borne in mind.

For each sample, ca. 2 g of dry sediment was dry- sieved through a 1 mm mesh. The sample was then transferred to a 50 ml plastic centrifuge tube with screw cap. Carbonate was dissolved by adding 50 ml 5% HCL (Analar made up with deionised water) for 12 hrs. Each sample was then filtered through Whatmans No. 1 filter papers using a vacuum filter pump. 50 ml of pH_2O was then passed through the sample. This step was performed three times. Filter papers were removed from the vacuum and oven dried for 12 hours, then placed in a desiccator to cool. Sediment was carefully removed from the filter papers and the samples crushed in an acetone-cleaned agate pestle and mortar. 50 ± 0.1 mg was then accurately weighed into small tin capsules (8 x 5 mm) using a Sautorius high precision balance.

$^{13}C/^{12}C$ ratios, % Carbon (C) and % Nitrogen (N) of bulk organic matter were then analysed at the NERC Isotope Geosciences Laboratory (Keyworth, UK) by combustion in a Carlo Erba 1500 on-line to a VG Triple-Trap and Optima dual-inlet mass spectrometer, $\delta^{13}C$ values were calculated to the VPDB scale using a within-run laboratory standard (BROC1) calibrated against NBS-19 and NBS-22. C/N ratios are calibrated against an Acetanilide standard.

4.4.4.4. $\delta^{18}O$ and $\delta^{13}C$ on Foraminifera

The isotopic compositions (oxygen and carbon) of deep-sea benthic foraminifera have been used extensively to examine secular changes in global ice volume, deep ocean circulation and temperature and nutrient cycling (Shackleton and Opdyke, 1973; Duplessy et al., 1980; Grossman et al., 1984a,b). This is due largely to the fact that the stable isotopic composition of foraminiferal carbonate reflects the isotopic composition of the water mass in which it lives. In this thesis, the $\delta^{18}O$ and $\delta^{13}C$ composition of foraminifera are used to investigate changes in lake hydrology associated with different ocean water masses (e.g. Ice Shelf Water and Upper Circumpolar Deep Water).

4.4.4.4.1. Oxygen Isotopes

The distribution of $\delta^{18}O$ in ocean waters is controlled primarily by the hydrological cycle, i.e. the ratio of evaporation and precipitation acting on the surface water masses and the amount of meteoritic water stored in continental ice caps (Mackensen et al., 1996). Additional factors such as sea-ice freezing and melting (MacDonald et al., 1995) the advection and mixing of water masses from different sources areas (Paren and Potter, 1984) and the addition of water enriched in ^{18}O (glacier/ice shelf ice) are also very important for the basic composition of $\delta^{18}O_{water}$ at any site. The ice volume effect is formidable such that the glacial to interglacial transition appears as a negative shift (on a profile of glacial-age to recent values) of between 0.3 and 1.3 ‰ (Anderson and Arthur, 1983), although the ice-volume effect is considered to be less important on Holocene time-scales.

Ocean temperature at the time of calcification plays an extremely important role in the isotopic composition of foraminifera. The overall reaction for precipitation of carbonate is based on a thermodynamic fractionation between ^{16}O and ^{18}O (Urey, 1947). This fractionation, which offsets the $\delta^{18}O$ of carbonate minerals relative to seawater by ca. + 30‰ is a logarithmic function of temperature with a slope over the oceanic temperature range of –2 °C to 30 °C, of between –0.20 and –0.27 ‰ per °C (Kim and O'Neil, 1997). Because the oxygen isotope proxy is based on a thermodynamic principle it is considered to be relatively robust and relatively unaffected by secondary kinetic effects (e.g. diffusion) (Lea, 2004), although secondary effects such as ontogenic (growth) are thought to be important. The temperature dependence of fractionation has led to the development of isotopic palaeothermometers or palaeotemperature equations (see Rohling and Cooke (1999) and Lea (2004) for more detailed reviews). The most significant complication in using the oxygen isotope to determine temperature is that $\delta^{18}O$ of carbonate solids reflects both temperature and the $\delta^{18}O$ of seawater. As noted above the $\delta^{18}O$ of seawater is controlled by continental ice volume and the evaporation-precipitation balance or 'salinity effect'. Both effects cast uncertainty on the use of oxygen isotope ratios for absolute and relative palaeothermometry (Lea, 2004). In

addition, there are several disequilibria effects, which influence the isotopic composition of benthic foraminiferal calcite such as vital effects (Duplessy et al., 1970), offsets due to ontogeny (growth) (Spero and Lea, 1996), and offsets due to carbonate ion concentration of seawaters (Spero et al., 1997). A more detailed account of these factors in provided by Rohling and Cooke, (1999). These factors must be borne in mind when interpreting the $\delta^{18}O$ signal.

4.4.4.4.2. Carbon Isotopes

The distribution of $\delta^{13}C$ in water mainly depends on the biological cycle of ^{13}C-depelted organic matter and the effects of gas exchange at the air-sea interface. Thus, the $\delta^{13}C$ signature of benthic foraminifera can be used to infer nutrient concentrations and changes in deep-sea circulation (Grossman, 1984a, b). However, disequilibrium effects also complicate the use of carbon isotopes for palaeoenvironmental reconstructions. Factors such as ambient pore water $\delta^{13}C$ at the species' preferred living depth of microhabitat (Grossman, 1984a, b; McCorkle et al., 1985) and respiratory CO_2 (vital effects) (Grossman, 1984a) are particularly important.

4.4.4.4.3. $\delta^{18}O$ and $\delta^{13}C$ analysis

The two most abundant foraminifera species in the sediment core (*Globocassidulina biora* and *Cibicides sp.*) were selected for isotopic ($\delta^{18}O$ and $\delta^{13}C$) analysis in order to reconstruct oceanographic conditions at the time of deposition. Both are calcareous benthic species and have been routinely used for isotopic analysis (Shackleton, 1974; Grossman, 1984a,b; Poole et al., 1994; Shackleton and Hall, 1994, 1997; Serjup et al., 1999). Between 15-30 handpicked tests of *Globocassidulina biora* and *Cibicides sp.* (after Igarashi et al., 2001) were transferred to plastic centrifuge tubes using a synthetic brush. 10 ml of deionised H_2O water was added to each sample. Tubes were then sonicated in an ultra sonic bath for two minutes to remove any internal/external impurities, such as clay. The overlying solution was removed using a pipette. This step was repeated until all visible contaminants were removed. Samples were then oven dried at 40°C. Once

dry, the samples were carefully transferred to an acetone-cleaned pestle and mortar and crushed to a fine powder. 50 μg of carbonate, weighed on a Sautorius balance were analysed for $\delta^{18}O$ and $\delta^{13}C$ at the NERC Isotope Geosciences Laboratory (Keyworth, UK) using a VG Isocarb on-line to a VG Triple-Trap and Optima dual-inlet mass spectrometer. Results are reported in $\delta^{18}O$ and $\delta^{13}C$ notation in per mil (‰) standardized to VPDB, based on calibration of the laboratory standards against NBS-19. Analytical precision was typically <2%. *Globocassidulina* species have been found to crystallise with isotopic values of –0.1 and 0.5‰ (Shackleton and Hall, 1997), whilst *Cibicides* species have been found to crystallise 0.58 ± 0.31‰ and 0.0‰ lighter than equilibrium (Poole et al., 1994; Shackleton and Hall, 1997) for $\delta^{18}O$ and $\delta^{13}C$ respectively. These corrections were applied to the data generated in this study.

4.5. Summary

This chapter has described the physical setting of the study site and has documented the limnology and bathymetry of Moutonnée and Ablation Lakes. This information has been largely based on work undertaken in the 1970's (e.g. Heywood, 1977). This chapter also outlined the field techniques used during 2000-1 and 2001-2 and has provided the rationale for the laboratory techniques employed in this thesis. This information will be used in the following chapters to reconstruct the environmental history of ML and AB with the primary aim of determining the Holocene history of George VI Ice Shelf.

Chapter 5

THE PRESENT DAY LIMNOLOGY AND SEDIMENTARY ENVIRONMENT OF MOUTONNÉE AND ABLATION LAKES: DEVELOPMENT OF A CONCEPTUAL MODEL FOR DETECTING ICE SHELF HISTORIES

5.1. Introduction

Chapter 4 provided a detailed description of the environmental setting and physical limnology of ML and AB that was based largely on work undertaken in the early 1970's (e.g. Heywood, 1977) and supplementary information collected in 2000-2001 and 2001-2002. The intention of this chapter is to provide a baseline study of the present day limnology of ML and AB (re-measured in 2000-1 and 2001-2) and to develop a conceptual model that will be used to help interpret the millennial scale history of GVI-IS. The conceptual model is necessary to provide the basis for the interpretation of proxy records from the lakes, presented in Chapter 4. An additional aim of this chapter is compare the physical limnological measurements made for this thesis with earlier data (e.g. Heywood's data from 1973) and thus provide a perspective on changes in these lakes over the last 30-years. It is hoped that this will provide a useful limnological data set to use as a baseline for possible GVI-IS collapse. Such a dataset was available at Disraeli Fiord, an epishelf lake on the northern coast of Ellesmere Island, Arctic Canada, which displayed very unique changes in its water chemistry prior to the break-up of the Ward Hunt Ice Shelf (Mueller et al., 2003).

5.2. Results

5.2.1. Vertical water chemistry profiles

5.2.1.1. CTD, DOx, pH

ML: In 2000 conductivity was relatively constant in the mixolimnion, increasing markedly across a halocline at 38-42, and then relatively constant in the monimolimnion (Fig. 5.1). Water temperature was low directly beneath the lake ice, stable until 30 m, followed by a thermocline to 44 m where it reached a minimum of –1.3°C. DOx levels were variable in the water column reaching a maximum at 12 m, sustained low levels between 26-40 m, and a brief increase at 42 m at the halocline. DOx levels then declined in the monimolimnion. Similar patterns were observed in 2001, but with a shallower halocline, thermocline and oxycline and higher (relative) oxygen concentrations in the lower parts of the mixolimnion. In 2001, pH (not measured in 2000) increased with depth reaching a maximum of 8.8 at 32 m before a stepwise decrease, reaching a minimum value of 7.61 directly above the sediment water interface.

AB: Water column chemistry was much more variable across years in AB with gradual haloclines occurring from c. 50 m water depth (Fig. 5.2). In 2001 the halocline was particularly weak with salinity rising to only 0.8 psu. Water temperature profiles were markedly different between years, with the only common factor being increases directly below the lake ice surface. In both years DOx decreased with depth but had a more marked oxycline below 60 m in 2001. In 2001, pH (not measured in 2000) increased from 7.55 – 7.82 in the mixolimnion with a marked increase at the halocline rising to a maximum of 8.09 at the sediment water interface.

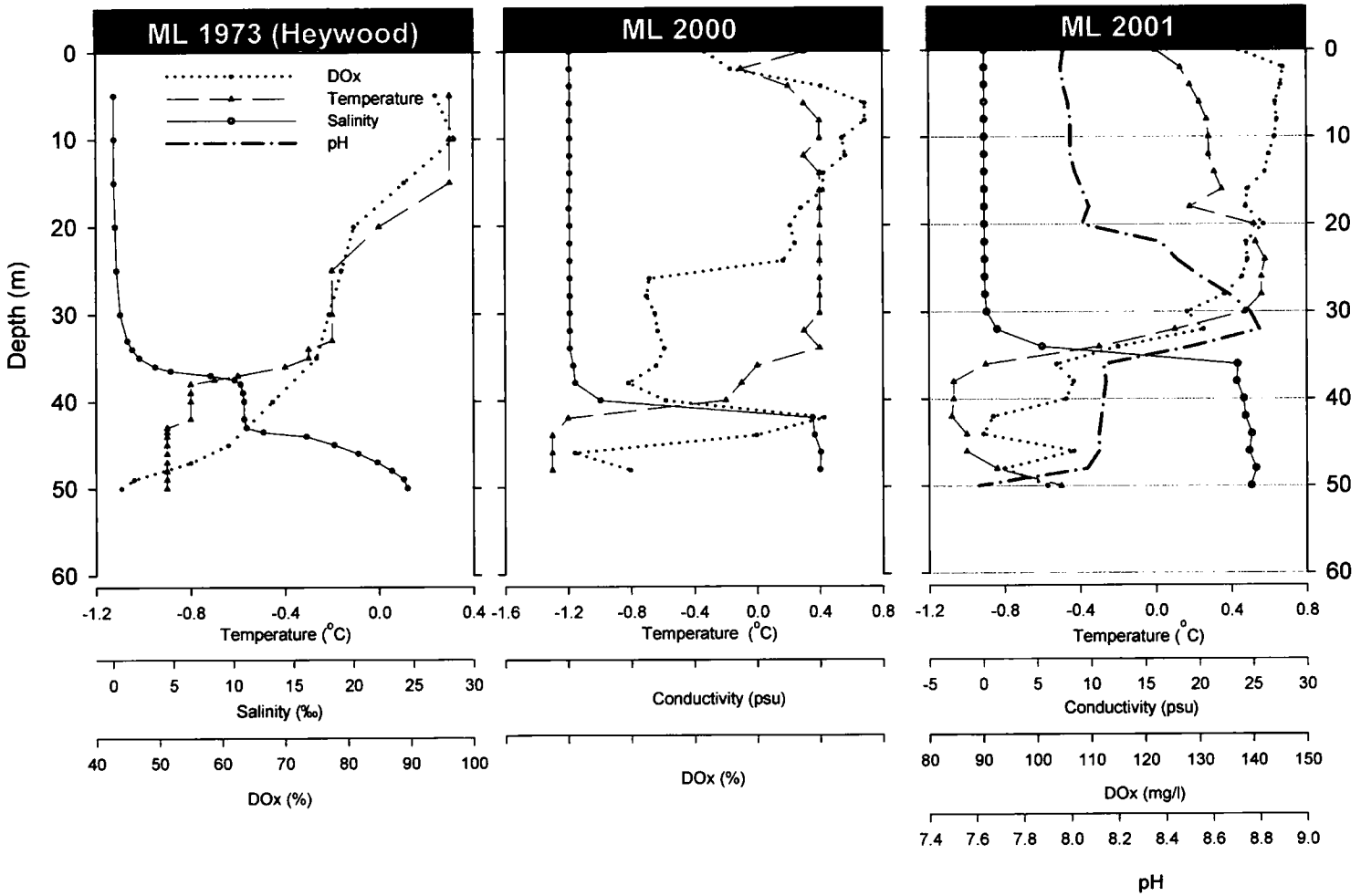

Figure 5.1. CTD profiles from Moutonnée Lake; (a) December 31st 1973 (Heywood, 1977); (b) 27th November 2000; and (c) 24th November 2001. Conductivity and DOx values are not shown on the x-axis for 2000 (discussed in the text) due to problems with CTD probe.

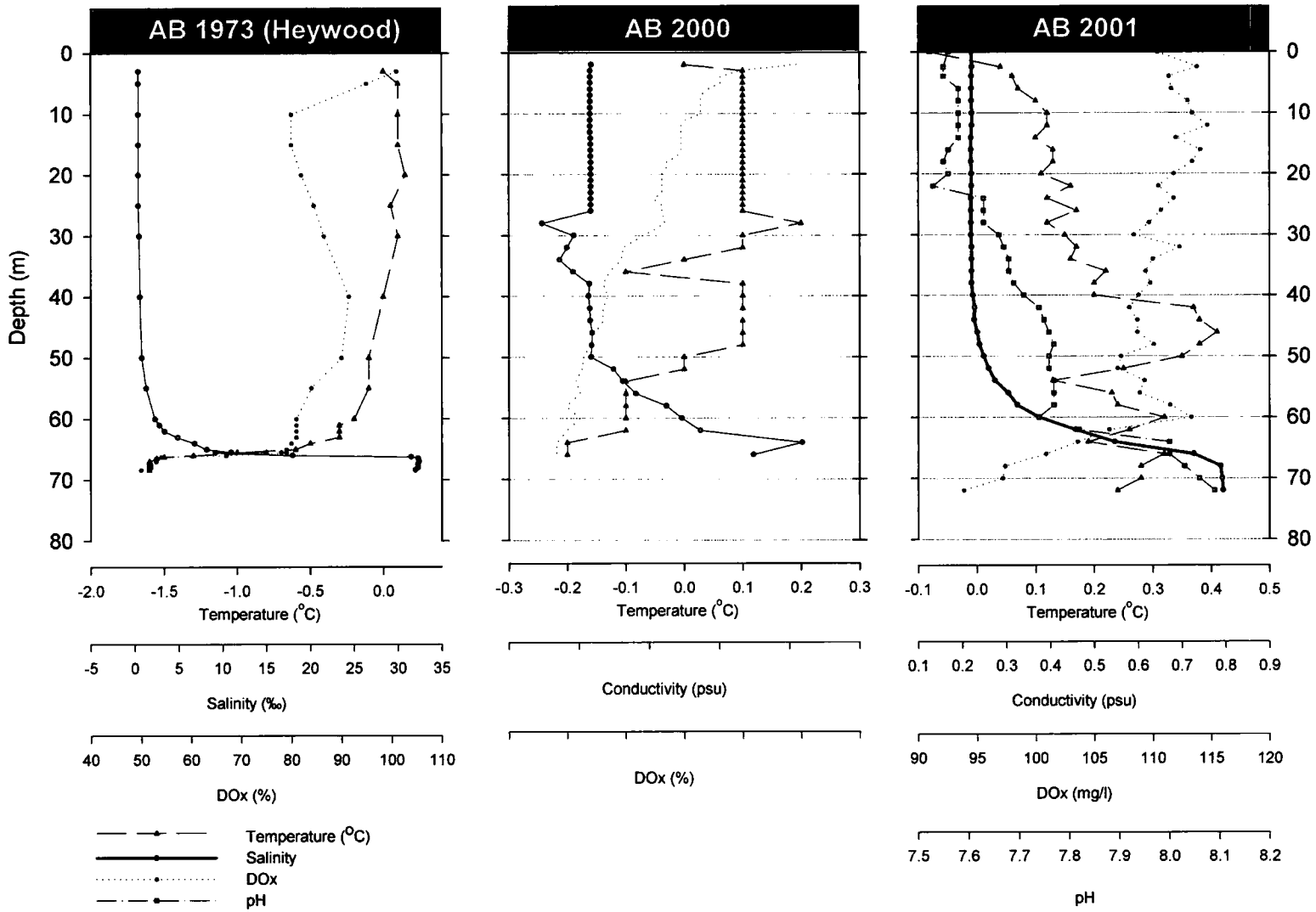

Figure 5.2. CTD profiles from Ablation Lake; (a) 30th November 1973 (Heywood, 1977); (b) 8th December 2000; and (c) 2nd December 2001. Conductivity and DOx values are not shown on the x-axis for 2000 (discussed in the text) due to problems with CTD probe.

5.2.1.2. Stable Isotopes ($\delta^{18}O$, $\delta^{2}H$, $\delta^{13}C_{TDIC}$) analysis – water samples

The lake water dataset contains 31 samples from Moutonnée and Ablation Lakes taken in 2000 and 2001. Values ranged from – 0.9 ‰ to –21.07 ‰ for $\delta^{18}O$ and from –9.2 ‰ to –149 ‰ for $\delta^{2}H$ (Fig. 5.3).

ML: $\delta^{2}H$ values remained constant at c. –148 ‰ through the mixolimnion but were much higher (– 9.2 ‰) below the halocline (Fig. 5.3). $\delta^{18}O$ values followed a similar pattern, being much higher below the halocline. In 2000, the $\delta^{13}C_{TDIC}$ (TDIC; Dissolved Inorganic Carbon; DIC) values were below detection, except in the surface layer (-2.4 ‰). In 2001 $\delta^{13}C_{TDIC}$ values ranged from –11.4 to –0.5 ‰ with a shift to more negative values at 35 m, coincident with the halocline.

AB: Both $\delta^{2}H$ and $\delta^{18}O$ values remained constant through the mixolimnion (Fig. 5.3), reflecting the presence of a strong halocline (*cf.* ML). In 2000, the $\delta^{13}C_{TDIC}$ values in the upper 25 m of the water column were characterized by decreasing $\delta^{13}C_{TDIC}$ from - 12.4 to - 19.4 ‰, increases at 35 and 45 m, and undetectable values at 55 and 65 m. In 2001 $\delta^{13}C_{TDIC}$ values ranged from –21 to 10.6 ‰ and were variable through the water column.

5.2.1.3. Plankton

Analyses of plankton in 2 litres of water from each of the sampling depths revealed no diatom plankton in ML or AB. The absence of plankton in the water samples suggests that both lakes are unproductive, a fact that is likely to reflect the presence of perennial lake ice and/or nutrient limitation. This is discussed further in the following sections. Bacteria and viruses were not studied.

5.2.1.4. Nutrients

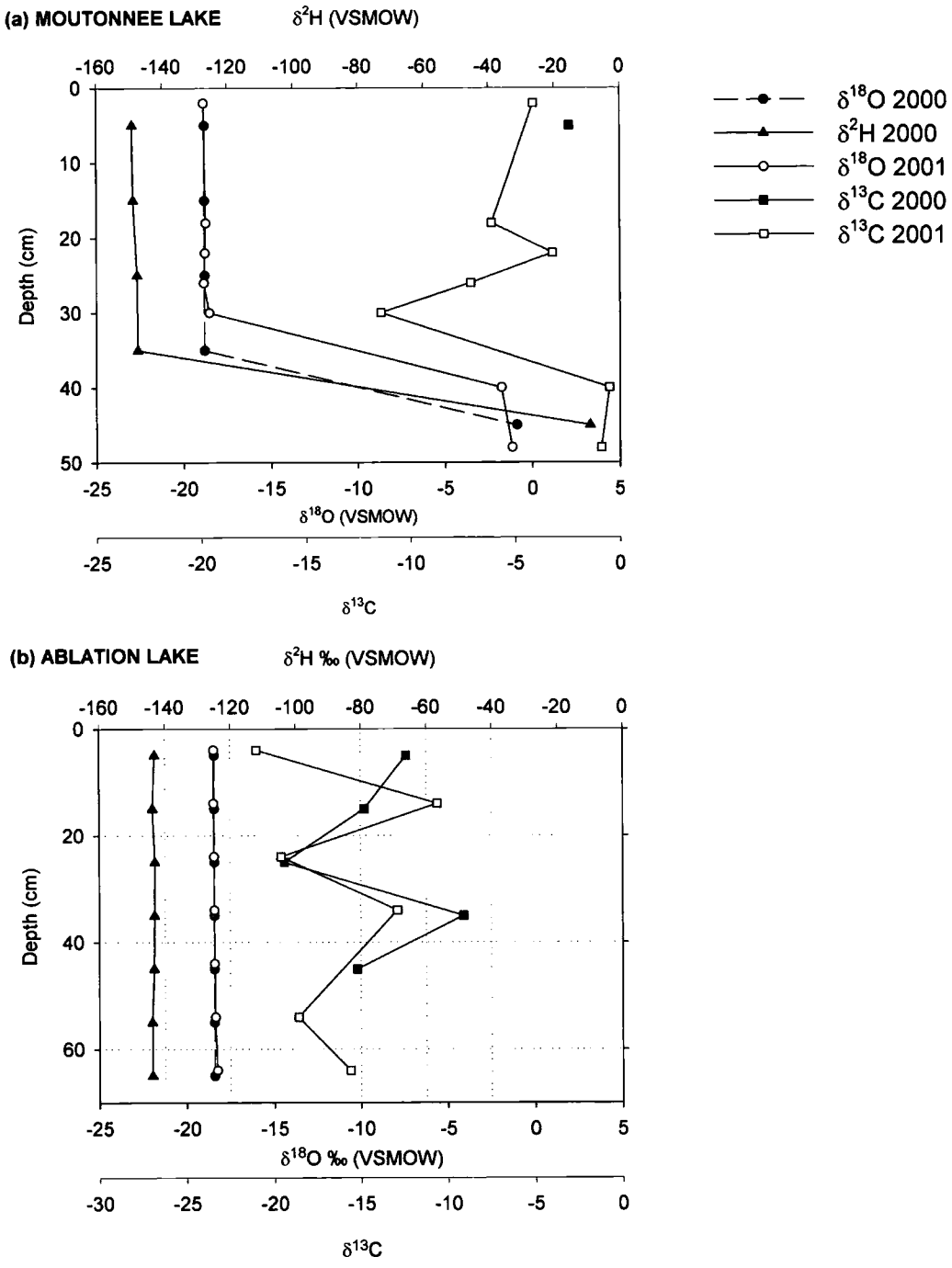

Figure 5.3. $\delta^{18}O$, $\delta^{2}H$ and $\delta^{13}C$ lake water profiles; (a) Moutonnée Lake; (b) Ablation Lake.

Nutrients were near, or below, detection limits in all samples (Table 5.1). Nitrate was only recorded in the upper 5 m of ML and at 65 m in AB. Nitrite was below detection limits in all samples. Ammonia was detected at 5 m in AB at 36.8 μM. Phosphate was present just above detection limits in the surface and basal samples in both lakes and at 35 m in AB. Silicate levels were below detection limits in both lakes.

5.2.2. Surface sediment transects and sediment traps

5.2.2.1. $\delta^{13}C_{org}$ and C/N ratios in surface sediments

ML: $\delta^{13}C_{org}$ values of the surface sediments ranged between –25.7 and –20.4 ‰ and were higher in the shallow water surface sediments (out to 450 m along surface sediment transect) and lower in the deeper water and near the ice shelf front (Fig. 5.4). C/N values ranged between 7.8 and 10.5 and were generally higher in the shallower surface sediment samples. C/N values decreased from 10.5 at transect point 1 (TP1) to 8.4 at TP4. Both $\delta^{13}C_{org}$ and C/N values increased towards TP6, with $\delta^{13}C_{org}$ reaching a maximum value of –20.4 ‰. $\delta^{13}C_{org}$ values then decreased rapidly, reaching a minimum of –25.6 ‰ at TP9. From this point $\delta^{13}C_{org}$ values remained constant along the rest of the transect.

AB: $\delta^{13}C_{org}$ values ranged between –25 and –15.5 ‰ and C/N values ranged between 7.8 and 9.7 (Fig. 5.5). Maximum values of both $\delta^{13}C_{org}$ (-15.5) and C/N (9.7) occured at TP1. Values of $\delta^{13}C_{org}$ and C/N both decreased towards TP4. From this point, C/N values fluctuated between 8 and 9 whilst $\delta^{13}C_{org}$ values increased slightly at TP5 before declining to a minimum value of –25.4 ‰ at TP9.

5.2.2.2. C_{org} and N_{org} in surface sediments

ML: C and N co-vary along the entire transect, fluctuating between 0.25-0.62 and 0.03-0.07 respectively (Fig. 5.4). As a general trend, values increase from TP1, and then decrease before increasing steadily towards TP12. From this point, values generally decrease reaching a minimum at TP18.

SITE NAME	SAMPLE DEPTH	ALKALINITY meq. L-1	NITRATE NO3 μN	NITRITE NO2 μN	AMMONIA NH4 μM	PHOSPHATE PO4 μM
Moutonnée	5	0.164	0.783	-0.013 bd	-1.55 bd	0.036
	15	0.168	bd	bd	0	bd
	25	0.175	bd	bd	-0.117 bd	bd
	35	0.18	bd	bd	-0.112 bd	bd
	45	3.127	bd	-0.385 bd	-1.54 bd	4.438
Ablation	5	0.041	-0.463 bd	-0.155 bd	36.789	0.021
	15	0.085	bd	bd	-0.05 bd	bd
	25	0.068	bd	bd	-0.554 bd	bd
	35	0.071	-0.106 bd	-0.011 bd		0.005
	45	0.072	bd	bd	-0.035 bd	bd
	55	0.075	bd	bd	-0.336 bd	bd
	65	0.079	0.161 bd	-0.002 bd	-0.233 bd	0.028

Table 5.1. Nutrient analysis of lake water (2000-01). Abbreviations (bd = below detection).

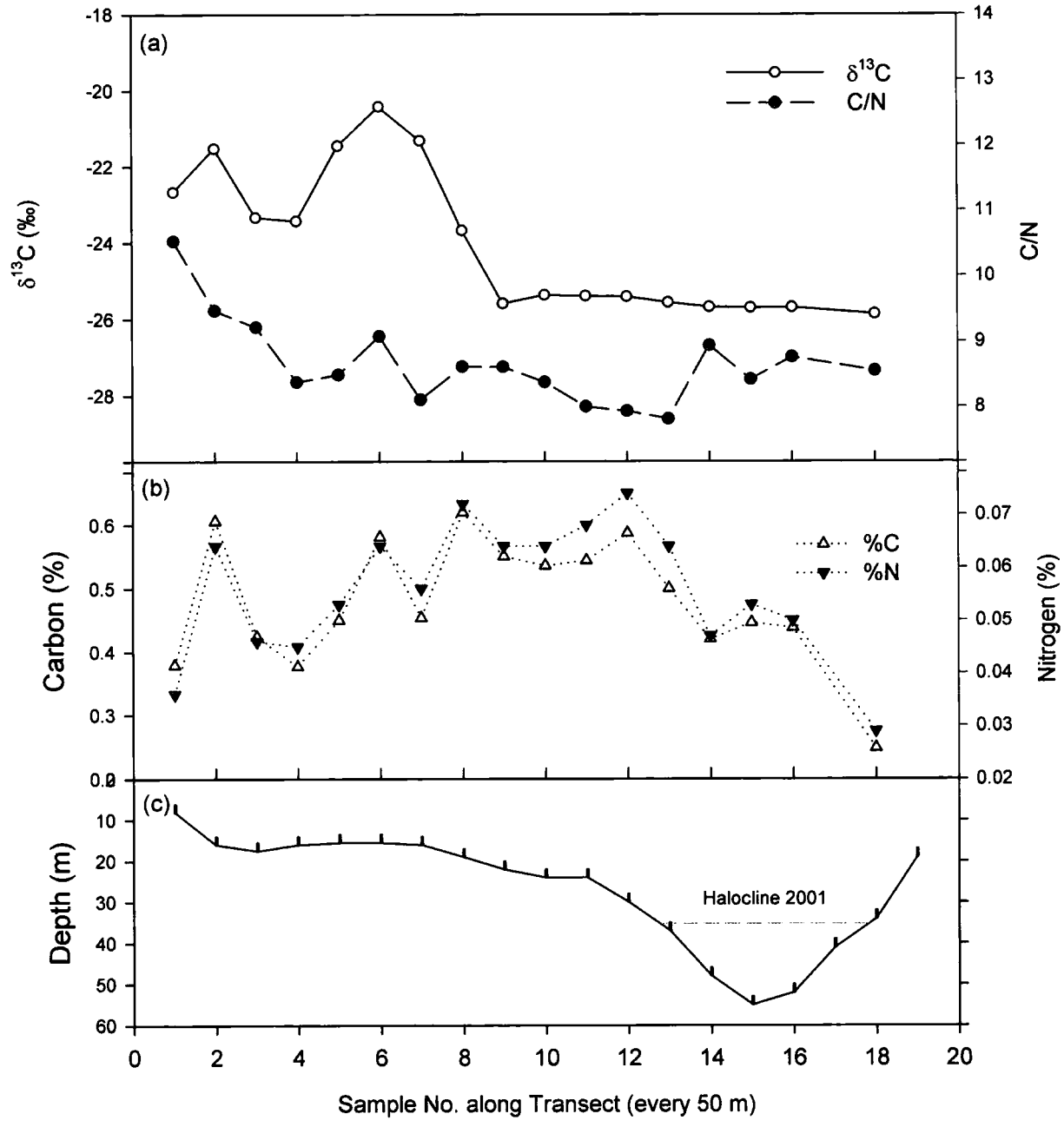

Figure 5.4. Showing Moutonnée Lake surface sediment transects: **(a)** $\delta^{13}C_{organics}$ and C/N; **(b)** %Carbon and % Nitrogen; **(c)** transect profile and water depth. Position of halocline in 2001 is also shown.

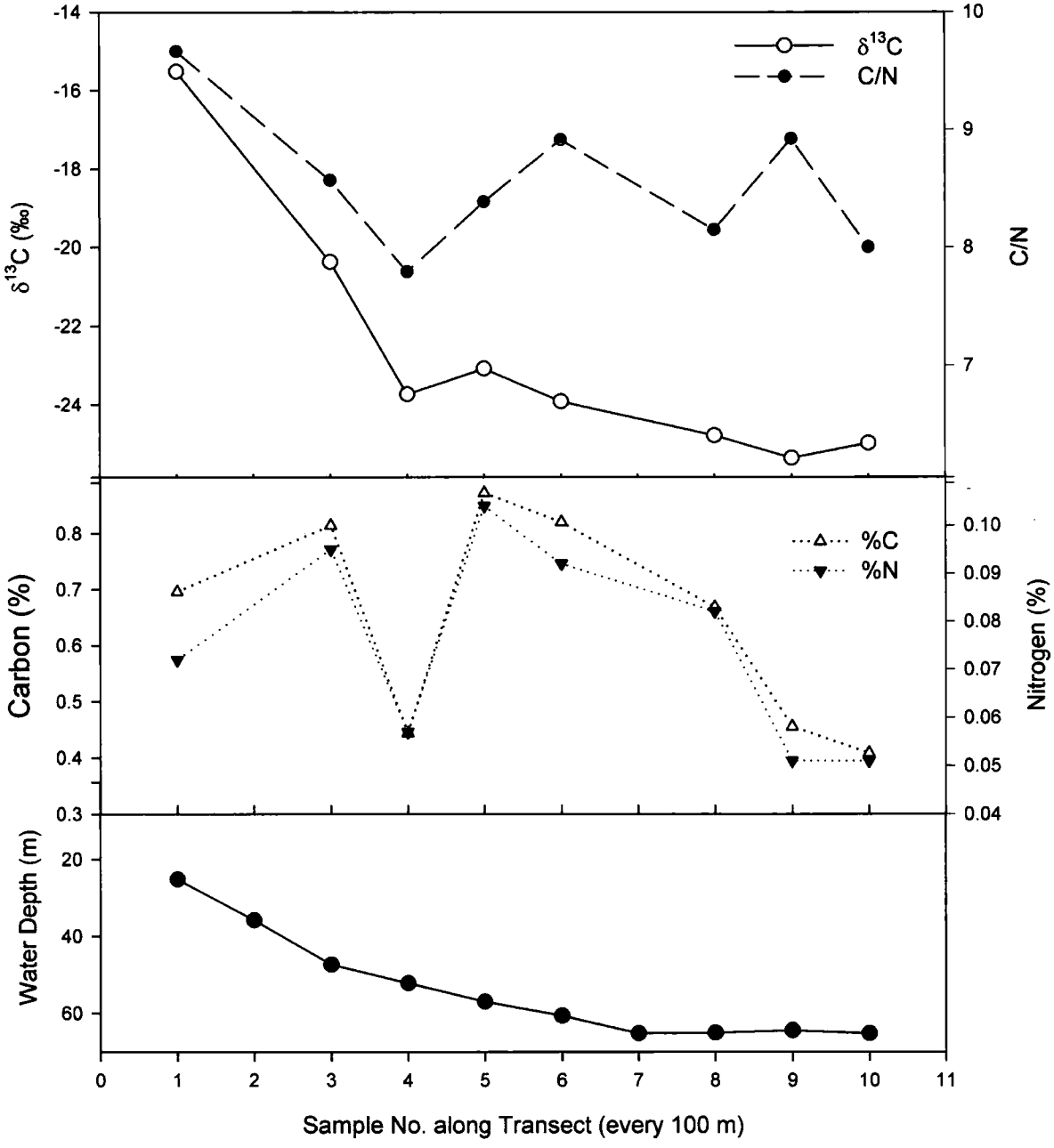

Figure 5.5. Showing Ablation Lake surface sediment transects: **(a)** $\delta^{13}C_{organics}$ and C/N; **(b)** %Carbon and % Nitrogen; **(c)** transect profile and water depth

AB: C and N co-vary along the entire transect, fluctuating between 0.41-0.87 and 0.05-0.10 respectively (Fig. 5.5). Values increase, and then decrease before increasing steadily reaching a maximum at TP5. Values then generally decrease towards TP10.

5.2.2.3. Diatoms in surface sediments

The diatom flora in the surface sediments from ML and AB consist of 23 taxa of which 4 could not be designated to species level. The assemblage compromises freshwater, brackish and marine taxa (halobian classification based on Wasell and Håkansson, 1994; Cremer et al., 2000; 2003).

ML: Quantitative counts of the diatom composition of sediment samples taken along a transect from the lake shoreline to the ice shelf front has been undertaken. The resulting diagram (Fig. 5.6) has been divided into four zones using CONISS (Grimm, 1987). Absolute diatom (valves g^{-1} sediment) abundance has also been calculated and is shown in Figure 5.6.

Zone 1 (TP1 (Lake shoreline) – 6). High relative abundances of freshwater taxa occurred in Zone 1, including *Achnanthes linkei* (61.9%), *Navicula cf. heufleriana* (10.8%), *Navicula molesta* (8.5%) and *Gomphonema angustatum/parvulu* (8%). Other significant taxa (>2%) included *Diadesmis perpusilla* (5.5%), and *Achnanthes taylorensis* (2.1%), which tolerates both fresh and brackish water. *A. Linkei*, was only present at >2% in the first three transect samples. Relative numbers of *N. cf. heufleriana*, *N. molesta* and *G.angustatum/parvulum* also decreased rapidly beyond TP3 and disappeared entirely at the boundary between Zone 1 and Zone 2. This was reflected in an overall decrease in the total number of valves (Fig. 5.6) from a maximum of 112082 valves g^{-1} sediment near the lake shoreline to 0 valves at the boundary between Zone 1 and 2 (Fig. 5.6).

Zone 2 (7-11). The boundary between Zones 1 and 2 was characterised by an increase in *A.taylorensis* and the disappearance of all the freshwater taxa present in Zone 1. *A. taylorensis*, dominated Zone 2 and reached a maximum of 91.2% at

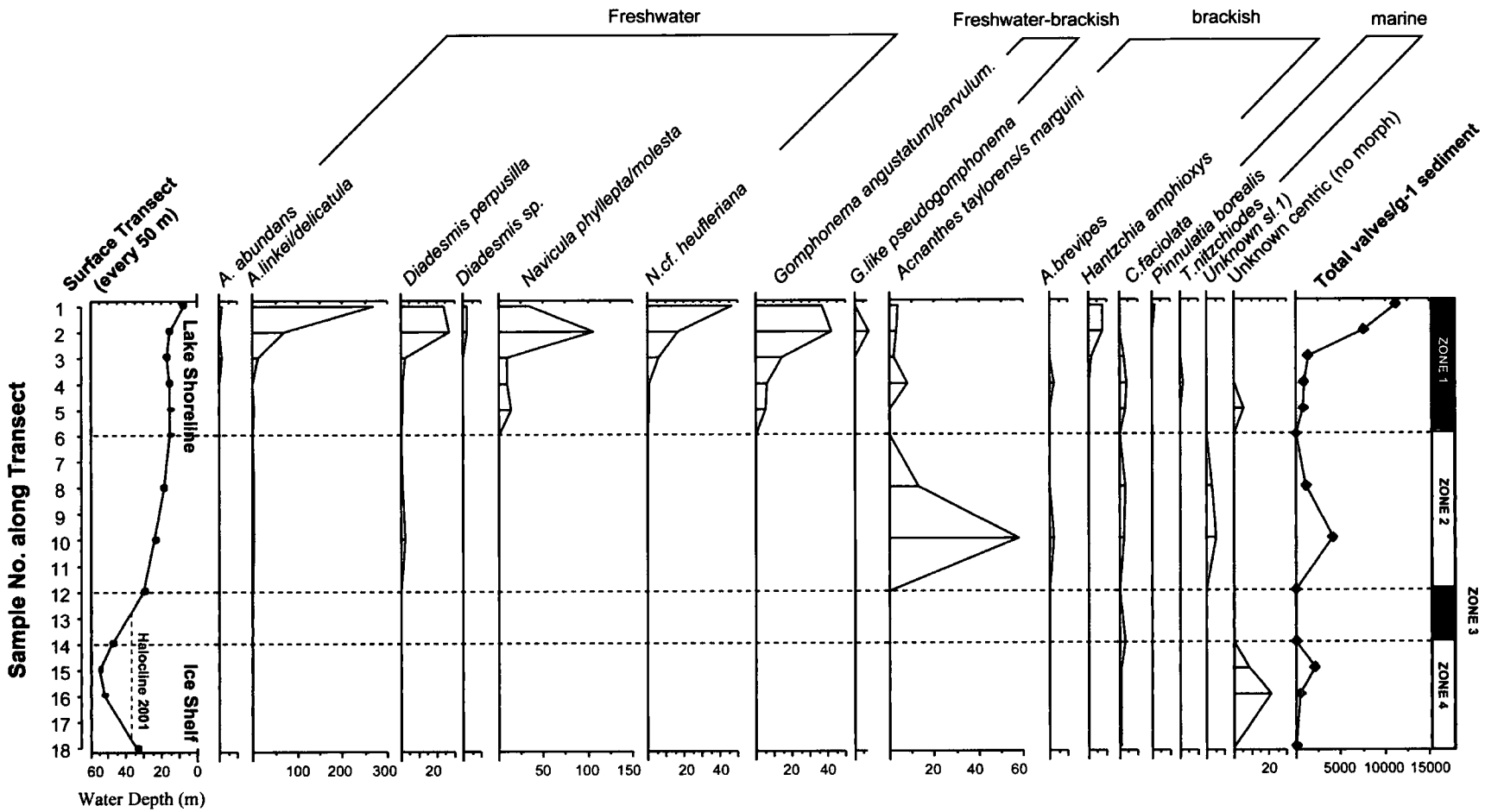

Figure 5.6. Diatom analysis of surface sediments from Moutonnée Lake and lake surface profile and sample number. Absolute diatom abundance (valves/g^{-1} sediment) is shown on the right of the diagram. Also shown is the position of the halocline recorded in 2001.

TP10 with 41298 valves g^{-1} sediment (Fig. 5.6). Low counts of *A. linkei* and the brackish-marine taxa, *Cocconeis faciolata* were also recorded. In Zone 3 there was a complete absence diatoms.

Zone 4 (15-18). The lower zone boundary was characterised by an unknown centric (Plate 1) diatom at 95.5% with minor contributions from the marine diatom *C. fasciolata.*

AB: Quantitative counts of the diatom composition of 10 sediment samples along a transect from the lake shoreline to the ice shelf front was undertaken. The resulting diagram has been divided into three zones using CONISS (Grimm, 1987) (Fig. 5.7). Absolute diatom (valves g^{-1} sediment) abundance has also been calculated and is shown in Figure 5.7.

Zone 1 (Shoreline (1)-4) was characterised by high concentrations of *A. taylorensis* (94-98%) which reached a peak relative abundance 300 m from the shoreline at TP 3 before declining at TP4 and then increasing towards the lower zone boundary. Absolute diatom abundance followed this pattern reaching a maximum of 204402 valves g^{-1} sediment at TP3 (Fig. 5.7). The freshwater taxa, *A. linkei* (2.3%) and *D. perpusilla* (2.3%) both decreased in abundance away from the lake shoreline.

Zone 2 (TP5-7) was characterised by increasing concentrations of marine taxa, notably *Diploneis sp.1* (10%), and *Unknown centric 1* (same as ML) (6.8%). *Achnanthes taylorensis* dominated the overall diatom composition (91.3%), but declined rapidly towards the boundary between Zone 2 and 3 and then disappeared.

Zone 3 (TP8-10) was defined by increasing concentrations of marine taxa, notably *Unknown centric 1, Diploneis sp. 1, Amphora copulata* and, *Achnanthes breviceps* all reaching maximum concentrations (*Unknown centric 1* (86.69%), *Diploneis sp. 1* (9.5%), *A. copulata* (3.4%)) at the last transect point beneath the ice shelf tongue. This also coincided with the highest absolute diatom abundance of 489780 valves g^{-1} sediment (Fig. 5.7).

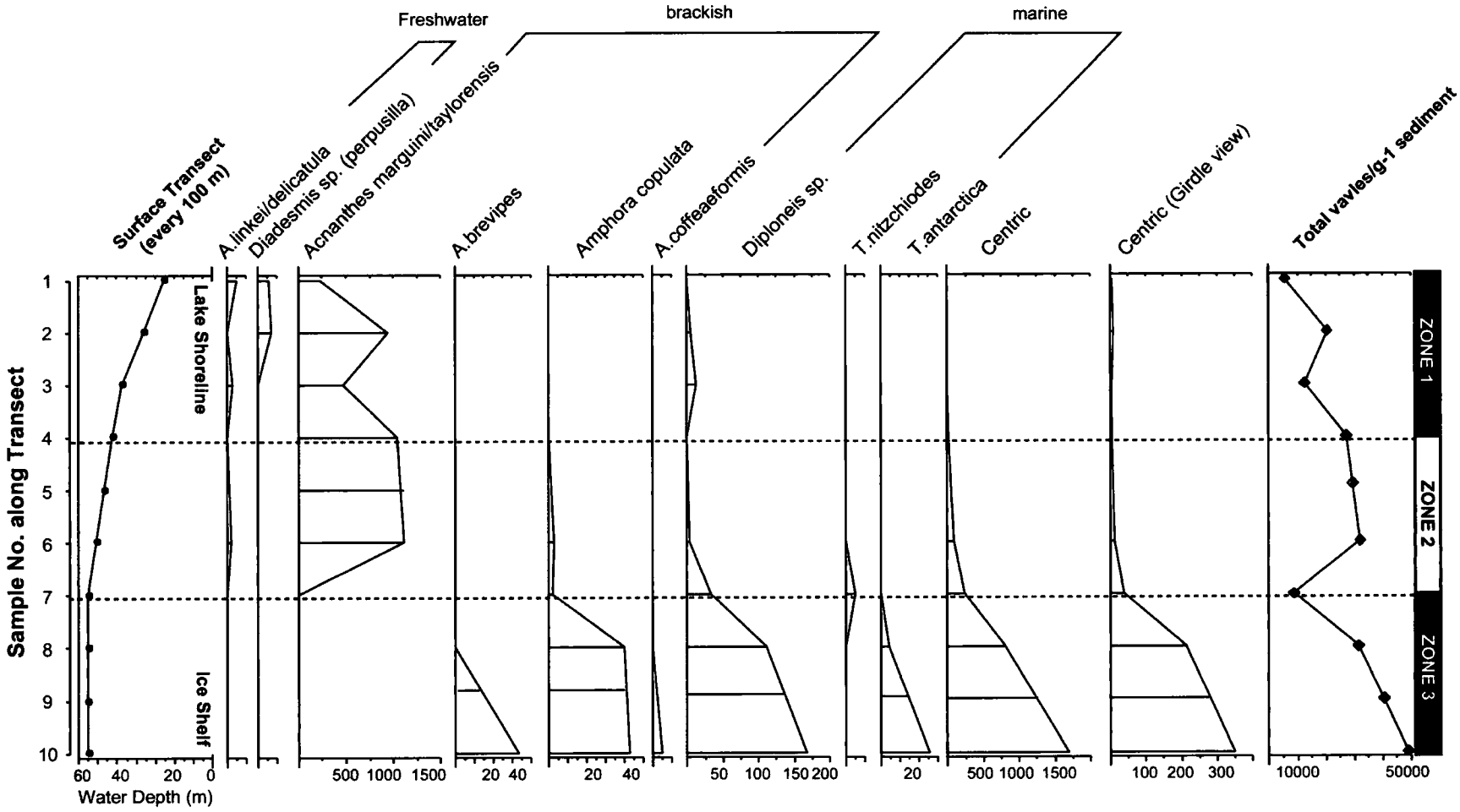

Figure 5.7. Diatom analysis of surface sediments from Ablation Lake and lake surface profile and sample number. Absolute diatom abundance (valves/g^{-1} sediment) is shown on the right of the diagram.

Grain-size fractions remained remarkably constant in both lakes (Fig. 5.8). In ML, sediment samples were dominated by clay and silt fractions, which have mean values of 56.3 % and 41.7 % respectively. Sand occurred in very low concentrations in the first two transect points (<0.77%), whilst clay increased slightly between TP6 and TP12. Gravel (>2 mm) was in low abundance throughout, but accounted for over 5% in TP6 (9.08%), TP11 (5.13%) and TP12 (6.90%). In AB sand occured in very low concentrations in the first two transect points, reaching a maximum value of 2.27% at TP4. Clay% increased slightly towards TP 5 and 6 and then decreased. Gravel decreased from a maximum at TP10 of 10.72% to 0.68% at TP5. A second gravel maximum occurred at TP4 (8.58%).

5.2.2.5. Sediment Traps

The dry sediment masses obtained from the inorganic component of the sediment trap are presented in Table 5.2, which also shows calculated sedimentation rate. Dry sediment mass is greater in the lower (40 m) traps, increasing from 0.1321 g at 22 m to 0.7899 g at 40 m (Table 5.2). Sediment from 48 m depth was used for Optically Stimulated Luminescence bleaching tests (S.J. Roberts) and the mass is unknown. The grain-size composition of one sample from the 22 m trap was analysed and revealed that sand (47.5%) and silt (43.8%) dominate the fraction, with clay contributing (8.6%).

TRAP DEPTH (M)	DRY SEDIMENT MASS (g-yr)	SEDIMENTATION RATE (g-cm²)
ML22	0.2434	0.0105
ML40	1.3986	0.0397
ML48	OSL	OSL

Table 5.2. Sediment trap dry mass and calculated sedimentation rate. OSL= samples used for Optical Luminescence dating bleaching test.

Detailed analysis (light microscope) of the water samples for diatom plankton and/or other microbiological remains collected from ML revealed the complete

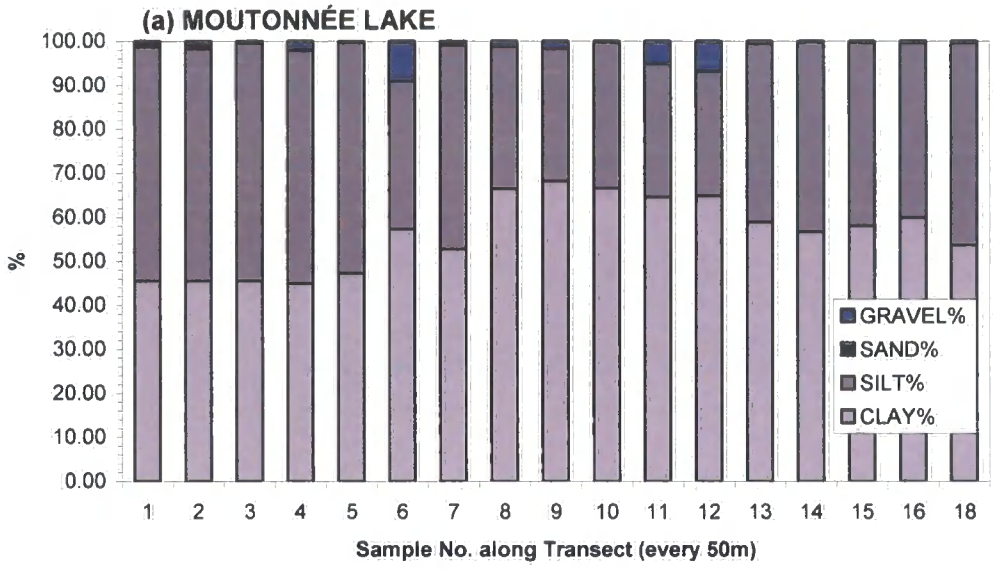

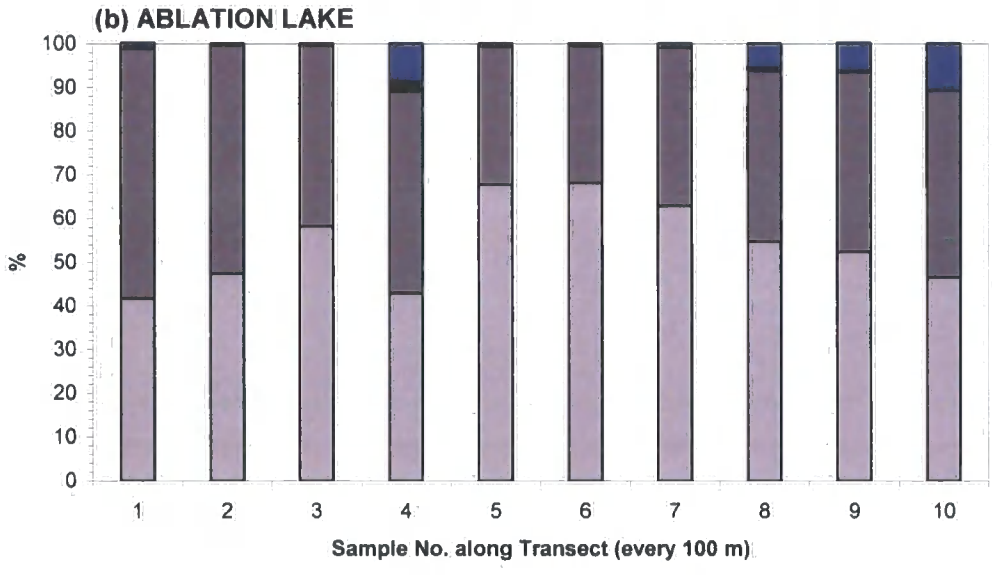

Figure 5.8. Grain-size variations for (a) Moutonnée Lake and (b) Ablation Lake surface sediments.

absence of plankton or other microbiological remains. This finding is consistent with the absence of plankton in the lake water samples.

5.2.3. Reference data set - constraining lake inputs and lake water source

5.2.3.1. δ^{18} O and δ^{2}H analyses of snow, lake ice, and ice shelf ice

The snow and ice reference dataset compromises 42 samples taken from snow, lake ice and ice shelf areas of ML and AB and has been used to investigate lake water source. Values range from –12.9 to - 21.3 ‰ for δ^{18}O and from –99 to -169 ‰ for δ^{2}H.

5.2.3.2. $\delta^{13}C_{org}$ and C/N ratio of soils, moss, and cyanobacteria

The dataset described in this section compromises a large group of mixed benthic samples including benthic cyanobacterial mats from meltpools, streams and wet seepage areas from the catchments on ML and AB. A detailed description of each sample is presented in Table 5.3 together with the result of $\delta^{13}C_{org}$ and C/N ratio. Values of $\delta^{13}C_{org}$ values in the reference data samples ranged between –26.0 and –14.1‰, and C/N values between 6.7 and 79.8 (Fig. 5.9). The samples form three main cluster groups, together with several important outliers. Cluster 1 compromise mixed benthos samples located in meltpools, or streams fed by meltpools. C/N values are relatively high (13.9 to 14.8), whilst $\delta^{13}C_{org}$ values (-25.4 to –23.2 ‰) are relatively light compared to cluster groups 2 and 3. Cluster 2 represents samples taken from benthic cyanobacterial mats and mixed benthos samples located in seepage and pool environments. These samples are characterised by lower C/N values (12.6-12) and heavier $\delta^{13}C_{org}$ (-19.2 to –17.8 ‰), relative to cluster group 1. Cluster 3 is composed of mixed benthos with epilithic and benthic cyanobacteria. C/N values are lower (10.5-9.7) compared to groups 2 and 3 whilst $\delta^{13}C_{org}$ values (-18.9 to –17.8 ‰) are similar to cluster group 2.

5.2.3.3. C_{org} and N_{org} of soils, moss, and cyanobacteria

SAMPLE CODE	*SITE*/ENVIRONMENT	MATERIAL	% N	% C	C/N	$\delta^{13}C$
1	ML North Inflow Stream	Green filamentous benthic cyanos	0.7	9.0	12.6	-14.1
2	ML North Inflow upstream of moraine	Benthic cyanobacteria mat	0.1	1.5	12.5	-19.2
3	ML Valley, NE meltpool on inner most moraine (ISM)	Mixed benthos	0.0	0.6	13.9	-25.4
4	ML Valley, NE meltpool on (ISM)	Mixed benthos	0.2	1.5	9.7	-18.6
5	ML Valley, NE stream between meltpools on ice shelf	Mixed benthos	0.3	4.1	14.8	-24.3
6	ML, NW inflow stream	Filamentous benthic cyanos	0.6	6.4	10.5	-17.8
8	ML Valley, South Inflow Stream	Green filamentous benthic cyano	1.0	9.5	9.8	-18.3
9	ML, South Inflow stream	Epilithic cyano adjacent to stream	0.4	3.8	10.0	-18.9
10	ML, Main inflow stream	Mixed benthos	0.3	3.9	14.0	-23.2
11	ML Valley, south inflow (IS proximal?)	Benthic cyanobacteria mat	0.1	0.9	9.6	-22.9
12	GVI-IS, marginal moraine	Moss in wet seepage	0.5	5.6	11.7	-23.5
13	AB Valley, 1Km upstream of camp nr. Cairn	Mixed benthos/cyano	0.2	2.2	10.1	-17.9
14	ML Valley - floor	Black epilithic cyanos	1.1	13.3	12.0	-19.1
15	ML Valley floor	Red/pink benthos	-	-	-	-17.3
16	ML Valley - pool	Fine grain seds	0.1	0.3	6.7	-
17	AB Valley, wet seepage adjacent to camp	Mixed benthos from pool	0.8	10.5	12.6	-17.8
18	AB Valley - 500 m W of camp - oil from sorted polygon	Soil	0.0	0.3	8.0	-26.6
19	ML	Gravel clast >10mm (Mudstone)	0.025	0.2	9.3	-25
20	Citadel - Fossil Wood	Fossil Wood	0.07	5.4	79.8	-23.6

Table 5.3: $\delta^{13}C_{org}$, and carbon and nitrogen values for catchment reference data set, showing sample type and environment. ISM= Ice shelf moraine; IS= Ice Shelf.

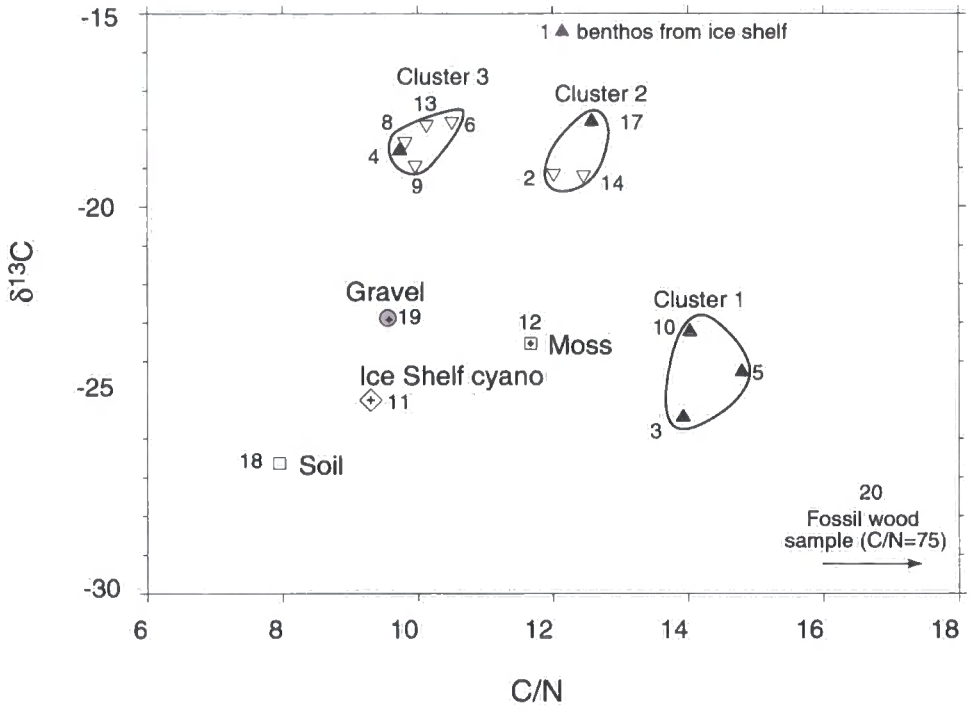

Figure 5.9. Showing $\delta^{13}C$ and C/N values for reference benthos, cyanobacteria, moss and catchment soil and rock. Numbers are referred to in table 5.3.

C_{org} values range from 0.2 to 13.3% N_{org} values range from 0.025 to 1.1% (Table. 5.3). The valley gravel sample from ML and the soil sample from AB yielded the lowest C and N content. Black epilithic cyanobacteria yielded the highest C and N values of 13.3% and 1.1% respectively. A fossil wood sample yielded high carbon content relative to nitrogen.

5.3. Interpretation

5.3.1. Vertical water chemistry profiles

5.3.1.1. CTD, DOx, pH

Since the first measurements of vertical water chemistry profiles in 1973 (Heywood, 1977) the gross chemical structures of both the ML and AB water column have experienced a number of changes, most notably in the depth of the chemoclines and, in particular the haloclines. In ML the two-step salinity profile present in 1973 is absent from 2000 and 2001 profiles and there has been a net increase in the volume of marine water. The first interpretation of the changes in ML is that the increase in the volume of marine water in ML represents a long-term trend similar to that observed in Disraeli Fiord prior to the break-up of the Ward Hunt Ice Shelf in the high Arctic (Mueller et al., 2003). This involved a steady decrease in the thickness of the freshwater layer from the early 1960s to 2002, which Mueller et al. (2003) interpreted as a result of a thinning of the Ward Hunt Ice Shelf (on the assumption that the depth of freshwater layer is equivalent to the draught of the ice shelf) in response to documented atmospheric warming. A similar explanation could apply at ML in response to the rapid regional atmospheric warming on the Antarctic Peninsula since the 1970's (e.g. Vaughan et al., 2003) similar to the documented thinning of other AP ice shelves (e.g. Larsen-B, Shepherd et al., 2003). The second interpretation is that these changes are simply a result of seasonal variation. Heywood's (1977) CTD profiles were taken in late December, over a month later than the profiles in the present study. Thus seasonal factors, such as the changing supply of meltwater, or changing tidal ranges may be involved in the shifting chemoclines. In other words, Heywood may have measured a deeper halocline

because the meltwater/freshwater layer was thicker due to a more advance melt-season. To determine which of these two competing hypotheses is correct would require a long-term monitoring study. It is worth noting however that the maximum change in halocline observed in ML (> 2 m) is greater than the maximum tidal range (72 cm) in ML.

Unlike ML, AB is partially grounded on a bedrock sill. Therefore the shifts in the halocline from 66.5 m on the 30th November 1973, to 64 m on the 8th December 2000 and then to a very weak halocline at 68 m on 2nd December 2001 are unlikely to be the result of anything more than changes in the seasonal supply of fresh meltwater, changing tidal ranges and the extent/distance to which marine water penetrates into the basin. It is unlikely to be related to thinning of the ice shelf as this would result in a net increase in the supply of marine water and the halocline becoming established higher in the water column. Given that the portions of the ice shelf reaching Ablation and Moutonnée Lakes are only a few km (~ 5 km) apart this may suggest that the changes in ML are more likely to be seasonal rather than long-term.

In both lakes, water temperature is within 1.5 °C of freezing at all depths. The similar depths of the thermoclines and haloclines is linked to the presence of cooler marine water which reaches a minimum temperature of –1.3 °C. It is interesting to note that the mean water temperature in AB has risen from –0.14 °C in 1973 to 0.05 °C and 0.19 °C in 2000 and 2001, coinciding with the weakening of the halocline, although the significance of this is questionable. DOx values fluctuate in both lakes and, in general decrease with depth. This is likely to the result of well oxygenated water entering the surface of the lake via inflow streams and from the littoral zone where photosynthesis occurs, whilst at depth, oxygen is depleted by oxidative processes (i.e. biological oxidation of organic matter). This occurs particularly at the sediment water interface where bacterial decomposition of any dissolved and particulate organic matter takes place.

5.3.1.2. Stable Isotopes

Stable isotope values also track the presence of fresh and marine water. Thus the $\delta^{18}O$ and $\delta^{2}H$ values in ML are distinctly different above and below the halocline, whilst samples from Ablation Lake are remarkably constant reflecting the complete dominance of fresh melt-water at the time of measurement. Conversely, higher $\delta^{18}O$ and $\delta^{2}H$ values below the ML halocline reflect the marine origin of the water. The dual source characteristics of water in ML are now investigated in more detail. This is not only important from a source point of view but it will also provide important contemporary isotopic information for any future palaeoclimatic study which aims to interpret the isotopic signal preserved within the lake sediment.

Generally, the $\delta^{18}O$ and $\delta^{2}H$ isotopic composition of lake water inherently reflects the air temperature and moisture source, but also contains information about various inputs (glacial-melt) and outputs (e.g. evaporation). Figure 5.10 shows the $\delta^{18}O$ and $\delta^{2}H$ values from samples collected from ML and AB plotted against the Global Meteoric Water Line (GMWL). The GMWL represents the correlation between $\delta^{18}O$ and $\delta^{2}H$ in precipitation worldwide (Craig, 1961). This relationship is further modified in arid climates such as the Antarctic by local evaporation lines (Gat and Gofiantini, 1981). Samples from this study plot close to the GMWL suggesting that the lake water is principally derived from the precipitation of snow and rainfall, but also the melting of yearly snow-patches. Together the lake water samples define a Local Meteoric Water Line (LMWL), which is very close to the meteoric water lines (derived from the isotopic composition of ppt) of nearby Antarctic stations, Halley (1965-2000) and Rothera (1996-2000) and Vernadsky (1964-2000) (IAEA, 2004). Linear regressions of the data (Fig. 5.10) give r^2 values, which are generally very high (>0.92), suggesting that the lake water has been little altered by local processes (e.g. evaporation) and largely reflects the isotopic signature of precipitation. Values also fall on a clear latitudinal gradient (Fig. 5.11) which principally relates to the temperature at which the precipitation formed (e.g. Dansgaard, 1964). Generally, the isotopic signature ($\delta^{18}O$ and $\delta^{2}H$) of lake water becomes progressively lighter as one moves southwards (e.g. Noon et al., 2002).

When plotted against regional reference data (Fig. 5.10), the $\delta^{18}O$ and $\delta^{2}H$ isotopic signature of water below the ML halocline plots close to marine water from the

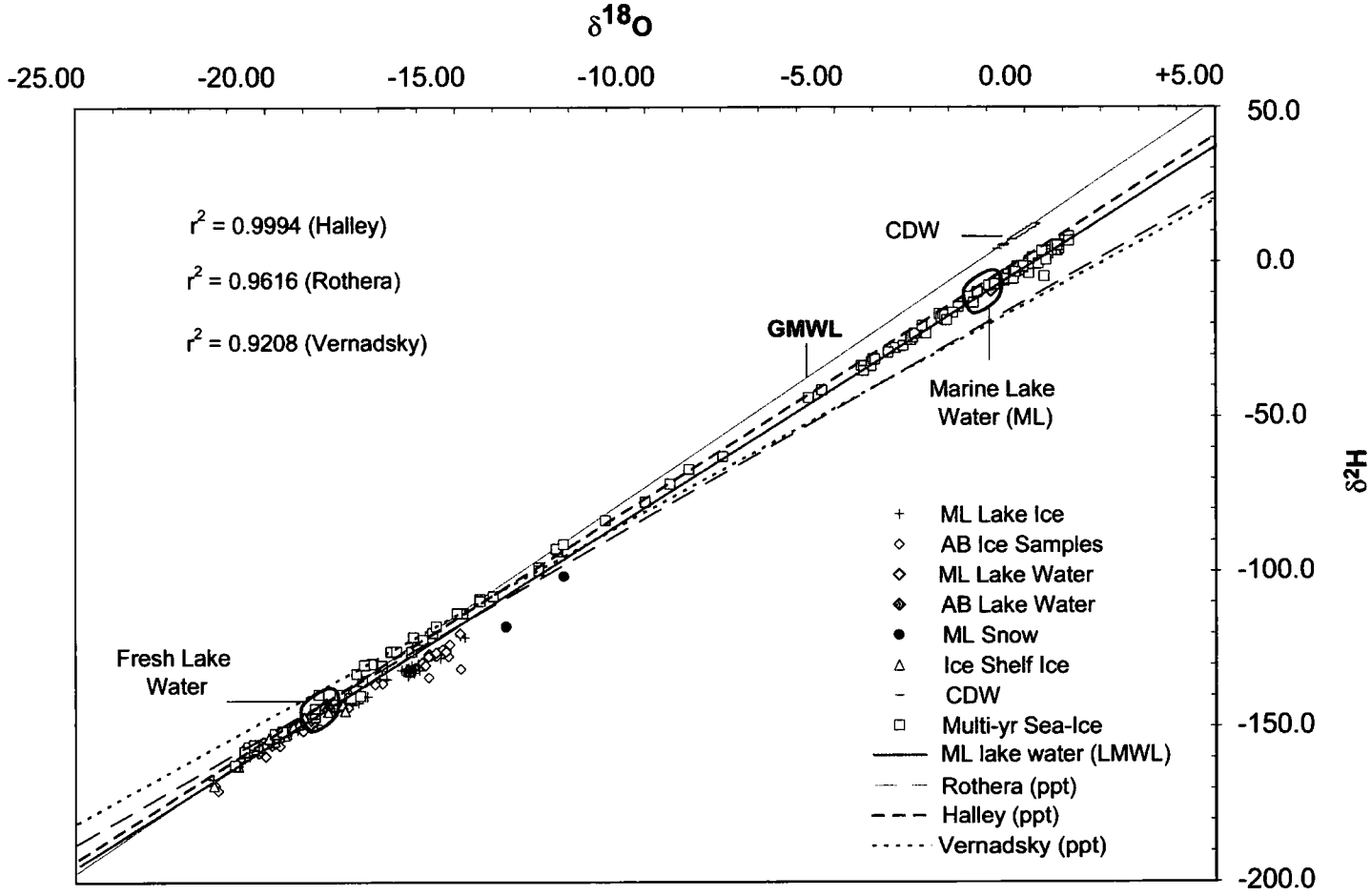

Figure 5.10. Co-isotopic plot of snow, ice and water samples from the Antarctic Peninsula and ML and AB. Snow samples from (Potter et al., 1984); multi-year sea-ice from the southern margin of George VI Ice Shelf (Tison et al., 1991) and December, January and February water column samples from the northern margin of GVI-IS (Potter and Paren, 1988) taken to be representative of Circumpolar Deep Water (CDW) (A. Jenkins pers.comm. 2004). Lake water samples are also plotted against; Global Meteoric Water Line (GMWL) (Dansgaard, 1964); and Local Meteoric Water Lines for ML and AB (black line) and nearby Antarctic Station, Halley (dashed line), Vernadsky (dotted line) and Rothera (grey line) (data from IAEA, 2003).

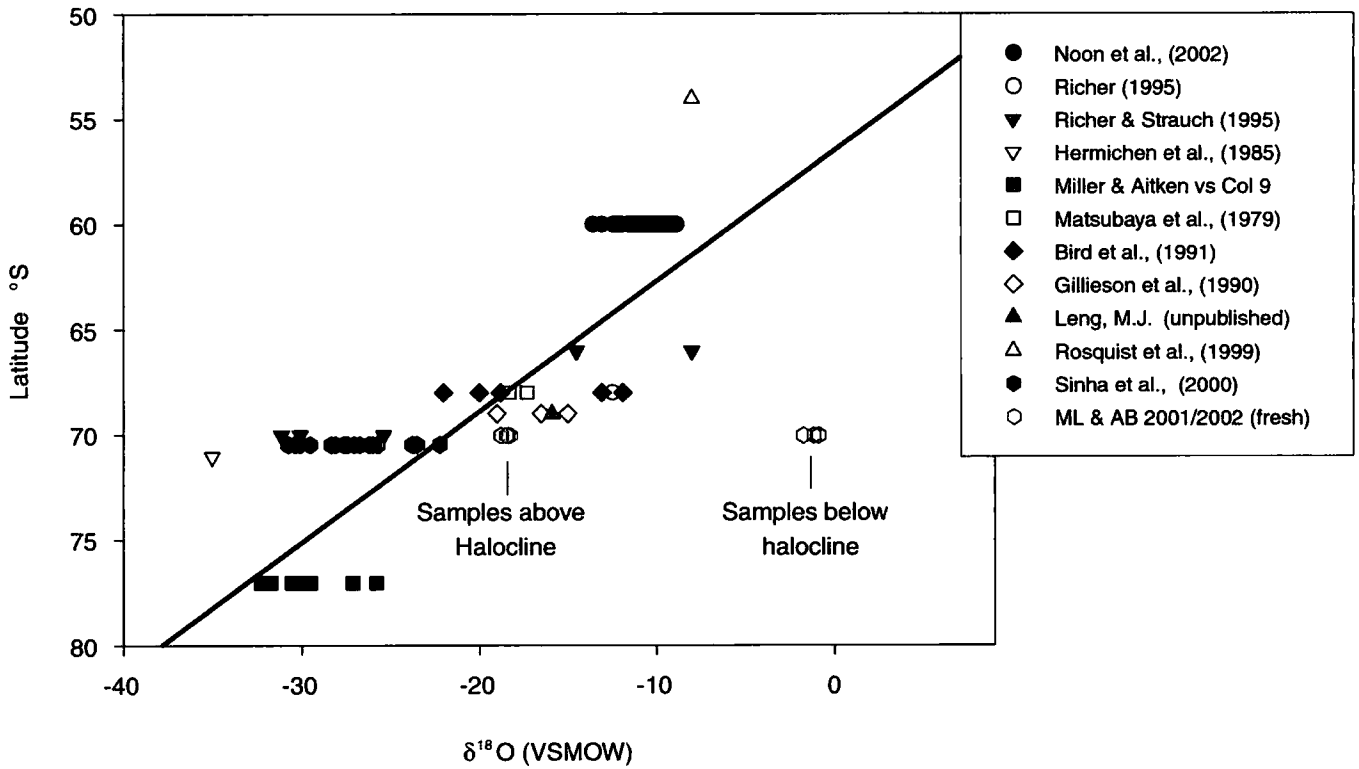

Figure 5.11. $\delta^{18}O$ from Antarctic Lakes vs. latitude. Freshwater samples from Moutonnée and Ablation Lakes (blue circles) fall on a clear latitudinal gradient. Black line defines GMWL. Data from; Signy Island (Noon et al., 2002), McMurdo Dry Valleys (Miller and Aitken, 1996), Vestfold Hills (Matsubaya et al., 1979; Bird et al., 1991) Larsemann Hills (Gillieson et al., 1990), Schirmacher Oasis (Hermichen et al., 1985; Richer, 1995; Richer and Strauch, 1995; Sinha et al., 2000); South Georgia (Rosqvist et al., 1999).

northern margin of GVI-IS and within the fields of multi-year sea-ice from the southern margin (Tison et al., 1991), which occupies the entire range of isotopic values presented in this study. The sea-ice values come from the base of a sea-ice core (Tison et al., 1991) and effectively represent frozen marine water mixed with fresh melt-water. It therefore seems likely that the isotopic signature of water below the halocline in ML is primarily marine in origin, with some dilution by fresh melt-water, as is common for marine water in this region.

The $\delta^{13}C_{TDIC}$ in ML and AB is distinctly different. In AB $\delta^{13}C_{TDIC}$ values are generally much lighter, having a range between –21 to –9.1 ‰, whilst $\delta^{13}C_{TDIC}$ values in ML range from –11.4 to –0.5 ‰. The heaviest $\delta^{13}C_{TDIC}$ values in ML occur below the halocline. TDIC comes from a wide variety of sources, but tends to be dominated by three processes: (1) $^{13}C/^{12}C$ of inflowing waters; (2) CO_2 exchange with the atmosphere; and (3) photosynthesis and respiration of lake biota (Leng and Anderson, 2003). In addition marine water tends to have high TDIC values (Gibson et al., 1999; Arrigo et al., 2000). Indeed the influence of marine TDIC is seen in ML, where water samples from below the halocline have higher $\delta^{13}C_{TDIC}$ values. Thus it seems likely that the $\delta^{13}C_{TDIC}$ profile in ML is dominated by the influx of marine TDIC. The picture is more complicated in Ablation. Since the AB is perennially ice covered, it is unlikely that CO_2 is able to exchange with the atmosphere. In addition, the lake water column has already been shown to be largely unproductive (e.g. low nutrient/absence of diatom plankton). As such, photosynthetic processes are also unlikely to control the $\delta^{13}C_{TDIC}$ variations in AB. In the absence of these processes, it is likely that the $\delta^{13}C_{TDIC}$ values in AB reflect the varying input of isotopically light carbon derived from catchment organic matter.

In summary, the water column chemistry (CTD and isotopes) of ML, and to a lesser extent AB, is dominated by the depth and strength of the halocline which marks the transition between fresh and marine water. All parameters measured respond either to the presence of these two water masses, or to the influx of fresh oxygenated meltwater from the catchment, or both. The water columns of both lakes were also

nutrient limited and as a result no phytoplankton were detected either by microscopic or pigment analysis (unpublished data).

5.3.2. Surface sediment transects and sediment traps

The salinity stratification strongly influences the parameters measured in the surface sediment transect and sediment traps. For example, the absence of plankton and phytoplankton in the filtered samples from the water column is mirrored by an absence of diatom remains in the ML sediment traps. This is consistent with studies of other ice-covered ultraoligotrophic Antarctic epishelf lakes, which are unproductive due to the near-absence of inorganic nutrients, low temperatures and low annual fluxes of photosynthetically active radiation (PAR) (Priddle, 1985; Henshaw and Laybourn-Parry, 2002; Cremer et al., 2004).

5.3.2.1. Lake ice conveyor model

A further interesting feature of the sediment traps recovered from Moutonnée Lake was their apparent in a WNW direction. This is a new and exciting result as it demonstrates for the first time that a rare lake-ice conveyor is operating at Moutonnée Lake (and by inference, probably at Ablation Lake too). A similar process has been observed at Trough Lake in the Dry Valleys of Antarctica (Fig. 5.12) (Hendy et al., 2000). Here, material is transported from the floating glacier tongue (in this case the Koettlitz Glacier) to the lake moat via the lake ice. The lake ice is pushed forward annually due to a cyclical relationship between glacier compression and moat development around the lake shoreline. During the winter season compressional stresses build up as the lake ice restricts the glacier flow. Once the summer melt season arrives and the moat is re-established, the stresses are released allowing the lake ice to be pushed forward (Hendy et al., 2000). Periodically icebergs are calved off the glacier front to form upstanding ridges locked in the lake ice cover (Fig. 5.12) (Hendy et al., 2000). As the icebergs ablate they release englacial material onto the lake-ice surface or directly into the lake water. Fine-grained material tends to melt through the lake ice under the influence of insolation and rains out onto the lake floor whilst coarser material (>1 cm) and

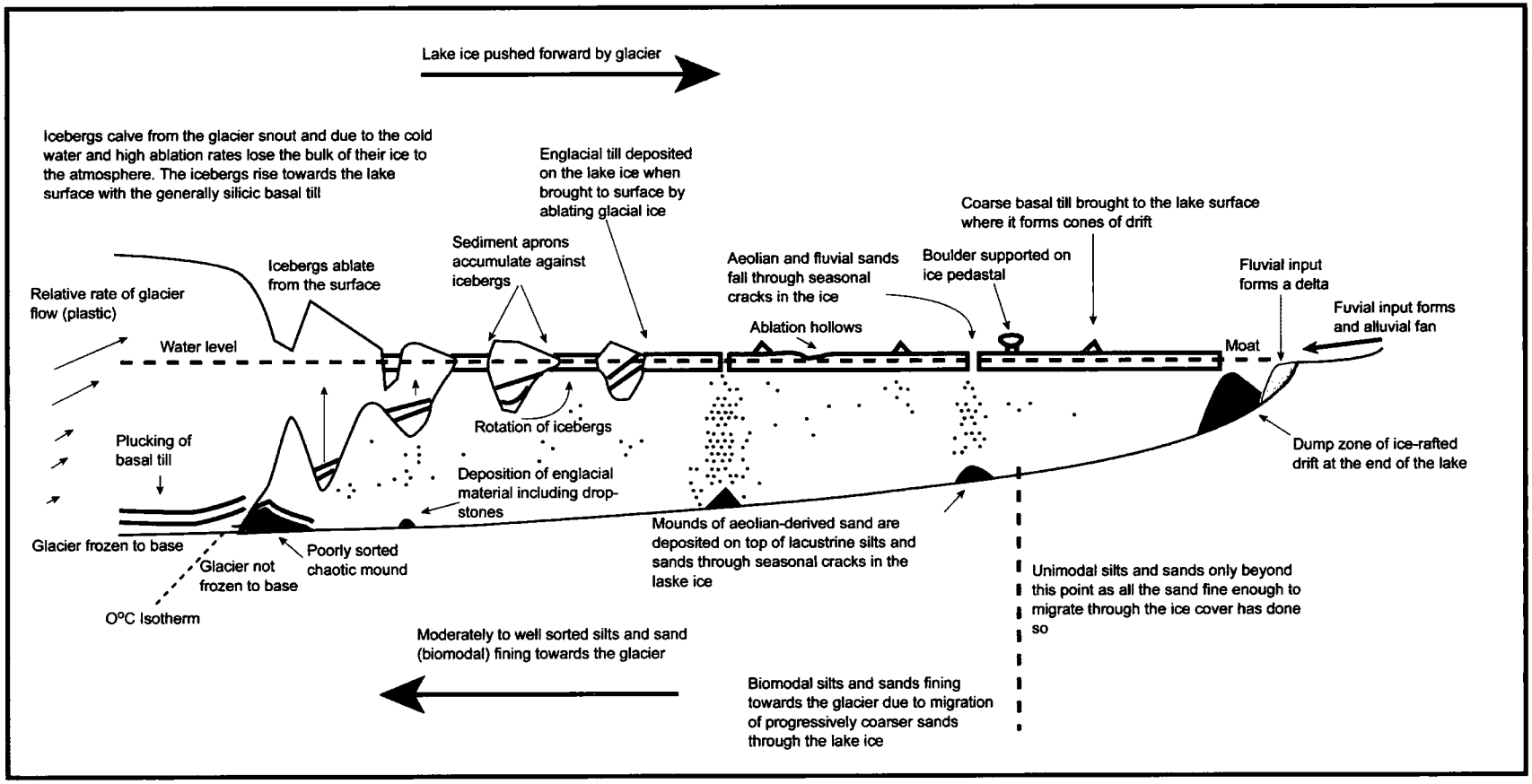

Figure 5.12. Lake ice conveyor model of drift deposition from a polar proglacial lake (Hendy et al., 2000).

occasional large boulders are carried on the lake surface to the moat where they are deposited either directly or by meltwater (Fig. 5.12). Once in the moat this material may be incorporated into ice-push structures and/or resorted by fluvial action.

As noted in Chapter's 3 and 4 Clapperton and Sugden (1982) first reported on the presence of Antarctic Peninsula erratics (granite) along the Moutonnée Lake shoreline. The erratics are easily distinguished from the rocks of Alexander Island, which are predominantly sedimentary. The only granitic rocks of Alexander Island are found in a conglomerate (Himalia Formation) but these are easily identified as being more weathered. Similar observations were made during the austral summer of 2002 where granite erratics were noted on the lake shoreline and also englacially within the ice shelf margin (Fig. 5.13). Thus it appears likely that granite from the AP is transported across the sound, by the ice shelf and then deposited on the lake ice surface where it is either transported to the lake shoreline or simply ablates through the lake ice eventually reaching the lake bottom. The important implication of the lake conveyor system is that the ice shelf, when in contact with Moutonnée and Ablation Lakes, leaves a lithological signature of its presence, which will be found in both the lake sediments and *palaeo-shorelines* (e.g. Fig. 5.13).

5.3.2.2. Diatoms

In contrast to the absence of plankton in the water column, the benthic environment does have a diatom flora, though with a very limited species diversity. The species in the ML and AB surface sediments include taxa common to Antarctica and the Antarctic Peninsula such as *Achnanthes breviceps*, *Amphora copulata*, *Hantzschia amphioxys*, and *Diadesmis sp.* (Oppenheim and Ellis-Evans, 1989; Oppenheim, 1990; Oppenheim and Greenwood, 1990; Schmidt et al., 1990; Wasell and Håkansson, 1992; Jones, 1993, Jones et al., 1993; Kawecka and Olech, 1993). The low diversity can be explained by the perennial ice cover, low temperatures, low photosynthetically active radiation (PAR) and nutrient limitation (cf. Spaulding et al., 1997, Jones, 1996; Spaulding and McKnight, 1999; Van de Vijver and Beyens, 1999, Le Cohu and Maillard, 1986). A general feature of both ML and AB was the absence of planktonic freshwater diatom taxa, both in the surface sediments but also the sediment traps. This finding is consistent with several other lake studies from

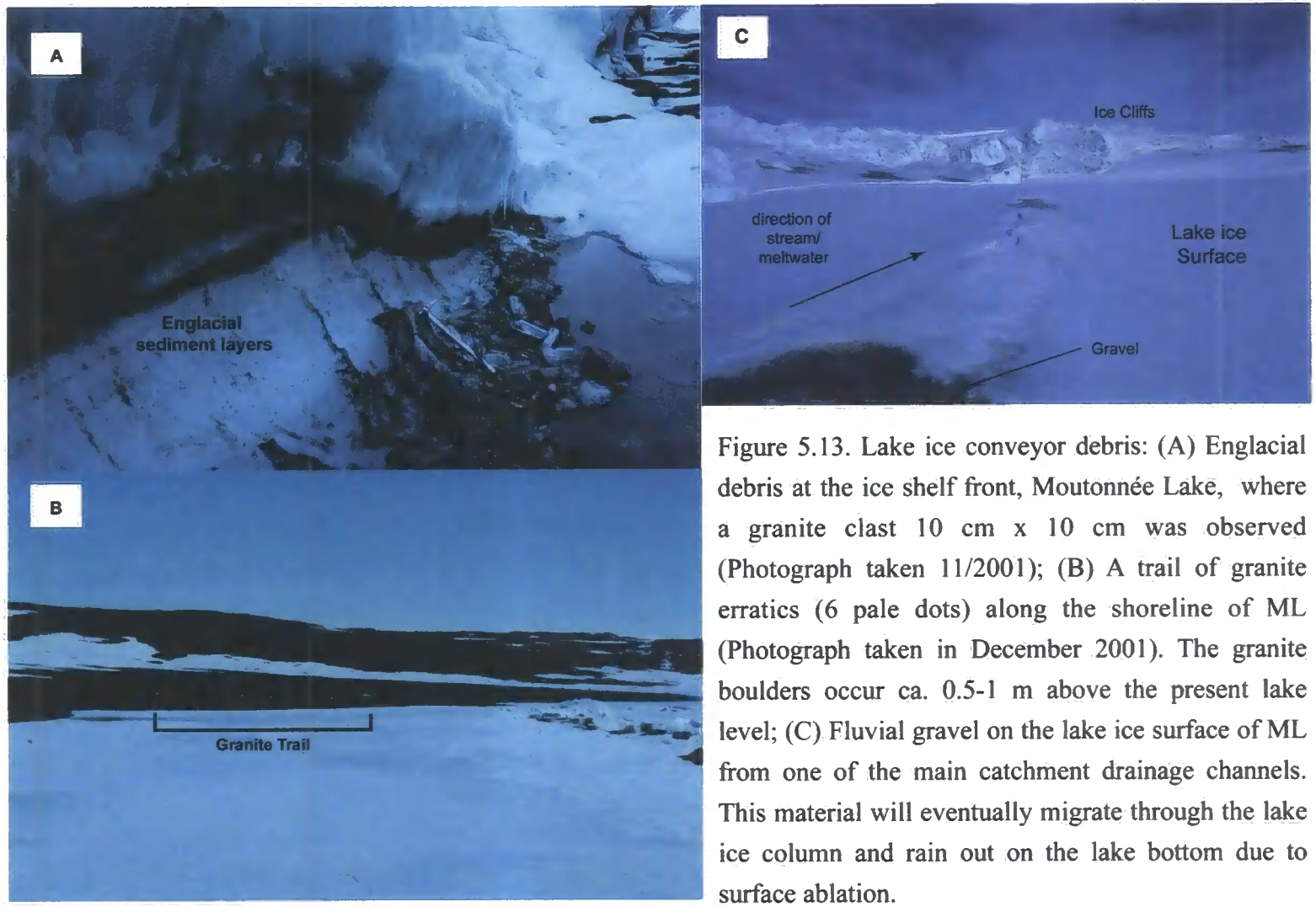

Figure 5.13. Lake ice conveyor debris: (A) Englacial debris at the ice shelf front, Moutonnée Lake, where a granite clast 10 cm x 10 cm was observed (Photograph taken 11/2001); (B) A trail of granite erratics (6 pale dots) along the shoreline of ML (Photograph taken in December 2001). The granite boulders occur ca. 0.5-1 m above the present lake level; (C) Fluvial gravel on the lake ice surface of ML from one of the main catchment drainage channels. This material will eventually migrate through the lake ice column and rain out on the lake bottom due to surface ablation.

the Antarctic and sub-Antarctic regions and is an issue that has been discussed by several authors (Jones, 1996; Spaulding and McKnight, 1999; Van de Vijver and Beyens, 1999). No single reason for this phenomenon has been presented, although trophic status has been suggested as an important factor (Le Cohu and Maillard, 1986). The benthic diatoms are likely to be associated with the biofilm reported by divers in AB (Heywood, 1977). This is a 'thin film of algae' extending to a depth of 15 m on the lake bottom. Evidence from this study suggests that these biofilms survive at greater depths, perhaps as deep as 24 m in ML.

In both lakes the change in species composition is related to changes in lake depth and the transition from freshwater to marine water. A notable exception in ML is Zone 3 (TP10-14), which contained no diatoms. This zone coincided with the upper limits of the measured chemoclines and it is therefore likely that the extreme variations in chemistry across this zone, coupled with the low light environment, are not favourable for diatom survival. In addition, pH could also be a factor as studies have shown that at higher pH (e.g. >9) diatom dissolution is rapid (Ryves, 1997). In the ML marine zone sediments, nearest the ice shelf front (Zone 4), there is an unknown centric diatom that is likely to be marine in origin and advected in by tides. A similar centric diatom occurs in relatively high numbers directly in front of the ice shelf tongue in Ablation Lake. In both cases, the limited diversity and low numbers of advected marine diatoms implies that there is very little diatom productivity beneath GVI-IS.

Diatoms in the AB transect show similar changes in species composition with depth and salinity but without the presence of true freshwater taxa. Instead, there is a change from freshwater-brackish taxa (e.g. *A. Linkei*) near the lake shoreline to marine diatoms close to the ice shelf front. Brackish water taxa, namely *Achnanthes taylorensis*, dominate the diatom assemblage and account for the greater absolute diatom abundance in AB compared with ML. Due to the relatively free exchange of water from underneath the ice shelf into AB there is a greater number/diversity of advected marine taxa (e.g. *T. antarctica, Diploneis sp.*, and *Unknown centric* and possibly some *in-situ* growth. The presence of these taxa suggest that marine water regularly enters the basin, but it does not penetrate beyond TP4, landward of which the water mass is predominantly freshwater.

5.3.2.3. $\delta^{13}C_{org}$ Isotopes and C/N

Similar to the diatoms, the salinity stratification also strongly influences the $\delta^{13}C$ isotope values along the surface sediment transect, with lighter $\delta^{13}C$ values (-25.7 to –25.4 ‰) below the halocline (i.e. under the influence of marine water) and heavier $\delta^{13}C$ values (-15.5 to –21.5 ‰) near the shore. C/N values also increase towards the shoreline. As a general rule (see Chapter 4) lacustrine algae have lighter $\delta^{13}C$ (c. –30 to –25 ‰) whilst marine-derived algae are often slightly heavier (c. –20 to –25 ‰, Meyers, 1997). However, in Antarctica this approximate partitioning often breaks down. As noted in Chapter 4, Doran et al. (1994b) have reported a very wide range of $\delta^{13}C$ values (-1.9 to –25.7 ‰) for sediments retrieved from Lake Hoare, an oligotrophic lake in Taylor Valley, Antarctica. Likewise, Gibson et al. (1999) have reported a range of –15 to –20 ‰ for Ross Sea sediments, whilst Rau et al. (1989) have reported values as low as –28 ‰ for marine algae in the Southern Ocean. An explanation for such negative values is that cold waters are capable of holding more dissolved CO_2 than temperate and tropical waters, thereby allowing greater isotopic discrimination by algae. On land only one study has reported $\delta^{13}C$ values for Antarctic terrestrial mosses, lichens and algae on Signy and the South Shetland Islands with values ranging from –28 and –18 ‰, but mostly between –25 to –21 ‰ (Galimov, 2000). The average of terrestrial plants is –27 ‰ (Ehleringer et al., 1993), but the observed impoverishment of plants studied by Galimov (2000) is likely to reflect species composition rather than geography. Lichens for example are known to have lighter ^{13}C than other terrestrial vegetation.

In addition to the biological influences, a comparison of $\delta^{13}C_{org}$ values from the catchment reference data set with the $\delta^{13}C$ and C/N values in the surface sediments (Fig. 5.14) shows that the two mineral samples (soil and catchment rock) have very similar values to those obtained from the surface sediments, specifically those below the halocline. The rock sample is an Upper Jurassic to lower Cretaceous mudstone that it is the most ubiquitous lithology in the catchment, and field observations have noted that gravel-sized clasts of this rock are transported onto the lake surface by summer melt streams. Once deposited on the lake surface, this

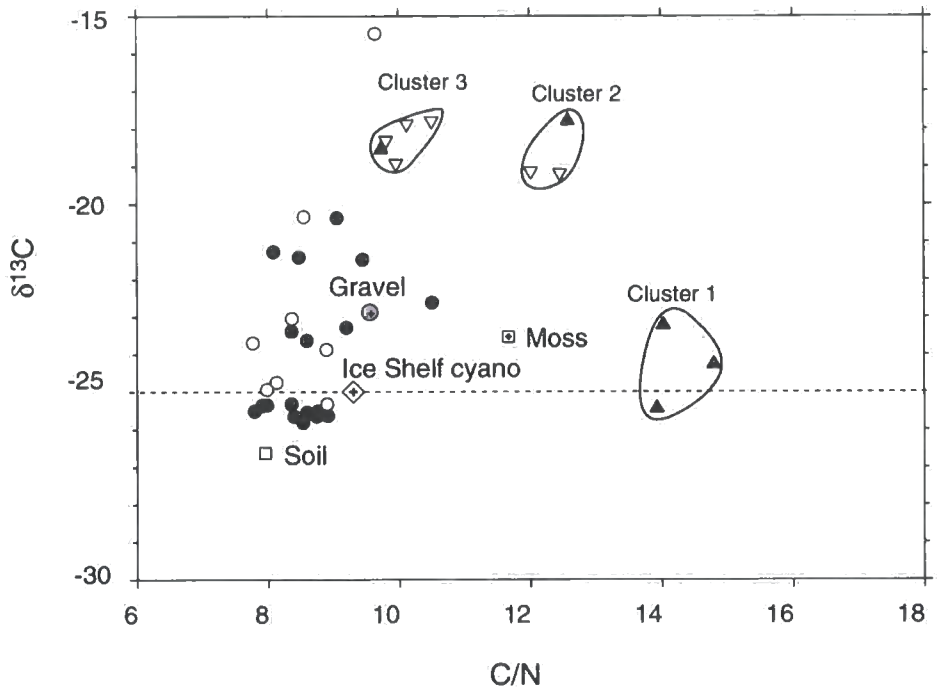

Figure 5.14. $\delta^{13}C$ versus C/N for reference samples collected from the catchments of Moutonnée and Ablation Lake; closed triangles = mixed benthos, open triangles = benthic cyanobacteria. Also plotted are $\delta^{13}Corg$ values from surface samples from Moutonnée (closed circles) and Ablation (open circles). Dotted line defines the theoretical division between marine (above line) and freshwater algae (below line) (Meyers, 1997).

material eventually ablates through the lake ice under the influence of insolation (e.g. Fig. 5.12; Hendy et al., 2000). This comparison with the reference data set suggests that at least part of $\delta^{13}C_{org}$ signature in the surface sediment may be derived from these allochthonous sources.

The source of heavier nearshore $\delta^{13}C_{org}$ values is less easy to determine from the reference data and could represent a mixture between partially degraded autochthonous organic material from the catchment, *in-situ* benthos and valley gravels. Bird et al. (1991) observed high $\delta^{13}C$ values for organic carbon in meltwater streams feeding lakes in the Vestfold Hills, which they attributed to extreme competition for available CO_2 by microbial autotrophs. The same process could be occurring at ML and AB and is supported by several organic reference samples collected from wet seepages and small pools that gave heavy $\delta^{13}C_{org}$ values, notably from the epilithic and benthic cyanobacteria samples (e.g. cluster group 3; Fig. 5.14).

In summary, the isotopic signature ($\delta^{13}C_{org}$) of surface sediment indicates that a substantial amount of material enters the lake from allochthonous sources. The deepest part of each lake is characterised by an isotopic signature (ca. –25.6 ‰) that closely resembles both that of the dominant catchment lithology (-25 ‰) and typical polar marine waters (Rau et al., 1989; Gibson et al, 1999), but it remains difficult to separate the two (biological and lithological) source signatures. In contrast the heavier isotopic signatures of surface sediments on the landward side of the lake shorelines are likely to reflect the influx of ^{13}C-enriched water.

5.3.2.4. Grain-size variations and sediment pathways

The grain-size composition of the surface sediments in both lakes is near uniform. On the basis of field observation three main sediment pathways have been identified: (1) fluvial; (2) aeolian; and (3) from the ice shelf. The absence of size-sorting away from these likely source regions, suggests that the lake-ice modulates the transport and deposition of sediment, for example via the lake-ice conveyor (e.g. Hendy et al., 2000) and by the rate at which particles migrate down the ice column due to surface ablation and insolation. Isotopically ($\delta^{13}C$) the surface sediments are

very similar to the valley-side gravels, which suggest a local catchment source is dominant. It is therefore likely that the majority of this sediment enters the lakes along fluvial and glacial routes, although it has been shown elsewhere in Antarctica, that aeolian processes are significant. For example, passive sediment traps in the McMurdo Dry Valleys of Antarctica have shown that strong winds transport significant quantities of sand (50 to 1000 μm) and silt and clay (<50 μm) sized material (Lancaster, 2002) with estimates of dust flux in Lake Bonney being 109 g m^{-2} yr^{-1} for sand and 1.1 g m^{-2} yr^{-1} for silt and clay (Lancaster, 2002). Although similar data is not available for Alexander Island, the Ablation Point massif is one of the largest ice-free areas on the Antarctic Peninsula, and the aeolian sediment flux is still likely to be important.

5.4. DISCUSSION

5.4.1. Evaluation of proxies to record periods of ice shelf loss

The data presented above has provided baseline information on the contemporary limnology of Moutonnée and Ablation and through the analysis of surface sediments provided a detailed signature of ice shelf presence. If the ice shelf were to disappear however, it would remove the lake ice dam, and ML and AB would become marine embayments. This would result in fundamental changes to the lake environment and leave a distinct (marine) depositional signature in the lake sediments. Of the parameters studied, stable isotopes clearly record the difference between freshwater and marine water both in the water column and in the surface sediments and are further supported by regional reference data. Therefore isotopic measurements have the potential to accurately discriminate the water source and help interpret the isotopic signal preserved within the lake sediment. Diatoms species composition is also linked to changes in salinity. However, the low nutrients measured in the water column and the layers of high pH (e.g. ML 2001) may influence preservation of frustules in the freshwater zone and hence in the sediments. Under marine conditions the sedimentary environment would favour preservation and thus it is likely that periods of marine water dominance would be faithfully recorded by the presence of marine diatoms. Lithological parameters are

also of value as the source region is likely to change from predominantly local rocks (and those rocks within specific flow lines within the ice shelf) during periods of ice shelf presence, to a variety of sources during periods of ice shelf absence when ice rafted debris (IRD) from multiple sources (i.e. multiple areas of Alexander Island/Palmer Land) would rain down to the sediments. The lake-ice conveyor system is also important as the ice shelf, when in contact with Moutonnée and Ablation Lakes, leaves a lithological signature of its presence, which will be found in both the lake sediments and in palaeo-shorelines.

5.4.2. Development of a conceptual Model

Based on what we now know about the modern day processes occurring in ML and AB and the signature it leaves in the sedimentary record, it is possible to develop a conceptual model of: (1) ice shelf presence and; (2) ice shelf absence. In the next section an overview of the two scenarios will be presented and the likely response, based on what is already known about the contemporary processes of key variables within the lake environment to ice shelf loss.

5.4.2.1.Ice Shelf Presence

Figure 15a shows the ice shelf presence scenario. Effectively this represents our understanding of modern-day conditions in Moutonnée and Ablation Lakes and is based upon the measured variables outlined above and what we already know from the work of Heywood (1977). These measurements have shown, for ML at least, that the water column is stratified with freshwater overlying marine water, the ice shelf is grounded on a bedrock sill and exotic lithologies are transported from the Antarctic Peninsula directly to the lake sediments and onto the lake shoreline.

Field measurements have shown that the modern day lake water column is unproductive, a feature that is likely to reflect the attenuation of sunlight by lake-ice and low nutrient levels. In ML diatom productivity is limited to areas close to the lake shoreline, where the assemblage is freshwater to freshwater-brackish species dominated The converse is true in Ablation Lake; where diatom productivity appears to be highest nearest the ice shelf with brackish and marine diatoms

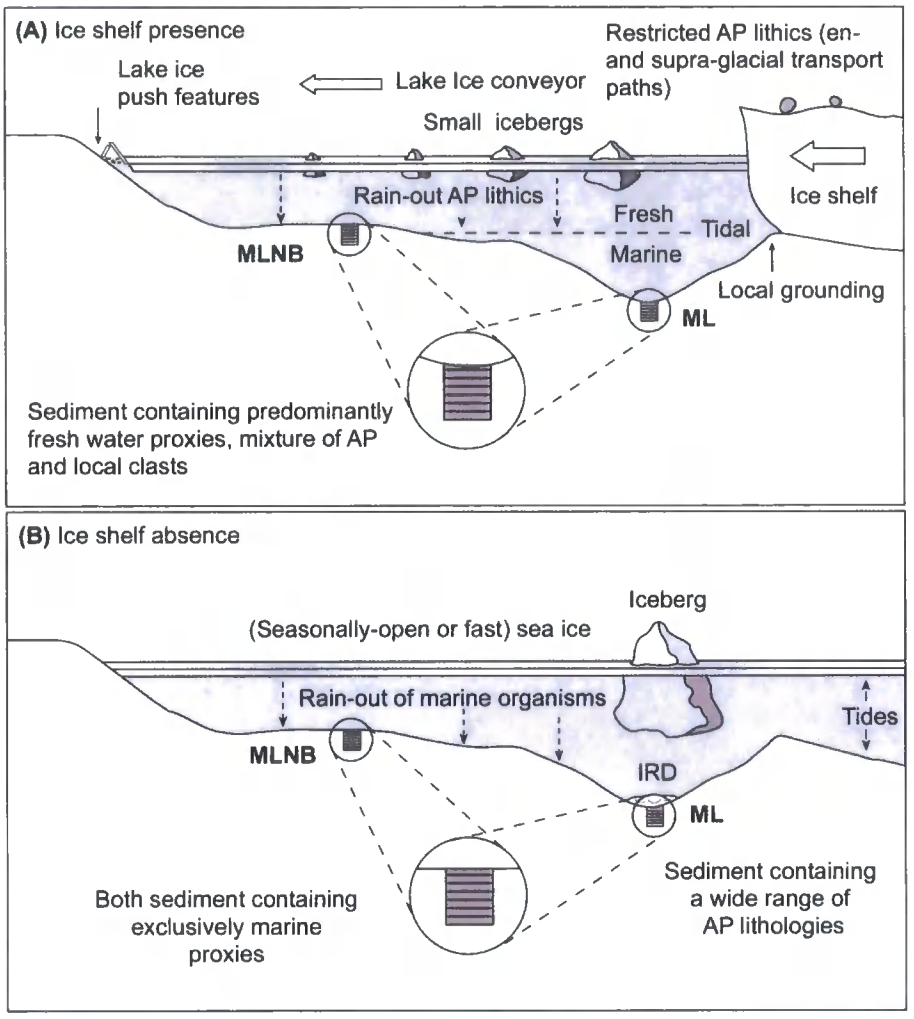

Figure 5.15. Conceptual model: **(a) Ice shelf presence.** Biologically the water column is stratified, with freshwater overlying marine water. Freshwater organisms dominate the biological assemblage and sedimentation is likely to be dominated by local fluvial and material transported by the ice shelf, a process driven by the 'lake ice conveyor' (e.g. Hendy et al., 2000). Material transported via the ice shelf is dominated by a restricted lithological assemblage, probably exploiting specific flow lines within the ice shelf. Isotopically, the sediments contain a freshwater signal; **(b) Ice shelf absence.** The stratified water column is replaced by a purely marine one. The biological assemblage is dominated by marine organism (e.g. diatoms), with the possible introduction of other marine organisms (e.g. foraminifera). Sedimentation is chaotic, with a wide range of lithological types being deposited as ice rafted debris (IRD). Isotopically the sediments are imprinted with a marine signal.

dominating the overall assemblage. This implies that some marine diatoms are advected beneath the ice shelf, but not in significant numbers. In both environments the biological signature during ice shelf presence is relatively weak or diffuse, since very little *in-situ* productivity takes place.

It has been shown in this Chapter (and Chapter 4) that the ratio of sedimentary organic carbon (C_{org}) to nitrogen (N_{org}) content of sediment can be used together with isotope ratios of organic carbon ($\delta^{13}C_{org}$) to differentiate between marine and terrestrial sources of organic matter and provide information on past productivity. In theory during ice shelf presence the C/N ratio will be dominated by terrestrial-derived C and N and will have a likely signature of 8-10 whilst the carbon isotopic composition of the sediment will be depleted in ^{13}C and characterized by freshwater algal values, yielding $\delta^{13}C_{org}$ values between –30 and -25‰. However, whilst a clear terrestrial signature has been detected in the surface sediments, a true marine signature remains unclear. The surface sediments of the main cores sites in both ML and AB yield $\delta^{13}C_{org}$ values of ca. –25 ‰, which is also thought to reflect a terrestrial source. Ice shelf presence is therefore characterised by $\delta^{13}C_{org}$ values of ca. –25 ‰.

The present day environment (i.e. ice shelf presence) is characterised by a relatively wide range in grain-sizes, but overall has an average mode, which probably reflects fluvially-derived material (<2 mm). Furthermore, the sediment appears to be dominated by local sedimentary lithologies (e.g. mudstone), which have a distinct carbon isotopic signature (ca. –25 ‰).

5.4.2.2. Ice Shelf Absence

Figure 15b shows the ice shelf absence scenario. Importantly, ice shelf loss would see the present stratified water column replaced by a purely marine one. Effectively, an epishelf lake would be replaced by a marine embayment. This would result in fundamental chemical, biological and sedimentological changes in the lake system.

It is the hypothesis of this PhD thesis that the present day diatom assemblage will be

replaced during periods of ice shelf loss by an exclusively marine assemblage. In addition to open marine diatom species one would expect to see the first appearance of sea-ice related taxa (e.g. *Fragilariopsis species*; Cremer et al., 2002). This change is likely to be rapid, owing to the sensitive ecologies of most freshwater forms. A similar scenario has been documented in a lake on Horseshoe Island, Antarctic Peninsula (Fig. 2.1b) where Wasell and Håkansson (1992) have shown the transition from marine conditions to a freshwater environment following isostatic isolation. Ice shelf collapse may also witness the appearance of other marine organisms (e.g. foraminifera).

A switch from a mainly freshwater water column to a marine-dominated environment will be reflected in the isotopic and elemental proxies. It is likely that during ice shelf absence, and a dominance of marine water, then the $\delta^{13}C$ signature of lake sediments is likely to fall to between –20 and –25 ‰, some ca. 5-7 ‰ lighter than present day (ice shelf presence) values. The C/N ratio is also likely to change, due to the influx of marine algae, which tend to be rich in nitrogen, thereby depressing the overall C/N ratio.

Significant changes in sedimentation are likely to follow any change in the configuration of George VI Ice Shelf. A coarsening of material is expected following ice shelf loss, in the form of ice-rafted debris. It has been documented above that the ice shelf transports exotic granite and metamorphic material from the Antarctic Peninsula to Moutonnée Lake. These differ from the rocks of Alexander Island, which are predominantly sedimentary in origin. Phases of ice shelf collapse should be marked by a clear depositional shift. Restricted ranges of igneous and metamorphic clasts, transported through George VI Ice Shelf to Alexander Island, and deposited with locally-derived sedimentary clasts, would be replaced, during periods of ice shelf loss, by a much broader lithological assemblage dominated by ice-rafted debris and locally derived sedimentary clasts from many different sources.

In summary, it is the hypothesis of this PhD thesis that any changes in the stability of the ice shelf should leave distinct biological, chemical and lithological signatures

in the lake sedimentary record. Biologically, ice shelf loss would see the present stratified water column replaced by a purely marine one with the consequent changes in biological assemblages. Significant changes in the mode of transport and abundance of clasts are also likely to follow any change in the configuration of George VI Ice Shelf. Ice shelf loss will be characterized by chaotic deposition of IRD with a wide variety of lithologies. Finally distinct changes in the chemical signature of the sediments are likely to follow any changes in the ice shelf. This is most likely to be reflected in the $\delta^{13}C$ values on organic matter, which should record any substantial changes in the lake hydrology. The thesis presented here is that through a combined biological, chemical and lithological approach it will be possible to provide an unambiguous record of ice shelf fluctuations. Agreement between the proxy records will clearly result in a robust record of Holocene ice shelf history, and thus environmental change.

5.5. Chapter Summary

The limnology of Moutonnée and Ablation Lakes has been re-evaluated after a period of 30 years. This has provided a long-term perspective on the changing chemistry and biology of these epishelf lakes. During this period the AP region has experienced a period of rapid regional warming that has resulted in the retreat and collapse of ice shelves north of 70 degrees latitude. Spanning 70-74.5° South, George VI ice shelf is now nearing its theoretical limit of stability. The role of the ice shelf in maintaining stratification of the water columns in these lakes means that they are uniquely placed to record periods of ice shelf loss both in the past (in their sediments) and in the future. This chapter has provided a perspective on changes in these lakes over the last 30 years and provides new baseline limnological data such as were available at Disraeli Fiord, an epishelf lake on the northern coast of Ellesmere Island, Arctic Canada, which displayed very clear changes in its water chemistry prior to the break-up of the Ward Hunt Ice Shelf (Mueller et al., 2003). In Moutonnée Lake for example, the halocline may have gradually risen over the 30-year period. It is uncertain at present however, whether these changes are associated with ice shelf thinning, or seasonal variability. To determine which of these two competing hypotheses is correct would require a long-term monitoring study.

In addition this chapter has used the reference data set presented above to develop a conceptual model for detecting ice shelf loss in epishelf lakes and has identified and evaluated a suite of proxies that are likely to change during ice shelf absence. Specifically, ice shelf loss is likely to cause significant changes in the biological (e.g. diatom), isotopic and elemental (e.g. $\delta^{13}C_{org}$ and C/N) and physical (e.g. grain-size/MS) signature of the lake sediments. The next chapter will present the results of the analysis of cores extracted from Moutonnée and Ablation Lakes.

Chapter 6

MULTI-PROXY CORE RESULTS FROM MOUTONNÉE AND ABLATION LAKES

6.1. Introduction

This chapter presents the biological, isotopic, elemental and physical data analyses of core material collected from Moutonnée and Ablation Lakes. These are used to develop a detailed palaeoenvironmental interpretation of each record in Chapter 7. Specifically, this chapter has three aims; Firstly, to identify key changes in each proxy record, which can then be associated with hydrological and/or physical changes in the lake system; secondly, to identify concurrent changes between individual proxies; and finally, to identify concurrent changes between cores from different lakes. This scaling-up from proxy to multi-proxy to multi-core is essential to provide a robust record of GVI-IS variability.

As will be shown in the following sections, distinct biological changes have been detected in Moutonnée Lake (both ML and MLNB cores), which are considered here to represent fundamental changes in the lake environment, recording periods of past ice shelf loss. In order to help focus the results and to achieve the aims outlined above, all data are presented and described with reference to the key diatom and foraminiferal zones, rather than separate zonation for each proxy record. Where appropriate, other significant patterns and changes are also highlighted.

The first section will present the results of the biological data from the sediment cores. The second section will present the isotopic and elemental analyses performed on the sediment cores and micropalaeontological remains within the sediments, whilst the third section will present the results of physical core analyses. The final section will present the core chronology and then summarise the key

patterns within and between the two lakes. The raw data presented in this chapter is also included as appendices (Appendix 2-5).

6.2 Biological Analysis

This section presents the results of diatom and foraminiferal analysis performed on core material from Moutonnée Lake. Analysis of sediment from the Ablation Lake cores (40 samples in total) revealed that they were devoid of micropalaeontological remains and suggests that the lake at the deeper core site is largely unproductive and /or corrosive (See Chapter 5).

6.2.1. Diatom Analysis

6.2.1.1. Moutonnée Lake (ML) Core

Of the 105 samples from the ML core prepared for quantitative diatom analysis, 40 samples contained diatoms. The diatom stratigraphy can be divided into five clear zones (Fig. 6.1) hereafter referred to as biota zones (BZ) I to V. The depths for these zones are: BZI (537–500 cm), BZII (499–485 cm), BZIII (484–302 cm), BZIV (301–236 cm) and BZV (235–0 cm). This five-fold zonation was established visually, since zonation using CONISS resulted in over-complicated zonation. Sediment from the other 65 samples (Zones I, III and V) were devoid of diatom and/or other micropalaeontological remains, despite the entire slide being analysed. Slides from Zones II and IV however, contained 30 diatom taxa (of which 1 could not identified to species level). All identified taxa are characteristic of marine and/or brackish water, with no freshwater taxa present (Table 6.1 and Plate 1). The diatom data is presented as number of valves per gram of sediment (valves g^{-1} sediment) rather than percentages. This is more useful for assessing changes in productivity. For comparison, percentage plots are shown in Appendix 1.

Zone II (485-500 cm)

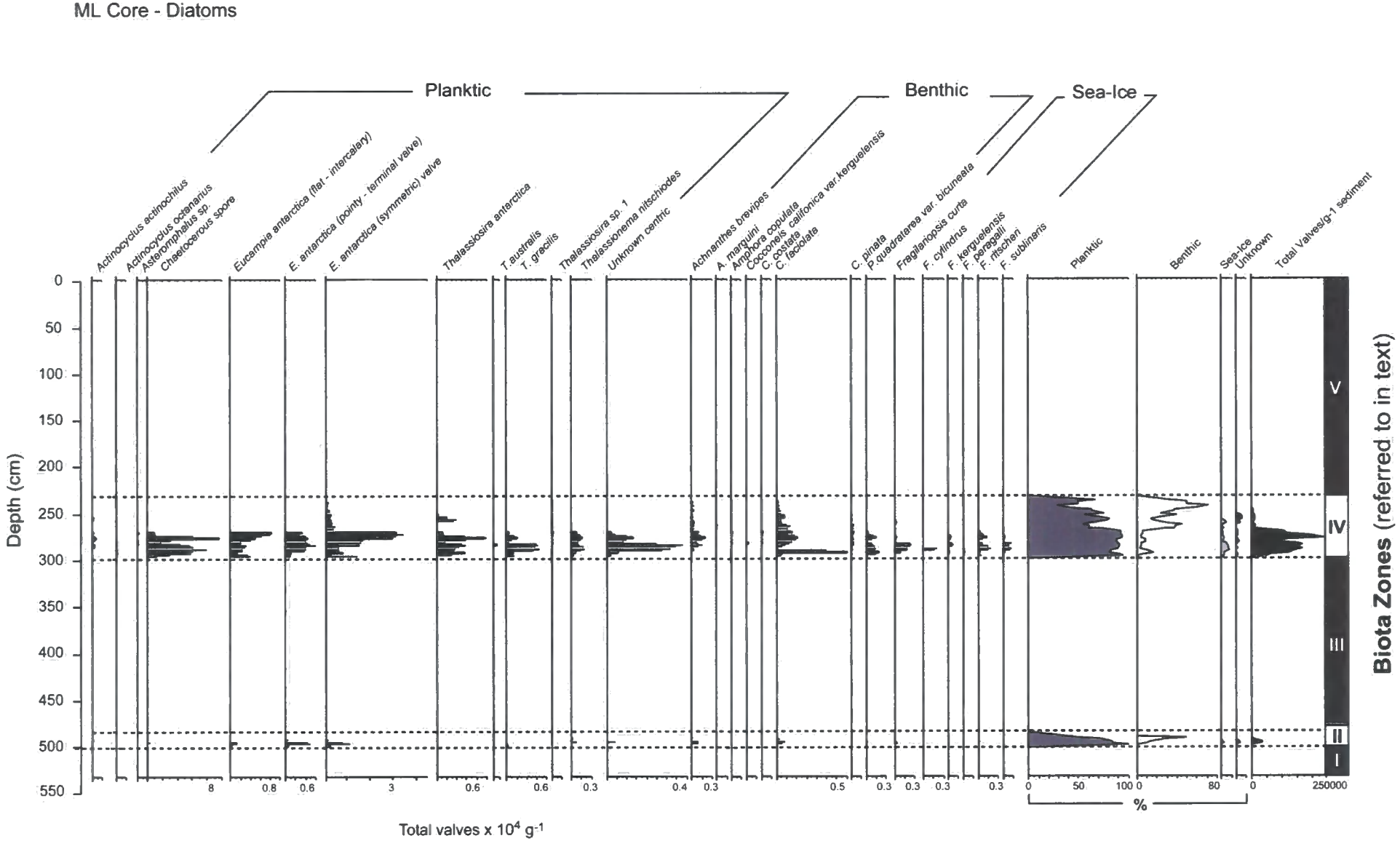

Figure 6.1. Diatom analysis of the ML core. Data presented as total number of valves x 10^4 g^{-1} sediment.

Species	References	Ecology/Salinity	Biogeography
Achnanthes hreviceps var.intermedia (Kutzing) Cleve	Ko-bayashi 1963, p.5, pls.1-3;n Kramer and Lange-Bertalot 1991, p.3, pl.1:4-8.	be/m,br?fr	cos
Achnanthes marguini/taylorensis		br/m	?
Actinocyclus actinochilus (Ehrenberg) Simonsen	Hustedt 1958, p. 126, figs 57-80 [as Charcotia actinochilus (Ehrenberg) nov. comb]; Simonsen 1982, p.105, figs 1-9; Krebs 1983, p.283, fig.6 [as Charcotia actinochilus].	pl/m	scw
Amphora copulata (Kutzing) Schoeman and Archibald	Schoeman and Archibald 1986, p.426, figs 14-53; Krammer and Lange-Bertalot 1997a, p.345, pl.149-3; 3-11 [as Amphora libyca Ehrenberg].	be/m, br	cos
Cocconies californica var. kerguelensis Heiden	Heiden and Kolbe 1928, p. 585, pl. 5:109; Simonsen 1992, p.32 pl. 32:9-15	be/m	circant
Cocconies costata var. antarctica Manguin	Manguin 1960, p.304, pl. 14:154-155a-c.	be,?pl/m	circant
Cocconeis faciolata (Ehrenberg) Brown	Krebs 1983, p.285, pl.2:1; Romero 1996, p. 380, figs 70-94.	be, pl/m	circant
Cocconeis pinnata Gregory	Romero 1996, p372/380-384	be/fr	?
Diploneis sp. 1 (sp b)	Roberts and McMinn 1999 p. 71, pl.3, fig.2	?	?
Diploneis splendida (Gregory) Cleve	Cleve 1894, p.87		
Diploneis stigmosa Heiden	Heiden and Kolbe 1928, p. 613, pl. 2:56; Manguin 1960, p. 308, pl. 30:363-364; Simonsen 1992, p. 50 pl. 51:3-4.	be/pl/m	circant
Eucampia antarctica var. recta (Castracane) Manguin	Hoban et al., 1980, p.592, figs. 1-14 [as E. balasutium Castracane]; Syvertsen and Hasle 1996 p. 172, pl. 33.	pl/m	scw
Fragilariopsis curta (Van Heurck) Hustedt	Hustsedt 1958, p. 160, figs 140-144, 159; Hasle 1965, p. 32, pls. 12:2-5, 13:1-6.	pl, cryo/m	scw
Fragilariopsis cylindrus (Grunow) Krieger	Hustsedt 1958, p. 162, figs 145-146; Hasle 1965, p. 32, pls. 12:6-12, 14:1-10, 17:2-4.	pl, cyro/m	ncw, scw
Fragilariopsis keruelenssis (O'Meara) Hustedt	Hustsedt 1958, p. 162, figs 121-127; Hasle 1965, p. 14, pls. 4:11-18, 5:1-11.	pl, cryo/m	scw
Fragilariopsis peragalii (Hasle) Cremer nov.comb	Hasle 1965, p. 41, pls 9:11-12, 15:1-5 [as Nitzschia peragallii]; Medlin and Priddle 1990, p.181, pls. 24, 4:11-12, 24,7:1-5 [as Nitzschia peragallii Hasle]	pl, cyro/m	scw
Fragilariopsis ritscheri Hustedt	Hustedt 1958, p. 164, 133-136, 153; Hasle 1965, p. 20 pls. 4:1-10, 5: 12-13	pl/m	scw
Fragilariopsis sublinearis (Van Heurck) Heiden	Heiden and Kolbe 1928, p. 554; Hasle 1965, p.27, pls. 7: 1, 11:1-10, 12:1	pl/m	
Navicula sp. 1	Unknown		
Pinnularia borealis Ehrenberg	Krammer and lange-Bertalot 1986	fr,br	cos
Pinnularia quadratarea var. bicuneata Heiden	Heiden and Kolbe 1928, p. 596, pl.2:33-35; Simonsen 1992, p.42, pl. 43:1-5; Tanimura 1992, p. 409, pl, 4:41-42 [as P . Quadratarea (Schmidt) Cleve]	be, cryo/m	circpol
Stauroneis anceps Ehrenberg	Krammer et al., 1986, p. 240, 614-617; Roberts and McMinn 1996 ??? [as Stauroneis cf. anceps]; Roberts and McMinn 1997, ???? [as Stauroneis cf. anceps]	pl/br, fr	circant
Thalassionema nitzschiodes (Grunow) Mereschkowsky	Heiden and Kolbe 1928, p. 564, pl. 5: 115 [as T. nitzschioides var. gracilis Heiden]; Simonsen 1992, p. 24, pl. 21: 1-4 [as T. nitzschiodes var. gracilis Heiden]; Hasle 2001, p. 9, figs 1-27;	pl/m	circant
Thalassiosira antarctica Comber	Hasle and Heimdal 1968, p. 359, figs 1-21; Johansen and Fryxell 1985, p. 158, figs 15-17, 37-39	pl, cryo/m	ncw, scw
Thalassiosira australis Peragallo	Fryxell 1977, p.96, figs 1-12; Johansen and Fryxell 1985, p. 158, figs 19-20, 46-48	pl/m	scw
Thalassiosira gracilis (Karsten) Hustedt	Hustedt 1958, p. 109, pl. 3: 4-7; Fryxell and Hasle 1979b, p. 382, figs 12-22; Johansen and Fryxell 1985, p. 170, figs 8, 58-59	pl/m	scw
Thalassiosira tumida (Janisch) Hasle	Rivera 1981, p. 127, pls. 61:378-383, 62: 384-389; Johansen and Fryxell 1985, p. 176	pl/m	scw
Thalassiosira sp.1	figs 28-32		
Thalassiosira sp. 2	Unknown	pl/m	-
Thalassiosira sp. 3	Unknown	pl/m	-
Chaetocerous spore (neglectus Karsten)	Priddle and Fyrxell 1985, p. 46-47; Hasle and Syvertsen 1996, p. 207, pl. 44.	pl/m	scw

Abbreviations: **Ecology**: be: benthic; cryo: in sea-ice and/or underneath the sea-ice; pl: planktonic; **Salinity**: fr: freshwater; in: marine; br: brackish water; **Biogeography**:cos: cosmopolitan; circant: circum-antarctic; circpol: circum-polar in the Arctic and Antarctic; ncw: northern cold water region; scw: southern cold water region (table modified from Cremer et al., 2003)

Table 6.1. Diatom taxa identified in the core sediments from Moutonnée Lake (after Cremer et al., 2003).

The diatom data (valves g^{-1} sediment) from Zone II in the ML core was further divided into two sub-zones by cluster analysis (CONISS) (Fig. 6.2). The characteristics of each are described in turn below.

Sub-zone IIa (500-493 cm) is dominated by planktic taxa, notably the various life history stages of *E. antarctica var. recta*, which account for between 93.75% (499 cm) and 54.84% (493 cm) of the assemblage (Fig. 6.1 and 6.2). Absolute diatom abundance in the sub-zone peaks at 497 cm, with a concentration of 27277 valves g^{-1} sediment. The upper sub-zone boundary is defined by a decrease in total valve concentration (Fig. 6.2).

Sub-zone IIb (492-485 cm) is characterised by uniformly low diatom counts (< 5 valves per slide). Notably *E. antarctica var. recta* and *Chaetoceros spp.* are absent (Fig. 6.1 and 6.2).

Zone IV (236-296 cm)

Zone IV in the ML core has been further was further divided into five sub-zones by cluster analysis (Fig. 6.3. The characteristics of each are described in turn below.

Sub-zone IVa (296-282 cm). The lower boundary of Zone IVa is characterised by high concentrations of planktic diatoms, notably various life history stages of *Eucampia antarctica var. recta* (59.52%), *Thalassiosira gracilis* (3.6%) and *Chaetoceros spores* (28.6%). There is an increase in the benthic marine species *Cocconeis faciolata* (14%) between 293-289cm. Concentrations of an Unknown centric (Plate 1) increase, which is also coincident with increases in the planktic taxa *E. antarctica var. recta, T. gracilis* and *Chaetoceros spores*. Sea-ice taxa, notably *Fragilariopsis curta* (2.5%) and *F. cylindrus* (2%) increase from 292 cm, reaching a maximum concentration of 7.3% at 290 cm. The upper boundary of sub-zone IVa is defined by a decrease in the total number of diatom valves, particularly planktic species, from a sub-zone maximum of 137376 valves g^{-1} sediment at 284 cm to 74936 valves g^{-1} sediment at the sub-zone boundary (Fig. 6.3). For example, *Chaetoceros spores* and the Unknown centric decline from 60.72% and 11.4% respectively in sub-zone IVa to 11.4% and 4.8% respectively at the boundary

ML Core - Zone II

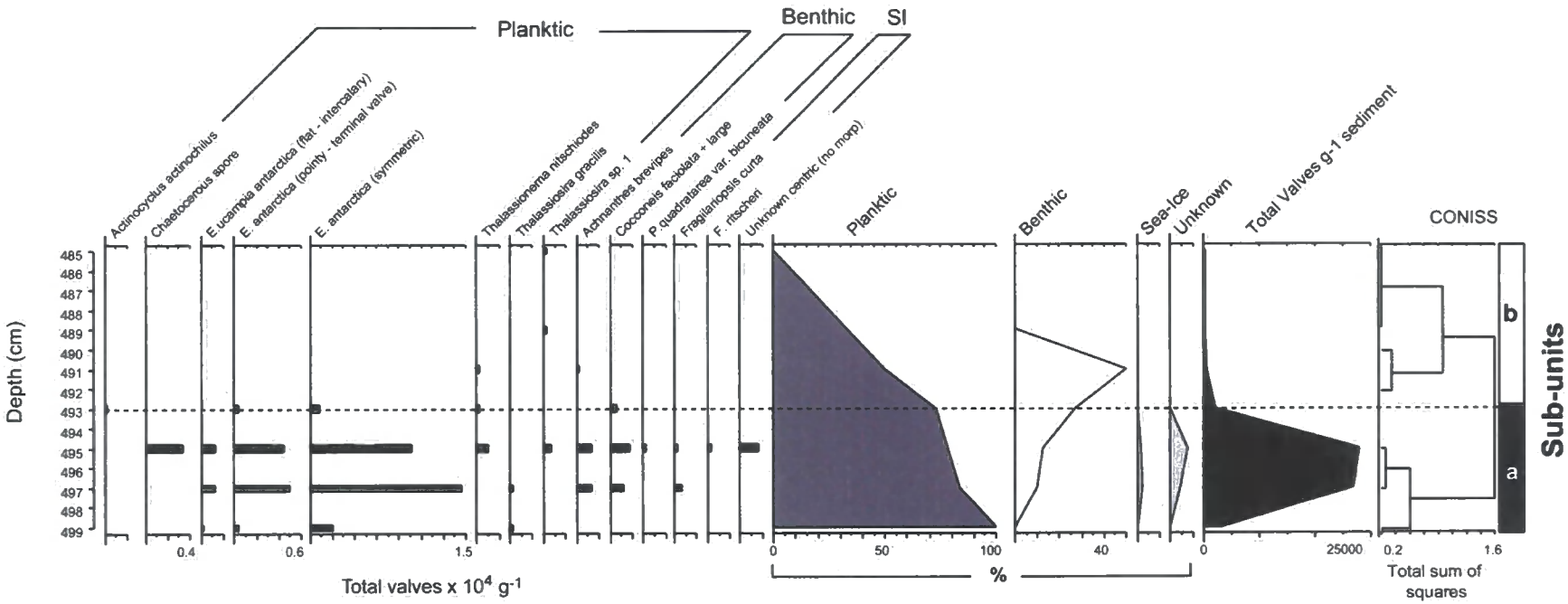

Figure 6.2 Diatom analysis of the ML core: Zone II. Data presented as valves x 10^4 g^{-1} sediment.

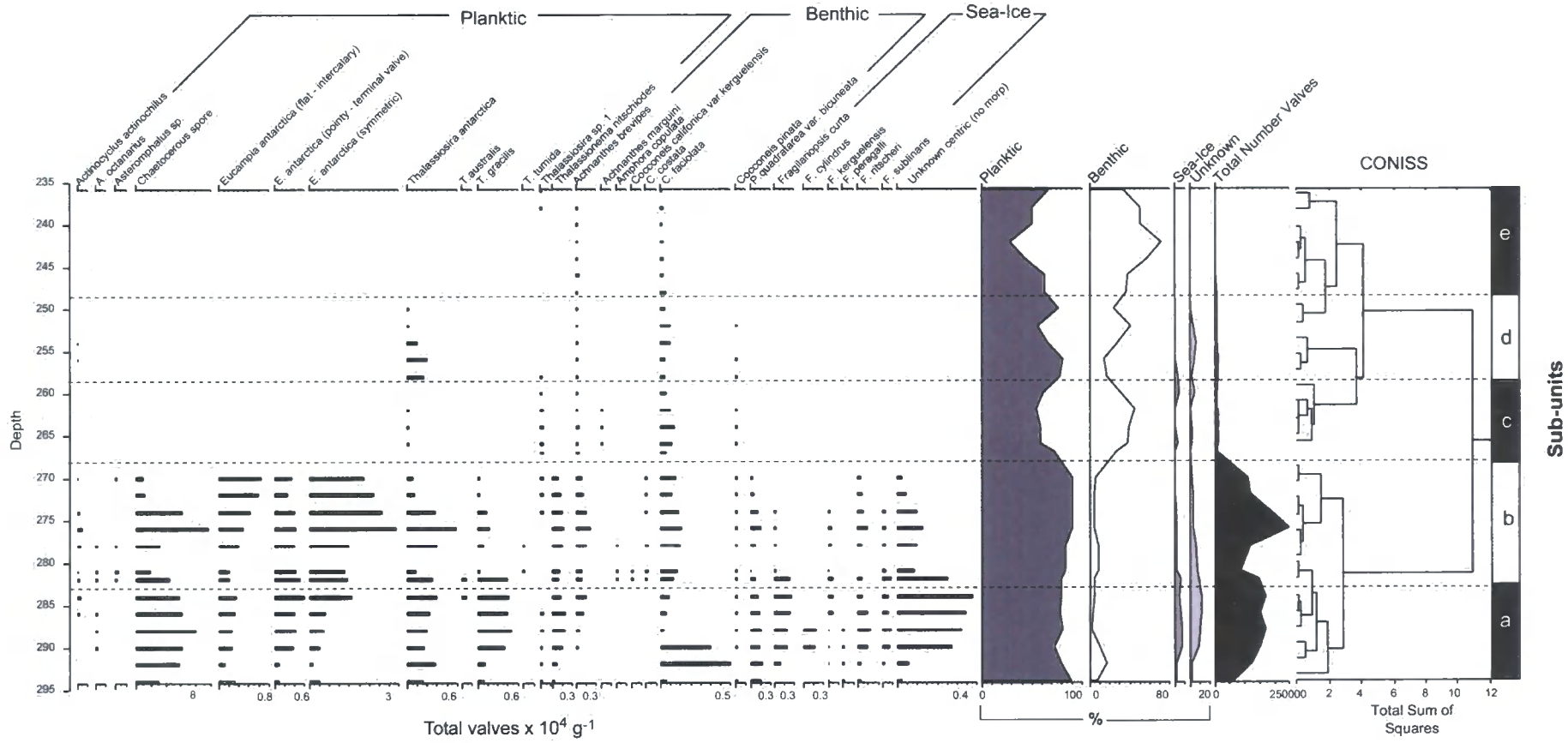

Figure 6.3. Diatom analysis of the ML core: Biota Zone IV. Data presented as valves x 10^4 g^{-1} sediment.

between sub-zone IVa and IVb. Other planktic taxa such as *T. antarctica* and *T. gracilis* also decline.

Sub-zone IVb (281-268 cm) is characterised by maximum diatom concentrations. Planktic marine and sea-ice diatoms, most notably *E. antarctica var. recta*, *T. antarctica* and *Chaetoceros* spores, increase from a minimum at the lower sub-zone boundary reaching a core maximum at 276 cm of 223925 valves g^{-1} sediment (Fig. 6.3). At this depth, the sub-zone is dominated by planktic taxa (90.8%) with benthic taxa accounting for 4.7% and sea-ice taxa 1.6%. Concentrations of *E. antarctica var. recta*, *Chaetoceros spores*, *Thalassiosira species* and general sea-ice taxa all decrease towards the upper sub-zone boundary. The upper sub-zone boundary is defined by a marked decline in the total number of valves, particularly the dominant planktonic taxa; *E. antarctica var. recta* and *Chaetoceros spores*.

Sub-zone IVc (267-259 cm) is characterised by an overall decrease in diatom abundance (Fig. 6.1 and 6.3), notably *Chaetoceros*, *E. antarctica var. recta* (intercalary, terminal and symmetric forms) and *T. antarctica*. The winter stage of *E. antarctica var. recta* (valve view of intercalary valve) still dominates the overall concentration, accounting for between 63% and 48% of the diatom assemblage. An overall decrease in planktic species coincides with an increase in benthic taxa, notably *C. faciolata*, which accounts for up to 27% of the assemblage in this sub-zone.

Sub-zone IVd (258-248 cm) is defined by an increase in *Thalassiosira antarctica*, which accounts for between 9.5% and 40.4% of the total assemblage. *E. antarctica var. recta* still dominates the sub-zone accounting for between 32.5% and 66.6%. The overall increase in benthic taxa, is the result of relative increases in *C. faciolata* and *Achnanthes breviceps*.

Sub-zone IVe (247-236 cm). The lower boundary of sub-zone IVe is defined by the disappearance of *T. antarctica*. The sub-zone is characterised by an increase in benthic taxa relative to planktic taxa, particularly *A. breviceps* and *C. faciolata*. Overall diatom abundance however continues to decrease, with diatoms disappearing entirely from the sediments at 236 cm (Fig. 6.3).

6.2.2.2. Moutonnée Lake North Basin (MLNB) Core

Of the 38 samples from the MLNB core prepared for quantitative diatom analysis, 15 samples contained diatoms. The resulting diagram shows two clear zones (Fig. 6.4). The depths for these zones are: BZ1 (172-135 cm) and BZII (134-0 cm). Sediment from BZII was devoid of diatom and/or other micropalaeontological remains, despite the entire slides from BZII being analysed. Slides from BZI contained 24 diatom taxa of which one could not be identified to species level. All identified taxa are characteristics of marine and/or brackish water, with no freshwater taxa present.

Zone 1 (171-120 cm)

Zone I in the MLNB core was further divided into two sub-zones by cluster analysis (Fig. 6.5). The characteristics of each are described in turn below.

Sub-zone Ia (171-153). The lower boundary (core bottom) is characterised by the highest abundance of diatom valves (78369 valves g^{-1} sediment) (Fig. 6.5) in MLNB. The overall assemblage is dominated by planktic taxa, particularly *Eucampia antarctica var. recta* (17.4%), *Thalassiosira sp.*1 (13.9%), *T. antarctica* (10.15%) and *Chaetoceros spores* (6.09%). Benthic taxa are dominated by *C. faciocolata* (19.03%) and *A. breviceps* (4.3%). Sea-ice taxa, notably *F. curta*, contribute 8.88% to the overall assemblage. From this depth, total valve abundance declines, which is largely the result of declining counts of the major planktic taxa. The upper boundary of sub-zone *Ia* is defined by significant decreases in *E. antarctica var. recta* and *Thalassiosira sp.* and also sea-ice taxa.

Sub-zone Ib (152-120) is characterised by declining valve abundances. The proportion of benthic taxa increases relative to planktic and sea-ice groups. *C. faciolata* constitutes between 45.6% and 100% of the overall diatom assemblage.

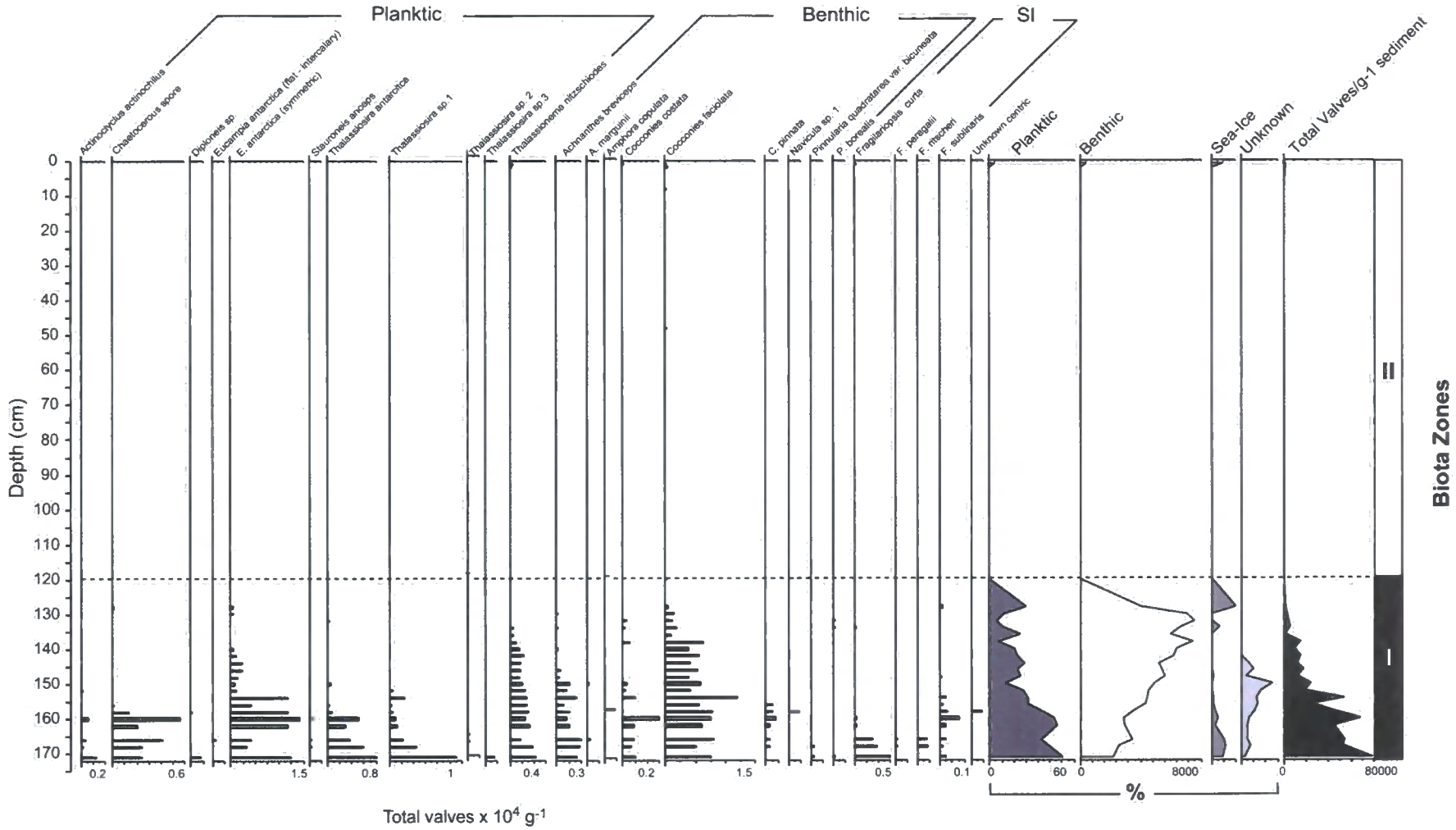

Figure 6.4. Diatom analysis of the MLNB core. Data presented as valves x 10^4 g^{-1} sediment

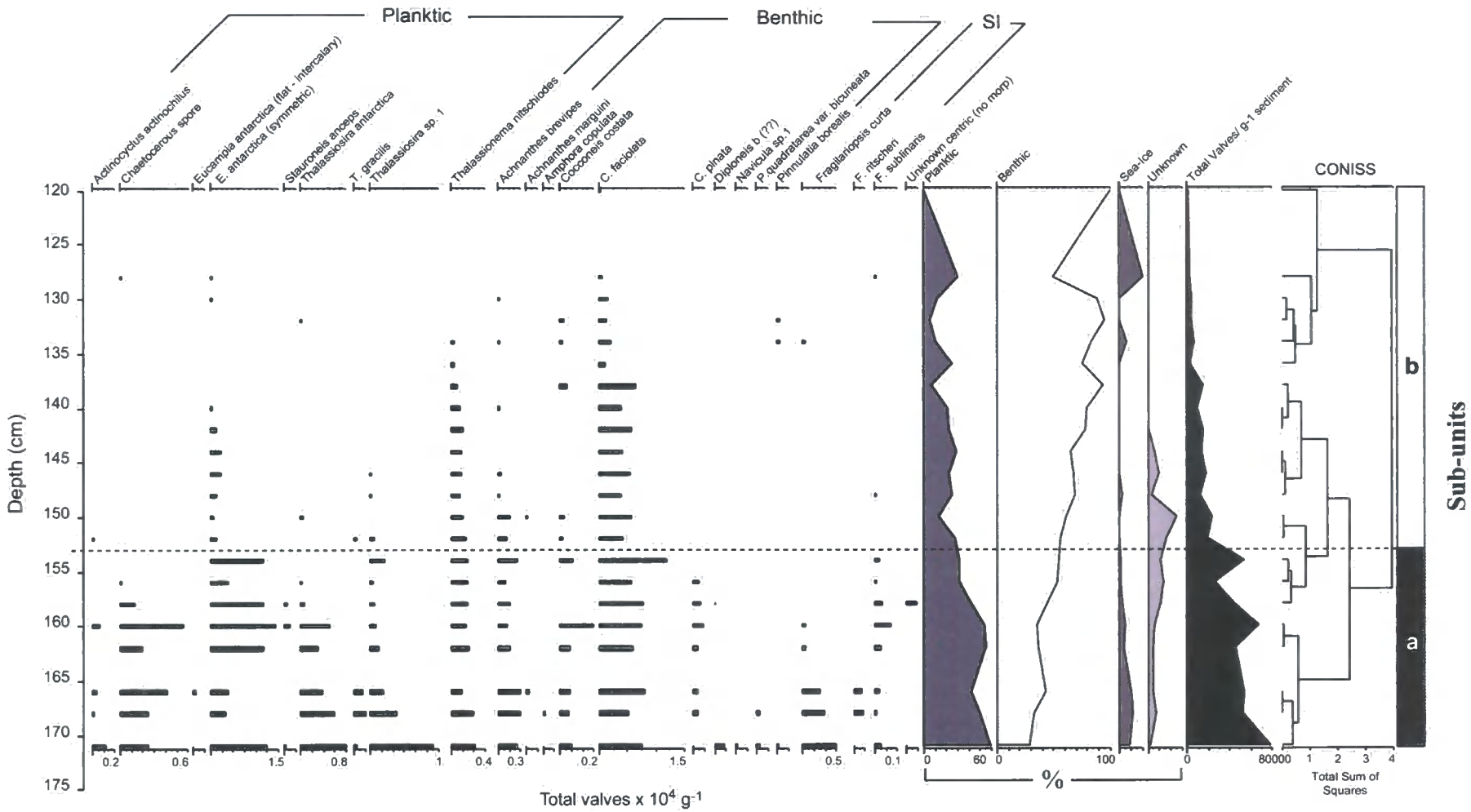

Figure 6.5. Diagram analysis of the MLNB core: Zone I. Data presented as valves x 10^4 g^{-1} sediment.

6.2.2.Foraminiferal Analysis

This section present the results of foraminiferal analysis performed on core material from the two principal sediment cores (ML and MLNB) from Moutonnée Lake. The data are presented as number of foraminifera per gram of sediment (foraminifera g^{-1}), with additional summary percentages of the most abundant genera. This is more useful for assessing overall changes in productivity. For comparison, percentage plots are shown in Appendix 1.

6.2.2.1. Moutonnée Lake (ML) Core

Of the 105 samples from the ML core prepared for quantitative foraminiferal analysis, 31 samples contained foraminifera. The resulting diagram also shows five clear zones (Fig. 6.6), which are directly comparable with the diatom zonation described in section 6.2.1. Like the diatom data, sediments from BZI, III and V were completely devoid of foraminifera, despite detailed inspection of the sediment. From the samples from BZII and IV, 12 distinct foraminiferal were identified (Plate 2). Of these, 4 were identified to species level, 7 to genus level and 1 could not be assigned a species name. All identified foraminifera are calcareous benthic marine species (Murray, 1991), with the assemblage being dominated by *Globocassidulina* species.

Zone II (497-491 cm)

Zone II in the ML core has been further split into three sub-zones using cluster analysis (Fig. 6.7). Each sub-zone coincides with the zonation suggested by each of the highest splits of CONISS (Grimm, 1987).

Sub-zone IIa (497-494.5 cm) is characterised by an overall dominance of *Globocassidulina* species. Total abundance reaches a maximum of 759 g^{-1} at 495 cm, composed mainly of *Globocassidulina sp.* From this depth total abundance declines (Fig. 6.7).

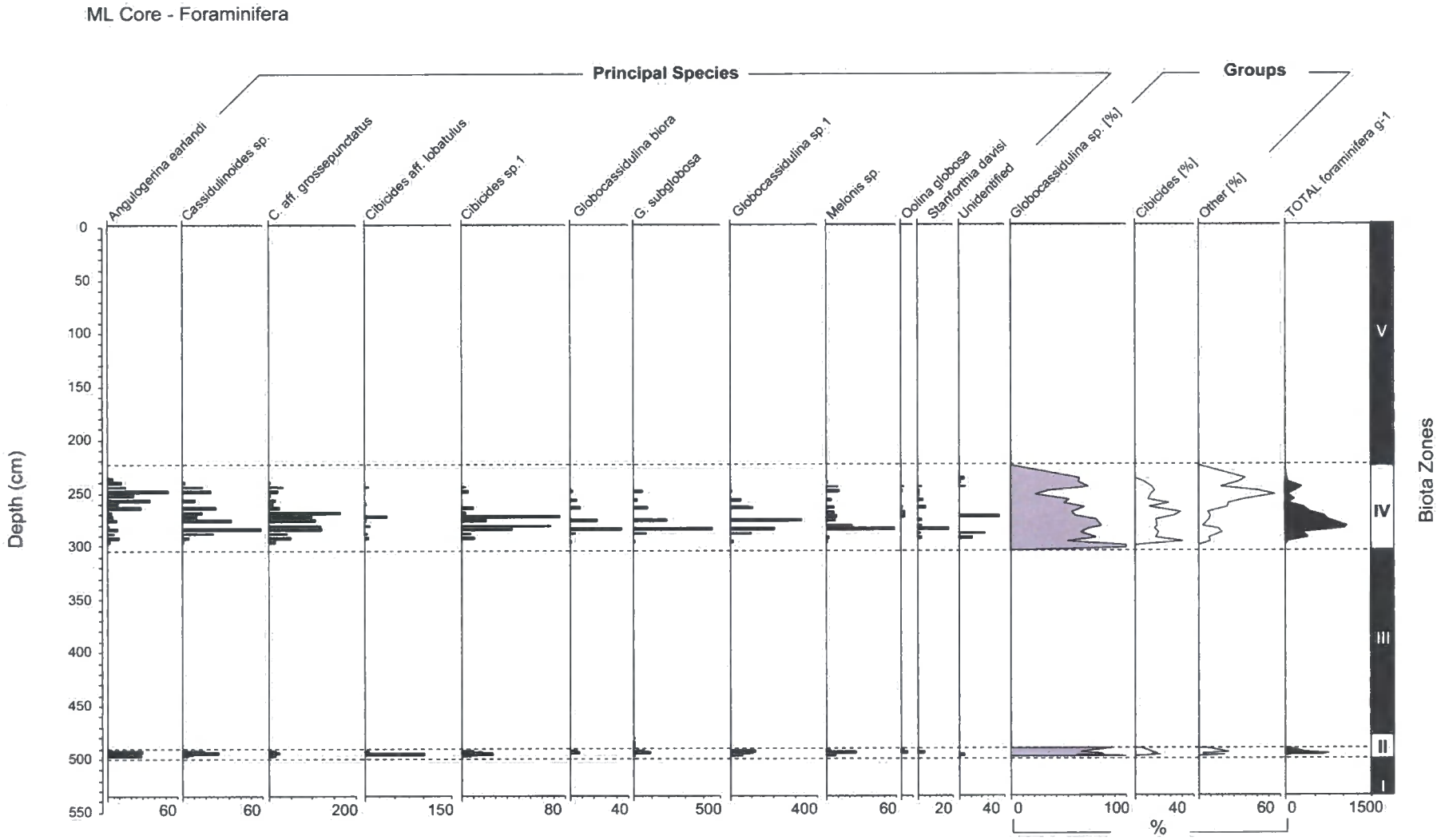

Figure 6.6. Foraminiferal analysis of the ML core. Data presented as total number of foraminifera per gram of sediment (n/g^{-1}). Summary percentages of principal genera groups are shown to the right of the diagram, together with total number of foraminifera g^{-1}.

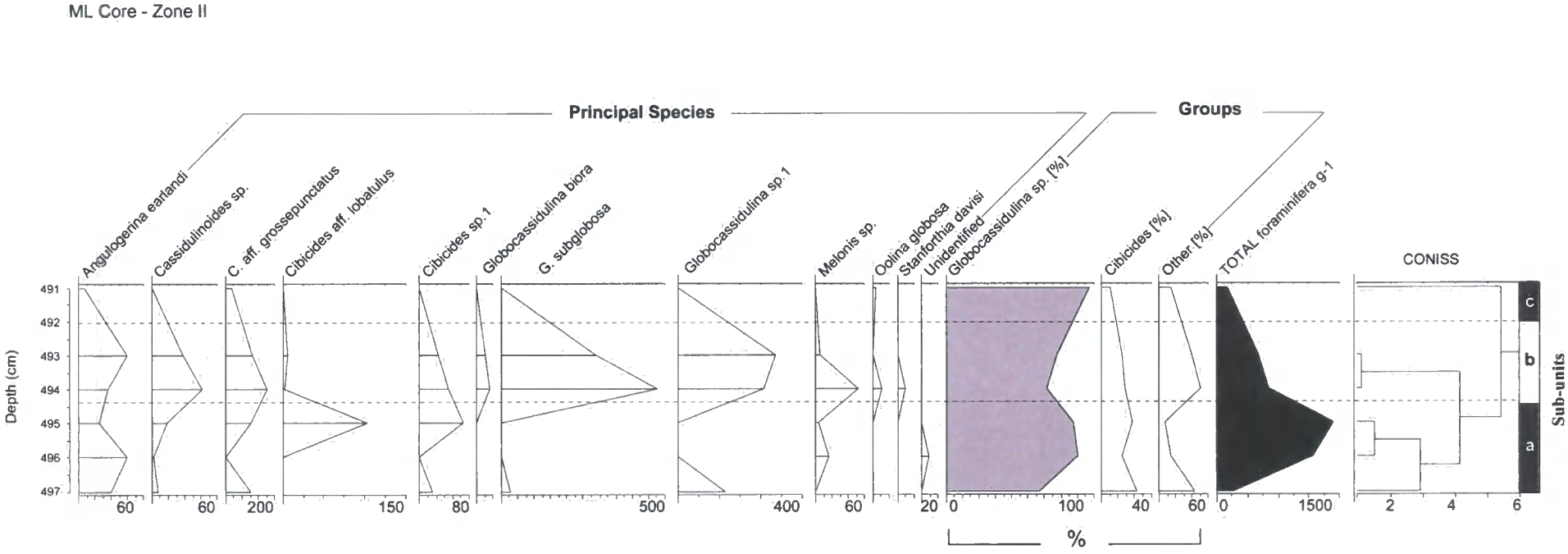

Figure 6.7. Foraminiferal analysis of the ML core zone II. Data presented as total number of foraminifera per gram of sediment (g^{-1}). Summary percentages of principal genera groups are shown to the right of the diagram, together with total number of foraminifera g^{-1}.

Sub-zone IIb (494-492.5 cm) is characterised by a continued decline in total foraminifera abundance. Other notable features include peaks in *Angulogerina earlandi* at 493 cm and *Melonis sp.*, *Oolina globosa* and *Stainforthia davisi* at 494 cm.

Sub-zone IIc (492-491 cm). All foraminifera species decline, except *Oolina globosa* which shows a small increase.

Zone IV (302-235 cm)

Zone IV in the ML core has been further split into four sub-zones (Fig. 6.8) suggested by each of the highest splits of the cluster analysis.

Sub-zone IVa (302-297 cm). The base of sub-zone IIa is characterised by low numbers of all species. *Globocassidulina species* dominate the assemblage.

Sub-zone IVb (296-266 cm) is characterised by increasing numbers of most foraminifera species. *Globocassidulina* species, notably *G. subglosa* and *G. biora* dominate the overall assemblage, accounting for between 50 and 78%. The rise in *Globocassidulina sp.* coincides with a maximum total foraminifera abundance of 1074 g^{-1} at 281 cm. Other notable peaks at this depth include maximum concentrations of *Cassidulinoides sp.*, *Melonis sp.*, and *Stainforthia davisi*. From this depth total abundance declines towards the upper sub-zone boundary. *Angulogerina earlandi* numbers remain low throughout the sub-zone.

Sub-zone IVc (265-243 cm). Zone IIc is characterised by low numbers of major species, notably and *G. subglosa*, *G.biora* and *C. aff. grossepunctatus* and relatively high numbers of *A. earlandi*, reaching a maximum of 52.4 g^{-1} (63%) at 248 cm. Total abundance increases slightly towards the upper sub-zone boundary (Fig. 6.8).

Sub-zone IVd (242-236 cm) is characterised by declining species numbers. *Globocassidulina species* (60%) are sub-dominant with *A. earlandi* accounting for 20% of the total assemblage.

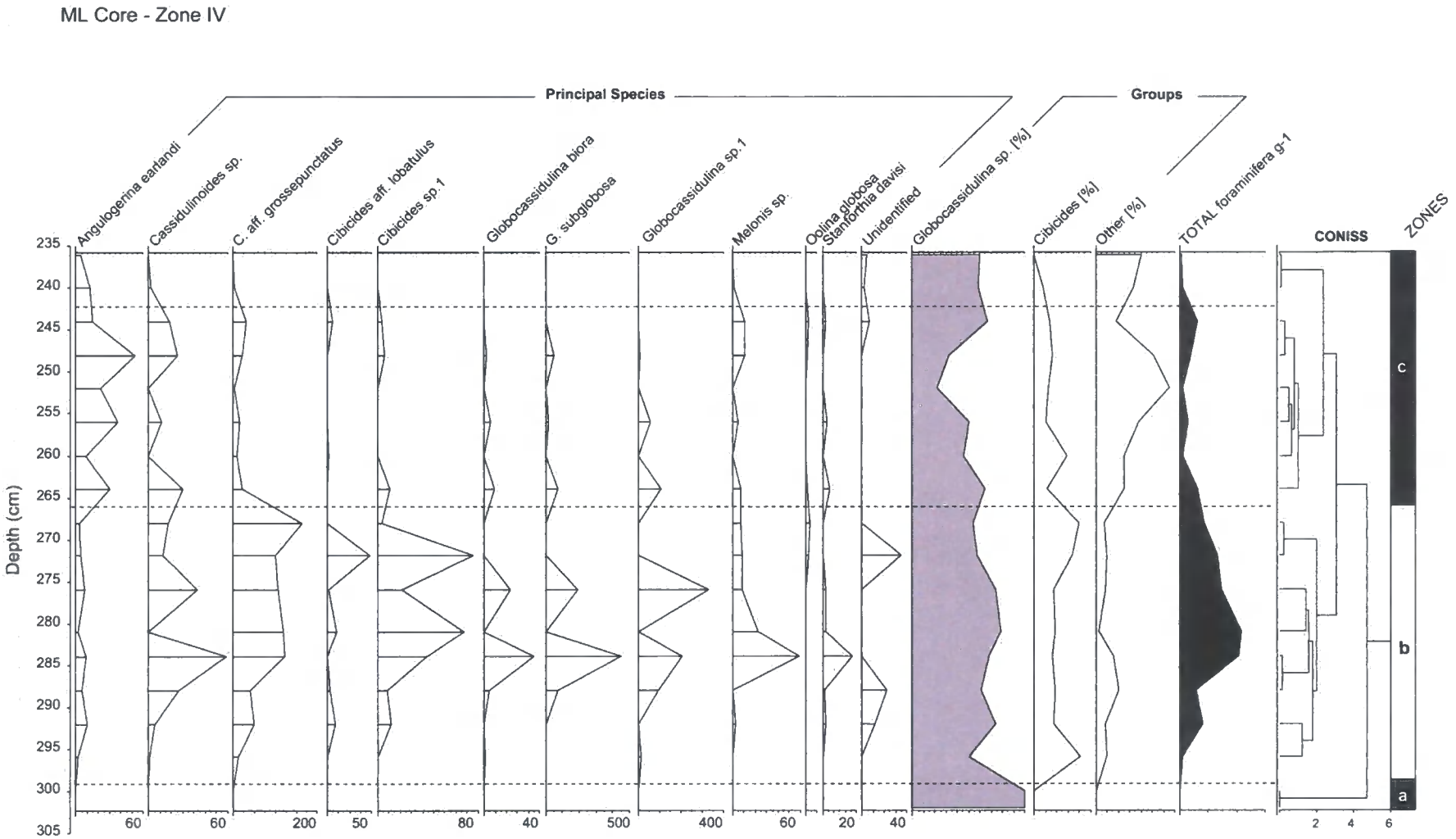

Figure 6.8. Foraminiferal analysis of the ML core zone IV. Data presented as total number of foraminifera per gram of sediment (g^{-1}). Summary percentages of principal genera groups are shown to the right of the diagram, together with total number of foraminifera g^{-1}.

6.2.2.2. Moutonnée Lake North Basin (MLNB) Core

Of the 34 samples from the MLNB core prepared for quantitative foraminiferal analysis, 20 samples contained foraminifera. The resulting diagram shows two clear zones (Fig. 6.9), which are directly comparable with the diatom zones in MLNB. Sediment from Zone II was devoid of foraminifera, despite detailed analysis. Samples from Zone I, contained 11 distinct foraminiferal species of which 8 were identified to genus level, 3 were identified to species level and 1 could not be assigned a species name. All identified foraminifera are calcareous benthic marine species (Murray, 1991). The foraminiferal assemblage within Zone I is now described in more detail.

Zone I (170-136 cm)

Zone I in the MLNB core has been further split into four sub-zones (Fig. 6.10) suggested by each of the highest splits of CONISS (Grimm, 1987).

Sub-zone Ia (170-164 cm) is characterised by an overall dominance of *Globocassidulina* species, notably *G. subglosa* and *G. biora.* Together *Globocassidulina* species account for ~81% of the total assemblage.

Sub-zone IIb (163-147 cm) is characterised by maximum total foraminiferal abundance of 47.33 g^{-1} at 162 cm and the continued dominance of *Globocassidulina* species (89-93%). Total (g^{-1}) abundance then declines before increasing towards a secondary peak of 45.89 g^{-1} at 154cm. The decline in overall foraminiferal abundance is attributed to a decline in the two major species, *G.biora* and *G. subglosa.* Other notable features include a relative decline in *C. aff. lobatulus* and *S. davisi.* Concentrations of *A. earlandi* remain low.

Sub-zone IIc (147-142 cm) is characterised by fluctuating total foraminifera superimposed on an overall decline towards the top of the sub-zone, which largely reflects the behaviour of *G.biora.* A peak in *Globocassidulina* and *Cibicides species* coincides with a decline in *C. porrectus.*

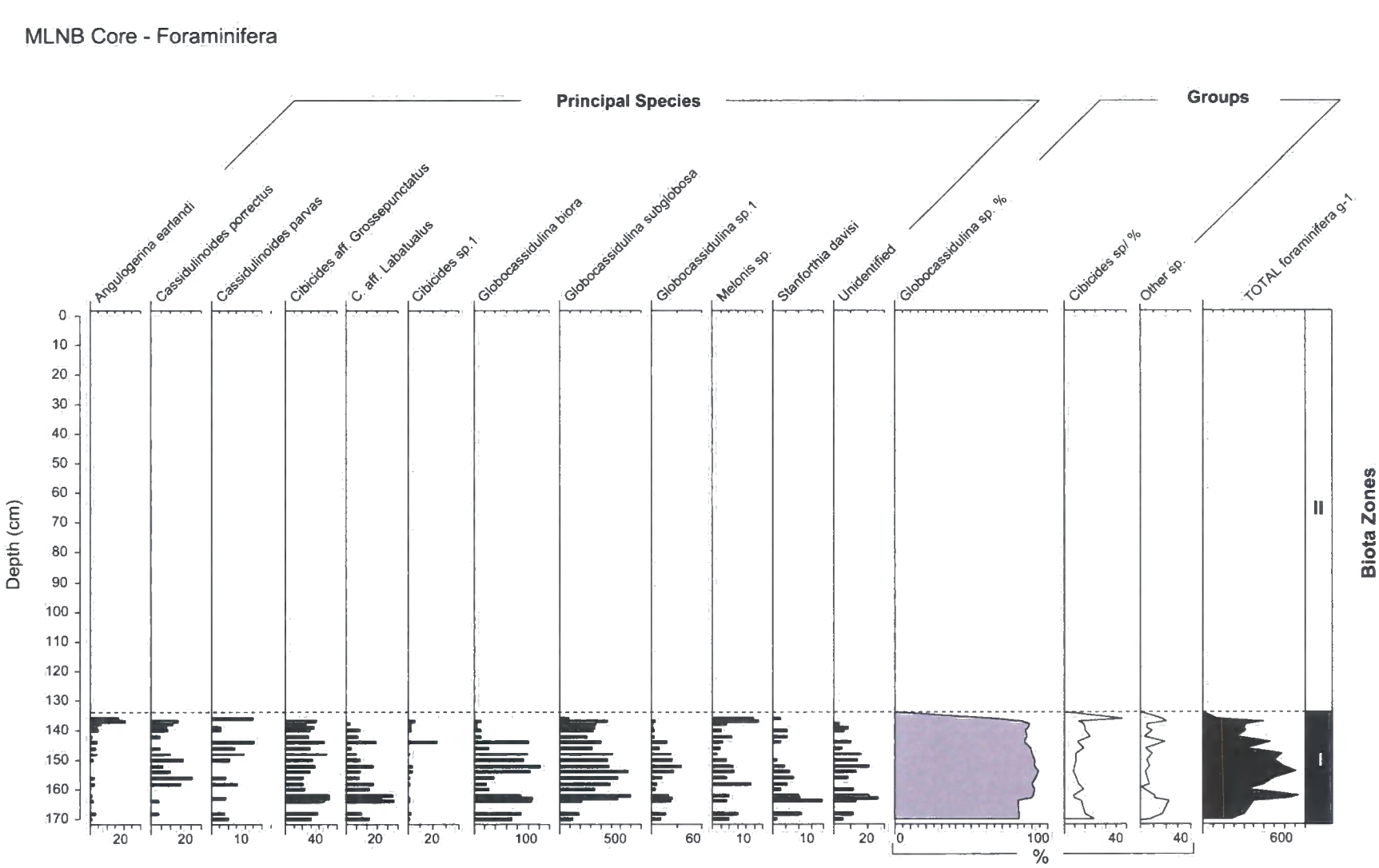

Figure 6.9. Foraminiferal analysis for the MLNB core. Data presented as total number of foraminifera per gram of sediment (g^{-1}). Summary percentages of principal genera groups are shown to the right of the diagram, together with total number of foraminifera g^{-1}.

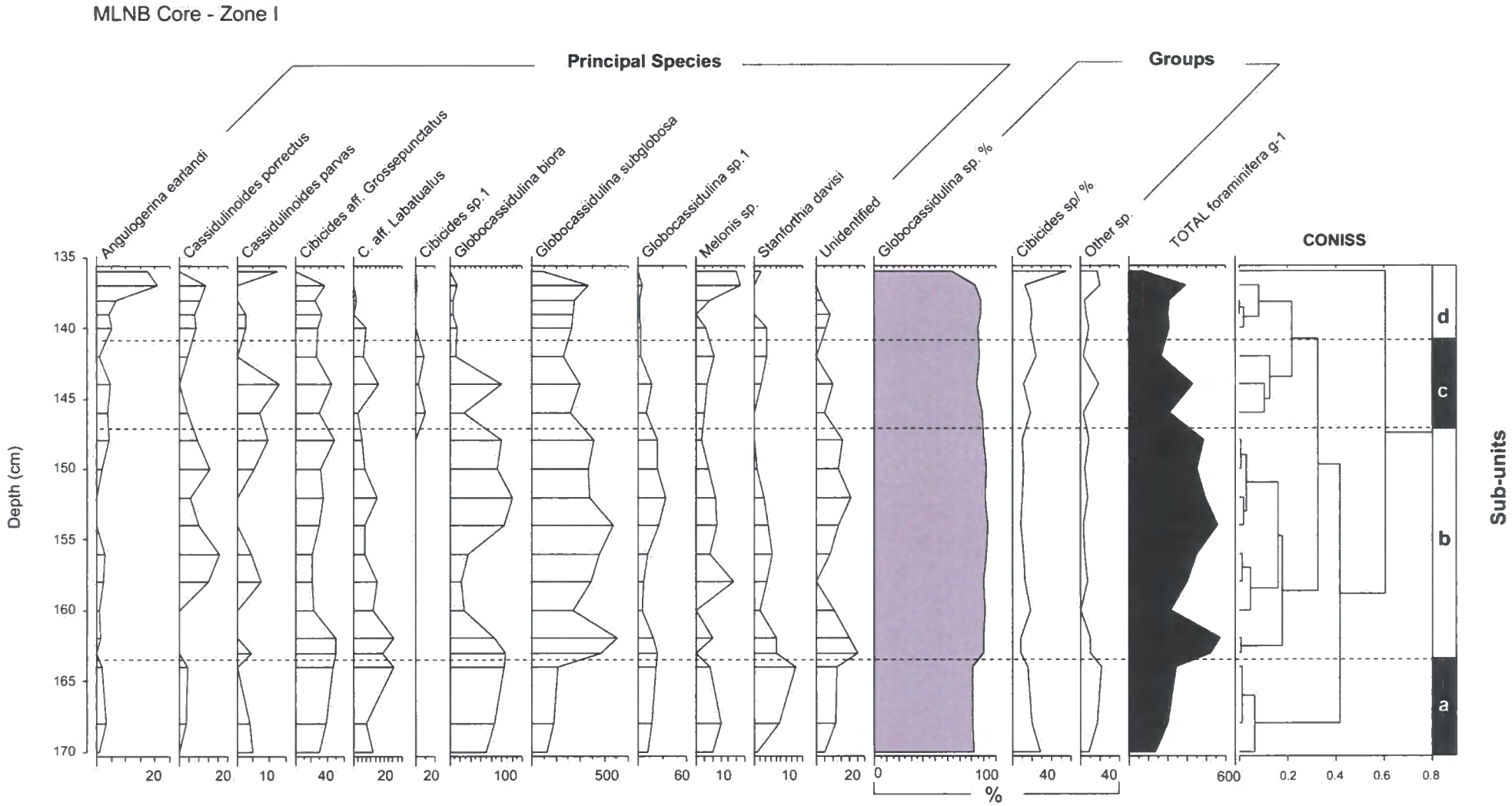

Figure 6.10. Foraminiferal analysis for the MLNB core zone I. Data presented as total number of foraminifera per gram of sediment (g^{-1}). Summary percentages of principal genera groups are shown to the right of the diagram, together with total number of foraminifera g^{-1}.

Sub-zone IId (141-136 cm) is characterised by an overall decrease in total abundance, although *G. subglosa* remains relatively high. Counts of *A. earlandi*, *C. parvas* and *Melonis sp.*, increase, reaching peak concentrations at 136 cm. *C. porrectus* also increases, whilst numbers of *G.biora* decline.

6.2.3. Summary: A combined biological zonation (BZ)

Moutonnée Lake (ML) Core: The ML core is defined by a five biological zones (referred to as BZI-V), with zones II and IV containing biological remains and I, III and V being devoid of biological remains (Fig. 6.1 and 6.6). In detail, BZII is characterised by a purely marine diatom assemblage, which is dominated by planktic diatoms, notably *Eucampia antarctica var. recta* whilst *Globocassidulina* species dominate the foraminiferal assemblage. Similarly, BZIV is dominated by planktic taxa, notably *Eucampia antarctica var. recta*, *Chaetoceros* species and *Thalassiosira* species. Total diatom abundance declines at 267 cm, which coincides with an increase in benthic diatom species. Similarly, total foraminiferal, notably *Globocassidulina* species declines rapidly at 268, whilst minor components of the assemblage (e.g. *A. earlandi*) begin to increase. This stepwise decline is also present in the $\delta^{13}C_{org}$ and LOI profiles presented below.

Moutonnée Lake North Basin (MLNB) Core: The MLNB core can be split into two-biological zones, with Biota Zone I containing biological remains and Biota Zone II being devoid of biological remains (Fig. 6.4 and 6.9). Like the ML core, the diatom assemblage is exclusively marine, being dominated by *C. faciolata* and *E. antarctica var. recta*. The diatoms in this zone are also characterised by a change form a planktic-dominated assemblage to a benthic-dominated assemblage. The foraminiferal assemblage is also dominated by *Globocassidulina* and *Cibicides species*, with *A. earlandi* becoming more abundant towards the upper zone boundary.

The overall structure of both the diatom and foraminiferal assemblages presented from Moutonnée Lake suggests that Zone IV from the ML core is contemporaneous with Zone I in the MLNB core. Specifically, the decrease in planktic diatoms and

increase in benthic taxa is common to both diatom zones. Likewise the foraminiferal assemblage is almost identical between the ML and MLNB cores. Notably, both cores show an overall decrease in *Globocassidulina* and *Cibicides* species and increase in *A. earlandi.* As will be shown later (section 6.5), this assumption is supported by the ^{14}C core chronology. These 'biota' zones are also correlated with near-simultaneous changes in the physical, isotopic and elemental data presented below.

Ablation Lake Cores (AB2 and AB4): Biological zones were absent in both sediment cores (AB2, AB4) retrieved from Ablation Lake. This suggests that the lake water column is largely unproductive and/or corrosive (see Chapter 5). Alternatively, it could suggest that we did not retrieve a complete sedimentary sequence from this site.

6.3. Isotopic and elemental analysis

This section presents the results of isotopic and elemental analysis performed on core material from ML and AB. The first section (6.4.1) presents oxygen and carbon isotope results performed on authigenic carbonate from the MLNB core. The second section (6.4.2) will present carbon isotope ($\delta^{13}C_{org}$) results together with total elemental carbon (C_{org}) and total nitrogen (N_{org}) percentage performed on the bulk organic fraction from core material from Moutonnée (ML and MLNB) and Ablation (AB2 and AB4) Lakes. The final section will present isotopic (carbon and oxygen) isotopic analyses performed on two foraminiferal species found within the ML and MLNB cores.

Each isotopic and elemental proxy is described relative to the biological zonation identified above (grey shading in each diagram). A summary and synthesis of all individual units will be provided at the end of the chapter.

6.3.1. Authigenic Carbonate

6.3.1.1. Moutonnée Lake North Basin (MLNB) Core

In this section, the results of a pilot authigenic carbonate (< 80 μm fraction) isotope ($\delta^{18}O_{auth}$ and $\delta^{13}C_{auth}$) study performed on bulk core material from MLNB are presented. The dataset comprises 16 samples taken at approximately 8 cm resolution (Fig. 6.11). Values range from –8.5 to 1.9 ‰ for $\delta^{18}O_{auth}$ and –13.0 to –1.2 ‰ for $\delta^{13}C_{auth}$ (Fig. 6.11). $\delta^{18}O_{auth}$ values increase at 136 cm, which is coincident with the upper boundary of the BZI. The overall trend is one of decreasing $\delta^{18}O_{auth}$ and $\delta^{13}C_{auth}$ values, before an increase in values at the core top (Fig. 6.11).

6.3.2. Organic Isotopes and Elemental analysis

In this section $\delta^{13}C_{org}$, C/N, $\%C_{org}$ and $\%N_{org}$ profiles are described collectively for each core.

6.3.2.1. Moutonnée Lake (ML) Core

Values for the ML core range from –26.4 to –22.6 ‰ for $\delta^{13}C_{org}$ from 6.8 to 12.3 for C/N, from 0.67 to 0.21 for $\%C_{org}$ and from 0 to 0.08 for $\%N_{org}$ (Fig. 6.12). BZI is characterised by stable $\delta^{13}C_{org}$, C_{org} and N_{org} values and decreasing C/N values. BZII is associated with rapidly increasing C_{org} and N_{org} values and a single sharp $\delta^{13}C_{org}$ peak. BZIII is characterised by relatively constant $\delta^{13}C_{org}$, C_{org}, N_{org} % and C/N values. Values in BZIV are characterised by elevated $\delta^{13}C_{org}$, C_{org} and N_{org} % and lower C/N values. BZIV is also characterised by a significant decrease in $\delta^{13}C_{org}$, C_{org} and N_{org} % at 260 cm, which is broadly coincident with an overall decrease in total diatom and total foraminifera between 267-268 cm. BZV is characterised by high and fluctuating C/N values, but relatively constant $\delta^{13}C_{org}$, C_{org} and N_{org} values.

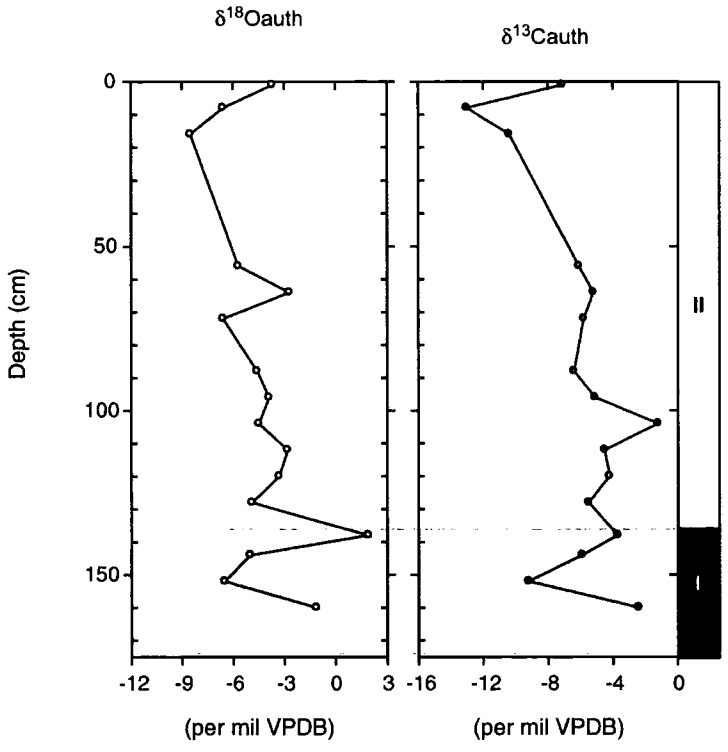

Figure 6.11. Moutonnée Lake North Basin (MLNB) core showing downcore variations in $\delta^{18}O$ and $\delta^{13}C$ performed on in-situ (core material) authigenic carbonate. Shaded box defines the biological zonation.

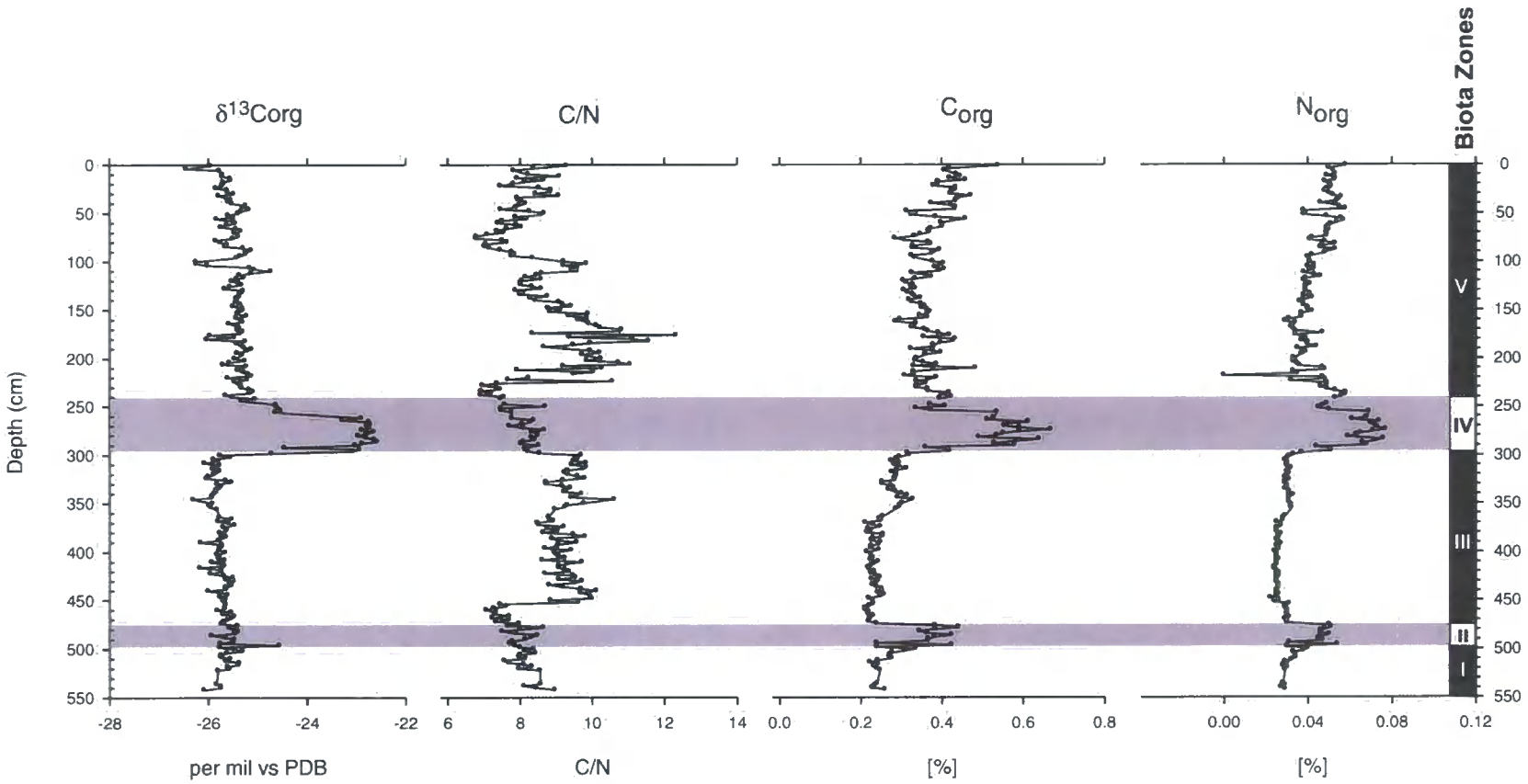

Figure 6.12 . Moutonnée Lake (ML) core showing downcore variations in $\delta^{13}C$, Carbon/Nitrogen ratio (C/N) % Carbon and % Nitrogen performed on bulk sediment samples. Grey shading represent biota zones II and IV.

6.3.2.2. Moutonnée Lake North Basin (MLNB) Core

Values for the MLNB core range from –28.1 to –23.2 ‰ for $\delta^{13}C_{org}$ from 6.7 to 12.1 for C/N, from 0.21 to 0.72 for $\%C_{org}$ and from 0.03 to 0.08 for $\%N_{org}$ (Fig. 6.13). BZI is associated with elevated $\delta^{13}C_{org}$, C_{org} and N_{org} values and low C/N (cf. Fig. 6.12 and 6.13). Between 133 and 32 cm $\delta^{13}C_{org}$ values decrease gradually. The $\delta^{13}C_{org}$ profile is also characterised by four sharp with heavier values at 136, 120, 102 and 76 cm. Values at 120 and 102 cm also coincide with sharp increases in C/N values. C/N values fluctuate along a gradually increasing trend, whilst $\%C_{org}$ and $\%N_{org}$ decrease. $\delta^{13}C_{org}$ values become more constant above 100 cm fluctuating around a mean of –25.7 ‰. Between ~ 30 and 9 cm $\%C_{org}$ and $\%N_{org}$ both increase whilst C/N values decrease. In the upper 8 cm of the core C/N, $\%C_{org}$ and $\%N_{org}$ rapidly increase, reaching core maxima in C_{org} and N_{org} of 0.72 % and 0.08 % respectively at the core top, whilst $\delta^{13}C_{org}$ values decrease.

6.3.2.3. Ablation Lake 4 (AB4) Core

Values for the AB4 core range from –28.79 to –23.82 ‰ for $\delta^{13}C_{org}$ from 1 to 22.8 for C/N, from 0.02 to 0.83 for $\%C_{org}$ and from 0.013 to 0.513 for $\%N_{org}$ (Fig. 6.14). Unlike the cores from ML, the sediment cores from AB were devoid of biological remains. Between 217-124 cm the core is characterised by relatively constant $\delta^{13}C_{org}$, C/N, $\%C_{org}$ and $\%N_{org}$ values, with mean values of –25.43 ‰, 8.7, 0.18 and 0.02 respectively. $\delta^{13}C_{org}$, C/N, and $\%C_{org}$ values fluctuate between 189-166 cm. Above 124 cm, $\delta^{13}C_{org}$ values decrease sharply at 123 cm, whilst C/N values increase. $\%N_{org}$ also increase whilst $\%C_{org}$ decreases. $\delta^{13}C_{org}$ values reach a core minimum of –28.79 ‰, whilst C/N reaches a core maximum of 22.8 at 76 cm. At ~ 70 cm $\%C_{org}$ and $\%N_{org}$ values suddenly decrease, whilst $\delta^{13}C_{org}$ values continue to fluctuate around a mean value of –26 ‰. The C/N profile continues to fluctuate. $\%N_{org}$ values remain relatively constant, only broken by one sudden increase in values at 54 cm. All values increase towards the core top. $\delta^{13}C_{org}$ and $\%C_{org}$ reach core maxima of –23.82 ‰ and 0.83 % respectively at 4 cm.

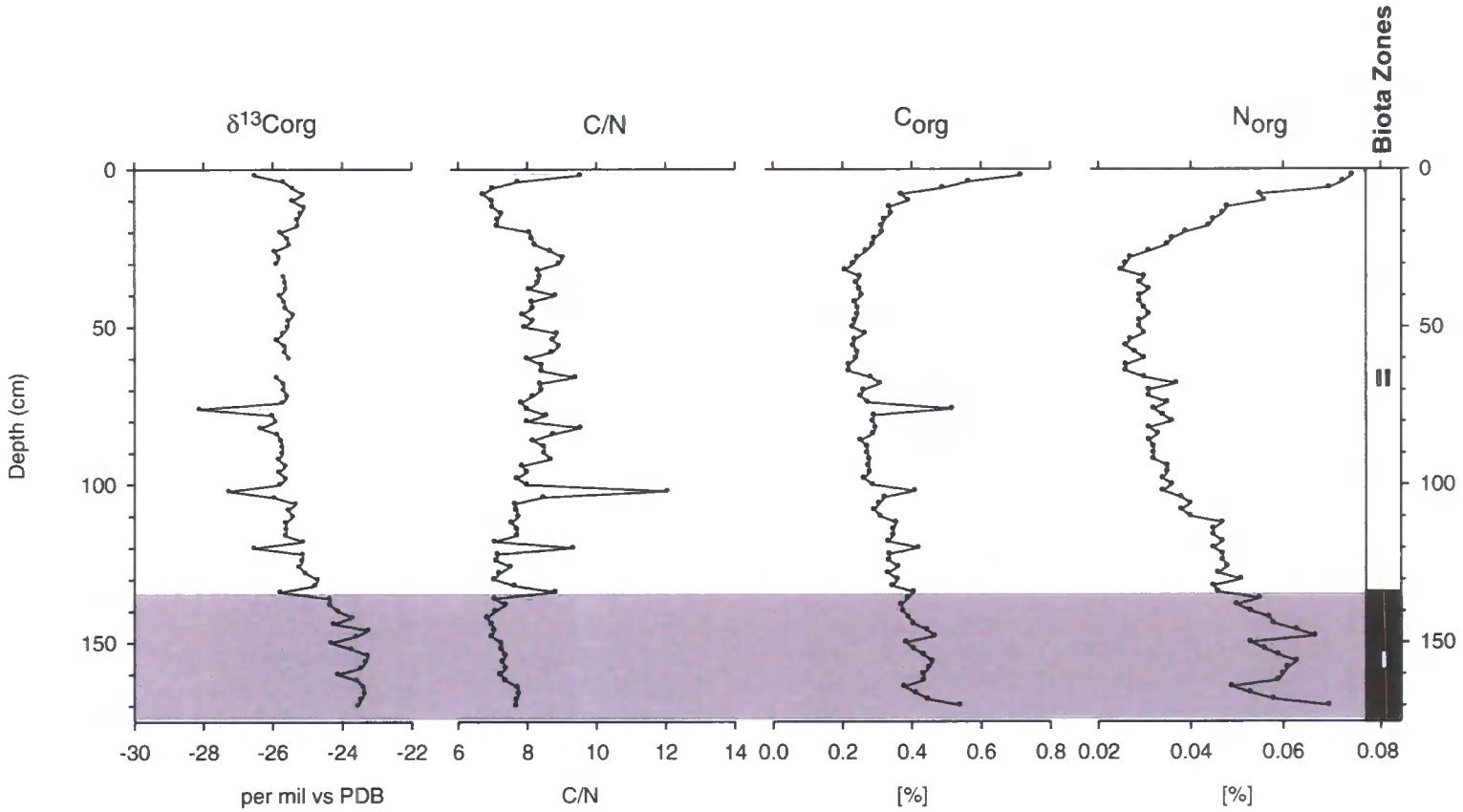

Figure 6.13. Moutonnée North Basin (MLNB) core showing downcore variations in $\delta^{13}C$, Carbon/nitrogen ratio (C/N), % Carbon and % Nitrogen performed on bulk sediment samples. Grey shading represent biota zones I.

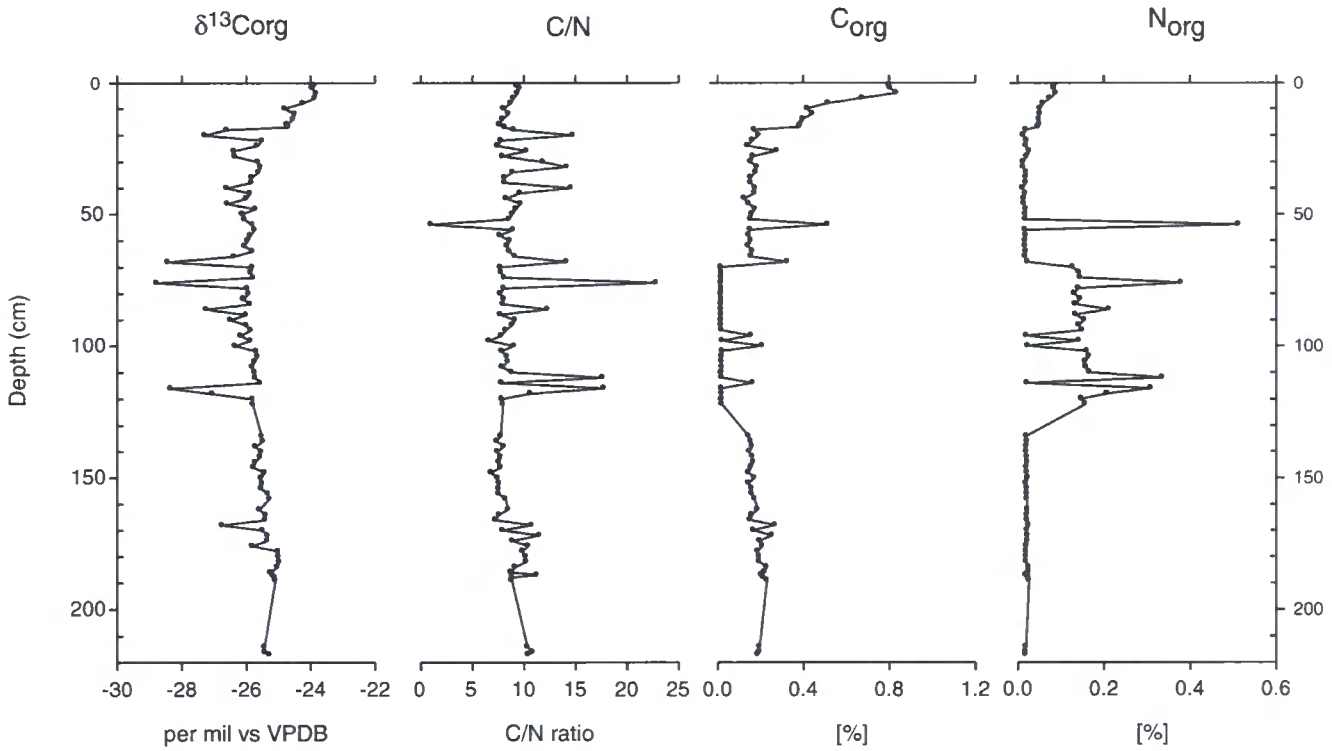

Figure 6.14. Ablation Lake 4 (AB4) core showing downcore variations in $\delta^{13}C$, Carbon/Nitrogen ratio (C/N), % Carbon and % Nitrogen performed on bulk sediment samples.

6.3.3. Foraminiferal $\delta^{18}O$ and $\delta^{13}C$

In this section the results of isotopic measurements ($^{18}O/^{16}O$ and $^{13}C/^{12}C$) performed on two benthic foraminiferal species (*Cibicides* and *Globocassidulina* sp.) are presented. Analysis is restricted to the foraminifera bearing zones in the ML and MLNB cores from Moutonnée Lake. Results from the ML core are presented first, then results from the MLNB core.

6.3.3.1. Moutonnée Lake (ML) Core

$\delta^{18}O$ *and* $\delta^{13}C$ *Cibicides sp.*

Values for *Cibicides* sp. range from 3.4 to 4.1 ‰ for $\delta^{18}O$ and from 0.9 to 1.3 ‰ for $\delta^{13}C$. In BZII (Table 6.2. and Fig. 6.15 a,b) $\delta^{18}O_{cibicides}$ and $\delta^{13}C_{cibicides}$ values co-vary with a large increase from the base followed by a small decrease.

In BZIV, $\delta^{18}O$ and $\delta^{13}C$ values initially co-vary but in anti-phase with peaks in $\delta^{18}O$ at 290 cm and 186 cm being associated with low points in $\delta^{13}C$ (Fig. 6.15b). Above 290 cm $\delta^{18}O$ values are more stable, declining gradually to 262 cm. $\delta^{13}C$ values on the other hand continue to fluctuate, reaching a zone maximum of 1.3 ‰ at 284 cm, before declining then increasing. Above 270 cm the $\delta^{18}O$ profile begins to fluctuate more markedly and is characterised by $\delta^{18}O$ peaks at 260 (4 .0 ‰) and 252 cm (4.1 ‰). This double peak is notable since it coincides with overall decreases in diatom and foraminifera abundance and $\delta^{13}C_{org}$ values. $\delta^{13}C$ values vary with a similar pattern, but changes occur out of phase with $\delta^{18}O$ values. Above 250 cm, $\delta^{18}O$ values become more stable whilst $\delta^{13}C$ values continue to fluctuate.

$\delta^{18}O$ *and* $\delta^{13}C$ *Globocassidulina sp.*

Values range from 3.6 to 4.7 ‰ for $\delta^{18}O$ and 0.3 to 1.2 ‰ for $\delta^{13}C$ (Fig. 6.16 a,b). BZII is characterised by generally decreasing $\delta^{18}O$ and $\delta^{13}C$ values, both reaching a zone minimum of 3.6 ‰ and 0.1 ‰ respectively at 492 cm.

Core	Depth	Cibicides sp.		Globocassidulina sp.		Core	Depth	Cibicides sp.		Globocassidulina sp.	
		d180	d13C	d18O	d13C			d180	d13C	d18O	d13C
ML Core	240	-	-	4.5	0.9	**MLNB Cor**	138	3.3	1.1	4.0	0.6
	242	3.5	0.9	4.6	0.8		140	3.4	1.1	3.7	0.4
	244	-	-	4.2	1.0		142	3.6	1.2	4.3	0.9
	246	3.6	1.2	4.4	1.2		144	3.5	1.5	4.1	0.7
	248	3.5	1.1	4.2	1.0		146	3.4	1.4	3.8	0.6
	250	4.0	1.0	4.3	0.8		148	3.5	1.3	4.0	1.0
	252	4.1	1.0	4.6	1.0		150	3.5	1.3	4.3	0.7
	254	3.4	1.2	4.2	0.9		152	3.5	1.4	4.5	1.2
	256	3.6	1.1	4.6	1.2		154	3.3	1.3	4.4	1.0
	258	3.6	1.0	4.6	1.0		156	3.5	1.4	4.4	0.8
	260	4.0	1.1	-	-		158	3.5	1.4	4.2	0.7
	262	3.9	1.2	4.4	0.9		160	3.4	1.4	4.3	1.1
	264	3.6	1.0	4.6	1.1		162	3.5	1.4	4.4	1.1
	266	3.6	1.0	4.5	1.0		164	3.2	1.3	-	-
	268	3.7	1.0	4.3	0.5		166	3.4	1.3	4.2	0.7
	270	3.6	1.0	4.5	1.1		168	3.4	1.3	4.2	0.3
	272	3.6	1.1	4.1	0.9		170	3.3	1.3	4.3	0.5
	274	3.6	0.9	4.6	0.5		171	3.4	1.3	-	-
	276	3.5	0.9	4.5	0.7						
	278	3.6	1.0	4.5	0.8						
	280	3.6	1.0	4.4	1.0						
	282	3.5	1.1	4.5	0.8						
	284	3.5	1.3	4.4	0.9						
	286	3.4	1.2	4.5	0.7						
	288	3.3	1.1	4.3	0.3						
	290	3.5	0.9	4.3	0.5						
	292	3.4	1.1	4.4	0.8						
	294	3.5	0.9	4.4	0.9						
	296	3.7	0.9	4.7	0.6						
	492	3.7	1.2	3.6	0.1						
	494	3.7	1.2	4.4	0.7						
	496	3.4	1.0	4.2	0.9						

Table 6.2. δ18O and δ13C results from two foraminiferal species, *Cibicides* and *Globocassidulina spp.*

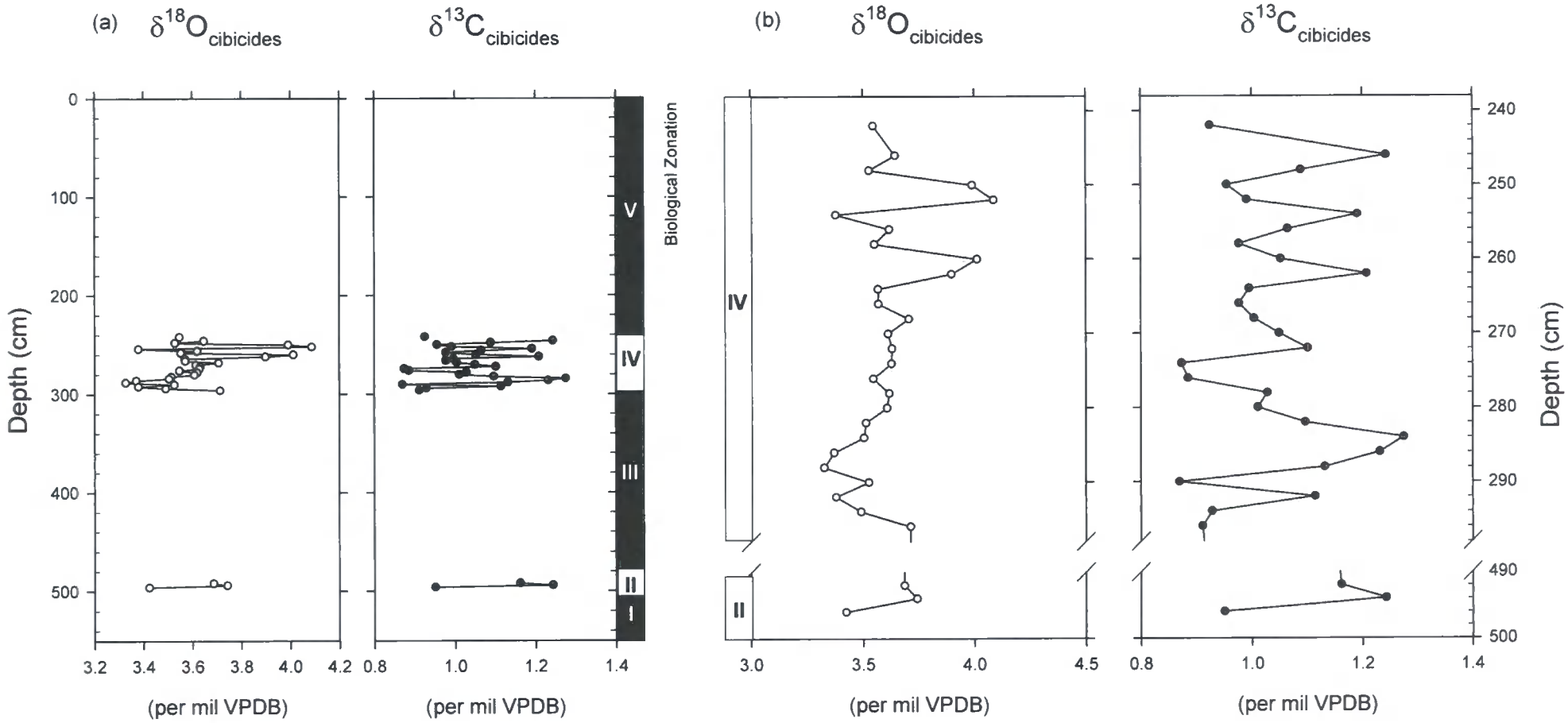

Figure 6.15. Moutonnée Lake (ML) core showing downcore variations in $\delta^{18}O$ and $\delta^{13}C$ performed on *Cibicides* sp. foraminifera; (a) whole core (b) $\delta^{18}O$ and $\delta^{13}C$ profiles from biological zones II and IV in more detail.

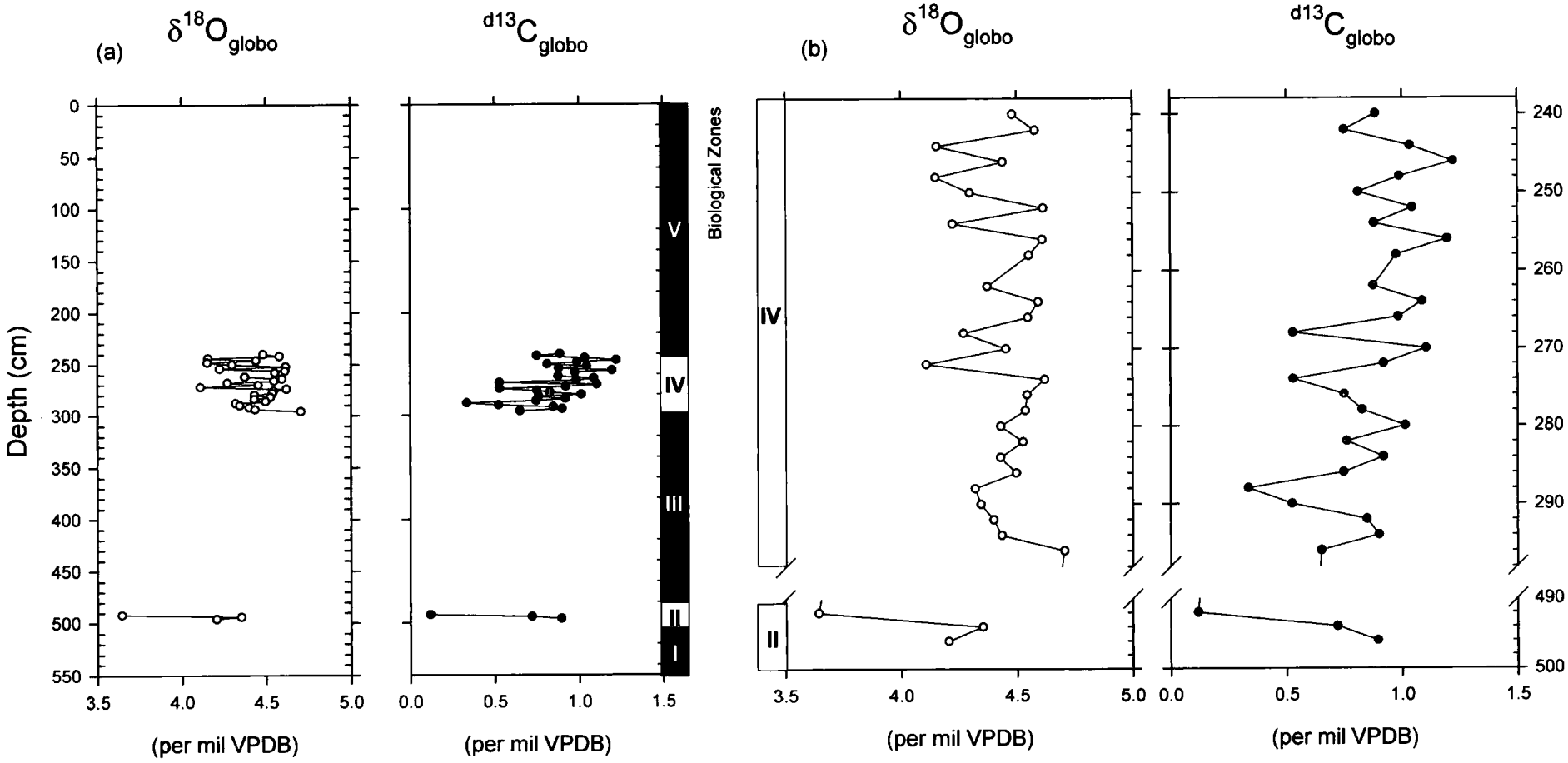

Figure 6.16 Moutonnée Lake (ML) core showing downcore variations in $\delta^{18}O$ and $\delta^{13}C$ performed on *Globocassidulina* sp. foraminifera; (a) shows whole core (b) shows detailed variations $\delta^{18}O$ and $\delta^{13}C$ profiles in biological zones II and IV.

BZIV is characterised by declining $\delta^{18}O$ and $\delta^{13}C$ values (Fig. 6.16b). BZIV is characterised by high $\delta^{18}O$ values until 292 cm, whilst $\delta^{13}C$ values are more variable. Between 274 cm and 268 cm $\delta^{18}O$ and $\delta^{13}C$ values become lighter, then heavier and lighter again. Above this depth both values are variable and show no significant pattern.

6.3.3.2. Moutonnée Lake North Basin (MNLB) Core

$\delta^{18}O$ *and* $\delta^{13}C$ *Cibicides sp.*

Values range from 3.3 to 3.6 ‰ for $\delta^{18}O$ and from 1.1 to 1.5 ‰ for $\delta^{13}C$ (Fig. 6.17 a,b). $\delta^{18}O$ and $\delta^{13}C$ values broadly co-vary, first decreasing then increasing, before decreasing again towards 162-cm (Table 6.2. and Fig. 6.17b). $\delta^{18}O$ values reach a minimum at 170 cm of 3.3 ‰, before. Values then decrease at 154 cm. $\delta^{13}C$ values reach a maximum of 1.5 ‰ at 144 cm whilst $\delta^{18}O$ peaks at 142 cm reaching a value of 3.6 ‰. Both $\delta^{18}O$ values and $\delta^{13}C$ values then fall reaching minimum values of 3.3 ‰ at 138 cm and 1.1 ‰ and 140 cm respectively.

$\delta^{18}O$ *and* $\delta^{13}C$ *Globocassidulina sp.*

Values range from 3.7 to 4.4 ‰ for $\delta^{18}O$ and from 0.3 to 1.2 ‰ for $\delta^{13}C$ (Fig. 6.18 a,b). $\delta^{18}O$ and $\delta^{13}C$ values co-vary throughout the core. Values first decrease then increase towards 152 cm (Fig. 6.18b). Above 152 cm $\delta^{13}C$ values fluctuate with a decreasing trend towards the upper zone limit. Similarly $\delta^{18}O$ values decrease, then increase at 142 cm before decreasing again, reaching a core minimum at 140 cm of 3.7 ‰.

6.4. Physical Analysis

Physical analysis was carried out on all long cores (ML, MLNB, AB2, AB4; raw data presented in Appendix 5) and included; magnetic susceptibility (MS), % loss-on-ignition (%LOI), % carbonate content (%$CaCO_3$) and grain-size (GS) analyses.

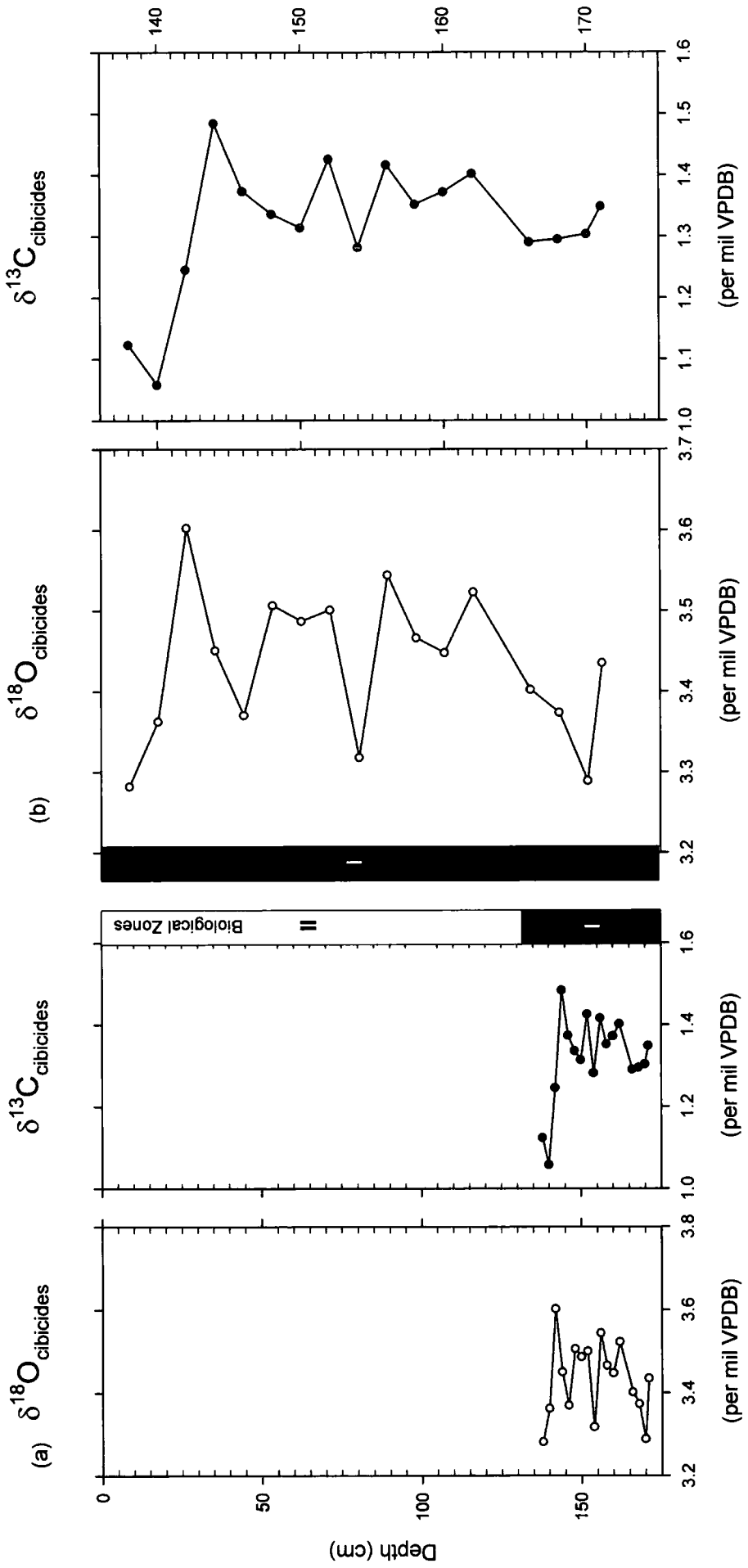

Figure 6.17. Moutonnée Lake North Basin (MLNB) core showing downcore variations in $\delta^{18}O$ and $\delta^{13}C$ performed on *Cibicides* sp. foraminifera; (a) whole core (b) $\delta^{18}O$ and $\delta^{13}C$ profiles from biological zone I in more detail.

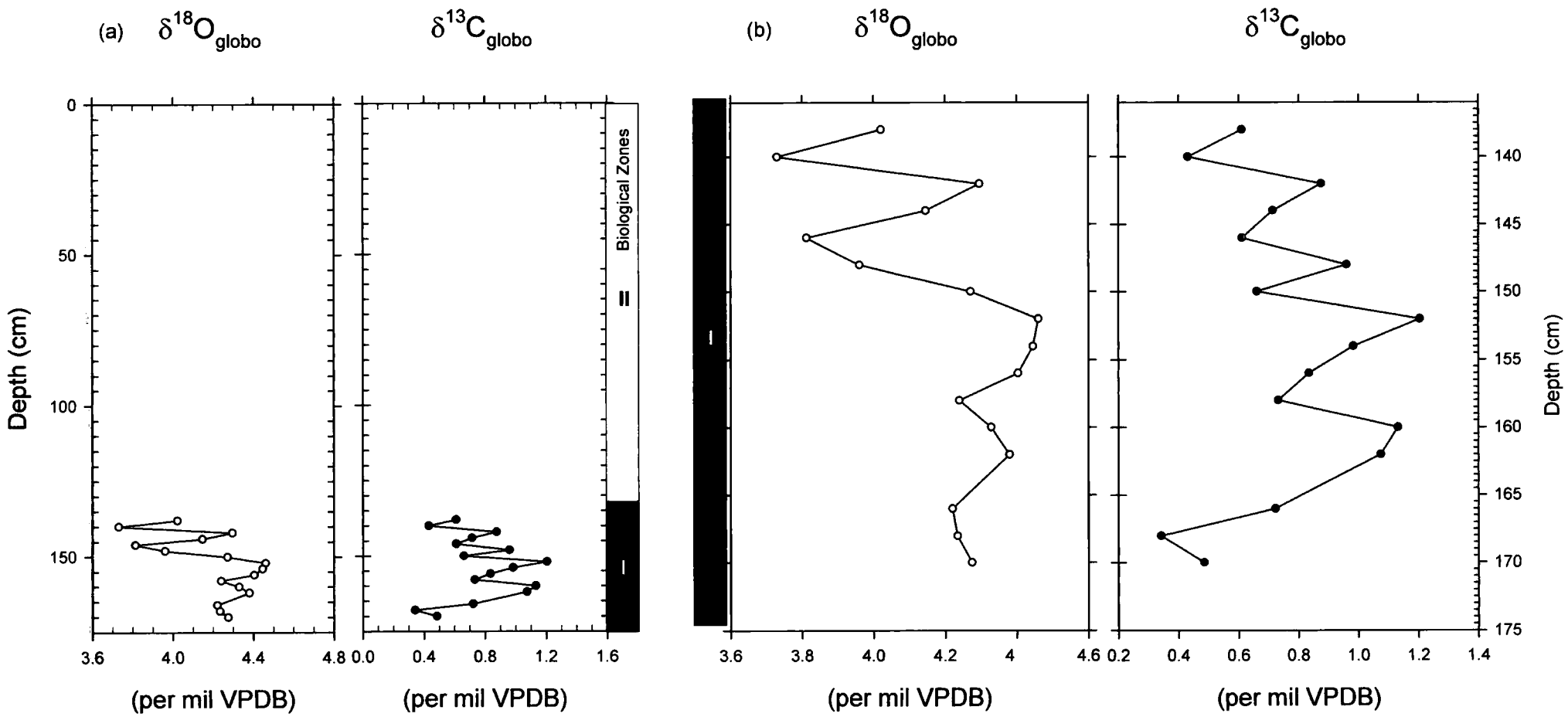

Figure 6.18. Moutonnée Lake North Basin (MLNB) core showing downcore variations in $\delta^{18}O$ and $\delta^{13}C$ performed on *Globocassidulina* sp. foraminifera: (a) whole core (b) $\delta^{18}O$ and $\delta^{13}C$ profile from biological zone I in more detail.

In each diagram, the grey shading represents the biological zonation derived from the biological data.

6.4.1. MS/LOI/$CaCO_3$ and $\%H_2O$

Magnetic susceptibility, % calcium carbonate, loss-on-ignition and % water content are described collectively for each core and compared directly with the biological zonation described in section 6.2. In several instances, however, anomalous MS readings, coincide with: (1) core boundaries (i.e. where two adjacent cores overlap in stratigraphical space); (2) where the core was sectioned in the field and; (3) tube 'edge effects' caused by difference in air pressure in the core tube between compacted core sediments and core tops (Fig. 6.19). The latter effect has already been discussed in Chapter 4. This would represent a significant problem if these changes only occurred where two adjacent cores were taken, as it could imply that cores did not overlap in stratigraphical space. This is however, not the case and is illustrated in Figure 6.19. The Magnetic Susceptibility profile from ML core shows that anomalous changes also coincide with intact 2 m long cores from single drives that have been cut in two. The changes that are seen are within the normal drift of the sensor, or in the case of core ends, the 'edge effect'. More importantly however, this problem does not appear to have influenced other physical, chemical and biological results. Any interpretation regarding environmental processes that is based on these physical core data must bear these factors in mind.

6.4.1.1. Moutonnée Lake (ML) Core

Values range from –7.3 to 31-mm^3 kg^{-1} for MS, from 0.04 to 0.4 % for H_2O, from 1.18 to 7.23 % for LOI and from 0.95 to 5.15 % for $CaCO_3$ (Fig. 6.20). In general, the biological zones are not well defined by these physical proxies. BZII is associated with elevated MS values, (although this could reflect the core boundary problem), together with increased $\%H_2O$ and %LOI values, whilst $\%CaCO_3$ remains unchanged. BZIV is also associated with elevated MS, $\%H_2O$ and %LOI values. The LOI profile shows a stepped decline in BZIV, which is also seen in the biological and isotopic data. BZIII is characterised by fluctuating MS values, which first show a decreasing trend followed by an increasing trend. In BZIV between ~

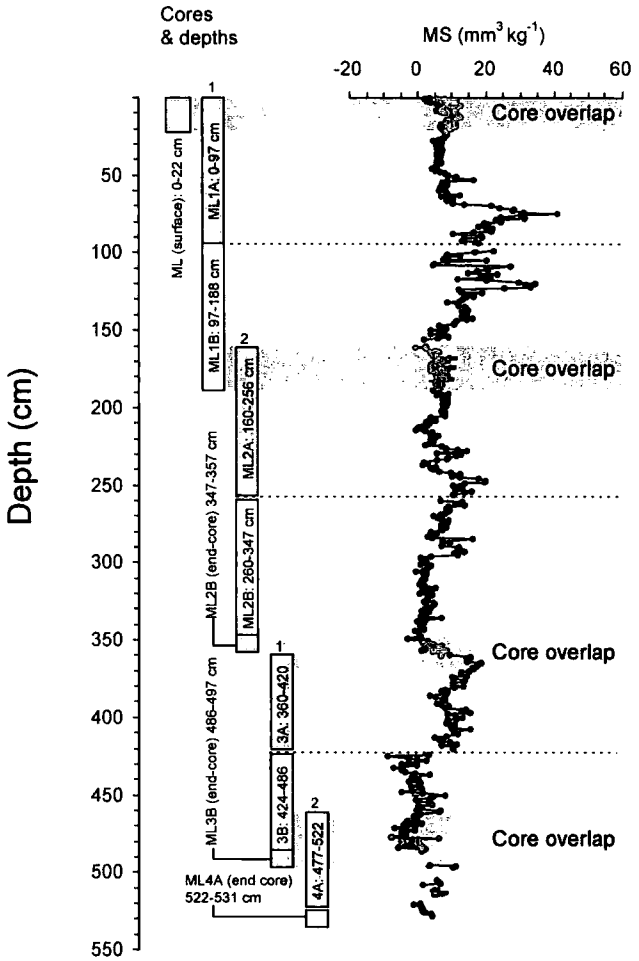

Figure 6.19. Downcore variation in Magnetic Susceptibility (MS) for the ML core showing the core sections (left), core drive hole (number above core) and core depths. Red curve represents duplicate MS readings performed on core overlap (e.g. between 1B and 2A). Horizontal shading highlights the core overlap, whilst horizontal dotted line represents core sectioning zones.

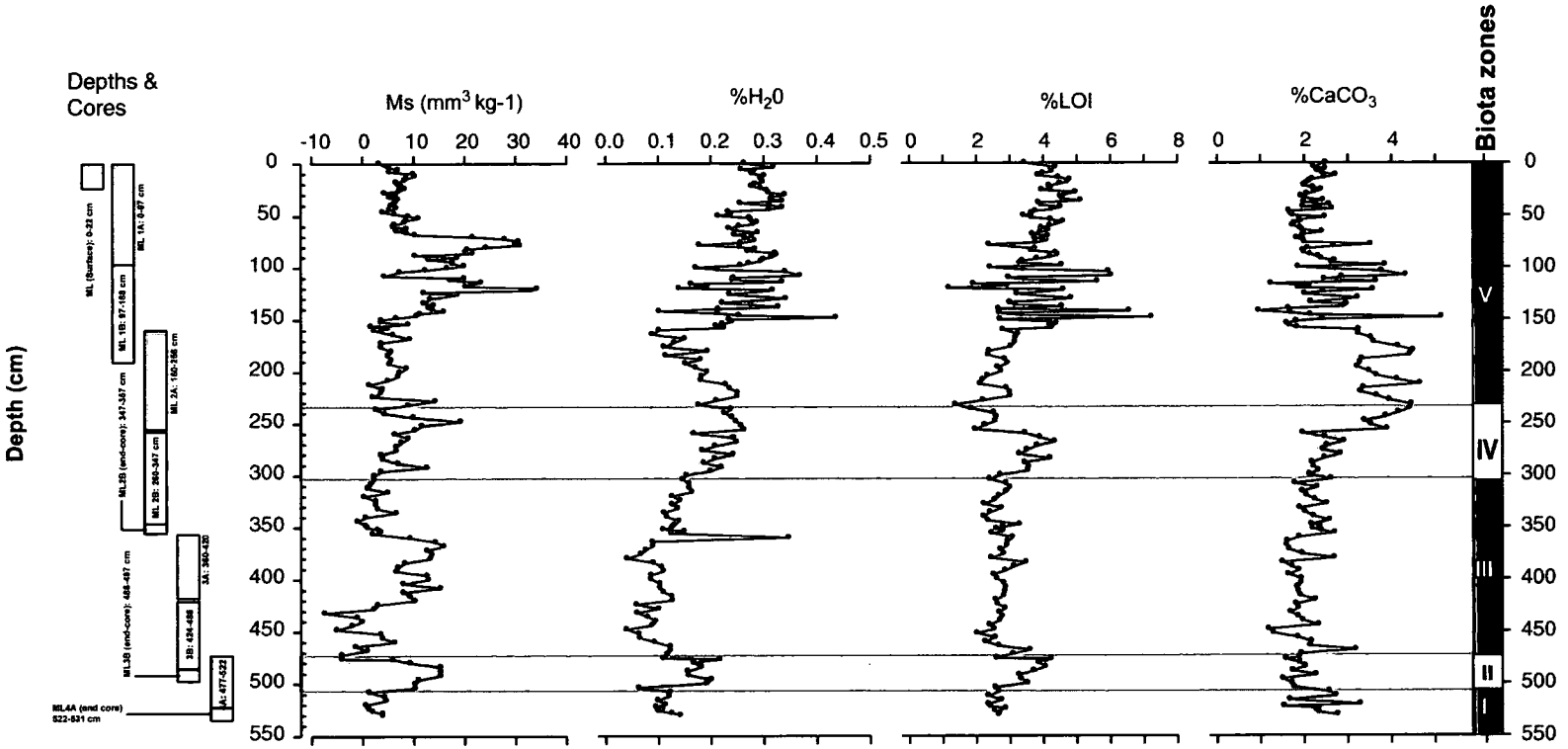

Figure 6.20. ML Core showing downcore variations in Magnetic Suceptibility (MS), % Water content (%H_2O), % Loss-on-ignition (LOI), and % Calcium carbonate (%$CaCO_3$). Cores, depths and core boundaries are shown on the left of the figure. Grey shading defines the biological zonation.

259-158 cm, $\%H_2O$ decreases, whilst %LOI begins to increase. $CaCO_3$ values fluctuate markedly at ca. 4%. The depth interval 157 to 62 cm is characterised by high amplitude, high frequency changes in all physical parameters. Above this, all values remain relatively stable from ~ 61 cm to the core top.

6.4.1.2. Moutonnée Lake North Basin (MLNB) Core

Values range from 26-to 52.8-mm3 kg^{-1} for MS, from 10.6 to 28.4 % for H_2O, from 1.6 to 4.4 % for LOI and from 2 to 4.12 % for $CaCO_3$ (Fig. 6.21). Biological Zone I is characterised by elevated MS and $CaCO_3$ values and depressed $\%H_2O$ and %LOI values (Fig. 6.21). Above BZ1 the core is characterised by decreasing MS and $CaCO_3$ values, whilst %H2O and %LOI values increase. MS and $CaCO_3$ reach core maxima of 52.8 mm^3 kg^{-1} and 4.3% at 170 and 154 cm respectively. MS, %LOI, $\%H_2O$ and $CaCO_3$ values then remain relatively constant, before %LOI and $\%H_2O$ increase and MS and $CaCO_3$ decrease beginning at ca. 30 cm.

6.4.1.3. Ablation Lake 2 (AB2) Core

Values range from 13.9 to 51.4 mm^3 $kg^{-1}$for MS, from 1.03 to 3.2 % for LOI, and from 1.36 to 2.48 for $\%CaCO_3$ (Fig. 6.22). All measured parameters are relative constant to a depth of ca.90 cm, when %LOI and $\%H_2O$ values begin to increase, whilst MS values decline then increase. The depth interval 51-0 cm is characterised by high amplitude fluctuations in H_2O and MS, whilst $\%CaCO_3$ and %LOI decrease steadily. The MS profile is striking; changing from low values (ca. 1-3) between 51 and 28 cm to high values (30-30.6 mm^3 kg^{-1}) between 24 and 22 cm. Values then fall close to the core mean (ca. 9.6-12.3).

6.4.1.4. Ablation Lake 4 (AB4) Core

Values range from 0.3-to 32.3-mm3 kg^{-1} for MS, from 0.01 to 0.26 for H_2O, from 0.46 to 4.02 % for LOI and from 0.32 to 3.86 % for $CaCO_3$ (Fig. 6.23). All measured parameters are relatively constant to a depth of 47 cm. The depth interval between 47-0 cm is characterised by a zone of increasing MS values between 51 cm

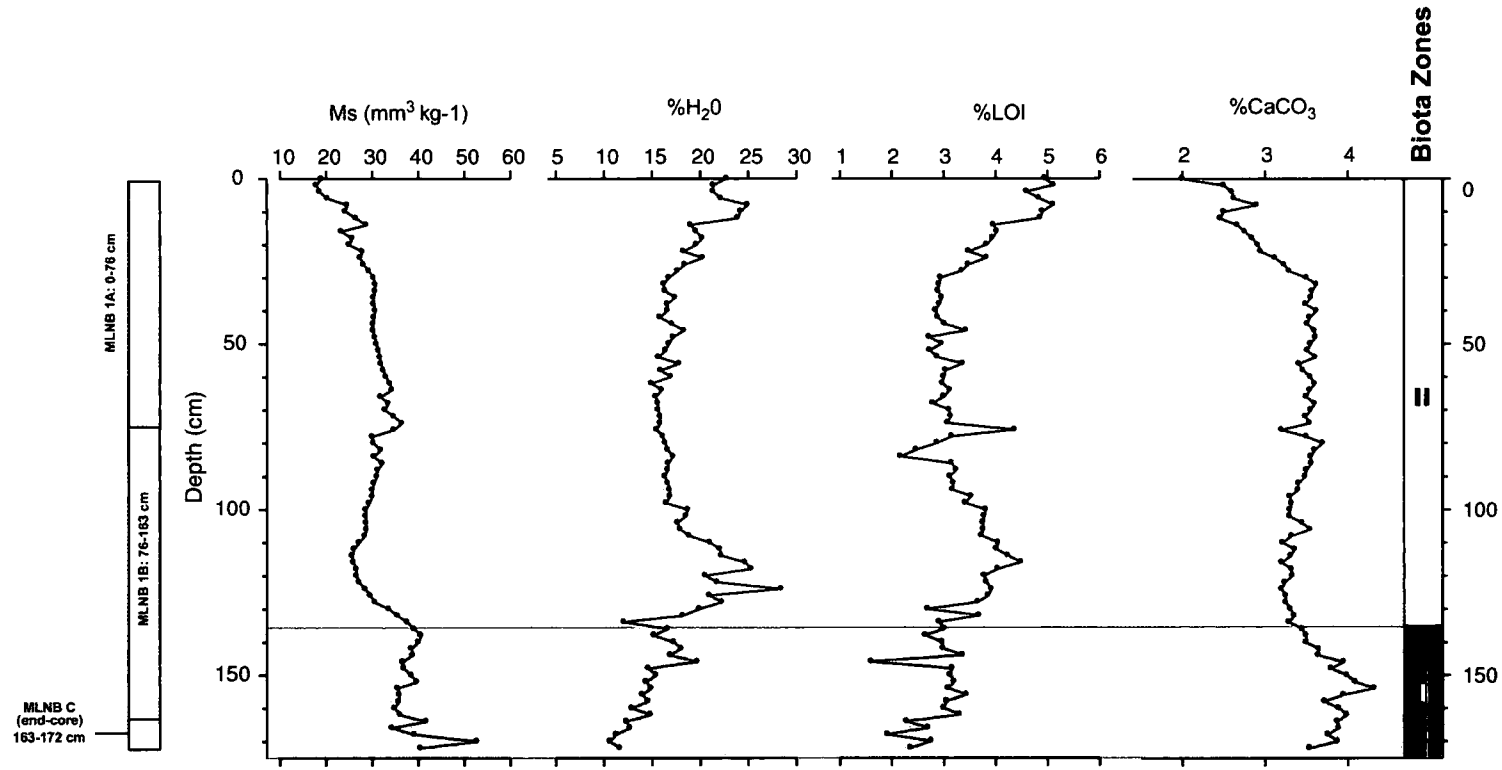

Figure 6.21. MLNB Core showing downcore variations in Magnetic suceptibility (MS), % Water content (%H_2O), % Loss-on-ignition (LOI), and %$CaCO_3$. Cores, depths and core boundaries are shown on the left of the figure. Grey shading defines the biological zonation.

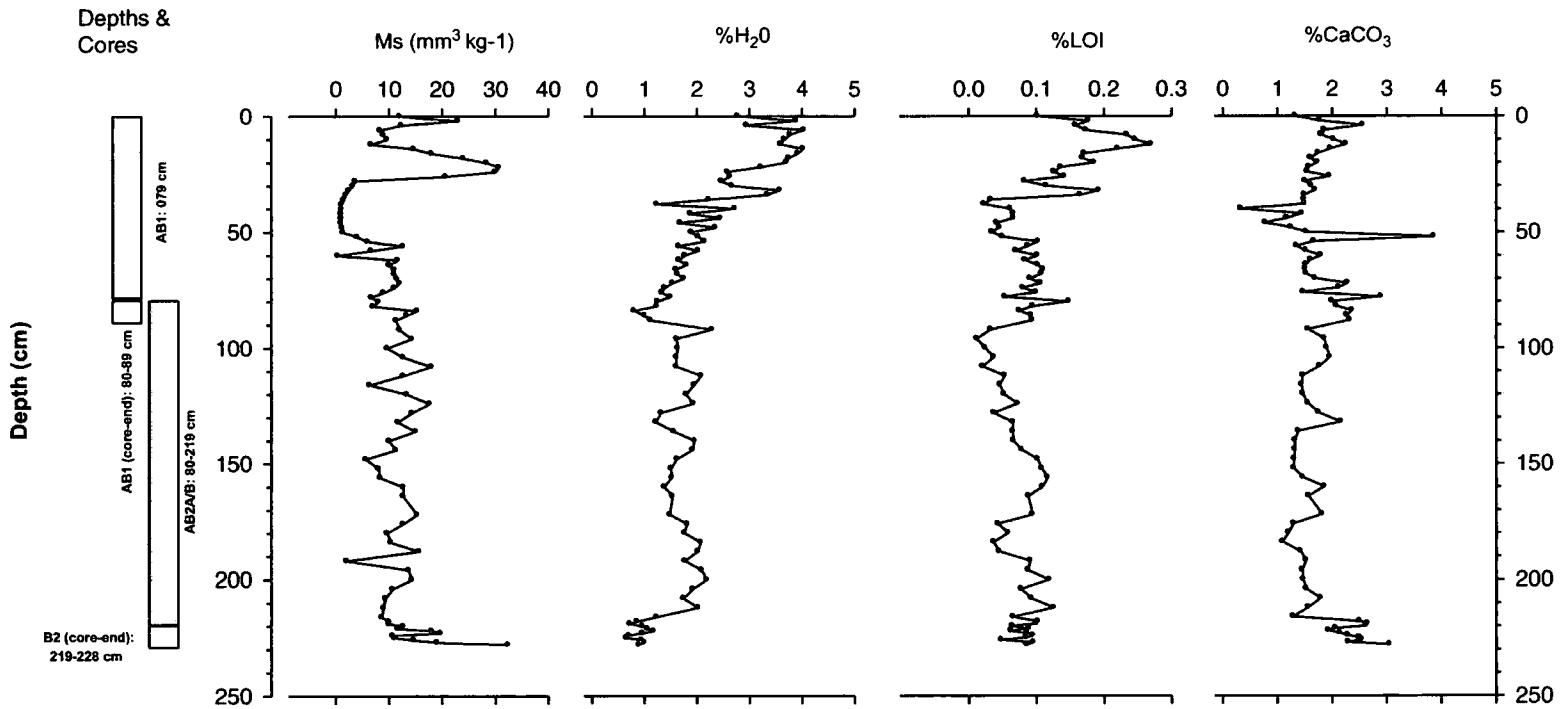

Figure 6.22. AB2 core showing downcore variations in Magnetic suceptibility (MS), % Water content (%H_2O), % Loss-on-ignition (LOI), and % Calcium carbonate (%$CaCO_3$). Cores, depths and core boundaries are shown on the left of the figure.

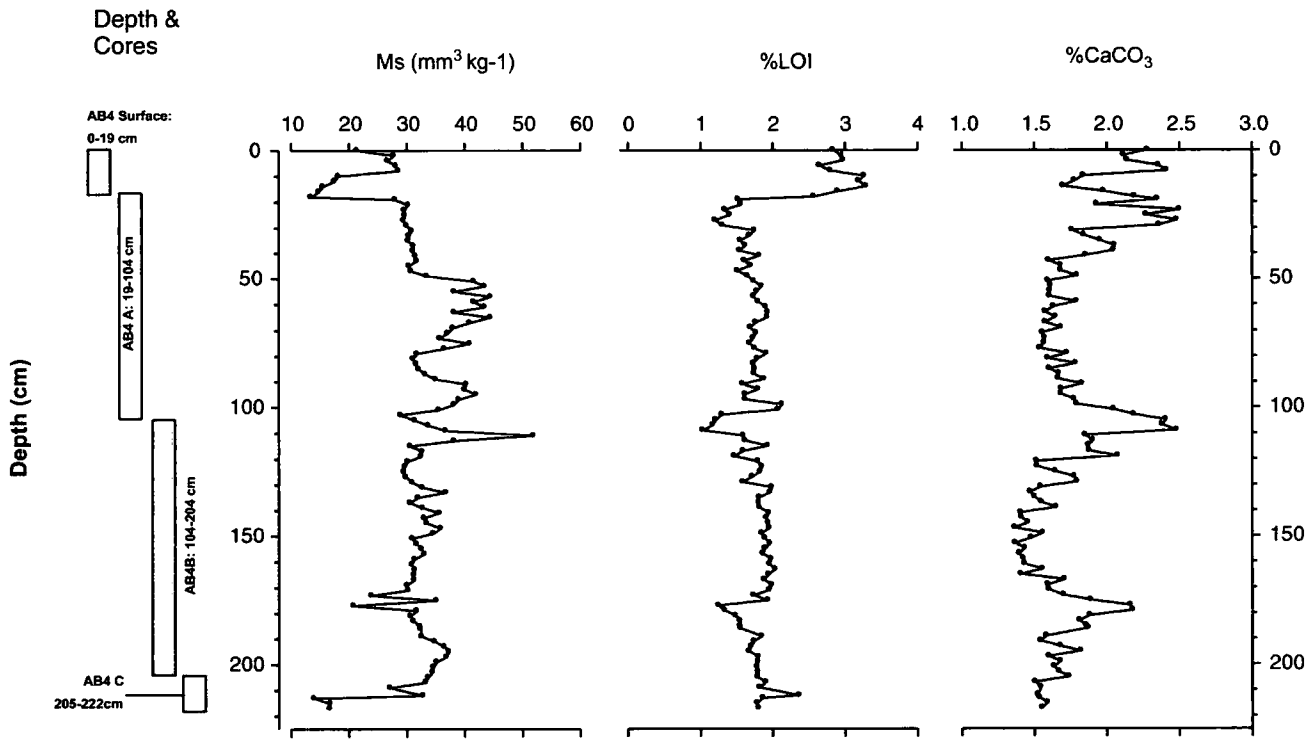

Figure 6.23. AB4 Core showing downcore variations in Magnetic suceptibility (MS), % Loss-on-ignition (LOI), and % Calcium carbonate (%$CaCO_3$). Cores, depths and core boundaries are shown on the left of the figure. %H_2O not meaured.

and 21 cm depth. MS values then decrease at 20 cm, which coincides with increasing %LOI and decreasing % $CaCO_3$.

6.4.2. Grain Size

This section presents the results of grain size analyses. In all cases, the <2 mm fraction was analysed. The > 2mm fraction has also been analysed for the ML and MLNB cores, in addition to the > 10 mm fraction in the ML core. Grain-size class data is presented in Appendix 5.

6.4.2.1. Moutonnée Lake (ML) Core

The >2 mm (obtained from wet sieving) and <2mm grain-size data are presented in Figure 6.24. BZII is characterised by a high proportion of >10 mm clast (Fig. 6.24), a decline in the 2-10 mm fraction and sand and an increase in % silt and clay. BZIV is characterised by a relative absence of >10 mm clasts, a decline in the 2-10 mm fraction. Percentage sand-silt-clay remains largely unchanged. BZIII is characterised by a decrease in >10 mm material and a rapid increase in 2-10 mm material from <5 % to >50% occurs. The percentage sand and percentage gravel increase, reaching a peak at 348 cm. % Clay and % silt fluctuate around 10% and 40% respectively. The sediment then fines from 347 cm to 304 cm, reflected by decreasing proportions of sand and gravel. Percentage clay and percentage silt remain constant, with only coarse silt showing a slight increase in abundance. BZV is characterised by increasing then decreasing coarse sediment fractions. Percentage gravel and percentage sand both increase from the upper boundary of BZIV reaching maximum concentrations at 124 cm of 22 % (gravel) and ca. 25 % sand. Percentage silt accounts for >40% of total sediment mass in this zone. Clay and fine silt percentages both increase steadily. From 124 cm, percentage gravel and sand fractions both decrease. The sediment surface is characterised by low gravel abundance and high abundances of the silt and clay fractions.

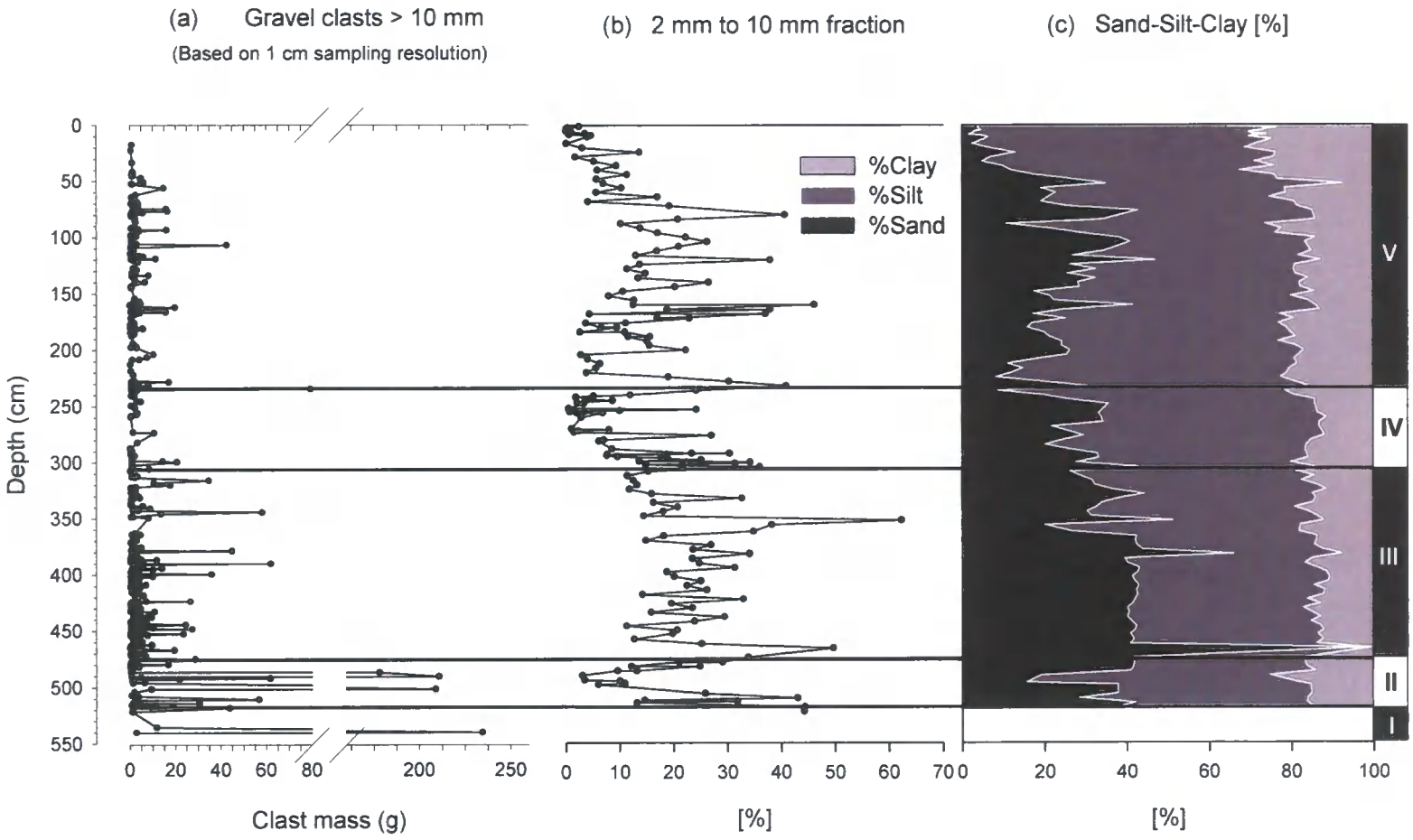

Figure 6.24. ML Core showing downcore variations in grain-size parameters (a) >10 mm clasts, (b) 2mm to 10mm clasts and (c) sand-silt-clay percentages. Solid black lines represent the biological zonation.

6.4.2.2. Moutonnée Lake North Basin (MLNB) Core

Biota Zone I is associated with an increase in coarse (>2mm and 63-2mm) material and a decrease in % silt and clay (Fig. 6.25). %Gravel then decreases rapidly in BZII (<135 cm), whilst fine-grained material increases. Fine-grained material (<63 μm) accounts for ca. 80% of the sample mass, with clay accounting for ca. 60% of this fraction. Between 27-0 cm there is a relative increase in percentage clay and silt and a decrease in %sand. The core top shows a modest increase in gravel sedimentation.

6.4.2.3. Ablation Lake 2 (AB2) Core

The sediment core is dominated by silt, accounting for ca. 60-70 %. (6.28) Clay remains relatively constant, whilst percentage sand fluctuates. Notable sand peaks occur at 147 cm, 70 and 50 cm, which correspond, to a clay and silt minima (Fig. 6.26). Percentage silt and clay then increase up to 23 cm before decreasing. Percentage gravel increases towards the sediment surface. Overall the unit is dominated by percentage silt (~ 20-70%).

6.4.2.4. Ablation Lake 4 (AB4) Core

AB4 is characterised by relatively constant sand-silt-clay proportions. Several notable fine layers occur at 160 cm, 106 cm, 40 cm and 30 cm and above 15 cm. In addition a prominent sand peak occurs at 20 cm. Overall, the sediment composed of clay (ca.40 %), silt (ca. 23-35 %), and sand (20-25 %).

6.5. Core Chronology

In this section the core chronologies for the Moutonnée and Ablation Lakes are presented. The ML and MLNB core chronologies are based on ten AMS ^{14}C dates performed on samples of monospecific foraminifera (Table 6.3). Eight are from *Globocassidulina* species with the remaining two performed on *Cibicides* species. Three other dates, two performed on the acid insoluble organic matter (AIOM)

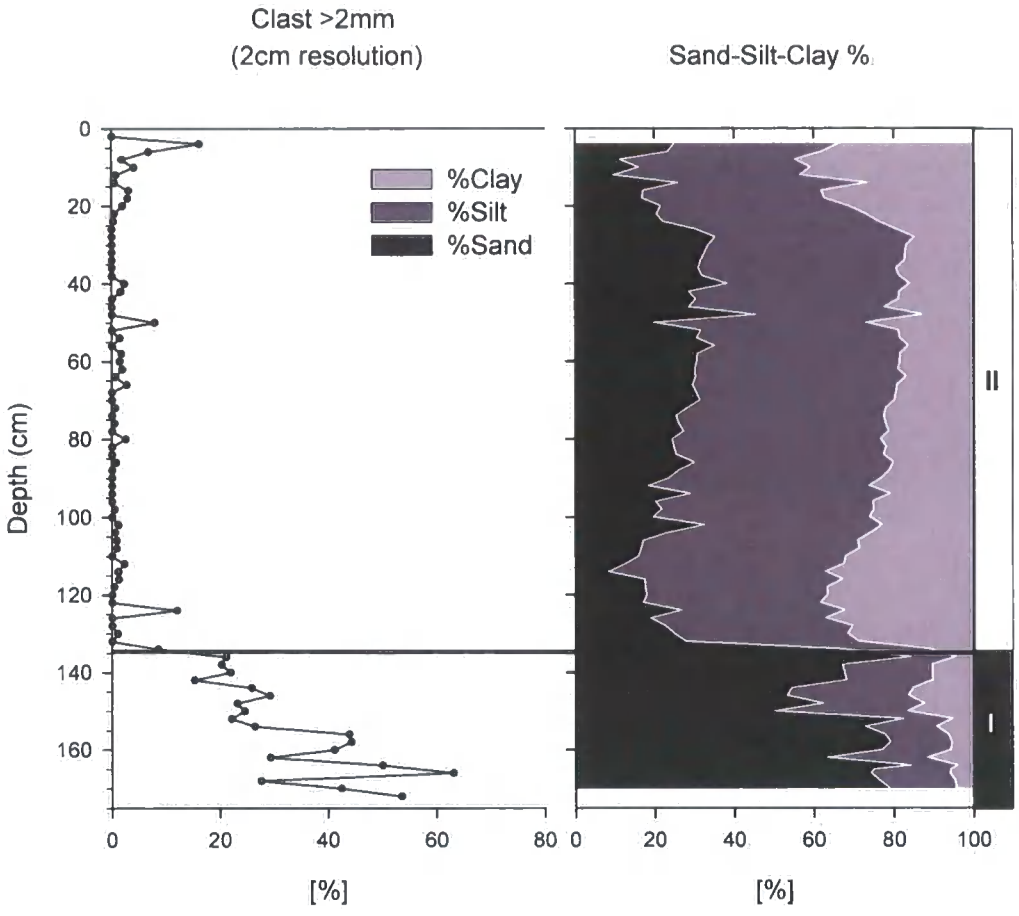

Figure 6.25. MLNB core showing downcore grain-size variations (a) <2mm to 10mm (b) sand-silt-clay percentages. Black line defines the biological zonation.

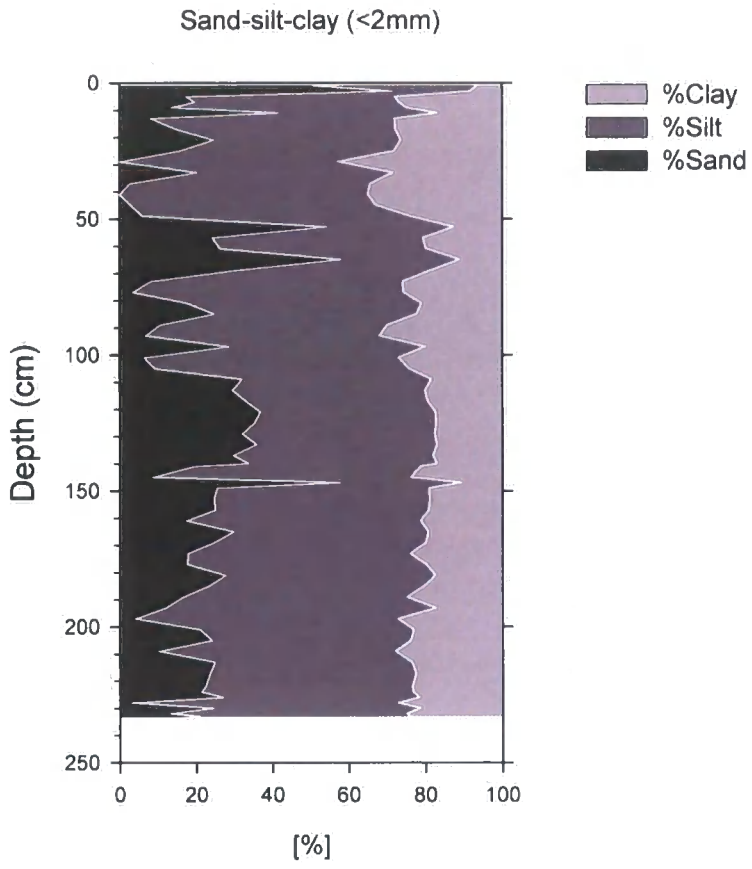

Figure 6.26. AB2 core showing sub-2mm grain size variations.

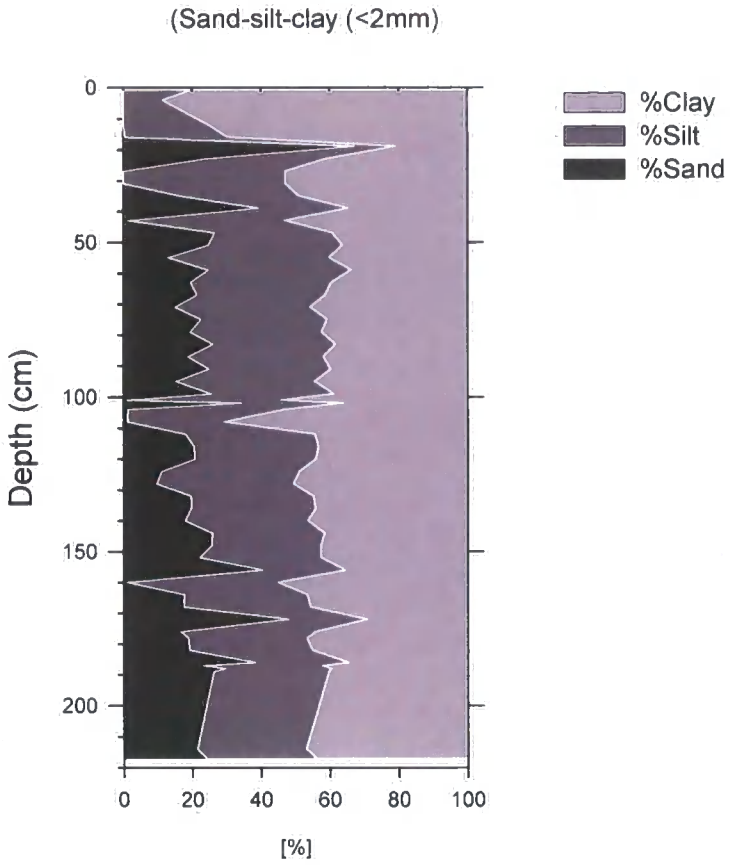

Figure 6.27. AB4 core showing sub-2mm grain size variations.

Material	Core	Lab. code	Core and depth (cm)	Conventional 14C age	δ13C (‰)	Marine reservoir corrected age	Calibrated age range (cal yr BP)	
							1-sigma	2-sigma range
Gb-Foraminifera	MLNB	SUERC-573	MLNB 138	8721±33	2.2	**7420±105**	8167-8370	8023-8479
Gb-Foraminifera	MLNB	SUERC-574	MLNB 163	8903±30	2.4	**7600±104**	8350-8573	8209-8747
Gb-Foraminifera	ML	SUERC-575	ML 243-246	8634±30	3.3	**7330±104 ****	8097-8311 (96%) 8061-8074 (4%)	7967-8372
Gb-Foraminifera	ML	SUERC-576	ML 252-255	8603±36	3.7	**7300±106**	8036-8269	7945-8355
Gb-Foraminifera	ML	SUERC-577	ML 270-272	9127±47	1.7	**7830±110 ****	8589-8851	8451-8941
Gb-Foraminifera	ML	SUERC-578	ML 280-281	9467±30	4.8	**8170±104**	8907-9088 (72%) 9243-9363 (28%)	8830-9434 9549-9595 (2%)
Cb-Foraminifera	ML	Beta-177300	ML 280-281	9430±40	-0.7	**8130±108**	8863-9083 (88%) 9245-9305 (12%)	8801-9425 9553-9591 (1%)
Gb-Foraminifera	ML	SUERC-579	ML 291-293	9403±33	4.4	**8100±105 ****	8843-9065 (95%) 9253-9275 (5%)	8742-9136 9188-9418 9554-9589 (1%)
Gb-Foraminifera	ML	AA-54874	ML 494-495	9260±110	0.6	**7960±149**	8656-8975	8445-9084 9242-9316 (3%) 9324-9361 (1%)
Cb-Foraminifera	ML	Beta-177301	ML 494-495	9400±40	-0.3	**8100±108 ****	8841-9067 (95%) 9253-9279 (5%)	8730-9138 9186-9419 9554-9589 (1%)
Algal Flakes	ML	AA-54875	ML 3-10	19720±160	-30.3	18420±354	X	X
AIOM	ML	CAMS-78992	ML Surface sediment	15100 ± 50	-25.9	13800±320	X	X
AIOM	ML	CAMS-78993	ML Basal sediment	28750 ± 180	-25.6	27450±364	X	X
AIOM	AB2	CAMS-78994	AB Surface sediment	14180 ± 50	-24.7	12880±320	X	X
AIOM	AB2	CAMS-78995	AB Basal sediment	30370 ± 220	-25.8	29070±385	X	X

Table 6.3. Radiocarbon dates from the ML, MLNB and AB cores. All dates were obtained on hand-picked specimens of Globocassidulina sp. (**Gb**) and Cibicides sp. (**Cb**). At two depths we obtained dates on both foraminiferal species: the dates are within 1-sigma of one another: **ML**=Moutonnée Lake main core; MLNB=Moutonnée Lake North Basin core; AB=Ablation Lake; **AIOM** = Acid insoluable Organic Matter fraction; **X** = beyond Calib calibration curve; ******denotes ages used in the age-depth model. Notes on calibration: Errors are reported as 1-sigma; dates are corrected by the commonly accepted value for Antarctic marine carbonate, 1300±100 yr (Berkman et al., 1998). Calibration was carried-out using the Calib program (v4.4) (Stuiver and Reimer, 1993), and a ΔR value of 900 yr. Where more than one calibrated range is given, the figure in parentheses indicates the percentage of the area under the probability distribution. All other ranges constitute 100% of the probability distribution over the stated 1- or 2-sigma range.

fraction and one performed on algal flakes assumed to be of freshwater origin are also presented. Two ^{14}C dates obtained from the AIOM fraction of core top and core bottom sediments from Ablation Lake are also presented. The construction of an age-depth model is discussed in Chapter 7, along with the environmental interpretation of the proxies.

Calibration was carried-out using the Calib 4.4.2 program (v4.4) (Stuiver and Reimer, 1993), using the marine/INTCAL98 calibration curve. Dates have been corrected for the southern ocean marine reservoir by the commonly accepted value for Antarctic marine carbonate, 1300 ± 100 yr (Berkman et al., 1998) and thus a ΔR value of 900 ± 100 yr was used together with a value of 100% for marine carbonate. Ages are reported as calibrated years before present (cal yr BP). Where more than one calibrated range is given, the figure in parentheses indicates the percentage of the area under the probability distribution. All other ranges constitute 100% of the probability distribution over the stated 1- or 2-sigma range.

6.5.1. Moutonnée Lake (ML) Core

The eight AMS ^{14}C dates on foraminiferal carbonate from ML core are presented in Table 6.3. Six of the ages are based on *Globocassidulina* remains, whilst the remaining two are from remains of *Cibicides* sp. Conventional ^{14}C ages range from 8603 ± 36 at 252-255 cm to 9403 ± 33 at 494-494. The calibrated ages fall between 8036-8269 (100%) and 8843-9065 (95%) cal yr BP at 1-sigma. The ages are in chronological order with any minor age-depth inversions falling within the cited (1-sigma) error. Figure 6.28 shows the conventional ^{14}C, marine reservoir corrected, and calibrated ages plotted against depth for the ML core.

Table 6.3 also shows the results of two 'range-finder' radiocarbon dated AIOM samples and one radiocarbon dated algal flake. Conventional ^{14}C ages for the CAMS-78992 sample of bulk sediment from the surface of the ML core yielded an age of 15100 ± 50 ^{14}C yrs, whilst sample CAMS-78993 from bulk sediment near the base of the ML core yielded an age of 28750 ± 180 ^{14}C yrs. The algal flake material taken from near the surface (3 cm sediment depth) in the ML core yielded an age of

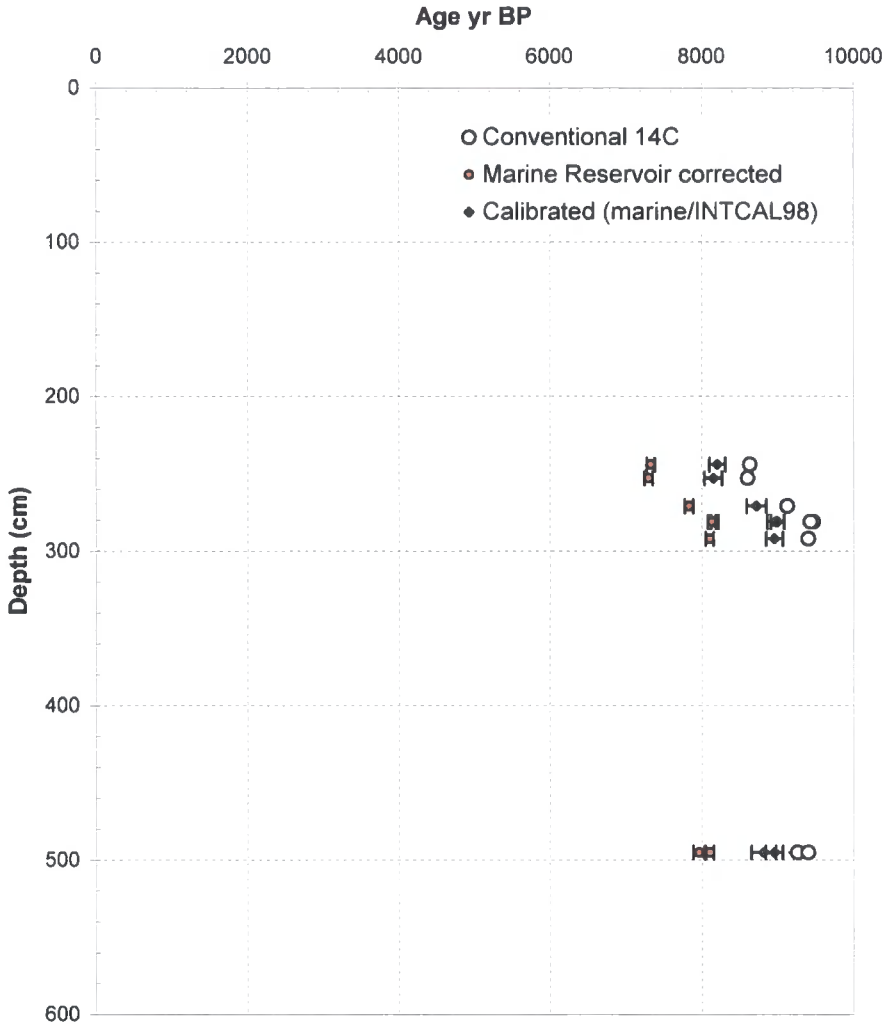

Figure 6.28. Depth versus conventional ^{14}C, marine reservoir corrected and calibrated (marine/INTCAL98) ages for the ML core, Moutonnée Lake. Unless error bars are shown, the size of the marker represents the total error. For calibrated ages, the mid-point between the calibrated ranges has been chosen. The attached error represents the total range.

19720 ± 160. These ages are surprisingly old in comparison to the ages derived from foraminiferal carbonate and clearly reflect some form of contamination in the bulk samples. The implication of these ages for the core chronology and local marine reservoir will be further discussed in Chapter 7.

6.5.2. Moutonnée Lake North Basin (MLNB) Core

The results of two AMS ^{14}C dates on foraminiferal carbonate from the MLNB core are presented in Table 6.2. Both ages are derived from *Globocassidulina* remains. The conventional ^{14}C ages are 8721 ± 33 at 138 cm and 8903 ± 30 at 163 cm. The calibrated ages fall between 8167-8370 and 8350-8573 cal yr BP at 1-sigma. Thus, both ages fall within the age-range defined by the foraminifera carbonate dates on the ML core. Figure 6.29 shows the conventional ^{14}C, marine reservoir corrected and calibrated ages these ages plotted against depth.

6.5.3. Ablation Lake 2 (AB2) Core

Table 6.3 also shows the results of two dates from Ablation Lake, performed on the AIOM fraction from bulk sediment samples near the surface and near the base of the AB2 core. The surface sediment yielded a conventional ^{14}C age of 14180 ± 50, whilst the basal sediment yielded an age of 30370 ± 220. The two bulk sediment ages are very similar to the 'old' ages obtained from the AIOM fraction of ML core material, and are likely to have been affected by similar contamination processes. The significance of this will be discussed further in Chapter 7.

6.5.4. ^{137}Cs and ^{210}Pb Chronology

A ^{137}Cs and ^{210}Pb pilot dating study was carried out on core top sediment (0-30 cm) from Moutonnée Lake with the aim of obtaining a core top chronology. The post detection analysis however revealed undetectable levels of ^{137}Cs or ^{210}Pb in the sediment. This may reflect one of several factors: (1) the lake ice cover retarded the accumulation of ^{137}Cs and ^{210}Pb fallout; (2) that the Moutonnée Lake catchment is not large enough to focus a sufficiently strong ^{137}Cs and ^{210}Pb signals; and (3) ^{137}Cs and ^{210}Pb fallout is uniformly low in this part of the AP.

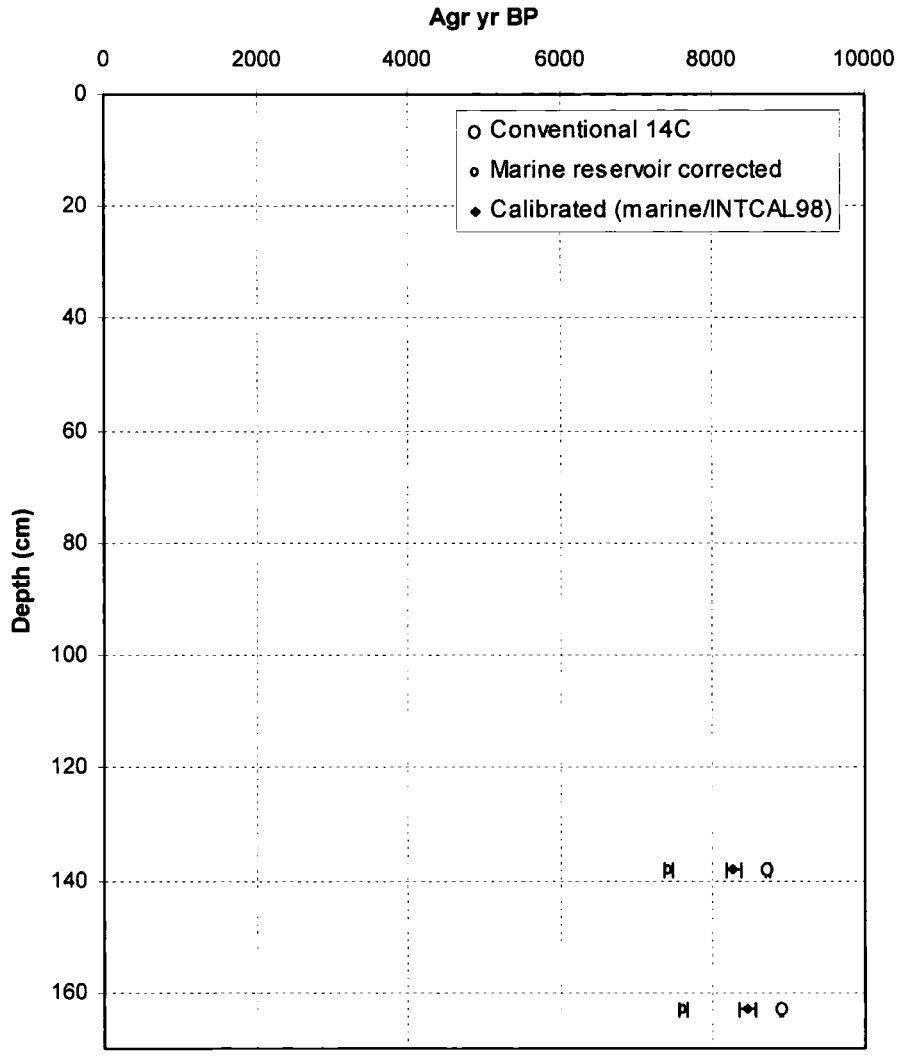

Figure 6.29. Depth versus conventional ^{14}C, marine reservoir corrected and calibrated (marine/INTCAL98) ages for the MLNB core, Moutonnée Lake. Unless error bars are shown, the size of the marker represents the total error. For calibrated ages, the mid-point between the calibrated ranges has been chosen. The attached error represents the total range.

The absence of a ^{137}Cs and ^{210}Pb in the surface sediment together with the erroneously old AIOM surface ages means that it is difficult to confidently assign a modern-day age to the ML and AB surface sediment. However, it is worth noting that in all cases, cores were extracted with the sediment-water interface intact. Because of this, the surface sediment of all core material is assumed to be 0 year BP.

6.5.5. Dates for the Biological Zones

The dates for the biological zones in the ML core show four key features:

(i) The dates (within error) are in their correct stratigraphical order

(ii) The biological zones (BZ) from the ML core (BZII and IV) date to the Early Holocene (8100±108 to 7300±106 ^{14}C yr BP) (8097-9067 cal yr BP) at the 1-sigma level.

(iii) The upper dates for BZII (7960±149 and 8100±108 ^{14}C yr BP) and the lower dates for BZIV (8100±105 ^{14}C yr BP) in the ML core are statistically indistinguishable (Fig. 6.30).

(iv) The dates for the top of BZIV (7330±104 ^{14}C yr BP) in the ML core, and the BZ I (7420±105 ^{14}C yr BP) in the MLNB core are statistically indistinguishable, showing chronological consistency between the two cores. This implies that, the biological zones from the ML and MLNB cores were deposited contemporaneously (Fig. 6.30).

In addition, and as will be discussed in more detail in the following chapter, the statistically indistinguishable dates for BZII and BZIV in the ML core imply that the intervening 1.88 m of sediment (BZIII) was deposited very rapidly, perhaps as an instantaneous dump of ice rafted debris (IRD) (Fig. 6.30). An important corollary of this is that the interval BZII to BZIV is interpreted as one environmental episode.

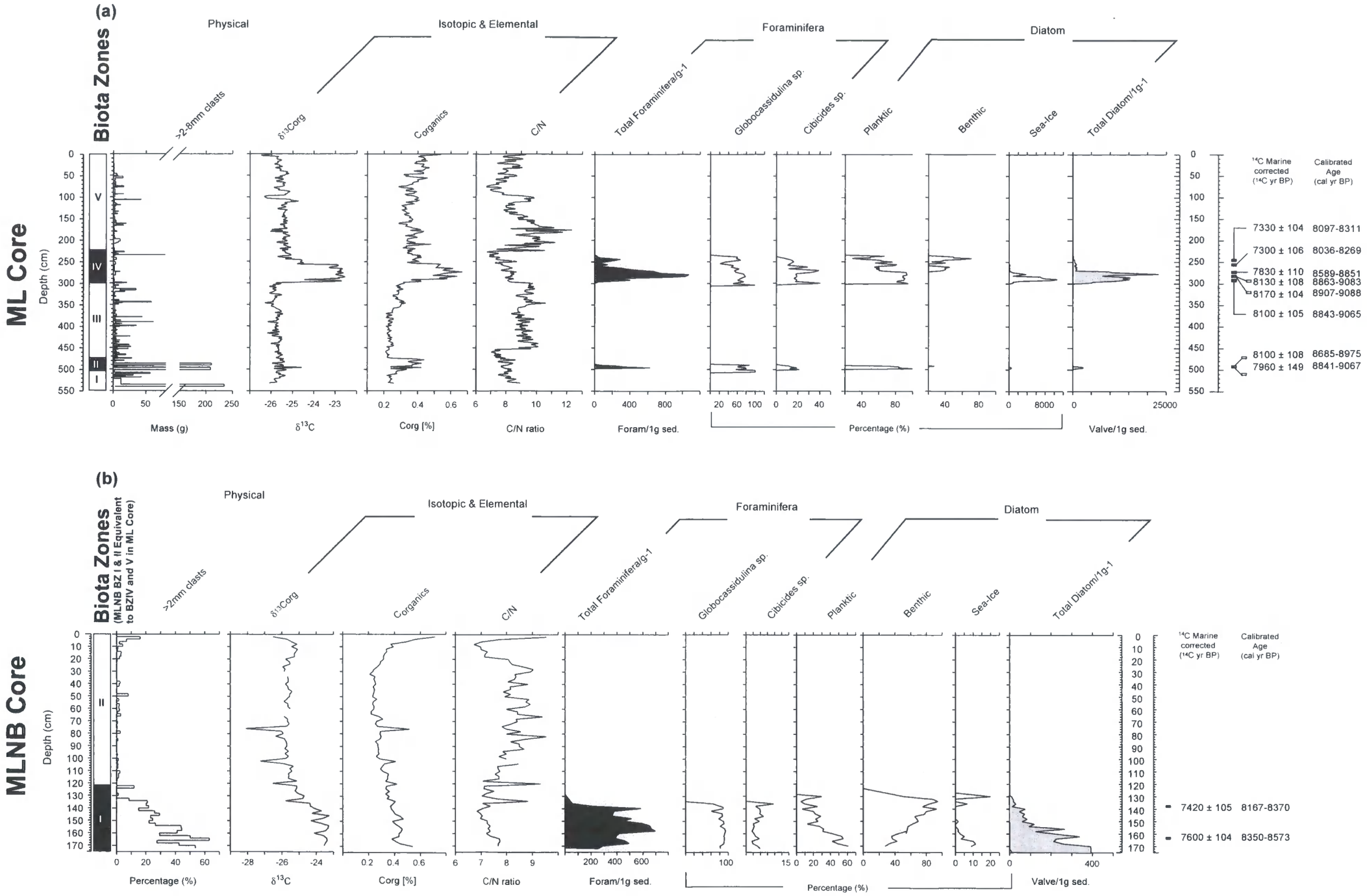

Figure 6.30. Summary diagram showing key multi-proxy data from (a) ML and (b) MLNB Cores from Moutonnée Lake. Proxies include: $\delta^{13}C$ on organic matter in bulk sediment ($\delta^{13}C$organics); %Corg and C/N ratio performed on bulk sediment; diatom and foraminiferal assemblages; and grain size data. Note that the overall ecological, physical and geochemical signatures of Biota Zones (BZ) IV and V are almost identical to BZ I and II in the MLNB core. Together with the ^{14}C chronology, this suggests that the zones are contemporaneous. BZ I, III and V (ML Core) and BZ II (MLNB Core) were entirely deviod of both diatoms and foraminifera.

6.6. Core Chronology - Construction of an Age Depth Model

Chapter 4 reviewed the problems associated with obtaining reliable core chronologies from bulk sediments in marine and/or lacustrine environments in the Antarctic. Dating problems are due primarily to the Antarctic marine reservoir effect (AMRE), the addition of old (or new) carbon and specific vital effects within some marine organisms (Melles et al., 1994; Berkman et al., 1998; Andrews et al., 1999). The strength of the ML core chronology is that it dates monospecific assemblages of well-preserved foraminifera and although species-specific reservoir corrections for *Globocassidulina* and *Cibicides* species have not yet been developed the general pre-bomb marine reservoir correction of 1300 years was considered to be most suitable for shells from the Antarctic Peninsula based on Berkman et al. (1998). This is consistent with the procedures established recently for the Antarctic Peninsula (Domack and McLennen, 1996; Domack et al., 2001) and the Ross Sea (Domack et al., 1999; Andrews et al., 1999).

The ^{14}C-dated ages derived from the bulk acid insoluble organic matter (AIOM) fraction (Table. 6.3) yielded consistently old ages, with surface sediments dated to 15100 ± 50 and 14180 ± 50 ^{14}C yr BP and basal sediments yielding ages of 28750 ± 180 and 30370 ± 220 ^{14}C yr BP for ML and AB respectively. Such old surface ages are not uncommon in Antarctica (see Andrews et al., 1999), since the AIOM fraction may be affected by reworked carbon from detrital humic macerals, kerogen from sedimentary rocks, CO_2 from meltwater and resuspended marine organic matter (Andrews et al., 1999; Domack et al., 1999; Hall and Denton, 2000; Brachfield et al., 2003). The old ages from ML and AB most likely reflect one or more of these factors – i.e. the introduction of old carbon from the catchment rocks (e.g. late Jurassic to Cretaceous mudstone or old CO_2 from glacial melt). An additional source of old carbon was also identified. An organic sample, originally considered to be a fragment of a freshwater biofilm, yielded a conventional radiocarbon age of 19720 ± 160 ^{14}C yr BP and this presumably inwashed old organic material is likely to have contributed to the old AIOM ages. The source of

this material however remains unclear, and its contribution downcore is thus difficult to quantify.

As a first approximation, Andrews et al. (1999) suggested that where a large surface error existed a reasonable radiocarbon chronology can be obtained by subtracting the surface age from subsequent dated samples. By subtracting the surface age from the basal age for each lake, the ML core spans the last ca. 13,650 ^{14}C years whilst the AB core spans the last ca. 16,190 ^{14}C years. This age range for the ML core however seems incompatible with the foraminiferal-derived ages. This factor may reflect variations in the marine reservoir over time (e.g. Crespin et al., 2004) and as such the AIOM fraction is not incorporated into the core chronology. Instead the core chronology from ML is based solely on the foraminiferal-derived ages, where the reservoir correction is more clearly understood (see Berkman et al., 1998).

The AB core was devoid of foraminifera (due to only partial core recovery at this site) and so the chronology of this site remains unresolved and will require further work on the AIOM fraction (or additional dating techniques) before it can be placed in a chronological framework.

6.6.1.Age Model Calibration

The foraminiferal derived ages of the ML core provide an opportunity to establish a calibrated marine radiocarbon stratigraphy for the entire core. The age depth model for the ML core has been constructed using four ages that occur in stratigraphical order (Table 6.3). A basal date of 8841-9067 cal yr BP has been used from BZII. In BZIV, the age model is developed using three ages (Table 6.3 and Fig. 6. 31). The sediment-water interface is assumed to be 0 cal yrs BP (see Chapter 6 for discussion). In all cases the age-depth model has been constructed using a linear interpolation between the arithmetic means of the calibrated age ranges (e.g. Telford et al., 2004). The use of a central point (or mean) of the calibrated age-range is common practice, but can result in large error (Telford et al., 2004a,b). Thus, the overall error associated with the calibrated range represent the entire range of the calibrated ^{14}C age. So for example, in BZII, 8841-9067 has an arithmetic mean of 8954 and an associated error ± 226 years. Where more than one calibrated range is

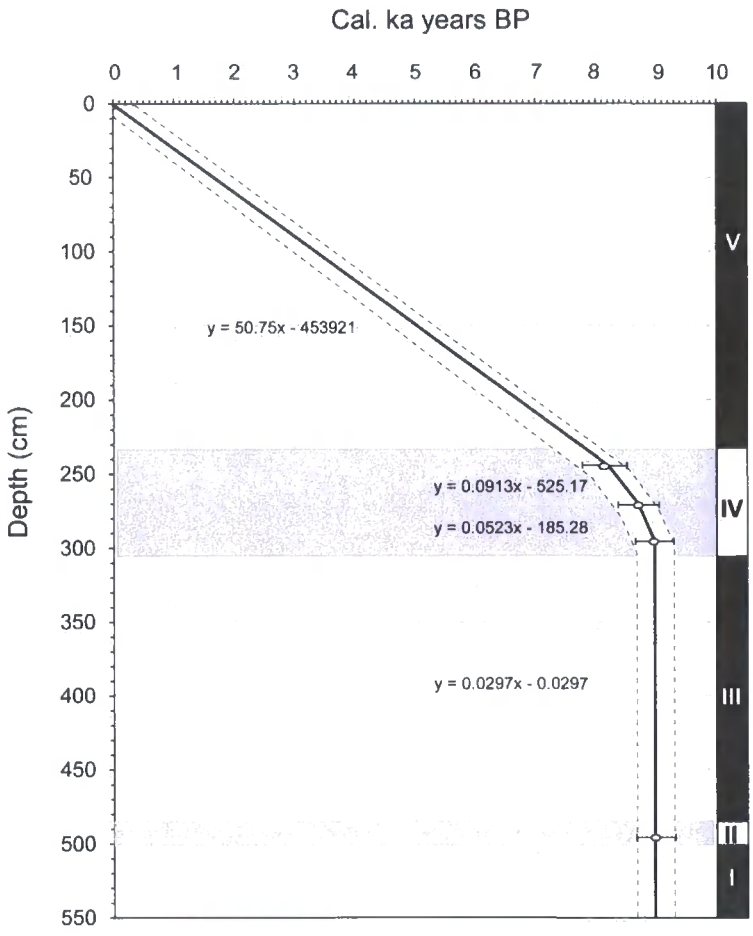

Figure 6.31. Depth versus calibrated radiocarbon age for the ML core. The ages are given as the arithmetic mean of the calibrated ranges (Table 6.3). The error bars (dotted line) represents the entire range of the calibrated age. The age-depth model uses simple linear interpolation between each mean age. The ages for BZI, III and V are based on linear interpolation.

given (Table 6.3) the ranges with the highest probability (1-sigma) have been used. Although this is not always statistically rigorous it is nevertheless thought to be a reasonable compromise (J.J.Lowe, pers. comm., 2004). Linear interpolation is most appropriate for the ML core since it forces the age-depth model to pass through the ^{14}C data points, which means that the model cannot deviate too far from 'reality' (Telford et al., 2004) (Figure. 6.31). However, no interpolation model can account for changes in sedimentation between two interpolated points.

Because the ML core lacks any dating control in units BZI, III and V, the ages for these units are based on linear interpolation (Fig. 6. 31). The age-depth model for the MLNB core was also constructed using linear interpolation. A summary of the important Biota Zone boundaries using the age-depth model is provided in Table 6.4. It is worth noting at this stage however, that whilst the ages from BZI, III and V are based on linear interpolation, BZII and BZIV are well constrained by the foraminiferal ages.

CORE	ZONE	DEPTH INTERVAL (CM)	CALIBRATED AGE RANGE (CAL YR B.P.)
ML	BZI	537-500	8964-8962
	BZII	499-485	8962-8962
	BZIII	485-302	8961-8959
	BZIV	301-236	8958-7946
	BZV	235-0	7912-0
MLNB	BZI	172-135	8533-8083
	BZII	134-0	8023-0

Table 6.4. Calibrated ages for key biological zonation in ML and MLNB cores.

6.7. Core summary and correlation

At the outset it was stated that this chapter had three fundamental aims. Firstly, to identify key changes in each proxy, which can then be associated with hydrological and/or other physical changes in the lake system; Secondly, to identify concurrent

changes between individual proxies; and finally, to identify concurrent changes between cores and lakes.

The key changes for each individual proxy have already been established and have been described in detail for each core. To highlight concurrent changes within cores, Figure 6.30 provides a summary of the key proxy data from ML and Figure 6.32 provides a summary of key data from AB. In ML significant and consistent environmental changes occurred between 500-490 cm (BZII) and 300-236 cm (BZIV) in the ML core and between 173-136 cm (BZ1) in the MLNB core (Fig. 6.30). These biological zones are associated with the influx of exclusively marine diatom and foraminiferal assemblages, elevated (marine) $\delta^{13}C_{org}$ and C_{org} values, depressed C/N values, and coarse (>2mm) sediment deposition. It is also clear from the mono-specific foraminiferal-based ^{14}C chronology that the biological zones were deposited during the early Holocene (8097-9067 cal yr BP). In addition, the core chronology suggests that the ML and MLNB biological zones were deposited contemporaneously. This is further supported by the similarity between the diatom and foraminiferal assemblages in each core. Other notable features from the ML core include a fluctuating C/N profile (Fig. 6.30) in BZV between 236-100 cm terminating at ca. 99 cm with a positive $\delta^{13}C_{org}$ and negative C/N excursion. This zone is also accompanied by rapid changes in LOI, $CaCO_3$ and H_2O (see Fig. 6.20). The palaeoenvironmental implications of the biological zones and the additional changes (e.g. BZV) are also discussed in Chapter 7.

In contrast to ML, biological remains were absent in the two cores (AB2, AB4) analysed from Ablation Lake (Fig. 6.32). This could suggest that: (1) the biological remains have been affected by post-depositional processes (i.e. dissolution) and/or; (2) only the upper portion (e.g. equivalent to BZV in the ML core and Zone I in the MLNB core) sedimentary sequence was recovered. Total dissolution of *all* silicate (diatom) and carbonate (foraminifera) remains seems unrealistic, although not impossible. For example, in Chapter 5 analysis of surface sediment in Moutonnée Lake revealed that in the vicinity of the halocline, the wide-ranging salinities appeared to prevent the growth of *in-situ* diatom valves (e.g. Fig. 5.6; Zone 3). However on present data and in the absence of a reliable core chronology, partial

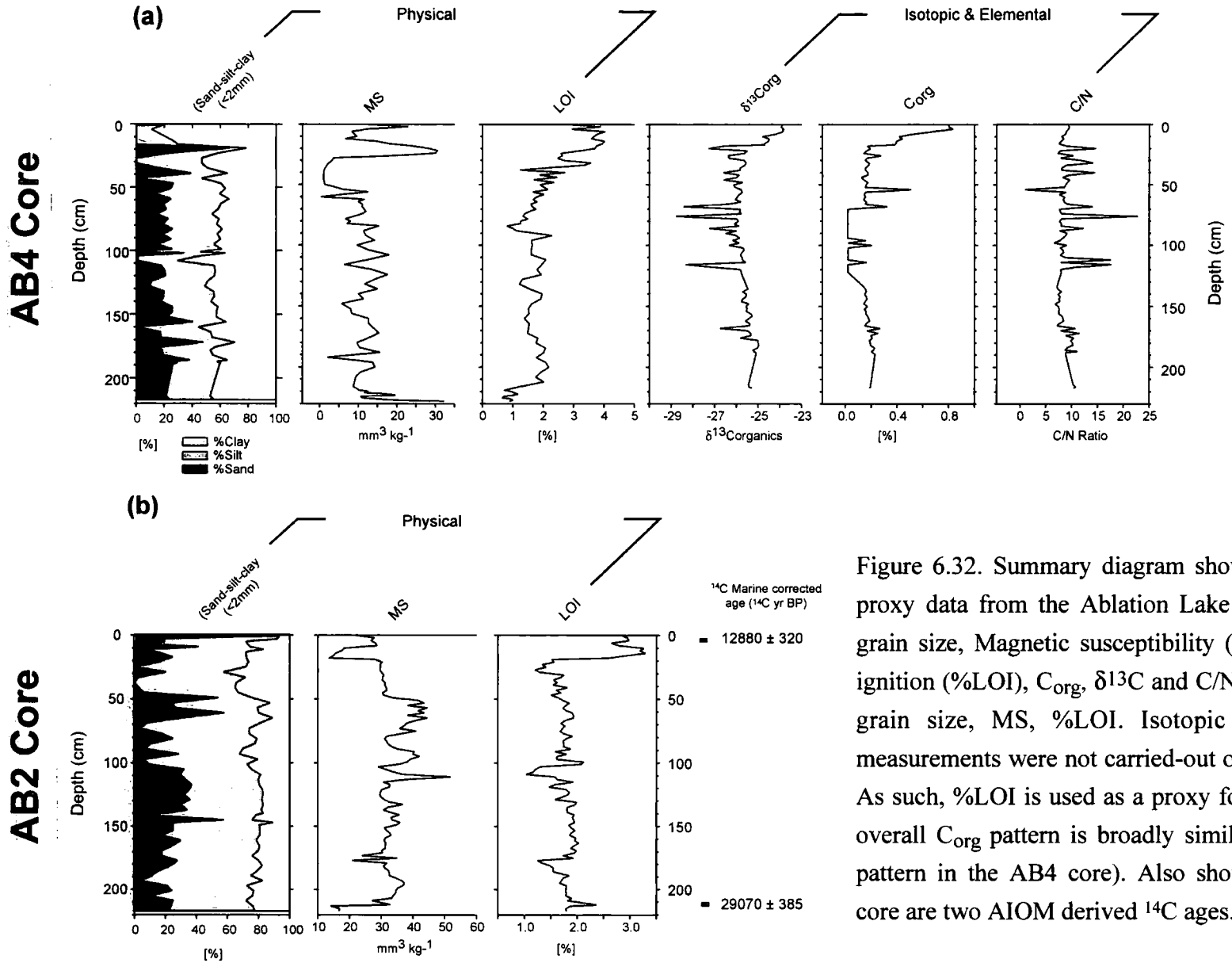

Figure 6.32. Summary diagram showing key multi-proxy data from the Ablation Lake cores **(a)** AB4: grain size, Magnetic susceptibility (MS), %Loss on ignition (%LOI), C_{org}, $\delta^{13}C$ and C/N ratio; **(b)** AB2: grain size, MS, %LOI. Isotopic and elemental measurements were not carried-out on the AB2 core. As such, %LOI is used as a proxy for C_{org} (NB: the overall C_{org} pattern is broadly similar to the %LOI pattern in the AB4 core). Also shown on the AB2 core are two AIOM derived ^{14}C ages.

retrieval of the sedimentary sequence is the favoured explanation. This interpretation is supported by our field observations. For example, the final drive of the ML core retrieved a bedrock disc, which implies that we reached the underlying bedrock and thus retrieved the entire sedimentary sequence. In contrast to ML, no clear evidence for reaching the base of the sequence was discovered. Instead the sediment became over consolidated towards the base of AB2 and AB4, which prevented further penetration.

Assuming that the cores extracted from Ablation Lake only represent the upper portion of the ML core (i.e. BZV) the available proxy data suggests there is no strong correlation between the sedimentary records obtained from Moutonnée and the records obtained from Ablation Lakes (see Fig. 6.30 and 6.32). The C_{org} proxy however, does appears to increase towards the sediment-water interface in all analysed cores. On a local-scale, this suggests that the different environmental records reflect site-specific changes, which will be largely determined by the processes occurring in the lake catchment. In this respect the size and the nature of the system (i.e. one is open (AB) and the other acts as a closed system (ML)) are probably the most important factors. As noted Chapter 5, ML is, largely a closed lake system, although tidal exchange does occur. As such, it is more likely to be influenced by local catchment-scale changes, unless it is influenced by large-scale external processes (e.g. the loss of the ice shelf dam). In contrast, available data suggests that Ablation Lake behaves as an open lake system that is able to exchange freely with the marine water beneath GVI-IS. Furthermore, the lake system (including the catchment) is much larger and has a more complex sedimentary regime. For example, in AB, the delivery of minerogenic material is likely to be modulated by the ice shelf 'tongue' and by local valley glaciers, which flow into the lake (Fig. 4.9 and 4.10, Chapter 4). Thus on a local valley scale, the sedimentary record within each lake may record different environmental processes.

6.8. Summary

In summary, BZII and IV identified in the ML core and BZI in the MLNB core represent a distinct suite of proxies. Within these zones there is a consistent

depositional signature in the $\delta^{13}C_{org}$, C_{org} and N_{org} values, together with the influx of foraminifera, and diatoms. In addition, there is a close replication of ecological, geochemical and sedimentological conditions in the upper biological zone of the ML core and the biological zone in the MLNB core (Fig. 6.30). In contrast biological zones were not detected in sediment cores from Ablation Lake (Fig. 6.32). This suggests that we did not retrieve a complete sedimentary sequence from Ablation Lake. In the next chapter the palaeoenvironmental implications of the biological zones identified in Moutonnée Lake are discussed in detail, specifically the evidence the present for ice shelf absence.

Chapter 7

EARLY HOLOCENE ABSENCE OF GEORGE VI ICE SHELF: IMPLICATIONS AND WIDER CONTEXT

7.1. Introduction

This chapter provides a detailed interpretation and discussion of the Holocene history of GVI-IS using the conceptual model developed in Chapter 5 and the core results presented in Chapter 6. Central to the discussion are the marine biological zones (BZII and IV in the ML core and BZI in the MLNB core) identified in sediment cores from Moutonnée Lake, which are interpreted here as representing a period of past ice shelf absence. This ice shelf absence is then placed in a regional context and compared with other palaeoclimatic records from the AP, before evidence of the mechanisms leading to the ice shelf absence and re-formation are discussed.

7.2. Environmental Interpretation of Core Data from Moutonnée Lake

Using the age model presented in the previous chapter the next section will discuss the palaeoenvironmental significance of sediments from Moutonnée Lake. Since BZIV in the ML core is directly comparable to BZI in the MLNB core (see Figure 6.30), both in age and overall biological and sedimentological character, the following interpretation and discussion will focus on the ML core, which provides a more detailed picture of the absence of George VI Ice Shelf and its subsequent re-formation. The sediment cores from Ablation Lake did not yield a record of ice shelf loss, which suggests that we did not retrieve a complete sediment sequence.

7.2.1. BZI (537-501 cm): Pre ice shelf absence

At the base of BZ1 (prior to 8964 cal yr BP) the multi-proxy core data suggest that the lake environment was similar to the present-day. In other words, the lake was perennially ice-covered, freshwater dominated and largely unproductive. There is an absence of biological microfossils and $\delta^{13}C_{org}$ values are similar to the modern day (e.g. - 25.7 ‰) (Fig. 7.1). The $\delta^{13}C_{org}$ values also suggest that the sediment was locally derived (see Chapter 5). There is no age-control at the very base of the core but applying a maximum and minimum sedimentation rate (based on dated units within the core) suggest a time interval of between 2 and 400 years for the deposition of this unit. A bedrock disc of local sedimentary material was retrieved from the final drive of the core, which suggest that the entire sedimentary sequence was extracted. An alternative possibility is that the disc of sedimentary rock is a large drop-stone and/or clast from a glacial till. However, if indeed the core bottom was close to bedrock then it would suggest that grounded ice existed in the basin prior to the deposition of BZI and had scoured-out any earlier sedimentary record. There is geomorphological evidence for both advance of valley glaciers over the lake site (valley stage advance) and expansion of the ice shelf sometime prior to 6500 ^{14}C yr BP, and most likely during the LGM or during deglaciation from it (Clapperton and Sugden, 1982).

7.2.2. BZII (522-490 cm): Onset of ice shelf absence

BZII provides the first evidence of ice shelf absence. Significantly, the unit is characterised by the incursion of an exclusively marine biological assemblage, elevated C_{org} and N_{org} values (Fig. 6.12 Chapter 6) and high abundances of >8 mm clasts (Fig. 7.1 and Fig. 6.12), probably deposited as ice-rafted debris (IRD). The lowermost foraminiferal-derived age from this unit suggests that the basin became an open marine embayment sometime before 8841-9067 cal yr BP. The modelled age for the base of BZII is 8962 cal yr BP. The interpretation of ice shelf break-up during this zone is supported by observations of the recent Arctic ice-shelf break-up where initial cracking of the ice shelf led to the draining of the epishelf lake, and the

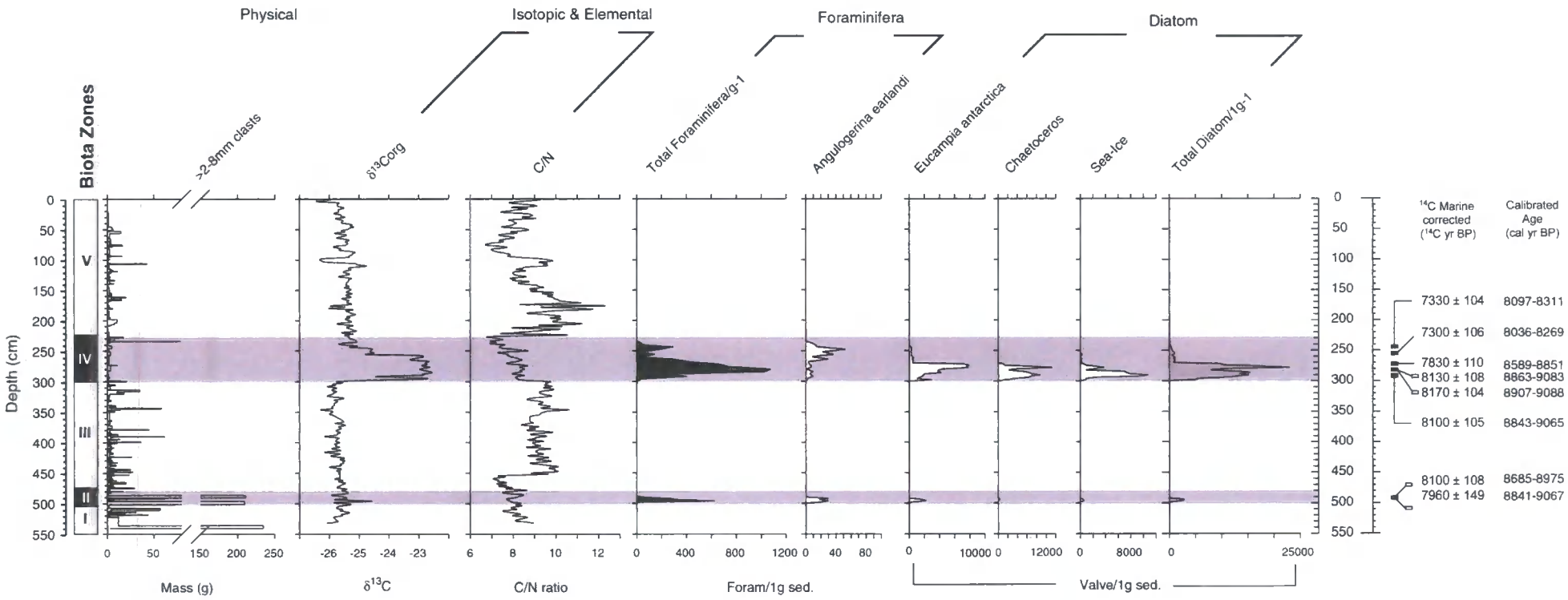

Figure 7.1. Summary diagram of key multi-proxy records from Moutonnée Lake (ML Core). ^{14}C ages and calibrated ^{14}C ages are shown on the right of the diagram.

influx of the first marine fauna and flora (e.g. Ward Hunt Ice Shelf, Arctic Canada; Mueller et al., 2003).

7.2.2.1. Diatom assemblage

The diatom assemblage in BZII (Fig. 7.1 and 6.1 Chapter 6) is dominated by planktic species, notably *Eucampia antarctica var. recta* and *Thalassiosira* species. The benthic marine species *Cocconeis fasciolata* is also present in high numbers at the base of the core. *Eucampia antarctica* var. *recta* often occurs adjacent to or beneath pack-ice (Fryxell and Prasad, 1990), and is generally associated with neritic (near-shore) environments, where floating ice is present and/or where significant melting leads to a meltwater-stratified water column (Cremer et al., 2003). The genus *Thalassiosira* is widespread in Antarctic waters and is associated with open water conditions (Taylor et al., 2001). *Thalassiosira antarctica* occurs commonly at sea-surface temperatures of between –2 to 1°C (Zielinski and Gersonde, 1997), and has been observed in newly formed platelet ice in polynas (Smetacek et al., 1992; Cunningham and Leventer, 1998) and in 'crack' pools formed by disintegrating ice during summer melting (Gleitz et al., 1996). Elsewhere, high abundances have been noted in sediments close to the front of the Ross Ice Shelf in association with the formation of platelet ice from super-cooled water masses that emerge from beneath ice shelf (Cunningham and Leventer, 1998). The benthic species *Cocconeis fasciolata* is also present in BZII. The ecology of *C. fasciolata* is largely unknown but has typically been found living in coastal-neritic environments in Antarctic waters (Frenguelli, 1943; Gilbert, 1991).

Together this diatom assemblage is indicative of a nearshore, marine environment associated with disintegrating ice. The assemblage also indicates the presence of a meltwater-stratified water column, which is consistent with the presence of a decaying ice shelf and large volumes of meltwater.

7.2.2.2. Foraminiferal assemblage

The foraminiferal assemblage in BZII is overwhelmingly dominated (>99%) by the calcareous benthic *Globocassidulina* spp., (*G. biora* and *G. subglobosa*). Overall, the assemblage present (both BZII and later in BZIV) is typical of continental shelf and slope environments (Murray, 1991). *Globocassidulina biora* is an infaunal, free-moving benthic foraminifera, which is typically found in Antarctic shallow waters with temperatures ranging from –1.95 to –1.14°C and salinities ranging from 33.96 to 34.99 ‰ (Crespin, 1960). It shows a strong association with high bottom current velocities (e.g. Mackensen et al., 1990) and has also been associated with coarse sediment substrate (e.g. Maxwell Bay, King George Island; Li et al., 2000). Similarly, *G. subglobosa* is an infaunal shelf species characteristic of sandy substrates on prominent submarine elevations that are influenced by strong bottom currents (Murray, 1991; Schmiedl et al., 1997). It has been documented in both shallow (0-100 m) and deeper waters (700-800 m) in the Ross Sea (Osterman and Kellogg, 1979). It forms part of the southern high productivity faunal assemblage described by Mackensen et al. (1993) between 55° and 49°S a zone that is influenced by lower Circumpolar Deep Water (LCDW) and Antarctic Bottom Water (AABW) (see Table 2.3 for water characteristics). It has also been found in association with *Bulimina aculeata* and *Fursenkoina* sp. (e.g. Domack et al., 1995) and appears to be related to Ross Sea Shelf Water (RSSW) in the Ross Sea (Osterman and Kellogg, 1979). RSSW is characteristically a saline (>34.7 ‰), oxygen-rich bottom water mass. Indeed *G. subglobosa* exhibits a significant positive correlation to dissolved oxygen content of water masses in the Southern Ocean (Schmiedl et al., 1997). In the Weddell Sea, *G. subglobosa* has been found in association with Fresh Shelf Water (<34.51 ‰, -1.89 to 1.5°C) to a depth of 550-700 m (Echols, 1971; Anderson 1975; Murray, 1991).

Cibicides lobatulus commonly occurs attached to a hard substrate (Nyholm, 1961; Loeblich and Tappan, 1964) and has been noted in surface samples on the continental margin in the Ross Sea between 100 and 400 m water depth (Osterman and Kellogg, 1979). In the Drake Passage *C. lobatulus* has been found in

association with strong currents and water temperatures ranging from 0 to –0.5°C (Jones and Pudsey, 1994). *Cibicides grossepunctatus* is an epifaunal species that is normally associated with hard substrates. It commonly occurs at 50-800 m water depths in the Weddell Sea (Anderson, 1975) and between 50 and 900 m in the Drake Passage (Herb, 1971).

The assemblage as a whole indicates open, relatively shallow, marine water conditions. Research elsewhere in Antarctica has shown that foraminiferal communities are not viable beneath ice shelves (Kellogg and Kellogg, 1988) as they require diatoms or other primary produces for food. In detail the assemblage is indicative of vigorous, well-oxygenated bottom currents, typical of an upwelling water mass (Murray, 1991). Vigorous ocean currents are also indicated by the faunal data and also the apparent size sorting (i.e. most tests in the assemblage are of similar size) in the *Globocassidulina* species (S. Ishman, pers. comm.). The assemblage also indicates a wide temperature range –1.95 to 1.5 °C, and high salinities (between 33.96 to 34.7 ‰).

7.2.2.3. Isotopic and Elemental data

Traditionally, the ratio of sedimentary carbon to nitrogen content has been used together with $\delta^{13}C_{org}$ to differentiate between marine and freshwater (or terrestrial) sources of organic matter (Macko et al., 1993; Meyers, 1994, 1997; Müller and Mathesius, 1999; Lamb et al., 2004). As a general rule, marine algae tend to yield lower C/N values (<8) (Bordovskiy, 1965; Thornton and McManus, 1994) and isotopically heavier $\delta^{13}C_{org}$ values when compared to freshwater algae (Meyers, 1997) (see Chapter 4). The C_{org}/N_{org} ratio reflects the amount of protein in organic matter, which is the most important nitrogen-containing component in living organisms (Müller, 1977; Müller and Voss, 1999b). Marine algae generally contain more protein than terrestrial or lacustrine algae (Owens, 1987; Meyers, 1994; Müller and Voss, 1999b; Westman and Hendenström, 2002), resulting in lower C/N values. The distinction between $\delta^{13}C_{org}$ in marine and lacustrine algae primarily relates to the way in which CO_2 is assimilated during photosynthesis. Photosynthesis in algae biochemically discriminates against ^{13}C to produce a shift

of ca. –20 ‰ from the isotope ratio of the inorganic carbon source. Freshwater algae utilises dissolved CO_2, which is often in equilibrium with the atmosphere (ca. –7 ‰), whilst marine algae uses marine bicarbonate, which has a $\delta^{13}C$ value of ca. 0 ‰. Thus typical values of $\delta^{13}C_{org}$ for freshwater plankton lie between –30 and –25 ‰, whereas marine plankton has $\delta^{13}C_{org}$ values between –20 and –25 ‰ (Meyers, 1997).

The isotopic and elemental data from BZII show a significant shift to higher C_{org} and N_{org} (Fig. 6.12 Chapter 6) values and sudden spike to lower $\delta^{13}C_{org}$ values. This change is interpreted as a result of the influx of marine algae following ice shelf absence. However, the absence of a well-defined $\delta^{13}C_{org}$ is surprising. It could suggest that majority of the material deposited during this period was locally derived (i.e. it has a similar $\delta^{13}C_{org}$ signature to surface sediments).

7.2.3. BZIII (489-303 cm): Ice Rafted Debris (IRD) phase

BZIII is characterised by the deposition of 1.87 m of coarse unsorted gravel (clasts > 8mm diameter) and is interpreted as a period of rapid sediment deposition within the marine embayment of ML (Fig. 7.1). The AMRE corrected foraminiferal dates from near the top of BZII (8100 ± 108 ^{14}C yr BP/8954 cal yr BP) unit and the base of BZIV (8105 ± 100 ^{14}C yr BP/8954 cal yr BP) are statistically indistinguishable confirming that BZIII was deposited very rapidly, perhaps as one, instantaneous ice rafted debris (IRD) dump. It is likely that the initial break-up of the ice shelf (BZII) would have generated large numbers of icebergs, and therefore melt-out and deposition of large amounts of coarse sediment as IRD in Moutonnée Lake (*cf.* conceptual model; Chapter 5). Unlike other Antarctic ice shelves, which are typically free of debris except near the grounding line (Drewry and Cooper, 1981; Powell, 1984) field observations (Pedley et al., 1988; and this study; see Chapter 4) have shown that coarse material is carried along englacial and supra-glacial pathways in (or on) George VI Ice Shelf. For example, Pedley et al. (1998) suggested that material is frozen onto the base of the ice shelf and is subsequently transported up through the ice shelf along well-defined flow lines. Initially this could not be reconciled with the very rapid basal melt rates of George VI Ice Shelf

(e.g. Potter and Paren, 1985), since any material entrained by the ice shelf would be quickly lost through basal melting. However, Pedley et al. (1988) provided evidence for localised areas of basal freezing (e.g. Hobbs Pool) where material is frozen onto the base of the ice shelf and gradually makes it way to the ice shelf surface. In addition, glacier ice leaving Palmer Land containing embedded rock debris will be first subjected to basal freezing, which would force material upwards followed by melting as it moves away from the coast and into George VI Sound (Bishop and Walton, 1981; Pedley et al., 1998). Material may also fall directly on the inflowing glaciers or ice shelf and is transported supra-glacially. These processes help to account for the presence of granite erratics on the present lake shorelines and in morainic ridges along the western margin of GVI-IS (Sugden and Clapperton, 1981; Pedley et al., 1988). Thus, break up of GVI-IS would release debris-bearing icebergs and as these melted within the basin this could account for the rapid deposition of IRD-sized material in BZII and BZIII.

In support of this interpretation, Gilbert and Domack (2003) have provided similar evidence based on the analysis of marine sediment cores from areas beneath the former Larsen-A and Prince Gustav ice shelves. They demonstrated that rates of sediment accumulation quadrupled several years prior to ice shelf disintegration, which they attributed to the draining of sediment-laden meltwater lakes and crevasses on the ice shelf surface followed by an influx of coarse gravel related to increased ice rafting during ice shelf disintegration (Gilbert and Domack, 2003).

The presence of icebergs in such a shallow bay needed to deposit substantial amounts of sediment requires further comment. At its deepest point Moutonnée Lake is presently ca. 55 m deep. It then shallows to ca. 35 m at the bedrock sill on which GVI-IS is grounded. This means that in the current configuration only relatively small icebergs could clear the bedrock sill and enter the lake. However, in the early Holocene, shortly after deglaciation it is likely that little isostatic recovery would have occurred following the unloading of the Last Glacial Maximum ice sheet over the AP. To the north (ca. 150 km) in Marguerite Bay, Bentley et al. (2005) have provided good evidence of 40-55 m of glacio-isostatic rebound since the early Holocene. In George VI Sound, where LGM ice thicknesses are thought to be even greater (e.g. Payne et al., 1989; Bentley et al., 1999), greater isostatic

depression is likely. Thus the sill could have been significantly deeper (ca. >80 m) at the time that the ice shelf was absent. A water depth of 80 m is very similar to the thickness of George VI Ice Shelf as it grounds along much of the west coast of Alexander Island (see Fig.3.2 Chapter 3). Thus many of the bergs from a disintegrating ice shelf would easily clear the bedrock sill and enter the lake basin. In addition, theoretical models suggest that icebergs tend to topple over during ice shelf absence, forming long elongate bergs (MacAyeal et al., 2003). This would also allow much larger bergs to enter the basin. It is also worth reiterating the likely rapidity of the dumping event: BZIII could have been deposited instantaneously, from one dump event, as evidenced by the lack of size sorting.

The absence of marine fauna and lack of a marine signature in the isotopic and elemental data in BZIII is also interesting, but perhaps not surprising. BZII (and certainly BZIV) are characterised by a marine fauna that indicate open marine conditions. Key to the argument regarding the dumping of ice-rafted material is the assumption that the embayment was dominated by marine water. At face value one might expect BZIII to contain some indication of open marine conditions, other than the presence of IRD. The absence of foraminifera and diatoms may reflect unfavourable environmental conditions or simply reflect the rapidity of deposition. The latter interpretation is favoured here since a large dump of what is likely to be terrestrially derived material is unlikely to contain marine foraminifera or marine diatoms. It is also possible that a freshwater surface layer, derived from large volumes of melted ice shelf ice and icebergs temporarily suppressed the marine signal (both biological and isotopic). Thus the surface waters of the basin would have been temporarily dominated in this period by meltwater produced from icebergs and freshly exposed glacier fronts along George VI Sound. This freshening effect has been measured at the base of melting ice shelves today (e.g. Potter and Paren, 1985). This hypothesis accounts for the absence of marine diatoms and foraminifera, since a meltwater-dominated environment would result in unfavourable conditions for marine biota and may also explain the absence of a marine isotopic signal. Thus it is most likely that BZIII represents an instantaneous dump (perhaps from one ice berg) of terrestrial derived debris.

The rapidity of deposition and its (likely) terrestrial source could also help to explain the absence of a marine $\delta^{13}C_{org}$ signal. It has already been shown in Chapter 5 that the $\delta^{13}C_{org}$ value of surface sediment in the modern day lake environment is likely to reflect the local sedimentary lithology. Whilst BZIII is composed of a wide range of lithologies, the *matrix* (from where material $\delta^{13}C_{org}$ is measured) is dominated by locally-derived sedimentary material. Thus in BZIII the $\delta^{13}C_{org}$ value reflects the character of the sediment, not the environment at the time of deposition.

One final scenario that needs to be considered is the possibility that BZIII represents a push of sediments as opposed to a dump. The environment at the time of deposition would have been unstable and high in energy. A grounded berg, ploughing over the bedrock sill may have pushed sediment from the ice shelf side of the lake over the core site. This would produce a large bulldozed diamicton corresponding to BZIII. However, if this were the case then one would expect to see traces of the reworked marine sediments (e.g. marine diatoms) and some degree of sediment sorting, which is not the case. Although this remains a possibility, it does not change the overall interpretation of ice shelf absence. What is important is that BZII and BZIV are separated from one another by a rapid/instantaneous depositional event.

7.2.4. BZIV (302-236 cm): Open marine conditions and ice shelf re-formation

BZIV is interpreted as a change from the high energy, IRD-dominated marine environment of BZIII to a more stable mode of sedimentation in an open marine embayment. It is characterised by a marine foraminiferal and diatom assemblage indicative of open water and proximal sea-ice and a clear shift from $\delta^{13}C_{org}$ values that reflect locally derived sediment in BZII and III to $\delta^{13}C_{org}$ values that are typical of marine algae. BZIV not only provides detailed evidence of the evolution of the marine phase but it also contains information about the processes and environment prior to the re-formation of the ice shelf.

7.2.4.1. Diatom Assemblage

Like BZII the diatom assemblage in BZIV is dominated by planktic species, notably *Chaetoceros* spores, *Eucampia antarctica var. recta* and *Thalassiosira species* (Fig. 7.2 and 6.1). In addition BZIV is characterised by the presence of sea-ice taxa (see Fig. 6.1 and 6.3). Total diatom abundance, notably of *Chaetoceros,* increases rapidly from the base of BZIV indicating a period of high productivity in an open marine embayment. *Chaetoceros* spores are widely regarded as an indicator of high primary productivity (Donegan and Schrader, 1972), but have also been connected with the presence of sea-ice (Leventer, 1992), with highest abundances occurring in water temperatures between –1 and 1°C (Zielinski and Gersonde, 1997). In the Palmer Deep, *Chaetoceros* resting spores have been associated with higher relative concentrations of other diatom taxa associated with sea-ice and sea-ice melt environments (Leventer et al., 2002) leading to the suggestion that melting sea-ice contributed to water column stratification, and thus the dominance of nutrient-depleting *Chaetoceros* blooms. This conclusion is also supported by sediment trap data, which shows that a high *Chaetoceros* resting spore flux is related to a nitrate-depleted, well-stratified water column (Leventer, 1991; Leventer et al., 1996). This is consistent with the idea that the water column in ML may have been stratified by meltwater during the deposition of this unit.

The base of BZIV is also characterised by small numbers of sea-ice taxa notably *Fragilariopsis curta* and *F. cylindrus*. *F. curta* often occurs where ice retreat has created a melt-water stratified surface water layer (Taylor et al., 2001). *Fragilariopsis cylindrus* has been observed amongst the dominant taxa in pack and fast ice (Garrison and Buck, 1989; Scott et al., 1994) and ice edge blooms (Kang and Fryxell, 1992), and has been also found in open water (Garrison et al., 1987; Leventer et al., 1993). The presence of *Fragilariopsis* species suggests that seasonal sea-ice was present near, or in Moutonnée Lake. It is unlikely that the sea-ice would have been perennial throughout the marine phase, since the presence of thick perennial sea-ice would act to suppress overall diatom productivity. For

example it has been shown in the Palmer Deep (e.g. Sjunneskog and Taylor, 2002), and elsewhere in Antarctica (e.g. Kaczmarska et al., 1993; Cremer et al., 2003; Whitehead et al., 2005) that thick sea-ice reduces diatom composition and abundance.

There is a significant decline in overall diatom abundance at 282 cm, (ca. 8840 cal yr BP) which implies a period of reduced productivity, perhaps cooling, related to increasing concentrations of fast or perennial sea-ice (Fig. 7.1). Absolute diatom abundance then briefly peaks at 276 cm (ca. 8775 cal yr BP). This phase is interpreted as a period of enhanced primary productivity and reduced sea-ice cover in ML. From ca. 270 cm (8705 cal yr BP) most diatom species decline almost disappearing entirely by 267 cm (8628 cal yr BP). Numbers of *Cocconeis* and other sea-ice related species (e.g. *E. antarctica*, *T. antarctica*) however persist until 236 cm (ca. 7946 cal yr BP) when diatoms disappear completely.

As a whole the diatom assemblage represents a highly productive marine water column in the initial phase of open-marine conditions between 300 cm (8958 cal yr BP) and 270 cm (8705 cal yr BP). Large amounts of ice-melt, both from icebergs and also catchment ice are likely to have resulted in a weakly stratified water column indicated by *Chaetoceros* and *F. curta*. The decline in productivity after 270 cm was could have been associated with the establishment of perennial sea-ice, and perhaps climatic cooling. This 'transition' phase between 270 cm (8705 cal yr BP) and 236 cm (ca. 7949 cal yr BP) is interpreted as representing the first signs of ice-shelf re-formation and the subsequent reversion of Moutonnée Lake to an epishelf lake.

7.2.4.2. Foraminiferal Assemblage

BZIV is characterised by a rapid increase in total foraminiferal abundance. Between 300 cm (8958 cal yr BP) and 270 cm (8705 cal yr BP) the assemblage is again dominated by *Globocassidulina* and *Cibicides* species indicative of an environment influenced by highly productive, oxygen-rich bottom waters (see BZII) (Mackensen et al., 1993). Like the diatom data, total foraminiferal abundances decrease rapidly at 270 cm suggesting a decrease in productivity and available food. The overall

decrease in foraminiferal abundance is coincident with increasing numbers of the minor component, *A. earlandi.* The ecology of *A. earlandi* (partly documented elsewhere as *Angulogerina angulosa* and *Trifarina angulosa*) is poorly known and thus the significance of this change is unclear. Where it has been documented, it tends to be associated with sandy and/or gravely substrate and strong bottom currents. It has been documented in relatively cold ocean water (–1.8 to 0.4 °C) with a salinity range between 34.43 and 34.72 ‰ (Mackensen et al., 1990). The increase in *A. earlandi* after 270 cm could suggest that it is more tolerant of low productivity conditions.

In terms of ocean water mass, the overall assemblage indicates that the early phase of ice shelf loss was characterised by a highly productive, saline deep-water mass that has a relatively wide temperature range (up to + 1.5 °C). The influence of this water mass then appears to decline at ca. 270 cm (8705 cal yr BP) when overall productivity declines. Cooler (?) and less productive marine water then persists in the basin until ca. 236 cm (ca. 7949 cal yr BP).

7.2.4.3. Isotopic and Elemental Data

BZIV is characterised by a rapid change to higher $\delta^{13}C_{org}$ values, lower C/N values and high C_{org} and N_{org} values (Fig. 7.1 and Fig. 6.12). The change in $\delta^{13}C_{org}$ and C/N strongly suggests a renewed dominance of marine water and subsequent deposition of nitrogen-rich marine algae following ice shelf loss. This mode of sedimentation dominates the core ca. 262 cm (ca. 8552 cal yrs BP), when $\delta^{13}C_{org}$, $\%C_{org}$ and N_{org} values decline rapidly. This is coincident with an overall decline in diatom and foraminiferal abundance and is consistent with the idea that this could represent the first signs of re-isolation of the epishelf lake in response to ice shelf re-formation. Interestingly the C/N ratio continues to be low beyond this depth, which might be interpreted as marine water existed in the basin until 236 cm (ca. 7949 cal yr BP). Alternatively it could simply reflect the persistence of a marine signal from a lower marine water layer once the basin became re-isolated as an epishelf lake.

7.2.4.4. Quantification of the marine environment

The data presented thus far suggests that Moutonnée Lake was characterised by high biological productivity in an open marine basin when BZIV was deposited. Marine productivity began to decline sometime between 270 and 262 cm (ca. 8705-8552 cal yr BP), perhaps in response to the re-isolation of the epishelf lake as the ice shelf reformed or in response to climatic cooling and/or increased sea-ice (or both). In addition, the foraminiferal data also implies a possible change in ocean water mass after ca. 270 cm (8705 cal yr BP). A more detailed quantification of the marine environment is required before these links can be further tested. The next section will therefore attempt to use semi-quantitative methods to investigate the marine environment during ice shelf loss and specifically addresses the following questions: (1) in what way did the environment change prior to the decline in $\delta^{13}C_{org}$ values, foraminifera and diatoms, and (2) can the presence of a specific ocean water mass/temperature (e.g. UCDW) be detected isotopically using foraminiferal calcite?

7.2.4.5. Quantifying sea-ice

Although the presence or absence of sea-ice related taxa provides evidence for the presence of sea-ice, several studies have sought to quantify the sea-ice-diatom relationships through the use of the 'Eucampia Index' (e.g. Kaczmarska et al., 1993; Leventer et al., 2003; Whitehead et al., 2005). Fryxell and Prasad (1990) identified two varieties of *Eucampia antarctica*, a 'southern' and a 'northern'. The southern variety, *Eucampia antarctica var. recta* is typically symmetric in broad girdle view whilst the northern form *Eucampia antarctica var. antarctica* is asymmetrical (Plate 1) (Fryxell, 1989; Fryxell and Prasad, 1990). In addition to these morphological criteria, the northern form is more likely to form longer chains than the southern variety. Fryxell and Prasad (1990) suggested that the northern form generally occurs in areas of less severe or thinner sea-ice allowing more cell division, leading to longer chains. In contrast the southern (or polar) form of *E. antarctica var. antarctica* occurs more often as short chains and doublets (Fryxell, 1989; Fryxell and Prasad, 1990). In the sedimentary record, chain length can be estimated by comparing the proportion of 'pointy' terminal valves (from the chain ends) to the

flat 'intercalary' valves (from the middle of the chain). The relationship between environmental conditions and chain length led Kaczmarska et al. (1990) to develop the Eucampia Index, to record oscillations in late-Pleistocene sea-ice on the Kerguelen Plateau. The Eucampia Index is the ratio of terminal to intercalary valves (Kaczmarska et al., 1993) (see Figure 1; Kaczmarska et al., 1993). In theory, warmer waters with less sea-ice should be characterised by more intercalary valves (i.e. lower Eucampia Index), since the northern form is likely to be dominant.

In this study the diatom assemblage is exclusively dominated by the southern form, *E. antarctica var. recta*. Although, the Eucampia index has traditionally been used to assess the relative importance of *E. antarctica var. recta* versus *E. antarctica var. antarctica*, and hence polar or sub-polar conditions (e.g. Kaczmarska et al., 1993; Leventer et al., 2003; Whitehead et al., 2005), it is still valid to use the Eucampia index as a proxy for sea-ice when dealing with a purely southern, polar assemblage (i.e. one dominated by *E. antarctica var. recta*) (e.g. Whitehead et al., 2005). This is because chain length is still a function of light availability and thus can be used as a proxy for the presence/absence or persistence of sea-ice (Fryxell and Prasad, 1990; Whitehead et al., 2005).

Figure 7.2 shows downcore variations in the Eucampia index for BZII & IV. These data clearly show that terminal valves (i.e. > sea-ice) were dominant in two phases, with the first occurring between 300 and 292 cm and the second between 267-276 cm. In contrast between 292 and 276 cm intercalary valves dominate the assemblage. This implies that sea-ice (or sea-ice related) conditions were characteristic of the early phase of ice shelf absence, followed by more open marine conditions, which coincides with a phase of maximum productivity observed in the diatom, foraminiferal and $\delta^{13}C_{org}$ data. The second peak in sea-ice (267-276 cm) occurs prior to the overall decline in diatom and foraminiferal abundance and could represent climatic cooling as perennial sea-ice becomes established and the ice shelf begins to reform.

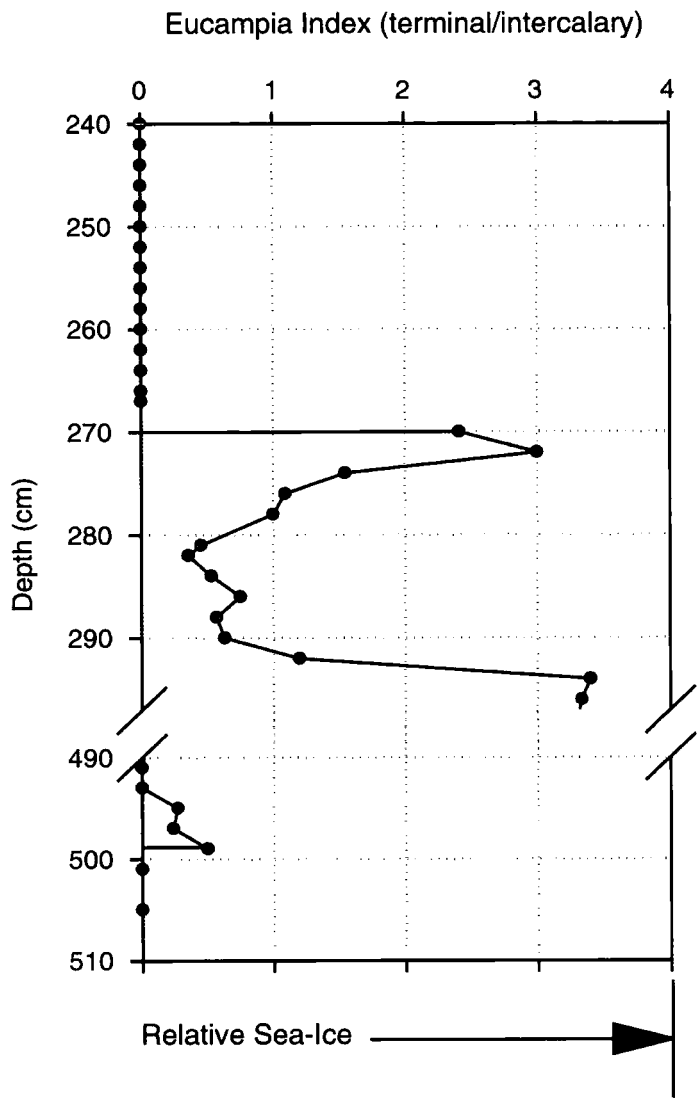

Figure 7.2. Distribution of terminal/intercalary valves of *Eucampia antarctica var. antarctica* in the marine zones (BZII and BZIV) in the ML core. High values indicate higher sea-ice cover.

7.2.4.6. Quantifying ocean water mass and temperature

One of the key questions that has arisen from this study is whether changes in ocean circulation influenced the early Holocene decay of GVI-IS through enhanced basal melting. The next section will use the $\delta^{18}O_{foram}$ and $\delta^{13}C_{foram}$ dataset from BZIV to examine this question further. This section has two main objectives: (1) can the foram-isotope data from ML be used to define the presence of specific water masses?, and (2) what can the foram-isotope data tell us about the transition from open marine conditions to re-isolation of the basin?

Section 4.4.4.4 (Chapter 4) reviewed the important factors, which control the isotope signature of benthic foraminifera. Generally, the $\delta^{18}O$ composition of benthic foraminiferal calcite is principally controlled by: (1) water temperature variations (ca. 1°C temperature change leads to a 0.23‰ shift in $\delta^{18}O$; Shackleton, 1974); (2) salinity (ca. 1‰ salinity change leads to a 0.61 ‰ shift in $\delta^{18}O$ (Craig and Gordon, 1965); and (3) global ice-volume (maximum glaciation leads to ca. 1.2‰ shift in $\delta^{18}O$; Chappell, 1996), whilst the $\delta^{13}C$ composition of benthic foraminifera is fundamentally controlled by (1) nutrient concentrations and (2) changes in deep-sea circulation (Grossman et al., 1984b; Duplessy et al., 1984).

Overall the carbon and oxygen isotope data presented in Chapter 6 from Moutonnée Lake (both ML and MLNB cores) is characterised by small and variable changes and do not appear to show any consistent pattern. However, one notable exception in the $\delta^{18}O_{cibicides}$ data set is the significant enrichment (+0.8 ‰) in $\delta^{18}O_{cibicides}$ starting at 264 cm in the ML core (Fig. 6.15, Chapter 6). A similar isotopic trend is also observed in the MLNB core, although the magnitude of change is not as large (+0.3 ‰) (Fig. 6.17, Chapter 6). The increase in $\delta^{18}O_{cibicdes}$ in the ML core coincides with a decrease in $\delta^{13}C_{org}$ values, absolute diatom and foraminiferal abundance and also important faunal changes in the foraminiferal data (e.g. increase in *A. earlandi*) (Fig.7.1).

Changes in ocean temperature and global ice volume are generally considered to exert the greatest influence on the isotope composition of benthic foraminifera,

although the 'salinity effect' and input of glacial water enriched in ^{18}O must also be considered (Rohling and Cooke, 1999; Schmidt, 1999). The effect of global ice volume can be immediately ruled out given the short (Holocene) time interval represented here. Thus if we assume that changes in $\delta^{18}O$ of foraminiferal carbonate are solely a function of temperature, then Shackleton's (1974) expression can be used to estimate changes in water temperature (data used is shown in Table 6.1):

$$\text{Temp (°C)} = 16.5 - 4.80*(\delta^{18}O_{carbonate} - \delta^{18}O_{water}) + 0.1*(\delta^{18}O_{carbonate} - \delta^{18}O_{water})^2$$

This equation gives a maximum temperature range of ca. 2.9 °C in ML and indicates that on a relative scale water temperature generally cooled towards the top of BZIV (Fig. 7.3). The major change in temperature occurs at ca. 266 cm (ca. 8628 cal yr BP). Such a large shift in water temperature seems unlikely over such a short period of time (ca.1000 yrs). However, a similar temperature and isotopic gradient has been recorded beneath the present George VI Ice Shelf (Potter and Paren, 1985) raising the possibility that the foraminiferal-$\delta^{18}O$ profile records a significant transition from relatively warm ocean water at the base of BZ II and IV to relatively cold ocean water consistent with the increase in perennial sea-ice between 267-276 cm. Essentially, the water below the present George VI Ice Shelf can be partitioned into two distinct water masses, which are separated by a transitional water mass on the basis of their isotopic and temperature characteristics (section 7.4). Super-cooled Ice Shelf Water (ISW) occurs directly beneath the ice shelf to a depth of ca. 45 m, and is characterised by temperature (-1.8 to -1.5 °C) and isotopic (-0.9 to -0.4 ‰) minima. In contrast below ca. 400 m relatively warm (+0.5 to 1 °C) isotopically distinct (+0-0.13 ‰) Upper Circumpolar Deep Water occurs. The water between ca. 45 and 400 m represents a mixture of ice shelf water and UCDW becoming warmer and isotopically heavier with depth (Fig. 7.4). ISW and UCDW thus have distinct temperature-salinity and $\delta^{18}O$ characteristics, with a maximum isotopic and temperature range of 1.0 ‰ and 2.8 °C respectively between ice shelf water and UCDW. These isotope and temperature ranges are remarkably similar to the recorded isotope profile and the calculated temperature change presented above. This could suggest that UCDW dominated the early phase of ice shelf absence and

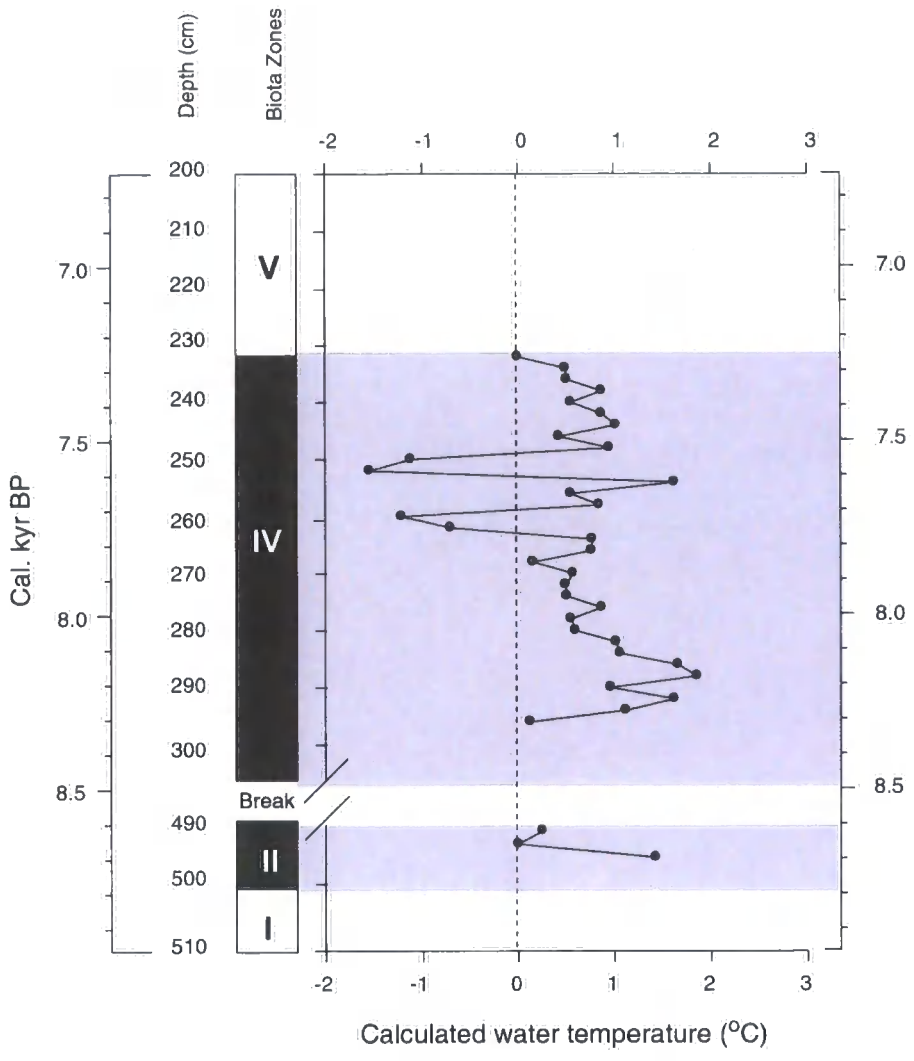

Figure 7.3. Reconstructed water temperature for BZ II and IV in the ML Core (*Cibicides* sp.) using the equation from Shackleton (1974). The equation was calculated using the $\delta^{18}O$ foraminiferal data in Table 6.1 and uses a $\delta^{18}O$ water value of -0.03 per mil (Potter and Paren, 1985).

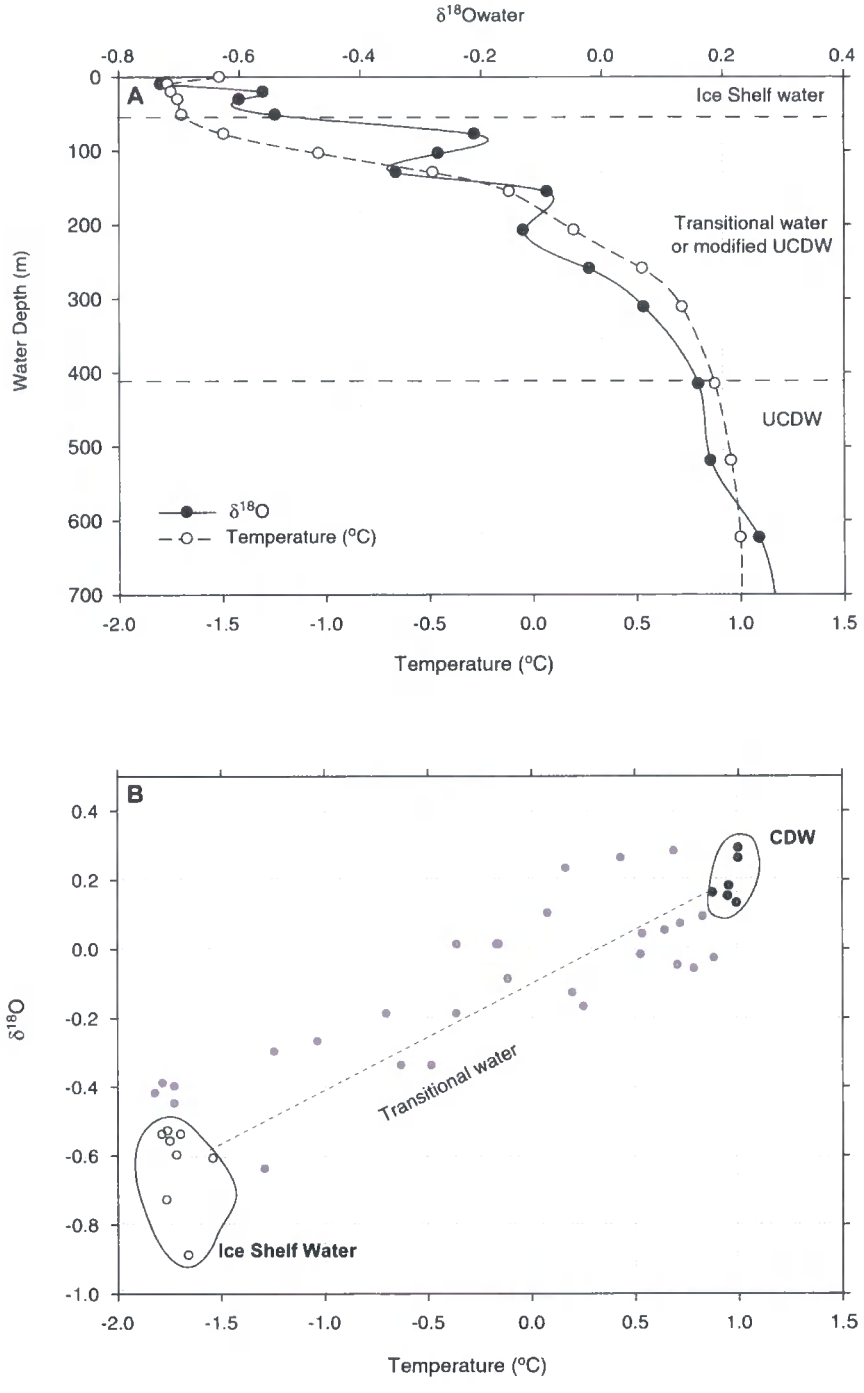

Figure 7.4. (a) Depth-temperature/$\delta^{18}O$ water profiles from the northern margin of George VI Ice Shelf showing the transition from unmodified ice shelf melt water directly below the ice shelf (above ca. 45 m) to Upper Circumpolar Deep Water (UCDW) (below ca. 400m). The water between these depths represents a mixture between ice shelf melt and UCDW. (b) The same data shown as a $\delta^{18}O$-temperature plot (data from Potter and Paren, 1985). The data shows a maximum isotopic shift from ice shelf water to UCDW of ca. 1.02 ‰ and a maximum temperature shift of ca. 2.8 °C.

was gradually replaced by cooler ice shelf water. As such this data is consistent with the idea that intrusions of warm UCDW played an important role in the absence of the ice shelf, through enhanced bottom melting and also in promoting increased marine productivity. It is also realistic to assume that eventually the UCDW isotopic signal would be diluted/replaced by large volumes of cooler, isotopically light meltwater, both from the melting ice shelf and local valley glaciers.

One argument against a change from UCDW to an environment dominated by ISW or local meltwater however is the overall structure of the $\delta^{13}C_{cibicides}$ profile, which shows no indication of a change in water mass characteristics. Not only is UCDW defined by temperature and salinity maxima, it is also considered to be nutrient-rich (Hofmann et al., 1996). Thus, one would expect a corresponding shift in the $\delta^{13}C_{cibicides}$ profiles, which is not seen. Furthermore, the isotopic profile obtained from the *Globocassidulina* species does not yield a comparable pattern. However, this can be explained by the different ecologies of the two species. *Cibicides* is an epifaunal species, which generally lives directly above the sediment-water interface, whilst *Globocassidulina* is an infaunal species living within the sediment. As a result, epifaunal species generally provide a more reliable record of changing water types since infaunal species can be more influenced by the nature of the sediment in which they live (Murray, 1991).

In addition to these factors, unpublished data from a marine core site in Marguerite Bay (Pope, 1991) suggests that the isotopic signature of UCDW as recorded in *Cibicides* species is unlike that obtained from ML. Pope (1991) obtained $\delta^{18}O_{cibicicdes}$ and $\delta^{13}C_{cibicides}$ values of between 3.8 to 4.5 ‰ and –0.2 to 1.2 ‰ respectively for Holocene age sediments (Pope, 1991). This compares with a range of 3.4 to 4.1 ‰ for $\delta^{18}O$ and from 0.9 to 1.5 ‰ for $\delta^{13}C$ for ML (Fig.7.5). Significantly, the core site in Marguerite Bay is currently bathed in UCDW and according to Pope (1991) probably has been during the Holocene. Working on the assumption that the Pope's (1991) foraminiferal isotopes data can be taken as a isotopic fingerprint for UCDW on the west coast of the AP then it suggests that if UCDW was present in/or near ML then its isotopic signature was slightly diluted. This could occur through the addition of large volumes of fresh meltwater, which is

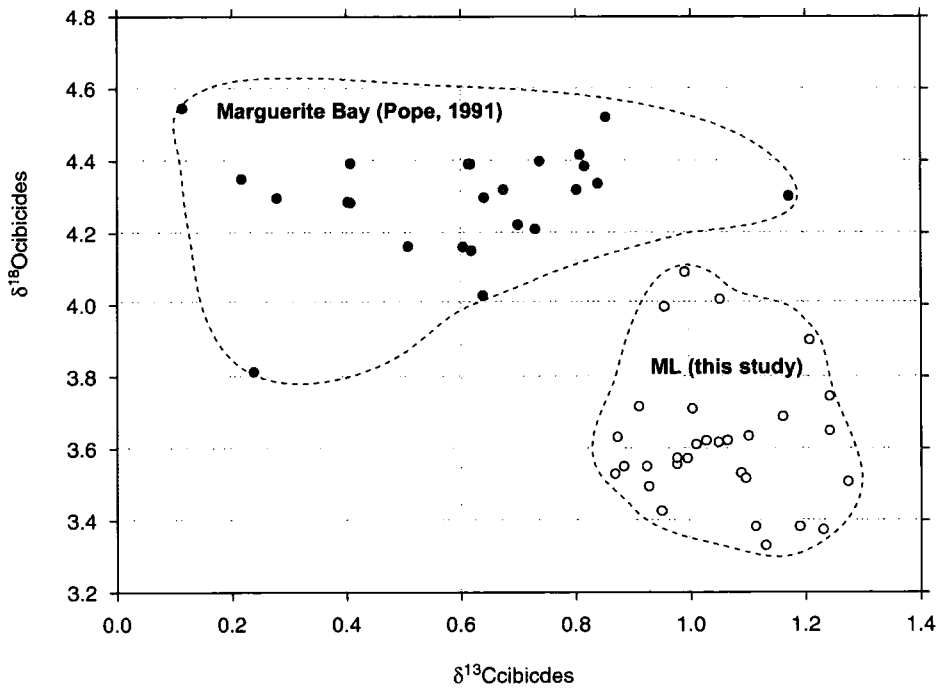

Figure 7.5. $\delta^{18}O$ versus $\delta^{13}C$ cross plot showing the isotope fields for *Cibicides* species from Marguerite Bay (Pope, 1991) and Moutonnée Lake (this study). The samples from Marguerite Bay were taken from a core site that is presently bathed in Upper Circumpolar Deep Water (UCDW) and used in this study to represent the isotope characteristics of UCDW.

generally isotopically lighter. For example, it is likely that the *Cibicides* species analysed by Pope (1991) survived at much greater water depths (the core site was at >700 m water depth) compared to the shells deposited in ML, which are likely to have survived either at the core site (50-80 m water depth) or on the shallow continental slope (<200). As such, the isotopic signature of foraminifera in ML would have been more readily influenced by meltwater than the Marguerite Bay samples, potentially modifying the isotopic signature. This could suggest that the $\delta^{18}O$ values from Marguerite Bay provide a more representative isotopic signature for UCDW, whilst the values taken to represent UCDW from ML are slightly modified by freshwater.

A further complication with a purely temperature-related interpretation is the possibility that several other environmental factors, notably changes in salinity and the addition of older ice shelf meltwater enriched in ^{18}O may have influenced the $\delta^{18}O_{cibicides}$ signature. For example, the water within and proximal to the ML embayment is likely to have experienced significant and rapid changes in salinity caused by the initial influx of marine water followed by the influx of large volumes of relatively fresh glacier and ice shelf meltwater. Generally changes in surface water conditions have little impact on benthic foraminifera in deep-sea sediments. *Cibicides* species however are known to survive at relatively shallow depths (<100 m) on the continental slope (Osterman and Kellogg, 1979) and as such, are more likely to be influenced by surface waters, especially if they are well mixed. Based on what is known about palaeosalinity calculations (e.g. Schmidt, 1999; Rohling, 1999) the $\delta^{18}O_{cibicides}$ record from ML shows a trend to more saline water conditions. This appears to be inconsistent however with other proxy data, which shows a gradual decline in the marine signal probably in response to the re-isolation of the basin and the renewed dominance of freshwater. Finally, in addition to changes in salinity, melting of (old) glacier and ice shelf ice may have contributed water that was enriched in ^{18}O (Charles and Fairbanks, 1990) leading to changes in the $\delta^{18}O_{cibicides}$ signal. However this relationship is difficult to quantify. Certainly the $\delta^{18}O$ profile becomes heavier towards the top of BZIV, which could suggest an input of ^{18}O rich water as the ice shelf melted.

In summary it remains difficult to precisely unravel the factors that have contributed to the observed changed in $\delta^{18}O_{cibicides}$. The present data suggests that the dominant factor controlling the $\delta^{18}O_{cibicides}$ records appears to have been water temperature. If water temperature change is the dominant factor then this equates to a ca. -2.9°C cooling in water temperature, which is almost identical to the observed temperature gradient between ISW directly beneath George VI Shelf and warmer UCDW. This could imply that UCDW was influential in the initial decay of George VI Ice Shelf and was gradually replaced by cooler, isotopically lighter ISW. This pattern is consistent with other proxy data, which shows a decline in marine productivity at ca. 270 cm and renewed dominance of freshwater possibly in response to the re-isolation of the epishelf lake as the ice shelf reformed. A change in water mass above 270 cm (8705 cal yr BP) is also indicated by the foraminiferal data which indicates a change from highly productive, saline water (e.g. UCDW) to less productive (cooler?) ocean water.

7.2.5. Lift-off/ advection hypothesis

One alternative scenario to ice shelf absence that needs to be explored is the possibility that the marine biological and isotopic signal recorded in BZII and BZIV is not the result of *in-situ* production during ice shelf absence, but instead results from advection of hemipelagic sediment from beneath the ice shelf. This scenario would require some kind of 'lifting off' of the ice shelf from the sill to enable larger quantities of water to enter the basin and also relies on the assumption that diatom and foraminifera communities exist (or are advected) beneath the ice shelf. It is commonly accepted, however, that phytoplankton communities are not viable beneath ice shelves because they need light for photosynthesis (Kellogg and Kellogg, 1986, 1987, 1988). Similarly foraminifera should also be absent because they require diatoms or other primary producers as food (Kellogg and Kellogg, 1988). It is possible however, that diatoms could have been advected in by ocean currents from areas of open water, although similar data has not been presented for foraminifera. Recently Hemer and Harris (2003) have suggested that *some* marine diatoms (e.g. *T. antarctica*) in sediments beneath the Amery Ice Shelf are likely to have been advected in by sub-ice shelf currents from the ice-free areas of Prydz

Bay; some 80 km away. Their study also implies that advection of diatoms may be species specific, since they later use the presence of sea-ice taxa (*F. curta* and *F. cylindrus*) from the same cores to suggest that the ice shelf must have retreated.

The Ablation Point Massif lies 100 km (northwards) and 334 km (southwards) from the open sea and thus it is possible that open-marine diatoms may have been advected from Marguerite Bay to the north. However, measurements have shown that currents beneath George VI Ice Shelf are extremely weak, except at the western margin of the northern ice front where a northward-flowing jet (i.e. *away* from the Ablation Point massif) of UCDW is present (Potter and Paren, 1985) and are thus unlikely to transport large quantities of hemipelagic sediments. Based on present data and without further field measurements however, this relationship cannot be quantified.

The strongest argument against the advection of large quantities of diatoms into Moutonnée and Ablation Lakes comes from the modern day lake data set and also the multi-proxy nature of this study. Firstly, despite Ablation Lake currently being an open system, which is able to exchange freely with water beneath George VI Ice Shelf (Heywood, 1977), no similar marine diatom assemblage is currently advected into the basin. The only marine diatoms found in Ablation Lake surface sediments are *Diploneis sp.*, and *T. antarctica*. Whilst the latter forms an important component of the BZIV assemblage, *Diploneis* species are entirely absent in core sediments. In addition, counts of *T. antarctica* are generally much lower in the Ablation Lake surface sediments, with a maximum abundance of 2,340 valves g^{-1}. This compares to a maximum of 11,500 valves g^{-1} in the ML core and suggests that advection is unlikely to account for the diatom assemblage in BZIV. The presence of *any* marine diatoms in surface sediments in AB and ML however, is difficult to reconcile without invoking some kind of advection. It is interesting to note that Hemer and Harris, (2003) use the presence of *T. antarctica* to argue for advection beneath the Amery Ice Shelf (also present in AB surface sediments). They note that past studies of diatom sinking rates have shown that *T. antarctica* is associated with lateral advection (e.g. Leventer and Dunbar, 1996; Cremer, 1999). They go on to suggest that *T. antarctica* may be better preserved on its path beneath the ice shelf because it is heavily silicified (Hemer and Harris, 2003). The *Diploneis sp.*, identified in this

study is also heavily silicified (see Plate 1). This implies that *some* advection of hemipelagic sediment is taking place beneath GVI-IS, but it is restricted to certain heavily silicified taxa. Secondly, the advection hypothesis cannot explain the occurrence of a full and varied diatom assemblage in sharply defined intervals (BZII and BZIV), at precisely the same time as major isotopic changes in $\delta^{13}C_{org}$ (related to *in situ* productivity), and parallel changes in several other proxies (e.g. foraminifera). Furthermore, the diatom evidence of an open water environment being replaced by sea-ice taxa as the ice shelf reformed is difficult to explain in terms of changing currents or advection (why would the species composition change?). Thus, a more robust interpretation is that the diatom assemblage reflects *in situ* productivity in Moutonnée Lake and the immediate region.

7.2.6. Evidence for ice shelf re-formation

Figure 7.6 shows the key palaeoenvironmental data from BZII and BZIV and allows the reconstruction of the environmental conditions prior to ice shelf re-formation. A consistent pattern within the data set is a reduction in a marine signal from ca. 270-cm (ca. 8705 cal yr BP). $\delta^{13}C_{org}$ values, for example, decrease to the more negative values similar to values found in modern day surface sediments. Significantly, the decline in marine fauna and the marine geochemical signal coincide with increasing levels of sea-ice inferred from the ratio of terminal to intercalary *Eucampia* valves and decreasing water temperature, possibly due to the dominance of cooler ISW. During this time interval atmospheric temperature inferred from the EPICA ice core (Masson-Delmotte et al., 2004) and Byrd ice core reveal a modest temperature rise (Fig.7.6). This slight temperature rise is however superimposed upon a longer term cooling trend following the early Holocene climatic optimum (Fig. 2.14 and 2.15 Chapter 2). Excluding the ice core data these data imply that marine productivity and/or the influence of marine water began to decline at 270 cm (ca. 8705 cal yr BP) disappearing entirely by 236 cm (ca.7950 cal yr BP). This suggests that the connection between the marine water in George VI Sound and the lake basin started to close at ca. 8705 cal yr BP cm becoming impounded completely by 7950 cal yr BP. For this to occur grounded ice must have been present on the bedrock sill. In other words the ice shelf must have reformed sufficiently to impound a standing

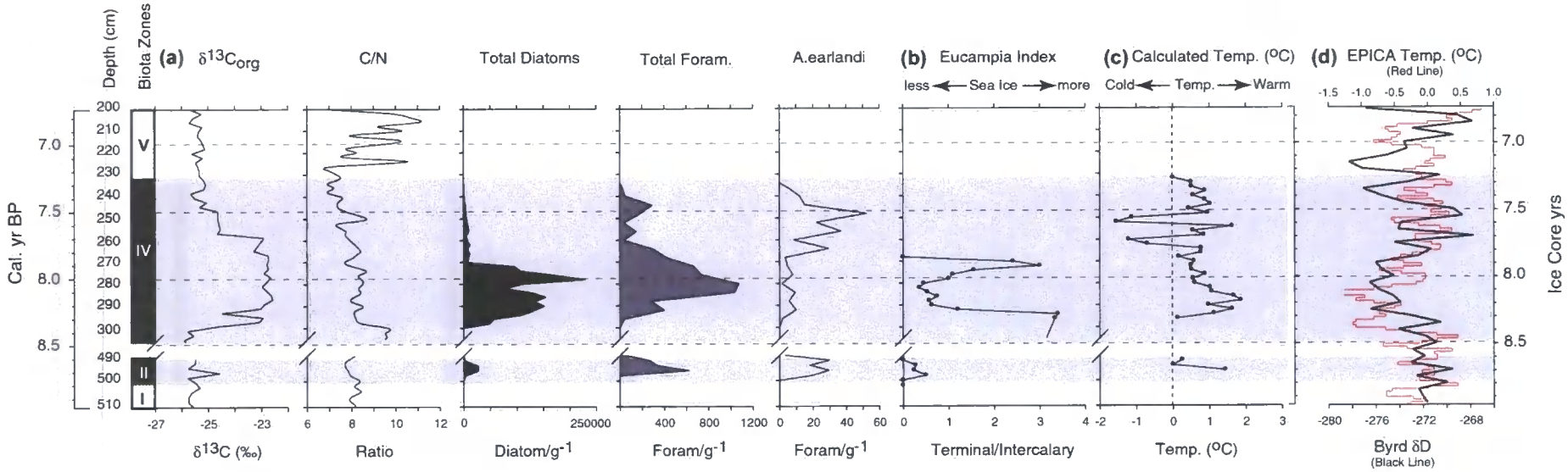

Figure 7.6. BZII and BZIV (grey shading) from Moutonnée Lake plotted against calibrated ^{14}C age using the age-depth model presented in Figure 7.1. The diagram shows **(a)** $\delta^{13}C_{org}$, C/N and key biological data; **(b)** relative sea-ice (Eucampia Index), calculated from the ratio of terminal valves to intercalary valves (after Kaczmarska et al., 1993); **(c)** relative water temperature infered from the benthic foraminfera (*Cibicides* sp.) using the equation from Shackleton (1974). The equation was calculated using the $\delta^{18}O$ foraminiferal data in Table 6.1 and uses a $\delta^{18}O$ water value of -0.03 per mil (Potter and Paren, 1985); **(d)** atmospheric temperature annomaly data from the EPICA ice core (Masson-Delmotte et al., 2004) together with Byrd δD profile (data from Hammer et al., 1994). Bryd δD data are corrected for elevation using 2.5‰ /1000 yr correction of Masson et al. (2000). Horizontal dashed line to show every 500 yrs.

body of freshwater, perhaps in response to the period of sustained climatic cooling recorded in several Antarctic ice cores (Fig. 2.14 and 2.15). It remains unclear however whether this data indicates full or partial re-formation of the ice shelf since the lake sediments provide no direct evidence for the geographical extent of the ice shelf at this time.

7.2.7. BZV (235-0 cm): Ice shelf presence phase

The upper most zone of the ML core (BZI) is interpreted here as a change back to a freshwater-dominated environment following the re-formation of the George VI Ice Shelf no later than ca. 7950 cal yr BP. In contrast to the $\delta^{13}C_{org}$ profile, which appears relatively stable, the C/N profile shows a significant degree of variability and is accompanied by changes in other physical parameters, notably %LOI, $\%CaCO_3$, MS and grain-size (Fig. 7.7). Assuming that the age-model for ML is broadly accurate, then BZV represents one of the longest lacustrine sequences on the AP and potentially offers a unique opportunity to study Holocene climatic change.

Following BZIV, C_{org} and N_{org} values continue to decline. The C/N profile then increases rapidly from 226 cm (ca. 7600 cal yr BP) reaching a core maximum of 12.3 at 176 cm depth (ca. 5900 cal yrs BP) before declining, then increasing to a secondary peak of 9.9 at 102 cm depth (ca. 3400 cal yrs BP). Both peaks (hereafter referred to peaks A and B; Fig.7.7) are associated with more negative $\delta^{13}C_{org}$ values and higher C_{org} values. From 76 cm (or ca. 2550 cal yrs BP) C/N values increase steadily.

In Chapter 4 the factors which control the Carbon and Nitrogen signature in lacustrine sediments were reviewed. Traditionally, total organic carbon (TOC equivalent to C_{org}) has been used as a proxy for productivity (e.g. Domack et al., 1993; Melles et al., 1997; Vilinski and Domack, 1998; Kulbe et al., 2001; McMinn et al., 2001), whilst C/N and $\delta^{13}C_{org}$ have been used to investigate carbon sources (Meyers, 1994, 1997; Mueller and Voss, 1999; Talbot and Laerdal, 2000; Lamb et al., 2004). It has already been speculated in Chapter 5 that changes in C_{org} and N_{org}

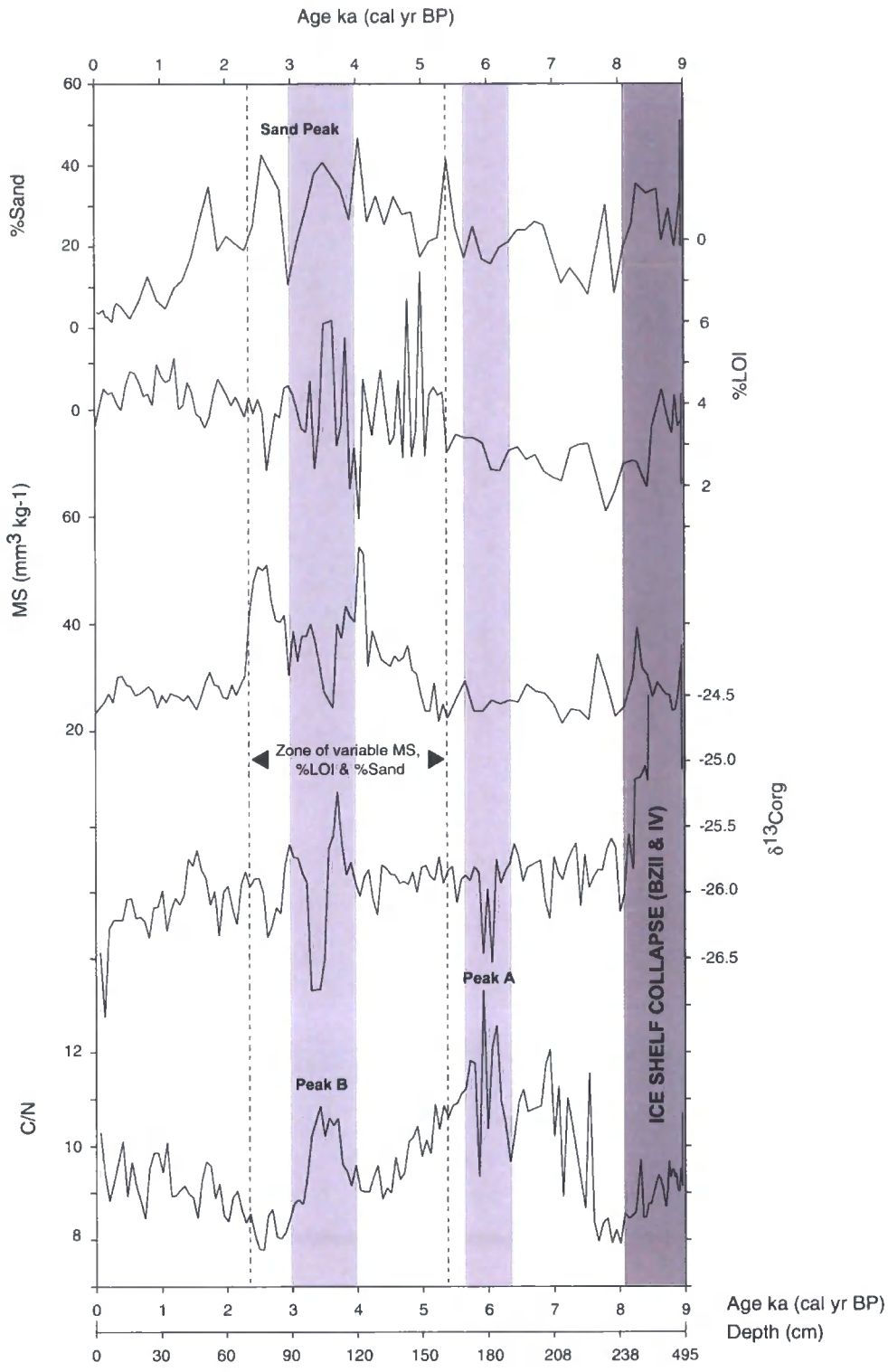

Figure 7.7. Key palaeo-environmental data from ML plotted against age (cal yr BP). C/N peaks A and B are highlighed in light grey and collapse of George VI Ice Shelf (BZII-IV) highlighted in dark grey. Age scale for this zone (BZV) is linear between the end of BZIV which is dated and the sediment-water interface which is assumed to be 0 ka BP.

content of surface sediments are likely to be controlled either directly by changes in lake productivity and/or indirectly by the rate of supply of nutrient-bearing meltwater streams (Chapter 5). Thus the major peaks in the C/N profile in the ML core are likely to reflect one or both of these scenarios.

Scenario 1: In Scenario 1 the C/N peaks and lower $\delta^{13}C_{org}$ values reflect changes in the supply of terrestrially derived C and N (e.g. increased precipitation). It has been shown from reference data in Chapter 5 that catchment benthos and cyanobacteria, in general, have higher C/N values (Fig. 5.14 Chapter 5). Thus, an increase in the flux of material entering ML caused by increased melting due to climatic warming or increased precipitation would result in a relative increase in carbon-rich organic material. This would lead to higher C/N values. However, the $\delta^{13}C$ of surface sediments in ML suggest that streams feeding ML are enriched in $^{13}C_{org}$, with samples nearest the lake shoreline yielding the heaviest $\delta^{13}C_{org}$ values (ca. -14 to -20 ‰). In other words material entering the lake from the catchment generally has high C/N values but higher $\delta^{13}C_{org}$ values. However, not all reference samples from the lake catchment yielded such high $\delta^{13}C_{org}$ values. Cluster group 1 (Figure 5.9 Chapter 5) for example has high C/N values and relatively low $\delta^{13}C_{org}$.

Scenario 2: In Scenario 2, the C/N peaks and low $\delta^{13}C_{org}$ values represent a period of enhanced lake productivity and the presence of an extensive littoral moat in summer owing to favourable climatic conditions (e.g. warming). Several studies have shown that increased C_{org} (leading to elevated C/N ratio) can be used as a reliable proxy for lake productivity (e.g. Melles et al., 1997; McMinn, 2001; Kulbe et al., 2001; Lamb et al., 2004). In addition, the $\delta^{13}C_{org}$ values (-26.2 ‰) are in the range commonly associated with lake algae and are lower than the core mean (ca. –25 ‰). Thus, peaks A and B could be explained by a period of enhanced lake productivity. However this scenario is complicated by the fact that increased productivity can also lead to elevated N_{org} values.

From a palaeoclimatological perspective it is likely that both scenarios reflect a warmer climate. Station records show that the recent regional warming on the Antarctic Peninsula has been accompanied by increased precipitation (Turner et al.,

1997). Thus it seems reasonable to assume that increased precipitation in the past was associated with warmer conditions. In addition, the flux of meltwater entering the lake would increase during periods of warming.

The MS, LOI and $CaCO_3$ profiles also show a high degree of variability between ca. 158 – 58 cm (ca. 5320 to 2150 cal yrs BP) (Fig. 7.7). This interval is also associated with increasing sand and gravel content, probably associated with an increase in mineral sedimentation rate. Together this would suggest that the lake catchment experienced some form of instability (e.g. pronounced seasonality) during this period. LOI, MS and $CaCO_3$ values then stabilize and remain stable through to the top of the core. Sand and gravel concentrations decrease, suggesting a change in sedimentation, perhaps related to reduced flux of coarser material under drier/cooler conditions. From this data it is apparent that C/N peak B was associated with a different suite of environmental indicators compared with C/N peak A. Generally peak A is associated with stable %LOI, MS, but higher C_{org} (Figure 6.12 Chapter 6) and reduced % sand values, whilst B is characterised by variable MS, LOI and high %Sand concentrations. Increased sand levels suggest greater minerogenic sedimentation, possibly associated with wetter conditions as sediment is transported into the lake from the surrounding catchment. Greater minerogenic sedimentation is also supported by the MS data. Magnetic susceptibility has long been used as a physical sedimentary proxy for variable biogenic and minerogenic sediment supply. Elsewhere in Antarctica, MS has been used as a regional proxy for changes in biogenic productivity (Leventer et al., 1996; Kirby et al., 1998; Brachfeld et al., 2000; Domack et al., 2001). Generally low magnetic signals have been interpreted as periods of high productivity when biogenic sedimentation is greater than minerogenic sedimentation. This is consistent with C/N peak B that shows a period of increased biogenic sedimentation is associated with low MS values. Together this data indicate that C/N peak B was associated with a period of increased sedimentation, which alternated between biogenic and minerogenic sources. As such, peak B compares more closely to scenario 2 and indicates a period of warmer/wetter conditions leading to an increased deposition of minerogenic and biogenic material from the catchment, whilst peak A could reflect a period of enhanced lake productivity in response to more favorable conditions similar to scenario 1.

Unlike the evidence for ice shelf absence, which was reproduced in both the ML and MLNB cores, some of the results from BZV do not, when plotted on a depth-scale, appear to be reproduced in the MLNB core. However, when the key data from the MLNB core is plotted against a common time-scale (assuming linear sedimentation), the major features such as C/N peaks A and B do appear to be replicated (Fig.7.8). This suggests that although some trends in the MLNB data differ from those displayed in the ML core, the key environmental changes (such as C/N peaks A and B) are reproduced. These discrepancies could be related to the relative positions of the cores in the lake basin. The ML core is situated in the middle of the lake basin and is likely to receive most of its minerogenic material from the alluvial fan deposits in the main valley floor and from a mixture of sediment from the north and south facing valley sides (Fig.7.9). During the summer the alluvial fan area is generally ice free and is colonised by well-developed moss patches and cyanobacterial mats which are dissected by prominent meltwater streams (Fig.7.9). Moss patches also occur on the north-facing valley slope (Heywood, 1977). In contrast the MLNB core site is situated in the lee of the bedrock sill and is close to a till-covered valley side. The valley side is south facing and as a consequence is snow covered for much of the year. The ML core is thus likely to reflect a catchment biological signal whilst the MLNB core in contrast is likely to reflect a more terrigeneous-dominated signal. This is supported by the C_{org} data and grain-size data. BZV in the ML core has a mean C_{org} value of 0.37 % whilst unit 2 in the MLNB core has a mean of 0.28 %. Similarly, the MLNB core has higher percentages of sand (mean 25%) compared with the ML core (mean 18%). This would suggest that the ML core more faithfully reflects biological activity in the catchment, which is fundamentally controlled by climate.

Finally, an additional feature of the core sediments from ML and AB (although absent in the ML core) is the increase in $\delta^{13}C_{org}$, C_{org} and N_{org} values at the core top/sediment-water interface (Figures 6.13 and 6.14). It is possible that this change could reflect an increase in the flux of marine water entering these lakes, leading to higher isotopic and elemental values (as is the case in BZIV). For ML, this is consistent with the limnological data (Chapter 5) which has shown a thickening of

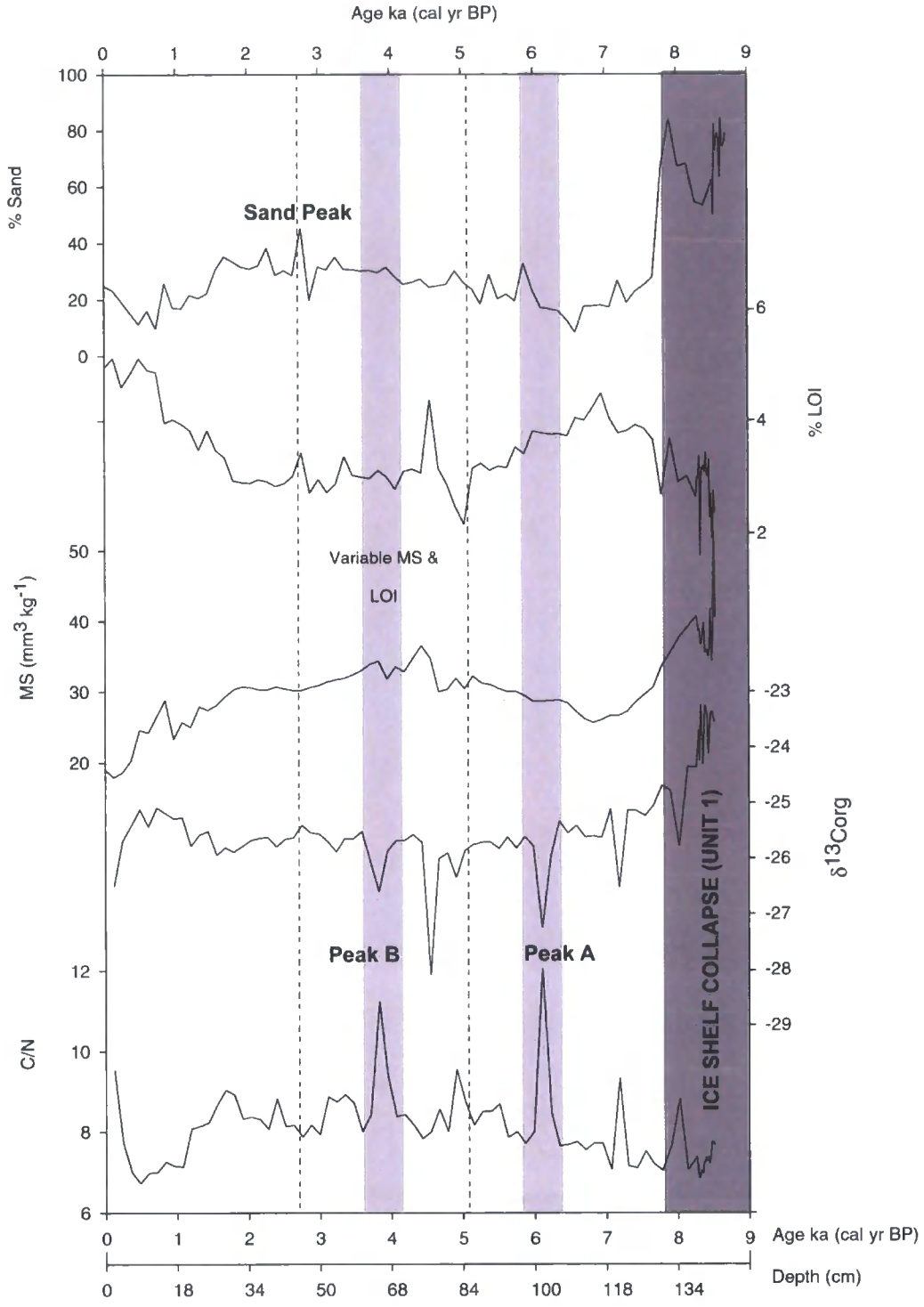

Figure 7.8. Key palaeoenvironmental data from the MLNB core plotted against age (cal yr BP) using a linear sedimentation rate. C/N peaks A and B from ML core are also observed in the MLNB core and occur in broadly during the same time-intervals (e.g. Peak A ca. 6 cal ka BP and Peak B ca. 4 cal ka BP).

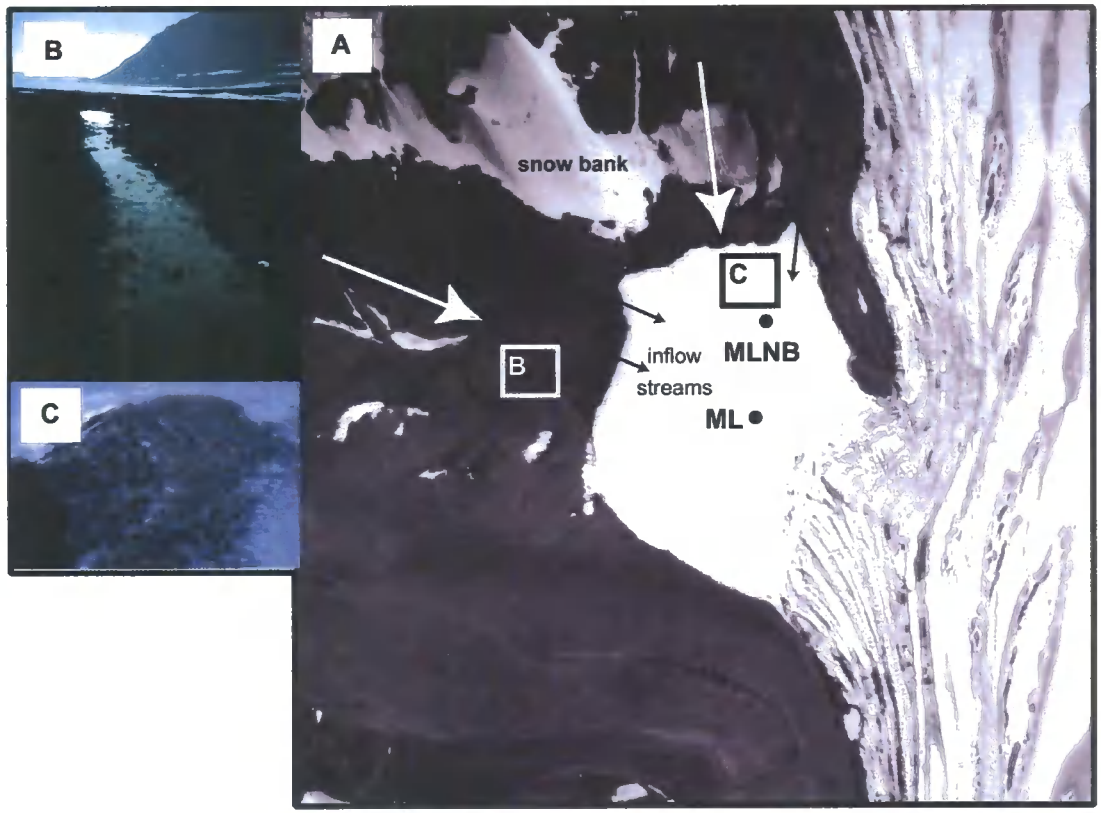

Figure 7.9. Relative sediment source areas for ML and MLNB core. (a) Aerial photograph of Moutonnée Lake showing ML and MLNB core site and observed sediment pathways (white arrows). Major inflow streams are also shown (black arrows). (b) shows an organic rich (cyanobacteria) stream flowing into ML. The lake can just be seen at the top of the photograph. (c) Gravel on the surface of the lake derived from the south facing valley side. The two photographs illustrate the different (biological vs minerogenic) lake sediment sources.

the marine layer over the last 30 years, perhaps in response to (recent) ice shelf thinning. As such, the change in isotopic and elemental proxies at the core top could provide evidence for the first signs of 20th/21st Century ice shelf break-up. An assessment of the significance of these changes will require the regular monitoring of ML and AB.

In summary, the sediment record in ML provides one of the longest lacustrine sequences on the AP. Shortly after the ice shelf began to reform (<8 ka yr BP) C/N values remain low until ca. 7600 cal yr BP. This is consistent with the proxy data from BZIV, which suggest that the ice shelf reformed in response to a period of climatic cooling. The C/N ratio values then begin to increase rapidly at ca. 7500 cal yr BP leading to C/N peak A at approximately 6000 cal yr BP. This may reflect a period of enhanced lake productivity in response to warmer environmental conditions. C_{org} levels then decline between C/N peaks A and B, which may imply a brief period of cooling and/or drier conditions. From ca. 158 cm (ca. 5320 cal yr BP), LOI, MS and $CaCO_3$ values fluctuate markedly. This interval also coincides with C/N peak B and an increase in sand-gravel sedimentation and is interpreted here as a period of wetter environmental conditions. This may reflect enhanced precipitation and/or climatic warming leading to increased snowmelt. Both of the latter scenarios are likely to reflect climatic warming. This period of instability ends at approximately 64 cm (ca. 2150 cal yr BP). From this depth proxy data indicates a period of relative stability, perhaps under cooler drier conditions. In addition, the core tops of MLNB and AB4 show increasing $\delta^{13}C_{org}$, C_{org} and N_{org} values, which could be interpreted as the first signs of 20th/21st Century ice shelf break-up.

7.2.8. Clast lithological data – further evidence for ice shelf loss

As part of the wider NERC-funded project, the conglomerate-grade (>8 mm) clasts in sediment from the ML core have been identified and their source characteristics investigated (Fig. 7.10) (Roberts et al., in prep.). It has already been noted (Chapter 3) that the Antarctic Peninsula is composed primarily of plutonic and volcanic rocks formed in a Cretaceous island arc, whereas Alexander Island is composed of

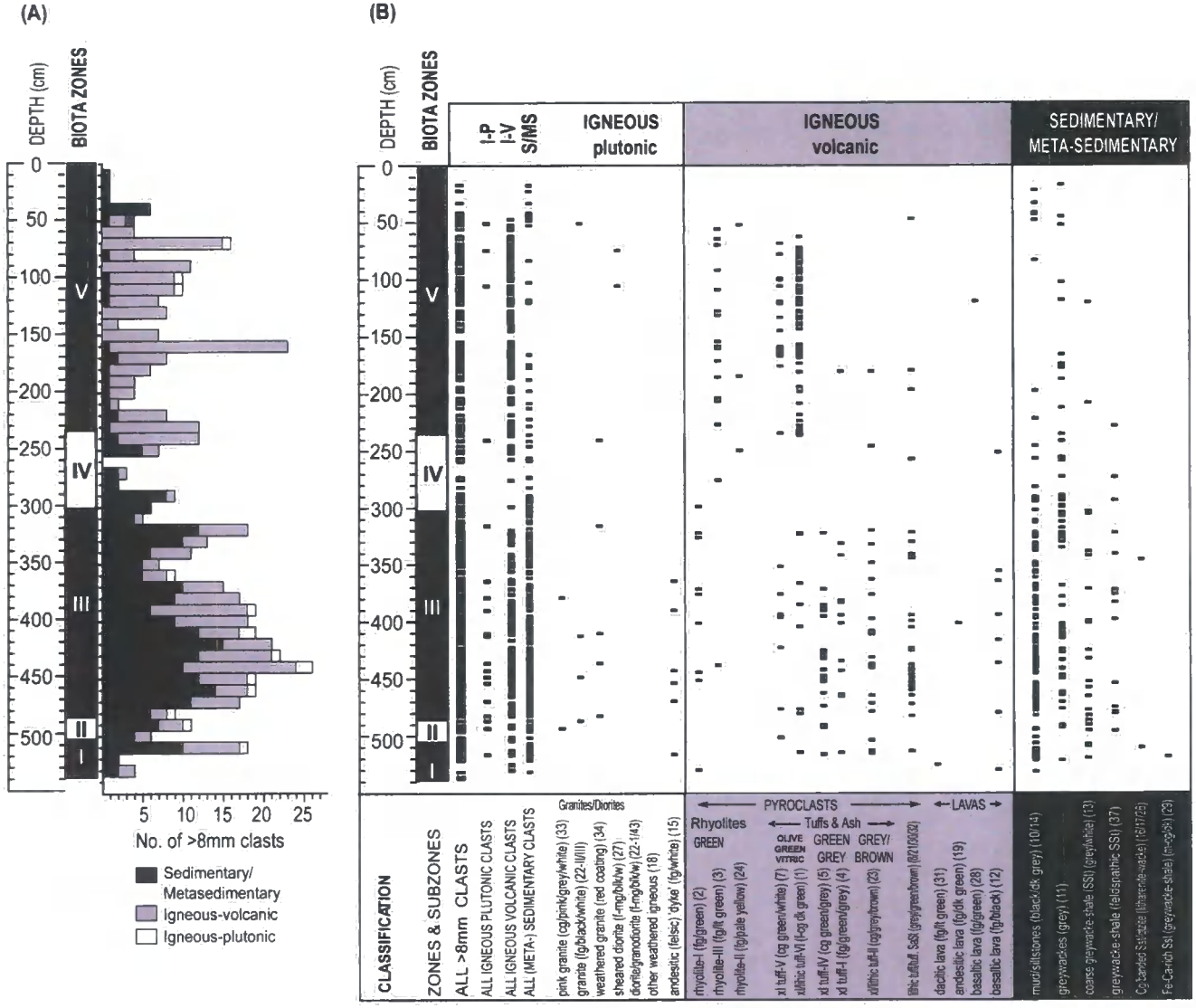

Figure 7.10. (a) Total number of > 8 mm clasts in the ML core. The clasts have been classified as sedimentary/metasedimentary, igneous-volcanic and igneous-plutonic. (b) Detailed classification of > 8 mm clasts in the ML core showing presence/absence of clasts. BZIII is characterised by the highest abundance and wide range of lithologies (Roberts et al., in prep).

sedimentary rocks deposited in a subduction-trench setting (Crabtree et al., 1985). It was also noted (Chapter 3 and 5) that George VI Ice Shelf transports plutonic material from the Antarctic Peninsula (along well defined flow lines) to Alexander Island where it is deposited either on the coastline, or in the case of ML, on the lake shoreline. On the basis of these observations, it was suggested (Chapter 5) that, when in contact with Alexander Island, the ice shelf leaves a distinct signature (plutonic and volcanic rocks) of its presence both on the coastline and potentially within the lake sediments of ML. An expected corollary of this is the removal of the ice shelf would change the composition of clasts reaching ML. It was hypothesised (Chapter 5) that during periods of ice-shelf absence a more diverse assemblage of clast lithologies would be deposited in the lake from debris-bearing icebergs from throughout George VI Sound.

The key data from this study are shown in Figure 7.10 classified into sedimentary-metasedimentary (i.e. local debris from Alexander Island), igneous-volcanic and igneous plutonic (i.e. exotic debris from Palmer Land) groups. Significantly, BZIII contains the maximum number and types of 'exotic', igneous and plutonic clasts. In addition, multivariate statistical analysis of geochemical (REE) and isotopic (Nd-Sr) data (data not shown) show many igneous clasts in BZIII have a close affinity with the igneous provinces of western Palmer Land (Roberts et al., in prep.). In contrast, the number of clast types in BZV (i.e. after the ice shelf had re-formed) is more limited and dominated by three clast types: (i) numerous 'exotic' olive-green vitric tuff clasts, (ii) pale green rhyolitic clasts, which are virtually absent in BZIII and whose geochemical/isotopic composition is different to Palmer Land derived (Jurassic) rhyolitic clasts in BZIII, (iii) a limited number of foliated diorite clasts known to originate from Palmer Land. While the exact provenance of the olive-green vitric tuff and pale green rhyolite clasts remains undetermined, a source in Palmer Land would appear most likely (Roberts et al., in prep.). The absence of these clasts in BZIII suggests that the flow regime and source of material changed following ice shelf reformation (Roberts et al., in prep). Importantly, the wide lithological diversity in BZIII suggests that icebergs were able to float freely in George VI Sound and deposit a wide-range of lithologies from several different sources throughout the sound.

7.3. Discussion

It has been demonstrated that GVI-IS was absent at ML in the early Holocene. In addition, the core sediments from ML provide information on the environmental conditions, which preceded ice shelf reformation and those, which post-dated it. What has emerged from these data is the possibility that GVI-IS may have disappeared in response to changes in ocean circulation and/or increased atmospheric warming. In the next section, the timing of ice shelf loss will be placed in a regional context and compared with other terrestrial and marine records from the AP. Following this, the post ice shelf environmental history obtained from ML will be discussed. The penultimate section will deal more explicitly with the mechanisms leading to the absence of GVI-IS and the factors, which lead to its re-formation. The final section will speculate on the likely future of GVI-IS.

7.3.1.The timing of Ice Shelf loss: a regional context

The ML core chronology shows that the GVI-IS disappeared in the early Holocene, with the onset of retreat occurring at 8100 ^{14}C yr BP (8962 cal yr BP) and complete or partial re-formation by 7300 ^{14}C yr BP (7945 cal yr BP). This coincides with the widespread deglaciation of coastal areas around the Antarctic Peninsula (Ingólfsson et al., 1998; 2003; see Chapter 2) and immediately post-dates ice core evidence of a widespread early Holocene climatic optimum ca. 11,500-9,000 cal yr BP (Fig. 7.11) (Masson et al., 2000; Masson-Delmotte et al., 2004). The timing of ice shelf absence also coincides with the inferred intial influx of Circumpolar Deep Water (UCDW) onto the Bellingshausen Sea shelf between ca. 9000 and 3600 cal yr BP (Shevenell and Kennet, 2002) and warm water conditions between 9000 and 6700 cal yr BP (Leventer et al., 2002). Thus, both atmospheric and oceanographic changes have been recorded immediately prior to, and coincident with, the ice shelf absence.

If we now consider the original evidence for absence of GVI-IS there appears to be an apparent mis-match between the dates presented here for ice shelf loss and those originally proposed by Clapperton and Sugden (1982) and later supported by Hjort et al. (2001). Clapperton and Sugden (1982) dated barnacle shells (*Bathylasma*

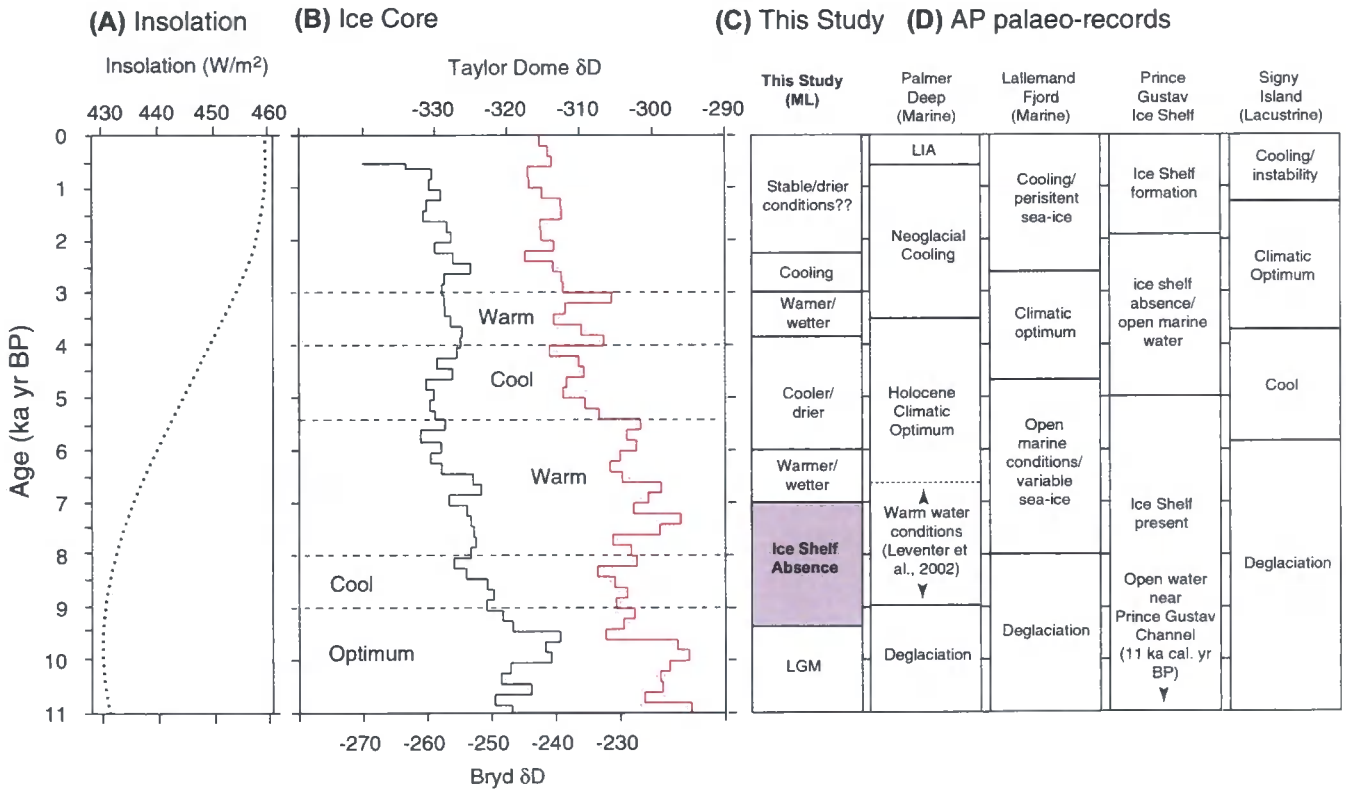

Figure 7.11. Synthesis of regional palaeoenvironmental change from the Antarctic Peninsula region: **(a)** solar insolation at 65°S for December (Berger and Loutre, 1991); **(b)** 200 yr average Byrd δD profile (black) (Hammer et al., 1994; corrected for elevation change after Masson et al., 2000) and 200 year average Taylor Dome δD profile (red) (Steig et al., 1998); **(c)** Inferred collapse (this study) of George VI Ice Shelf highlighted in grey; **(d)** important palaeoclimatic records from the Antarctic Peninsula. Data from Palmer Deep (Domack et al., 2001); Lallemand Fjord (Shevenell et al., 1996); Prince Gustav Ice Shelf (Pudsey and Evans, 2001); Signy Island (Jones et al., 2000; Noon et al., 2003). LGM= Last Glacial Maximum; LIA= Little Ice Age.

corolliforme) from an ice shelf moraine deposited on the western margin of George VI Ice Shelf at Two Step Cliffs (Fig. 2.1 Chapter 2). They obtained an age of ca. 7200 ^{14}C yr BP, which corresponds to ca. 5900 ^{14}C yr BP after the 1300 yr AMRE correction suggested by Berkman et al. (1998). This age was later confirmed by Hjort et al. (2001) who re-dated several shells from the same site. Their dates ranged between 5750 and 6000 ^{14}C yrs BP (or ca. 6550-6859 cal yr BP). Since no modern shells were found in the ice shelf moraine, Clapperton and Sugden (1982) concluded that the most likely explanation to account for the presence of *Bathylasma corolliforme* was that George VI Sound was seasonally free of water at Two Step Cliffs around 6550-6859 cal yr BP. Thus, the age range for seasonally open water in George VI Sound suggested by Clapperton and Sugden (1982) and Hjort et al. (2001) is ca. 1000 years younger than the youngest age from ML. The difference in age could be due to one of several factors; (1) the Antarctic marine reservoir effect (AMRE) is variable between foraminiferal calcite of the lake site and the barnacle calcite at Two Step Cliffs; (2) that *Bathylasma corolliforme* is able to survive beneath portions of George VI Ice Shelf and/or is able to survive in isolated marine habitats (e.g. polynas/shallow ice free areas such as Hobbs Pool; Fig. 2.1b); (3) that the ice shelf did not fully reform until 6550 cal yr BP in the region of Two Step Cliffs ca. 1000 years after re-formation at Ablation Point; (4) different glaciological behaviour of GVI-IS at the Ablation Point Massif and Two Step Cliffs.

The question of whether the AMRE is variable between Ablation Point and Two Step Cliffs is a difficult one to answer. Given the close proximity of the two sites it seems unlikely that the difference in age between the foraminifera and barnacle samples are related to changes in the rate of upwelling. However, on present data this assumption cannot be tested. It is also unlikely that the 1000 yr age difference is the result of different vital effects between the two marine species. It has been suggested that differences between Antarctic marine taxa can be estimated by the similarity of their δ^{13}C values (Harkness, 1979; Gordon and Harkness, 1992) relative to seawater which is around 0 ‰. Both species yield δ^{13}C values between –0.9 and +4.4 ‰, which is within the range of most Antarctic carbonate species (Gordon and Harkness, 1992). Thus on the basis of the geographical proximity of

the two sites and the isotopic data it would seem unlikely that the younger age from Two Step Cliffs results from a variable AMRE or specific vital effects between the two dated species.

The second possibility is that communities of *Bathylasma corolliforme* were able to survive beneath George VI Ice Shelf in isolated refugia and as such do not reflect fully-open marine conditions near Two Step Cliffs. *Bathylasma corolliforme* is generally considered a deep-sea Antarctic barnacle which rarely survives in waters shallower than 100 m (Dayton et al., 1982). Whilst there is no evidence to suggest that *B. corolliforme* exists beneath ice shelves and grounded ice margins (Dayton et al., 1982) Hains and Melles (1994) have shown that some shells (e.g. *Adamussium colbecki*) survive in coastal refuges beneath ice shelves. However, unlike *B. corolliforme*, *A. colbecki* are common in littoral or shallow Antarctic waters (Dell, 1990). Thus their presence on the shallow shelf beneath thin portions of an ice shelf should not be surprising. As noted above *B. corolliforme* generally survives at much greater depths (>1000 m; Dayton et al., 1982). However, for *B. corolliforme* to be entrained by the ice shelf and deposited within the ice shelf moraine, it must have survived at relatively shallow depths (e.g. <100 m). In addition to the apparent ecological preferences of *B. corolliforme* it is unlikely that it survived beneath George VI Ice Shelf given the original evidence that no modern shells were (or have been) discovered in the ice shelf moraine (Hjort et al., 2001). It is still possible however that *B. corolliforme* survived in isolated areas of open water. At present the upwelling of warm deep water on the west of George VI Sound at the northern ice front results in a discrete polyna (Potter et al., 1988). It is possible that a similar feature once existed farther south near Two Step Cliffs in response to some oceanographic change. This is also supported by observational evidence, which suggests that *B. corolliforme* is not distributed uniformly along the western coast of George VI Sound (M.J. Bentley pers. comm.). It is worth noting however, that no systematic search for *B. corolliforme* along the entire ice shelf moraine has been performed.

Whilst the presence of *B. corolliforme* dated to 6000-6500 cal yr BP remains something of an enigma there is no clear evidence to suggest that the age is incorrect. Indeed the initial explanation for its presence within an ice shelf moraine

along the western margin of GVI-IS still remains the most plausible interpretation. Certainly a longer period of ice shelf absence is consistent with the diatom data from Palmer Deep, which indicates the early Holocene presence of warmer UCDW between ca. 9000 and 6700 cal yr BP (Leventer et al., 2002). One final problem is that if the barnacle age from Two Step Cliffs is taken to represent an extended period of ice shelf absence (between 8962 and 6500 cal yr BP) then it becomes problematic that no barnacles/shells of equivalent age to the ML ages were discovered in any of the moraines analysed along George VI Sound. One would expect to find barnacles, which span the entire age range from the inception of ice shelf break-up at ML lake of ca. 8962 cal yr BP to full (or partial) re-formation at Two Step Cliffs by ca. 6000 cal yr BP. One way to reconcile these ages would be to invoke a gradual retreat of the George VI Ice Shelf from the north. The present day ice shelf is retreating relatively slowly in response to the southward progression of the –9 °C isotherm. It is likely that if atmospheric temperatures continue to rise then the northern margin of the ice shelf will eventually recede as far south as the Ablation Point Massif and then sometime later, Two Step Cliffs. In other words Moutonnée Lake would experience open marine conditions before Two Step Cliffs. However, this hypothesis is largely dependent on how the ice shelf retreated during the early Holocene, which is discussed in more detail below. Before this is investigated however, the environmental history following ice shelf reformation (ca. 8000 ka to present) is discussed in more detail.

7.3.2. A 8000 yr Climatic Record from Alexander Island

The data presented in this thesis also provides evidence of long-term environmental change in ML following ice shelf re-formation. Multi-proxy data from ML indicate that marine sedimentation had been replaced by sedimentation in an epishelf lake by 236 cm (or 7946 cal yr BP). Assuming that the age-model for Moutonnée Lake is broadly accurate, then this interval represents one of the longest lacustrine sequences on the AP.

At present, the AP is characterised by a relative paucity of high-resolution (Holocene) climatic records. This has made it difficult to assess the regional significance of climatic events during Holocene and to compare relative forcing

factors. Recent studies from the Palmer Deep however have provided a detailed marine record of Holocene oceanic changes on the west side of the AP (Domack et al., 2001). The relative completeness of the record (ca. 13000 yrs) and its firm chronology has, for the first time, provided an initial framework against which ideas about forcing mechanism can be tested (Domack et al., 2003a). The Palmer Deep record shows deglaciation was underway by ca. 13000 cal yr BP. The site was then characterised by warm water intrusion between 9000 and 6700 yrs BP, which coincided with the loss of GVI-IS, followed by neoglacial cooling after 3600 yrs BP (Fig.7.11 and Fig. 2.11 Chapter 2) (Domack et al., 2001). The latter time interval is also characterised by strong century-scale (ca. 200 yr) oceanic variability (Shevenell and Kennett, 2002). The intention of the next section is to place the climatic events recorded in the ML core in a regional context. However these comparisons must remain tentative until the core chronology is further improved.

The ML core provides evidence (peaks in C/N etc) for two periods of climatic warming; the first centred around ca. 6000 cal yr BP and the second between ca. 3850 and 3000 cal yr BP (Fig. 7.7 and 7.11). These two events are followed by cooler/drier phases between ca. 6000 to 4000 cal yr BP and ca. 3000 and 2000 cal yr BP respectively. The first warm interval is broadly contemporaneous with warm water conditions recorded in the diatom flora at Palmer Deep between 9000 and 6700 cal yr BP and other geochemical data from the same site, which shows a warm oceanographic interval at approximately 6,000 cal yr BP (Domack pers. comm.). This event also coincides with the widespread deglaciation of the sub-Antarctic Peninsula Islands (Björck et al., 1991a,b, 1996; Jones et al., 2000; Noon et al., 2003). The cooler/drier period between approximately 6000 and 4000 cal yr BP is comparable to a period of cooler temperatures and seasonally variable sea-ice conditions between 6200 and 4000 cal yr BP recorded in Lallemand Fiord (Shevenell et al., 1996) and cool conditions between 5900 and 3800 cal yr BP on Signy Island (Jones et al., 2000; Noon et al., 2003). The second period of warmer/wetter conditions in the ML core coincides with the widespread mid-Holocene climatic optimum (or hypsithermal) recorded in several lake, moss bank, ice core and marine records (see Jones et al., 2000; Hodgson et al., in press and references therein). Specifically Shevenell et al. (1996) recorded a climatic optimum in the Lallemand Fiord between 4200 and 2700 cal yr BP (Shevenell et al., 1996),

whilst the Palmer Deep record shows a major change in sedimentation at 3600 cal yr BP, which has been interpreted as the beginning of cooling and the so-called neoglacial period (Domack et al., 2001) (Fig.7.11 and 2.11 Chapter 2).

On the basis of the limited chronological model, it would appear that the changes in the C/N profile from ML are broadly contemporaneous with regional climatic trends on the west coast of the AP as recorded in marine, lake and ice core records. The next logical step is to assess whether the ML record is comparable to other climatic records from beyond the AP. Recent studies have provided evidence for strong links between Holocene climatic changes on the AP and oceanic/atmospheric changes in the tropical Pacific (Shevenell and Kennett, 2002; Lamy et al., 2001, 2002; Domack et al., 2003a). Specifically, Domack et al. (2003a) have suggested a possible link between the Palmer Deep marine record and the intensity of the Peru-Chile Current (PCC) (Lamy et al., 2002). The PCC is the direct northward continuation of the Antarctic Circumpolar Current (ACC). The southern most edge of the ACC abuts the Antarctic Peninsula shelf as it is funnelled through the Drake Passage by the Southern Westerlies and eventually into the Atlantic sector of the Southern Ocean (Fig.7.12). The impingement of the ACC on the tip of the AP is thought to play a fundamental role in the climate of the west coast of the AP and is also associated with the upwelling of warm UCDW (Smith et al., 1999; Smith and Klinck, 2002). Lamy et al. (2002) have reconstructed the PCC over the last ca. 8000 yrs based on a multi-proxy approach including sea-water palaeotemperature and palaeosalinity reconstructions derived from alkenone and planktic foraminiferal oxygen isotopes as well as palaeoproductivity indicators (opal and organic carbon). It is thought that the ACC delivers cold nutrient rich waters to the southeastern Pacific leading to high productivity in the PCC (Hebbeln et al., 2000). Thus on Holocene timescales, high palaeotemperatures and salinities are thought to reflect decreased advection of subpolar water masses by the ACC (Lamy et al., 2002).

Figure 7.13 shows the C/N profile from ML (a) plotted against palaeoprecipitation (Fe content) (b), sea surface temperature record of the PCC (c); and the Taylor Dome δD ice core record (d). The PCC data set is characterised by two prominent excursions to higher palaeotemperatures and palaeosalinities and decreased

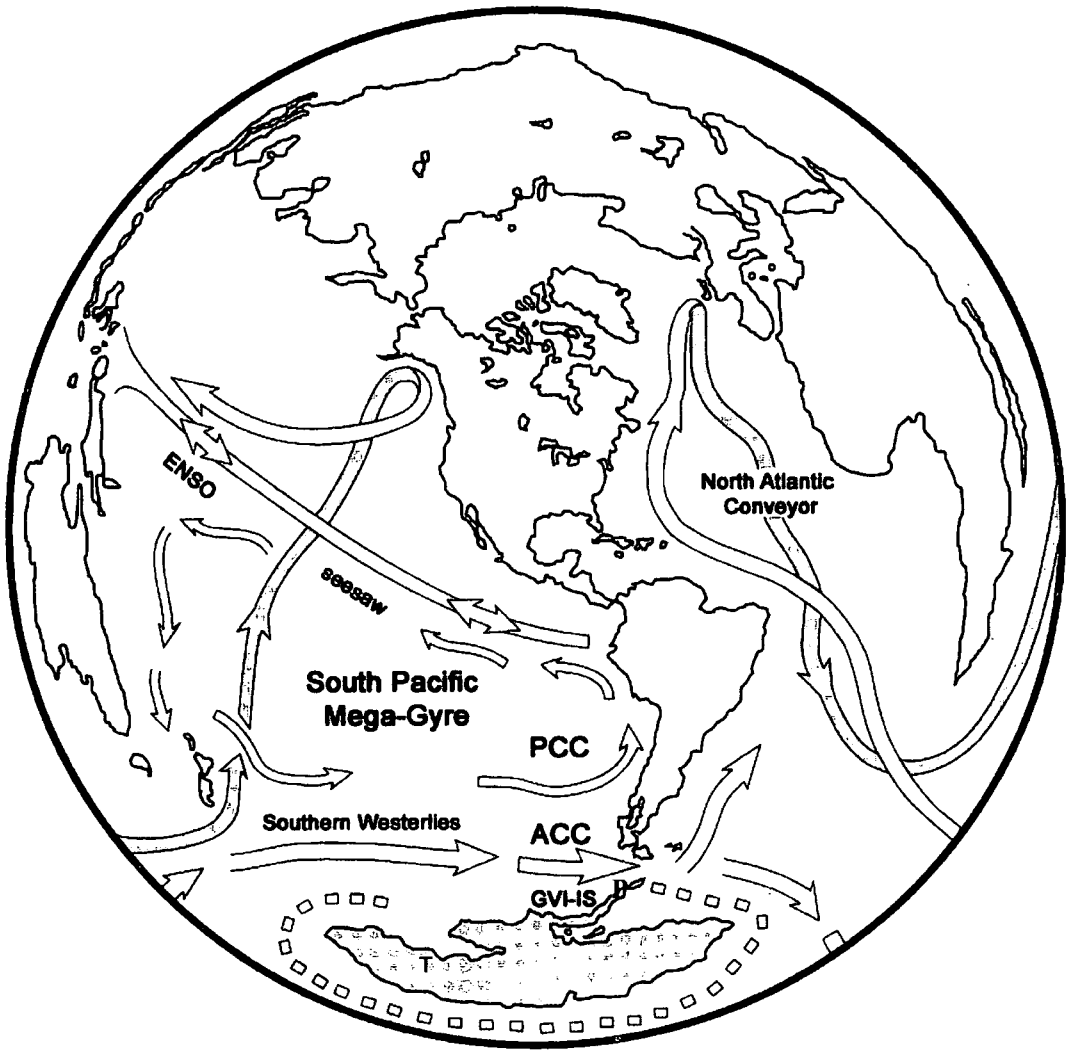

Figure 7.12. Global oceanographic circulation in context of Antarctic Peninsula and southern Pacific Ocean processes such as El Nino-Southern Oscillation (ENSO), South Pacific Gyre, the Antarctic Circumpolar Current (ACC) and deep water flow contributed by North Atlantic thermohaline processes. Location of the Peru-Chile Current (PCC) is also shown together with the location of George VI Ice Shelf (GVI-IS), Taylor Dome ice core (T) and Palmer Deep (P). The northerly limit of sea-ice is indicated by a bold dashed line (approximate) (modified from Domack and Mayewski, 1999).

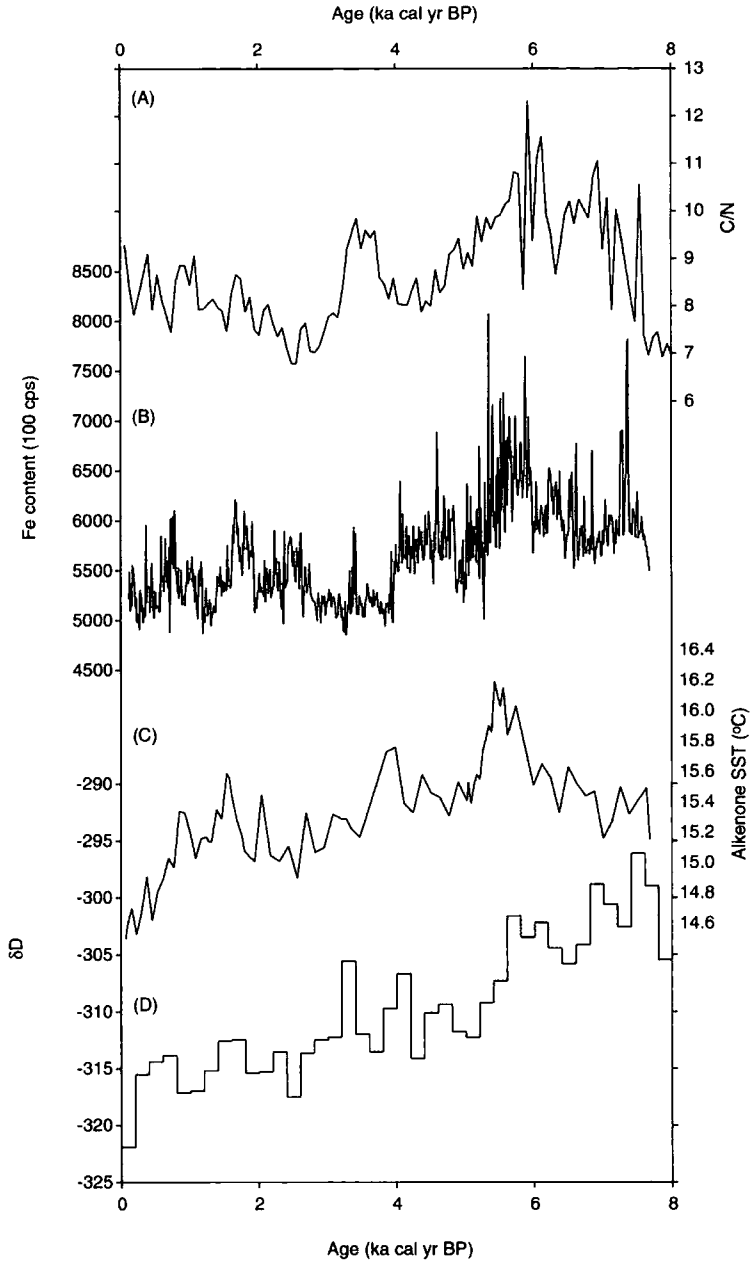

Figure 7.13. Compilation of palaeoclimatic data sets from Moutonnée Lake, Peru-Chile Current and Antarctic ice core data (a) C/N profile from ML; (b) Iron content from PCC core used as a proxy for precipitation and the position of the Southern Westerlies (Lamy et al., 2001). High iron content imply increased contribution of iron rich volcanic Andean source rocks and decreased supply of iron-poor Coastal range rocks. Such conditions indicate decreased rainfall most likely induced by a southward shift in the South Westerlies (Lamy et al., 2001); (c) alkenone based palaeotemperature reconstruction that traces the advection of subpolar water by the ACC (Lamy et al., 2002); (d) 200-year averages of δD from the Taylor Dome ice core record (Steig et al., 1998).

precipitation between 6,000 and 5000 cal yr BP and at 3,860 cal yr BP (Lamy et al., 2002). These data are consistent with the two (warm) events recorded in ML and as such provide evidence for links between climatic-related oceanographic changes on the Antarctic Peninsula and those occurring in the tropical Pacific. Lamy et al. (2001, 2002) have suggested that the long-term (Holocene) evolution of the PCC has been controlled by latitudinal shifts of the Antarctic Circumpolar Current (ACC), which are in turn driven by the Southern Hemisphere westerly wind field (Southern Westerlies). Thus according to Lamy et al. (2001, 2002) higher palaeotemperatures and salinities in the PCC recorded at ca. 6000 cal yr BP and ca. 3850 cal yr BP most likely reflect a decreased advection of cold and nutrient rich water via the ACC. Lamy et al. (2001, 2002) attribute these changes in the PCC and precipitation to a latitudinal displacement of the ACC and the Southern Westerly wind belt, possibly in response to insolation-induced changes in Southern Hemisphere atmospheric circulation patterns (e.g. Hadley Cell). The modern location of the Southern Westerly wind belt is related to steep SST gradients within the ACC and ENSO-related changes. It is thought that less advection of the ACC-derived water masses imply a more southerly location of this system (Lamy et al., 2002). A southward shift of both the Southern Westerlies and the ACC during the middle Holocene is supported by other data. For example ice core (Thompson et al., 1998) and lake records (Cross et al., 2000) from the South American Altiplano indicates increased aridity, which could relate to a more intense Hadley cell. According to Lamy et al. (2001) the intensification of the Hadley cell could have resulted in a further southward shift of the Southern Westerlies. Conversely, Lamy et al. (2002) go on to argue that decreasing palaeotemperatures and increasing continental precipitation after ca. 4000 yrs suggests a northward shift of both the ACC and the southern westerly wind belt.

So, how are the changes in the PCC connected to climatic variability on the AP? The simplest connection involves the strength and position of the westerly wind belt and its associated impact on the ACC. The western AP is situated within the zone of strongest Southern Hemisphere westerly winds (Kreutz et al., 1998) and as such is likely be sensitive to any perturbations in its intensity or position. At present the westerly winds bring warm, moist air to the west side of the AP. Thus it is possible that a poleward displacement of the Southern Westerlies during the Mid-Holocene

(e.g. Lamy et al., 2002) led to higher temperatures on the west coast of the AP and specifically increased precipitation or warmer conditions at Moutonnée Lake. This is consistent with ice core data from Taylor Dome (Stager and Mayeswki, 1997; Steig et al., 1998) and the sediment record from the Palmer Deep (Domack et al., 2001; Leventer et al., 2002), which indicate higher atmospheric and oceanographic temperatures at ca. 6000 cal yr BP. In the case of the Taylor Dome ice core record there is also an indication of warmer climatic conditions between 4 and 3,000 cal yr BP. In addition Cunningham et al. (1999) have provided evidence for a warm event in Ross Sea between 6000 and 3000 cal yr BP, which may suggest that the mid-Holocene warming may have been a circum-Antarctic event.

The precise mechanism linking displacement of the Southern Westerlies and warming at ML during the Mid-Holocene period is not easily determined. It has been suggested that the western AP hydrography is sensitive to westerly wind strength and El Nino-Southern Oscillation (ENSO)-like climatic variability (Shevenell and Kennett, 2002). Shevenell and Kennett (2002) have demonstrated strong links between late Holocene oceanographic perturbations in the Palmer Deep record and the strength of the Southern Westerlies. Between ca. 9000 and 3700 ka BP the PD record is devoid of foraminifera, which Shevenell and Kennett (2002) attribute to the presence of corrosive UCDW. They argue that the presence of sustained UCDW on the continental shelf during this time interval resulted in warmer regional atmospheric temperatures, decreased sea-ice cover and increased primary productivity. They go on to suggest that the presence of UCDW was directly related to decreased westerly wind strength related to ENSO variability. Shevenell and Kennett (2002) also note that intervals of increased UCDW in the PD also correlates with less intense westerly winds, inferred from the sea-salt record of the Siple Dome Ice Core (e.g. Kreutz et al., 1997). As noted already there is also strong evidence from the Southern Ocean (Pacific sector) for decreased meridional wind strength (or ENSO) (Lamy et al., 2001) and decreased West Antarctic sea ice during this time period (Stager and Mayewski, 1997). After 3700 ka BP the PD sequence exhibits a significant shift in sedimentary character, which is coincident with a southward shift in the Intertropical Convergence Zone (ITCZ) (e.g. Baker et al., 2000; Haug et al., 2001) and an increase in ENSO strength and low-latitude climate variability (Sandweiss et al., 1996; Rodbell et al., 1999). In the PD record,

Shevenell and Kennett (2003) suggest that this may have resulted in a general increase in shelf water (replacing UCDW) and westerly wind strength between ca. 3600 and 500 ka yr BP resulting in a general cooling. They suggest that predominantly offshore winds could push the southern boundary of the ACC off the western AP continental shelf, thereby depressing the volume of UCDW in PD (e.g. Hoffman et al., 1996; Smith et al., 1999). It is therefore possible that the environmental conditions at ML during the Holocene were forced by changes in UCDW, associated with changes in the ACC and Southern Westerlies. This also raises the possibility that the early Holocene appearance of UCDW on the continental shelf was controlled by atmospheric changes in the southeastern tropical Pacific.

In summary, lake sediment records from BZV in the ML core provide evidence for two periods of warmer and/or wetter conditions during the last ca. 8,000 yrs. These two events appear to correlate with changes in other AP records and also appear to correlate with changes in the Peru-Chile Current. This is consistent with records from the Palmer Deep, which have also demonstrated strong links between climatic variations on the west cost of the AP and atmospheric-oceanic perturbations in the Pacific Ocean (Domack and Mayewski, 1999; Shevenell and Kennett, 2002; Domack et al., 2003a). More important in the context of the main aim of this thesis is whether the absence of GVI-IS was associated with a climatic forcing originates from the tropical Pacific? However, this idea cannot be tested with present data.

7.3.3. Mechanism for ice shelf absence vs. mechanism for ice shelf re-formation

High-resolution multi-proxy sediment records from ML provide evidence that GVI-IS was absent from ca. 8962 cal yr BP and had partially or fully reformed by 7945 cal yr BP. Chapters 2 and 3, reviewed the factors likely to contribute to ice shelf loss, with specific reference to GVI-IS. Research has shown that other AP ice shelves are sensitive to atmospheric temperature and their present distribution is largely controlled by the position of the –9 °C mean annual isotherm (Morris and Vaughan, 2003) boundary but as yet shows only modest retreat. In addition to atmospheric warming, several recent studies have highlighted the importance of enhanced basal melting caused by changes in ocean circulation (Domack et al.,

1995; Rignot, 2002; Williams et al., 2002; Shepherd et al., 2003). It was suggested in Chapter 3 that changes in ocean circulation could play an important role in the future stability of GVI-IS and may have been key to any changes that have occurred on Holocene timescales.

Previous research has suggested that the present day GVI-IS is relatively insensitive to atmospheric warming and is unlikely to collapse in a Larsen-style, melt-pool triggered fashion (Vaughan and Doake, 1996; Scambos et al., 2002). However, as noted above the early Holocene absence of GVI-IS not only coincides with widespread early Holocene warming (11,500-9000) in Antarctica (Masson et al., 2001) but also, and importantly, the influx of warm Upper Circumpolar Deep Water (UCDW) onto the AP continental shelf (Leventer et al., 1996; Taylor and Sjunneskog, 2002). Based on the ice core evidence, early Holocene temperatures were warmer than the present day and there is also a suggestion that UCDW flow was more vigorous at this time (Howe and Pudsey, 1999). Doake and Vaughan (1991) speculated that small changes in temperature could cause a significant change in the net balance of an ice shelf, effectively changing the balance from accumulation to ablation. They suggested that successive years of net ablation, through increased temperature would lead to deterioration of the ice shelf surface. In addition, rifts and crevasses would no longer be 'healed or glued' by winter accumulation. Laboratory experiments also show that the fracture toughness of ice is reduced at higher temperatures and by the presence of water (Lui and Miller, 1979; Sabo and Schulson, 1989). It seems likely that George VI Ice Shelf underwent similar changes following a period (1000 + yrs) of early Holocene atmospheric warming. Although not sufficient to destabilise the ice shelf alone, when combined with the introduction of UCDW at ca. 9000 yrs BP, the George VI Ice Shelf became susceptible to cracking and large scale-failure. Whether this led to partial or complete disintegration of the ice shelf in the Holocene is open to debate. The clast data from the ML core implies that icebergs were able to float freely in George VI Sound between 8964 and 7945 cal yr BP, depositing a wide range of lithologies from a wide variety of sources (Roberts et al., in prep.). In addition there is evidence from much further south, at Two Step Cliffs for seasonally open water at ca. 6500 cal yr BP (Hjort et al., 2001).

In general, the mechanisms for early Holocene warming observed in Antarctic ice cores are not fully understood (Masson-Delmotte et al., 2004). It has been speculated that at the end of Northern Hemisphere deglaciation, reduced North Atlantic Deep Water (NADW) formation could result in warmer conditions over Antarctica (Blunier et al., 1997; 1998). In effect, shutdown of the NADW would mean that warm ocean water was no longer drawn away from high southern latitudes (Broecker, 1998; Blunier et al., 1998). The 'switching on' of the thermohaline circulation following the end of Northern Hemisphere deglaciation would act to remove the heat from high southern latitudes thereby ending the early Holocene optimum in Antarctica (Broecker, 1998). Circumpolar Deep-Water is the most voluminous water mass in the Antarctic circum-polar current (ACC) (Smith et al., 1999) and its circulation is intrinsically linked to NADW formation (Whitworth and Nowlin, 1987). It is possible, although currently speculative, that the switching-on of NADW following the end of Northern Hemisphere deglaciation led to the reinvigoration of UCDW on the AP. However few studies have provided a long-term perspective on UCDW variability and its connection to variations in NADW are unclear (Ishman and Sperling, 2002). Based on the size distribution of fine (< 63 μm) sediments in the Scotia Sea, Howe and Pudsey (1999) suggested that UCDW flow was unstable between ca. 17000 and 12500 ka yr BP. At approximately 12280 ka yr they noted an increase in size sorting which they interpreted as indicating strong flow of CDW. During deglaciation and into the early Holocene however they suggested that CDW flow became more stable (Howe and Pudsey, 1999).

Shevenell and Kennett (2002) have provided a more detailed picture of Holocene changes in UCDW, from their marine isotope study at Palmer Deep. They argued that between 9000 and 3600 ka yr BP a sustained presence of UCDW at this site resulted in warmer regional atmospheric and sea-surface temperature, decreased sea-ice cover and increased primary production. This conclusion is consistent with other proxy evidence (e.g. diatom) from the Palmer Deep, which indicates the presence of 'warm water conditions' between 9000 and 6700 ka yr BP (Leventer et al., 2002; Taylor and Sjunneskog, 2002), but is at odds with the foraminiferal

assemblage study of Ishman and Sperling (2002), which suggests that UCDW was absent on the western AP shelf during this time interval.

A consistent theme to have emerged from some of these studies is the suggestion that UCDW variability could be associated with atmospheric circulation (Pudsey and Howe, 1999; Shevenell and Kennett, 2002; Ishman and Sperling, 2002) and not the reorganisation of thermohaline circulation associated with NADW. As discussed above, regional Southern Ocean ventilation changes may result from low- to high-latitude atmospheric teleconnections involving Southern Hemisphere westerly wind field fluctuations (Klinck and Smith, 1993; Charles et al., 1996; Labeyrie et al., 1996; Ninnemann et al., 1999; Lamy et al., 2002; Shevenell and Kennett, 2002). From their foraminiferal-based isotope study from the Palmer Deep, Shevenell and Kennett, (2002) have also proposed that Holocene changes in UCDW were controlled by the strength or position of the Southern Hemisphere westerly wind field and not thermohaline reorganisation. They suggest that these atmospheric changes may originate in the tropical pacific and could be associated with high-frequency ENSO variability. There is also an indication that environmental changes in Moutonnée Lake are closely coupled to climatic changes in the southeastern Pacific (e.g. Lamy et al., 2002). This raises the possibility that the absence of GVI-IS was linked to climatic changes in the tropical Pacific.

The prospect of a combined atmospheric-oceanic mechanism for ice shelf absence is an exciting (and plausible) hypothesis and it is possible that it was driven by changes associated with: (i) oceanic reorganisation associated with NADW; and/or (ii) changes in the southeastern Pacific. It remains difficult however, to test this hypothesis on the basis of present data. At present the only evidence for a combined atmosphere-ocean mechanism is based on the relative timing of climatic events (atmospheric warming/influx of warm UCDW). The data presented here suggests links between the presence of UCDW (e.g. isotopic and faunal) and absence of GVI-S and it has also demonstrated possible links between changes in the C/N ratio in ML over the last ca. 8000 yr BP and changes in the Peru-Chile Current associated with latitudinal shifts of the Antarctic Circumpolar Current (ACC) (e.g. Lamy et al., 2002). Whether the appearance of UCDW on the western AP continental shelf is connected to changes in the PCC remains unclear.

If a combined atmospheric-ocean mechanism caused the early Holocene absence of GVI-IS then this raises several interesting questions about Holocene climate in Antarctica and the future stability of GVI-IS. Firstly the combination of significant atmospheric warming and vigorous CDW circulation appears to be unique, at least on Holocene timescales. Second, if George VI Ice Shelf was absent during this time interval then we should see evidence for the retreat/collapse of other AP ice shelves. At the present day George VI Ice Shelf marks the southernmost extent of ice shelf retreat on the western side of the AP whilst the Larsen-B Ice Shelf marks the limit on the east side. Both limits coincide with the –9 °C mean annual isotherm. All ice shelves on the western side if the AP north of this boundary have collapsed or retreated in recent years. It is logical to suggest therefore that several other ice shelves north of GVI-IS (e.g. Wordie, Mueller, Prince Gustav Channel) retreated and/or collapsed during this phase of exceptional climate warming. However, only one other study has provided evidence for ice shelf retreat on the AP (e.g. Pudsey and Evans; Prince Gustav Ice Shelf) and this suggests the ice shelf was absent between 5000-2000 cal yr BP. Thus until the early Holocene history of other AP ice shelves is determined (e.g. Wordie, Wilkins) it will be difficult to assess the significance of the early Holocene absence of George VI Ice Shelf. Finally, if the present distribution of ice shelves is climatically controlled, the disappearance of GVI-IS in the early Holocene would imply that the climate was warmer during this time-interval than the present day as is shown in the ice core data (Masson-Delmotte et al., 2004). If current atmospheric (e.g. Vaughan et al., 2003) and oceanic (Gille, 2002) warming continues however then the GVI-IS will eventually disappear entirely.

The next logical question is, if atmospheric warming and ocean-circulation contributed to the early Holocene absence of GVI-IS, how and why did this change, and allow the ice shelf to reform? Multi-proxy evidence suggests that the ice shelf may have reformed in response to cooler climatic conditions. Shortly after this the C/N profile from ML indicates that the climate became warmer and/or wetter at approximately 6000 cal yr BP. This is consistent with Antarctic ice core data, which show an extended period of warmer temperature in the early Holocene followed by a temperature minimum (cold event) at ca. 8000 yr BP, then a secondary warm

event around 6000 yr BP (Masson et al., 2000; Masson et al., 2004). In contrast, the Palmer Deep marine record implies an extended oceanic Holocene optimum between ca. 9000-3300 ka cal yr BP, which has been attributed to the presence (and then absence after ca. 3300 ka yr BP) of warmer UCDW on the western continental shelf (Shevenell and Kennett, 2002; Taylor and Sjunneskog, 2002; Domack et al., 2003a). Irrespective of the relative impacts of atmospheric warming versus oceanic warming, it is likely that ice shelf reformation would have been largely dependent on the behaviour of the input glaciers and ice streams following ice shelf loss.

Whilst there is a growing body of literature relating to the factors controlling ice shelf collapse there is relatively little information on how an ice shelf reforms and over what kind of time scales since these processes have never been observed by glaciologists. In their study of the Holocene history of the Prince Gustav Channel ice shelf, Pudsey and Evans (2001) suggested that the channel was ice free between ca. 5000 and 2000 cal yr BP and started to reform after 1900 cal yr BP as the climate began to cool. This places a maximum constraint of 1900 years on the time taken for the ice shelf to re-form, but does not provide a minimum time period, nor suggest how the ice shelf reformed. For all AP ice shelves there are three possible sources of mass input; glacier input, *in situ* surface accumulation and basal accretion (Vaughan, in press). It is likely that the Prince Gustav Channel ice shelf re-formed after many years of snow accumulation on fast ice (sea ice attached to a land mass or grounded ice sheet) (e.g. Hughes, 1987; Vaughan, in press) and thus its re-formation can be adequately explained by the inferred widespread climatic cooling (neoglacial) on the AP after ca. 2000 cal yr BP (e.g. Björck et al., 1991a, 1991b; Domack and McClennen, 1996; Jones et al., 2001; Domack et al., 2003a).

The re-formation of GVI-IS is likely to have been controlled by similar processes to the re-formation of the Prince Gustav Channel Ice Shelf, but also, and more importantly, the behaviour of the glaciers feeding into George VI Sound. Unfortunately the behaviour of input glaciers following the retreat of other AP ice shelves is not straightforward. Vaughan (1992, 1995) reported that glaciers, which fed the Wordie Ice Shelf, did not show any appreciable change after its disintegration whilst several recent studies have shown that some ice streams, which fed the Larsen-A/B ice shelf, have accelerated following its demise (Rott et al.,

2002; De Angelis and Skvarca, 2003; Rignot et al., 2004; Scambos et al., 2004). Thus it is possible that the removal of George VI Ice Shelf would have been followed by the accelerated discharge of glacier ice from the AP and Alexander Island ice catchments into George VI Sound where it would be glued together by sea-ice. It is possible that this process would have been relatively rapid although this question cannot be answered satisfactorily using the present data set.

Whilst it is difficult to provide a definitive answer on how the ice shelf reformed the data presented here can constrain the maximum and minimum time period for this process to take place. If the oldest age from BZII (ca. 8962 cal yr BP) indicates the initial absence of GVI-IS and the *Bathylasma* ^{14}C date (Hjort et al., 2001) of 5750 ^{14}C yr BP (ca. 6550 cal yr BP) represents the maximum age for ice shelf re-formation, this gives a 2412 year window in which the ice shelf had reformed sufficiently to entrain and deposit the shells within the ice shelf moraine at Two Step Cliffs. This is of course the maximum length of time, and relies on the assumption that the ages from the barnacles from Two Step Cliffs are correct and/or represent ice shelf loss at this site. The evidence from Moutonnée Lake suggests that ice shelf re-formation at this site was much quicker. Thus the maximum age range for ice shelf reformation at Moutonnée Lake would be 1000 years from the first signs of ice shelf absence at ca. 8962 cal yr BP to the age at the top of BZIV (ca. 7964 cal yr BP), taken to represent the re-isolation of ML and therefore ice shelf re-formation. However if we take the decline in diatom and foraminifera at ca. 270 cm in the BZIV to represent the beginning of ice re-formation (ca. 8705 cal yr BP) whilst retaining the upper age from BZIV for ice re-formation we get ca. 740 years for ice shelf re-formation. Thus on the basis of data from ML re-formation of George VI Ice Shelf took between 740-1000 years, which is approximately half the time allowed by Pudsey and Evans's (2001) data. It is worth noting however that grounded ice, sufficient to re-dam Moutonnée Lake does not necessarily mean the entire re-formation of GVI-IS. Whilst these are not absolute values for ice shelf re-formation they could provide useful time constraints for any future modelling studies.

7.3.5. The Future behaviour of George VI Ice Shelf

The northern and southern margins of George VI Ice Shelf are presently retreating. This retreat appears to be related to the recent 20th/ 21st Century atmospheric warming on the AP and more specifically, to the southward progression of the –9 °C mean annual isotherm (Morris and Vaughan, 2003). A further interesting feature of the present day GVI-IS is the presence of warm UCDW beneath the ice shelf, which drives high basal melt rates beneath the ice shelf. In the context of the results presented in this thesis, the critical combination of enhanced atmospheric warming and the presence of warm UCDW imply that George VI Ice Shelf will soon decay completely. Whether the present day ice shelf will collapse rapidly (< decade) in a series of large break-up events or as slow, gradual (> centuries) retreat remains unclear.

7.4. Chapter summary

The data presented in this thesis provides robust evidence for the absence of George VI Ice Shelf during the early Holocene. The timing of ice shelf absence has been constrained by 10 AMS ^{14}C dates performed on mono-specific foraminifera samples. These dates suggest that GVI-IS was absent at ML between ca. 8962 cal. yr B.P., and ca. 7946 cal. yr B.P. The spatial extent of ice shelf absence however remains unclear. Evidence from father south (Two Step Cliffs), suggests that the ice shelf was absent at ca. 6500 cal yr BP, 1500 years later than at Moutonnée Lake. This discrepancy may reflect varying marine reservoirs, spatial variability in ice shelf retreat and reformation phases, or errors in the way that the data from Two Step Cliffs has been interpreted. The early Holocene absence of GVI-IS recorded in ML immediately followed a period of maximum Holocene warmth that is recorded in some Antarctic ice cores and coincides with an influx of warmer ocean water onto the western AP shelf at ca. 9000 cal. yr B.P. This thesis has suggested that it was the critical combination of both early Holocene atmospheric warming acting to thin and weaken the ice shelf and then enhanced basal melting by UCDW that led to the absence of the ice shelf. The precise mechanisms linking climatic warming and the influx of warm deep water onto the continental shelf are unclear. It has been suggested (e.g. Shevenell and Kennett, 2002) that the tropical Pacific may have played an important role in modulating oceanographic changes on the western side

of the AP. Whether this teleconnection played an influential role in the initial retreat of GVI-IS, as yet, untested, although it has been demonstrated that links between the climatic record in ML and the southeastern Pacific exist at least on Holocene time scales. The re-formation of the ice shelf is also uncertain, although this thesis has speculated upon the environmental conditions immediately prior to ice shelf reformation and has also provided useful time-constraints over which the process take place. Fundamentally, the subsequent reformation of the ice shelf is a glaciological question and is dependent on rates of snow accumulation on fast ice and the behaviour of the input glaciers and how they transfer mass into George VI Sound. If the outlet glaciers flow unimpeded into the sound, eventually they will coalesce and enable the ice shelf to reform. In George VI Sound, which is a narrow channel this process could take place relatively rapidly. Finally, the absence of the ice shelf during this time interval suggests that early Holocene ocean-atmosphere variability in the Antarctic Peninsula was greater than that measured in recent decades.

Chapter 8

CONCLUSION: KEY FINDINGS, LIMITATIONS AND RECOMMENDATIONS FOR FUTURE WORK

8.1. Introduction

In Chapter 1, the overall aims of the thesis were defined as:

1. To provide a baseline study of the present-day limnology of Moutonnée and Ablation Lakes in order to develop a conceptual model for detecting ice shelf histories from the sediment record in epishelf lakes

2. To determine the Holocene history of George VI Ice Shelf.

To address the above aims, this thesis has sought:

1. To understand the present day dynamics of George VI Ice Shelf

2. The retrieval and analyses of contemporary water samples, lake surface sediments and lake catchment reference material to understand the contemporary lake environment and its depositional signature.

3. To develop a conceptual model for detecting ice shelf loss from the sediment record in epishelf lakes.

4. To retrieve and analyse sediment cores from Moutonnée and Ablation Lakes and to measure their physical, chemical and biological characteristics.

5. To interpret the sediment core data using the conceptual model and thereby identify periods of ice shelf presence or absence.

6. To investigate the mechanisms for any periods of ice shelf absence within the wider context of AP environmental change.

This chapter concludes this thesis by reviewing the main findings of the work in the context of the original aims stated above. It also reflects on limitations of this PhD study and makes recommendations for future research on the western Antarctic Peninsula.

8.2. Main findings of the PhD study

1. To understand the present day dynamics of George VI Ice Shelf

Chapter 3 provided a review of the dynamics of GVI-IS. It was noted that GVI-IS is the largest ice shelf on the western AP and its northern margin marks the southernmost limit of recent ice shelf retreat. The dynamics of the present day ice shelf are strongly influenced by the presence of warm Upper Circumpolar Deep Water (UCDW) beneath the ice shelf, which drives one of the highest basal melt rates in Antarctica. Presently, the mass balance of the ice shelf is maintained by input of glacier ice from the Antarctic Peninsula and Alexander Island. However, it is unknown how long UCDW has been on the shelf and for how long such high melt rates can be sustained.

One of the most interesting features about GVI-IS is the presence of a well-defined region of surface melt-ponding, which appears on the ice shelf surface each summer between 70°15' and 72°00'S. The distribution of melt-ponding remains something of an enigma but the ponds tend to occur where mean annual temperature lies between –6 °C and –10 °C and in areas where the ice shelf is under compression. The compressive nature of GVI-IS is also important since it means that it is unlikely to become susceptible to melt-pool induced collapse through crevasse deepening, a

hypothesis that has been used to explain the demise of other AP ice shelves (e.g. Larsen-B). It therefore seems likely that in the future the ice shelf will be more sensitive to changes in ocean circulation (e.g. intensity of UCDW) and to prolonged periods of atmospheric warming leading to ice shelf thinning by bottom melting and surface melting, respectively.

2. *The retrieve and analyses contemporary water samples, lake surface sediments and lake catchment reference material to understand the contemporary lake environment and its depositional signature.*
3. *To develop a conceptual model for detecting ice shelf loss from the sediment record in epishelf lakes.*

A key component of this research has been to provide new information on the present day limnology and sedimentary environment of ML and AB (Chapters 4 and 5). To achieve this, vertical water column chemistry measurements were taken over two successive field seasons and compared with earlier measurements taken in the 1970's (e.g. Heywood, 1977). In addition, a detailed analysis of surface sediments was undertaken. Analysis of the surface sediments included diatom, $\delta^{13}C_{org}$, C/N and grain-size parameters. The vertical water chemistry measurements revealed that the physical, chemical and biological limnology of the lakes is dominated by the position of the halocline. In ML, the position of the halocline has changed over the 30-year period, but it is not yet clear whether these changes are a result of ice shelf thinning or reflect seasonal changes (e.g. tides, or build-up of a summer meltwater layer). The lake water stratification also strongly influences the biological and chemical characteristics of the surface sediments. Samples nearest the ice shelf margin, and below the halocline, are generally characterised by the presence of marine diatoms and higher $\delta^{13}C_{org}$ values. Together with earlier limnological studies, these data have provided a 30-year perspective on the limnology of ML and AB, and new baseline data. Such data were available at Disraeli Fiord, an epishelf lake on the northern coast of Ellesmere Island, Arctic Canada, which displayed unique changes in its water chemistry prior to the break-up of the Ward Hunt Ice Shelf (Mueller et al., 2003). The data in this thesis can now be used to assess

possible future changes in lake water chemistry, which may be related to changes in GVI-IS.

The role of the ice shelf in maintaining stratification of the water columns in these lakes means that the lakes are uniquely placed to record periods of ice shelf loss both in the past (in their sediments) and in the future (though changes in water chemistry). As such the baseline data has been used to develop a conceptual model for detecting ice shelf loss in epishelf lakes, and has identified several proxies that are likely to change during ice shelf absence (Chapter 5). The conceptual model was necessary to provide the basis for the interpretation of the core-derived proxy records from the lakes. Specifically, the model shows that ice shelf loss is likely to cause significant changes in the biological (e.g. diatom), isotopic and elemental (e.g. $\delta^{13}C_{org}$ and C/N) and physical (e.g. grain-size/MS) signature of the lake sediments.

4. *To retrieve and analyse sediment cores from Moutonnée and Ablation Lakes and to measure their physical, chemical and biological characteristics.*

5. *To interpret the sediment core data using the conceptual model and thereby identify periods of ice shelf presence or absence.*

The project retrieved a number of sediment cores from Ablation and Moutonnée Lakes, including Moutonnée Lake (ML) core, Moutonnée Lake North Basin (MLNB) Ablation Lake 2 and 4. Two key findings have emerged from the analysis of these cores (Chapter 6, 7). Firstly, core results indicate a dramatic shift to open marine conditions in ML which has been interpreted using the conceptual model as representing a period of past ice shelf absence. During this period there is a clear marine depositional signature in the $\delta^{13}C_{org}$, C_{org} and N_{org} values, together with foraminifera, and diatoms showing that marine waters dominated the site and that there were both sea ice and open marine water conditions. There is a close replication of ecological and sedimentological conditions in the upper biological zone of the ML core and the biological zone in the MLNB core. This period of ice shelf loss has been constrained by 11 AMS ^{14}C dates performed on mono-specific

foraminifera samples. These dates suggest that GVI-IS was absent between ca. 8962 cal. (calibrated) yr B.P. and ca. 7945 cal. yr B.P. This early Holocene collapse immediately followed a period of maximum Holocene warmth that is recorded in some Antarctic ice cores and coincides with an influx of warmer ocean water onto the western Antarctic Peninsula shelf at ca. 9000 cal. yr B.P. The absence of the ice shelf during this time interval suggests that early Holocene ocean-atmosphere variability in the Antarctic Peninsula was greater than that measured in recent decades.

Secondly, the ML core also provides palaeoenvironmental data spanning the last ca. 8000 cal. years BP. Significantly, changes in the C/N profile in ML appear to reflect oceanic-atmospheric changes occurring in the tropical western Pacific, and specifically changes in the Peru-Chile Current (PCC) and the strength of the southern Westerlies (Lamy et al. 2001, 2002). The existence of a link between the western AP and the PCC has also been recently highlighted by Domack et al. (2003) based on palaeoenvironmental records from the Palmer Deep marine core. This raises the possibility that environmental changes (including the loss of GVI-IS) were in part driven by changes in the western tropical Pacific. However, the ability to test these ideas is limited, at present, by a poor core chronology for the upper 236 cm of the core.

6. *To investigate the mechanisms for any periods of ice shelf absence within the wider context of AP environmental change.*

Within the literature there are only two other studies that have provided a detailed reconstructions of past ice shelf variation on the AP. Pudsey and Evans (2001) provided a long-term perspective on the Holocene history of the Prince Gustav Ice Shelf and Domack et al. (2001) and Brachfeld et al. (2003) have provided a Holocene perspective on the Larsen-A Ice Shelf. Both records suggest that ice shelf retreat/absence occurred sometime between ca. 5000 and 2000 cal yr BP. Whilst these studies have provided compelling evidence for ice shelf absence, they have provided little information on the mechanisms leading to ice shelf collapse. A unique aspect of this thesis has been the detailed investigation of possible mechanisms that contribute to ice shelf collapse (Chapter 7). It has been previously

noted that the early Holocene collapse of GVI-IS followed a period of maximum Holocene warmth recorded in several Antarctic ice cores and the appearance of warm ocean water on the western shelf of the Antarctic Peninsula. It has been argued in this thesis that it was the critical combination of a prolonged period of atmospheric warming combined with the intrusion of warm water onto the continental shelf and beneath GVI-IS, which led to its early Holocene collapse. This thesis has also attempted to take this link one step further by using the $\delta^{18}O$ signature of benthic foraminifera to fingerprint the presence of UCDW and thereby provide a direct link between the appearance of UCDW and the collapse of GVI-IS. Although not conclusive, the $\delta^{18}O$ record shows a transition from warmer water (UCDW?) during the early stages of ice shelf loss to cooler water (Ice Shelf Water?), prior to the re-isolation of the epishelf lake presumably due to ice shelf re-formation. This provides an important step forwards in our understanding of the mechanisms, which control ice shelf collapse and reformation.

In summary, this thesis has successfully achieved its six objectives. In doing so it has achieved the twin aims of the thesis, namely:

1. To provide a baseline study of the present-day limnology of Moutonnée and Ablation Lakes in order to develop a conceptual model for detecting ice shelf histories from the sediment record in epishelf lakes.

2. To determine the Holocene history of George VI Ice Shelf.

8.3. Limitations of the PhD study

It is appropriate at this juncture to reflect on some of limitations of this PhD research, since they provide important constraints on the main findings of this work, and also useful pointers as to possible directions for future research.

8.3.1. Core chronology

One of the strengths of this study has been the ability to date well-preserved mono-specific foraminifera samples. The foraminiferal-based chronology has allowed this

thesis to accurately date the period of ice shelf absence, which so far has not been achieved in other marine-based studies. However, whilst a period of ice shelf absence has been well constrained by several ^{14}C dates on foraminifera, it has not been possible to obtain a core chronology for the upper 236 cm of the ML core, and specifically, the sediment-water interface and also the entire Ablation Lake core. The AIOM surface ages from ML and AB were erroneously old (ca. 15100 ^{14}C yr BP and 14180 ^{14}C yr BP) and are likely to reflect some form of contamination from old carbon. In an attempt to overcome this problem, a pilot ^{137}Cs and ^{210}Pb was attempted in ML in order to confirm a surface age of 0 yr BP for the core top. However, the pilot study revealed undetectable levels of ^{137}Cs and ^{210}Pb in core sediments from ML. Thus until the chronology of these cores is improved the palaeoclimatic interpretations, particularly those based on the upper 236 cm in the ML (Chapter 7) are chronologically limited. It is worth noting however, that such challenges are far from unique to this study and the issue of obtaining reliable core chronologies is a challenge faced by all marine (and some terrestrial) palaeoenvironmental studies on the Antarctic Peninsula. This study has provided a more robust core chronology than many other Antarctic investigations because it has dated monospecific foraminifera samples, rather than the AIOM used in many other foram-barren studies.

8.3.2.Assessing the spatial pattern of ice shelf collapse in George VI Sound

Whilst the data presented in this thesis provides a robust record of ice shelf loss at Moutonnée Lake, it does not provide clear constraints on the spatial nature of ice shelf presence or absence in George VI Sound. As noted in Chapter 7, there is some evidence for a period of open water conditions farther south dated to ca. 6500 cal yr BP, 1500 years after ice shelf absence at Moutonnée Lake. This implies one of three things. First there is a variable radiocarbon marine reservoir between the Ablation Point Massif and Two Step Cliffs, leading to different ages for the same period of ice shelf loss. Second, collapse and reformation of George VI Ice Shelf was spatially variable, with collapse occurring much earlier at ML. This is supported to a certain extent by the fact that the ice shelf moraine does not contain a uniform distribution of fossil barnacles along the coast of Alexander Island. Finally, that the ecology of the dated fossils is poorly understood.

It is worth noting here however, that an attempt to extend the spatial extent of the data presented in this study is in progress. As part of the wider NERC-funded project the group (D.A Hodgson, M.J. Bentley, J.A. Smith) did retrieve a lake sediment in 2001-02 from 'Citadel-Bastion Lake' (72°00'S, 68°29'W) (Fig. 2.1b). Citadel-Bastion Lake is situated ~ 125 km south of the Ablation Point Massif, and approximately 10 km south of Two Step Cliffs on Alexander Island. It is a perennially ice covered, entirely fresh water lake, dammed on its northern side by the Saturn glacier, which lies approximately 1 km upstream of the current position of George VI Ice Shelf. The > 3.5 m long sediment record from Citadel-Bastion Lake shows that the lake has remained freshwater dominated and has not experienced a marine incursion during the period of deposition. Furthermore, the core could not be reliably dated with ^{14}C, although other dating techniques are being investigated (Roberts, unpublished data). Importantly however, one of our key findings was that although it has a similar appearance to some of the epishelf lakes further north, survey data in 2003 confirmed that the lake is 5 m above sea level. As a result, it is not an epishelf lake and so the loss of GVI-IS in the past will not have left a signature in the sedimentary record.

8.3.3 Ablation Lake record

The absence of a detailed record of ice shelf collapse from Ablation Lake suggests that we did not core the entire sedimentary sequence from this lake. It is likely therefore that both records from Ablation Lake are equivalent to some part of the upper 236 cm in the ML core and/or the upper 125 cm in the MLNB core in relative age. However, the available proxy data do not show any degree of correlation between the two lakes. This suggests that during ice shelf presence, the records in the two lakes may be influenced by local valley-scale changes. However, until a better core chronology from Ablation Lake is obtained it remains difficult to test these ideas.

8.3.4. Mechanisms for ice shelf collapse

The data presented in this thesis has enabled key ideas about the factors which contributed to the early Holocene disappearance of GVI-IS to be investigated. Specifically, this thesis has explored the possibility that UCDW played an important role in the disappearance of the ice shelf, through the $\delta^{18}O$ signature of benthic foraminifera. However, this evidence would be considerably strengthened by additional $\delta^{18}O$ and $\delta^{13}C$ data for both ocean water (i.e. different water masses) and foraminiferal data from the AP region with which to compare the ML record.

8.4. Recommendations for future work

8.4.1. Improving core chronologies in Moutonnée and Ablation Lakes

A recommendation for future research would be to investigate the sources of old carbon contamination in sediments from ML and AB that have contributed to old AIOM ages. For instance, it has already been noted that algal flakes within the sediment in the ML core yielded old (19720 ^{14}C yr BP) ^{14}C ages. If one can isolate the old carbon fraction(s) within the core, it may be possible to obtain reliable ages (e.g. biomarker-specific dating as is being developed for other Antarctic samples at Woods Hole Oceanographic Institute and University of Arizona). It may also be possible to apply alternative dating techniques to the sediment cores from ML and AB such as the geomagnetic techniques recently developed by Brachfeld et al. (2003).

8.4.2. Investigate the spatial extent of the early Holocene collapse of George VI Ice Shelf

As noted above, the data presented in this thesis does not fully constrain the spatial extent of the early Holocene collapse of George VI Ice Shelf. As such the acquisition of sediment cores from along George VI Sound would help to further

elucidate the spatial extent of ice shelf collapse as would a more systematic study of the ice shelf moraines for marine shells. This type of study could be combined with oceanographic studies, which are concerned with understanding the circulation beneath ice shelves (e.g. Hemmer and Harris, 2003). There have been previous suggestions (A. Jenkins, pers. comm.) to (hot-water) drill through the ice shelf for glaciological and oceanographic research but this thesis has shown that it would be useful to add sediment coring to the objectives of such a study.

8.4.3. Moutonnée Lake – long term monitoring

To judge whether the changes observed in the position of the halocline in Moutonnée Lake are significant, future work should aim to monitor the lake water column chemistry and tides in ML (e.g. permanent moorings). To some extent this might act as a predictive tool for assessing changes in the ice shelf and to provide an early warning system for any future ice shelf collapse.

8.4.5. Ablation Lake – a longer record

It is likely that only a partial sedimentary sequence was extracted from Ablation Lake. Whilst this does not undermine the case for ice shelf loss recorded in Moutonnée Lake, a comparable record from Ablation Lake would certainly strengthen further the argument for ice shelf loss. Thus a recommendation for future work would involve the retrieval of longer cores from Ablation Lake.

8.4.6. Reconstructing Ice Shelf histories in Antarctica

As noted above, at present there are relatively few studies that have successfully demonstrated the past behaviour of Antarctic Peninsula ice shelves (e.g. Pudsey and Evans, 2001; Domack et al., 2001; Brachfeld et al., 2003). As a result there is huge potential to extend the techniques developed in this thesis and those previously established in East Antarctica (e.g. Hemer and Harris, 2003) to obtain detailed histories of many Antarctic ice shelves and glaciers. This is particularly important if we are to judge the significance of the early Holocene collapse of George VI Ice Shelf and investigate further the forcing mechanism. Antarctic Peninsula ice shelf

collapse seems set to continue, with implications for global sea level, and so it is vitally important that we continue to use techniques, such as those developed in this thesis, to provide the clearest possible understanding of past Antarctic ice shelf variability and its driving mechanisms.

References

Andersen, T. F. and Arthur, M. A. (1993). Stable isotopes of oxygen and carbon and their application to sedimentological and palaeoenvironmental problems. *In* "Stable isotopes in Sedimentary Geology." SEPM Short Course 10.

Anderson, J. B. (1975). Ecology and distribution of foraminifera in the Weddell Sea of Antarctica. *Micropaleontology* 21, 69-96.

Anderson, J. B. and Bartek, L. R. (1992). Cenozoic glacial history of the Ross Sea revealed by intermediate resolution seismic reflection data combined with drill site information. *In* "The Antarctic Palaeoenvironment: A perspective on global change." (J.P. Kennett and D.A. Warnke, Eds.), pp. 231-62. Antarctic Research Series 56, American Geophysical Union.

Anderson, J. B. andrews, B. A., Bartek, L. R. and Truswell, E. M. (1991). Petrology and palynology of glacial sediments: implications for subglacial geology of the eastern Weddell Sea, Antarctica. *In* "Geological Evolution of Antarctica." (M. R. A. Thompson, J. A. Crame, and J. W. Thompson, Eds.), pp. 231-235. Cambridge University Press, New York.

Anderson, J. B., Shipp, S. S., Lowe, A. L., Wellner, J. S. and Mosola, A. B. (2002). The Antarctic Ice Sheet during the Last Glacial Maximum and its subsequent retreat history: a review. *Quaternary Science Reviews* 21, 49-70.

Andrews, J. T., Domack, E. W., Cunningham, W. L., Leventer, A., Licht, K. J., Jull, A. J. T., DeMaster, D. J. and Jennings, A. E. (1999). Problems and possible solutions concerning radiocarbon dating of surface marine sediments, Ross Sea, Antarctica. *Quaternary Research* 52, 206-216.

Appleby, P. G., Jones, V. J. and Ellis-Evans, J. C. (1995). Radiometric Dating of Lake-Sediments from Signy Island (Maritime Antarctic) - Evidence of recent climatic-change. *Journal of Paleolimnology* 13, 179-191.

Aristarain, A. J., Jouzel, J. and Lorius, C. (1990). A 400 years isotope record of the Antarctic Peninsula Climate. *Geophysical Research Letters* 17, 2369-2372.

Arrigo, K. R., G. R. DiTullio, et al. (2000). Phytoplankton taxonomic variability in nutrient utilization and primary production in the Ross Sea. *Journal of Geophysical Research-Oceans* 105(C4): 8827-8845.

Baker, P. A., Seltzer, G. O., Fritz, S. C., Dunbar, R. B., Grove, M. J., Tapia, P. M., Cross, S. L., Rowe, H. D. and Broda, J. P. (2001). The history of South American tropical precipitation for the past 25,000 years. *Science* 291, 640-643.

Bamber, J. L., Vaughan, D. G. and Joughin, I. (2000). Widespread complex flow in the interior of the Antarctic Ice Sheet. *Science* 287, 1248-1250.

Banfield, L. A. and Anderson, J. B. (1995). Seismic facies investigation of the late Quaternary glacial history of Bransfield Basin, Antarctica. *In* "Geology and Seismic Stratigraphy of the Antarctic Margin." (A. K. Cooper, P. F. Barker, and G. Branncolini, Eds.), pp. 123-140. Antarctic Research Series. American Geophysical Union, Washington, D.C.

Barcena, M. A., Gersonde, R., Ledesma, S., Fabres, J., Calafat, A. M., Canals, M., Sierro, F. J. and Flores, J. A. (1998). Record of Holocene glacial oscillations in Bransfield Basin as revealed by siliceous microfossil assemblages. *Antarctic Science* 10, 269-285.

Bard, E., Hamelin, B., Fairbanks, R. G. and Zindler, A. (1990). Calibration of the C-14 Timescale over the past 30,000 years using mass-spectrometric U-Th ages from Barbados corals. *Nature* 345, 405-410.

Barker, P. F. (1982). The Cenozoic subduction history of the Pacific margin of the Antarctic Peninsula: ridge crest-trench interactions. *Journal of the Geological Society, London* 139, 787-801.

Barker, P., Fontes, J. C., Gasse, F. and Druart, J. C. (1994). Experimental dissolution of diatom silica in concentrated salt- solutions and implications for paleoenvironmental reconstruction. *Limnology and Oceanography* 39, 99-110.

Baroni, C. and Orombelli, G. (1991). Holocene raised beaches at Terra Nova Bay, Victoria Land, Antarctica. *Quaternary Research* 36, 157-177.

Baroni, C. and Orombelli, G. (1994). Abandoned penguin rookeries as Holocene paleoclimatic indicators in Antarctica. *Geology* 22, 23-26.

Baroni, C. and Orombelli, G. (1994). Holocene glacier variations in the Terra Nova Bay area (Victoria Land, Antarctica). *Antarctic Science* 6, 497-505.

Bart, P. J. and Anderson, J. B. (1996). Seismic expression of depositional sequences associated with expansion and contraction of ice sheets on the northwestern Antarctic Peninsula continental shelf. *In* "Geology of siliciclastic seas." (M. De Batist, and P. Jacobs, Eds.), pp. 171-186. Geological Society London.

Battarbee, R. W. (1986). Diatom Analysis. *In* "Handbook of Holocene Palaeoecology and Palaeohydrology." (B. E. Berglund, Ed.), pp. 527-570. John Wiley and Son Ltd., New York.

Baum, S. K. (2001). Glossary of Physical Oceanography and Related Disciplines. Department of Oceanography, Texas A&M University.

Bell, C. M. (1973). Structural geology of parts of Alexander Island. *British Antarctic Survey Bulletin* 41-42, 43-58.

Benson, L. V., Meyers, P. A. and Spencer, R. J. (1991). Change in the size of Walker Lake over the past 5000 years. *Palaeogeography, Palaeoclimatology, Palaeoecology* 81, 189-214.

Bentley, M. J. (1999). Volume of Antarctic Ice at the Last Glacial Maximum, and its impact on global sea level change. *Quaternary Science Reviews* 18, 1569-1595.

Bentley, M. J. and Anderson, J. B. (1998). Glacial and marine geological evidence for the ice sheet configuration in the Weddell Sea-Antarctic Peninsula Region during the Last Glacial Maximum. *Antarctic Science* 10, 307-323.

Bentley, M. J., Hodgson, D. A., Smith, J. A. and Cox, N. J. (2005). Preliminary relative sea level curves for South Shetlands and Marguerite Bay regions, Antarctic Peninsula. *Quaternary Science Reviews* 24, 1203-1216.

Berger, A. and Loutre, M. F. (1991). Insolation values for the climate of the last 10000000 years. *Quaternary Science Reviews* 10, 297-317.

Berkman, P. A. and Forman, S. L. (1996). Pre-bomb radiocarbon and the reservoir correction for calcareous marine species in the Southern Ocean. *Geophysical Research Letters* 23, 363-366.

Berkman, P. A. Andrews, J. T., Björck, S., Colhoun, E. A., Emslie, S. D., Goodwin, I. D., Hall, B. L., Hart, C. P., Hirakawa, K., Igarashi, A., Ingólfsson, O., López-Martínez, J., Lyons, W. B., Mabin, M. C.

G., Quilty, P. G., Taviani, M. and Yoshida, Y. (1998). Circum-Antarctic coastal environmental shifts during the Late Quaternary reflected by emerged marine deposits. *Antarctic Science* 10, 345-362.

Bird, M. I., Chivas, A. R., Radnell, C. J. and Burton, H. R. (1991). Sedimentological and Stable-Isotope Evolution of Lakes in the Vestfold Hills, Antarctica. *Palaeogeography, Palaeoclimatology, Palaeoecology* 84, 109-130.

Birkenmajer, K. (1981). Lichenometric dating of raised marine beaches at Admiralty Bay, King George Island (South Shetland Island, West Antarctica). *Bulletin de l'Academie Polonaise des Sciences* 29, 119-127.

Bishop, J. F. and Walton, J. L. W. (1977). Problems encountered when monitoring tidal movements in extremely cold conditions. *Polar Record* 18, 502-505.

Bishop, J. F. and Walton, J. L. W. (1981). Bottom melting under George VI Ice Shelf, Antarctica. *Journal of Glaciology* 27, 429-447.

Björck, S., Hakansson, H., Zale, R., Karlen, W. and Johnson, B., L. (1991a). A late Holocene lake sediment sequence from Livingston Island, S. Shetland Islands. *Antarctic Science* 3, 61-72.

Bjorck, S., Malmer, N., Hjort, C., Sandgren, P., Ingolfsson, O., Wallen, B., Smith, R. I. L. and Jonsson, B. L. (1991b). Stratigraphic and paleoclimatic studies of a 5500-year-old moss bank on Elephant Island, Antarctica. *Arctic and Alpine Research* 23, 361-374.

Björck, S., Olsson, S., Ellis-Evans, J. C., Hakansson, H., Humlum, O. and de Lirio, J. (1996). Late Holocene climate records from lake sediments on James Ross Island. *Palaeogeography, Palaeoclimatology, Palaeoecology* 113, 195-220.

Blott, S. J. and Pye, K. (2001). GRADISTAT: a grain size distribution and statistics package for the analysis of unconsolidated sediments. *Earth Surface Processes and Landforms* 26, 1237-1248.

Blunier, T., Chappellaz, J., Schwander, J., Dallenbach, A., Stauffer, B., Stocker, T. F., Raynaud, D., Jouzel, J., Clausen, H. B., Hammer, C. U. and Johnsen, S. J. (1998). Asynchrony of Antarctic and Greenland climate during the last glacial period. *Nature* 394, 739-743.

Blunier, T., Schwander, J., Stauffer, B., Stocker, T., Dallenbach, A., Indermuhle, A., Tschumi, J., Chappellaz, J., Raynaud, D. and Barnola, J. M. (1997). Timing of the Antarctic cold reversal and the atmospheric CO2 increase with respect to the Younger Dryas event. *Geophysical Research Letters* 24, 2683-2686.

Bond, G., Showers, W., Cheseby, M., Lotti, R., Almasi, P., deMenocal, P., Priore, P., Cullen, H., Hajdas, I. and Bonani, G. (1997). A pervasive millennial-scale cycle in North Atlantic Holocene and glacial climates. *Science* 278, 1257–1266.

Bordovskiy, O. K. (1965). Accumulation and transformation of organic substances in marine sediments. *Marine Geology* 3, 3-114.

Bormann, P. and Fritzche, D. (1995). Queen Maud Land, East Antarctica and its surroundings., pp. 448. Justus Perthes Gotha, Darmstadt.

Brachfeld, S., Acton, G. D., Guyodo, Y. and Banerjee, S. K. (2000). High-resolution paleomagnetic records from Holocene sediments from the Palmer Deep, Western Antartic Peninsula. *Earth and Planetary Science Letters* 181, 429-441.

Brachfeld, S., Domack, E., Kissel, C., Laj, C., Leventer, A., Ishman, S., Gilbert, R., Camerlenghi, A. and Eglinton, L. B. (2003). Holocene history of the Larsen-A Ice Shelf constrained by geomagnetic paleointensity dating. *Geology* 31, 749-752.

British Antarctic Survey (1982). British Antarctic Territory, Geological Map, 1:500,000, Palmer Land, Series BAS 500G, Sheet 5. British Antarctic Survey, Cambridge.

Broecker, W. S. (1963). Radiocarbon ages of Antarctic materials. *Polar Record* 11, 472-473.

Broecker, W. S. (1998). Paleoceanographic circulation during the last deglaciation: A bipolar seesaw? *Paleoceanography* 13, 119-121.

Broecker, W. S., Peng, T. H., Ostlund, G. and Stuiver, M. (1985). The Distribution of Bomb Radiocarbon in the Ocean. *Journal of Geophysical Research-Oceans* 90, 6953-6970.

Bromwich, D. H. and Rogers, A. N. (2001). El-Nino-Southern Oscillation Modulation of West Antarctic Precipitation. *In* "The West Antarctic Ice Sheet, Behaviour and Environment." (R. B. Alley, and R. Bindschadler, Eds.). AGU, Antarctic Research Series, Washington DC.

Canals, M., Urgeles, R. and Calafat, A. M. (2000). Deep sea-floor evidence of past ice streams off the Antarctic Peninsula. *Geology* 28, 31-34.

Cartwright, D. E. (1980). Analysis of British Antarctic Survey tidal records. *British Antarctic Survey Bulletin* 49, 167-179.

Chappell, J., Omura, A., Esat, T. M., McCulloch, M., Pandolfi, J., Ota, Y. and Pillans, B. (1996). Reconciliation of late Quaternary sea levels derived from coral terraces at Huon Peninsula with deep sea oxygen isotope records. *Earth and Planetary Science Letters* 141, 227-236.

Charles, C. D. and Fairbanks, R. G. (1990). Glacial to interglacial changes in the isotopic gradient of the southern ocean surface waters. *In* "Geological history of the polar oceans: Arctic vs. Antarctic." (U. Bleil, and T. Theide, Eds.), pp. 519-538. Kluwer Academic Publishers.

Charles, C. D., Lynch-Stieglitz, J., Ninnemann, U. S. and Fairbanks, R. G. (1996). Climate connections between the hemisphere revealed by deep sea sediment core ice core correlations. *Earth and Planetary Science Letters* 142, 19-27.

Chen, T. C. and Yen, M. C. (1997). Interdecadal variations of the Southern Hemisphere circulation. *Journal of Climate* 10, 805-812.

Ciais, P., Jouzel, J., Petit, J. R., Lipenkov, V. and White, J. W. C. (1994). Holocene temperature variations inferred from six Antarctic ice cores. *Annals of Glaciology* 20, 427-436.

Clapperton, C. (1990). Quaternary Glaciations in the Southern Ocean and Antarctic Peninsula area. *Quaternary Science Reviews* 7, 229-252.

Clapperton, C. M. and Sugden, D. E. (1982). Late Quaternary glacial history of George VI Sound area, West Antarctica. *Quaternary Research* 18, 243-267.

Clapperton, C. M. and Sugden, D. E. (1983). Geomorphology of the Ablation Point massif, Alexander Island, Antarctica. *Boreas* 12, 125-135.

Clapperton, C. M. and Sugden, D. E. (1988). Holocene glacier fluctuations in South-America and Antarctica. *Quaternary Science Reviews* 7, 185-198.

Clapperton, C. M., Sugden, D. E., Birnie, J. and Wilson, M. J. (1989). Late-Glacial and Holocene Glacier Fluctuations and Environmental-Change on South Georgia, Southern-Ocean. *Quaternary Research* 31, 210-228.

Clement, A. C., Seager, R. and Cane, M. A. (1999). Orbital controls on the El Nino/Southern Oscillation and the tropical climate. *Paleoceanography* 14, 441-456.

Clement, A. C., Seager, R. and Cane, M. A. (2000). Suppression of El Nino during the mid-Holocene by changes in the Earth's orbit. *Paleoceanography* 15, 731-737.

Clesceri, L. S., Greenberg, A. E. & Eaton, A. D. *Standard Methods for the Examination of Water and Wastewater (20th Edition)* (American Public Health Association, American Water Works Association and Water Environment Federation, 1998).

Colhoun, E. A., Mabin, M. C. G., Adamson, D. A. and Kirk, R. M. (1992). Antarctic ice volume and contribution to sea level fall at 20,000 yr BP from raised beaches. *Nature* 358, 316-318.

Convey, P. (2001). Terrestrial Ecosystem Response to Climate Changes in the Antarctic. *In* "Fingerprints of Climate Change - Adapted Behaviour and Shifting Species Range." (G.-R. Alther, C. A. Burga, and P. J. Edwards, Eds.), pp. 17-42. Kluwer, New York.

Corliss, B. H. (1983). Distribution of Holocene deep-sea benthonic foraminifera in the southwest Indian Ocean. *Deep-Sea Research* 30, 95-117.

Corliss, B. H. and Chen, C. (1988). Morphotype patterns of Norwegian deep-sea benthonic foraminifera and ecological implications. *Geology* 16, 716-719.

Corr, H. F. J., Jenkins, A., Nicholls, K. W. and Doake, C. S. M. (2002). Precise measurement of changes in ice-shelf thickness by phase- sensitive radar to determine basal melt rates. *Geophysical Research Letters* 29, (8).

Crabtree, R. D., Storey, B. C. and Doake, C. S. M. (1985). The structural evolution of George VI Sound, Antarctic Peninsula. *In* "Geophysics of the Polar Regions." (E. S. Husebye, G. L. Johnson, and Y. Kristoffersen, Eds.), pp. 431-442. *Tectonophysics*.

Craig, H. (1961). Isotopic variations in meteoric waters. *Science* 133, 1833-1834.

Craig, H. and Gordon, L. (1965). Deuterium and oxygen-18 variations in the ocean and marine atmosphere. *In* "Stable isotopes in oceanographic studies and palaeotemperatures." (E. Tongiorgi, Ed.). pp. 78. CNR, Pisa.

Cremer, H. (1999). Distribution patterns of diatom surface sediment assemblages in the Laptev Sea (Arctic Ocean). *Marine Micropaleontology* 38, 39-67.

Cremer, H., Roberts, D., McMinn, A., Gore, D. and Melles, M. (2003). The Holocene diatom flora of marine bays in the Windmill Islands, East Antarctica. *Botanica Marina* 46, 82-106.

Cremer, H., Gore, D., Hultzsch, N., Melles, M. and Wagner, B. (2004). The diatom flora and limnology of lakes in the Amery Oasis, East Antarctica. *Polar Biology* 27, 513-531.

Crespin, I. (1960). Some recent foraminifera from Vestfold Hills, Antarctica. *Science reports of the Tohoku University (2nd Series): Special Volume, 4*, 19-31.

Crespin, J., Crosta, X., Masson-Delmotte, V. and Leventer, A. (2004). Evolution of Holocene reservoir ages off Adelie Land, East Antarctica (abstract). *8th International conference on paleoceanography, Biarittz.*

Cullather, R. I., Bromwich, D. H. and VanWoert, M. L. (1996). Interannual variations in Antarctic precipitation related to El Nino southern oscillation. *Journal of Geophysical Research-Atmospheres* 101, 19109-19118.

Cunningham, W. L. and Leventer, A. (1998). Diatom assemblages in surface sediments of the Ross Sea: relationship to present oceanographic conditions. *Antarctic Science* 10, 134-146.

Cunningham, W. L., Leventer, A. andrews, J. T., Jennings, A. E. and Licht, K. J. (1999). Late Pleistocene-Holocene marine conditions in the Ross Sea, Antarctica: evidence from the diatom record. *Holocene* 9, 129-139.

Curl, J. E. (1980). A glacial history of South Shetland Islands, Antarctica. *Ohio State University, Institute of Polar Studies Report* 63, 47pp.

Curry, W. B., Duplessy, J. C., Labeyrie, L. and Shackleton, N. J. (1988). Changes in the distribution of d13C of deep water CO2 between the last glaciation and the Holocene. *Paleoceanography* 3, 317-341.

Dansgaard, W. (1964). Stable isotopes in precipitation. *Tellus* 16, 436-468.

Dayton, P. K., Newman, W. A. and Oliver, J. (1982). The Vertical Zonation of the Deep-Sea Antarctic Acorn Barnacle, Bathylasma-Corolliforme (Hoek) - Experimental Transplants from the Shelf into Shallow-Water. *Journal of Biogeography* 9, 95-109.

De Angelis, H. and Skvarca, P. (2003). Glacier surge after ice shelf collapse. *Science* 299, 1560-1562.

Dean, W. E. (1974). Determination of carbonate and organic matter in calcareous sediments and sedimentary rocks by Loss on Ignition: comparison with other methods. *Journal of Sedimentary Petrology* 44, 242-248.

Dearing, J. A. (1999). Holocene environmental change from magnetic proxies in lake sediments. *In* "Quaternary Climates, Environments, and Magnetism." (B. A. Maher, and R. Thompson, Eds.). Cambridge University Press, Cambridge.

Dell, R. K. (1990). Antarctic Mollusca: with special reference to the fauna of the Ross Sea. *Bulletin of the Royal Society of New Zealand* 27, 311.

Doake, C. S. M. (1978). Dissipation of tidal energy by Antarctic ice shelves. *Nature* 275, 304-305.

Doake, C. S. M. and Vaughan, D. G. (1991). Rapid disintegration of the Wordie Ice Shelf in response to atmospheric warming. *Nature* 350, 328-330.

Doake, C. S. M., Corr, H. F. J., Rott, H., Skvarca, P. and Young, N. (1998). Breakup and conditions for stability of the northern Larsen Ice Shelf, Antarctica. *Nature* 391, 778-780.

Domack, E. W. and Ishman, S. (1993). Oceanographic and Physiographic Controls on Modern Sedimentation within Antarctic Fjords. *Geological Society of America Bulletin* 105, 1175-1189.

Domack, E. W. and McClennen, C. E. (1996). Accumulation of glacial marine sediments in fjords of the Antarctic Peninsula and their use as late Holocene paleoenvironmental indicators. *In* "Foundations for Ecological Research West of the Antarctic Peninsula." (R. M. Ross, E. E. Hofmann, and L. B.

Quetin, Eds.), pp. 135-154. American Geophysical Union, Antarctic Research Series, Washington, D.C.

Domack, E. W. and Mayewski, P. A. (1999). Bi-polar ocean linkages: evidence from late-Holocene Antarctic marine and Greenland ice-core records. *Holocene* 9, 247-251.

Domack, E. W., Jull, A. J. T. anderson, J. B., Linick, T. W. and Williams, C. R. (1989). Application of tandem accelerator mass-spectrometer dating to Late Pleistocene-Holocene sediments of the East Antarctic continental shelf. *Quaternary Research* 31, 277-287.

Domack, E. W., Mashiotta, T. A. and Burkley, L. A. (1993). 300-year cyclicity in organic matter preservation in Antarctic fjord sediments. *In* "The Antarctic Palaeoenvironment: a perspective on global change." pp. 265-272. Antarctic Research Series.

Domack, E. W., Ishman, S. E., Stein, A. B., McClennen, C. E. and Jull, A. J. T. (1995). Late Holocene Advance of the Muller Ice Shelf, Antarctic Peninsula - Sedimentological, Geochemical and Paleontological Evidence. *Antarctic Science* 7, 159-170.

Domack, E. W., Taviani, M. and Rodriguez, A. (1999). Recent sediment remolding on a deep shelf, Ross Sea: implications for radiocarbon dating of Antarctic marine sediments. *Quaternary Science Reviews* 18, 1445-1451.

Domack, E., Leventer, A., Dunbar, R., Taylor, F., Brachfeld, S. and Sjunneskog, C. (2001). Chronology of the Palmer Deep site, Antarctic Peninsula: a Holocene palaeoenvironmental reference for the circum-Antarctic. *Holocene* 11, 1-9.

Domack, E., Burnett, A. and Leventer, A. (2003a). Environmental Setting of the Antarctic Peninsula. *In* "Antarctic Peninsula Climate Variability: Historical and Paleoenvironmental Perspectives." (E. Domack, A. Leventer, A. Burnett, R. Bindschadler, P. Convey, and M. Kirby, Eds.), pp. 1-13. American Geophysical Union, Washington.

Domack, E., Leventer, A., Root, S., Ring, J., Williams, E., Carlson, D., Hirshorn, E., Wright, W., Gilbert, G. and Burr, G. (2003b). Marine Sedimentary Record of Natural Environmental Variability and Recent Warming in the Antarctic Peninsula. *In* "Antarctic Peninsula Climate Variability: Historical and Paleoenvironmental Perspectives." (E. Domack, A. Leventer, A. Burnett, R. Bindschadler, P. Convey, and M. Kirby, Eds.). American Geophysical Union, Washington.

Donegan, D. and Schrader, H. (1982). Biogenic and abiogenic components of laminated and hemipelagic sediments in the central Gulf of California. *Marine Geology* 48, 215-237.

Donnici, S. and Barbero, R. S. (2002). The benthic foraminiferal communities of the northern Adriatic continental shelf. *Marine Micropaleontology* 44, 93-123.

Doran, P. T., Wharton, R. A. and Lyons, W. B. (1994a). Paleolimnology of the McMurdo Dry Valleys, Antarctica. *Journal of Paleolimnology* 10, 85-114.

Doran, P.T., Wharton, R. A., Spaulding, S.A. and Foster, J.S., (1994b). McMurdo LTER: Paleolimnology of Taylor Valley, Antarctica. *Antarctic Journal of United States*, 234-237.

Doran, P. T., McKay, C. P., Meyer, M. A. andersen, D. T., Wharton, R. A. and Hastings, J. T. (1996). Climatology and implications for perennial lake ice occurrence at Bunger Hills oasis, east Antarctica. *Antarctic Science* 8, 289-296.

Doran, P. T., Wharton, R. A., Des Marais, D. J. and McKay, C. P. (1998). Antarctic paleolake sediments and the search for extinct life on Mars. *Journal of Geophysical Research-Planets* 103, 28481-28493.

Doran, P. T., Berger, G. W., Lyons, W. B., Wharton, R. A., Davisson, M. L., Southon, J. and Dibb, J. E. (1999). Dating Quaternary lacustrine sediments in the McMurdo Dry Valleys, Antarctica. *Palaeogeography, Palaeoclimatology, Palaeoecology* 147, 223-239.

Doran, P. T., Wharton, R. A., Lyons, W. B., Des Marais, D. J. and Andersen, D. T. (2000). Sedimentology and geochemistry of a perennially ice-covered epishelf lake in Bunger Hills Oasis, East Antarctica. *Antarctic Science* 12, 131-140.

Douglas, R. G. and Woodruff, F. (1981). Deep sea benthic foraminifera. *In* "The oceanic lithosphere." (C. Emiliani, Ed.), pp. 1233-1327. Wiley-Interscience, New York.

Drewry, D. J. and Cooper, A. P. R. (1981). Processes and models of Antarctic glaciomarine sedimentation. *Annals of Glaciology* 2, 117-122.

Dunbar, R. B. and Leventer, A. (1992). Seasonal variation in carbon isotopic composition of Antarctic sea ice and open water plankton communities. *Antarctic Journal of the United States* 27, 79-81.

Duplessy, J. C., Lalou, C. and Vinot, A. C. (1970). Differential isotopic fractionation in benthic foraminifera and palaeotemperatures reassessed. *Science* 168, 250-251.

Duplessy, J. C., Moyes, J. and Pujol, C. (1980). Deep water formation in the North Atlantic Ocean during the last ice age. *Nature* 286, 479-482.

Duplessy, J. C., Shackleton, N. J., Matthews, R. K., Prell, W., Ruddiman, W. F., Caralp, M. H. and Hendy, C. H. (1984). ^{13}C record of benthic foraminifera in the last interglacial ocean: implications for the carbon cycle and the global deep water circulation. *Quaternary Research* 21, 225-243.

Echols, R. J. (1971). Distribution of foraminifera in sediments of the Scotia Sea area. *In* "Antarctic Oceanology." (J. L. Reid, Ed.), pp. 93-168. Antarctic Research Series.

Eglinton, T. I., Benitez-Nelson, B. C., Pearson, A., McNichol, A. P., Bauer, J. E. and Druffel, E. R. M. (1997). Variability in radiocarbon ages of individual organic compounds from marine sediments. *Science* 277, 796-799.

Ehlenringer, J. R., Hall, A. E. and Farquar, G. D. (1993). "Stable isotopes and plant Carbon-Water relationships." Academic Series.

Elliot, M. H. (1974). Stratigraphy and sedimentary petrology of the Ablation Point area, Alexander Island. *British Antarctic Survey Bulletin* 39, 87-113.

Emeis, K. C., Struck, U., Blanz, T., Kohly, A. and Voss, M. (2003). Salinity changes in the central Baltic Sea (NW Europe) over the last 10 000 years. *Holocene* 13, 411-421.

Emslie, S. D. (2001). Radiocarbon dates from abandoned penguin colonies in the Antarctic Peninsula region. *Antarctic Science* 13, 289-295.

Fabres, J., Calafat, A., Canals, M., Barcena, M. A. and Flores, J. A. (2000). Bransfield Basin fine-grained sediments: late-Holocene sedimentary processes and Antarctic oceanographic conditions. *Holocene* 10, 703-718.

Fahrbach, E., Rohardt, G., Scheele, N., Schroder, M., Strass, V. and Wisotzki, A. (1995). Fornation and discharge of deep and bottom water in the northwestern Weddell Sea. *Journal of Marine Research* 53, 515-538.

Fleming, W. L. S., Stephenson, A., Roberts, B. B. and Bertram, G. C. L. (1938). Notes on the scientific work of the British Graham Land expedition. *Geographical Journal* 91, 508-532.

Folk, R. L. and Ward, W. C. (1957). Brazos River bar: a study in the significance of grain size parameters. *Journal of Sedimentary Petrology* 27, 3-26.

Folland, C., Karl, T., Christy, J., Clarke, R., Gruza, G., Jouzel, J., Mann, M. E., Oerlemans, J., Salinger, M. and Wang, S.-W. (2001). Observed Climate Variability and Change. *In* "Climate Change 2001: The Scientific Basis." (J. T. Houghton, Y. Ding, D. J. Griggs, M. Noguer, P. J. van den Linden, X. Dai, K. Maskell, and A. C. Johnson, Eds.), pp. 99-182. Cambridge University Press, Cambridge.

Fontugne, M. R. and Jouanneau, J. M. (1987). Modulation of the particulate organic carbon flux to the ocean by a macrotidal estuary — evidence from measurements of carbon isotopes in organic matter from the Gironde system. *Estuarine, Coastal Shelf Science* 24, 377-387.

Fowbert, J. A. and Lewis-Smith, R. I. (1994). Rapid population increases in native vascular plants in the Argentine Islands, Antarctic Peninsula. *Arctic and Alpine Research* 26, 290-296.

Fox, A. J. and Cooper, A. P. R. (1998). Climate-change indicators from archival aerial photography of the Antarctic Peninsula. *Annals of Glaciology*, 27, 636-642.

Fox, A. J. and Vaughan, D. G. (in press). The retreat of the Jones Ice Shelf, Antarctic Peninsula. *Journal of Glaciology.*

Fraser, W. R., Trivelpiece, W. Z., Ainley, D. G. and Trivelpiece, S. G. (1992). Increases in Antarctic Penguin Populations - Reduced competition with whales or a loss of sea ice due to environmental warming. *Polar Biology* 11, 525-531.

Fryxell, G. A. (1989). Marin phytoplankton at the Weddell Sea ice edge: seasonal changes at the specific level. *Polar Biology* 10, 1-18.

Fryxell, G. A. and Prasad, A. (1990). Eucampia-Antarctica var recta (Mangin) stat nov (Biddulphiaceae, Bacillariophyceae) - life stages at the Weddell Sea ice edge. *Phycologia* 29, 27-38.

Fryxell, G. A., Prasad, A. and Fryxell, P. A. (1989). Eucampia-Antarctica (Castracane) Mangin (Bacillariophyta) - complex nomenclatural and taxonomic history. *Taxon* 38, 638-640.

Gal'chenko, V. F. (1994). Sulphate reduction, methane production and methane oxidation in various water bodies of the Bunger Hills oasis of Antarctica. *Microbiology* 63, 388-396.

Galimov, E. M. (2000). Carbon isotope composition of Antarctic plants. *Geochimica et Cosmochimica Acta* 64, 1737-1739.

Garrison, D. L. and Buck, K. R. (1989). The biota of Antarctic pack ice in the Weddell Sea and Antarctic Peninsula regions. *Polar Biology* 10, 211-219.

Garrison, D. L., Buck, K. R. and Fryxell, G. A. (1987). Algal assemblages in Antarctic pack ice and ice-edge plankton. *Journal of Phycology* 23, 564-572.

Gat, J. R. (1995). Stable isotopes of fresh and saline lakes. *In* "Physics and chemistry of lakes." (A. Lerman, D. Imboden, and J. Gat, Eds.), pp. 139-165. Springer, Berlin.

Gat, J. R. and Gonfiantini, R. (1981). "Stable Isotope Hydrology: Deuterium and Oxygen-18 in the Water Cycle, IAEA Technical Report Series #210." Vienna.

Gibson, J. A. E. (1999). The meromictic lakes and stratified marine basins of the Vestfold Hills, East Antarctica. *Antarctic Science* 11, 175-192.

Gibson, J. A. E. and Andersen, D. T. (2002). Physical structure of epishelf lakes of the southern Bunger Hills, East Antarctica. *Antarctic Science* 14, 253-261.

Gibson, J. A. E., Trull, T., Nichols, P. D., Summons, R. E. and McMinn, A. (1999). Sedimentation of C-13-rich organic matter from Antarctic sea- ice algae: A potential indicator of past sea-ice extent. *Geology* 27, 331-334.

Gibson, J. A. E., Vincent, W. F., Van Hove, P., Belzile, C., Wang, X. W. and Muir, D. (2002). Geochemistry of ice-covered, meromictic Lake A in the Canadian High Arctic. *Aquatic Geochemistry* 8, 97-119.

Gilbert, R. and Domack, E. W. (2003). Sedimentary record of disintegrating ice shelves in a warming climate, Antarctic Peninsula. *Geochemistry, Geophysics, Geosystems* 4, art. no.-1038.

Gille, S. T. (2003). Warming of the Southern Ocean since the 1950's. *Science* 295, 1275-1277.

Gillieson, D., Burgess, J., Spate, A. and Cochrane, A. (1990). An atlas of the lakes of the Larsemann Hills, Princess Elizabeth Land, Antarctica. *ANARE Notes* 74, 173pp.

Gleitz, M., Grossmann, S., Scharek, R. and Smetacek, V. (1996). Ecology of diatom and bacterial assemblages in water associated with melting summer sea ice in the Weddell Sea, Antarctica. *Antarctic Science* 8, 135-146.

Goodwin, I. D. (1993). Holocene deglaciation, sea-level change, and the emergence of the Windmill Islands, Budd Coast, Antarctica. *Quaternary Research* 40, 70-80.

Gordon, J. E. and Harkness, D. D. (1992). Magnitude and geographic-variation of the radiocarbon content in Antarctic marine life - implications for reservoir corrections in radiocarbon dating. *Quaternary Science Reviews* 11, 697-708.

Gore, D. B. (1997). Blanketing snow and ice; constraints on radiocarbon dating deglaciation in East Antarctic oases. *Antarctic Science* 9, 336-346.

Graf, W., Moser, H., Oerter, H., Reinwarth, O. and Stichler, W. (1988). Accumulation and ice core studies on the Filchner-Ronne Ice Shelf, Antarctica. *Annals of Glaciology* 11, 23-31.

Grossman, E. L. (1984a). Stable Isotope Fractionation in Live Benthic Foraminifera from the Southern-California Borderland. *Palaeogeography, Palaeoclimatology, Palaeoecology* 47, 301-327.

Grossman, E. L. (1984b). Carbon isotopic fractionation in live benthic foraminifera - comparison with inorganic precipitate studies. *Geochimica et Cosmochimica Acta* 48, 1505-1512.

Hain, S. and Melles, M. (1994). Evidence for a marine molluscan fauna beneath ice shelves in the Lazarev and Weddell Seas, Antarctica, from Shells of Adamussium-Colbecki and Nacella (Patinigera) cf. Concinna. *Antarctic Science* 6, 29-36.

Hall, B. L. and Denton, G. H. (2000). Radiocarbon chronology of Ross Sea drift, eastern Taylor Valley, Antarctica: Evidence for a grounded ice sheet in the Ross Sea at the last glacial maximum. *Geografiska Annaler Series a-Physical Geography* 82A, 305-336.

Hall, B. L. and Denton, G. H. (2000). Radiocarbon chronology of Ross Sea drift, eastern Taylor Valley, Antarctica: Evidence for a grounded ice sheet in the Ross Sea at the last glacial maximum. *Geografiska Annaler Series a-Physical Geography* 82A, 305-336.

Hammer, C. U., Claussen, H. B. and Langway, C. C., Jr. (1994). Electrical conductivity method (ECM) stratigraphic dating of the Byrd station ice core, Antarctica. *Annals of Glaciology* 20, 115-120.

Hansen, J., Ruedy, R., Glascoe, J. and Sato, M. (1999). GISS analysis of surface temperature change. *Journal of Geophysical Research-Atmospheres* 104, 30997-31022.

Hansom, J. D. and Flint, C. P. (1989). Holocene ice fluctuations on Brabant Island, Antarctic Peninsula. *Antarctic Science* 1, 165-166.

Harangozo, S. A., Colwell, S. R. and King, J. C. (1997). An analysis of a 34-year air temperature record from Fossil Bluff (71°S, 68°W), Antarctica. *Antarctic Science* 9, 355-363.

Harangozo, S. A., Colwell, S. R. and King, J. C. (1997). An analysis of a 34-year air temperature record from Fossil Bluff (71°S, 68°W), Antarctica. *Antarctic Science* 9, 355-363.

Harden, S. L., Demaster, D. J. and Nittrouer, C. A. (1992). Developing sediment geochronologies for high-latitude continental shelf deposits - a radiochemical approach. *Marine Geology* 103, 69-97.

Harkness, D. D. (1979). Radiocarbon dates from Antarctica. *British Antarctic Survey Bulletin* 47, 43-59.

Harris, P. T., O'Brien, P. E., Sedwick, P. and Truswell, E. M. (1996). Late Quaternary history of sedimentation on the Mac Robertson Shelf, East Antarctica: problems with 14C dating of marine sediment cores. *Paper Proceedings of the Royal Society of Tasmania* 130, 47-53.

Haug, G. H., Hughen, K. A., Sigman, D. M., Peterson, L. C. and Rohl, U. (2001). Southward migration of the Intertropical convergence zone through the Holocene. *Science* 293, 1304-1308.

Heiri, O., Lotter, A. F. and Lemcke, G. (2001). Loss on ignition as a method for estimating organic and carbonate content in sediments: reproducibility and comparability of results. *Journal of Paleolimnology* 25, 101-110.

Hemer, M. A. and Harris, P. T. (2003). Sediment core from beneath the Amery Ice Shelf, East Antarctica, suggests mid-Holocene ice-shelf retreat. *Geology* 31, 127-130.

Hendy, C. H. (2000). The role of polar lake ice as a filter for glacial lacustrine sediments. *Geografiska Annaler Series a-Physical Geography* 82A, 271-274.

Hendy, C. H., Sadler, A. J., Denton, G. H. and Hall, B. L. (2000). Proglacial lake-ice conveyors: A new mechanism for deposition of drift in polar environments. Geografiska Annaler Series a-Physical Geography 82A, 249-270.

Henshaw, T. and Laybourn-Parry, J. (2002). The annual patterns of photosynthesis in two large, freshwater, ultra-oligotrophic Antarctic lakes. *Polar Biology* 25, 744-752.

Herb, R. (1971). Distribution of recent benthonic foraminifera in the Drake Passage. *American Geophysical Union, Antarctica Research Series* 17, 251-300.

Hermichen, W. D., Kowski, P. and Wand, U. (1985). Lake Untersee, a 1st Isotope Study of the Largest Fresh-Water Lake in the Interior of East Antarctica. *Nature* 315, 131-133.

Herron, M. J. and Anderson, J. B. (1990). Late Quaternary glacial history of the South Orkney Plateau. *Quaternary Research* 33, 265-275.

Herterich, K. (1987). Dynamics of the West Antarctic Ice Sheet (C. J. van der Veen, and J. Oerlemans, Eds.), pp. 185-202. Reidel, Dordrecht, Netherlands.

Heywood, R. B. (1977). A limnological survey of the Ablation Point area, Alexander Island, Antarctica. *Philosophical Transactions of the Royal Society of London* B279, 39-54.

Heywood, R. B. and Light, J. J. (1975). First direct evidence of life under Antarctic shelf ice. *Nature* 254, 591-592.

Hindmarsh, R. (1997). Deforming beds: Viscous and plastic scales of deformation. *Quaternary Science Reviews* 16, 1039-1056.

Hindmarsh, R. C. A. and Le Meur, E. (2001). Dynamical processes involved in the retreat of marine ice sheets. *Journal of Glaciology* 47, 271-282.

Hjort, C., Ingólfsson, O., Moller, P. and Lirio, J. M. (1997). Holocene glacial history and sea-level changes on James Ross Island, Antarctic Peninsula. *Journal of Quaternary Science* 12, 259-273.

Hjort, C., Bentley, M. J. and Ingólfsson, O. (2001). Holocene and pre-Holocene temporary disappearance of the George VI Ice Shelf, Antarctic Peninsula. *Antarctic Science* 13, 296-301.

Hjort, C., Ingólfsson, O., Bentley, M. J. and Björck, S. (2004). Late Pleistocene and Holocene glacial and climate history of the Antarctic Peninsula regions: A brief overview of land and lake sediments. *In* "Antarctic Peninsula Climate Variability: Historical and Paleoenvironmental Perspectives." (E. Domack, A. Leventer, A. Burnett, R. Bindschadler, P. Convey, and M. Kirby, Eds.). American Geophysical Union, Washington.

Hodgson, D. A., Dyson, C. L., Jones, V. J. and Smellie, J. L. (1998). Tephra analysis of sediments from Midge Lake (South Shetland Islands) and Sombre Lake (South Orkney Islands), Antarctica. *Antarctic Science* 10, 13-20.

Hodgson, D. A., Noon, P. E., Vyverman, W., Bryant, C. L., Gore, D. B., Appleby, P., Gilmour, M., Verleyen, E., Sabbe, K., Jones, V. J., Ellis-Evans, J. C. and Wood, P. B. (2001a). Were the Larsemann Hills ice-free through the Last Glacial Maximum? *Antarctic Science* 13, 440-454.

Hodgson, D. A., Vyverman, W. and Sabbe, K. (2001b). Limnology and biology of saline lakes in the Rauer Islands, eastern Antarctica. *Antarctic Science* 13, 255-270.

Hodgson, D. A., McMinn, A., Kirkup, H., Cremer, H., Gore, D., Melles, M., Roberts, D. and Montiel, P. (2003). Colonization, succession, and extinction of marine floras during a glacial cycle: A case study from the Windmill Islands (east Antarctica) using biomarkers. *Paleoceanography* 18, 1067.

Hodgson, D.A., Doran, P.T., Roberts, D., McMinn, A. (2004) Paleolimnological studies from the Antarctic and sub Antarctic islands. *In*: Pienitz R, Douglas MSV, Smol JP (eds) Developments in Palaeoenvironmental Research. Volume 8. Long-term Environmental Change in Arctic and Antarctic Lakes, Volume 8. Kluwer, Dordrecht, pp. 550.

Hoffman, E. E. and Klinck, J. M. (1998). Thermohaline variability of the waters overlying the West Antarctic Peninsula continental shelf. *In* "Ocean, Ice and Atmosphere Interactions at the Antarctic

continental margin." (S. Jacobs, and R. F. Weiss, Eds.), pp. 67-82. AGU, Antarctic Research Series, Washington D.C.

Hofman, E. E., Klinck, J. M., Lascara, C. M. and Smith, D. A. (1996). Water Mass Distribution and circulation west of the Antarctic Peninsula and including the Bransfield Strait. *In* "Foundations for Ecological Research West of the Antarctic Peninsula." (R. M. Ross, E. E. Hoffman, and L. B. Quetin, Eds.), pp. 61-80. American Geophysical Union, Washington.

Holdsworth, G. (1977). Tidal interaction with ice shelves. *Annals of Geophysics* 33, 133-146.

Houghton, J. T., Ding, Y., Griggs, D. J., Noguer, M., van den Linden, P. J., Dai, X., Maskell, K. and Johnson, C. A. (2001). "Climate Change 2001: The Scientific Basis." Cambridge University Press, Cambridge.

Howe, J. A. and Pudsey, C. J. (1999). Antarctic circumpolar deep water: A Quaternary paleoflow record from the northern Scotia Sea, South Atlantic ocean. *Journal of Sedimentary Research* 69, 847-861.

Hughes, T. J. (1987). The marine ice transgression hypothesis. *Geografiska Annaler* 69A, 237-250.

Hurd, D. C., Pankratz, H. S., Asper, V., Fugate, J. and Morrow, H. (1981). Changes in the physical and chemical properties of biogenic silica from the central Equatorial pacific. Part III. Specific pore volume, mean pore size and skeletal ultra-structure of acid cleaned samples. *American Journal of Science* 281, 833-895.

Hurrell, J. W. and van Loon, H. (1994). A modulation of the atmospheric annual cycle in the Southern Hemisphere. *Tellus* 46A, 325-338.

Huybrechts, P. and de Wolde, J. (1999). The dynamic response of the Greenland and Antarctic ice sheets to multiple-century climatic warming. *Journal of Climate* 12, 2169-2188.

Igarashi, A., Numanami, H., Tsuchiya, Y. and Fukucki, M. (2001). Bathymetric distribution of fossil foraminifera within marine sediment cores from the eastern part of Lutzow-Holm Bay, East Antarctica, and its paleoceanographic implications. *Marine Micropaleontology* 42, 125-162.

Ikehara, M., Kawamura, K., Ohkouchi, N., Kimoto, K., Murayama, M., Nakamura, T., Oba, T. and Taira, A. (1997). Alkenone sea surface temperature in the Southern Ocean for the last two deglaciations. *Geophysical Research Letters* 24, 679-682.

Ingólfsson, O., Hjort, C., Berkman, P. A., Bjorck, S., Colhoun, E., Goodwin, I. D., Hall, B., Hirakawa, K., Melles, M., Moller, P. and Prentice, M. L. (1998). Antarctic glacial history since the Last Glacial Maximum: an overview of the record on land. *Antarctic Science* 10, 326-344.

Ingólfsson, A. and Hjort, C. (2002). Glacial history of the Antarctic Peninsula since the Last Glacial Maximum - a synthesis. *Polar Research* 21, 227-234.

Ingólfsson, O., Hjort, C. and Humlum, O. (2003). Glacial and climate history of the Antarctic Peninsula since the Last Glacial Maximum. *Arctic Antarctic and Alpine Research* 35, 175-186.

Ishman, S. E. and Domack, E. W. (1994). Oceanographic Controls on Benthic Foraminifers from the Bellingshausen Margin of the Antarctic Peninsula. *Marine Micropaleontology* 24, 119-155.

Ishman, S. E. and Sperling, M. R. (2002). Benthic foraminiferal record of Holocene deep-water evolution in the Palmer Deep, western Antarctic Peninsula. *Geology* 30, 435-438.

Jacka, T. H. and Budd, W. F. (1998). Detection of temperature and sea-ice-extent changes in the Antarctic and Southern Ocean, 1949-96. *Annals of Glaciology*, 27, 553-559.

Jacobs, S. S. and Comiso, J. C. (1993). A recent sea-ice retreat west of the Antarctic Peninsula. *Geophysical Research Letters* 20, 1171-1174.

Jacobs, S. S. and Comiso, J. C. (1997). Climate variability in the Amundsen and Bellingshausen Seas. *Journal of Climate* 10, 697-709.

Jacobs, S. S., Fairbanks, R. G. and Horibe, Y. (1985). Origin and evolution of water masses near the antarctic continental margin: Evidence from H218O/H216O ratios in sea water. *In* "Oceanology of the antarctic Continental Shelf (Antarctic Research Series)." (S. S. Jacobs, Ed.). American Geophysical Union., Washington, D.C.

Jacobs, S. S., Helmer, H. H., Doake, C. S. M., Jenkins, A. and Frolich, R. M. (1992). Melting of ice shelves and the mass balance of Antarctica. *Journal of Glaciology* 38, 375-382.

Jezek, K. C. (1984). Recent changes in the dynamic condition of the Ross Ice Shelf, Antarctica. *Journal of Geophysical Research* 89, 409-416.

Joerg, W. L. G. (1937). The topographical results of Ellsworth's Trans-Antarctic flight of 1935. *American Geographical Society*, New York.

John, B. S. (1972). Evidence from South Shetland Islands towards a glacial history of West Antarctic. *Institute of British Geographers, Special Publication* 4, 75-89.

John, B. S. and Sugden, D. E. (1971). Raised marine features and phases of glaciation in the South Shetland Islands. *British Antarctic Survey Bulletin* 24, 45-111.

Jones, P. D., Marsh, R., Wigley, T. M. L. and Peel, D. A. (1993). Decadal timescale links between Antarctic Peninsula ice core oxygen-18, deuterium and temperature. *Holocene* 3, 14-26.

Jones, R. W. and Pudsey, C. J. (1994). Recent benthonic foraminifera from the Western Antarctic Ocean. *Journal of Micropalaeontology* 13, 17-23.

Jones, V. J. (1993). The use of diatoms in lake sediments to investigate environmental history in Maritime Antarctica: an example from Sombre Lake, Signy Island. *Antarctic Science Special Topic*, 91-95.

Jones, V. J. (1996). The diversity, distribution and ecology of diatoms from Antarctic inland waters. *Biodiversity and Conservation* 5, 1433-1449.

Jones, V. J., Juggins, S. and Ellisevans, J. C. (1993). The Relationship between Water Chemistry and Surface Sediment Diatom Assemblages in Maritime Antarctic Lakes. *Antarctic Science* 5, 339-348.

Jones, V. J., Hodgson, D. A. and Chepstow-Lusty, A. (2000). Palaeolimnological evidence for marked Holocene environmental changes on Signy Island, Antarctica. *Holocene* 10, 43-60.

Joughin, I. and Padman, L. (2003). Melting and freezing beneath Filchner-Ronne Ice Shelf, Antarctica. *Geophysical Research Letters* 30, 1477.

Jouzel, J., Vaikmae, R., Petit, J. R., Martin, M., Duclos, Y., Stievenard, M., Lorius, C., Toots, M., Melieres, M. A., Burckle, L. H., Barkov, N. I. and Kotlyakov, V. M. (1995). The 2-step shape and timing of the Last Deglaciation in Antarctica. *Climate Dynamics* 11, 151-161.

Kaczmarska, I., Barbrick, N. E., Ehrman, J. M. and Cant, G. P. (1993). Eucampia Index as an Indicator of the Late Pleistocene Oscillations of the Winter Sea-Ice Extent at the ODP Leg 119 Site 745b at the Kerguelen Plateau. *Hydrobiologia* 269, 103-112.

Kang, S. and Fryxell, G. A. (1992). *Fragilariopsis cylindrus* (Grunow) Krieger: the most abundant diatom in water column assemblages of Antarctic marginal ice-edge zones. *Polar Biology* 12, 609-627.

Kawecka, B. and Olech, M. (1993). Diatom communities in the vanishing and Ornithologist Creek, King George Island, South Shetland, Antarctica. *Hydrobiologia* 269, 327-333.

Keigwin, L. D. (1996). The Little Ice Age and Medieval warm period in the Sargasso Sea. *Science* 274, 1504-1508.

Keil, R. G., Tsamakis, E., Fuh, C. B., Giddings, J. C. and Hedges, J. I. (1994). Mineralogic and textural controls on the organic composition of coastal marine sediments. Hydrodynamic spearation using SPLITT-fraction. *Geochemica et Cosmochimica Acta* 58, 879-893.

Kellogg, D. E. and Kellogg, T. B. (1986). Diatom biostratigraphy of sediment cores from beneath the Ross Ice Shelf. *Micropaleontology* 32, 74-94.

Kellogg, D. E. and Kellogg, T. B. (1987a). Diatoms of the McMurdo Ice Shelf, Antarctica - implications for sediment and biotic reworking. *Palaeogeography, Palaeoclimatology, Palaeoecology* 60, 77-96.

Kellogg, D. E. and Kellogg, T. B. (1987b). Microfossil distributions in modern Amundsen Sea sediments. *Marine Micropaleontology* 12, 203-222.

Kellogg, T. B. and Kellogg, D. E. (1988). Antarctic cryogenic sediments - biotic and inorganic facies of ice shelf and marine-based ice-sheet environments. *Palaeogeography, Palaeoclimatology, Palaeoecology* 67, 51-74.

Kennedy, D. S. and Anderson, J. B. (1989). Glacial-marine sedimentation and Quaternary glacial history of Marguerite Bay, Antarctic Peninsula. *Quaternary Research* 31, 255-276.

Khim, B. K., Yoon, H. I., Kang, C. Y. and Bahk, J. J. (2002). Unstable climate oscillations during the late Holocene in the eastern Bransfield Basin, Antarctic Peninsula. *Quaternary Research* 58, 234-245.

Kim, S.-T. and O'Neil, J. R. (1997). Equilibrium and non-equilibrium oxygen isotopes effects in synthetics calcites. *Geochemica et Cosmochimca Acta* 61, 3461-3475.

King, J. C. (1994). Recent Climate Variability in the Vicinity of the Antarctic Peninsula. International *Journal of Climatology* 14, 357-369.

King, J. C. and Harangozo, S. A. (1998). Climate change in the western Antarctic Peninsula since 1945: observations and possible causes. *Annals of Glaciology,* 27, 571-575.

King, J. C. and Turner, J. (1998). "Antarctic Meteorology and Climatology." Cambridge University Press.

King, J. C. and Comiso, J. C. (2003). The spatial coherence of interannual temperature variations in the Antarctic Peninsula. *Geophysical Research Letters* 30, art. no.-1040.

King, J. C., Turner, J., Marshall, G. J., Connolley, W. M. and Lachlan-Cope, T. (2004). Antarctic Peninsula climate variability and its causes as revealed by analysis of instrumental records. *In* "Antarctic Peninsula Climate Variability: Historical and Paleoenvironmental Perspectives." (E. Domack, A. Leventer, A. Burnett, R. Bindschadler, P. Convey, and M. Kirby, Eds.), American Geophysical Union, Washington.

Kirby, M. E., Domack, E. W. and McClennen, C. E. (1998). Magnetic stratigraphy and sedimentology of Holocene glacial marine deposits in the Palmer Deep, Bellingshausen Sea, Antarctica: implications for climate change? *Marine Geology* 152, 247-259.

Kitagawa, H. and van der Plicht, J. (1998). Atmospheric radiocarbon calibration to 45,000 yr BP: Late glacial fluctuations and cosmogenic isotope production. *Science* 279, 1187-1190.

Klinck, J. M. and Smith, D. A. (1993). Effect of wind changes during the Last Glacial Maximum on the circulation in the Southern-Ocean. *Paleoceanography* 8, 427-433.

Klokov, V. D., Kaup, E., Zierath, R. and D., H. (1990). Lakes of the Bunger Hills (East Antarctica): chemical and ecological properties. *Polish Polar Research* 11, 147-159.

Kreutz, K. J., Mayewski, P. A., Meeker, L. D., Twickler, M. S., Whitlow, S. I. and Pittalwala, II. (1997). Bipolar changes in atmospheric circulation during the Little Ice Age. *Science* 277, 1294-1296.

Kreutz, K. J., Mayewski, P. A., Whitlow, S. I. and Twickler, M. S. (1998). Limited migration of soluble ionic species in a Siple Dome, Antarctica, ice core. *Annals of Glaciology* 27, 371-377.

Kroopnick, P. (1985). The distribution of 13C of total CO2 in the world oceans. *Deep-Sea Research I* 32, 57-84.

Kulbe, T., Melles, M., Verkulich, S. R. and Pushina, Z. V. (2001). East Antarctic climate and environmental variability over the last 9400 years inferred from marine sediments of the Bunger Oasis. *Arctic Antarctic and Alpine Research* 33, 223-230.

Kwok, R. and Comiso, J. C. (2002). Spatial patterns of variability in Antarctic surface temperature: Connections to the Southern Hemisphere Annular Mode and the Southern Oscillation. *Geophysical Research Letters* 29, art. no.-1705.

Labeyrie, L., Labracherie, M., Gorfti, N., Pichon, J. J., Vautravers, M., Arnold, M., Duplessy, J. C., Paterne, M., Michel, E., Duprat, J., Caralp, M. and Turon, J. L. (1996). Hydrographic changes of the Southern Ocean (southeast Indian sector) over the last 230 kyr. *Paleoceanography* 11, 57-76.

Lamb, A. L., Leng, M. J., Mohammed, M. U. and Lamb, H. F. (2004). Holocene climate and vegetation change in the Main Ethiopian Rift Valley, inferred from the composition (C/N and delta C-13) of lacustrine organic matter. *Quaternary Science Reviews* 23, 881-891.

Lamy, F., Hebbeln, D., Rohl, U. and Wefer, G. (2001). Holocene rainfall variability in southern Chile: a marine record of latitudinal shifts of the Southern Westerlies. *Earth and Planetary Science Letters* 185, 369-382.

Lamy, F., Ruhlemann, C., Hebbeln, D. and Wefer, G. (2002). High- and low-latitude climate control on the position of the southern Peru-Chile Current during the Holocene. *Paleoceanography* 17, art. no.-1028.

Lamy, F., Kaiser, J., Ninnemann, U., Hebbeln, D., Arz, H. W. and Stoner, J. (2004). Antarctic timing of surface water changes off Chile and Patagonian ice sheet response. *Science* 304, 1959-1962.

Lancaster, N. (2002). Flux of eolian sediment in the McMurdo Dry Valleys, Antarctica: a preliminary assessment. *Arctic Antarctic and Alpine Research* 34, 318-323.

Larter, R. D. and Barker, P. F. (1991). Effects of Ridge Crest Trench Interaction on Antarctic Phoenix Spreading - Forces on a Young Subducting Plate. *Journal of Geophysical Research-Solid Earth* 96, 19583-19607.

Larter, R. D. and Vanneste, L. E. (1995). Relict subglacial deltas on the Antarctic Peninsula outer shelf. *Geology* 23, 33-36.

Last, W. M. and Smol, J. (2001). An introduction to basin analysis, coring and chronological techniques used in paleolimnology. *In* "Tracking Environmental Change Using Lake Sediments: Basin Analysis, Coring and Chronological Techniques." (W. M. Last, and J. Smol, Eds.). Kluwer, Dordrecht.

Lawrence, M. J. F. and Hendy, C. H. (1989). Carbonate deposition and Ross Sea ice advance, Fryxell Basin, Taylor Valley, Antarctica. *New Zealand Journal of Geology and Geophysics* 32, 267-277.

Laybourn-Parry, J., Quayle, W. C., Henshaw, T., Ruddell, A. and Marchant, H. J. (2001). Life on the edge: the plankton and chemistry of Beaver Lake, an ultra-oligotrophic epishelf lake, Antarctica. *Freshwater Biology* 46, 1205-1217.

Laybourn-Parry, J., Henshaw, T., Jones, D. J. and Quayle, W. (2004). Bacterioplankton production in freshwater Antarctic lakes. *Freshwater Biology* 49, 735-744.

Le Cohu, R. and Maillard, R. (1986). Diatomeés d'eau douce de îles Kerguelen (à l'exclusion de Monoraphideés). *Annales Limnologie* 22., 99-118.

Lea, D. W. (2004). Elemental and isotopic proxies of past ocean temperatures. *In* "Treatise on Geochemistry." (H. Elderfield, Ed.). Elservier.

Leng, M., Barker, P., Greenwood, P., Roberts, N. and Reed, J. M. (2001). Oxygen isotope analysis of diatom silica and authigenic calcite from Lake Pinarbasi, Turkey. *Journal of Palaeolimnology* 25, 343-349.

Leng, M. J. and N. J. Anderson (2003). Isotopic variation in modern lake waters from western Greenland. *Holocene* 13(4): 605-611.

Leng, M. J. and J. D. Marshall (2004). Palaeoclimate interpretation of stable isotope data from lake sediment archives. *Quaternary Science Reviews* 23(7-8): 811-831.

Lennon, P. W., Loynes, J., Paren, J. G. and Potter, J. R. (1982). Oceanographic observations from George VI Ice Shelf, Antarctic Peninsula. Annals of Glaciology 3, 178-183.

Leventer, A. (1991). Sediment trap diatom assemblages from the Northern Antarctic Peninsula region. *Deep-Sea Research Part a-Oceanographic Research Papers* 38, 1127-1143.

Leventer, A. (1992). Modern distribution of diatoms in sediments from the George-V- Coast, Antarctica. *Marine Micropaleontology* 19, 315-332.

Leventer, A. and Dunbar, R. B. (1996). Factors influencing the distribution of diatoms and other algae in the Ross Sea. *Journal of Geophysical Research-Oceans* 101, 18489-18500.

Leventer, A., Dunbar, R. B. and Demaster, D. J. (1993). Diatom Evidence for Late Holocene Climatic Events in Granite Harbor, Antarctica. *Paleoceanography* 8, 373-386.

Leventer, A., Domack, E. W., Ishman, S. E., Brachfeld, S., McClennen, C. E. and Manley, P. (1996). Productivity cycles of 200-300 years in the Antarctic Peninsula region: Understanding linkages among the sun, atmosphere, oceans, sea ice, and biota. *Geological Society of America Bulletin* 108, 1626-1644.

Leventer, A., Domack, E., Barkoukis, A., McAndrews, B. and Murray, J. (2002). Laminations from the Palmer Deep: A diatom-based interpretation. *Paleoceanography* 17, art. no.-1027.

Lewin, J. C. (1961). The dissolution of silica from diatom walls. *Geochimica et Cosmochimica Acta* 21, 182-198.

Lewis, D. W. and McConchie, D. M. (1994a). "Analytical Sedimentology." Chapman & Hall, New York.

Lewis, D. W. and McConchie, D. M. (1994b). "Practical Sedimentology." Chapman & Hall, New York.

Li, B. H., Yoon, H. I. and Park, B. K. (2000). Foraminiferal assemblages and CaCO3 dissolution since the last deglaciation in the Maxwell Bay, King George Island, Antarctica. *Marine Geology* 169, 239-257.

Lindenberg, H. G. and Auras, A. (1984). Distribution of arenaceous foraminifera in depth profiles of the Southern-Ocean (Kerguelen Plateau Area). *Palaeogeography, Palaeoclimatology, Palaeoecology* 48, 61-106.

Lipenkov, V., Ekaykin, A. A., Barkov, N. I. and Pourchet, M. (1998). On the relation between surface snow density in Antarctica and wind speed. *Data of Glaciological Studies 85, 148–158.*

Loeblich, A., R. Jr. , and Tappan, H. (1964). Foraminiferal classification and evolution. *Journal of the Geological Society of India* 5, 5-39.

Loeblich, A. J. and Tappan, H. (1988). "Foraminiferal genera and their classification." Van Nostrand Reinhold, New York.

Lopez-Martinez, J., Thomson, M. R. A., Arche, A., Bjorck, S., Ellis-Evans, J. C., Hathway, B., Hernandez-Cifuentes, E., Serrano, E., Zale, R. and King, S. (1996). Geomorphological Map of Byers Peninsula, Livingston Island. British Antarctic Survey, Cambridge.

Lorius, C., Jouzel, J., Raynaud, D., Hansen, J. and Letreut, H. (1990). The ice-core record - climate sensitivity and future Greenhouse warming. *Nature* 374, 139-145.

Lorius, C., Merlivat, L., Jouzel, J. and Pourchet, M. (1979). A 30,000 yr isotope climatic record from Antarctic ice. *Nature* 280, 644-648.

Loynes, J., Potter, J. R. and Paren, J. G. (1984). Current, temperature, and salinity beneath George VI Ice Shelf, Antarctica. *Deep-Sea Research Part I-Oceanographic Research Papers* 31, 1037-1055.

Lucchitta, B. K. and Rosanova, C. E. (1998). Retreat of northern margins of George VI and Wilkins Ice Shelves, Antarctic Peninsula. *Annals of Glaciology* 27, 41-46.

Lui, H. W. and Miller, K. J. (1979). Fracture toughness of fresh-water ice. *Journal of Glaciology* 22, 135-143.

Lutze, G. F. and Coulbourn, W. T. (1984). Recent benthic foraminifera from the continental margin of north west Africa: community structure and distribution. *Marine Micropaleontology* 8, 361-401.

Lyons, W. B., Tyler, S. W., Wharton, R. A., McKnight, D. M. and Vaughn, B. H. (1998). A Late Holocene desiccation of Lake Hoare and Lake Fryxell, McMurdo Dry Valleys, Antarctica. *Antarctic Science* 10, 247–256.

Lythe, M. B. and Vaughan, D. G. (2001). BEDMAP: A new ice thickness and subglacial topographic model of Antarctica. *Journal of Geophysical Research-Solid Earth* 106, 11335-11351.

MacAyeal, D. R., Scambos, T. A., Hulbe, C. L. and Fahnestock, M. A. (2003). Catastrophic ice-shelf break-up by an ice-shelf-fragment- capsize mechanism. *Journal of Glaciology* 49, 22-36.

Macdonald, R. W., Paton, D. W., Carmack, E. C. and Omstedt, A. (1995). The fresh-water budget and under-ice spreading of Mackenzie River water in the Canadian Beaufort Sea based on salinity and O-18/O-16 measurements in water and Ice. *Journal of Geophysical Research-Oceans* 100, 895-919.

Mackensen, A., Fuetterer, D. K., Grobe, H. and Schmiedl, G. (1993). Benthic foraminiferal assemblages from the eastern South Atlantic Polar front region 35 and 75oS: Distribution, ecology and fossilization potential. *Marine Micropaleontology* 22, 33-69.

Mackensen, A., Grobe, H. and Fuetterer, D. K. (1990). Benthic foraminiferal assemblages from the eastern Weddell Sea between 68 and 73S: Distribution, ecology and fossilzation potential. *Marine Micropaleontology* 16, 241-283.

Mackensen, A., Hubberten, H. W., Scheele, N. and Schlitzer, R. (1996). Decoupling of delta C-13 (Sigma CO2) and phosphate in recent Weddell Sea deep and bottom water: Implications for glacial southern ocean *Palaeogeography, Palaeoclimatology, Palaeoecology* 11, 203-215.

Macko, S. A., Engel, M. H. and Parker, P. L. (1993). Early diagenesis of organic matter in sediments. *In* "Organic Geochemistry." (M. H. Engel, and S. A. Macko, Eds.), pp. 211-224, New York.

Marshall, G. J. (2002). Analysis of recent circulation and thermal advection change in the northern Antarctic Peninsula. *International Journal of Climatology* 22, 1557-1567.

Marshall, G. J. and King, J. C. (1998). Southern hemisphere circulation anomalies associated with extreme Antarctic Peninsula winter temperatures. *Geophysical Research Letters* 25, 2437-2440.

Marshall, G. J., Turner, J. and Miners, W. D. (1998). Interpreting recent accumulation records through an understanding of the regional synoptic climatology: an example from the southern Antarctic Peninsula. *Annals of Glaciology*, 27, 610-616.

Marshall, G. J., Lagun, V. and Lachlan-Cope, T. A. (2002). Changes in Antarctic Peninsula tropospheric temperatures from 1956 to 1999: A synthesis of observations and reanalysis data. *International Journal of Climatology* 22, 291-310.

Marshall, W. M. and Warakomski, J. M. (1980). Amorphous silica solubillities II. Effects of aqueous salt solution at 25oS. *Geochimica et Cosmochimica Acta* 44, 915-924.

Martinez-Macchiavello, J. C., Tatur, A., ServantVildary, S. and DelValle, R. (1996). Holocene environmental change in a marine-estuarine-lacustrine sediment sequence, King George Island, South Shetland Islands. *Antarctic Science* 8, 313-322.

Maslanyj, M. P. (1987). Seismic bedrock depth measurements and the origin of George VI Sound, Antarctic Peninsula. British Antarctic Survey Bulletin 75, 51-56.

Maslanyj, M. P. (1988). Gravity and aeromagnetic evidence for the crustal structure of George VI Sound, Antarctic Peninsula. British Antarctic Survey Bulletin 79, 1-16.

Masson, V., Vimeux, F., Jouzel, J., Morgan, V., Delmotte, M., Ciais, P., Hammer, C., Johnsen, S., Lipenkov, V. Y., Mosley-Thompson, E., Petit, J. R., Steig, E. J., Stievenard, M. and Vaikmae, R. (2000). Holocene climate variability in Antarctica based on 11 ice-core isotopic records. *Quaternary Research* 54, 348-358.

Masson-Delmotte, V., Stenni, B. and Jouzel, J. (2004). Common millennial-scale variability of Antarctic and Southern Ocean temperatures during the past 5000 years reconstructed from the EPICA Dome C ice core. *Holocene* 14, 145-151.

Matsubaya, O., Sakai, H., Torii, T., Burton, H. R. and Kerry, K. (1979). Antarctic saline lakes: stable isotope ratios, chemical composition and evolution. *Geochimica et Cosmochimica Acta* 43, 7-25.

Mausbacher, R. (1991). Die Jungkvartare Relief - und Klimageschichte im Bereich der Fildeshlbinsl, Sud-Shetland_inseln, Antarktis. *Heidelberger Geographische Arbeiten* 89, 207.

Mayewski, P., Lyons, W., Zielinski, G., Twickler, M., Whitlow, S., Dibb, J., Grootes, P., Taylor, J., Wung, P., Fosberry, K., Wake, C. and Welsh, K. (1995). An ice-core-based late Holocene history for the Transantarctic Mountains, Antarctica. *Antarctic Research Series, Contributions to Antarctic, Research IV 67*, 33–45.

McCorkle, D. C., Martin, P. A., Lea D, W. and Klinkhammer, G. P. (1995). Evidence of a dissolution effect on benthic shell chemistry: d13C, Cd/Ca, Ba/Ca, and Sr/Ca from the Ontong Java Plateau. *Paleoceanography* 10, 699-714.

McCrea, J. M. (1950). On the isotopic chemistry of carbonates and a paleotemperature scale. *Journal of Chemical Physics* 18, 185-195.

McKenzie, J. (1985). Carbon Isotopes and productivity in the lacustrine and marine environment. *In* "Chemical processes in Lakes." (W. Stumm, Ed.), pp. 99-118. Wily, New York.

McMinn, A. (2000). Late Holocene increases in sea ice extent in fjords of the Vestfold Hills, eastern Antarctica. *Antarctic Science* 12, 80-88.

McMinn, A., Heijnis, H. and Hodgson, D. (1994). Minimal effects of UVB-radiation on Antarctic diatoms over the past 20 Years. *Nature* 370, 547-549.

McMinn, A., Heijnis, H., Harle, K. and McOrist, G. (2001). Late-Holocene climatic change recorded in sediment cores from Ellis Fjord, eastern Antarctica. *Holocene* 11, 291-300.

McMinn, A., Skerratt, J., Trull, T., Ashworth, C. and Lizotte, M. (1999). Nutrient stress gradient in the bottom 5 cm of fast ice, McMurdo Sound, Antarctica. *Polar Biology* 21.

Mead, G. A. (1985). Recent benthic foraminifera in the Polar Front Region of the Southwest Atlantic. *Micropaleontology* 31, 221-248.

Mead, G. A. and Kennett, J. P. (1987). The Distribution of Recent Benthic Foraminifera in the Polar Front Region, Southwest Atlantic. *Marine Micropaleontology* 11, 343-360.

Melles, M., Kulbe, T., Verkulich, S. R., Pushina, Z. V. and Hubberten, H.-W. (1997). Late Pleistocene and Holocene environmental history of Bunger Hill, East Antarctica, as revealed by freshwater epishelf lake sediments. *In* "The Antarctic Region: Geological evolution and Processes." (C. A. Ricci, Ed.), pp. 809-820. Terra Antarctic Publications, Sienna.

Melles, M., Verkulich, S. R. and Hermichen, W. D. (1994). Radiocarbon dating of lacustrine and marine sediments from the Bunger Hills, East Antarctica. *Antarctic Science* 6, 375-378.

Menking, K. M., Bischoff, J. L., Fitzpatrick, J. A., Burdette, J. W. and Rye, R. O. (1997). Climatic/hydrologic oscillations since 155,000 yr BP at Owens Lake, California, reflected in abundance and stable isotope composition of sediment carbonate. *Quaternary Research* 48, 58-68.

Mercer, J. H. (1968). Antarctic Ice and Sangamon Sea Level. *International Association of Scientific Hydrology Symposia* 79.

Mercer, J. H. (1976). Glacial history of southernmost South America. *Quaternary Research* 6, 125-166.

Mercer, J. H. (1978). West Antarctic Ice Sheet and CO2 greenhouse effect: a threat of disaster. *Nature* 271, 321-325.

Mercer, J. H. and Laugenie, C. (1973). Glacier in Chile ended a major readvance about 36,000yrs ago: some global comparisons. *Science* 182, 1017-1019.

Meredith, M. P., Grose, K. E., McDonagh, E. L., Heywood, K. J., Frew, R. D. and Dennis, P. F. (1999). Distribution of oxygen isotopes in the water masses of Drake Passage and South Atlantic. *Journal of Geophysical Research* 104, 20949-20962.

Meyers, P. A. (1994). Preservation of elemental and isotopic source identification of sedimentary organic-matter. *Chemical Geology* 114, 289-302.

Meyers, P. A. (1997). Organic geochemical proxies of paleoceanographic, paleolimnologic, and paleoclimatic processes. *Organic Geochemistry* 27, 213-250.

Meyers, P. A. and Ishiwatari, R. (1993). Lacustrine organic geochemistry - an overview of indicators of organic-matter sources and diagenesis in lake-sediments. *Organic Geochemistry* 20, 867-900.

Meyers, P. A. and Teranes, J. L. (2001). Sediment organic matter. *In* "Tracking Environmental Change Using Lake Sediments. Volume 2: Physical and Geochemical Methods." (W. M. Last, and J. Smol, Eds.). Kluwer Academic Publishers, Dordrecht, The Netherlands.

Mikkelson, N. (1980). Experimental dissolution of Pliocene diatoms. *Nova Hedwigia* 33, 893-907.

Miller, K. J., Fairbanks, R. G. and Mountain, G. S. (1987). Tertiary oxygen isotope synthesis, sea level history and continental margin erosion. *Paleoceanography* 2, 1-19.

Miller, L. G. and Aiken, G. R. (1996). Effects of glacial meltwater inflows and moat freezing on mixing in an ice-covered Antarctic lake as interpreted from stable isotope and tritium distributions. *Limnology and Oceanography* 41, 966-976.

Morgan, V. I., Wookey, C. W., Li, J., Ommen, T. D. V., Skinner, W. and Fitzpatrick, M. F. (1997). Site information and initial results from deep ice drilling on Law Dome. *Journal of Glaciology* 43, 3-10.

Morris, E. M. and Vaughan, D. G. (1994). Snow surface temperatures in West Antarctica. *Antarctic Science* 6, 529-535.

Morris, E. M. and Vaughan, D. G. (2003). Spatial and temporal variation of surface temperature on the Antarctic Peninsula and the limit of variability of ice shelves. *In* "Antarctic Peninsula Climate Variability: Historical and Paleoenvironmental Perspectives." (E. Domack, A. Leventer, A. Burnett, R. Bindschadler, P. Convey, and M. Kirby, Eds.). American Geophysical Union.

Mosley-Thompson, E. (1992). Palaeoenvironmental conditions in Antarctica since A.D. 1500: Ice core evidence. *In* "Climate since A.D. 1500." (R. S. Bradley, and J. P.D., Eds.), pp. 572-591. Routledge, London.

Mosley-Thompson, E. (1996). Holocene climate changes recorded in and East Antarctic ice core. *In* "Climate variations and forcing mechanisms of the last 2000 years." (P. D. Jones, R. S. Bradley, and J. Jouzel, Eds.), pp. 263-279. Springer-Verlag, Heidelberg, Berlin.

Mosley-Thompson, E. and Thompson, L. G. (2003). Ice core paleoclimate histories for the Antarctic Peninsula: Where do we go from here? *In* "Antarctic Peninsula Climate Variability: Historical and Paleoenvironmental Perspectives." (E. Domack, A. Leventer, A. Burnett, R. Bindschadler, P. Convey, and M. Kirby, Eds.). American Geophysical Union.

Mosley-Thompson, E., Dai, J., Thompson, L. G., Grootes, P. M., Arbogast, J. K. and Paskievitch, J. F. (1991). Glaciological studies at siple station (Antarctica) - potential ice-core palaeoclimatic record. *Journal of Glaciology* 37, 11-22.

Moy, C. M., Seltzer, G. O., Rodbell, D. T. and Anderson, D. M. (2002). Variability of El Nino/Southern Oscillation activity at millennial timescales during the Holocene epoch. *Nature* 420, 162-165.

Muller, A. and Mathesius, U. (1999). The palaeoenvironments of coastal lagoons in the southern Baltic Sea, I. The application of sedimentary C-org/N ratios as source indicators of organic matter. *Palaeogeography, Palaeoclimatology, Palaeoecology* 145, 1-16.

Muller, A. and Voss, M. (1999). The palaeoenvironments of coastal lagoons in the southern Baltic Sea, - II. delta C-13 and delta N-15 ratios of organic matter - sources and sediments. *Palaeogeography, Palaeoclimatology, Palaeoecology* 145, 17-32.

Mueller, D. R., Vincent, W. F. and Jeffries, M. O. (2003). Break-up of the largest Arctic ice shelf and associated loss of an epishelf lake. *Geophysical Research Letters* 30, 2031.

Muller, P. J. (1977). C/N ratios in Pacific deep-sea sediments: effects of inorganic ammonium and organic nitrogen compounds sorted by clays. *Geochimica et Cosmochimica Acta* 41, 765-776.

Mulvaney, R., Oerter, H., Peel, D. A., Graf, W., Arrowsmith, C., Pasteur, E. C., Knight, B., Littot, G. C. and Miners, W. D. (2002). 1000 year ice-core records from Berkner Island, Antarctica. *Annals of Glaciology,* 35, 45-51.

Murray, J. W. (1991). "Ecology and Palaeoecology of Benthic Foraminifera." Longman Scientific & Technical, London.

Nakai, N. (1972). Carbon isotopic variations and the palaeoclimate from lake Biwa. *Proceedings of the Japanese Academy* 48, 516-521.

Nesje, A., Matthews, J. A., Dahl, S. O., Berrisford, M. S. and Andersson, C. (2001). Holocene glacier fluctuations of Flatebreen and winter- precipitation changes in the Jostedalsbreen region, western Norway, based on glaciolacustrine sediment records. *Holocene* 11, 267-280.

Nicholls, K. W. and Paren, J. G. (1993). Extending the Antarctic meteorological record using ice-sheet temperature profiles. *Journal of Climate* 6, 141-150.

Nichols, R. L. (1953). Geomorphology of Marguerite Bay, Palmer Peninsula, Antarctica. Department of the Navy, Office of Naval Research, Washington D.C.

Nichols, R. L. (1968). Coastal geomorphology, McMurdo Sound, Antarctica. *Journal of Glaciology* 7, 449-478.

Nikolaiev, V. I., Kotlyakov, V. M. and Smirnov, K. E. (1988). Isotopic studies of the ice core from the Komsomolskaia station, Antarctica. *Data of Glaciological Studies of the USSR Academy of Sciences* 63, 97–102.

Ninnemann, U. S., Charles., C. D. and Hodell, D. A. (1999). Origin of global millennial-scale climate events: Constraints from the Southern Ocean deep sea sedimentary record. *In* "Mechanisms of Global Climate Change at Millennial Time Scales." (P. U. Clark, R. S. Webb, and L. D. Keigwin, Eds.). Geophysical Monograph. Series., 112, 99– 112, AGU, Washington, D.C.

Noon, P. E., Birks, H. J. B., Jones, V. J. and Ellis-Evans, J. C. (2001). Quantitative models for reconstructing catchment ice-extent using physical-chemical characteristics of lake sediments. *Journal of Paleolimnology* 25, 375-392.

Noon, P. E., Leng, M. J., Arrowsmith, C., Edworthy, M. G. and Strachan, R. J. (2002). Seasonal observations of stable isotope variations in a valley catchment, Signy Island, South Orkney Islands. *Antarctic Science* 14, 333-342.

Noon, P. E., Leng, M. J. and Jones, V. J. (2003). Oxygen-isotope (delta O-18) evidence of Holocene hydrological changes at Signy Island, maritime Antarctica. *Holocene* 13, 251-263.

Nyholm, K. G. (1961). Morphogensis and biology of the foraminifer *Cibicides labatulus*. *Zoologiska Bidrag fran Uppsala* 33, 89-93.

O'Neil, J. R., Clayton, R. N. and Mayeda, T. K. (1969). Oxygen isotope fractionation in divalent metal carbonates. *Journal of Chemical Physics* 5, 5547-5548.

Oerlemans, J. (1982). A model of the Antarctic Ice Sheet. *Nature* 297, 550-553.

Oppenheim, D. R. and Greenwood, R. (1990). Epiphytic diatoms in two freshwater maritime Antarctic lakes. *Freshwater Biology* 24, 303-314.

Oppenheimer, D. R. (1990). A preliminary study of benthic diatoms in contrasting lake environments. *In* "Antarctic ecosystems. Ecological change and conservation." (K. R. Kerry, and G. Hempel, Eds.), pp. 91-99. Springer-Verlag, Berlin.

Oppenheimer, D. R. and Ellis-Evans, J. C. (1989). Depth-related changes in benthic diatom assemblages of a maritime Antarctic lake. *Polar Biology* 9, 525-532.

Oppenheimer, M. (1998). Global Warming and the stability of the West Antarctic Ice Sheet. *Nature* 393, 325-332.

Osterman, L. and Kellogg, D. E. (1979). Recent benthic foraminifera distributions from the Ross Sea, Antarctica: relation to ecologic and oceanographic conditions. *Journal of Foraminiferal Research* 9, 250-269.

Owens, N. J. P. (1987). Natural variations in 15N in the marine environment. *Advances in Marine Biology* 24, 411-451.

Paren, J. G. and Cooper, S. (1988). Thermal regime of George VI Ice Shelf, Antarctic Peninsula. *Annals of Glaciology* 11, 206.

Payne, A. J., Sugden, D. E. and Clapperton, C. M. (1989). Modeling the growth and decay of the Antarctic Peninsula Ice Sheet. *Quaternary Research* 31, 119-134.

Pearson, M. R. and Rose, I., H. (1983). The dynamics of George VI Ice Shelf. *British Antarctic Survey Bulletin* 52, 205-220.

Peck, L. S. and Brey, T. (1996). Bomb signals in old Antarctic brachiopods. *Nature* 380, 207-208.

Pedley, M., Paren, J. G. and Potter, J. R. (1986). The tidal spectrum underneath Antarctic Ice Shelves. *Journal of Geophysical Research* 91, 13001-13009.

Pedley, M., Paren, J. G. and Potter, J. R. (1988). Localized basal freezing within George Vi Ice Shelf, Antarctica. *Journal of Glaciology* 34, 71-77.

Peel, D. (1992). Ice core evidence from the Antarctic Peninsula region. *In* "Climate since A.D. 1500." (R. S. Bradley, and P. D. Jones, Eds.), pp. 549-571. Routledge, London.

Peel, D. A. and Clausen, H. B. (1982). Oxygen-Isotope and total beta-radioactivity measurements on 10 m ice cores from the Antarctic Peninsula. *Journal of Glaciology* 28, 43-55.

Peel, D., Mulvaney, R. and Davison, B. M. (1988). Stable-Isotope/Air-Temperature relationships in ice cores from Dolleman Islands and the Palmer Land Plateau, Antarctic Peninsula. *Annals of Glaciology* 10, 130-136.

Peel, D., Mulvaney, R., Pasteur, E. C. and Chenery, C. (1996). Climate changes in the Atlantic Sector of Antarctica over the Past t 500 years from ice cores and other evidence. *In* "Climatic variations and forcing mechanisms of the last 2000 years, NATO ASI series." (P. D. Jones, R. S. Bradley, and J. Jouzel, Eds.). Sringer-Verlag, Heidelberg, Berlin.

Petit, J. R., Jouzel, J., Raynaud, D., Barkov, N. I., Barnola, J. M., Basile, I., Bender, M., Chappellaz, J., Davis, M., Delaygue, G., Delmotte, M., Kotlyakov, V. M., Legrand, M., Lipenkov, V. Y., Lorius, C., Pepin, L., Ritz, C., Saltzman, E. and Stievenard, M. (1999). Climate and atmospheric history of the past 420,000 years from the Vostok ice core, Antarctica. *Nature* 399, 429-436.

Phillips, H. A. (1998). Surface meltstreams on the Amery Ice Shelf, East Antarctica. *Annals of Glaciology* 27, 177-181.

Pollard, D. (1980). A simple parameterization of ice sheet ablation rate. *Tellus* 32, 384-388.

Poole, D. A. R., Saettem, J. and Vorren, T. O. (1994). Foraminiferal stratigraphy, paleoenvironments and sedimentation of the glacigenic sequence southwest of Bjornoya. *Boreas* 23, 122-138.

Pope, P. G. (1991). "Late Quaternary Glacial History of the Northern Antarctic Peninsula : Evidence from the Bellingshausen Continental Shelf." Unpublished PhD thesis, Rice University.

Pope, P. G. and Anderson, J. B. (1992). Late Quaternary glacial history of the northern Antarctic Peninsula's western continental shelf: evidence from the marine record. *In* "The Antarctic Palaeoenvironment: A perspective on global change." (J.P. Kennett and D.A. Warnke, Eds.), pp. 63-91. Antarctic Research Series 56, American Geophysical Union.

Potter, J. R. and Paren, J. G. (1985). Interaction between ice shelf and ocean in George VI Sound, Antarctica. *In* "Oceanology of the Antarctic continental shelf." (S. S. Jacobs, Ed.), pp. 35-58. American Geophysical Union, Washington D.C.

Potter, J. R., Paren, J. G. and Loynes, J. (1984). Glaciological and oceanographic calculations of the mass balance and oxygen isotope ratio of a melting ice shelf. *Journal of Glaciology* 30, 161-170.

Potter, J. R., Paren, J. G. and Pedley, M. (1985). Tidal behaviour under an Antarctic Ice Shelf. *British Antarctic Survey Bulletin* 68, 1-18.

Potter, J. R., Talbot, M. H. and Paren, J. G. (1988). Oceanic regimes at the ice fronts of George-Vi Sound, Antarctic Peninsula. *Continental Shelf Research* 8, 347-362.

Powell, R. D. (1984). Glaciomarine processes and inductive lithofacies modeling of ice shelf and tidewater glacier sediments based on Quaternary examples. *Marine Geology* 57, 1-52.

Prahl, F. G., Ertel, J. R., Goni, M. A., Sparrow, M. A. and Eversmeyer, B. (1994). Terrestrial organic-carbon contributions to sediments on the Washington Margin. *Geochimica et Cosmochimica Acta* 58, 3035-3048.

Priddle, J. (1985). Species composition of net phytoplankton from Drake Passage, Bransfield Strait and Scotia Sea during summer, 1982. *Meeresforschung-Reports on Marine Research* 30, 240-250.

Pudsey, C. J. and Evans, J. (2001). First survey of Antarctic sub-ice shelf sediments reveals mid- Holocene ice shelf retreat. *Geology* 29, 787-790.

Pudsey, C. J., Barker, P. F. and Larter, R. D. (1994). Ice-sheet retreat from the Antarctic Peninsula shelf. *Continental Shelf Research* 14, 1647-1675.

Quayle, W. C., Peck, L. S., Peat, H., Ellis-Evans, J. C. and Harrigan, P. R. (2002). Extreme responses to climate change in Antarctic lakes. *Science* 295, 645-645.

Rau, G. H., Takahashi, T. and Marais, D. J. D. (1989). Latitudinal variations in plankton delta-C-13 - implications for CO_2 and productivity in past oceans. *Nature* 341, 516-518.

Rebesco, M., Camerlenghi, A., De Santis, L., Domack, E. and Kirby, M. (1998). Seismic stratigraphy of Palmer Deep: a fault-bounded late Quaternary sediment trap on the inner continental shelf, Antarctic Peninsula Pacific margin. *Marine Geology* 151, 89-110.

Redfield, A. C., Ketchum, B. and Richards, F. A. (1963). The influence of organisms on the composition of seawater. *In* "The Sea." (M. N. Hill, Ed.). Wiley-Interscience, New York.

Renberg, I. (1990). A procedure for preparing large sets of diatom slides from sediment cores. *Journal of Paleolimnology* 4, 87-90.

Reynolds, J. M. (1981a). Lakes on George VI Ice Shelf, Antarctica. *Polar Record* 20, 425-432.

Reynolds, J. M. (1981b). The distribution of mean annual temperatures in the Antarctic Peninsula. *British Antarctic Survey Bulletin* 54, 123-133.

Reynolds, J. M. and Hambrey, M. J. (1988). The Structural Glaciology of George-Vi Ice Shelf, Antarctic Peninsula. *British Antarctic Survey Bulletin,* 79-95.

Richter, W. (1995). Isotope hydrological considerations. *In* "The Schirmacher Oasis, Queen Maud Land, East Antarctic and its surroundings." (P. Bormann, and D. Fritzsche, Eds.), pp. 296-300, Gotha:Perhtes.

Richter, W. and Strauch, G. (1983). Deuterum and 18-oxygen variations in lakes of the Schirmacher Oasis (East Antarctica). *Isotopenpraxis* 19, 145-153.

Richter, W. and Bormann, P. (1995). The Schirmacher Oasis, Queen Maud Land, East Antarctica, and its surroundings. *In* "Hydrology." (P. Bormann, and D. Fritzsche, Eds.), pp. 259–319. Perthes, Gotha.

Ridley, J. (1993). Surface Melting on Antarctic Peninsula Ice Shelves Detected by Passive Microwave Sensors. *Geophysical Research Letters* 20, 2639-2642.

Riedinger, M. A., Steinitz-Kannan, M., Last, W. M. and Brenner, M. (2002). A ca. 6100 C-14 yr record of El Nino activity from the Galapagos Islands. *Journal of Paleolimnology* 27, 1-7.

Rignot, E. and Jacobs, S. S. (2002). Rapid bottom melting widespread near Antarctic ice sheet grounding lines. *Science* 296, 2020-2023.

Rignot, E., Braaten, D., Gogineni, S. P., Krabill, W. B. and McConnell, J. R. (2004). Rapid ice discharge from southeast Greenland glaciers. *Geophysical Research Letters* 31, art. no.-L10401.

Roberts, D., McMinn, A. and Zwartz, D. (2000). An initial palaeosalinity history of Jaw Lake, Bunger Hills based on a diatom-salinity transfer function applied to sediment cores. *Antarctic Science* 12, 172-176.

Roberts, S.J., Miller, I,L., Hodgson, D.A., Bentley, M.J., Smith, J.A. (in prep). Early Holocene collapse/reformation of George VI Sound ice shelf: clast-provenance analysis of lake sediments from Alexander Island, Antarctica Peninsula

Robertson, R., Visbeck, M., Gordon, A. L. and Fahrbach, E. (2002). Long-term temperature trends in the deep waters of the Weddell Sea. *Deep-Sea Research Part Ii-Topical Studies in Oceanography* 49, 4791-4806.

Robin, G. d. Q. and Adie, R. J. (1964). The Ice Cover. *In* "Antarctic Research." (R. Preistly, J., G. d. Q. Robin, and R. J. Adie, Eds.), pp. 1001-1117. Butterworths, London.

Rodbell, D. T., Seltzer, G. O. anderson, D. M., Abbott, M. B., Enfield, D. B. and Newman, J. H. (1999). An similar to 15,000-year record of El Nino-driven alluviation in southwestern Ecuador. *Science* 283, 516-520.

Rohling, E. J. and Cooke, S. (1999). Stable oxygen and carbon isotopes in foraminiferal carbonate shells. *In* "Modern Foraminifera." (B. V. Sen Gupta, Ed.), pp. 239-258. Kluwer Academic Press.

Rosqvist, G. C., Rietti-Shati, M. and Shemesh, A. (1999). Late glacial to middle Holocene climatic record of lacustrine biogenic silica oxygen isotopes from a Southern Ocean island. *Geology* 27, 967-970.

Rott, H., Skvarca, P. and Nagler, T. (1996). Rapid collapse of Northern Larsen Ice Shelf, Antarctica. *Science* 271, 788-792.

Ruttenberg, K. C. and Goni, M. A. (1997). Phosphorus distribution, C:N:P ratios, and delta C-13(oc) in arctic, temperate, and tropical coastal sediments: Tools for characterizing bulk sedimentary organic matter. *Marine Geology* 139, 123-145.

Rymill, J. R. (1938). British Graham Land expedition 1934-1937. *Geographical Journal* 91, 424-438.

Ryves, D. B., Juggins, S., Fritz, S. C. and Battarbee, R. W. (2001). Experimental diatom dissolution and the quantification of microfossil preservation in sediments. *Palaeogeography, Palaeoclimatology, Palaeoecology* 172, 99-113.

Ryves, D.B. (1997). Palaeolimnology list-server query and response. http://www.indiana.edu/~diatom

Sabbe, K., Verleyen, E., Hodgson, D. A., Vanhoutte, K. and Vyverman, W. (2003). Benthic diatom flora of freshwater and saline lakes in the Larsemann Hills and Rauer Islands, East Antarctica. *Antarctic Science* 15, 227-248.

Sabo, S. A. and Schulson, E. M. (1989). The fracture toughness of ice in contact with fresh water. *Journal of Glaciology* 35, 191-192.

Sandgren, P. and Snowball, I. (2001). Application of mineral magnetic techniques to paleolimnology. *In* "Tracking Environmental Change Using Lake Sediments. Volume 2: Physical and Geochemical Methods." (W. M. Last, and J. Smol, Eds.). Kluwer Academic Publishers, Dordrecht, The Netherlands.

Sandweiss, D. H., Richardson, J. B., Reitz, E. J., Rollins, H. B. and Maasch, K. A. (1996). Geoarchaeological evidence from Peru for a 5000 years BP onset of El Nino. *Science* 273, 1531-1533.

Sandweiss, D. H., Maasch, K. A. and Anderson, D. G. (1999). Climate and culture - Transitions in the mid-Holocene. *Science* **283,** 499-500.

Sandweiss, D. H., Maasch, K. A., Burger, R. L., Richardson, J. B., Rollins, H. B. and Clement, A. (2001). Variation in Holocene El Nino frequencies: climate records and cultural consequences in ancient Peru. *Geology* 29, 603-606.

Savin, S. M., Douglas, R. G., Keller, G., Killingley, J. S., Shaugnessy, K., Sommer, M. A., Vincent, E. and Woodruff, F. (1981). Miocene benthic foraminiferal isotope records: a synthesis. *Marine Micropaleontology* 6, 423-450.

Scambos, T. A., Bohlander, J. A., Shuman, C. A. and Skvarca, P. (2004). Glacier acceleration and thinning after ice shelf collapse in the Larsen B embayment, Antarctica. *Geophysical Research Letters* 31, 1-4.

Scambos, T. A., Hulbe, C., Fahnestock, M. and Bohlander, J. (2000). The link between climate warming and break-up of ice shelves in the Antarctic Peninsula. *Journal of Glaciology* 46, 516-530.

Scambos, T., Hulbe, C.L. and Fahnestock, M.A. (2002). Characterising ice shelf response to climate change in Antarctica. A historical and palaeoenvironmental Perspective. Hamilton College, 2002.

Schelske, C. L. and Hodell, D. A. (1995). Using Carbon Isotopes of Bulk Sedimentary Organic-Matter to Reconstruct the History of Nutrient Loading and Eutrophication in Lake Erie. *Limnology and Oceanography* 40, 918-929.

Schlosser, P., Bayer, R., Foldvik, A., Gammelrod, T., Rohardt, G. and Munnich, K. O. (1990). Oxygen-18 and helium as tracers of ice shelf water and water/ice interactions in the Weddell Sea. *Journal of Geophysical Research* 95, 3253-3263.

Schmidt, G. A. (1999). Error analysis of paleosalinity calculations. *Paleoceanography* 14, 422-429.

Schmidt, R., Mausbacher, R. and Muller, J. (1990). Holocene diatom flora and stratigraphy from sediment cores of two Antarctic Lakes (King George Island). *Journal of Paleolimnology* 3, 55-90.

Schmiedl, G., Mackensen, A. and Mueller, P. J. (1997). Recent benthic foraminifera from the eastern South Atlantic Ocean: Dependence on food supply and water masses. *Marine Micropaleontology* 32, 249-287.

Schumm, S. A. (1977). "The Fluvial System." New York, Wiley.

Schwerdtfeger, W. (1984). "Weather and Climate of the Antarctic." Elsevier, Amsterdam.

Scott, P., McMinn, A. and Hosie, G. (1994). Physical parameters influencing diatom community structure in eastern Antarctic sea ice. *Polar Biology* 14, 507-517.

Sejrup, H.-P., Iversen, M., Larsen, E., Landvik, J. Y. and Janocko, J. (1999). A stage 7 marine interglacial record (the Grodeland Interglacial) on Jaeren, southwestern Norway; foraminiferal, stable isotopes and amino acid evidence. *Boreas* 28, 326-347.

Shackleton, N. J. (1974). Attainment of isotpoic equilibrium between ocean water and the benthonic genus Uvigerina: isotopic changes in the ocean during the last glacial. *Colloq. International C.N.R.S.* 219, 203-209.

Shackleton, N. J. and Opdyke, N. D. (1973). Oxygen isotope and paleomagnetic stratigraphy of equatorial Pacific core V28-238: oxygen isotope temperatures and ice volumes on a 10-5 and 10-6 year scale. *Quaternary Research* 3, 39-55.

Shackleton, N. J. and Kennett, J. P. (1975). Palaeotemperature history of the Cenozoic and the initiation of Antarctic glaciation: oxygen and carbon isotope analyses in DSDP Sites 277, 279 and 281. *In* "Initial reports of the DSDP." (J. P. Kennett, and R. E. Houtz, Eds.), pp. 743-755. Government Printing office, Washington.

Shackleton, N. J. and Hall, M. A. (1997). The late Miocene stable isotope record, site 926. *In* "Proceedings of the Ocean Drilling Program, Scientific Results." (N. J. Shackleton, W. B. Curry, C. Richter, and T. J. Bralower, Eds.).

Shepherd, A., Wingham, D., Payne, T. and Skvarca, P. (2003). Larsen ice shelf has progressively thinned. *Science* 302, 856-859.

Shevenell, A. E. and Kennett, J. P. (2002). Antarctic Holocene climate change: A benthic foraminiferal stable isotope record from Palmer Deep. *Paleoceanography* 17, 1019.

Shevenell, A. E., Domack, E. and Kernan, G. M. (1996). Record of Holocene palaeoclimate change along the Antarctic Peninsula: Evidence from glacial marine sediments, Lallemand Fjord. *Paper Proceedings of the Royal Society of Tasmania* 130, 55-64.

Siegenthaler, U. and Eicher, U. (1986). Stable oxygen and carbon isotope analyses. *In* "Handbook of Holocene palaeoecology and palaeohydrology." (B. E. Berglund, Ed.), pp. 407-422. Wiley, Chichester.

Simmonds, I. (2003). Regional and large-scale Influences on Antarctic Peninsula Climate. *In* "Antarctic Peninsula Climate Variability: Historical and Paleoenvironmental Perspectives." (E. Domack, A. Leventer, A. Burnett, R. Bindschadler, P. Convey, and M. Kirby, Eds.). American Geophysical Union, Washington.

Simmonds, I. and Jacka, T. H. (1995). Relationships between the interannual variability of Antarctic Sea-Ice and the Southern Oscillation. *Journal of Climate* 8, 637-647.

Simmonds, I. and Keay, K. (2000). Mean Southern Hemisphere extratropical cyclone behavior in the 40-year NCEP-NCAR reanalysis. *Journal of Climate* 13, 873-885.

Sinha, R., Navada, S. V., Chatterjee, A., Kumar, S., Mitra, A. and Nair, A. R. (2000). Hydrogen and oxygen isotopic analysis of Antarctic lake waters. *Current Science* 78, 992-995.

Sjunneskog, C. and Taylor, F. (2002). Postglacial marine diatom record of the Palmer Deep, Antarctic Peninsula (ODP Leg 178, Site 1098) 1. Total diatom abundance. *Paleoceanography* 17, art. no.-8003.

Sloan, B. J., Lawer, L. A. and Anderson, J. B. (1995). Seismic stratigraphy of the Palmer Basin. *In* "Antarctic Research Series." American Geophysical Union.

Smetacek, V., Scharek, R., Gordon, L. I., Eicken, H., Fahrbach, E., Rohardt, G. and Moore, S. (1992). Early Spring Phytoplankton Blooms in Ice Platelet Layers of the Southern Weddell Sea, Antarctica. *Deep-Sea Research Part a-Oceanographic Research Papers* 39, 153-168.

Smith, A. M., Vaughan, D. G., Doake, C. S. M. and Johnson, A. C. (1998). Surface lowering of the ice ramp at Rothera Point, Antarctic Peninsula, in response to regional climate change. *In* "Annals of Glaciology, Vol 27, 1998." pp. 113-118. Annals of Glaciology.

Smith, D. A. and Klinck, J. M. (2002). Water properties on the west Antarctic Peninsula continental shelf: a model study of effects of surface fluxes and sea ice. *Deep-Sea Research Part Ii-Topical Studies in Oceanography* 49, 4863-4886.

Smith, D. A., Hofmann, E. E., Klinck, J. M. and Lascara, C. M. (1999). Hydrography and circulation of the west Antarctic Peninsula continental shelf. *Deep-Sea Research Part I-Oceanographic Research Papers* 46, 925-949.

Smith, G. I. and Friedman, I. (1990). Lithology and palaeoclimatic implications of lacustrine deposits around lake Vanda and Don Juan pond, Antarctica. *In* "Physical and biochemical processes in Antarctic Lakes." (W. Green, and I. Friedman, Eds.). Antarctic Research Series, AGU, Washington DC.

Spaulding, S. A. and McKnight, D. (1998). Diatoms as indicators of environmental change in Antarctic freshwaters. *In* "The Diatoms: applications for the Environmental and Earth Sciences." (J. Smol, and E. F. Stoermer, Eds.), pp. 249-263. Cambridge University Press, Cambridge.

Spaulding, S. A., McKnight, D. M., Stoermer, E. F. and Doran, P. T. (1997). Diatoms in sediments of perennially ice-covered Lake Hoare, and implications for interpreting lake history in the McMurdo dry valleys of Antarctica. *Journal of Paleolimnology* 17, 403-420.

Spero, H. J. and Lea, D. W. (1996). Experimental determination of stable isotope variability in Globigerina bulloides: Implications for paleoceanographic reconstructions. *Marine Micropaleontology* 28, 231-246.

Spero, H. J., Bijma, J., Lea, D. W. and Bemis, B. E. (1997). Effect of seawater carbonate concentration on foraminiferal carbon and oxygen isotopes. *Nature* 390, 497-500.

Stager, J. C. and Mayewski, P. A. (1997). Abrupt early to mid-Holocene climatic transition registered at the equator and the poles. *Science* 276, 1834-1836.

Steig, E. J., Brook, E. J., White, J. W. C., Sucher, C. M., Bender, M. L., Lehman, S. J., Morse, D. L., Waddington, E. D. and Clow, G. D. (1998). Synchronous climate changes in Antarctica and the North Atlantic. *Science* 282, 92-95.

Steig, E. J., Fastook, J. L., Zweck, C., Goodwin, I. D., Licht, K. J., White, J. and Ackert, R. P. (2001). West Antarctic Ice Sheet Elevation changes. *In* "The West Antarctic Ice Sheet, Behaviour and Environment." (R. B. Alley, and R. Bindschadler, Eds.). AGU, Antarctic Research Series, Washington DC.

Steinitz-Kannan, M., Riedinger, M., Last, W., Brenner, M. and Miller, M. (1999). A six thousand year history of El Niño events in the Galapagos: Evidence from lake cores. *Proceedings of the American Association for the Advancement of Science, Pacific Division 18 (1): 84.*

Storey, B. C. and Garrett, S. W. (1985). Crustal growth of the Antarctic Peninsula by accretion, magmatism and extension. *Geological Magazine* 122, 5-14.

Stuiver, M. and Reimer, P. J. (1993). Extended 14C database and revised CALIB radiocarbon calibration program. *Radiocarbon* 35, 215-230.

Stuiver, M., Quay, P. D. and Ostlund, H. G. (1983). Abyssal water C-14 distribution and the age of the World Oceans. *Science* 219, 849-851.

Stuut, J-B, W., Crosta, X., van der Borg, K. and Schneider, R. 2004. Relationship between Antarctic sea ice and southwest African climate during the late Quaternary. *Geology*, 32, 10, 909-912.

Suarez, M. (1976). Plate-tectonic model for southern Antarctic Peninsula and its relation to southern Andes. *Geology* 4, 211-214.

Sugden, D. E. and Clapperton, C. M. (1980). West Antarctic Ice Sheet fluctuations in the Antarctic Peninsula area. *Nature* 286.

Sugden, D. E. and Clapperton, C. M. (1981). An ice-shelf moraine, George VI Sound, Antarctica. *Annals of Glaciology* 2, 135-141.

Sugden, D. E. and Clapperton, C. M. (1988). Holocene glacier fluctuations in South America and Antarctica. *Quaternary Science Reviews* 7, 185-198.

Swithinbank, C. W. M. (1988). Satellite image atlas of Glaciers of the World. *USGS professional paper, 1386-B.*

Syvitski, J. P. M. (1991). "Principles, Methods of Application of Particle Size Analysis." Cambridge University Press, New York.

Talbot, M. H. (1988). Oceanic environment of George VI Ice Shelf, Antarctic Peninsula. *Annals of Glaciology* 11, 161-164.

Talbot, M. R. (1990). A review of the paleohydrological interpretation of carbon and oxygen isotopic ratios in primary lacustrine carbonates. *Isotope Geosciences*, 261–80.

Talbot, M. R. and Laerdal, T. (2000). The Late Pleistocene-Holocene palaeolimnology of Lake Victoria, East Africa, based upon elemental and isotopic analyses of sedimentary organic matter. *Journal of Paleolimnology* 23, 141-164.

Taylor, B. J., Thomson, M. R. A. and Willey, L. E. (1979). The geology of Ablation point-Keystone Cliffs area, Alexander Island. *British Antarctic Survey Bulletin* 82, 85.

Taylor, F. and McMinn, A. (2001). Evidence from diatoms for Holocene climate fluctuation along the East Antarctic margin. *Holocene* 11, 455-466.

Taylor, F. and Sjunneskog, C. (2002). Postglacial marine diatom record of the Palmer Deep, Antarctic Peninsula (ODP Leg 178, Site 1098) 2. Diatom assemblages. *Paleoceanography* 17, art. no.-1026.

Taylor, F., Whitehead, J. and Domack, E. (2001). Holocene paleoclimate change in the Antarctic Peninsula: evidence from the diatom, sedimentary and geochemical record. *Marine Micropaleontology* 41, 25-43.

Telford, R. J., Heegaard, E. and Birks, H. J. B. (2004a). All age-depth models are wrong: but how badly? *Quaternary Science Reviews* 23, 1-5.

Telford, R. J., Heegaard, E. and Birks, H. J. B. (2004b). The intercept is a poor estimate of a calibrated radiocarbon age. *Holocene* 14, 296-298.

Tenzer, G. E., Meyers, P. A. and Knoop, P. (1997). Sources and distribution of organic and carbonate carbon in surface sediments of Pyramid lake, Nevada. *Journal of Sedimentary Research* 67, 884-890.

Thomas, R. H., Sanderson, T. J. O. and Rose, K. E. (1979). Effects of a climate warming on the West Antarctic Ice Sheet. *Nature* 227, 355-358.

Thompson, L. G., Peel, D. A., Mosley-Thompson, E., Mulvaney, R., Dai, J., Lin, P. N., Davis, M. E. and Raymond, C. F. (1994). Climate since ad 1510 on Dyer Plateau, Antarctic Peninsula: evidence for recent climate change. *Annals of Glaciology* 20, 420-426.

Thompson, R. and Oldfield, F. (1986). "Environmental Magnetism." George Allen and Unwin, London.

Thompson, S. and Eglinton, G. (1978). The fractionation of a recent sediment for organic geochemical analysis. *Geochemica et Cosmochimica Acta* 42, 199-207.

Thornton, S. F. and McManus, J. (1994). Applications of organic carbon and nitrogen stable isotopes and C/N ratios as source indicators of organic matter provenance in estuarine systems: evidence from the Tay estuary, Scotland. *Estuarine, Coastal and Shelf Science* 38, 219-233.

Tison, J. L., Morris, E. M., Souchez, R. and Jouzel, J. (1991). Stratigraphy, stable isotopes and salinity in multiyear sea ice from the rift area, South George-VI Ice Shelf, Antarctic Peninsula. *Journal of Glaciology* 37, 357-367.

Trenberth, K. E. and Caron, J. M. (2000). The Southern Oscillation revisited: Sea level pressures, surface temperatures, and precipitation. *Journal of Climate* 13, 4358-4365.

Turner, J., Colwell, S. R. and Harangozo, S. (1997). Variability of precipitation over the coastal western Antarctic Peninsula from synoptic observations. *Journal of Geophysical Research-Atmospheres* 102, 13999-14007.

Urey, H. C. (1947). The thermodynamic properties of isotopic substances. *Journal of Chemical Society*, 562-581.

Van de Vijver, B. and Beyens, L. (1999a). Biogeography and ecology of freshwater diatoms in sub-Antarctica: a review. *Journal of Biogeography* 26, 993-1000.

Van de Vijver, B. and Beyens, L. (1999b). Freshwater diatoms form Ile de la Possession (Crozet Archipelago, sub-Antarctica): an ecological assessment. *Polar Biology* 22, 178-188.

van den Broeke, M. R. (1998). The semi-annual oscillation and Antarctic climate. Part 2: Recent changes. *Antarctic Science* 10, 184-191.

van den Broeke, M. R. (2000). On the interpretation of Antarctic temperature trends. *Journal of Climate* 13, 3885-3889.

van der Veen, C. J. (1998). Fracture Mechanics approach to investigating conditions leading to ice shelf break-up. *In* "Chapman conference on the West Antarctic Ice Sheet. 13-18 September 1998." AGU, Washington.

Van Hove, P., Swadling, K. M., Gibson, J. A. E., Belzile, C. and Vincent, W. F. (2001). Farthest north lake and fjord populations of calanoid copepods *Limnocalanus macrurus* and *Drepanopus bungei* in the Canadian high Arctic. *Polar Biology* 24, 303-307.

van Loon, H. (1984). Interannual variations in the half-yearly cycle of pressure gradients and zonal winds at sea-level on the Southern Hemisphere. *Tellus* 36A, 76-86.

Vaughan, D. G. (1992). *In* "The contribution of Antarctic Peninsula to sea level rise." (E. M. Morris, Ed.), pp. 35-44. British Antarctic Survey, Cambridge.

Vaughan, D. G. (1993). Implications of the break-up of Wordie ice shelf, Antarctica for sea level. *Antarctic Science* 5, 403-408.

Vaughan, D. G. (1995a). "Dynamic and climatic controls on Antarctic ice shelves." Unpublished PhD thesis, The Open University.

Vaughan, D. G. (1995b). Tidal flexure at ice shelf margins. *Journal of Geophysical Research* 100 (B4), 6213-6224.

Vaughan, D. G. (in press). A new classification scheme for ice shelves based on mechanisms of mass gain and loss. *Polar Record.*

Vaughan, D. G. and Doake, C. S. M. (1996). Recent atmospheric warming and retreat of ice shelves on the Antarctic Peninsula. *Nature* 379, 328-331.

Vaughan, D. G., Marshall, G. J., Connolley, W. M., Parkinson, C., Mulvaney, R., Hodgson, D. A., King, J. C., Pudsey, C. J. and Turner, J. (2003). Recent rapid regional climate warming on the Antarctic Peninsula. *Climatic Change* 60, 243-274.

Verleyen, E., Hodgson, D. A., Vyverman, W., Roberts, D., McMinn, A., Vanhoutte, K. and Sabbe, K. (2003). Modelling diatom responses to climate induced fluctuations in the moisture balance in continental Antarctic lakes. *Journal of Paleolimnology* 30, 195-215.

Verleyen, E, Hodgson, D.A, Sabbe, K, Vanhoutte, K, Vyverman, W. (2004) Coastal oceanographic conditions in the Prydz Bay region (East Antarctica) during the Holocene recorded in an isolation basin. *Holocene* 14 (2): 246-257

Villalba, R., Cook, E. R., Jacoby, G. C., D'Arrigo, R. D., Veblen, T. T. and Jones, P. D. (1998). Tree-ring based reconstructions of northern Patagonia precipitation since AD 1600. *Holocene* 8, 659-674.

Villinski, J. C. and Domack, E. (1998). Temporal changes in sedimentary organic carbon from Ross Sea Antarctica: inferred changes in ecosystem and climate. *EOS (Transactions, American Geophysical Union)* 79, 150-157.

Vincent, W. F., Gibson, J. A. E. and Jefferies, M. O. (2001). Ice shelf collapse, climate change and habitat loss in the Canadian High Arctic. *Polar Record* 37, 131-136.

Wand, U., Hermichen, W.-D., Bruggemann, E., Zierath, R. and Klokov, V. D. (1988). Stable isotope and hydrogeochemical studies of Beaver Lake and Radok Lake, MacRobertson Land, East Antarctica. *ZFI Mitteilungen* 143, 99-111.

Ward, C. G. (1995). The mapping of ice front changes on Muller Ice Shelf, Antarctic Peninsula. *Antarctic Science* 7, 197-198.

Wassell, A. and Hankinson, H. (1992). Diatom stratigraphy in a lake on Horseshoe Island, Antarctica. *Diatom Research* 7, 157-194.

Weatherly, J. W., Walsh, J. E. and Zwally, H. J. (1991). Antarctic Sea Ice Variations and Seasonal Air-Temperature Relationships. *Journal of Geophysical Research-Oceans* 96, 15119-15130.

Weertman, J. (1973). Can a water filled crevasse reach the bottom surface of a glacier? *In* "International Association of Scientific Hydrology Publication 95:Hydrology of Glaciers." Cambridge.

Weertman, J. (1974). Stability of the junction of an Ice Sheet and Ice Shelf. *Journal of Glaciology* 13, 3-11.

Weertman, J. (1976). Glaciology's Grand Unsolved Problem. *Nature* 260, 284-286.

Wefer, G. and Berger, W. H. (1991). Isotope Paleontology - growth and composition of extant calcareous species. *Marine Geology* 100, 207-248.

Westman, P. and Hedenstrom, A. (2002). Environmental changes during isolation processes from the Litorina Sea as reflected by diatoms and geochemical parameters - a case study. *Holocene* 12, 531-540.

Wharton, R. A., Lyons, W. B. and Marais, D. J. D. (1993). Stable Isotopic Biogeochemistry of Carbon and Nitrogen in a Perennially Ice-Covered Antarctic Lake. *Chemical Geology* 107, 159-172.

Whitehead, J. M., Wotherspoon, S. and Bohaty, S. M. (2005). Minimal Antarctic Sea Ice During the Pliocene. *Geology*, 33, 137-140.

Whitworth, T. I. and Nowlin, J., W.D. (1987). Water masses and currents of the Southern Ocean at the Greenwich Meridian. *Journal of Geophysical Research* 92, 6462-6476.

Williams, M. J. M., Warner, R. C. and Budd, W. F. (2002). Sensitivity of the Amery Ice Shelf, Antarctica, to changes in the climate of the Southern Ocean. *Journal of Climate* 15, 2740-2757.

Wright, M. R. (1994). "The offshore sedimentary record of the late Quaternary record, Hong Kong." Unpublished MSc thesis, University of Liverpool.

Ye, Z. and Cuihua, X. (1997). 210Pb distribution characteristics in the lake sediment cores at Great Wall station, Antarctica. *Journal of Polar Science* 8, 33-36.

Yoon, H. I., Park, B. K., Kim, Y. and Kang, C. Y. (2002). Glaciomarine sedimentation and its paleoclimatic implications on the Antarctic Peninsula shelf over the last 15 000 years. *Palaeogeography, Palaeoclimatology, Palaeoecology* 185, 235-254.

Yoon, H. I., Park, B. K., Kim, Y. and Kim, D. (2000). Glaciomarine sedimentation and its paleoceanographic implications along the fjord margins in the South Shetland Islands, Antarctica during the last 6000 years. *Palaeogeography, Palaeoclimatology, Palaeoecology* 157, 189-211.

Yuan, X. J. and Martinson, D. G. (2000). Antarctic sea ice extent variability and its global connectivity. *Journal of Climate* 13, 1697-1717.

Zale, R. (1994). C-14 Age Corrections in Antarctic Lake-Sediments Inferred from Geochemistry. *Radiocarbon* 36, 173-185.

Zale, R. (1994). Changes in Size of the Hope Bay Adelie Penguin Rookery as Inferred from Lake Boeckella Sediment. *Ecography* 17, 297-304.

Zale, R. and Karlen, W. (1989). Lake Sediment Cores from the Antarctic Peninsula and Surrounding Islands. *Geografiska Annaler Series a-Physical Geography* 71, 211-220.

Zielinski, U. and Gersonde, R. (1997). Diatom distribution in Southern Ocean surface sediments (Atlantic sector): Implications for paleoenvironmental reconstructions. *Palaeogeography, Palaeoclimatology, Palaeoecology* 129, 213-250.

Plate 1 – Key diatoms species x1000

1. *Cocconeis faciolata* (Ehrenberg) Brown
2. *Chaetoceros spore* (neglectus Karsten)
3. Diploneis sp.
4. *Eucampia antarctica var. recta* (Castracane) Manguin – Intercalary
5. *Eucampia antarctica var. recta* (Castracane) Manguin – Symmetric
6. *Eucampia antarctica var. recta* (Castracane) Manguin – Pointy/terminal
7. *Thalassiosira antarctica* Comber
8. *Thalassiosira gracilis* (Karsten) Hustedt
9. *Unknown centric*

Plate 2 – Key foraminiferal species

1. *Angulogerina earlandi* Parr
2. *Cibicides aff. grossepunctatus* Earland
3. *Cibicides lobatulus* (Walker and Jacob)
4. *Globocassidulina biora* (Crespin)Stainforthis davisi (Chapman and Parr)
5. *Melonis* sp.
6. *Cassidulinoides parvas* (Earland)

Plate 1

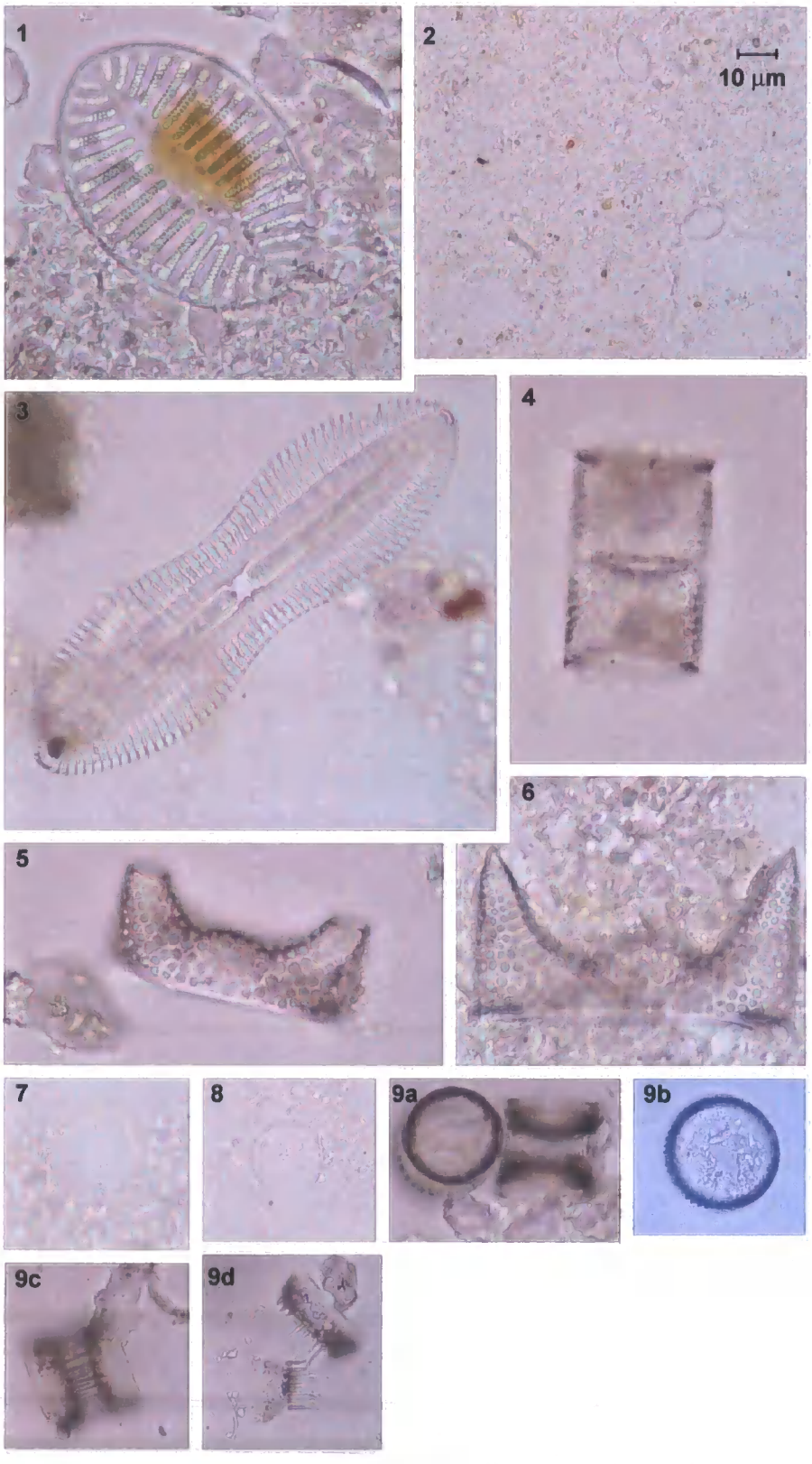

Plate 2

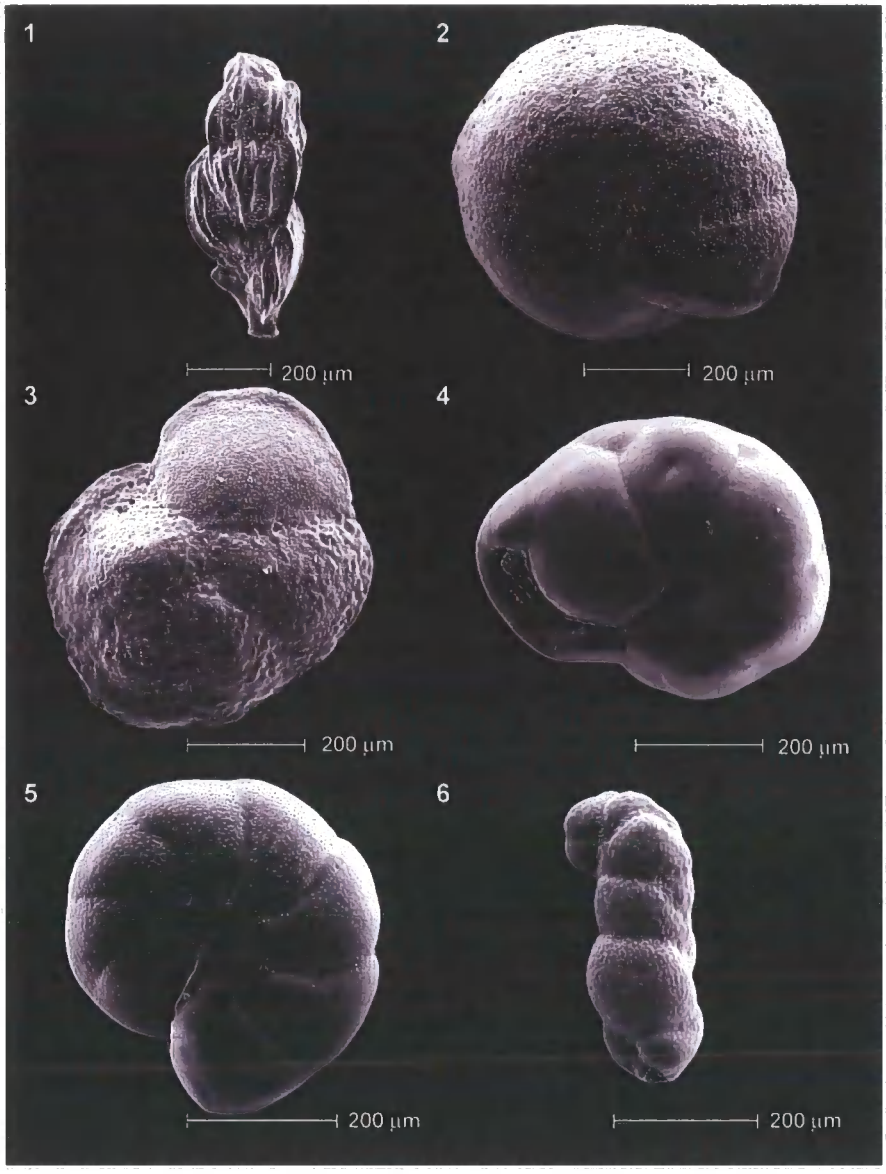

APPENDIX ONE – PERCENTAGE PLOTS

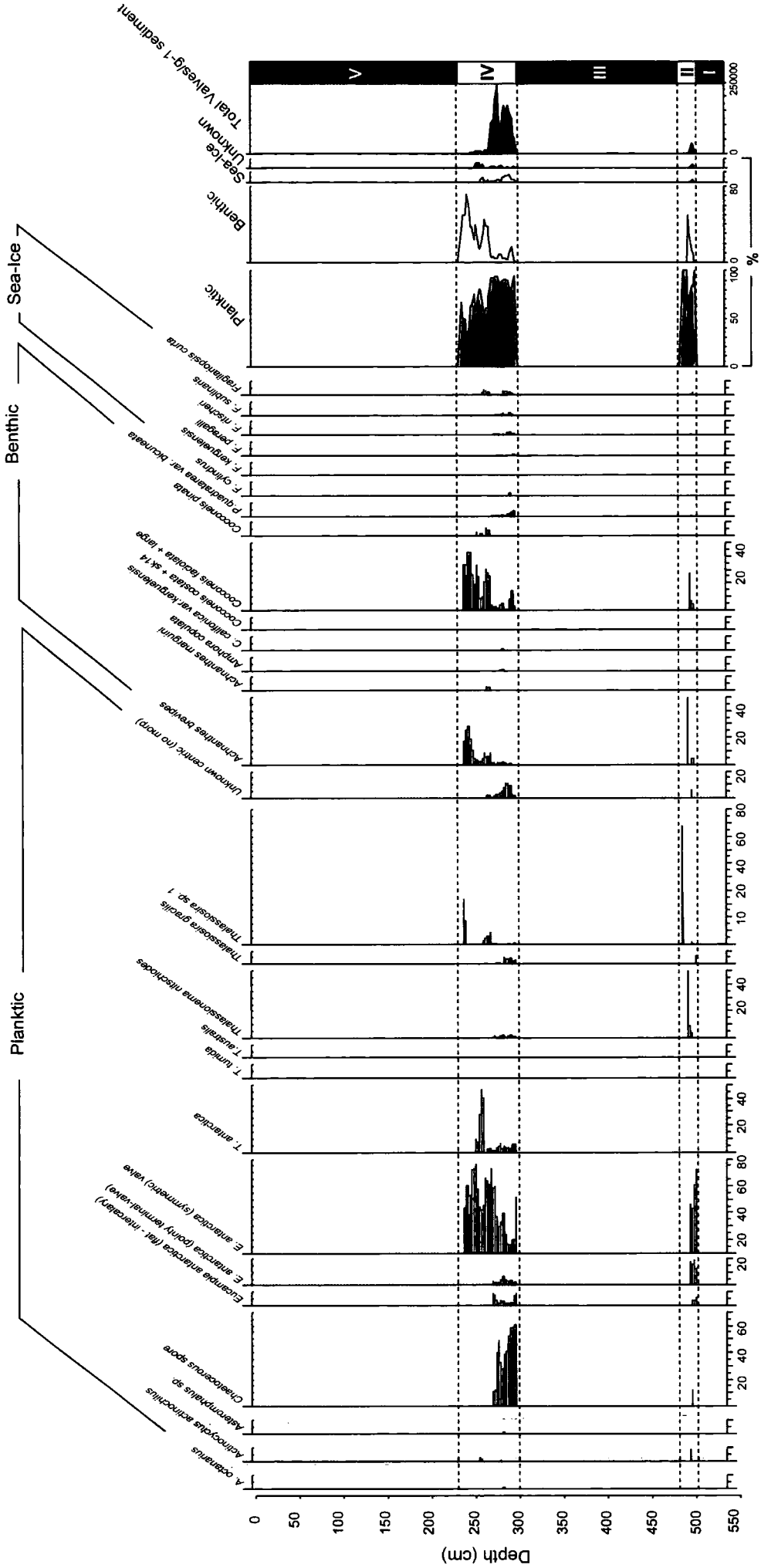

Appendix 1. Diatom analysis of the ML core. Data presented as percentages.

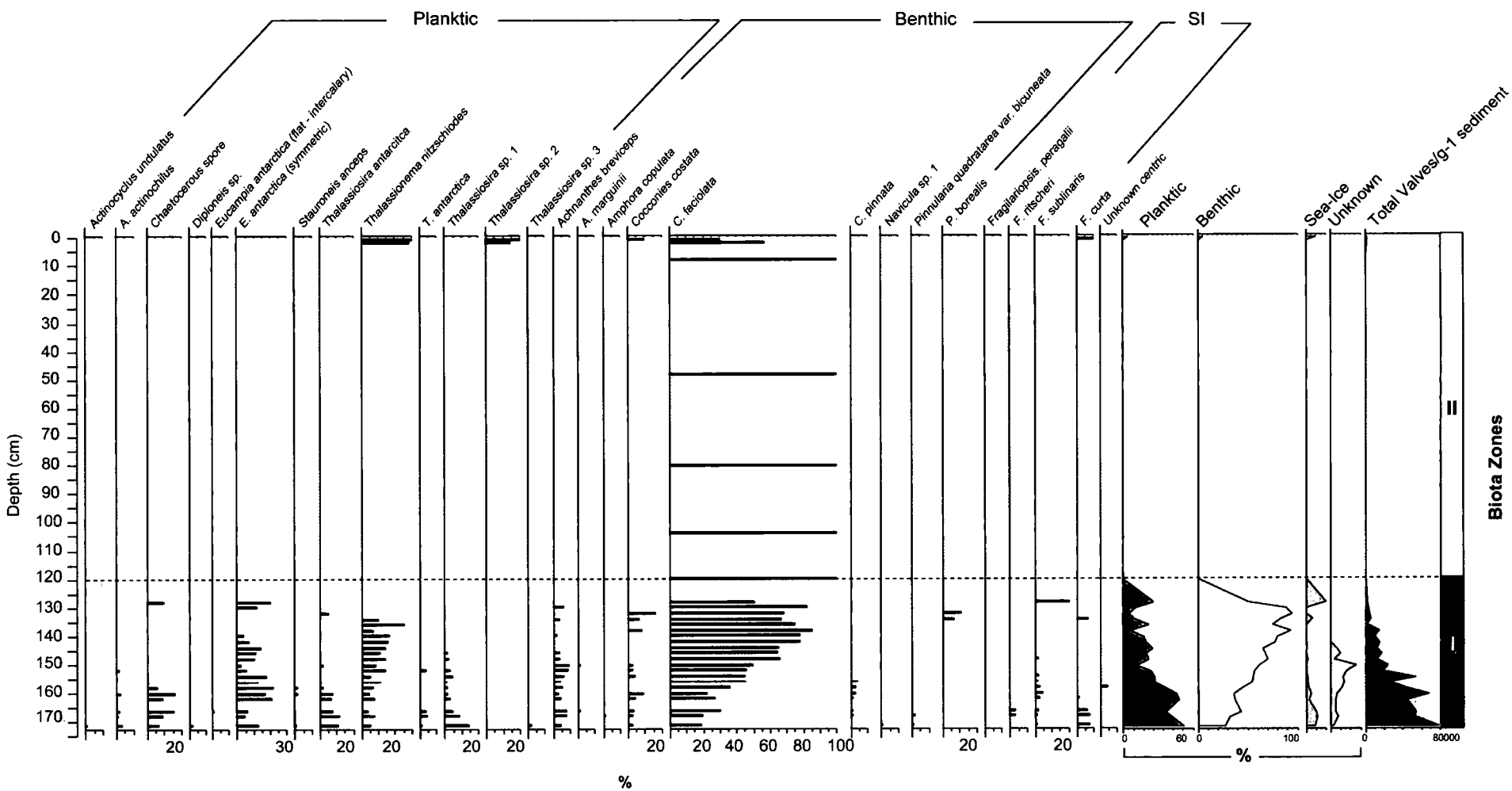

Appendix 1. Diatom analysis of the MLNB core. Data presented as percentages

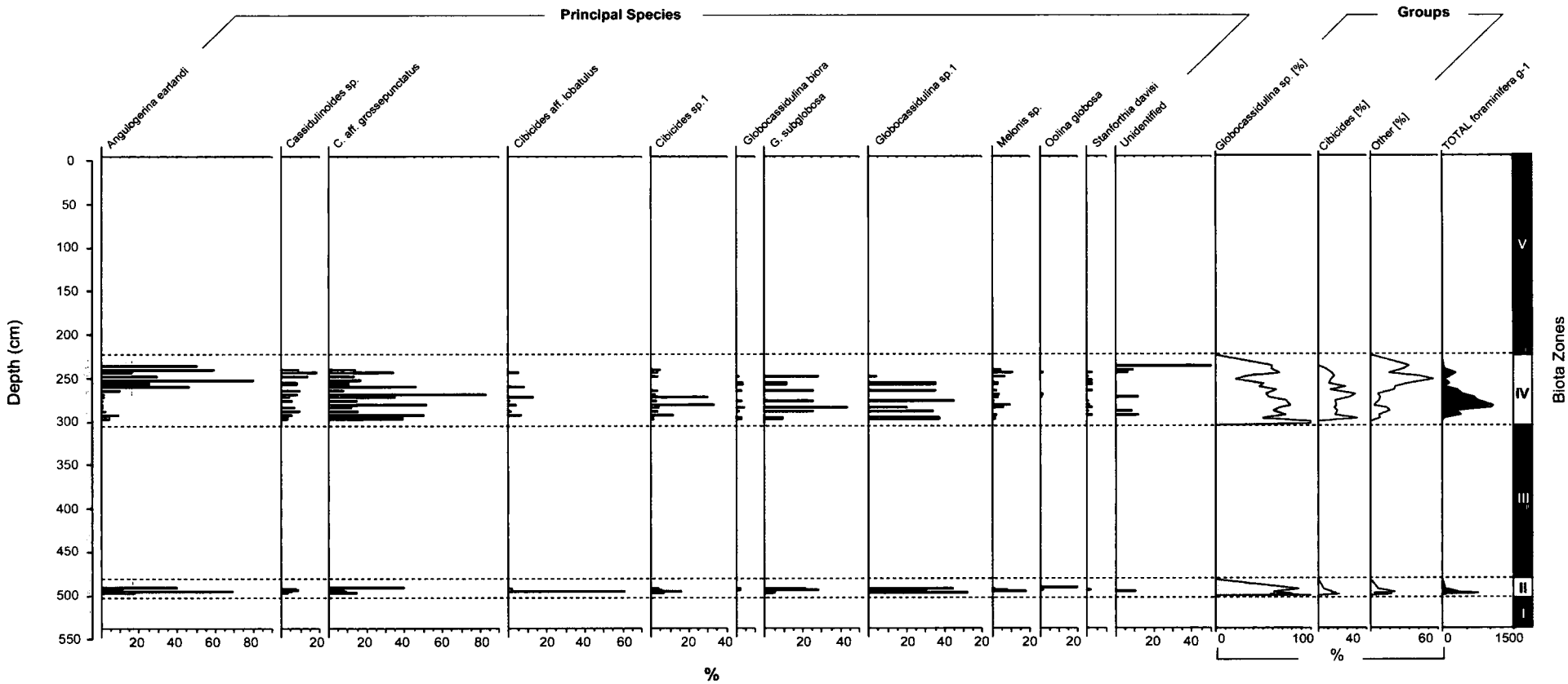

Appendix 1. Foraminiferal analysis of the ML core. Data presented as percentages

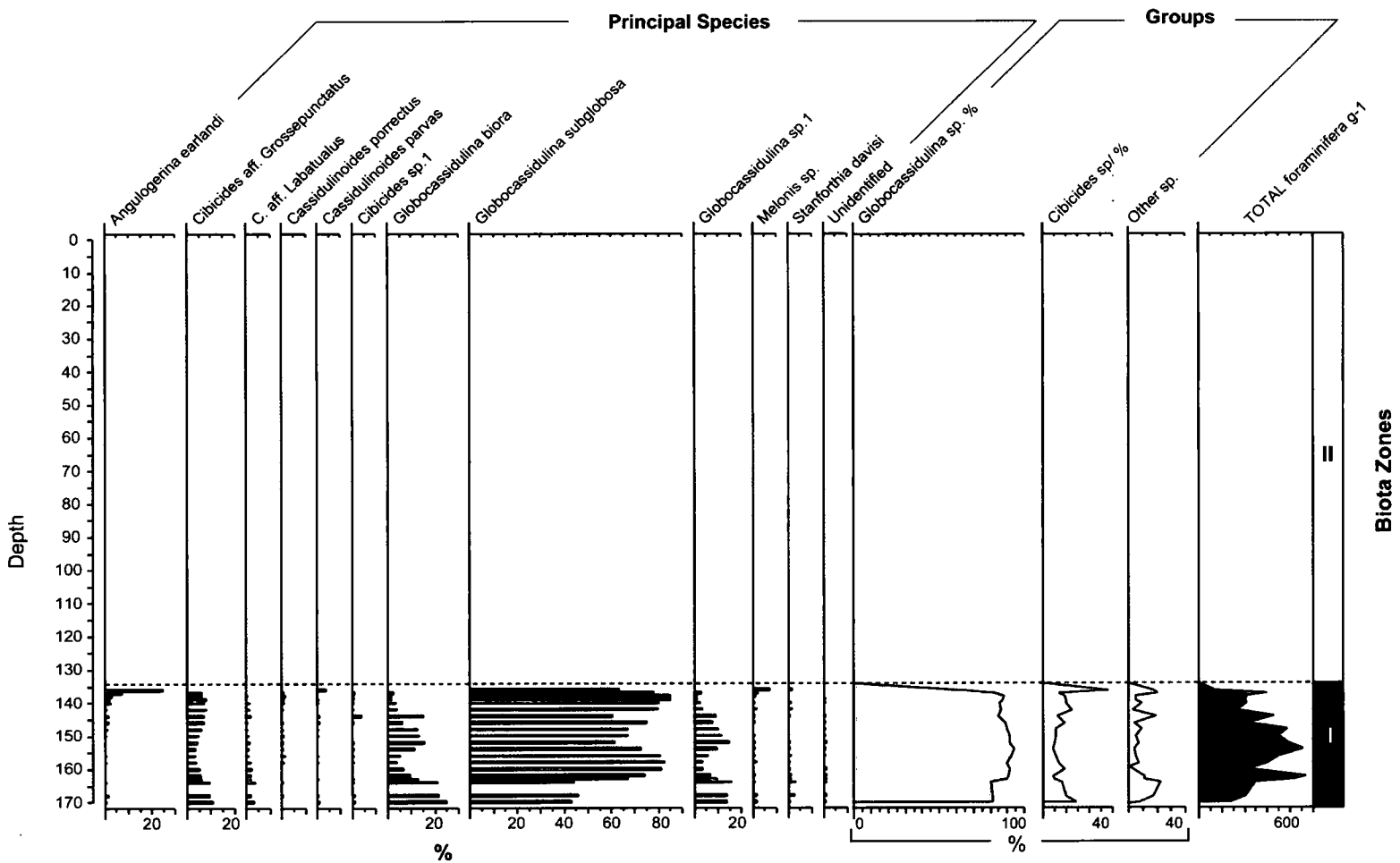

Appendix 1. Foraminiferal analysis of the MLNB core. Data presented as percentages